

SAFETY ANALYSIS REPORT
OF
JRF-90Y-950K

2019
Kyoto University

CONTENTS

	<u>Page</u>
(I) Description of nuclear fuel package	(I)
A. Purpose and conditions	(I)-A-1
B. Kinds of package	(I)-B-1
C. Packaging	(I)-C-1
D. Contents of packaging	(I)-D-1
 (II) Safety analysis of nuclear fuel package	 (II)
A. Structural analysis	(II)-A-1
A.1 Structural design	(II)-A-1
A.1.1 General description	(II)-A-1
A.1.2 Design standards	(II)-A-2
A.2 Weight and center of gravity	(II)-A-33
A.3 Mechanical properties of materials	(II)-A-33
A.4 Requirements of the package	(II)-A-50
A.4.1 Chemical and electrical reactions	(II)-A-50
A.4.2 Low temperature strength	(II)-A-51
A.4.3 Sealing device	(II)-A-52
A.4.4 Hoisting accessory	(II)-A-53
A.4.5 Tightening device	(II)-A-58
A.4.6 Pressure	(II)-A-66
A.4.7 Vibration	(II)-A-68
A.5 Normal test conditions	(II)-A-71
A.5.1 Thermal test	(II)-A-71
A.5.1.1 Outline of temperature and pressure	(II)-A-71
A.5.1.2 Thermal expansion	(II)-A-73

A. 5.1.3	Stress calculation	·····	(II)-A-74
A. 5.1.4	Comparison of allowable stress	·····	(II)-A-82
A. 5.2	Water spray	·····	(II)-A-84
A. 5.3	Free drop	·····	(II)-A-84
A. 5.4	Stacking test	·····	(II)-A-201
A. 5.5	Penetration	·····	(II)-A-207
A. 5.6	Corner or edge drop	·····	(II)-A-209
A. 5.7	Summary of results and evaluation	·····	(II)-A-209
A. 6	Accident test conditions	·····	(II)-A-210
A. 6.1	Mechanical test - Drop test I (9m drop)	·····	(II)-A-210
	or mechanical test - Drop III (dynamic pressure pickles)		
A. 6.1.1	Vertical drop	·····	(II)-A-216
A. 6.1.2	Horizontal drop	·····	(II)-A-230
A. 6.1.3	Corner drop	·····	(II)-A-237
A. 6.1.4	Inclined drop	·····	(II)-A-240
A. 6.1.5	Summary of the results	·····	(II)-A-244
A. 6.2	Mechanical test --- DropII (1m drop)	·····	(II)-A-246
A. 6.2.1	Summary of results	·····	(II)-A-252
A. 6.3	Thermal test	·····	(II)-A-253
A. 6.3.1	Summary of temperatures and pressure	·····	(II)-A-253
A. 6.3.2	Thermal expansion	·····	(II)-A-253
A. 6.3.3	Comparison of allowable stresses	·····	(II)-A-254
A. 6.4	Water immersion	·····	(II)-A-256
A. 6.5	Summary of result and evaluation	·····	(II)-A-265
A. 7	Reinforced immersion test	·····	(II)-A-267
A. 8	Radioactive content	·····	(II)-A-267
A. 9	Fissile package	·····	(II)-A-268
A. 9.1	Normal test conditions	·····	(II)-A-268
A. 9.2	special test conditions for	·····	(II)-A-270
	fissionable transported articles		

A.10	Appendix	(II)-A-275
B.	Thermal analysis	(II)-B-1
B.1	General description	(II)-B-1
B.2	Thermal properties of the materials	(II)-B-6
B.3	Specifications of components	(II)-B-10
B.4	Normal test conditions	(II)-B-11
B.4.1	Thermal analytical model	(II)-B-11
B.4.1.1	Analytical model	(II)-B-11
B.4.1.2	Test model	(II)-B-13
B.4.2	Maximum temperatures	(II)-B-13
B.4.3	Minimum temperatures	(II)-B-14
B.4.4	Maximum internal pressure	(II)-B-14
B.4.5	Maximum thermal stress	(II)-B-14
B.4.6	Summary of results and evaluation	(II)-B-15
B.5	Accident test conditions	(II)-B-16
B.5.1	Thermal analytical model	(II)-B-16
B.5.1.1	Analytical model	(II)-B-16
B.5.1.2	Test model	(II)-B-20
B.5.2	Evaluation conditions for packages	(II)-B-21
B.5.3	Temperatures of packages	(II)-B-21
B.5.4	Maximum internal pressure	(II)-B-23
B.5.5	Maximum thermal stresses	(II)-B-23
B.5.6	Summary of results and evaluation	(II)-B-24
B.6	Appendix	(II)-B-26
C.	Containment analysis	(II)-C-1
C.1	General	(II)-C-1
C.2	Containment system	(II)-C-1
C.2.1	Containment system	(II)-C-1

C.2.2	Penetration of containment system	(II)-C-4
C.2.3	Gasket and weldings of the containment system	(II)-C-4
C.2.4	Lid	(II)-C-5
C.3	Normal test conditions	(II)-C-6
C.3.1	Leakage of radioactive materials	(II)-C-6
C.3.2	Pressurization of the containment system	(II)-C-19
C.3.3	Coolant contamination	(II)-C-19
C.3.4	Loss of coolant	(II)-C-19
C.4	Accident test conditions	(II)-C-20
C.4.1	Fissile gas	(II)-C-20
C.4.2	Leakage of radioactive materials	(II)-C-21
C.5	Summary of the results and the evaluation	(II)-C-24
C.6	Appendix	(II)-C-25
D.	Shield analysis	(II)-D-1
D.1	Outline	(II)-D-1
D.2	Radiation source specification	(II)-D-1
D.2.1	Gamma radiation source	(II)-D-2
D.2.2	Neutron source	(II)-D-11
D.3	Model specification	(II)-D-14
D.3.1	Analysis model	(II)-D-14
D.3.2	Numeric density of atoms in each area of analysis model	(II)-D-20
D.4	Shield evaluation	(II)-D-22
D.5	Summary of the results and evaluation	(II)-D-27
D.6	Appendix	(II)-D-29
E.	Criticality analysis	(II)-E-1
E.1	General	(II)-E-1
E.2	Parts to be analyzed	(II)-E-3
E.2.1	Content	(II)-E-3

E.2.2	Packaging	(II)-E-3
E.2.3	Neutron absorbing materials	(II)-E-7
E.3	Model specification	(II)-E-8
E.3.1	Calculation model	(II)-E-8
E.3.2	Regional densities for each analyzed model region	(II)-E-10
E.4	Evaluation for subcriticality	(II)-E-28
E.4.1	Calculation conditions	(II)-E-28
E.4.2	Water immersion into package	(II)-E-29
E.4.3	Calculation method	(II)-E-29
E.4.4	Results	(II)-E-31
E.5	Benchmark test	(II)-E-34
E.6	Summary of results and evaluation	(II)-E-44
E.7	Appendix	(II)-E-45

F.	Assessment of the compliance with	
	the regulation and the notification	(II)-F

(III)	Basic policy for quality management	(III)
A.	Quality management system	(III)-1
A.1	General requirement	(III)-1
A.2	Requirements for documentation	(III)-2
B.	Responsibility of the management	(III)-4
B.1	Commitment of the management	(III)-4
B.2	Responsibility and authority	(III)-4
B.3	Management review	(III)-5
C.	Education and training	(III)-9
C.1	Securing resources	(III)-9
C.2	Section personnel	(III)-9
C.3	Education and training, etc.	(III)-9

D.	Design control	(III)-10
D.1	Planning of processes required by individual operations	(III)-10
D.2	Determination of individual operations requirements	(III)-10
D.3	Review of individual operations requirements	(III)-11
D.4	Transmission of information to external parties	(III)-11
D.5	Design and development planning	(III)-11
D.6	Input related to design and development	(III)-12
D.7	Output related to design and development	(III)-12
D.8	Design and development review	(III)-13
D.9	Design and development verification	(III)-13
D.10	Validation of design and development	(III)-14
D.11	Control of design and development changes	(III)-14
E.	Manufacturing order of transport packaging	(III)-16
E.1	Quality management plan	(III)-16
E.2	Procurement process	(III)-16
E.3	Evaluation of the Manufacturer of Transport Packaging	(III)-16
E.4	Quality Management Requirement to the Manufacturer	(III)-17
E.5	Verification of manufacturing of transport packaging	(III)-18
E.6	Schedule management and certification of special processes	(III)-18
E.7	Measurement, analysis and improvement	(III)-18
E.8	Content of quality management system by manufacturer of transport packaging	(III)-24
F.	Handling and Maintenance	(III)-33
F.1	Handling Management	(III)-33
F.2	Maintenance and storage management	(III)-33
(IV)	Handling methods and maintenance of nuclear fuel package	
A.	Package handling methods	(IV)-A-1
A.1	Method of loading	(IV)-A-1
A.2	Package inspection prior to shipment	(IV)-A-2

A.3	Method of unloading	(IV)-A-2
A.4	Preparation of empty packaging	(IV)-A-2
B.	Maintenance requirements	(IV)-B-1
B.1	Visual appearance inspection	(IV)-B-1
B.2	Pressure durability inspection	(IV)-B-1
B.3	Airtight leakage inspection	(IV)-B-1
B.4	Shielding inspection	(IV)-B-1
B.5	Subcriticality inspection	(IV)-B-1
B.6	Thermal inspection	(IV)-B-1
B.7	Lifting inspection	(IV)-B-1
B.8	Actuation check/inspection	(IV)-B-1
B.9	Maintenance of auxiliary systems	(IV)-B-2
B.10	Maintenance of the valves, gaskets, etc. of sealing devices	(IV)-B-2
B.11	Storage of the transport packaging	(IV)-B-2
B.12	Retention of records	(IV)-B-2
B.13	Others	(IV)-B-2
(V)	Important Notice about a safe design	
	and the safe transportation	(V)

List of Figures

	<u>Page</u>
Chapter I	
(I)-Fig. A. 1 Rough drawing of package	(I)-A-7
(I)-Fig. C. 1 Rough drawing of package	(I)-C-2
(I)-Fig. C. 2 Package under transport condition	(I)-C-3
(I)-Fig. C. 3 Package under transport condition	(I)-C-4
(I)-Fig. C. 4 Seal boundary of package	(I)-C-5
(I)-Fig. C. 5 General drawing of package	(I)-C-9
(I)-Fig. C. 6 Main body	(I)-C-10
(I)-Fig. C. 7 Inner lid	(I)-C-11
(I)-Fig. C. 8 Basket for box type fuel	(I)-C-12
(I)-Fig. C. 9 Outer shell lid	(I)-C-13
(I)-Fig. D. 1 Metal spacer	(I)-D-4
(I)-Fig. D. 2 JRR-3 standard type fuel element	(I)-D-8
(uranium silicon aluminum dispersion alloy)	
(I)-Fig. D. 3 JRR-3 follower type fuel element	(I)-D-9
(uranium silicon aluminum dispersion alloy)	
(I)-Fig. D. 4 JRR-4B type fuel element	(I)-D-10
(I)-Fig. D. 5 JRR-4L type fuel element	(I)-D-11
(I)-Fig. D. 6 JRR-4 fuel element	(I)-D-12
(uranium silicon aluminum dispersion type alloy)	
(I)-Fig. D. 7 JMTR standard fuel element	(I)-D-13
(I)-Fig. D. 8 JMTR follower type fuel element	(I)-D-14
(I)-Fig. D. 9 KUR standard and half-loaded fuel element	(I)-D-15
(uranium silicon aluminum dispersion type alloy)	
(I)-Fig. D. 10 KUR special fuel element	(I)-D-16
(uranium silicon aluminum dispersion type alloy)	
(I)-Fig. D. 11 JMTRC standard fuel element	(I)-D-17
(A type, B type, C type)	
(I)-Fig. D. 12 JMTRC standard fuel element (pin fix type)	(I)-D-18
(C type)	
(I)-Fig. D. 13 JMTRC special fuel element (special A type)	(I)-D-19
(I)-Fig. D. 14 JMTRC special fuel element (special B type)	(I)-D-20
(I)-Fig. D. 15 JMTRC special fuel element	(I)-D-21

	(special C type, special D type)	
(I)-Fig. D. 16	JMTRC fuel follower (HF type)	(I)-D-22
(I)-Fig. D. 17	JMTRC standard fuel element (MA, MB, MC type)	(I)-D-23
(I)-Fig. D. 18	JMTRC special fuel element	(I)-D-24
	(special MB type, special MC type)	
(I)-Fig. D. 19	JMTRC fuel follower (MF type)	(I)-D-25
(I)-Fig. D. 20	KUCA Coupon type fuel	(I)-D-26
(I)-Fig. D. 21	KUCA flat type fuel	(I)-D-27

Chapter II

(II)-Fig. A. 1	Position of center of gravity ······	(II)-A-33
(II)-Fig. A. 2	Variations in mechanical properties of ······ SUS304 according to changes in temperature (1/5)	(II)-A-37
(II)-Fig. A. 2	Variations in mechanical properties of ······ SUS304 according to changes in temperature (2/5)	(II)-A-38
(II)-Fig. A. 2	Variations in mechanical properties of ······ SUS304 according to changes in temperature (3/5)	(II)-A-39
(II)-Fig. A. 2	Variations in mechanical properties of ······ SUS304 according to changes in temperature (4/5)	(II)-A-40
(II)-Fig. A. 2	Variations in mechanical properties of ······ SUS304 according to changes in temperature (5/5)	(II)-A-41
(II)-Fig. A. 3	Variations in mechanical properties of ······ SUS630 according to changes in temperature (bolt material) (1/4)	(II)-A-42
(II)-Fig. A. 3	Variations in mechanical properties of ······ SUS630 according to changes in temperature (bolt material) (2/4)	(II)-A-43
(II)-Fig. A. 3	Variations in mechanical properties of ······ SUS630 according to changes in temperature (bolt material) (3/4)	(II)-A-44
(II)-Fig. A. 3	Variations in mechanical properties of ······ SUS630 according to changes in temperature (bolt material) (4/4)	(II)-A-45
(II)-Fig. A. 4	Variations in mechanical properties of ······ SUS630 according to changes in temperature (1/1)	(II)-A-46
(II)-Fig. A. 5	Variations in mechanical properties of ······ AG3NE according to changes in temperature (1/1)	(II)-A-47
(II)-Fig. A. 6	Design fatigue curve (austenitic type stainless steel and high nickel alloy) ······	(II)-A-48
(II)-Fig. A. 7	Design fatigue curve ······ (high tensile strength bolt)	(II)-A-48
(II)-Fig. A. 8	Stress-strain curve of shock absorber ······	(II)-A-49
(II)-Fig. A. 9	Analytical model for eye-plate ······	(II)-A-53
(II)-Fig. A. 10	Analytical model of welded part on eye-plate ······	(II)-A-56
(II)-Fig. A. 11	Acceleration during transportation ······	(II)-A-58
(II)-Fig. A. 12	Analytical model for eye-plate ······	(II)-A-60
(II)-Fig. A. 13	Analytical model for welded part of eye-plate ······	(II)-A-63
(II)-Fig. A. 14	Vibration analytical model of packaging ······	(II)-A-68
(II)-Fig. A. 15	Analytical model of thermal expansion ······	(II)-A-73

(II)-Fig. A. 16	Stress evaluation position under	(II)-A-75
	normal test conditions	
(II)-Fig. A. 17	Stress analysis model of inner shell	(II)-A-76
	center portion	
(II)-Fig. A. 18	Stress analysis model of inner shell bottom plate ..	(II)-A-77
(II)-Fig. A. 19	Stress analysis model of inner lid center portion ..	(II)-A-78
(II)-Fig. A. 20	Analytical model of inner lid O-ring displacement ..	(II)-A-79
(II)-Fig. A. 21	Stress analysis model of bolt of the inner lid	(II)-A-80
	(initial clamping stress)	
(II)-Fig. A. 22	Stress analysis model of bolt of inner lid	(II)-A-81
	(stress due to internal pressure)	
(II)-Fig. A. 23	Stress analysis model of bolt of inner lid	(II)-A-82
	(stress due to thermal expansion)	
(II)-Fig. A. 24	Acceleration evaluation position of steel plate	(II)-A-88
	for horizontal drop	
(II)-Fig. A. 25	Acceleration analysis model of outer shell plate ...	(II)-A-89
	for horizontal drop	
(II)-Fig. A. 26	Cross section of outer shell lid flange	(II)-A-92
(II)-Fig. A. 27	Acceleration analysis model of outer shell head	(II)-A-95
	plate for horizontal drop	
(II)-Fig. A. 28	Cross section of partition plate	(II)-A-97
(II)-Fig. A. 29	Deformation analysis model of eye plate	(II)-A-99
(II)-Fig. A. 30	Analytical model of eye-plate fixing-plate	(II)-A-100
(II)-Fig. A. 31	Analytical model of flange of outer shell	(II)-A-102
(II)-Fig. A. 32	Analytical model of eye-plate fixing lug	(II)-A-104
(II)-Fig. A. 33	Acceleration analysis model of steel plate	(II)-A-106
	for vertical drop	
(II)-Fig. A. 34	Acceleration analysis model of steel plate	(II)-A-108
	for corner drop	
(II)-Fig. A. 35	Stress evaluation position for 1.2m	(II)-A-111
	horizontal drop (main body of inner shell)	
(II)-Fig. A. 36	Analytical model of interference to inner shell	(II)-A-112
	due to shock absorber deformation for 1.2m	
	horizontal drop	
(II)-Fig. A. 37	Stress analysis model of inner shell for	(II)-A-113
	1.2m horizontal drop	
(II)-Fig. A. 38	Stress analysis model of inner shell	(II)-A-114
	bottom plate for 1.2m horizontal drop	
(II)-Fig. A. 39	Stress analysis model of inner shell	(II)-A-115
	upper part for 1.2m horizontal drop	

(II)-Fig. A. 40	Stress analysis model for inner lid·····	(II)-A-117
	clamping bolt for 1.2m horizontal drop	
(II)-Fig. A. 41	Analytical model of section·····	(II)-A-118
	modulus of rectangular fuel basket	
(II)-Fig. A. 42	Evaluation of fuel elements for 1.2m·····	(II)-A-122
	horizontal drop	
(II)-Fig. A. 43	Analytical model of rectangular fuel elements for··	(II)-A-123
	1.2m horizontal drop perpendicular to fuel plate	
(II)-Fig. A. 44	Analytical model of rectangular fuel element for··	(II)-A-124
	1.2m horizontal drop parallel to fuel plate	
(II)-Fig. A. 45	Analytical model of holder·····	(II)-A-129
(II)-Fig. A. 46	Analytical model of fuel plate for·····	(II)-A-130
	1.2m horizontal drop parallel to fuel plate	
(II)-Fig. A. 47	Analytical model of coupon fuel for·····	(II)-A-131
	1.2m horizontal drop	
(II)-Fig. A. 48	Analytical model of flat fuel plate for 1.2 m·····	(II)-A-132
	horizontal drop in the plane direction of the fuel plate	
(II)-Fig. A. 49	Analytical model of flat fuel plate for 1.2 m·····	(II)-A-133
	horizontal drop in the direction parallel to the fuel plate	
(II)-Fig. A. 50	Stress evaluation position for 1.2m lower·····	(II)-A-141
	side vertical drop (main body of packaging)	
(II)-Fig. A. 51	Analytical model of interference to inner shell····	(II)-A-142
	due to shock absorber deformation for 1.2m lower side vertical drop	
(II)-Fig. A. 52	Stress analysis model of inner shell for·····	(II)-A-143
	1.2m lower side vertical drop	
(II)-Fig. A. 53	Stress analysis model of inner shell bottom·····	(II)-A-144
	plate for 1.2m lower side vertical drop	
(II)-Fig. A. 54	Stress analysis model of inner lid for·····	(II)-A-146
	1.2m lower side vertical drop	
(II)-Fig. A. 55	Stress analysis model of rectangular fuel·····	(II)-A-148
	element for 1.2m lower side vertical drop	
(II)-Fig. A. 56	Analytical model of 1.2m lower portion·····	(II)-A-150
	vertical drop of lowly irradiated fuel element	
(II)-Fig. A. 57	Analytical model of 1.2m lower portion vertical····	(II)-A-152
	drop of lowly irradiated fuel element	
(II)-Fig. A. 58	Analytical model of hold down part·····	(II)-A-153
(II)-Fig. A. 59	Analytical model of 1.2m vertical drop: ·····	(II)-A-155
	coupon fuel	

(II)-Fig. A. 60	Analytical model of 1.2m vertical drop: coupon fuel flat fuel	(II)-A-156
(II)-Fig. A. 61	Stress evaluation position for 1.2m lid side vertical drop (main body of a packaging)	(II)-A-164
(II)-Fig. A. 62	Analytical model of interference inner shell due to shock absorber deformation for 1.2m lid side vertical drop	(II)-A-165
(II)-Fig. A. 63	Stress analysis model of inner shell for 1.2m lid side vertical drop	(II)-A-166
(II)-Fig. A. 64	Stress analysis model of inner shell bottom plate for 1.2m lid side vertical drop	(II)-A-167
(II)-Fig. A. 65	Stress analysis model of inner lid for 1.2m lid side vertical drop	(II)-A-169
(II)-Fig. A. 66	Stress analysis model of rectangular fuel element for 1.2m lid side vertical drop	(II)-A-175
(II)-Fig. A. 67	Analytical model of 1.2m upper portion vertical drop of lowly irradiated fuel element	(II)-A-177
(II)-Fig. A. 68	Analytical model for 1.2m upper portion vertical drop of lowly irradiated fuel element	(II)-A-179
(II)-Fig. A. 69	Analytical model of hold down part	(II)-A-180
(II)-Fig. A. 70	Analytical model of interference to inner shell due to shock absorber deformation for 1.2m corner drop	(II)-A-191
(II)-Fig. A. 71	Analytical model of stress on inner lid clamping bolts for lid side corner drop	(II)-A-193
(II)-Fig. A. 72	Analytical model of interference with inner shell due to shock absorber deformation for 1.2m lower side inclined drop	(II)-A-197
(II)-Fig. A. 73	Relationship between acceleration and drop angle for 1.2m lower side inclined drop	(II)-A-198
(II)-Fig. A. 74	Analytical model of interference with inner shell due to shock absorber deformation for 1.2m upper side inclined drop	(II)-A-199
(II)-Fig. A. 75	Relationship between acceleration and drop angle for 1.2m upper side inclined drop	(II)-A-200
(II)-Fig. A. 76	Stress evaluation position for compressive load	(II)-A-202
(II)-Fig. A. 77	Analytical model of inner lid under compressive load	(II)-A-202
(II)-Fig. A. 78	Analytical model of inner shell under compressive load	(II)-A-204
(II)-Fig. A. 79	Penetration model	(II)-A-207
(II)-Fig. A. 80	Shearing model	(II)-A-208

(II)-Fig. A. 81	Analytical model of interference to inner shell ···· (II)-A-216 due to shock absorber deformation for 9m lower side vertical drop
(II)-Fig. A. 82	Analytical model of interference to inner shell ···· (II)-A-223 due to shock absorber deformation for 9m upper side vertical drop
(II)-Fig. A. 83	Analytical model of interference to inner shell ···· (II)-A-230 due to shock absorber deformation for 9m horizontal drop
(II)-Fig. A. 84	Analytical model of interference to inner shell ···· (II)-A-237 due to shock absorber deformation for 9m corner drop
(II)-Fig. A. 85	Analytical model of interference to inner shell ···· (II)-A-240 due to shock absorber deformation for 9m lower side inclined drop
(II)-Fig. A. 86	Relationship between acceleration and drop angle ··· (II)-A-241 for 9m lower side inclined drop
(II)-Fig. A. 87	Analytical model of interference to inner shell ···· (II)-A-242 due to shock absorber deformation for 9m upper side inclined drop
(II)-Fig. A. 88	Relationship between acceleration and drop angle ··· (II)-A-243 for 9m upper side inclined drop
(II)-Fig. A. 89	Analytical model for drop test II ··········· (II)-A-246
(II)-Fig. A. 90	Analytical model for penetration strength ········· (II)-A-248 under conditions of drop test II
(II)-Fig. A. 91	Stress evaluation position of inner shell ········· (II)-A-256 for 15m immersion test
(II)-Fig. A. 92	Analytical model of allowable buckling ········· (II)-A-257 pressure for frame of inner shell
(II)-Fig. A. 93	Curve representing buckling behavior factor ······· (II)-A-258 of inner shell under external pressure
(II)-Fig. A. 94	Stress analysis model of center of inner shell ···· (II)-A-259
(II)-Fig. A. 95	Stress analysis model of bottom plate ········· (II)-A-260 of inner shell
(II)-Fia. A. 96	Stress analysis model of center of inner lid ····· (II)-A-261
(II)-Fig. A. 97	Displacement analysis model of O-rings of ······· (II)-A-262 inner lid under external pressure
(II)-Fig. A. 98	Normal test conditions ··················· (II)-A-268
(II)-Fig. A. 99	Accident test condition ··················· (II)-A-270
(II)-Fig. A. 100	Drop attitude and test order ··············· (II)-A-272
(II)-Fig. A. 101	Analytical model of shock absorber ··········· (II)-A-276

(II)-Fig. A. 102	Analytical model by uniaxial displacement method ···	(II)-A-277
(II)-Fig. A. 103	Compressive stress/strain relationship of materials	(II)-A-278
(II)-Fig. A. 104	Proportion of shock absorber ·········	(II)-A-281
(II)-Fig. A. 105	Analytical model of inner lid for 1.2m ········· lid side vertical drop	(II)-A-283
(II)-Fig. A. 106	Stress/strain characteristics curves for ········· shock absorber at low temperatures	(II)-A-288
(II)-Fig. A. 107	Stress/strain curves for hard polyurethane foam ···	(II)-A-289
(II)-Fig. A. 108	Low temperature strength of SUS 304 ·········	(II)-A-290
(II)-Fig. A. 109	Low temperature impact value of SUS 304 ·········	(II)-A-291
(II)-Fig. A. 110	Low temperature impact value of SUS 630·H1150 ·····	(II)-A-292
(II)-Fig. A. 111	Analytical model for initial clamping force ······· of inner lid clamping bolts	(II)-A-293
(II)-Fig. A. 112	Triangle diagram for inner lid clamping bolt ·····	(II)-A-298
(II)-Fig. B. 1	Component of packaging ·········	(II)-B-3
(II)-Fig. B. 2	Concept of thermal transmission ·········	(II)-B-4
(II)-Fig. B. 3	Two dimensional axis symmetrical model ·········	(II)-B-17
(II)-Fig. B. 4	Temperature time history under accident ········· test conditions	(II)-B-22
(II)-Fig. B. 5	“TRUMP” flowchart (1/3)··········	(II)-B-32
(II)-Fig. B. 5	“TRUMP” flowchart (2/3)··········	(II)-B-33
(II)-Fig. B. 5	“TRUMP” flowchart (3/3)··········	(II)-B-34
(II)-Fig. B. 6	Fuel basket model ·········	(II)-B-35
(II)-Fig. B. 7	Comparison of prototype packaging test results ····· with analysis results	(II)-B-43
(II)-Fig. C. 1	Containment boundary of packaging ·········	(II)-C-3
(II)-Fig. D. 1	Neutron fission energy spectrum ·········	(II)-D-12
(II)-Fig. D. 2	Gamma radiation shield calculation model ·········	(II)-D-16
(II)-Fig. D. 3	Relationship between packaging surface angles ····· flux and calculation point of packaging surface	(II)-D-17

(II)-Fig. D. 4	Neutron shield calculation model ·····	(II)-D-19
(II)-Fig. D. 5	Mesh distribution drawing ·····	(II)-D-31
(II)-Fig. E. 1	Calculation model of arrayed packages for ····· criticality with 10 box type fuel elements (except KUR)	(II)-E-11
(II)-Fig. E. 2	Calculation model of arrayed packages for ····· criticality with 10 box type fuel elements (KUR and KUCA fuel)	(II)-E-12
(II)-Fig. E. 3	Calculation model of package for criticality ····· with 10 box type fuel elements	(II)-E-13
(II)-Fig. E. 4	Calculation model of package for criticality ····· with HEU and MEU	(II)-E-14
(II)-Fig. E. 5	Criticality calculation model of JRR-3 ····· standard fuel element	(II)-E-15
(II)-Fig. E. 6	Criticality calculation model of JRR-4B type ····· fuel element	(II)-E-16
(II)-Fig. E. 7	Criticality calculation model of JRR-4L type ····· fuel element	(II)-E-17
(II)-Fig. E. 8	Criticality calculation model JRR-4 type ····· fuel element	(II)-E-18
(II)-Fig. E. 9	Criticality calculation model of JMTR standard ····· type fuel element	(II)-E-19
(II)-Fig. E. 10	Criticality calculation model of JMTRC standard ··· type fuel element (HEU)	(II)-E-20
(II)-Fig. E. 11	Criticality calculation model of JMTRC standard ··· type fuel element (MEU)	(II)-E-21
(II)-Fig. E. 12	Criticality calculation model of KUR standard ····· type fuel element	(II)-E-22
(II)-Fig. E. 13	Criticality calculation model of KUCA coupon ····· type fuel	(II)-E-23
(II)-Fig. E. 14	Criticality calculation model of KUCA flat ····· type fuel element	(II)-E-24
(II)-Fig. E. 15	Schematic flow of criticality analysis ·····	(II)-E-30
(II)-Fig. E. 14	Relationship between effective multiplication ····· factor ($k_{eff} \pm 3\sigma$) and water density (contained ten JRR-3 standard type fuel elements (uranium silicon aluminum dispersion type alloy))	(II)-E-32
(II)-Fig. E. 16	Configuration of TCA criticality experiments ·····	(II)-E-38
(II)-Fig. E. 17	SPERT-D fuel ·····	(II)-E-39

(II)-Fig. E. 18	SPERT-D fuel (continued)	(II)-E-40
(II)-Fig. E. 19	Core arrangement	(II)-E-41
(II)-Fig. E. 20	Fuel element	(II)-E-42
(II)-Fig. E. 21	Core arrangement	(II)-E-43
(II)-Fig. E. 22	Relationship between effective multiplication factor ($k_{eff} \pm 3\sigma$) and water density type fuel element (contained ten JRR-3 standard type fuel elements (uranium silicon Aluminum dispersion type alloy))	(II)-E-48

Chapter III

(III)-Fig. B. 1	Quality assurance organization for design of the transport packaging	(III)-8
-----------------	--	---------

List of Tables

Chapter I

(I)-Table A.1	Specification of fuel enclosed in package ·····	(I)-A-3
(I)-Table C.1	Material of packaging ·····	(I)-C-15
(I)-Table C.2	Dimension of packaging ·····	(I)-C-16
(I)-Table C.3	Weight of packaging ·····	(I)-C-17
(I)-Table D.1	Specification of fuel element ····· (fresh fuel element)	(I)-D-5
(I)-Table D.2	Specification of fuel element ····· (lowly irradiated fuel element)	(I)-D-6
(I)-Table D.3	Specification of fuel element ····· (fresh fuel for KUCA)	(I)-D-7

Chapter II

(II)-Table A.1	Design standard for structural analysis ·····	(II)-A-4
(II)-Table A.2	Design load, combination of load (1/2) ·····	(II)-A-5
(II)-Table A.2	Design load, combination of load (2/2) ·····	(II)-A-6
(II)-Table A.3	Load condition (1/2) ·····	(II)-A-7
(II)-Table A.3	Load condition (2/2) ·····	(II)-A-8
(II)-Table A.4	Design conditions, analytical methods ····· of structural analysis (1/24)	(II)-A-9
(II)-Table A.4	Design conditions, analytical methods ····· of structural analysis (2/24)	(II)-A-10
(II)-Table A.4	Design conditions, analytical methods ····· of structural analysis (3/24)	(II)-A-11
(II)-Table A.4	Design conditions, analytical methods ····· of structural analysis (4/24)	(II)-A-12
(II)-Table A.4	Design conditions, analytical methods ····· of structural analysis (5/24)	(II)-A-13
(II)-Table A.4	Design conditions, analytical methods ····· of structural analysis (6/24)	(II)-A-14
(II)-Table A.4	Design conditions, analytical methods ····· of structural analysis (7/24)	(II)-A-15
(II)-Table A.4	Design conditions, analytical methods ····· of structural analysis (8/24)	(II)-A-16

(II)-Table A.4	Design conditions, analytical methods ······	(II)-A-17 of structural analysis (9/24)
(II)-Table A.4	Design conditions, analytical methods ······	(II)-A-18 of structural analysis (10/24)
(II)-Table A.4	Design conditions, analytical methods ······	(II)-A-19 of structural analysis (11/24)
(II)-Table A.4	Design conditions, analytical methods ······	(II)-A-20 of structural analysis (12/24)
(II)-Table A.4	Design conditions, analytical methods ······	(II)-A-21 of structural analysis (13/24)
(II)-Table A.4	Design conditions, analytical methods ······	(II)-A-22 of structural analysis (14/24)
(II)-Table A.4	Design conditions, analytical methods ······	(II)-A-23 of structural analysis (15/24)
(II)-Table A.4	Design conditions, analytical methods ······	(II)-A-24 of structural analysis (16/24)
(II)-Table A.4	Design conditions, analytical methods ······	(II)-A-25 of structural analysis (17/24)
(II)-Table A.4	Design conditions, analytical methods ······	(II)-A-26 of Structural analysis (18/24)
(II)-Table A.4	Design conditions, analytical methods ······	(II)-A-27 of structural analysis (19/24)
(II)-Table A.4	Design conditions, analytical methods ······	(II)-A-28 of structural analysis (20/24)
(II)-Table A.4	Design conditions, analytical methods ······	(II)-A-29 of structural analysis (21/24)
(II)-Table A.4	Design conditions, analytical methods ······	(II)-A-30 of structural analysis (22/24)
(II)-Table A.4	Design conditions, analytical methods ······	(II)-A-31 of structural analysis (23/24)
(II)-Table A.4	Design conditions, analytical methods ······	(II)-A-32 of structural analysis (24/24)
(II)-Table A.5	Mechanical properties of materials ······	(II)-A-35
(II)-Table A.6	Mechanical properties of materials to be used ····	(II)-A-36 as design standards
(II)-Table A.7	List of different materials contacted ······	(II)-A-50
(II)-Table A.8	Minimum temperatures of parts of package ······	(II)-A-51
(II)-Table A.9	Summary of analyses under routine transport ······	(II)-A-65

(II)-Table A.10	Stresses evaluation under changed pressure ·····	(II)-A-67
(II)-Table A.11	Design temperature under normal test conditions ··	(II)-A-71
(II)-Table A.12	Design pressure under normal test conditions ·····	(II)-A-72
(II)-Table A.13	Stress evaluation under normal test conditions ··· (thermal test)	(II)-A-83
(II)-Table A.14	Deformation and acceleration of shock ········· absorber under normal test conditions	(II)-A-87
(II)-Table A.15	Design acceleration under normal test conditions ·	(II)-A-110
(II)-Table A.16	Stress evaluation for 1.2m horizontal drop (1/6) ··	(II)-A-135
(II)-Table A.16	Stress evaluation for 1.2m horizontal drop (2/6) ··	(II)-A-136
(II)-Table A.16	Stress evaluation for 1.2m horizontal drop (3/6) ··	(II)-A-137
(II)-Table A.16	Stress evaluation for 1.2m horizontal drop (4/6) ··	(II)-A-138
(II)-Table A.16	Stress evaluation for 1.2m horizontal drop (5/6) ··	(II)-A-139
(II)-Table A.16	Stress evaluation for 1.2m horizontal drop (6/6) ··	(II)-A-140
(II)-Table A.17	Stress evaluation for 1.2m bottom side ········· vertical drop(1/6)	(II)-A-158
(II)-Table A.17	Stress evaluation for 1.2m bottom side ········· vertical drop(2/6)	(II)-A-159
(II)-Table A.17	Stress evaluation for 1.2m bottom side ········· vertical drop(3/6)	(II)-A-160
(II)-Table A.17	Stress evaluation for 1.2m bottom side ········· vertical drop(4/6)	(II)-A-161
(II)-Table A.17	Stress evaluation for 1.2m bottom side ········· vertical drop(5/6)	(II)-A-162
(II)-Table A.17	Stress evaluation for 1.2m bottom side ········· vertical drop(6/6)	(II)-A-163
(II)-Table A.18	Stress evaluation for 1.2m lid side ········· vertical drop (1/6)	(II)-A-185
(II)-Table A.18	Stress evaluation for 1.2m lid side ········· vertical drop (2/6)	(II)-A-186
(II)-Table A.18	Stress evaluation for 1.2m lid side ········· vertical drop (3/6)	(II)-A-187
(II)-Table A.18	Stress evaluation for 1.2m lid side ········· vertical drop (4/6)	(II)-A-188
(II)-Table A.18	Stress evaluation for 1.2m lid side ········· vertical drop (5/6)	(II)-A-189

(II)-Table A. 18	Stress evaluation for 1.2m lid side ······	(II)-A-190 vertical drop (6/6)
(II)-Table A. 19	Design acceleration for corner drops ······	(II)-A-192
(II)-Table A. 20	Stress evaluation for 1.2m lid side ······	(II)-A-196 corner drop
(II)-Table A. 21	Relationship between drop angle and acceleration ·	(II)-A-198
(II)-Table A. 22	Relationship between drop angle and acceleration ·	(II)-A-199
(II)-Table A. 23	Stress evaluation for stacking test ······	(II)-A-206
(II)-Table A. 24	Deformation and acceleration of shock absorber ···	(II)-A-214 under accident test conditions
(II)-Table A. 25	Design acceleration under accident ······	(II)-A-215 test conditions
(II)-Table A. 26	Stress evaluation for 9m lower side ······	(II)-A-217 vertical drop (1/6)
(II)-Table A. 26	Stress evaluation for 9m lower side ······	(II)-A-218 vertical drop (2/6)
(II)-Table A. 26	Stress evaluation for 9m lower side ······	(II)-A-219 vertical drop (3/6)
(II)-Table A. 26	Stress evaluation for 9m lower side ······	(II)-A-220 vertical drop (4/6)
(II)-Table A. 26	Stress evaluation for 9m lower side ······	(II)-A-221 vertical drop (5/6)
(II)-Table A. 26	Stress evaluation for 9m lower side ······	(II)-A-222 vertical drop (6/6)
(II)-Table A. 27	Stress evaluation for 9m upper side ······	(II)-A-224 vertical drop (1/6)
(II)-Table A. 27	Stress evaluation for 9m upper side ······	(II)-A-225 vertical drop (2/6)
(II)-Table A. 27	Stress evaluation for 9m upper side ······	(II)-A-226 vertical drop (3/6)
(II)-Table A. 27	Stress evaluation for 9m upper side ······	(II)-A-227 vertical drop (4/6)
(II)-Table A. 27	Stress evaluation for 9m upper side ······	(II)-A-228 vertical drop (5/6)
(II)-Table A. 27	Stress evaluation for 9m upper side ······	(II)-A-229 vertical drop (6/6)
(II)-Table A. 28	Stress evaluation for 9m horizontal drop (1/6) ···	(II)-A-231
(II)-Table A. 28	Stress evaluation for 9m horizontal drop (2/6) ···	(II)-A-232

(II)-Table A. 28	Stress evaluation for 9m horizontal drop (3/6) ···	(II)-A-233
(II)-Table A. 28	Stress evaluation for 9m horizontal drop (4/6) ···	(II)-A-234
(II)-Table A. 28	Stress evaluation for 9m horizontal drop (5/6) ···	(II)-A-235
(II)-Table A. 28	Stress evaluation for 9m horizontal drop (6/6) ···	(II)-A-236
(II)-Table A. 29	Design acceleration for corner drop ·········	(II)-A-238
(II)-Table A. 30	Stress evaluation for 9m upper corner drop ·····	(II)-A-239
(II)-Table A. 31	Relationship between drop angle and acceleration ·	(II)-A-241
(II)-Table A. 32	Relationship between drop angle ········· and acceleration for drop test I	(II)-A-243
(II)-Table A. 33	Relationship between drop angle ········· and acceleration for drop test II	(II)-A-244
(II)-Table A. 34	Evaluation of penetration for drop test II ·····	(II)-A-252
(II)-Table A. 35	Design temperatures used for ········· accident test condition	(II)-A-253
(II)-Table A. 36	Design pressure of package under accident ·····	(II)-A-253
(II)-Table A. 37	Stress analysis and evaluation under accident ···	(II)-A-255
(II)-Table A. 38	Stresses evaluated for 15m water immersion test ·	(II)-A-264
(II)-Table A. 39	Damages of the fissile package under the normal ·	(II)-A-269
(II)-Table A. 40	Compliance with requirements for fissile package under normal test conditions	(II)-A-269
(II)-Table A. 41	Deformations and design accelerations of shock ···	(II)-A-273
(II)-Table A. 42	Damage of the fissile package under special test ·	(II)-A-274
(II)-Table A. 43	Comparisons of analytical values ········· by “CASH-II” and experimental values	(II)-A-281
(II)-Table A. 44	Comparison of analytical and experimental ·····	(II)-A-282
(II)-Table A. 45	Analysis results of displacement of ········· inner O-rings of inner lid	(II)-A-287
(II)-Table B. 1	Conditions of thermal analyses ·········	(II)-B-5
(II)-Table B. 2	Methods of thermal analyses ·········	(II)-B-6

(II)-Table B.3	Thermal properties of stainless steel	(II)-B-7
(II)-Table B.4	Thermal properties of air	(II)-B-7
(II)-Table B.5	Thermal properties of shock absorber (balsa)	(II)-B-8
(II)-Table B.6	Thermal properties of heat insulator	(II)-B-9
	(hard polyurethane foam)	
(II)-Table B.7	Specifications of silicone rubber O-ring	(II)-B-10
(II)-Table B.8	Specifications of fusible plug	(II)-B-10
(II)-Table B.9	Thermal conditions under normal test conditions ..	(II)-B-12
(II)-Table B.10	Maximum temperatures of each part of package	(II)-B-13
(II)-Table B.11	Thermal conditions under accident test conditions ..	(II)-B-19
(II)-Table B.12	Maximum temperatures of package under accident ...	(II)-B-21
	test conditions	
(II)-Table B.13	Maximum pressure in packaging under accident	(II)-B-25
	test conditions	
(II)-Table B.14	Convection heat transfer coefficient between	(II)-B-37
	package surface and ambient environment	
(II)-Table B.15	Radiation factor and radiation morphological	(II)-B-37
	coefficient	
(II)-Table B.16	Calculation result for packaging internal	(II)-B-40
	pressure	
(II)-Table B.17	Design pressures for specific test conditions	(II)-B-41
(II)-Table B.18	Comparison of prototype packaging test results ...	(II)-B-42
	with analysis results	
II)-Table C.1	Design pressure and design temperature of	(II)-C-2
	containment system	
(II)-Table C.2	The dimensions and material of the gasket	(II)-C-5
(II)-Table C.3	Inner shell clamping bolt	(II)-C-5
(II)-Table C.4	Maximum permissible leakage rate of the air	(II)-C-7
(II)-Table C.5	The maximum radius of leak hole on leakage rate ..	(II)-C-10
	test	
(II)-Table C.6	The maximum gas leakage rate under normal test ...	(II)-C-11
	conditions	
(II)-Table C.7	Weight proportions of ^{234}U and ^{236}U used for	(II)-C-13
	caluculations	
(II)-Table C.8	Surface contamination level per fuel element	(II)-C-14

(II)-Table C.9	Leakage rate of radioactive substances under ·····	(II)-C-15
	normal test condition	
(II)-Table C.10	Nuclide of JMTRC fuel surface water and ·····	(II)-C-16
	radioactive concentration	
(II)-Table C.11	Surface activity per one fuel element of lowly ··	(II)-C-17
	irradiated fuel element	
(II)-Table C.12	Leak rate of the radioactivity under normal ·····	(II)-C-18
	test condition	
(II)-Table C.13	The maximum gas leakage rate under the accident ·	(II)-C-21
	test conditions	
(II)-Table C.14	Leakage rate of radioactive substances under ···	(II)-C-23
	normal test conditions	
(II)-Table C.15	Leakage rate of radioactive substances under ····	(II)-C-23
	accident test condition	
(II)-Table D.1	Gamma radiation emission rate of uranium ·····	(II)-D-3
	isotope	
(II)-Table D.2	Gamma radiation source intensity for one fuel ····	(II)-D-3
	element	
(II)-Table D.3	Specific activity used for calculation ·····	(II)-D-4
(II)-Table D.4	²³⁴ U and ²³⁶ U weight rate used for calculation ·····	(II)-D-4
(II)-Table D.5	Radioactive nuclide weight per one element used ··	(II)-D-4
	in calculation	
(II)-Table D.6	Gamma radiation emission rate of uranium isotope ·	(II)-D-7
(II)-Table D.7	Gamma radiation source intensity per ·····	(II)-D-7
	one mixed fuel element (actinoids)	
(II)-Table D.8	Specific activity used for calculation ·····	(II)-D-8
(II)-Table D.9	²³⁴ U and ²³⁶ U weight rate used for calculation ·····	(II)-D-8
(II)-Table D.10	Radioactive nuclide weight per one element ·····	(II)-D-8
	used in calculation	
(II)-Table D.11	Radioactivity rate of the fission products ·····	(II)-D-10
	obtained by ORIGEN	
(II)-Table D.12	Uranium isotope spontaneous fission speed ·····	(II)-D-11
(II)-Table D.13	Emission rate of spontaneous fission of ·····	(II)-D-13
	uranium isotope	
(II)-Table D.14	Material and density ·····	(II)-D-20

(II)-Table D. 15	Volumetric rate of shield material for each ·····	(II)-D-20
	area used in shield calculation	
(II)-Table D. 16	Atom density for each material ·····	(II)-D-21
(II)-Table D. 17	Gamma radiation energy group structure and ·····	(II)-D-23
	dose-equivalent rate calculation factor	
(II)-Table D. 18	Dose-equivalent rate by gamma radiation ·····	(II)-D-24
	(fresh fuel elements loading)	
(II)-Table D. 19	Dose-equivalent rate by gamma radiation ·····	(II)-D-24
	(lowly irradiated fuel elements loading)	
(II)-Table D. 20	Neutron dose-equivalent rate ·····	(II)-D-25
(II)-Table D. 21	Dose-equivalent rate of neutron irradiation ·····	(II)-D-26
	(lowly irradiated fuel elements loading)	
(II)-Table D. 22	Package dose-equivalent rate ·····	(II)-D-27
	(fresh fuel element loading)	
(II)-Table D. 23	Package dose-equivalent rate ·····	(II)-D-28
	(lowly irradiated fuel elements loading)	
(II)-Table E. 1	Specifications of fuel element ·····	(II)-E-4
(II)-Table E. 2	Specification of fuel plate (1/2) ·····	(II)-E-5
(II)-Table E. 2	Specification of fuel plate (2/2) ·····	(II)-E-6
(II)-Table E. 3	Distance from the surface of the inner shell ·····	(II)-E-7
	to the surface of the packaging	
(II)-Table E. 4	Requirements defined in the regulation ·····	(II)-E-25
	And analysis condition	
(II)-Table E. 5	Atom density of regions used in ·····	(II)-E-26
	criticality calculation (atoms/barn·cm)	
(II)-Table E. 6	Atom density of fuel element used in ·····	(II)-E-27
	criticality calculation (atoms/barn·cm)	
(II)-Table E. 7	Fuel elements to be analyzed ·····	(II)-E-28
(II)-Table E. 8	Results of criticality analysis when immersed ····	(II)-E-33
(II)-Table E. 9	Analysis result of benchmark criticality test ····	(II)-E-37
(II)-Table E. 10	Effective multiplication factor for various ·····	(II)-E-47
	water density [contained ten JRR-3 standard type	
	fuel elements (uranium silicon aluminum	
	dispersion type alloy) and	
	(300 KUCA flat plates in a package)]	

(II)-Table F.1	Assessment of the compliance with the technical standards stipulated in the regulation and the notification	(II)-F-2
----------------	---	----------

Chapter III

Chapter IV

(IV)-Table A.1	Procedures for pre-shipment inspection of the package	(IV)-A-3
----------------	---	----------

(I) Description of nuclear fuel package

A Purpose and conditions

(I) Description of nuclear fuel package

(I)-A. Purpose and conditions

This packaging is intended for carrying fresh fuel elements to be charged into Kyoto University Research Reactor (KUR) and Kyoto University Critical Assembly (KUCA) installed at the Institute for Integrated Radiation and Nuclear Science, Kyoto University, from fabrication plants, domestic and overseas, to KUR and KUCA.

In addition, this packaging is intended for carrying fresh fuel elements to be charged into JRR-3 installed at the Tokai Research Institute of the Japan Atomic Energy Agency (JAEA) and into JMTR and JMTRC installed at the Oarai Research Institute, from fabrication plants, domestic and overseas, to JRR-3 etc.

Moreover, this is also intended to transport JRR-4 installed at the Nuclear Science Research Institute and the JMTR's new fuel elements installed at the Oarai Research and Development Center, as well as fuels low-irradiated in the JMTRC of the Oarai Research and Development Center to overseas countries or regions.

The conceptual drawing of this packaging is shown in (I)-Fig. A. 1.

(1) Name of packaging	JRF-90Y-950K
(2) Type	BU type fissile package
(3) Allowable number of packages	Unlimited
(4) Allowable arrangement of packages	Not specified
(5) Transport index	1.9
(6) Criticality safety index	0
(7) Weight of package	950kg or less
(8) Size of packaging	
(a) Diameter	approx. 840mm
(b) Height	approx. 1800mm
(9) Maximum weight of packaging (Rectangular fuel element loaded)	approx. 860kg

(10) Main materials for packaging

- (a) Main body : Stainless steel, Balsa wood, Hard polyurethane foam
- (b) Outer lid : Stainless steel, Balsa wood, Hard polyurethane foam
- (c) Inner lid : Stainless steel, Silicone rubber
- (d) Fuel basket : Stainless steel, Silicone rubber

(11) Nuclear fuels contained in packaging

The packaging may contain low-enriched uranium (called “LEU fuel” here in after), medium-enriched uranium and high-enriched uranium (referred to “HEU fuel” hereafter) **fuel elements for research reactor**. These fuels are **categorized as, based on their usage purpose, the standard fuel element, the half-loaded fuel element, the special fuel element and the fuel follower. In addition, coupon type and flat type fuels using low-enriched uranium may be contained as fuels for critical assembly.**

- (a) Fresh fuels : 10 or less

The fresh fuels having the equal nominal enrichment only are contained.

- (b) Lowly irradiated fuels : 10 or less

The lowly irradiated fuels, HEU and MEU, are contained together.

- (c) **KUCA fuel**

Coupon type fuels : 1200 or less

Flat type fuels : 300 or less

The KUCA fuels having same fuel type only are contained.

(12) Specifications for nuclear fuels contained in packaging

The specification for fuel is shown in (I)-Table A.1.

(13) Form of shipment

- (a) Transport method

Sea transport is done by seagoing vessels and transport over land is done by carrier. Each is exclusively loaded.

- (b) Loading method

The packaging is tightly fastened with specially designed tools.

(I)-Table A.1 Specification of nuclear material contained in shipping container (1/4) (Fresh Fuel Element)

Reactor		KUR (Kyoto University Research reactor)		
Fuel Element		KUR Standard Fuel Element	KUR Special Fuel Element	KUR Half-loaded Fuel Element
Number of Fuel Elements (element/package)		10 or less		
Fuel Type		LEU fuel		
Materials of Nuclear Fuel		Uranium-silicon -aluminum dispersion alloy		
Weight	²³⁵ U weight (g or less/package)	2,180	1,090	1,090
	U weight (g or less/package)	11,150	5,580	5,580
	²³⁵ U weight (g or less/element)	218	109	109
	U weight (g or less/element)	1,115	558	558
Enrichment (wt% or less)		19.95		
Activity of Contents	Total (GBq or less/package)	29.8		
	Principal Radionuclide (GBq or less/package)	²³⁴ U : 28.6 ²³⁵ U : 0.38 ²³⁶ U : 0.59 ²³⁸ U : 0.24		
Physical State		Solid		
Burn-up (% or less)		0 (Fresh Fuel)		
Total Heat Generation Rate (W or less/package)		0 (Fresh Fuel)		
Cooling Time (days)		0 (Fresh Fuel)		

-Loading a transport package with different types of nuclear fuel material is allowed for each reactor only when all the fuel elements contained are the same type having the same enrichment level. For the nuclear fuel material from JMTRC, however, mixed loading of fuel elements of different types and different enrichment levels is allowed.

- The values of weight and heat generation are calculated proportionally from the maximum weight and heat generation for each type of fuel element according to the number of assemblies contained.

(I)-Table A.1 Specification of nuclear material contained in shipping container (2/4) (Fresh Fuel Element)

Reactor		JRR-3		JRR-4			JMTR		
Fuel Element		JRR-3 standard fuel element	JRR-3 follower type fuel element	JRR-4B type fuel element	JRR-4L type fuel element	JRR-4 type fuel element	JMTR standard fuel element	JMTR fuel followers	
Number of Fuel Elements (element/package)		10 or less							
Fuel Type		LEU fuel		HEU fuel	LEU fuel		MEU fuel	LEU fuel	
Materials of Nuclear Fuel		Uranium-silicon -aluminum dispersion alloy		Uranium -aluminum alloy	Uranium-aluminum dispersion alloy	Uranium-silicon -aluminum dispersion alloy	Uranium-aluminum dispersion alloy	Uranium-silicon -aluminum dispersion alloy	
Weight	²³⁵ U weight (g or less/package)	4, 850	3, 100	1, 700	2, 300	2, 100	3, 200	4, 250	2, 800
	U weight (g or less/package)	24, 810	15, 860	1, 830	11, 770	10, 750	7, 280	21, 740	14, 330
	²³⁵ U weight (g or less/element)	485	310	170	230	210	320	425	280
	U weight (g or less/element)	2, 481	1, 586	183	1, 177	1, 075	728	2, 174	1, 433
Enrichment (wt% or less)		19. 95		93. 3	19. 95		46. 0	19. 95	
Activity of Contents	Total (GBq or ess/package)	29. 8							
	Principal Radionuclide (GBq or less/package)	²³⁴ U: 28. 6 ²³⁵ U: 0. 38 ²³⁶ U: 0. 59 ²³⁸ U: 0. 24							
Physical State		Solid							
Burn-up (% or less)		0 (Fresh Fuel)							
Total Heat Generation Rate (W or less/package)		0 (Fresh Fuel)							
Cooling Time (days)		0 (Fresh Fuel)							

-Loading a transport package with different types of nuclear fuel material is allowed for each reactor only when all the fuel elements contained are the same type having the same enrichment level. For the nuclear fuel material from JMTRC, however, mixed loading of fuel elements of different types and different enrichment levels is allowed.

- The values of weight and heat generation are calculated proportionally from the maximum weight and heat generation for each type of fuel element according to the number of assemblies contained.

(I)-Table A.1 Specification of nuclear material contained in shipping container (3/4) (Low Irradiated Fuel Element)

Reactor		JMTRC					
Fuel Element		JMTRC Standard	JMTRC Special	JMTRC Follower	JMTRC Standard	JMTRC Special	JMTRC Follower
Number of Spent Fuel Elements (element/package)		10 or less					
Fuel Type		HEU fuel			MEU fuel		
Materials of Nuclear Fuel		Uranium-aluminum alloy			Uranium-aluminum dispersion alloy		
Weight	²³⁵ U weight (g or less/package)	2, 850		1, 990	3, 170	2, 860	2, 100
	U weight (g or less/package)	3, 180		2, 220	7, 210	6, 500	4, 780
	²³⁵ U weight (g or less/element)	285		199	317	286	210
	U weight (g or less/element)	318		222	721	650	478
Enrichment (wt% or less)		90. 0			46. 0		
Activity of Contents	Total (GBq or ess/package)	17. 3					
	Principal Radionuclide (GBq or less/package)	(a) ²³⁴ U: 16. 2 (b) ²³⁵ U: 0. 25 (c) ²³⁶ U: 0. 29 (d) ²³⁸ U: 0. 05 (e) Others: 0. 52					
Physical State		Solid					
Burn-up (% or less)		7. 23×10 ⁻⁵			1. 76×10 ⁻⁵		
Total Heat Generation Rate (W or less/package)		4. 30×10 ⁻⁵			3. 29×10 ⁻⁵		
Cooling Time (days)		5, 475 or more			1, 460 or more		

-Loading a transport package with different types of nuclear fuel material is allowed for each reactor only when all the fuel elements contained are the same type having the same enrichment level. For the nuclear fuel material from JMTRC, however, mixed loading of fuel elements of different types and different enrichment levels is allowed.

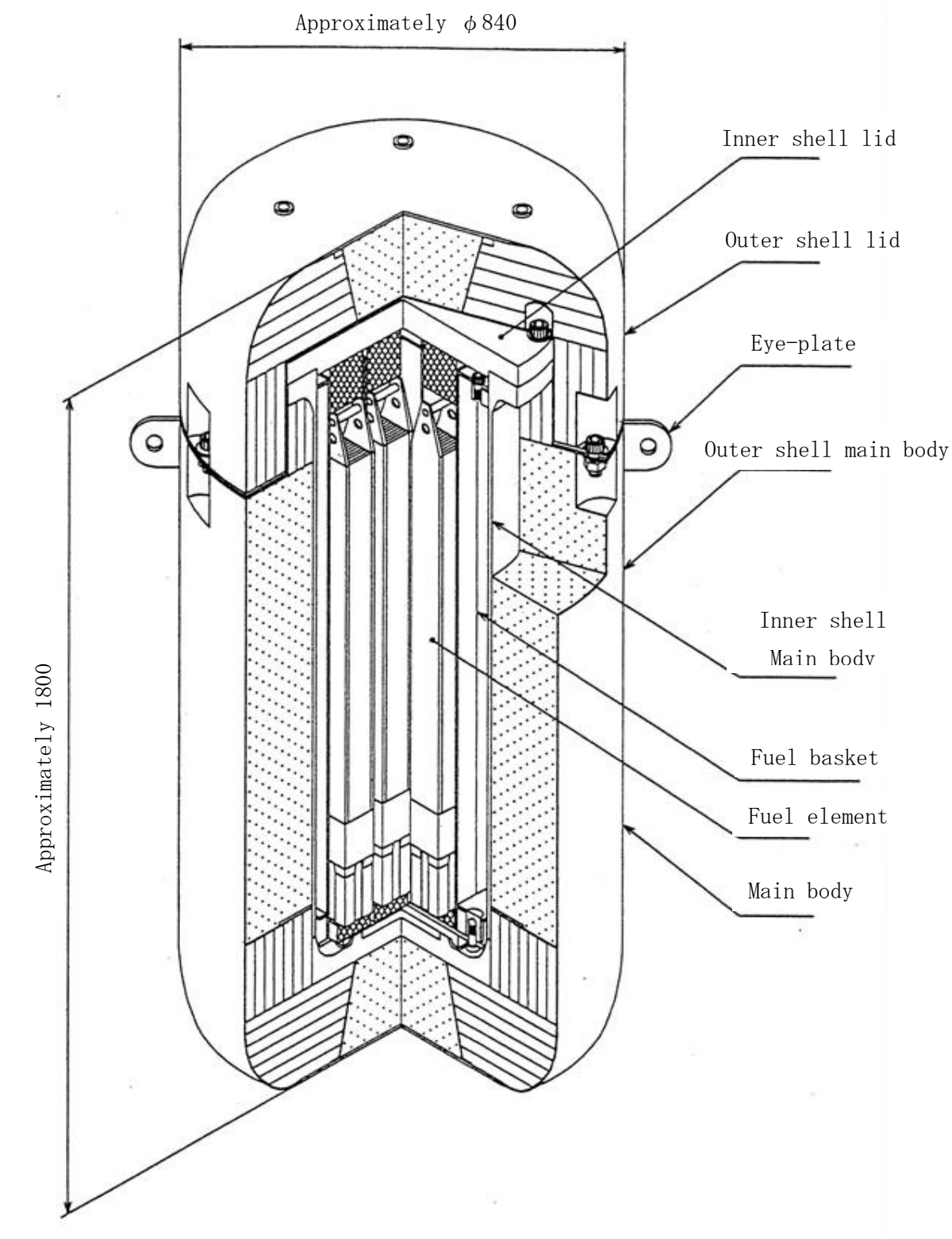
- The values of weight and heat generation are calculated proportionally from the maximum weight and heat generation for each type of fuel element according to the number of assemblies contained.

(I)-Table A.1 Specification of nuclear material contained in shipping container (4/4) (Fresh Fuel Element)

Reactor		KUCA (Kyoto University Critical Assembly)	
Fuel Element		Coupon	Flat
Number of Fuel Elements (element/package)		1, 200 or less	300 or less
Fuel Type		LEU Fuel	
Materials of Nuclear Fuel		Uranium-molybdenum -aluminum dispersion alloy	Uranium-silicon -aluminum dispersion alloy
Weight	²³⁵ U weight (g or less/package)	4, 800	4, 500
	U weight (g or less/package)	24, 600	23, 400
	²³⁵ U weight (g or less/element)	4	15
	U weight (g or less/element)	20. 5	78
Enrichment (wt% or less)		19. 95	
Activity of Contents	Total (GBq or less/package)	15. 5	
	Principal Radionuclide (GBq or less/package)	²³⁴ U : 14. 5	
		²³⁵ U : 0. 38	
		²³⁶ U : 0. 27	
		²³⁸ U : 0. 24	
Physical State		Solid	
Burn-up (% or less)		0 (Fresh Fuel)	
Total Heat Generation Rate (W or less/package)		0 (Fresh Fuel)	
Cooling Time (days)		0 (Fresh Fuel)	

-Loading a transport package with different types of nuclear fuel material is allowed for each reactor only when all the fuel elements contained are the same type having the same enrichment level. For the nuclear fuel material from JMTRC, however, mixed loading of fuel elements of different types and different enrichment levels is allowed.

- The values of weight and heat generation are calculated proportionally from the maximum weight and heat generation for each type of fuel element according to the number of assemblies contained.



(I)-Fig.A.1 Rough drawing of package

B Kinds of package

(I)-B. Kinds of package

(1) Requirements for different kinds of package

Since the radioactive substances stored are fresh fuel plates of uranium fuel and the radioactivity level exceeds the value of A_2 , this package must satisfy requirements for type BU package.

(2) Requirements for a fissile package

Since this package contains fuel with an enrichment level between 19.95wt% to 93.3wt% and more than 15g of ^{235}U , it must satisfy requirements for fissile package.

Accordingly, this package corresponds to a “type BU fissile package”.

C Packaging

(I) -C

(I)-C. Packaging

1. Outline of packaging

This packaging is a cylindrical type in the form, which is maintained in vertical posture during both transport and handling.

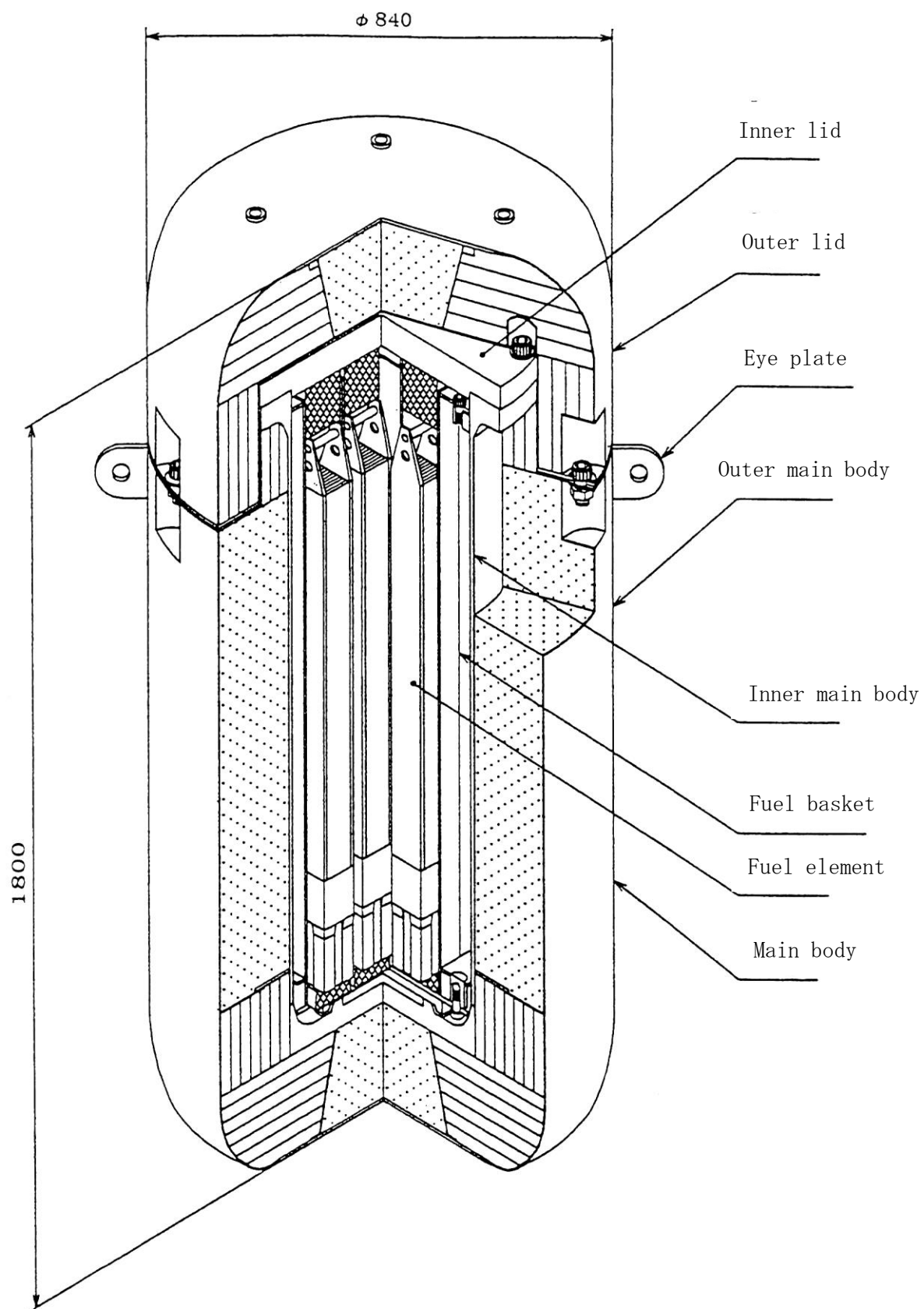
The package outline is shown in (I)-Fig.C.1.

The package tie down condition os shown in (I)-Fig.C.2.

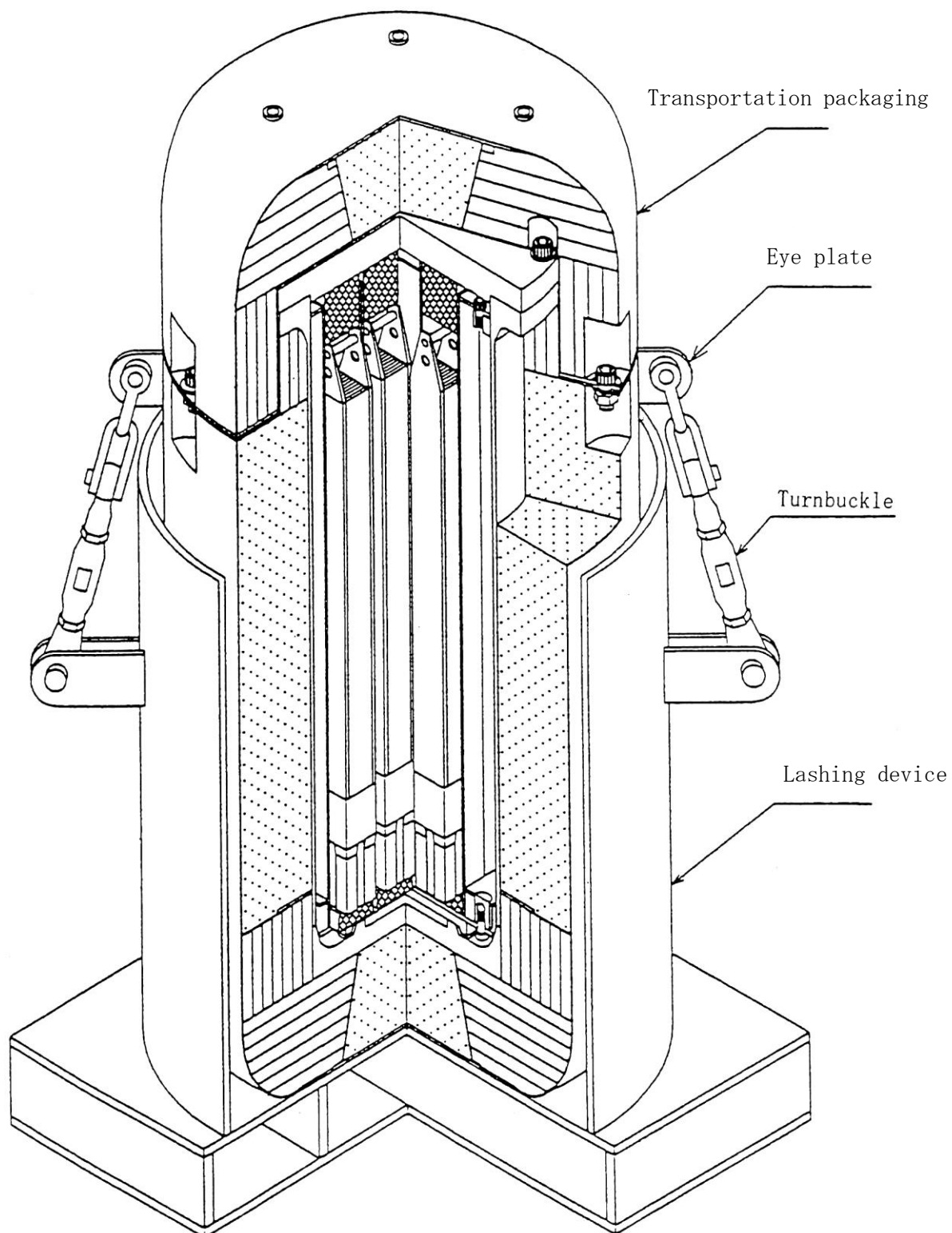
The package under transport condition is shown in (I)-Fig.C.3.

The general feature of the packaging is as follows.

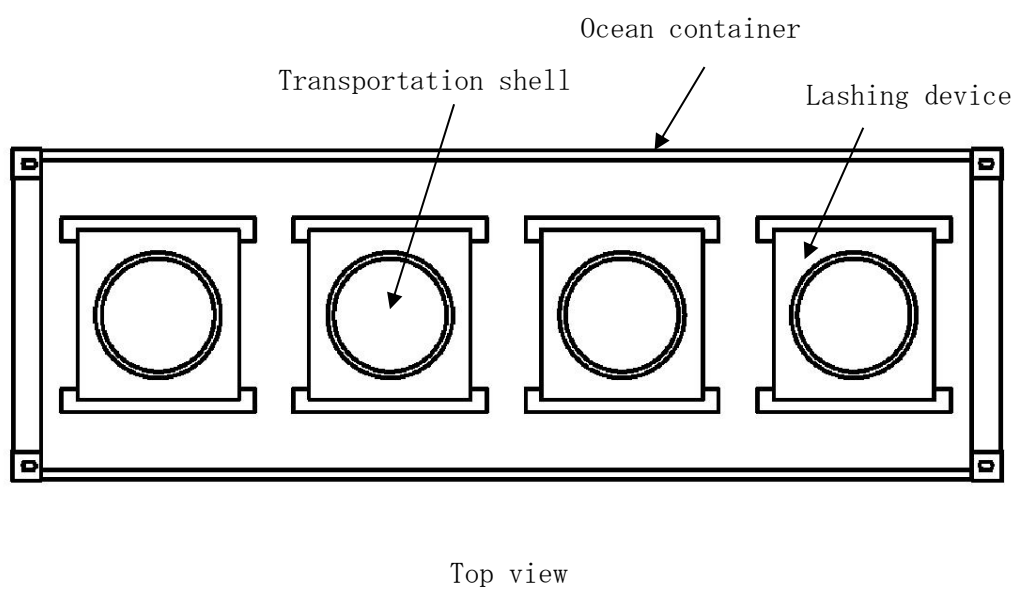
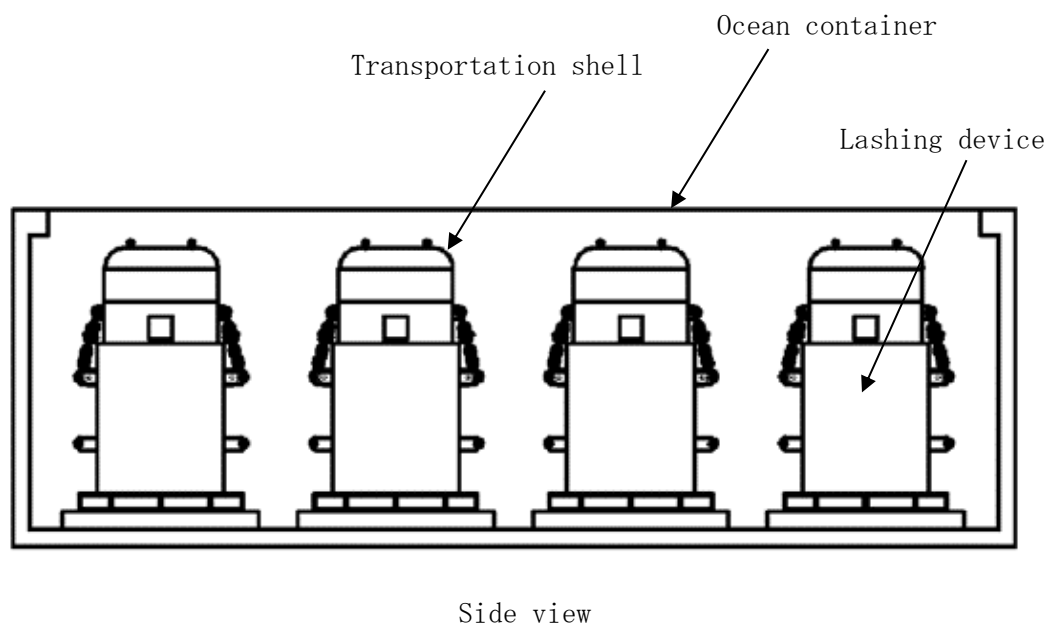
- (1) The fuel basket of this packaging is designed to be rectangular type so that the rectangular fuel can be loaded.
- (2) The inner shell is designed as a pressure vessel against the design pressure of 9.81×10^{-2} MPa. [Gauge]
- (3) This packaging is handled by a crane using the eye-plate installed on the main body.
- (4) To absorb impact energy caused by drop, there are the shock absorbers at the upper and lower parts of the packaging.
- (5) To reduce the heat gain caused by fire, there are the heat insulators at the upper and lower parts of the packaging and shell.
- (6) The containment boundary of this packaging is shown in (I)-Fig.C.4.



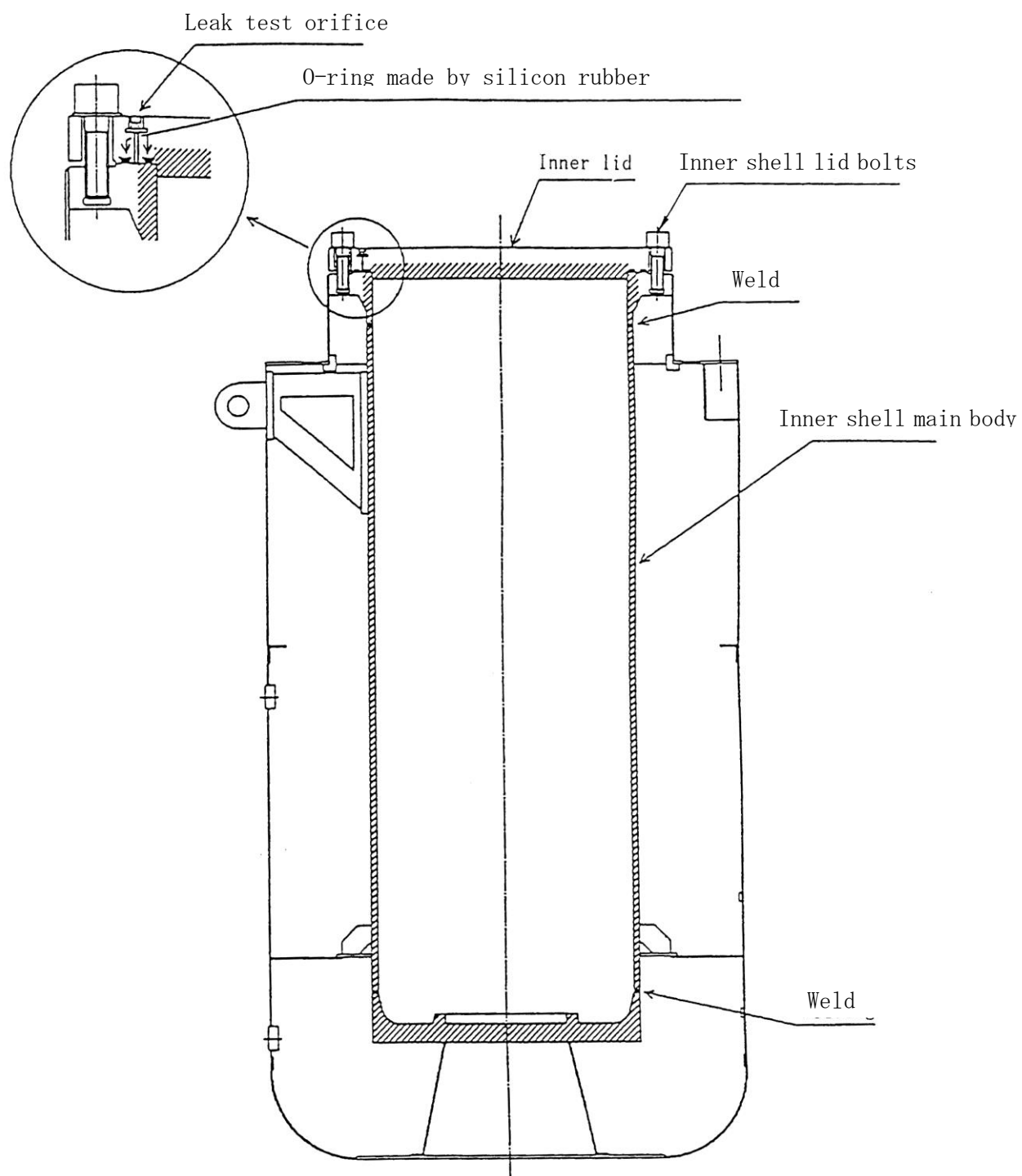
(I)-Fig.C.1 Rough drawing of package

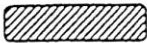


(I)-Fig.C.2 Package under transport condition



(I)-Fig.C.3 Package under transport condition



 : The range that the surrounded with a slanted line shows a seal border.

(I)-Fig.C.4 Seal boundary of package

2. Structure of packaging (Refer to (I)-Fig.C.5)

This packaging consists of 4 main parts:

- (1) Main body
- (2) Inner lid
- (3) Fuel basket
- (4) Outer lid

Following is the description of each part.

2.1 Main body (Refer to (I)-Fig.C.6)

The main body is in the cylindrical shape of 1,559mm in height and 840mm in outer diameter and consists of the outer shell and inner shell.

The outer shell consists of 3mm thick stainless steel and 6mm thick stainless steel at the bottom. The inner shell consists of 10mm thick stainless steel and 35mm thick stainless steel at the bottom.

The shell and bottom plate is welded completely.

The space between the outer and inner shells, heat insulators and shock absorbers are applied to reduce the heat gain caused by fire and to absorb impact energy caused by drop.

At the upper side of the main body, the eye-plates are welded at 4 places to lift the packaging.

Eight fusible plugs is provided on the outer shell. These plugs are provided to avoid the pressure raise by steam or gas generated from the heat insulator and shock absorber due to heat during fire.

The inner shell is provided with three bosses at the upper side of the inner surface and the convex section at the bottom, in order to fix the fuel basket.

The boss and fuel basket upper part are fixed with bolts, and the fuel basket lower part is inserted into the convex section.

When fixing, to avoid metal contact of the inner shell and fuel basket, the cushion rubber is provided.

2.2 Inner lid (Refer to (I)-Fig.C.7)

The inner lid is in the cylindrical shape, 620mm in outer diameter and 55mm in thickness.

The inner lid is tied down with the main body, using 16 inner lid tightening bolts, and the contact section of the inner lid and inner shell is constructed so that leaktightness is maintained with O-ring. This O-ring is doubly provided to assure leaktightness, and a leak test hole between the double O-ring is provided to make it possible to perform a leak test.

2.3 Fuel basket (Refer to ((I)-Fig C.8))

The fuel basket is manufactured to locate each fuel element in the specified position of the packaging and maintain its relative position, and 10 fuel elements can be contained. The fuel basket is shown in (I)-Fig.C.8 rectangular pipes to enclose the fuel elements, are assembled by welding, and the upper and the lower portions of the rectangular pipes, are welded to the flanges and basket bottom is attached to the flange bottom by the three bolts. The inside dimension of the rectangular pipe is 94mm×94mm, the outside diameter of the fuel basket is 459mm, and the height is 1293mm.

And also, the fuel basket is fixed to the three bosses located at the upper inside portion of the inner shell by bolt, the movements to the vertical and circumferential direction are restricted, and the vibration is also restricted.

2.4 Outer lid (Refer to (I)-Fig. C. 9)

The outer lid is in of the cylindrical shape 398mm in height and 840mm in outer diameter.

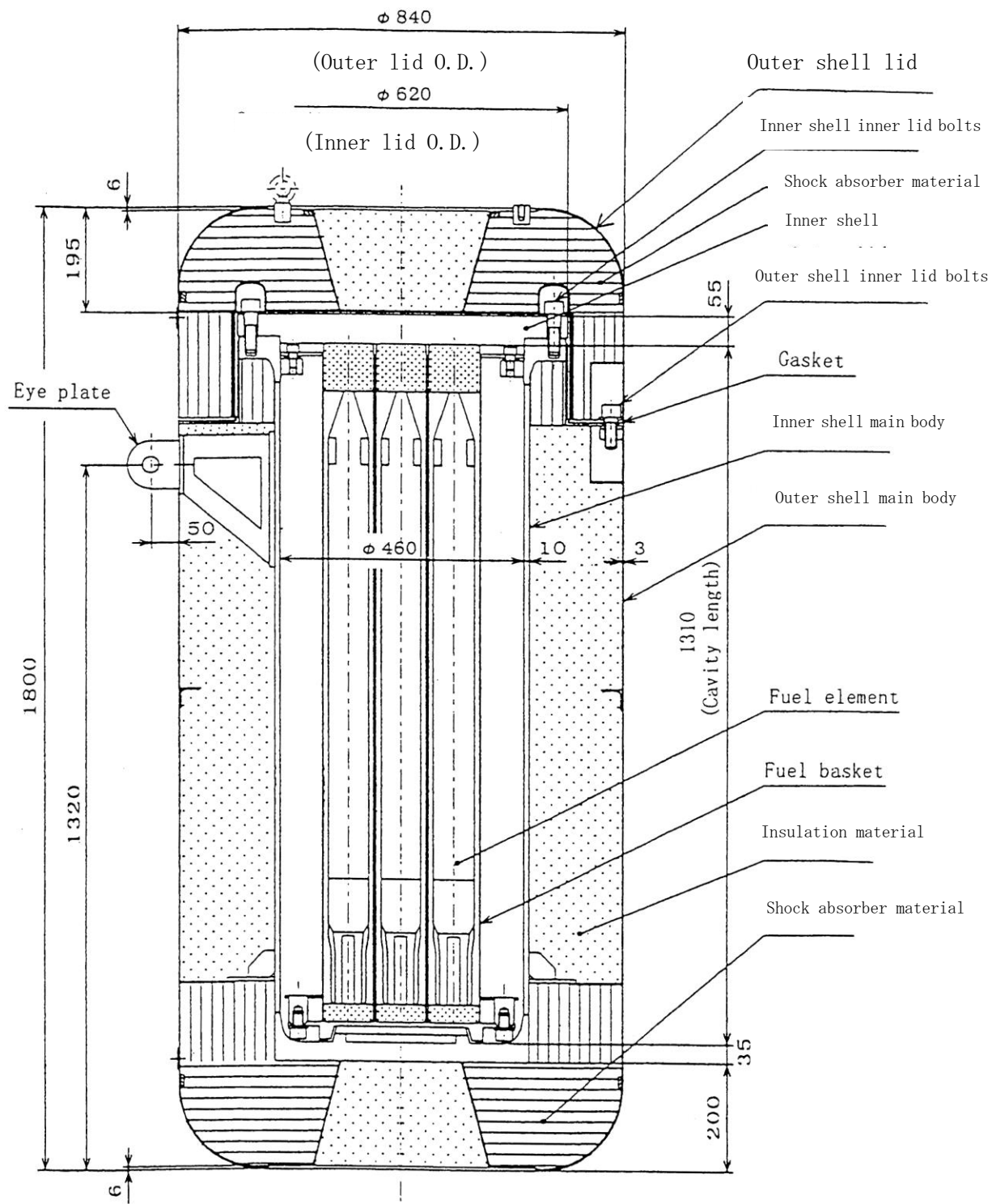
The outer cover plate consists of 3mm thick stainless steel shell and 6mm thick stainless steel upper plate. The inner cover plate consists of 3mm thick stainless steels.

The space between the outer and inner cover plates, the heat insulators and shock absorbers are applied to reduce the heat gain caused by fire and to absorb impact energy caused by drop.

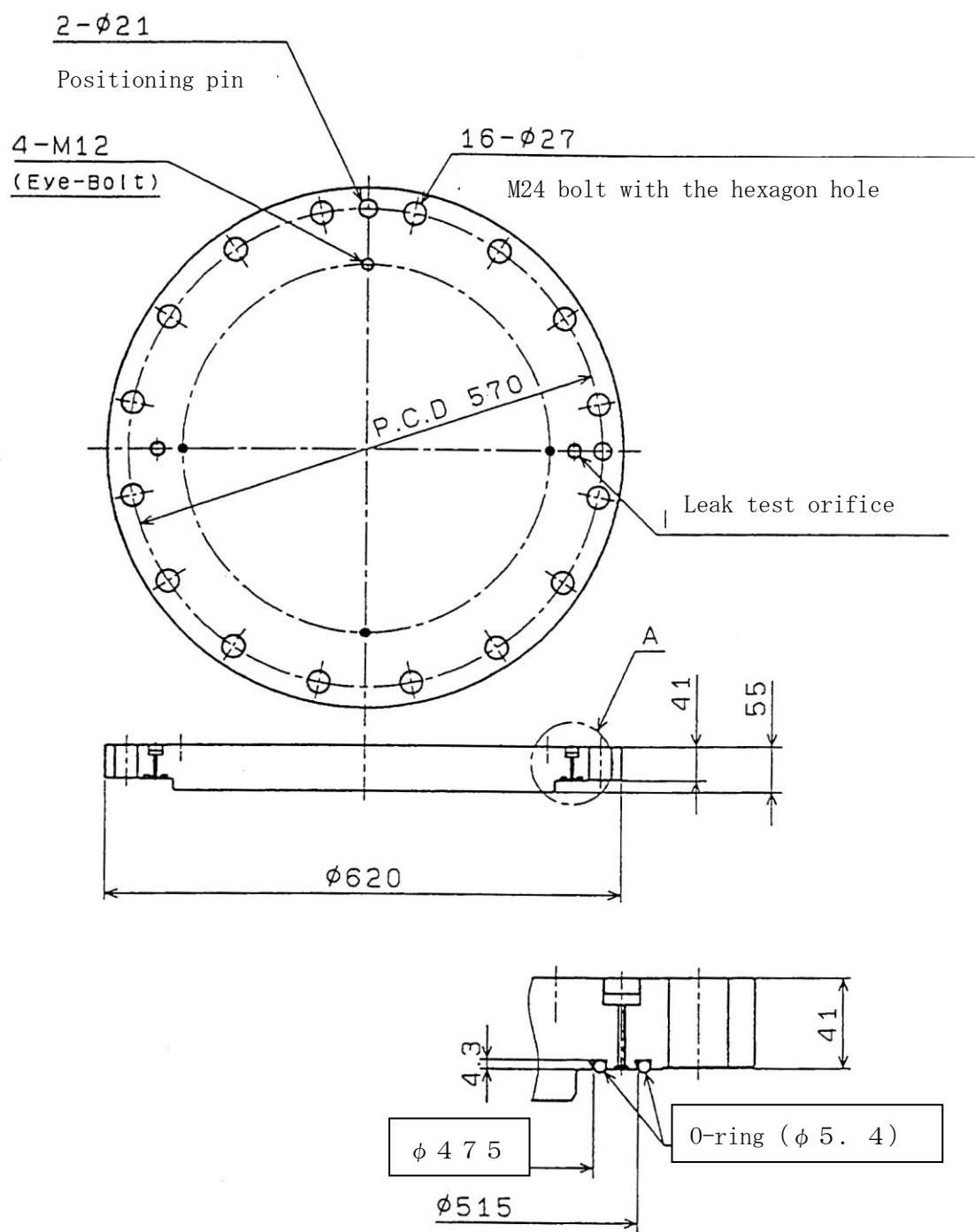
4 eye-bolt bosses for lifting are welded to the outer lid. 4 fusible plugs are provided on the outer cover plate. These plugs are used to avoid the pressure raise by steam or gas generated from the heat insulator and shock absorber due to heat during fire.

The outer lid is tied down with the outer lid tightening bolts through the rubber packing to the upper part of the main body in such a manner that it covers the inner lid. Such a structure prevents water from intruding into the clearance between the main body and the outer lid.

Also, the tightened section between the main body and outer lid can he sealed and locked.

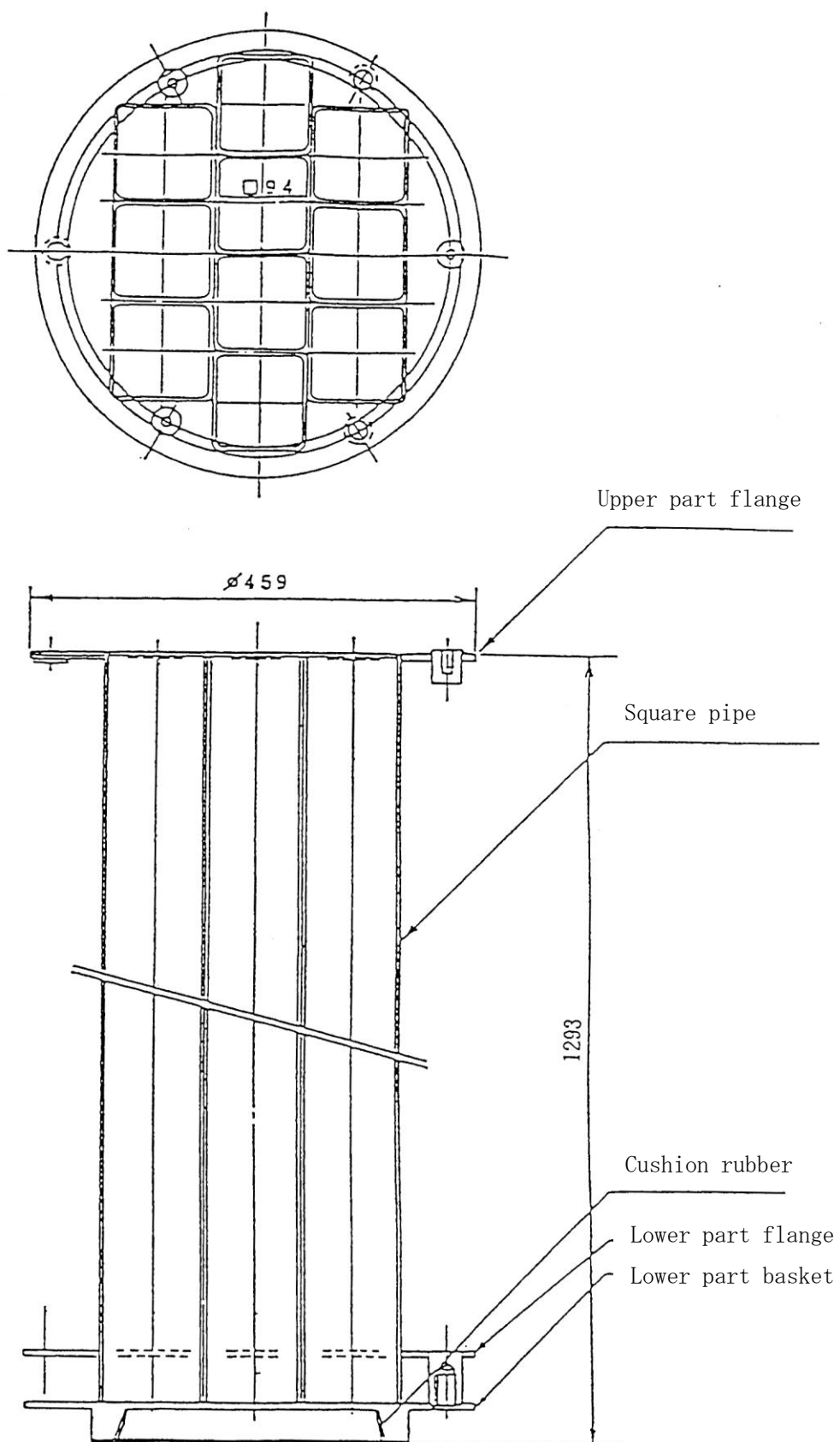


(I)-Fig.C.5 General drawing of package

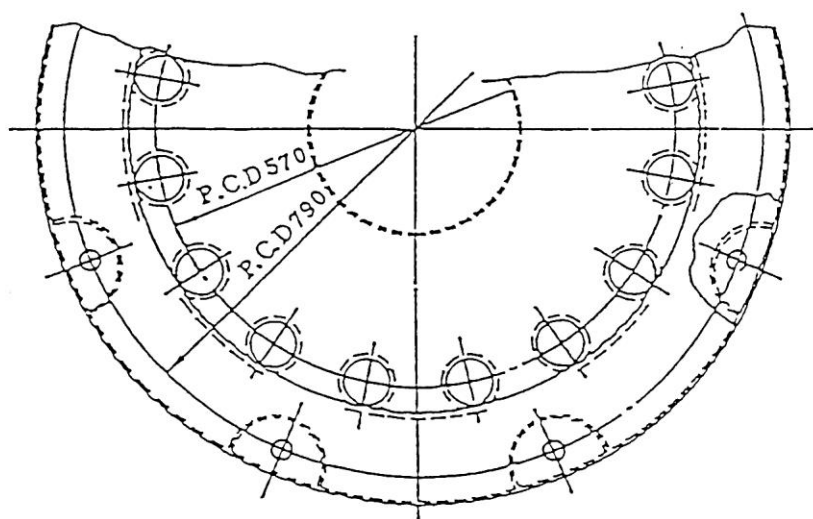
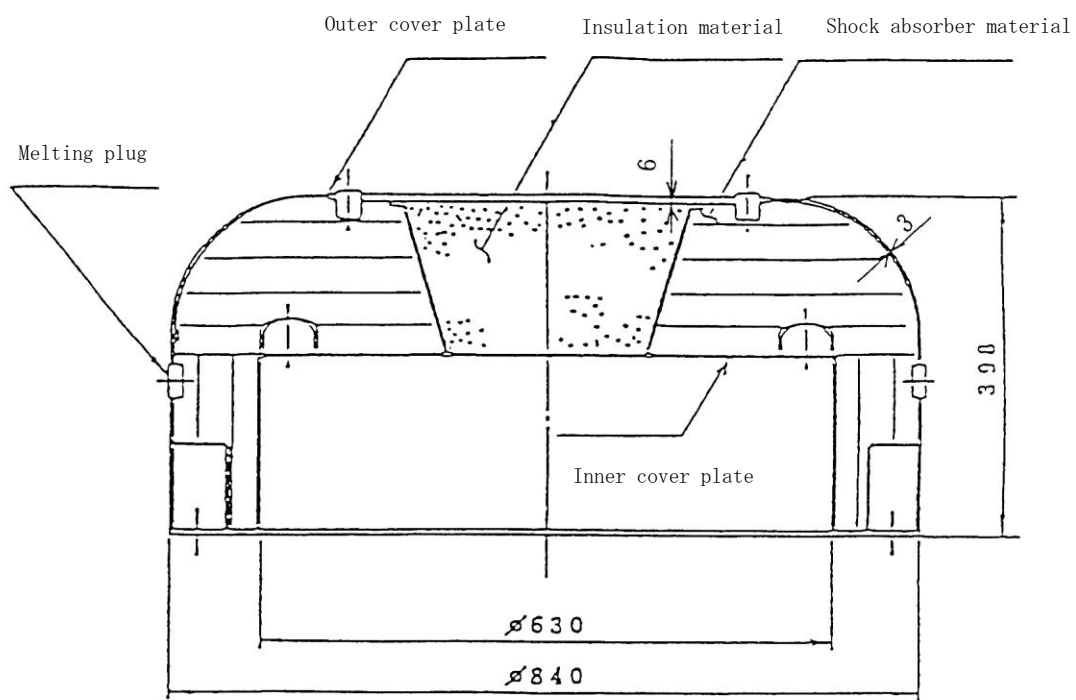


: The A part details

(I)-Fig.C.7 Inner shell lid



(I)-Fig.C.8 Basket for box type fuel



(I)-Fig.C.9 Outer shell lid

3. Material of packaging

(I) -Table C.1 shows the material of the packaging.

4. Dimension of packaging

(I) -Table C.2 shows the dimension of the packaging.

5. Weight of packaging

(I) -Table C.3 shows the weight of the packaging.

(I)-Table C.1 Material of packaging

Name of Part	Material	Number	Notes
(1) Main body			
• Outer shell	Stainless steel	1 ^s	
• Inner shell	Stainless steel	1 ^s	
• Eye plate	Stainless steel	4	
• Boss	Stainless steel	3	
• Heat insulator	Hard polyurethane foam	1 ^s	
• Shock absorber	Balsa wood	1 ^s	
• O-ring	Silicone rubber	1 ^s	
• Fusible plug	Solder, Stainless steel	8 ^s	
• Gasket	Ethylene propylene rubber	1	
(2) Inner Lid			
• Inner Lid	Stainless steel	1	
(3) Fuel Basket			
• Rectangular pipe	Stainless steel	10	
• Upper flange	Stainless steel	1	
• Lower flange	Stainless steel	1	
• Cushion rubber	Silicone rubber	1	
(4) Outer Lid			
• Outer cover plate	Stainless steel	1 ^s	
• Inner cover plate	Stainless steel	1 ^s	
• Heat insulator	Hard polyurethane foam	1 ^s	
• Shock absorber	Balsa wood	1 ^s	
• Fusible plug	Solder, Stainless steel	4 ^s	

(I)-Table C.2 Dimension of packaging

Name of Part	Item	Dimension(nominal)	Notes
(1) Main body	Outer Diameter	840	
	Inner Diameter	460	
	Height	1,559	
(2) Inner Lid	Outer Diameter	620	
	Thickness	55	
	Size of Bolt	M24	
(3) Fuel Basket	Outer Diameter	459	
	Height	1,293	
	Inner width	94×94	
(4) Outer Lid	Outer Diameter	840	
	Inner Diameter	630	
	Height	398	
	Size of Bolt	M24	

(I)-Table C.3 Weight of packaging

No.	Name	Weight (kg)	Notes
1	Inner shell main body	480	
2	Inner shell lid	120	
3	Fuel Basket	138	
4	Outer shell lid	120	
5	Total	858	

The weights of the contents are shown in (I)-Table D.1 and (I)-Table D.2, the weight becomes maximum of 92kg when the ten JRR-3 standard fuel elements are contained and the maximum weight of the package is 950kg.

D Contents of packaging

(I)-D. Contents of packaging

D.1 Fresh fuel

Among the contents of packaging, fresh fuel elements for research reactors are plate type fuels to be charged in JRR-3, JRR-4, JMTR and KUR. There are three kind of enrichment, high-enriched uranium fuel (HEU fuel), medium-enriched uranium fuel (MEU fuel), and low-enriched uranium fuel (LEU fuel).

The fuel meat is uranium aluminum alloy for HEU fuel, uranium aluminum dispersion type alloy for MEU fuel, and uranium aluminum dispersion type alloy or uranium silicon aluminum dispersion type alloy for LEU fuel.

Fuel plates are processed as follows : a fuel meat sandwiched by a frame and cover (cladding material) of aluminum alloy is hot-rolled. After being cold-rolled to the required thickness, it is cut longitudinally and transversely while being monitored by fluoroscopy so that the fuel meat can be located within the required zone.

On side plate or mounting plate of the aluminum alloy, the required number of grooves are provided for mounting the fuel plates. The width of a groove is equal to the thickness of the plate. Fuel plates are inserted into these grooves and mechanically fixed so that the fuel plates can resist a tensile stress of 265N/cm.

Required mounting parts are fixed by welding and other methods to complete a standard type fuel elements and follower type fuel elements (referred to as “fuel elements” hereinafter).

The fuel element is wrapped by some buffer, such as polyurethane foam, then put into an organic high-molecular compound bag such as polyethylene (Protective sheets), and loaded into the fuel basket of packaging.

When the fuel element are loaded, silicone rubber spacers are used to the upper and lower sides of the fuel element in order to absorb possible impact energy during transport, and also to fix the fuel element. For the KUR fuel elements, metal spacers (outer dimension : 84 x 90 x 875mm or 954mm) shown in (I)- Fig. D.1 are inserted into the fuel basket, and the fuel elements are loaded into the metal spacers.

The specifications of fuel elements loaded in the packaging are shown in (I)-Table D. 1.

D.2 Lowly irradiated fuel

Among the contained fuels in the packaging, the lowly irradiated fuels are the plate type fuels loaded in the JMTRC, consisting of 61 HEU fuels and 31 MEU fuels. The core material of the fuel is the uranium-aluminum alloy for HEU fuel and is the uranium-aluminum dispersion type alloy for MEU. On the side plate or attachment plate made of aluminum alloy, are provided for the required number of the grooves corresponding to the thickness of the fuel plate. The fuel plate inserted is mechanically fixed by roll swage or fixed by the aluminum alloy pin to withstand the tensile force of more than 265N/cm.

The required parts are welded to the fuel plates to complete the standard fuel element, the special fuel element and the fuel follower (referred to as “fuel elements etc.” hereinafter).

The special fuel element has the structure where a part of the fuel plates are not mechanically fixed and can be removed. The fuel elements etc. are charged after cutting the unnecessary upper and lower portions to reduce the weight. For the special fuel elements, they are provide with a hold-down for fuel plate as shown in (I)-Fig.D. 13 through (I)-Fig.D. 15 and in (I)-Fig.D. 18.

The fuel elements etc. are packed with the shock absorber such as polyurethane foam etc. and is put in the bag made of organic high molecular compound such as polyethylene (protection sheet), and is enclosed in the fuel basket of the packaging. In case the fuel element etc. are loaded, the spacers of silicone rubber are used at the top and bottom of the fuel element etc. in order to absorb the impact in the transportation and to fix the fuel element etc. by adjusting the position. The specification of the fuel element etc., used for the safety analysis of packaging is shown in (I)-Table D. 2.

D.3 Fresh fuel for KUCA

Among the contents of packaging, fuels for critical assembly are fuel plate to be charged in KUCA. There are two types of fuels, a square plate fuel (coupon) and a flat plate fuel (flat), both of which are low-enriched uranium fuels (LEU fuel).

The fuel meat is a uranium molybdenum aluminum dispersion type alloy for coupon type, and a uranium silicon aluminum dispersion type alloy for flat type.

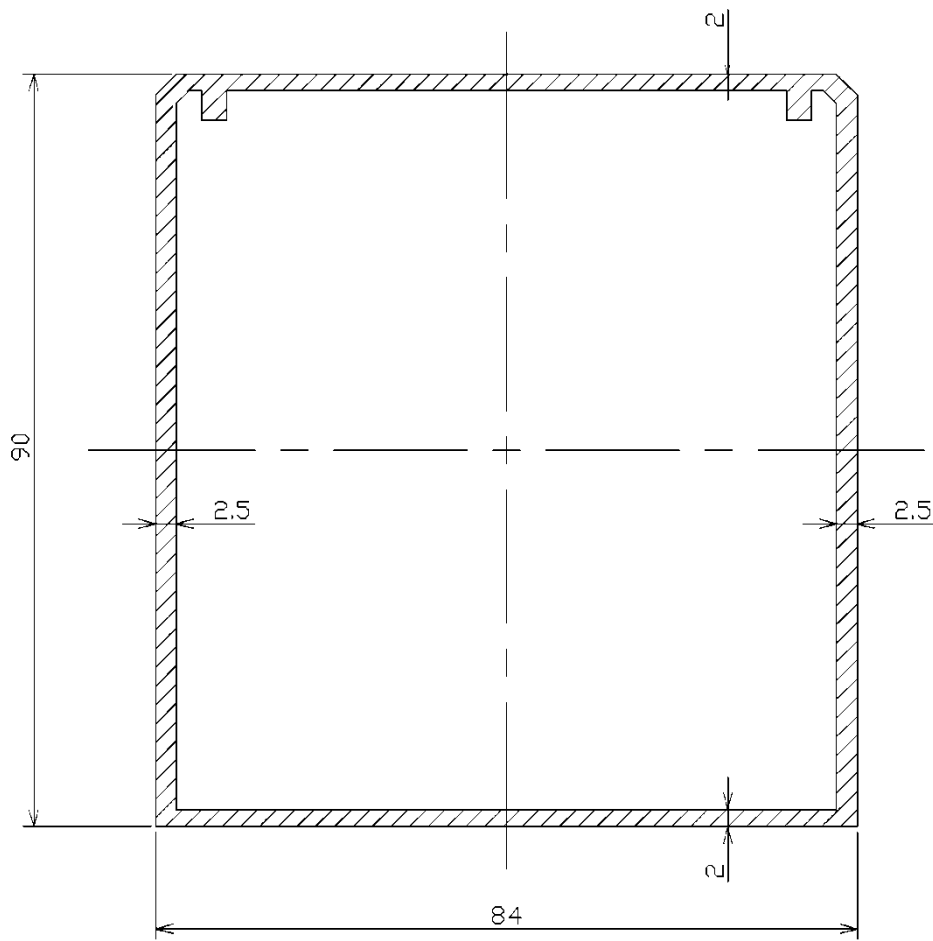
Coupon plates are processed as follows : a fuel meat is enclosed in a case and a cover (covering material) made of an aluminum alloy.

Flat plates are processed as follows : a fuel meat sandwiched by a frame and cover (cladding material) of aluminum alloy is hot-rolled. After being cold-rolled to the required thickness, it is cut longitudinally and transversely while being monitored by fluoroscopy so that the fuel meat can be located within the required zone.

The coupon plates are inserted into the aluminum sheath after sandwiching the cushion material such as aluminum sheet for protection between the fuel plates, and it is wrapped by some buffer such as polyurethane foam, then loaded into the fuel basket of packaging. The flat plates are wrapped by some buffer such as polyurethane foam after sandwiching the cushion material such as aluminum sheet for protection between the fuel plates, then loaded into the fuel basket of packaging.

When the KUCA fuels are loaded, silicone rubber spacers are used to the upper and lower sides of the fuel plates in order to absorb possible impact energy during transport, and also to fix the fuel plates.

The specifications of fuel elements loaded in the packaging are shown in (I)-Table D.3.



(I)-Fig.D.1 Metal Spacer

(I)-Table D.1 Specification of fuel element (fresh fuel element)

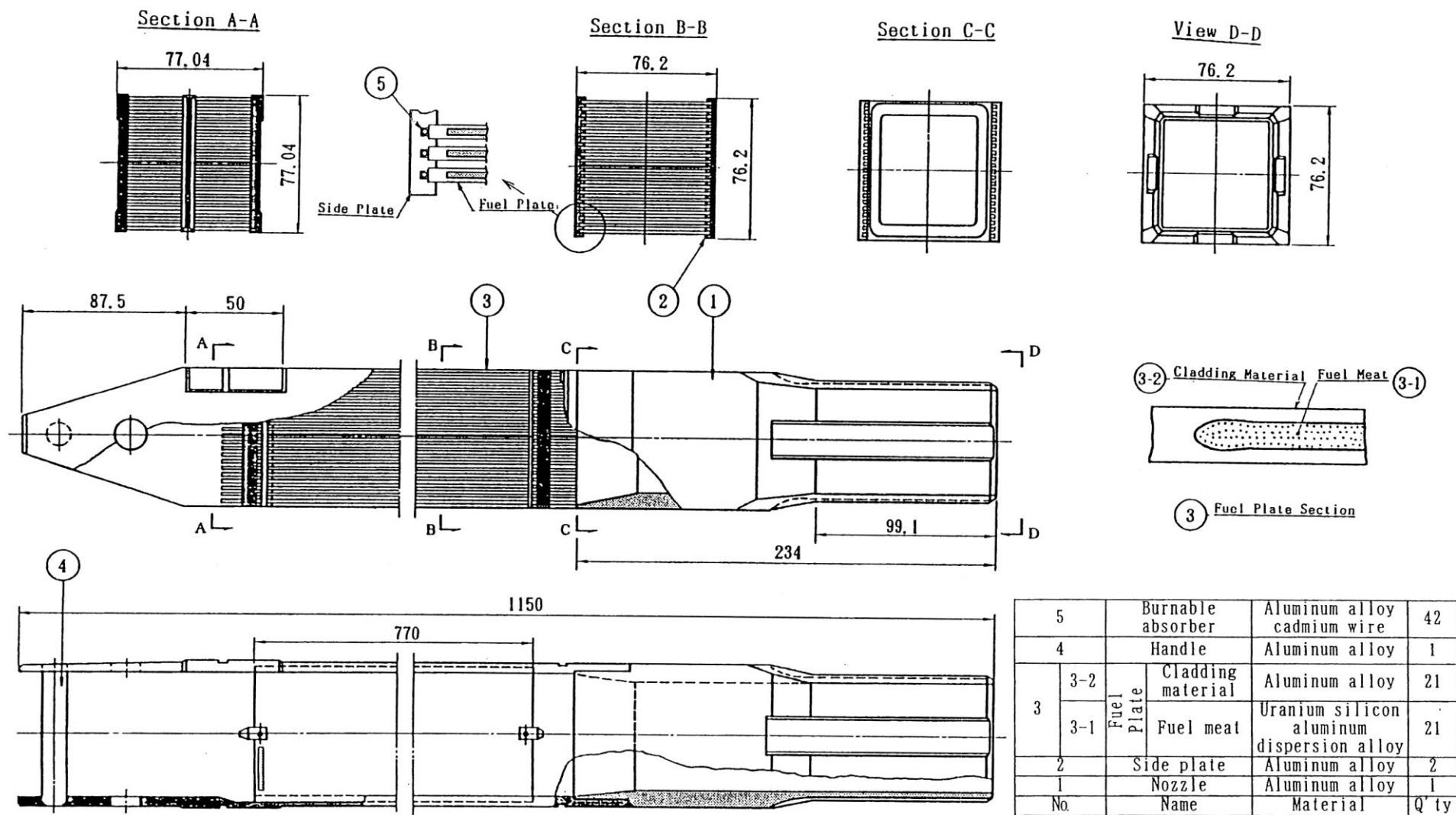
Fuel Basket Type		Box										
Type	Reactor	JRR-3		JRR-4			JMTR			KUR		
	Fuel Element	JRR-3 Standard	JRR-3 Follower	JRR-4 B	JRR-4 L	JRR-4	JMTR Standard	JMTR Follower	KUR Standard	KUR Special	KUR Half-loaded	
Type		Plate fuel										
Total no. of loaded (fuel/Package)		10 or less										
Kind		LEU fuel		HEU fuel	LEU fuel		MEU fuel	LEU fuel		LEU fuel		
Nuclear spec.	U-235 enrichment (wt%)	19.95 or less		93.3 or less	19.95 or less		46.0 or less	19.95 or less		19.95 or less		
	U-235 contained (g/one element)	485 or less	310 or less	170 or less	230 or less	210 or less	320 or less	425 or less	280 or less	218 or less	109 or less	109 or less
	U contained (g/one element)	2481 or less	1586 or less	183 or less	1177 or less	1075 or less	728 or less	2174 or less	1433 or less	1115 or less	558 or less	558 or less
Burnup (%)		0 (Fresh fuel)										
Heat generation(w/container)		0 (Fresh fuel)										
Cooling down days(day)		0 (Fresh fuel)										
Radioactivity (GBq/Package)		29.8 or less										
Material	Core material	Uranium silicon alminum dispersion alloy	Uranium silicon alminum dispersion alloy	Uranium alminum alloy	Uranium alminum dispersion alloy	Uranium silicon alminum dispersion alloy	Uranium alminum dispersion alloy	Uranium silicon alminum dispersion alloy	Uranium silicon alminum dispersion alloy	Uranium silicon alminum dispersion alloy	Uranium silicon alminum dispersion alloy	Uranium silicon alminum dispersion alloy
	Clad material	Aluminum alloy										
	Side plate, Attached plate	Aluminum alloy										
	Burnable absorber	Cadmium wire			-				Cadmium wire		-	
Shape	Fuel cross section shape	Rectangular type										
	Ref. drawing	(I)-Fig.D.2	(I)-Fig.D.3	(I)-Fig.D.4	(I)-Fig.D.5	(I)-Fig.D.6	(I)-Fig.D.7		(I)-Fig.D.8	(I)-Fig.D.9	(I)-Fig.D.10	(I)-Fig.D.9
Fuel weight(kg/one element)		9.2	6.0	6.3	7.9	6.5	7.6	8.4	5.8	6.0	5.5	5.5

(I)-Table D.2 Specification of fuel element (lowly irradiated fuel element)

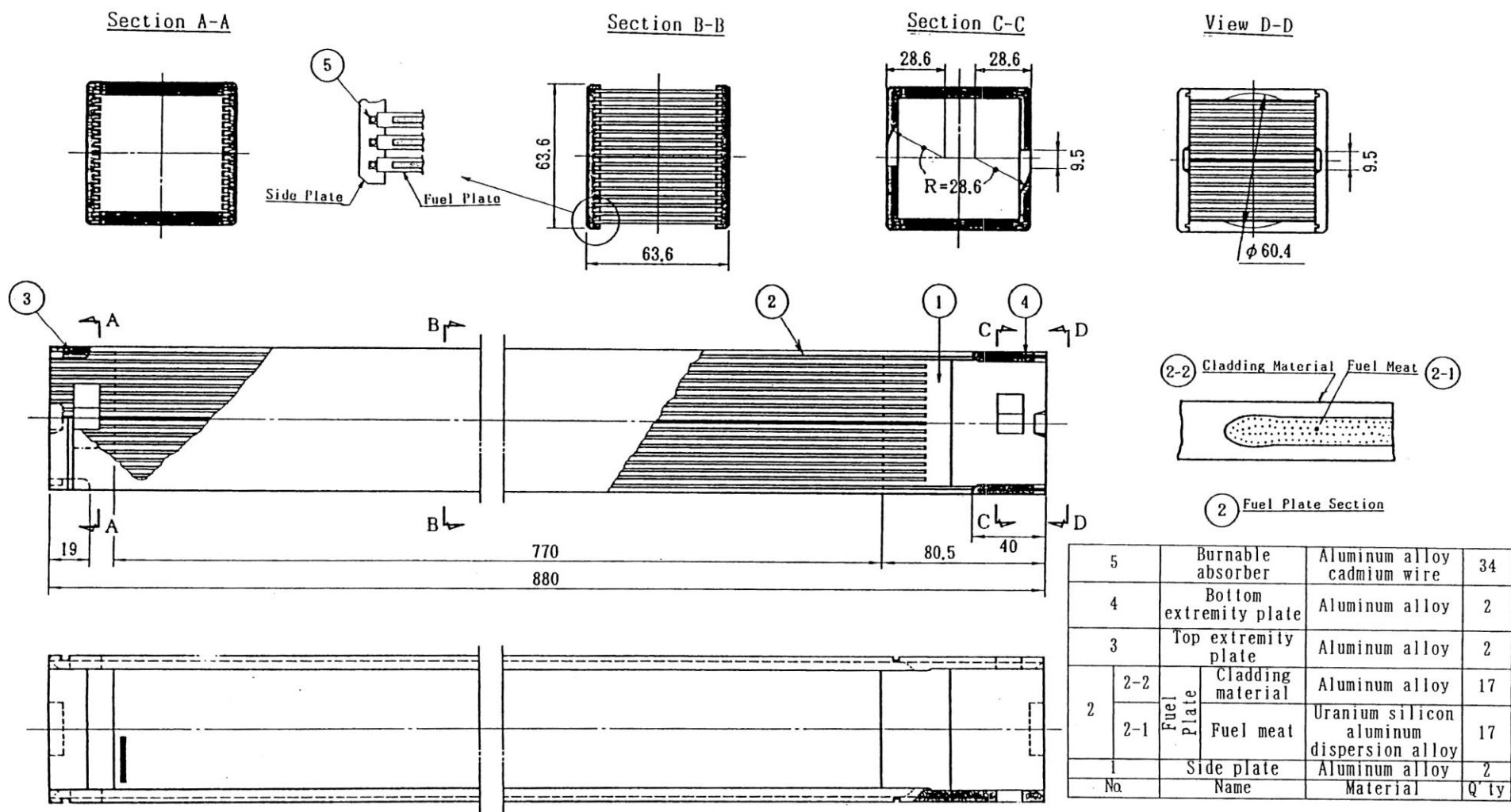
Fuel Basket Type		Box								
Type	Reactor	JMTRC								
	Fuel Element	JMTRC Standard		JMTRC Special		JMTRC Follower	JMTRC Standard	JMTRC Special	JMTRC Follower	
Type		Plate fuel								
Total no. of loaded (fuel/Package)		10 or less								
Kind		HEU fuel					MEU fuel			
Nuclear spec.	U-235 enrichment (wt%)	90.0 or less					46.0 or less			
	U-235 contained (g/one element)	285 or less	285 or less		199 or less	317 or less	286 or less	210 or less		
	U contained (g/one element)	318 or less	318 or less		222 or less	721 or less	650 or less	478 or less		
Burnup (%)		7.23×10 ⁻⁵ or less					1.76×10 ⁻⁵ or less			
Heat generation(w/container)		4.30×10 ⁻⁵ or less								
Cooling down days(day)		5475 or more					1460 or more			
(GBq/Package)		17.3 or less								
Material	Core material	Uranium Alminum alloy	Uranium Alminum alloy		Uranium Alminum alloy	uranium alminum dispersion type alloy	uranium alminum dispersion type alloy	uranium alminum dispersion type alloy		
	Clad material	Alminum alloy								
	Side plate, Attached plate	Alminum alloy								
	Burnable absorber	-					-			
Shape	Fuel cross section shape	Rectangular type								
	Ref. drawing	(I)-Fig. D. 11	(I)-Fig. D. 12	(I)-Fig. D. 13	(I)-Fig. D. 14	(I)-Fig. D. 15	(I)-Fig. D. 16	(I)-Fig. D. 17	(I)-Fig. D. 18	(I)-Fig. D. 19
Fuel weight (kg/one element)		6.3	6.6	2.0	6.9	4.1	6.7	6.9	4.4	
Holder	Ref. drawing	-	(I)-Fig. D. 13	(I)-Fig. D. 14	(I)-Fig. D. 15	-	-	(I)-Fig. D. 18	-	
	Weight (kg/one element)	-	1.4	2.6	1.4	-	-	1.4	-	

(I)-Table D.3 Specification of fuel element (fresh fuel for KUCA)

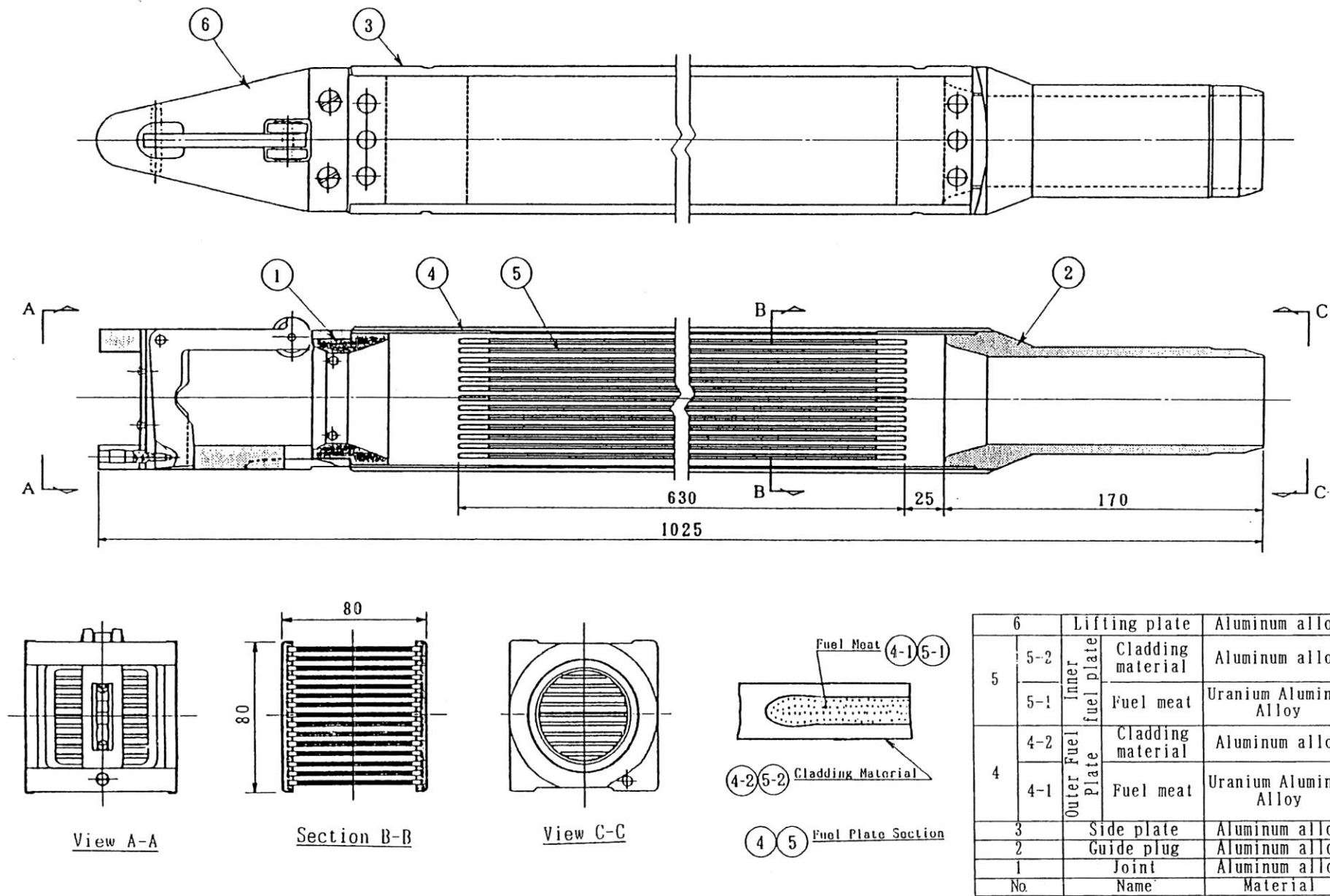
Fuel Basket Type		Box	
Type	Reactor	KUCA	
	Fuel Element	Coupon	Flat
Type		Plate fuel	
Total no. of loaded (fuel/Package)		1200 or less	300 or less
Kind		LEU fuel	
Nuclear spec.	U-235 enrichment (wt%)	19.95 or less	
	U-235 contained (g/one plate)	4 or less	15 or less
	U contained (g/one plate)	20.5 or less	78 or less
Burnup (%)		0 (Fresh fuel)	
Heat generation(w/package)		0 (Fresh fuel)	
Cooling down days(day)		0 (Fresh fuel)	
(GBq/Package)		15.5 or less	15.5 or less
Material	Core material	Uranium molybdenum aluminum dispersion alloy	Uranium silicon aluminum dispersion alloy
	Clad material	Aluminum alloy	
	Side plate, Attached plate	-	
	Burnable absorber	-	
Shape	Fuel cross section shape	Rectangular type	
	Ref. drawing	(I)-Fig. D. 20	(I)-Fig. D. 21
Fuel weight(kg/one plate)		36	230



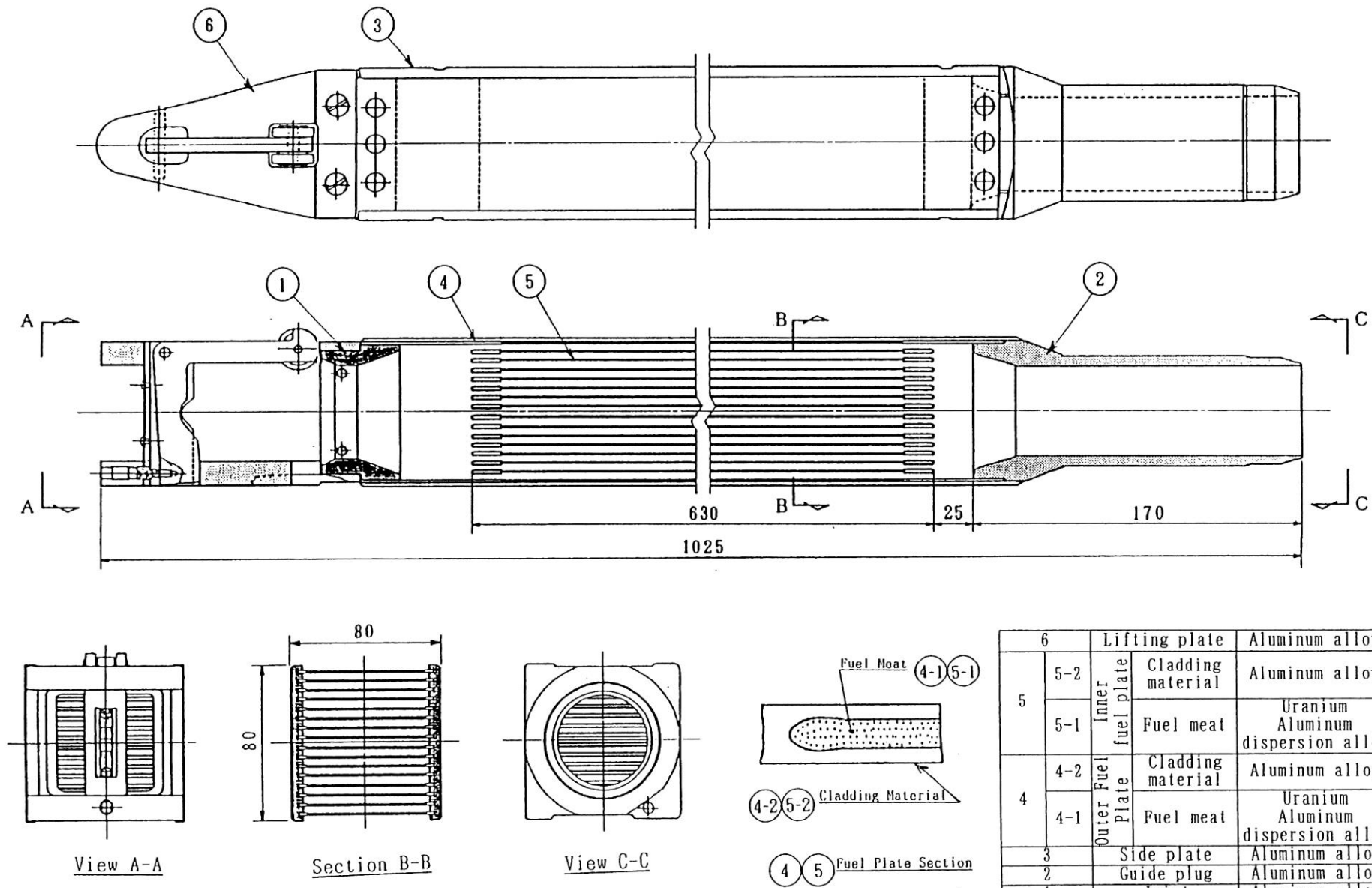
(I)-Fig.D.2 JRR-3 standard type fuel element (uranium silicon aluminum dispersion alloy)



(I)-Fig.D.3 JRR-3 follower type fuel element (uranium silicon aluminum dispersion alloy)

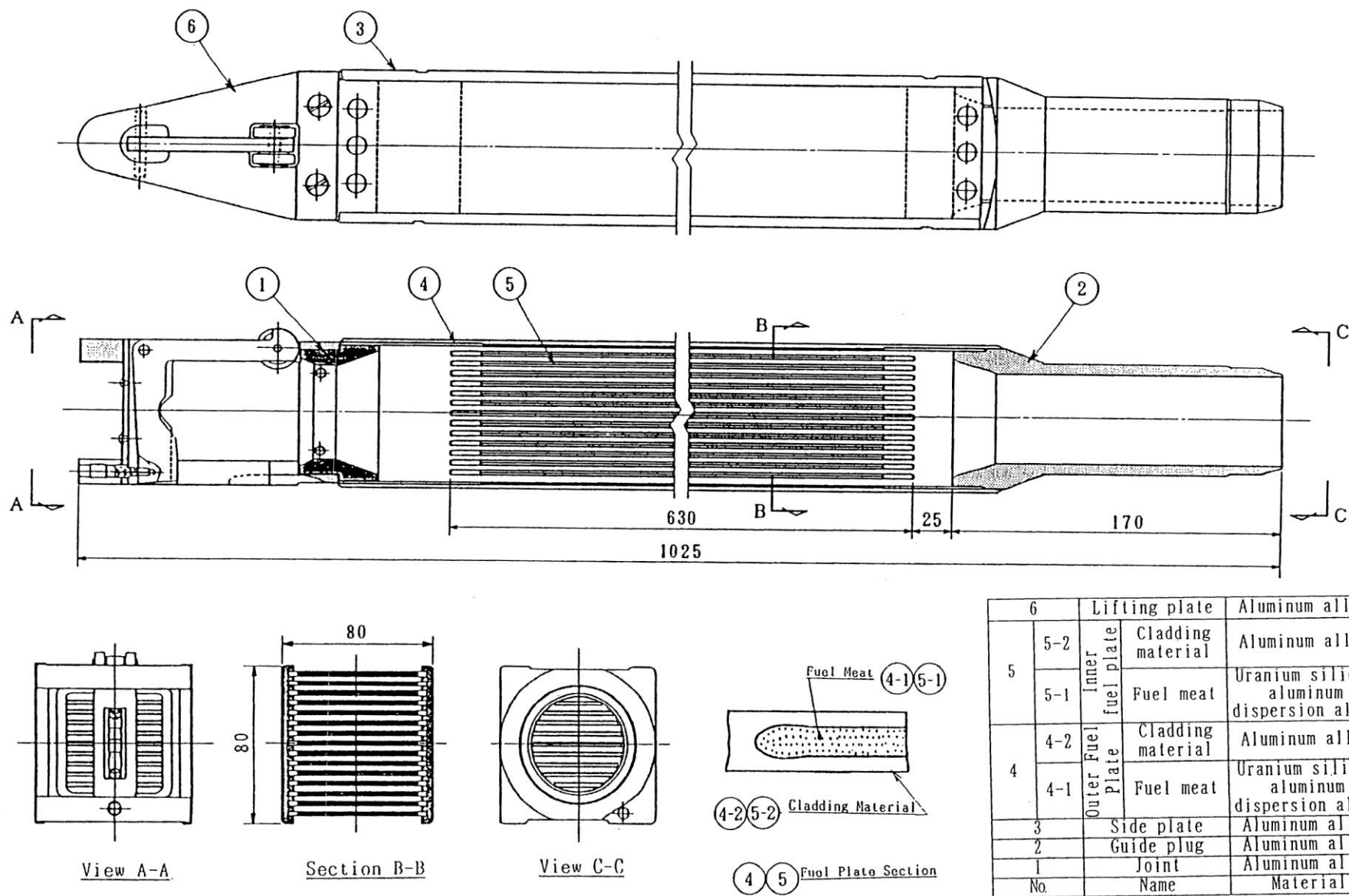


(I)-Fig.D.4 JRR-4B type fuel element

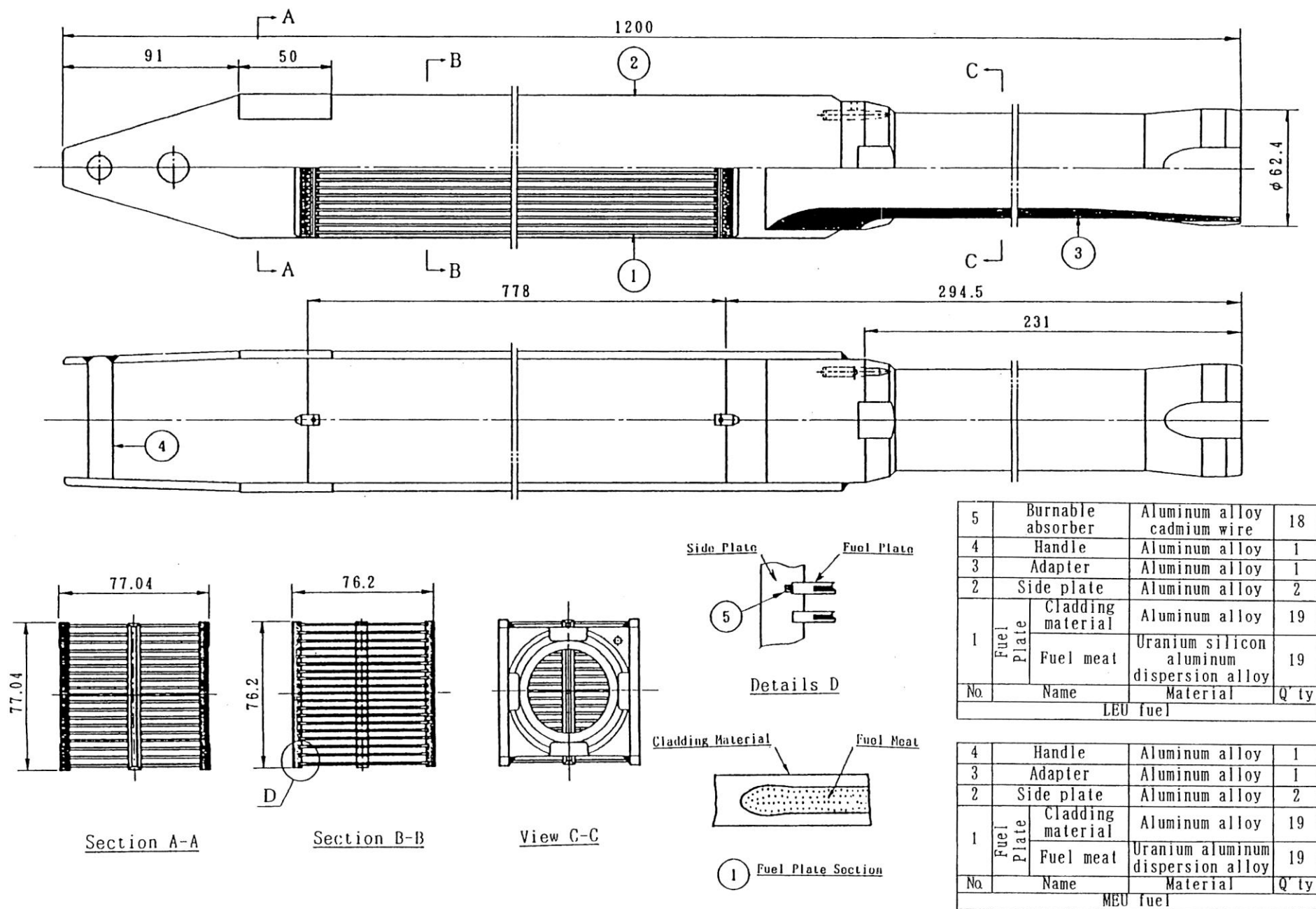


6		Lifting plate	Aluminum alloy	1
5	5-2	Inner fuel plate	Cladding material	Aluminum alloy
	5-1	Inner fuel plate	Fuel meat	Uranium Aluminum dispersion alloy
4	4-2	Outer fuel plate	Cladding material	Aluminum alloy
	4-1	Outer fuel plate	Fuel meat	Uranium Aluminum dispersion alloy
3		Side plate	Aluminum alloy	2
2		Guide plug	Aluminum alloy	1
1		Joint	Aluminum alloy	1
No.		Name	Material	Q'ty

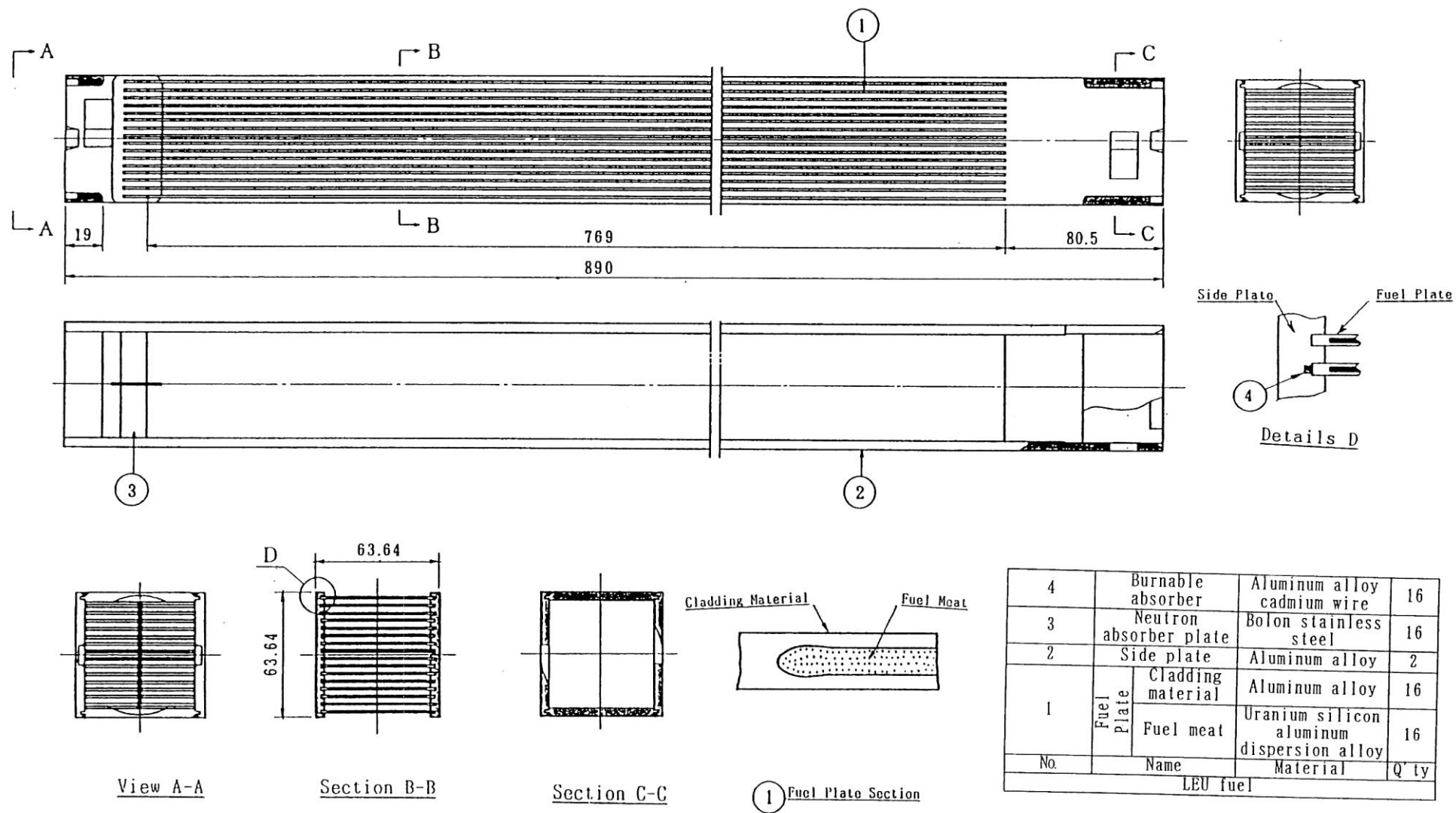
(I)-Fig.D.5 JRR-4L type fuel element



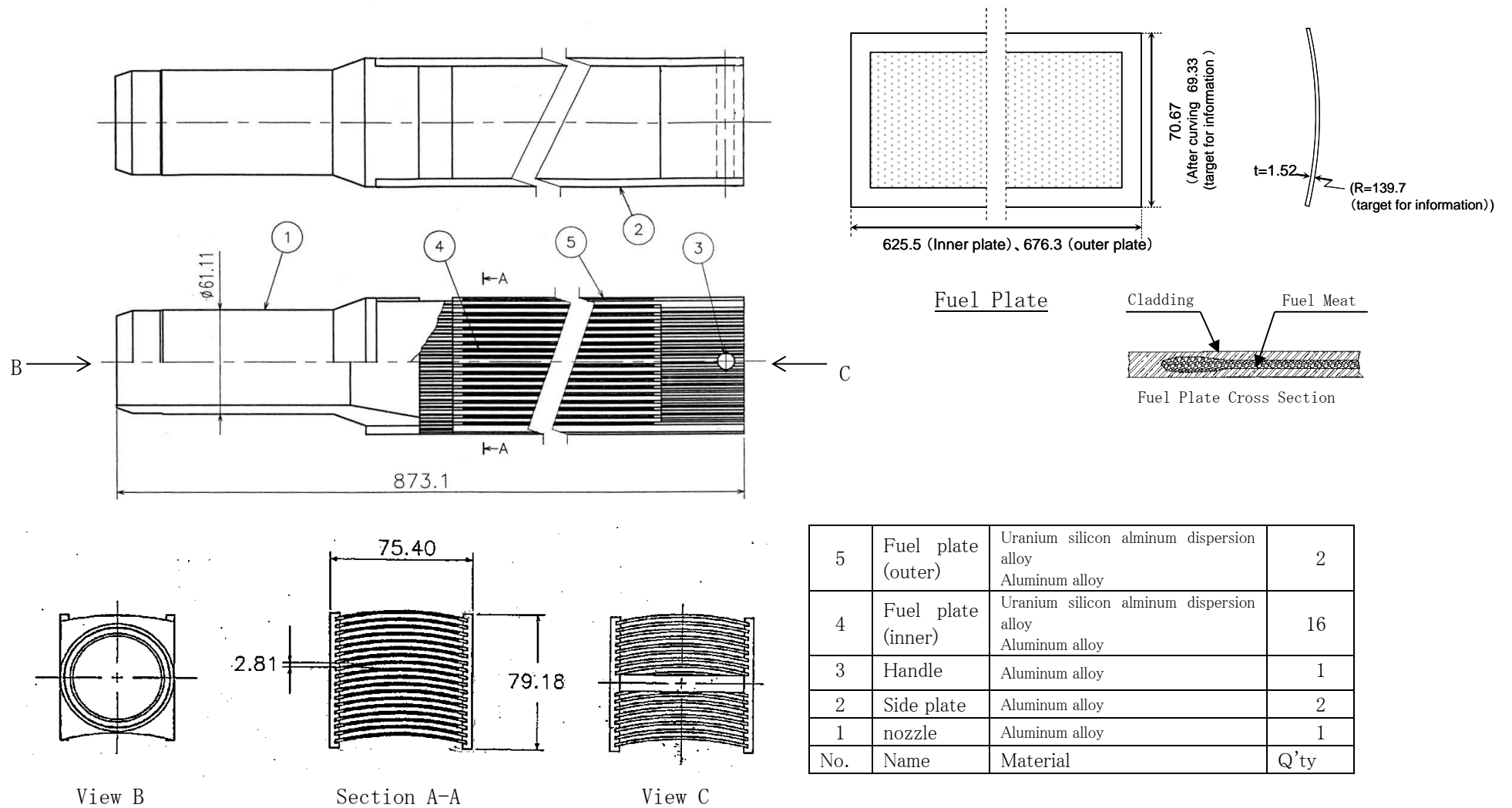
(I)-Fig.D.6 JRR-4 fuel element (uranium silicon aluminum dispersion type alloy)



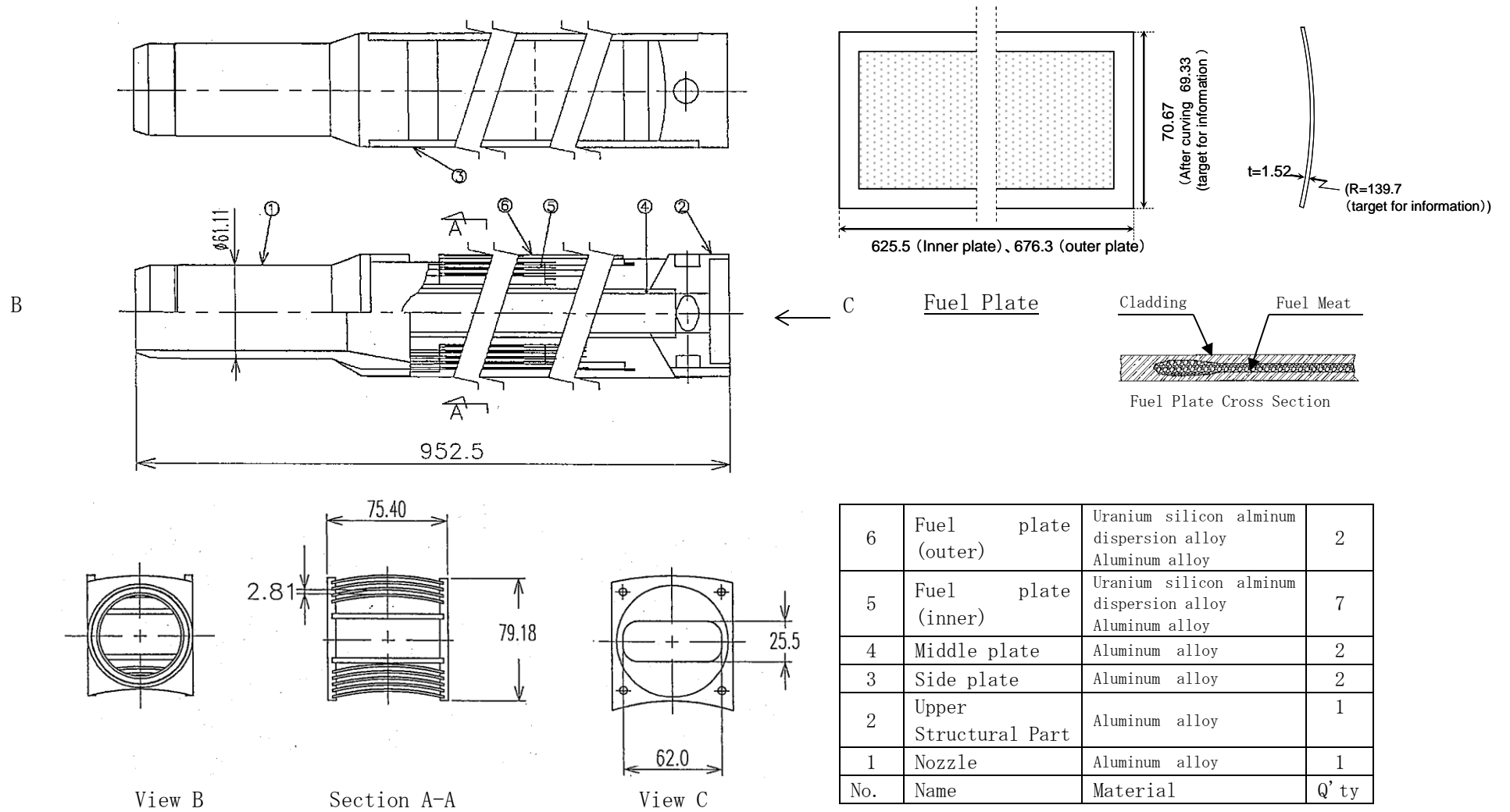
(I)-Fig.D.7 JMTR standard fuel element



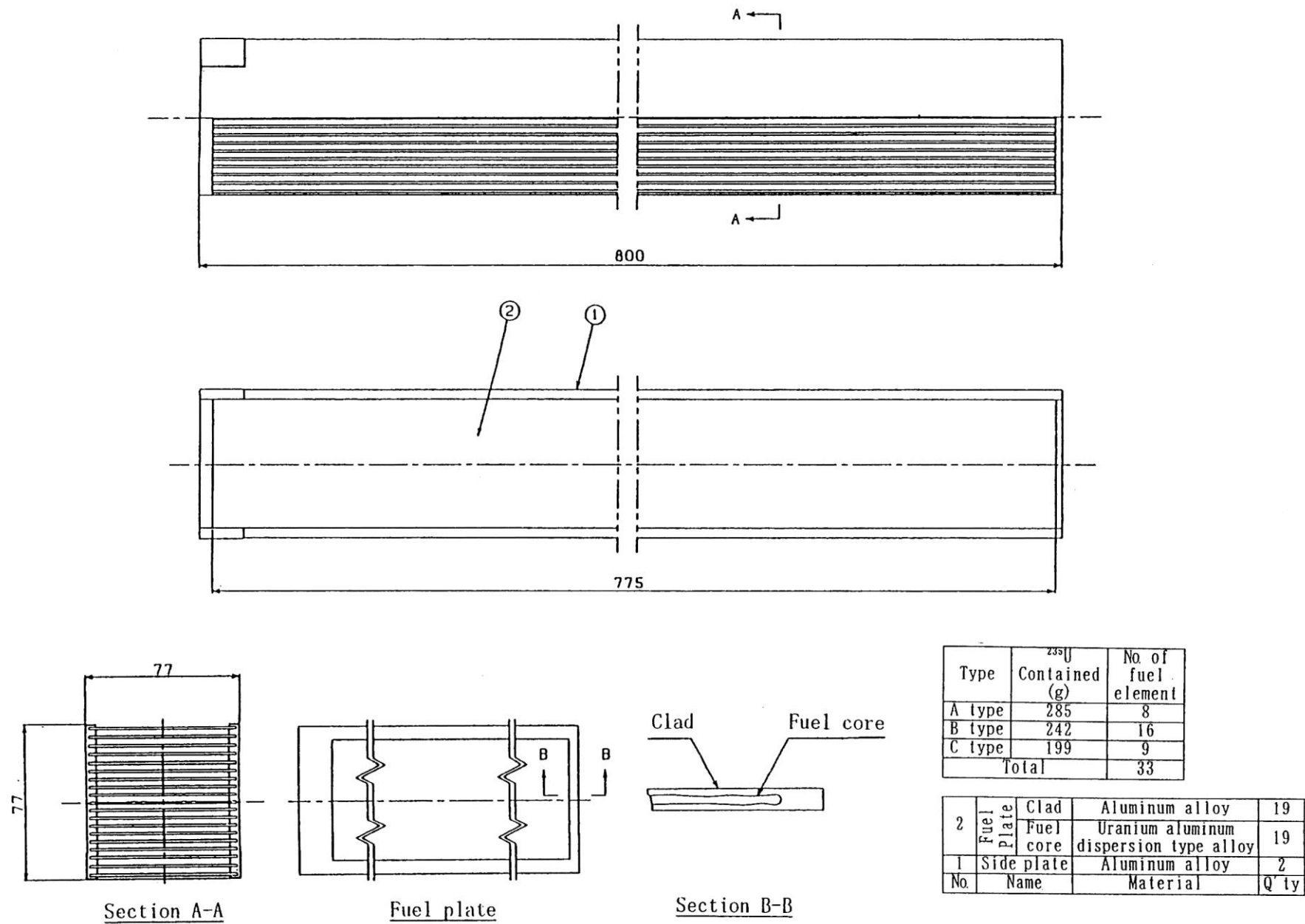
(I)-Fig.D.8 JMTR follower type fuel element



(I)-Fig.D.9 KUR Standard and Half-loaded fuel elements (Uranium silicon aluminum dispersion alloy)

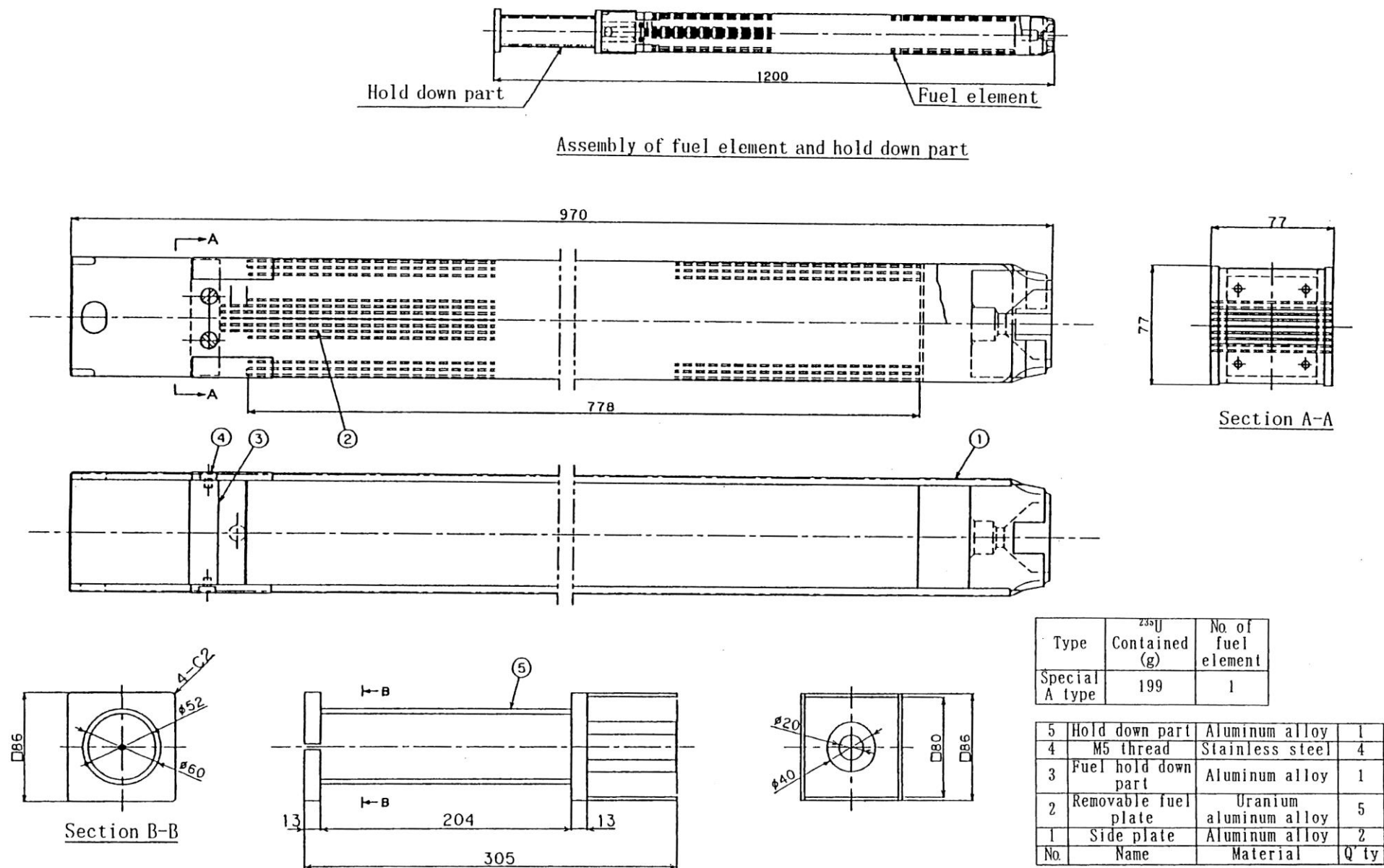


(I)-Fig.D.10 KUR Special fuel element (Uranium silicon alminum dispersion alloy)

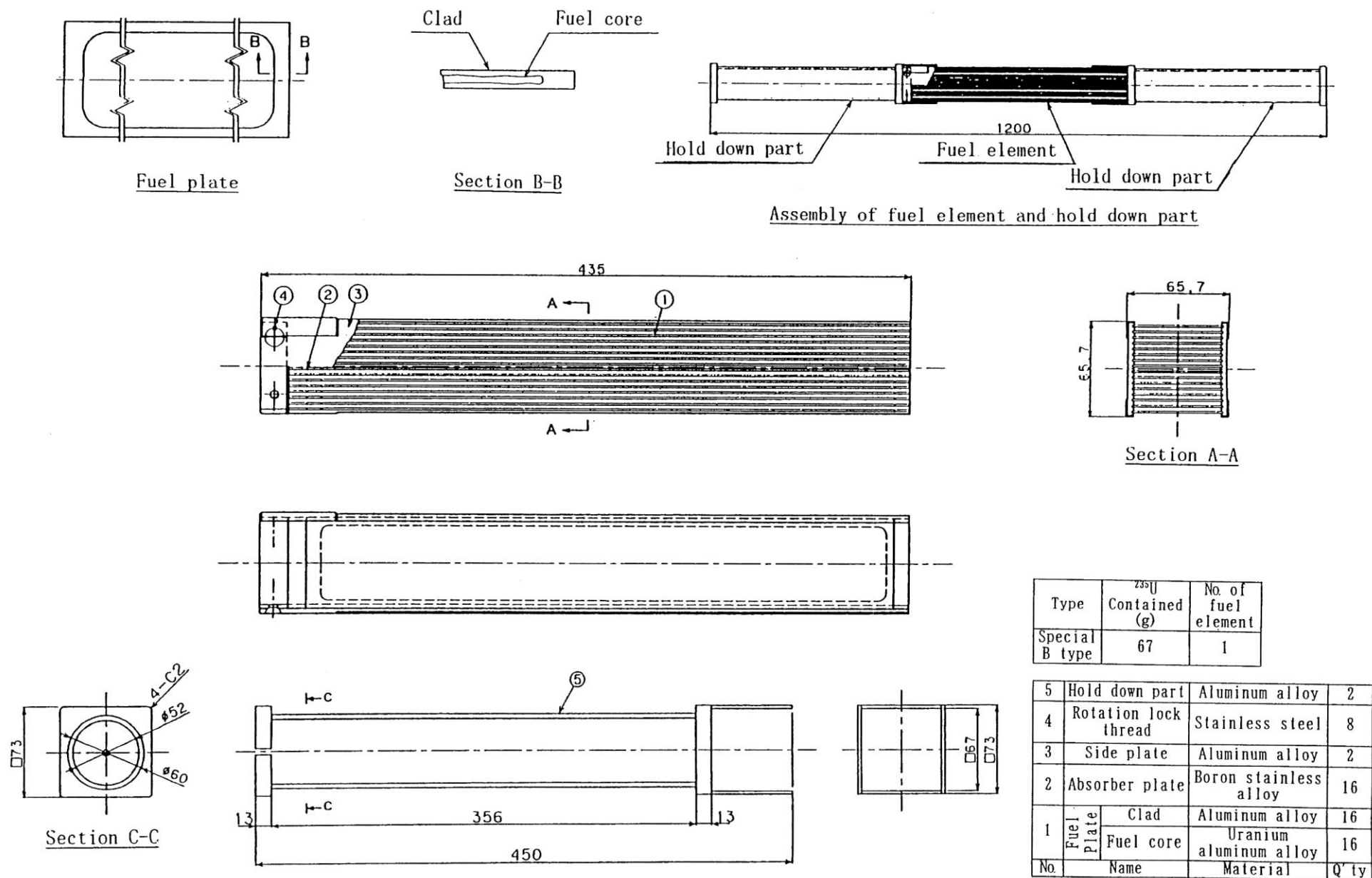


(I)-Fig.D.11 JMTRC standard fuel element (A type, B type, C type)

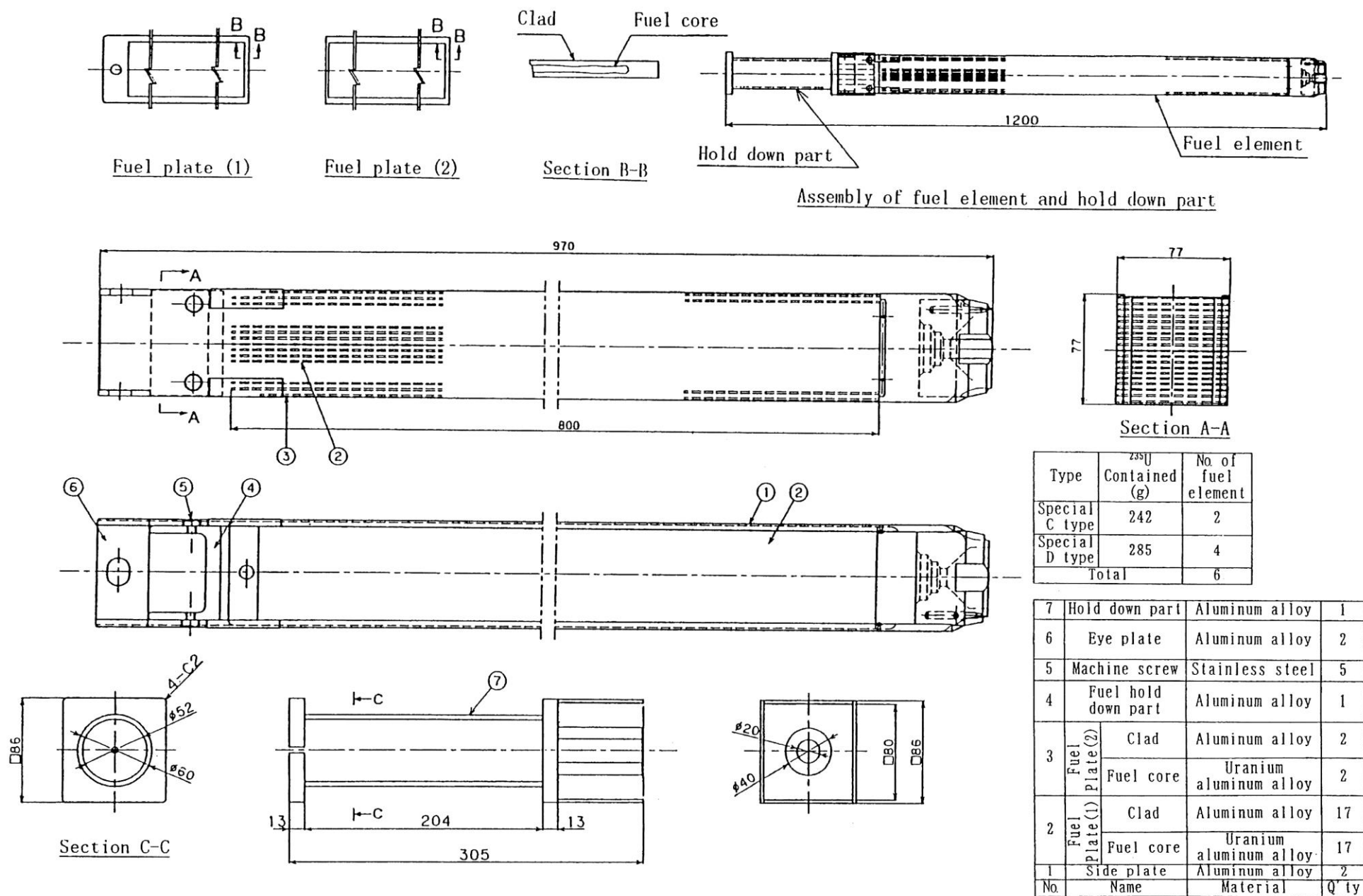
(I)-Fig.D.12 JMTRC standard fuel element (pin fix type) (C type)



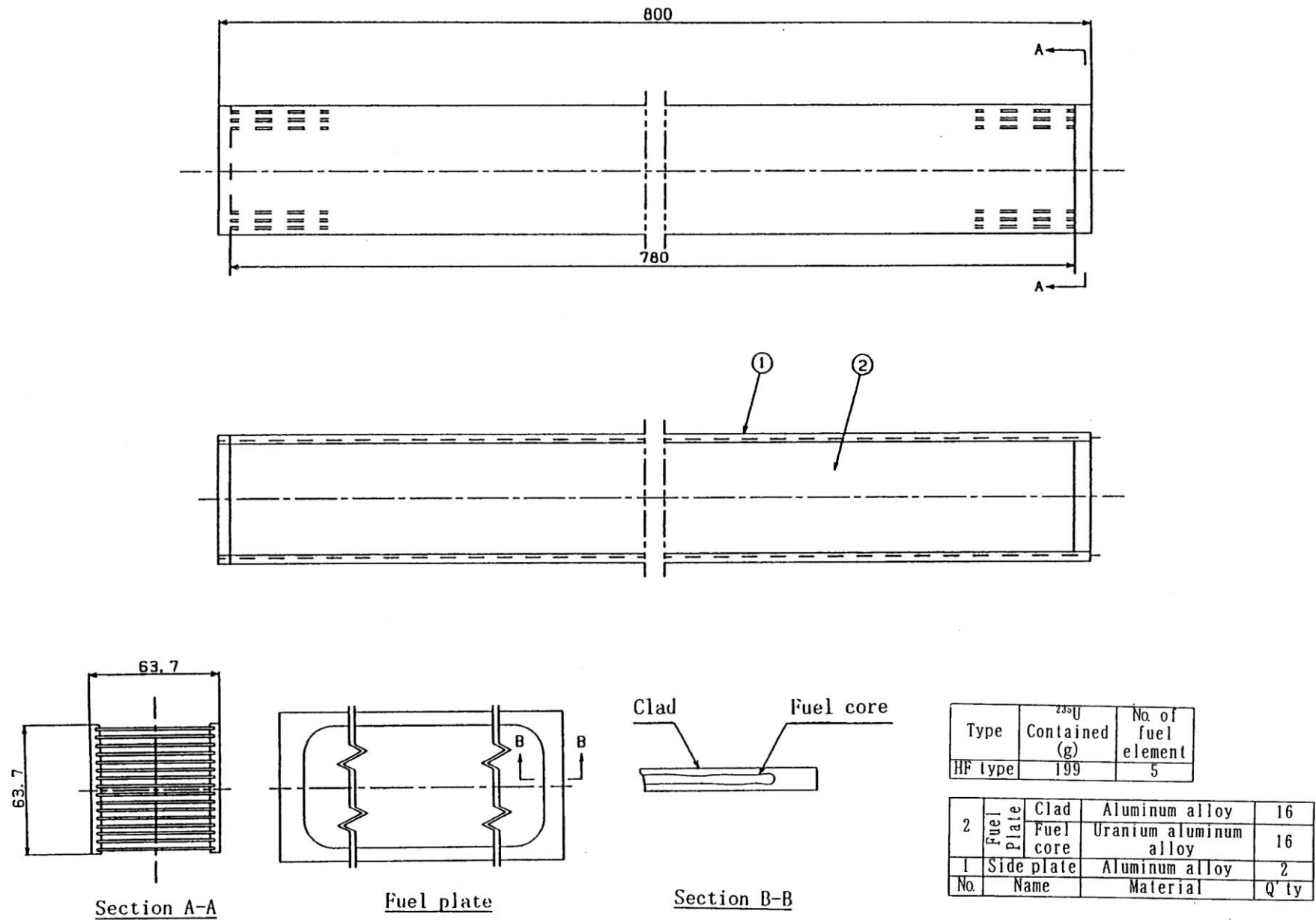
(I)-Fig.D.13 JMTRC special fuel element (special A type)



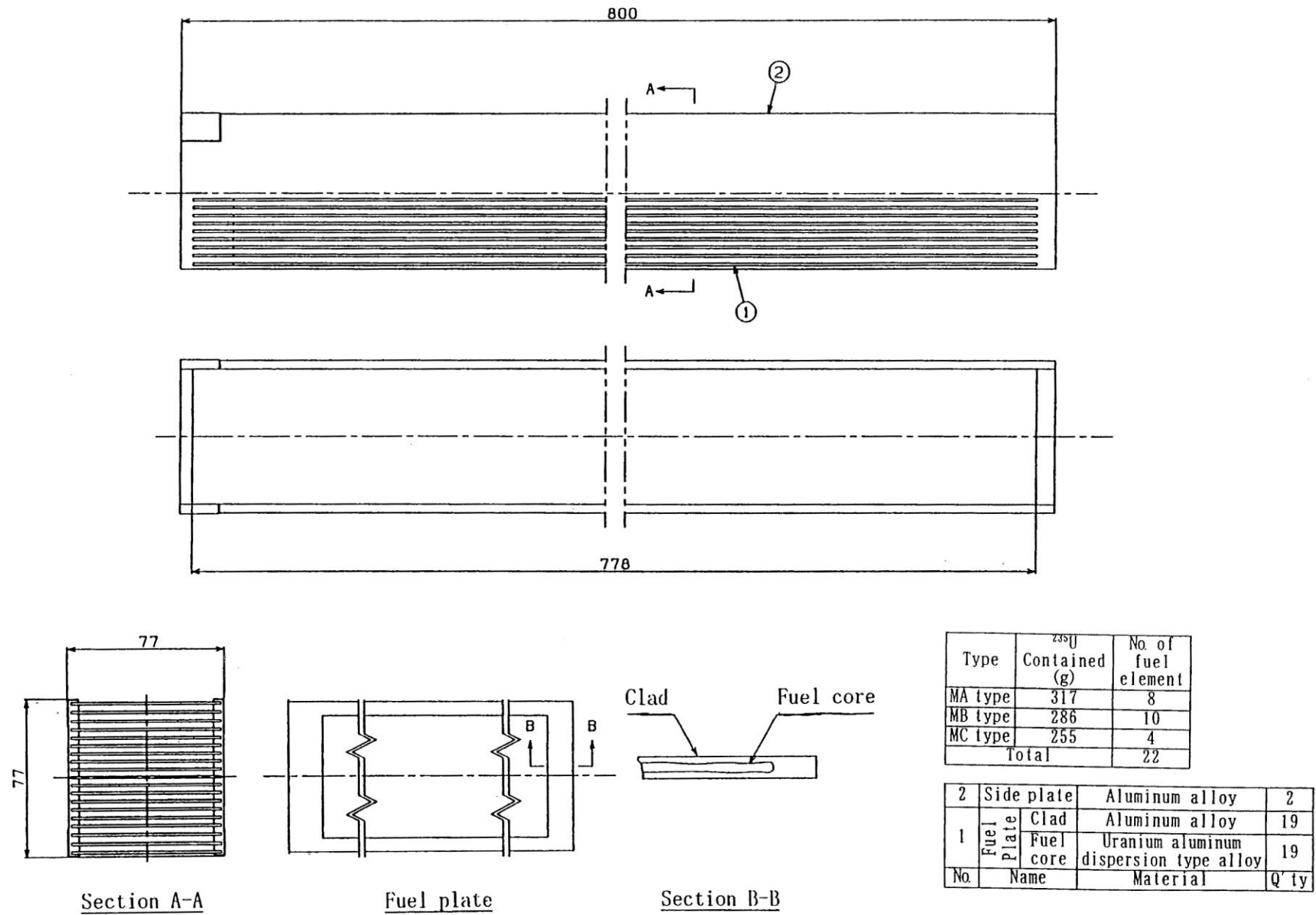
(I)-Fig.D.14 JMTRC special fuel element (special B type)



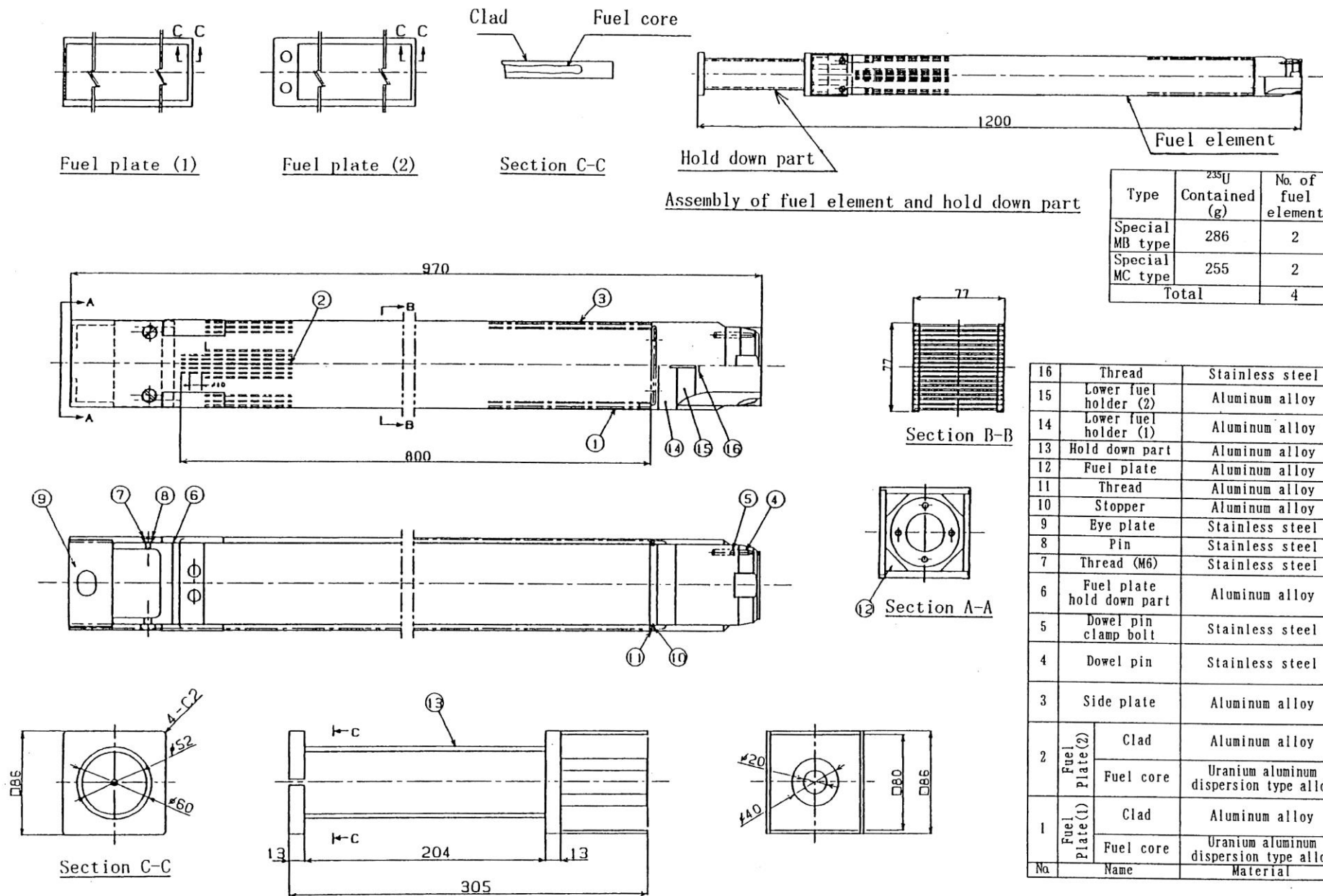
(I)-Fig.D.15 JMTRC special fuel element (special C type, special D type)



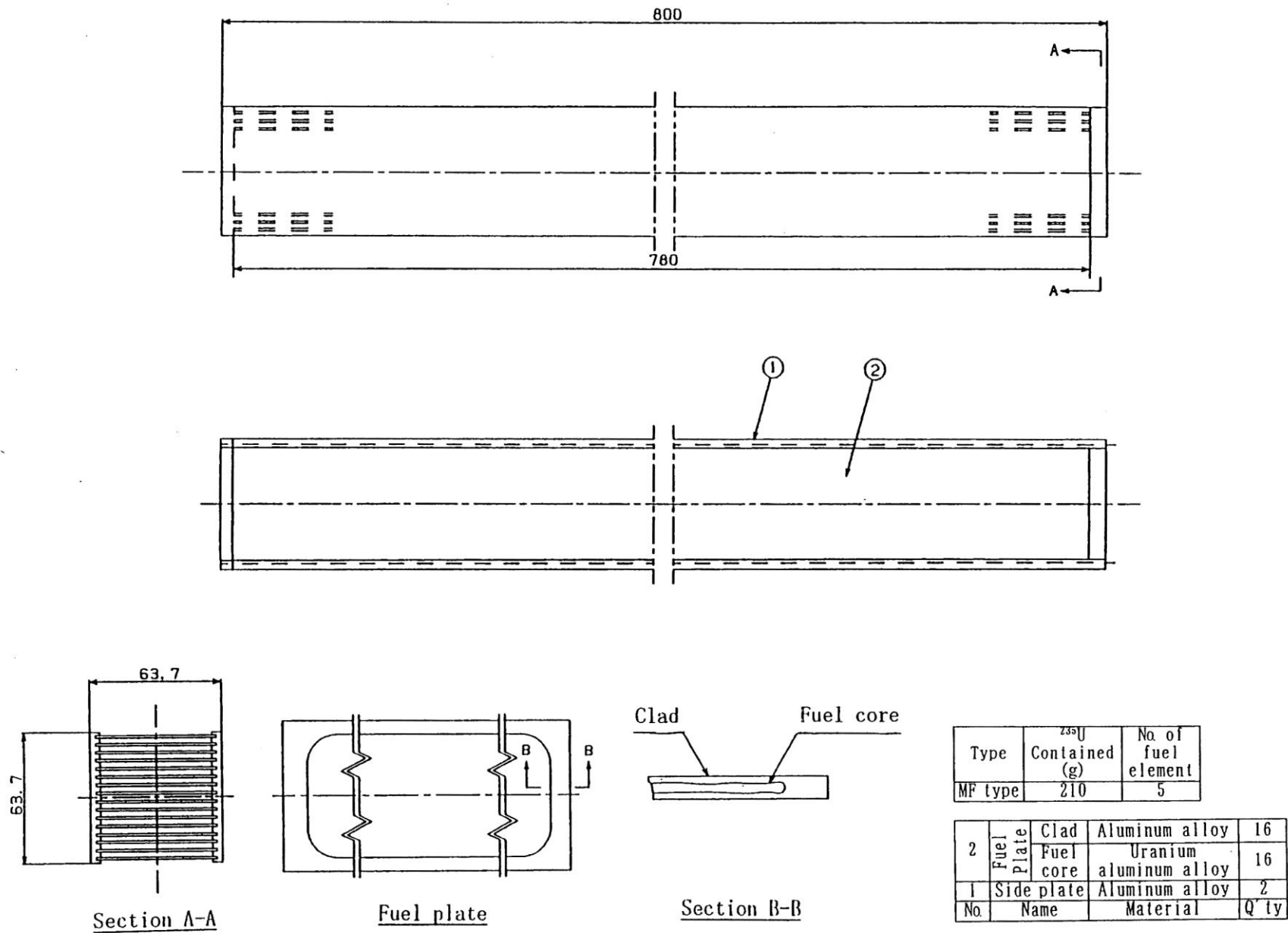
(I)-Fig.D.16 JMTRC fuel follower (HF type)



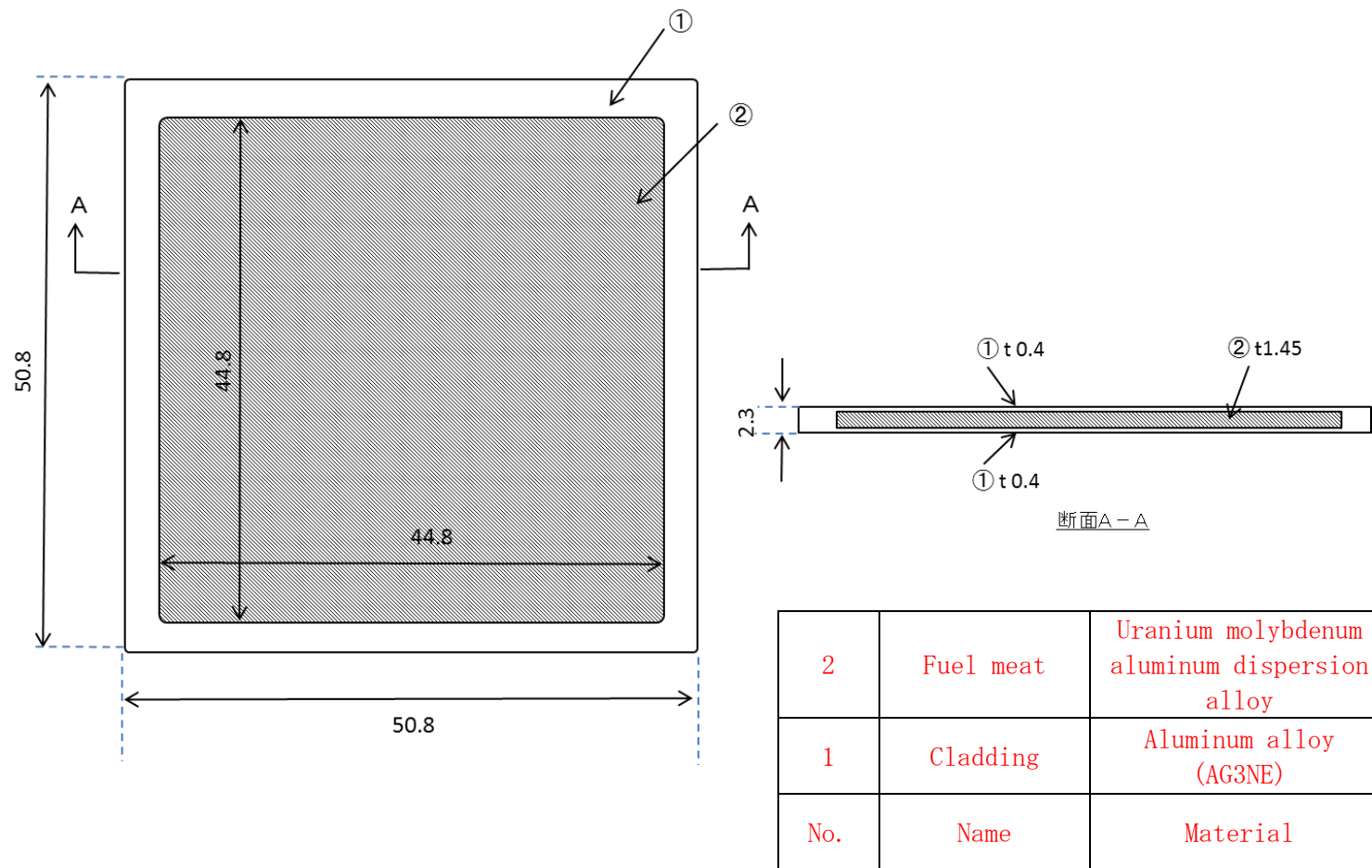
(I)-Fig.D.17 JMTRC standard fuel element (MA, MB, MC type)



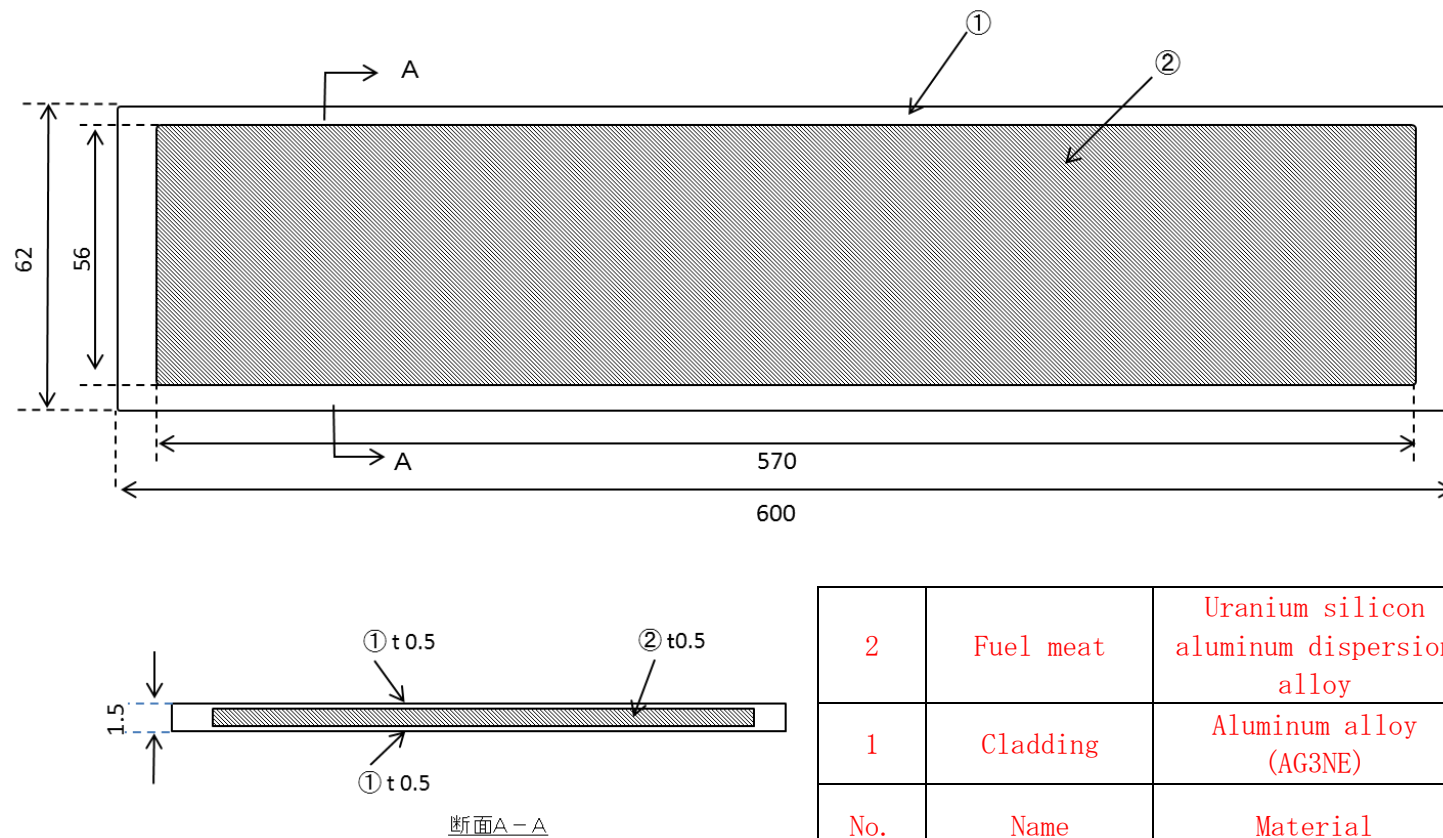
(I)-Fig.D.18 JMTRC special fuel element (special MB type, special MC type)



(I)-Fig.D.19 JMTRC fuel follower (MF type)



(I)-Fig.D.20 KUCA Coupon type fuel



(I)-Fig.D.21 KUCA flat type fuel

(II) Safety analysis of nuclear fuel package

(II) Safety analysis of nuclear fuel packages

The safety analysis for this transported article will be conducted in order to show that the transported article complies with the technical standards as a BU-type fissionable transported article in accordance with the “Rules on Transporting Nuclear Fuel Materials outside the Plant or Place of Business” (Prime Minister’ s Office Order No. 57 of 1978) (hereafter called the “Rules”) and the “Science and Technology Agency’ s Notice No. 5 of 1990 [Notice on the Details of Technical Standards for Transport of Nuclear Fuel Materials Etc. Outside Plants]” (hereafter called the “Notice”).

The safety analysis on the present package is performed to demonstrate compliance of the package with the technical standards in accordance with the following Regulations:

1. Structural analysis

In the structural analysis, besides the confirmation of the fact that any particular anomalies such as cracks, fissures etc. Would not be produced on the packages during the normal transportation, verification shall be conducted of the integrity of containment devices, which is to be the prerequisite for containment analysis, both under normal and accident test conditions.

And also to obtain the conditions for evaluation of the thermal and shielding analysis, the features and integrity of the packages under the normal and accident test conditions were evaluated. Further considering the fact that this packages are the particular BU type fissile packages, the status and integrity of packages under the normal and accident test conditions regarding the fissile packages, were evaluated in order to verify the subcritical assurance.

2. Thermal analysis

In the thermal analysis, considering the results of structural analysis above

mentioned, the temperature and pressure of each part of packages under the normal condition of transport and under, the normal and accident test conditions, are evaluated to provide for the conditions for evaluating the structural integrity, containment, shielding and criticality analysis. And also the compatibility of the packages was confirmed with the accessible surface temperature standards (85°C) of the packages under the normal test conditions.

3. Containment analysis

In the containment analysis, on the basis of the above-mentioned conditions 1 and 2 and also on the basis of allowable release rate of leakage tests before shipment the leak rate of radioactive materials under the normal and accident test conditions was evaluated to show that the standard values were duly satisfied.

4. Shield analysis

In the shielding analysis, considering the above-mentioned conditions 1 and 2, the dose equivalent rate at the surface of packages, or at the locations 1 meter apart from the surface of the packages during the normal condition of transport, under the normal and accident test conditions, was evaluated to show that the standard values were duly satisfied.

5. Criticality analysis

In the criticality analysis, it is indicated that no structural change or the like that may affect the criticality assessment will occur under the general test conditions for fissionable transported articles based on the result of 1 cited above, and that subcriticality will be ensured in cases of both isolated-system and arranged-system transported articles, under the general test conditions and special test conditions for transported articles during normal transport,

transported articles in an isolated system, and fissionable transported articles.

6. Evaluation of the compliance with the regulation and the notification

Based on the above-cited results and descriptions regarding the nuclear fuel packages given in chapter A, it was duly ensured that the design of this packages were compliance with the technical standards which was established by the regulation and the notification. In the following, chapter (II)-A through (II)-F will show particulars for each of analyses and evaluations.

(II) -A Structural analysis

(II)-A. Structural analysis

A.1 Structural design

A.1.1 General description

A Type B(U) packaging consists of an inner shell, an outer shell, and a fuel basket as shown in (I)-Fig.C.1.

The inner shell consists of a shell containing a fuel basket and a lid.

Fuel baskets are the rectangular type as shown in (I)-Fig.C.7. A basket for rectangular elements **or wrapped KUCA fuels** can contain up to ten elements,

After being placed in the fuel basket, the fuel elements **and wrapped KUCA fuels** are fixed by a spacer made of silicone rubber.

Inner shell combined with its lid forms containment boundary as shown in (I)-Fig.C.3 and also works as a pressure vessel against inner pressure. Inner lid attached to inner shell by inner lid bolts keep containment of its joint using double O-ring system.

Outer shell with its lid forms containment boundary as shown in (I)-Fig.C.4.

Heat insulator and shock absorber are filled between inner shell and outer shell. Outer lid attached to outer shell with outer lid bolts keep containment of its joint using Gasket.

Inner lid would never be opened by any possible contingency since it is covered by outer lid during transport. Outer lid bolt has a lock and a seal so that they would show evidence that it has not been opened.

This packaging is lifted and tied down with 4 eye-plates shown in (I)-Fig.C.5.

The package is tie_down to tie down device shown in (I)-Fig.C.2 with eye-plates during transport.

A.1.2 Design standards

The design standards for the packaging are based on the “Public Notification and Section III-Subsec, NB of ASME. Analytical standard are determined for each set of test conditions.

(1) Analytical standards

(II)-Table A.1 shows the various test conditions for the design standards corresponding to the items being analyzed. The analytical standards will be determined on the basis of the mechanical properties of the materials shown in section (II)-A.3 and the temperatures shown in section (II)-B.

The design standard value in which distortion level has no influence on the packaging's containment under accident test conditions is used for the inner lid clamping bolts, which are essential for the containment boundary. Yield stress is used as the analytical standard for the hoisting and clamping device in accordance with the “Public Notification”. Penetration resistance is chosen as the analytical standard for the collision during the penetration test.

Welding efficiency is 1.0 for welding parts inspected by radiation method and 0.45 for other welding parts.

Symbols of the design standard value in Tables are as follows;

S_m ; Design stress intensity value

S_y ; Yield point of the designh

S_u ; Design tensile strength

S_a ; Alternative peak stress

N ; Number of cycles

N_a ; Allowable number of cycles

DF ; Accumulative usage factor ($= N/N_a$)

(2) Combinations of design load

Combinations of design load are determined on conditions (structure temperature, material, safety factor, etc.) of each components shown in (II)-Table.A.2 and (II)-Table.A.3.

(3) Margin for safety

Margin of safety (MS) is obtained as follows.

$$\text{Margin for safety (MS)} = \frac{\text{The design standard value}}{\text{Analytical value}} - 1$$

According to the design standards described above, (II)-Table A.4 (1/24) ~(24/24) shows conditions of structural analysis, analytical item and method, etc.

(II)-Table A.1 Design standard for structural analysis

Pm; General primary membrane stress

Q ; Secondary stress

PL; Local primary membrane stress

F ; Peak stress

Pb; Primary bending stress

DF; Accumulative usage factor

Condition	Item	Component Position to be evaluated	Primary stress		Primary+secon -dary Stress	Primary+secon -dary+peak stress
			Pm(PL)	PL+Pb	PL+Pb+Q	PL+Pb+Q+F
Routine transport	Lifting device	Eye plate	<Sy	<Sy	—	—
	Tie-down device	Eye plate	<Sy	<Sy	—	—
	Pressure	Package	Withstanding the effect of changing ambient pressure.			
	Vibration	Package	Withstanding the effect of vibration during transport.			
Normal conditions of transport	Thermal test	Inner shell	<Sm	<1.5Sm	<3Sm	Fatigue evaluation (DF<1)
		Inner lid	<2/3Sy	<Sy	<Sy	
		Inner lid bolt				
	Water spray test	Package	Withstanding the water spray test.			
	Free drop test (1.2m height)	Inner shell	<Sm	<1.5Sm	<3Sm	—
		Fuel basket				
		Inner lid	<2/3Sy	<Sy	<Sy	—
		Inner lid bolt				
		Fuel element/plate				
	Stacking test	Inner shell	<Sm	<1.5Sm	<3Sm	—
		Inner lid	<2/3Sy	<Sy	<Sy	
	Penetrating test	Outer shell	No penetration			
Accident conditions of transport	Drop test I (9m height)	Inner shell	$<\frac{2}{3} Su$	<Su	—	—
		Fuel basket				
		Inner lid	<2/3Sy	<Sy	—	—
		Inner lid bolt				
		Fuel element/plate				
	Drop test II (1m height penetration)	Outer shell	No penetration			
		Inner shell	$<\frac{2}{3} Su$	<Su	—	—
		Inner lid	<2/3Sy	<Sy	—	
	Thermal test	Inner shell	$<\frac{2}{3} Su$	<Su	—	—
		Inner lid	<2/3Sy	<Sy	—	
		Inner lid bolt				
	Water immersion (15m depth)	Inner shell	$<\frac{2}{3} Su$	<Su	—	—
		Inner lid	<2/3Sy	<Sy	—	

Note: The same criteria for stress evaluation are used for both Type B(U) packages and fissile packages.

(II)-Table A.2 Design load, combination of load (1/2)

Requirement	Condition	Item	Component Position to be evaluated	Load				
				Mass*	Internal pressure	External pressure	Thermal expansion	Other
B(U) package	Routine transport	Lifting device	Eye plate	△	—	—	—	—
		Tie-down device	Eye plate	△	—	—	—	—
		Pressure	Package	—	○	○	—	○
		Vibration	Package	—	—	—	—	△
	Normal conditions of transport	Thermal test	Inner shell	—	△	—	—	—
			Inner lid	—	△	—	—	—
			Inner lid bolt	—	○	—	○	○
		Water spray test	Package	—	—	—	—	△
		Free Drop test (1.2m height)	Inner shell	○	○	—	—	—
			Fuel basket	△	—	—	—	—
			Inner lid	○	○	—	—	—
			Inner lid bolt	○	○	—	○	○
			Fuel element/plate	△	—	—	—	—
		Penetrating test	Outer shell	—	—	—	—	△
		Stacking test	Inner shell	○	○	—	—	—
	Accident conditions of transport	Drop test I (9m height)	Inner shell	○	○	—	—	—
			Fuel basket	△	—	—	—	—
			Inner lid	○	○	—	—	—
			Inner lid bolt	○	○	—	—	○
			Fuel element/plate	△	—	—	—	—
		Drop test II (1m height penetration)	Outer shell	△	—	—	—	—
			Inner shell	○	○	—	—	—
			Inner lid	○	○	—	—	—
		Thermal test	Inner shell	—	△	—	—	—
			Inner lid	—	△	—	—	—
			Inner lid bolt	—	○	—	—	○
		Water immersion (15m depth)	Inner shell	—	—	△	—	—
			Inner lid	—	—	△	—	—

○: Analyzed under combination of load. △: Analyzed under single load.

*: Mass does not mean weight simply but means mass (force) considering impact force such as given (mass) × (acceleration).

(II)-Table A.2 Design load, combination of load (2/2)

Requirement	Condition	Item	Component Position to be evaluated	Load				
				Mass*	Internal pressure	External pressure	Thermal expansion	Other
Fissile packages	Normal conditions of transport	Water spray test	Package	—	—	—	—	△
		Free drop test (1.2m height)	Inner shell	○	○	—	—	—
			Fuel basket	△	—	—	—	—
			Inner lid	○	○	—	—	—
			Inner lid bolt	○	○	—	○	○
			Fuel element/plate	△	—	—	—	—
		Stacking test	Inner shell	○	○	—	—	—
		Penetrating test	Outer shell	—	—	—	—	△
	Accident conditions of transport	Drop test I (9m height)	Inner shell	○	○	—	—	—
			Fuel basket	△	—	—	—	—
			Inner lid	○	○	—	—	—
			Inner lid bolt	○	○	—	—	○
			Fuel element/plate	△	—	—	—	—
		Drop test II (1m height penetration)	Outer shell	△	—	—	—	—
			Inner shell	○	○	—	—	—
			Inner lid	○	○	—	—	—
		Thermal test	Inner shell	—	△	—	—	—
			Inner lid	—	△	—	—	—
			Inner lid bolt	—	○	—	—	○
		Water immersion (0.9m depth)	Inner shell	—	—	△	—	—
			Inner lid	—	—	△	—	—

○: Analyzed under combination of load. △: Analyzed under single load.

*: Mass does not mean weight simply but means mass (force) considering impact force such as given (mass) × (acceleration).

(II)-Table A.3 Load conditions (1/2)

Requirement	Condition	Item	Component Position to be evaluated	Load				
				Mass*	Internal pressure	External pressure	Thermal expansion	Other
B(U) Package	Routine transport	Lifting device	Eye plate	$\times 3$ times $=6.99 \times 10^3 \text{N}$	—	—	—	—
		Tie-down device	Eye plate	$\times 2$ [g] (up, down, front, back) $\times 1$ [g] (Left, right)	—	—	—	—
		Pressure	Package	—	$9.81 \times 10^{-2} \text{MPa}$	60kPa	—	Initial clamping force $5.89 \times 10^4 \text{N}$
		Vibration	Package	—	—	—	—	—
	Normal conditions of transport	Thermal test	Inner shell	—	$9.81 \times 10^{-2} \text{MPa}$	—	—	—
			Inner lid	—	$9.81 \times 10^{-2} \text{MPa}$	—	—	—
			Inner lid bolt	—	$9.81 \times 10^{-2} \text{MPa}$	—	75(°C)	Initial clamping force $5.89 \times 10^4 \text{N}$
		Water spray test	Package	—	—	—	—	—
		Free drop test (1.2m height)	Inner shell	\times Acceleration	$9.81 \times 10^{-2} \text{MPa}$	—	—	—
			Fuel basket	$=254.1$ [g]	—	—	—	—
			Inner lid	(for horizontal drop)	$9.81 \times 10^{-2} \text{MPa}$	—	—	—
			Inner lid bolt	$=250.6$ [g] (for vertical drop)	$9.81 \times 10^{-2} \text{MPa}$	—	75(°C)	Initial clamping force $5.89 \times 10^4 \text{N}$
				$=90.8$ [g] (for corner drop)	—	—	—	—
		Stacking test	Inner shell	$\times 5$ times+Self weight	$9.81 \times 10^{-2} \text{MPa}$	—	—	—
		Penetrating test	Outer shell	—	—	—	—	6kg Bar drop
	Accident conditions of transport	Drop test I (9m height)	Inner shell	\times Acceleration	$9.81 \times 10^{-2} \text{MPa}$	—	—	—
			Fuel basket	$=367.0$ [g]	—	—	—	—
			Inner lid	(for horizontal drop)	$9.81 \times 10^{-2} \text{MPa}$	—	—	—
			Inner lid bolt	$=388.4$ [g] (for vertical drop)	$9.81 \times 10^{-2} \text{MPa}$	—	—	Initial clamping force $5.89 \times 10^4 \text{N}$
				$=310.9$ [g] (for corner drop)	—	—	—	—
		Drop test II (1m height penetration)	Outer shell	Self weight $\times 1\text{m}$ drop on mild steel bar	—	—	—	—
			Inner shell	\times Acceleration	$9.81 \times 10^{-2} \text{MPa}$	—	—	—
			Inner lid	$=72.1\text{g}$ (Horizontal) $=147.1$ [g] (Vertical)	$9.81 \times 10^{-2} \text{MPa}$	—	—	—
		Thermal test	Inner shell	—	$9.81 \times 10^{-2} \text{MPa}$	—	—	—
			Inner lid	—	$9.81 \times 10^{-2} \text{MPa}$	—	—	—
			Inner lid bolt	—	$9.81 \times 10^{-2} \text{MPa}$	—	—	Initial clamping force $5.89 \times 10^4 \text{N}$
		Water immersion (15m depth)	Inner shell	—	—	147kPa	—	—
			Inner lid	—	—	147kPa	—	—

* : Mass does not mean weight simply but means mass (force) considering impact force such as given (mass) \times (acceleration).

(II)-Table A.3 Load conditions (2/2)

Requirement	Condition	Item	Component	Load				
			Position to be evaluated	Mass*	Internal pressure	External pressure	Thermal expansion	Other
Fissile package	Normal conditions of transport	Water spray test	Package	—	—	—	—	Water spray
		Free drop test (1.2m height)	Inner shell	×Acceleration	9.81×10^{-2} MPa	—	—	—
			Fuel basket	=254.1[g]	—	—	—	—
			Inner lid	(for horizontal drop)	9.81×10^{-2} MPa	—	—	—
			Inner lid bolt	=250.6[g] (for vertical drop)	9.81×10^{-2} MPa	—	75(°C)	Initial clamping force 5.89×10^4 N
				=90.8[g] (for corner drop)				
		Stacking test	Inner shell	×5 times+Self weight	9.81×10^{-2} MPa	—	—	—
		Penetrating test	Outer shell	—	—	—	—	6kg bar drop
	Accident conditions of transport	Drop test I (9m height)	Inner shell	×Acceleration =379.0[g] (for horizontal drop)	9.81×10^{-2} MPa	—	—	—
			Fuel basket		—	—	—	—
			Inner lid		9.81×10^{-2} MPa	—	—	—
			Inner lid bolt	=446.2[g] (for vertical drop)	9.81×10^{-2} MPa	—	—	Initial clamping force 5.89×10^4 N
				=332.3[g] (for corner drop)				
		Drop test II (1m height penetration)	Outer shell	Self weight 1m drop on mild steel bar	—	—	—	—
			Inner shell	×Acceleration =72.1g(Horizontal) =147.0[g](Vertical)	9.81×10^{-2} MPa	—	—	—
			Inner lid		9.81×10^{-2} MPa	—	—	—
		Thermal test	Inner shell	—	9.81×10^{-2} MPa	—	—	—
			Inner lid	—	9.81×10^{-2} MPa	—	—	—
			Inner lid bolt	—	9.81×10^{-2} MPa	—	—	Initial clamping force 5.89×10^4 N
		Water immersion (0.9m depth)	Inner shell	—	—	9 kPa	—	—
			Inner lid	—	—	9 kPa	—	—

* : Mass does not mean weight simply but means mass (force) considering impact force such as given (mass) × (acceleration).

(II)-Table A.4 Design conditions, analytical methods of structural analysis (1/24)

Symbols:

σ : Principal stress τ_t : Torsional stress
 σ_b : Bending stress F : Load
 σ_c : Compressive stress P : Pressure
 τ : Shear stress A : Cross section

Requirement	Condition	Item	Design condition						Analytical methods		Remark
			Reference figure	Material	Temp.	Design load			Applied formula or element	Standard	
						Type	Loading factor	Element			
B(U) package	Routine transport	1. <u>Chemical and galvanic reaction</u>						Activation difference of electric position			
		(1) Chemical reaction	—	—	—	Corrosion	—		no chemical reaction	Nil	
		(2) Galvanic reaction	—	—	—	Corrosion	—		no galvanic reaction	Nil	
		2. <u>Strength at low temperature</u>									
		(1) Body	—	SUS304	−40℃	Material	1	Degradation	Allowable lowest temperature	No brittle fracture −40℃	
		(2) Bolt	—	SUS630	−40℃	Material	1	Degradation	Allowable lowest temperature		
		(3) O-ring	—	Silicon-rubber	−40℃	Material	1	Degradation	Allowable lowest temperature		
		3. <u>Containment system</u>									
		(1) Inner lid	(I)-Fig. C. 3	SUS630	75℃	Opening due to contingency	—	Possibility of contingency	—	Nil	
		4. <u>Lifting device</u>							M:Bending moment t:Plate thickness b:Width of eye plate		
		(1) Eye plate	(II)-Fig. A. 9	SUS304	75℃	Mass of package	3	Bending stress	$\sigma_b = \frac{6M}{tb^2}$	Sy	
							3	Shear stress	$\tau = \frac{F}{A}$	0.6Sy	
								Combined stress	$\sigma = \sqrt{\sigma_b^2 + 4\tau^2}$	S	
		5. <u>Tie-down device</u>									
		(1) Eye plate	(II)-Fig. A. 11	SUS304	75℃	Mass of package	2	Bending stress	$\sigma_b = \frac{6M}{tb^2}$	Sy	
			(II)-Fig. A. 12				2	Shear stress	$\tau = \frac{F}{A}$	0.6Sy	
								Combined stress	$\sigma = \sqrt{\sigma_b^2 + 4\tau^2}$	S	

Requirement	Condition	Item	Design condition						Analytical methods		Remark							
			Reference figure	Material	Temp.	Design load			Applied formula or element	Standard								
						Type	Loading factor	Element										
B(U) package	Routine transport	<u>6. Pressure</u>																
		(1) Frame of Inner shell	—	SUS304	75℃	Reduction of ambient pressure 60kPa	1	Combined stress	$\sigma_{\theta} = \frac{P \cdot Dm}{2t}$ $\sigma_z = \frac{P \cdot Dm}{4t}$ $\sigma_r = -\frac{P}{2}$	Formula for thin cylinder	Note 1	Note 1: Design standard of each stress component is determined using Sm.						
		(2) Inner bottom plate	—	SUS304	75℃		1	Combined stress	$\sigma_{\theta} = \pm 0.225 \frac{P \cdot a^2}{h^2}$ $\sigma_r = \pm 0.75 \frac{P \cdot a^2}{h^2}$ $\sigma_z = -P$				Formula for fixed disc	Note 2: Analysis standard of each stress component is determined using Sy.				
		(3) Inner shell lid	—	SUS630	75℃		1	Combined stress	$\sigma_{\theta} = \sigma_r = \mp 1.24 \frac{P \cdot a^2}{h^2}$ $\sigma_z = -P$						Formula for simply supported disc	Note 2: Initial margin of tightening is about 1.1mm.		
		(4) Inner shell lid bolt	—	SUS630	75℃		Initial bolt load	1	Tensile stress								$\sigma_t = \frac{F}{Ar}$	Note 3
					Internal pressure		1	Tensile stress	$\sigma_t = \frac{F}{n \cdot Ar}$									
		(5) Displacement of inner O-ring part of inner shell lid	—	SUS630	75℃	Internal pressure	1	Displacement	$\omega = \frac{P \cdot a^4}{64}$ $\times \left(1 - \frac{r^2}{a^2}\right)$ $\times \left(\frac{5+\nu}{1+\nu} - \frac{r^2}{a^2}\right)$	Formula for displacement of O-ring part								
		<u>7. Vibration</u>																
		(1) Package	(II)-Fig. A. 14	SUS304	75℃	Vibration	1	Resonance	$f_u = \sqrt{\frac{1}{2\pi}} \cdot \sqrt{\frac{k}{m}}$		No resonance							
		(2) Fuel basket							f_u :characteristic frequency									

(II)-Table A.4 Design conditions, analytical methods of structural analysis (3/24)

Symbols:

σ : Principal stress τ_t : Torsional stress
 σ_b : Bending stress F : Load
 σ_c : Compressive stress P : Pressure
 τ : Shear stress A : Cross section

Requirement	Condition	Item	Design condition						Analytical methods		Remark
			Reference figure	Material	Temp.	Design load			Applied formula or element	Standard	
						Type	Loading factor	Element			
B(U) package	Normal test conditions	<u>1. Thermal condition</u>									
		1.1 Thermal expansion									
		(1) Gap between basket and inner shell	(Ⅱ)-Fig. A. 15	SUS304	approx. 62/63℃	Thermal expansion	1	Compression	Presense of gap between inner shell and basket.	Free	—
		1.2 Stress Calculation									
		(1) Frame of Inner shell	(Ⅱ)-Fig. A. 16 (Ⅱ)-Fig. A. 17	SUS304	75℃	Internal pressure	1	Combined Stress	Formula for thin cylinder	} Note 1	Note 1: Design standard of each stress component is determined using Sm.
		(2) Inner bottom plate	(Ⅱ)-Fig. A. 18	SUS304	75℃	Internal pressure	1	Combined Stress	Formula for fixed disc		
		(3) Inner shell lid	(Ⅱ)-Fig. A. 19	SUS630	75℃	Internal pressure	1	Combined Stress	Formula for simply supported disc	} Note 2	Note 2: Analysis standard of each stress component is determined using Sy.
		(4) Inner shell lid bolt	(Ⅱ)-Fig. A. 21	SUS630	75℃	Initial bolt load Internal pressure Thermal expansion	1	Tensile stress $\sigma_t = \frac{F}{A_i}$ Tensile stress $\sigma_t = \frac{F}{n \cdot A_i}$ Tensile stress Negrigible			
		(5) Displacement of 0-ring part of inner lid	(Ⅱ)-Fig. A. 20	SUS630	75℃	Internal pressure	1	Displacement	Formula for displacement of 0-ring part		
		<u>2. Water spray test</u>					Water spray	1	Absorption Water-repellent	Absorption Water-repellent	Nil Good

(II)-Table A.4 Design conditions, analytical methods of structural analysis (4/24)

Symbols:

σ : Principal stress τ_t : Torsional stress
 σ_b : Bending stress F : Load
 σ_c : Compressive stress P : Pressure
 τ : Shear stress A : Cross section

Requirement	Condition	Item	Design condition						Analytical methods		Remark
			Reference figure	Material	Temp.	Design load			Applied formula or element	Standard	
						Type	Loading factor	Element			
B(U) package	Normal test conditions	3. Free drop									
		3.1 Horizontal drop									
		(1) Deformation of shock absorber	(Ⅱ)-Fig. A. 35 (Ⅱ)-Fig. A. 36	—	—	Horizontal drop from 1.2m height	1	Deformation	$\delta = \delta_0 - \delta_H$ δ_0 : Minimum thickness before drop δ_H : Deformation δ : Thickness after drop	Note 1	Note 1: Effect of deformation will be judged in thermal test.
		(2) Frame of Inner shell	(Ⅱ)-Fig. A. 37	SUS304	75℃	ditto	1	Bending stress	$\sigma_b = \frac{M}{Z}$		
		(3) Inner bottom plate	(Ⅱ)-Fig. A. 38	SUS304	75℃	ditto	1	Shear stress	$\tau = \frac{F}{A}$		
		(4) Upper part of inner shell (Inner lid)	(Ⅱ)-Fig. A. 39	SUS630	75℃	ditto	1	Shear stress	$\tau = \frac{F}{A}$	Note 2	Note 2: Analytical standard of each stress component is determined using Sm.
		(5) Inner shell lid bolt	(Ⅱ)-Fig. A. 40	SUS630	75℃	ditto	1	Bending stress	$\sigma_b = \frac{M \cdot L_{max}}{I}$		
		(6) Fuel basket	(Ⅱ)-Fig. A. 41	SUS304	75℃	ditto	1	Bending stress	$\sigma_b = \frac{M}{Z}$		
		(7) Fuel element/plate	(Ⅱ)-Fig. A. 42~44	AG3NE	75℃	ditto	1	Bending stress	$\sigma_b = \frac{M}{Z}$	Note 3	Note 3: Analysis standard of each stress component is determined using Sy.
					1	Compression stress	$\sigma_c = \frac{W}{a(h_2 - h_1)}$				
					1	Buckling stress	$\sigma_y = \sigma_{cr} (1 + \frac{e}{r} \sec \frac{L}{2K} \sqrt{\frac{\sigma_{cr}}{E}})$ σ_y : Yield stress σ_{cr} : buckling stress E : modulus of direct elasticity K : radius-of-gyration of area L : length r : section modulus/cross section e : eccentricity	Note 4	Note 4: Analysis standard is Sy.		
		(8) Fuel element hold down part	(Ⅱ)-Fig. A. 45	A6061P	75℃	ditto	1	Bending stress	$\sigma_b = \frac{M}{Z}$	Note 5	Note 5: Analysis standard of each stress component is determined using Sy.

Note: Bolt stress due to internal pressure and initial bolt load is obtained from the design condition and formula described in “1.2 Stress calculation”.

(II)-Table A.4 Design conditions, analytical methods of structural analysis (5/24)

Symbols:

σ : Principal stress τ_t : Torsional stress
 σ_b : Bending stress F : Load
 σ_c : Compressive stress P : Pressure
 τ : Shear stress A : Cross section

Requirement	Condition	Item	Design condition						Analytical methods		Remark	
			Reference figure	Material	Temp.	Design load			Applied formula or element	Standard		
						Type	Loading factor	Element				
B(U) package	Normal test conditions	3.2 Vertical drop (Bottom side)	(Ⅱ)-Fig. A. 46									Note 1: Effect of deformation will be judged in thermal test.
		(1) Deformation of shock absorber	(Ⅱ)-Fig. A. 47	—	—	Vertical drop (Bottom side) from 1.2m height	1	Deformation	$\delta = \delta_0 - \delta_v$ δ_0 : Minimum thickness before drop δ_v : Deformation δ : Thickness after drop	Note 1		
		(2) Frame of Inner shell	(Ⅱ)-Fig. A. 48	SUS304	75℃	ditto	1	Compression stress	$\sigma_c = \frac{F}{A}$	Note 2	Note 2: Analytical standard of each stress component is determined using Sm.	
		(3) Inner bottom plate	(Ⅱ)-Fig. A. 49	SUS304	75℃	ditto	1	Combined stress	Formula for fixed disc			
		(4) Inner shell lid	(Ⅱ)-Fig. A. 50	SUS630	75℃	ditto	1	Combined stress	Formula for simply supported disc	Note 3	Note 3: Analysis standard of each stress component is determined using Sy.	
		(5) Inner shell lid bolt	—	SUS630	75℃	ditto	1	—	—			
		(6) Fuel Element/plate	(Ⅱ)-Fig. A. 51~53	AG3NE	75℃	ditto	1	Shear stress	$\tau = \frac{F}{2(h_2 - h_1) b}$	Note 3		
							1	Tensile stress	$\sigma_t = \frac{W_o}{A}$			
							1	Compression stress	$\sigma_c = \frac{W}{A}$			
		(7) Fuel element hold down part	(Ⅱ)-Fig. A. 54	A6061P	75℃	ditto	1	Compression stress	$\sigma_c = \frac{W}{A}$			

(II)-Table A.4 Design conditions, analytical methods of structural analysis (6/24)

Symbols:

σ : Principal stress τ_t : Torsional stress
 σ_b : Bending stress F : Load
 σ_c : Compressive stress P : Pressure
 τ : Shear stress A : Cross section

Requirement	Condition	Item	Design condition						Analytical methods		Remark	
			Reference figure	Material	Temp.	Design load			Applied formula or element	Standard		
						Type	Loading factor	Element				
B(U) package	Normal test condition	3.3 Vertical drop (Lid side)	(Ⅱ)-Fig. A. 55									Note 1: Effect of deformation will be judged in thermal test. Note 2: Analytical standard of each stress component is determined using Sm. Note 3: Analysis standard of each stress component is determined using Sy.
		(1) Deformation of shock absorber	(Ⅱ)-Fig. A. 56	—	—	Vertical drop (Lid side) from 1.2m height	1	Deformation	$\delta = \delta_0 - \delta_v$ δ_0 : Minimum thickness before drop δ_v : Deformation δ : Thickness after drop	Note 1		
		(2) Frame of Inner shell	(Ⅱ)-Fig. A. 57	SUS304	75℃	ditto	1	Compression stress	$\sigma_c = \frac{F}{A}$	Note 2		
		(3) Inner bottom plate	(Ⅱ)-Fig. A. 58	SUS304	75℃	ditto	1	Combined stress	Formula for fixed disc			
		(4) Inner shell lid	(Ⅱ)-Fig. A. 59	SUS630	75℃	ditto	1	Combined stress	Formula for simply supported disc			
		(5) Inner shell lid bolt		SUS630	75℃	ditto	1	Tensile stress	$\sigma_t = \frac{R}{n \cdot A_i}$	Note 3		
		(6) Fuel Element/plate	(Ⅱ)-Fig. A. 60～62	AG3NE	75℃	ditto	1	Shear stress	$\tau = \frac{F}{2(h_2 - h_1) b}$			
							1	Tensile stress	$\sigma_t = \frac{W_o}{A}$			
							1	Compression stress	$\sigma_c = \frac{W}{A}$	Note 3		
		(7) Fuel element hold down part	(Ⅱ)-Fig. A. 63	A6061P	75℃	ditto	1	Compression stress	$\sigma_c = \frac{W}{A}$			
		3.4 Corner drop	(Ⅱ)-Fig. A. 63			Corner drop from 1.2m drop		Analyzed for each item of para. 5.1～5.3 above from horizontal and vertical component of impact				
		(1) Inner shell lid bolt	(Ⅱ)-Fig. A. 64	SUS630	75℃	(Lid side)	1	Bending stress	$\sigma_{max} = \sigma_v + \sigma_H$ $\sigma_v = \frac{N_v \cdot W \cdot L_v \cdot \ell_{vMAX}}{2 \Sigma \ell^2 \cdot A_r}$ $\sigma_H = \frac{N_H \cdot W \cdot L_H \cdot \ell_{HMAX}}{2 \Sigma \ell^2 \cdot A_r}$	Note 3		
		3.5 Inclined drop	(Ⅱ)-Fig. A. 65～68	—	—	Inclined drop from 1.2m height		Analyzed for each item of para. 5.1～5.3 above from horizontal and vertical component of impact				

(II)-Table A.4 Design conditions, analytical methods of structural analysis (7/24)

Symbols;

σ : Principal stress

σ_b : Bending stress

σ_c : Compressive stress

 τ : Shear stress τ_t : Torsional stress

F : Load

P : Pressure

A : Cross section

[illegible]

(II)-Table A.4 Design conditions, analytical methods of structural analysis (8/24)

Symbols:

 σ : Principal stress τ_t : Torsional stress σ_b : Bending stress

F : Load

 σ_c : Compressive stress

P : Pressure

 τ : Shear stress

A : Cross section

Requirement	Condition	Item	Design condition						Analytical methods		Remark												
			Reference figure	Material	Temp.	Design load			Applied formula or element	Standard													
						Type	Loading factor	Element															
B(U) package	Accident test conditions	1. Drop test I	(II)-Fig. A. 75	—	—	Vertical drop (Bottom side) from 9m height	1	Deformation	$\delta = \delta_0 - \delta_v$ δ_0 : Minimum thickness before drop δ_v : Deformation δ : Thickness after drop	}	Note 1	Note 1: Effect of deformation will be judged in thermal test.											
		1.1 Vertical drop (Bottom side)																					
		(1) Deformation of shock absorber																					
		(2) Frame of Inner shell											SUS304	75℃	ditto	1	Compression stress	$\sigma_c = \frac{W}{A}$	}	Note 3	Note 2: Analytical standard of each stress component is determined using Su.		
		(3) Inner bottom plate											SUS304	75℃	ditto	1	Combined stress	Formula for fixed disc					
		(4) Inner shell lid											SUS630	75℃	ditto	1	Combined stress	Formula for simply supported disc	}	Note 2		Note 3: Analysis standard of each stress component is determined using Sy.	
		(5) Inner shell lid bolt											SUS630	75℃	ditto	1	—	—					
		(6) Fuel element/plate											AG3NE	75℃	ditto	1	Shear stress	$\tau = \frac{F}{2(h_2 - h_1) b}$	}	Note 2			
																					1		Tensile stress
																						1	
(7) Fuel element hold down part	A6061P	75℃	ditto	1	Compression stress	$\sigma_c = \frac{W}{A}$	}	Note 2															

(II)-Table A.4 Design conditions, analytical methods of structural analysis (9/24)

Symbols:

σ : Principal stress τ_t : Torsional stress
 σ_b : Bending stress F : Load
 σ_c : Compressive stress P : Pressure
 τ : Shear stress A : Cross section

Requirement	Condition	Item	Design condition						Analytical methods		Remark												
			Reference figure	Material	Temp.	Design load			Applied formula or element	Standard													
						Type	Loading factor	Element															
B(U) package	Accident test conditions	1.2 Vertical drop (Lid side)	(Ⅱ)-Fig.A. 76	—	—	Vertical drop (Lid side) from 9m height	1	Deformation	$\delta = \delta_0 - \delta_v$ δ_0 : Minimum thickness before drop δ_v : Deformation δ : Thickness after drop	}	Note 1	Note 1: Effect of deformation will be judged in thermal test.											
		(1) Deformation of shock absorber																					
		(2) Frame of Inner shell											SUS304	75℃	ditto	1	Compression stress	$\sigma_c = \frac{F}{A}$	}	Note 2	Note 2: Analytical standard of each stress component is determined using Su.		
		(3) Inner bottom plate											SUS304	75℃	ditto	1	Combined stress	Formula for fixed disc					
		(4) Inner shell lid											SUS630	75℃	ditto	1	Combined stress	Formula for simply supported disc	}	Note 3		Note 3: Analysis standard of each stress component is determined using Sy.	
		(5) Inner shell lid bolt											SUS630	75℃	ditto	1	Tensile stress	$\sigma_t = \frac{F}{n \cdot A_i}$					
		(6) Fuel element/plate											AG3NE	75℃	ditto	1	Shear stress	$\tau = \frac{F}{2(h_2 - h_1) b}$					
																	1	Tensile stress					$\sigma_t = \frac{W_o}{A}$
																	1	Compression stress					$\sigma_c = \frac{W}{A}$
		(7) Fuel element hold down part											A6061P	75℃	ditto	1	Compression stress	$\sigma_c = \frac{W}{A}$					

(II)-Table A.4 Design conditions, analytical methods of structural analysis (10/24)

Symbols:

 σ : Principal stress τ_t : Torsional stress σ_b : Bending stress

F : Load

 σ_c : Compressive stress

P : Pressure

 τ : Shear stress

A : Cross section

Requirement	Condition	Item	Design condition						Analytical methods		Remark							
			Reference figure	Material	Temp.	Design load			Applied formula or element	Standard								
						Type	Loading factor	Element										
B(U) package	Accident test conditions	1.3 Horizontal drop	(II)-Fig.A.77	—	—	Horizontal drop from 9m height	1	Deformation	$\delta = \delta_0 - \delta_H$ δ_0 : Minimum thickness before drop δ : Thickness after drop δ_H : Deformation	Note 1	Note 1: Effect of deformation will be judged in thermal test.							
		(1) Deformation of shock absorber																
		(2) Frame Of Inner shell							SUS304			75℃	ditto	1	Bending stress	$\sigma_b = \frac{M}{Z}$	Note 3	Note 2: Analytical standard of each stress component is determined using Su.
		(3) Inner bottom plate							SUS304	75℃		ditto	1	Combined stress	Formula for fixed disc			
		(4) Upper part of inner shell (Inner lid)							SUS630	75℃		ditto	1	Shear stress	$\tau = \frac{F}{A}$			
		(5) Inner shell lid bolt							SUS630	75℃		ditto	1	Bending stress	$\sigma_b = \frac{M \cdot \ell_{\max}}{I}$	Note 2	Note 3: Analytical standard of each stress component is determined using Sy.	
		(6) Fuel basket							SUS304	75℃		ditto	1	Bending stress	$\sigma_b = \frac{M}{Z}$			
		(7) Fuel element/plate							AG3NE	75℃		ditto	1	Bending stress	$\sigma_b = \frac{M}{Z}$			
												1	Compression stress	$\sigma_c = \frac{W}{a(h_2 - h_1)}$	Note 4	Note 4: Analysis standard is σ_{cr} .		
												1	Buckling stress	$\sigma_y = \sigma_{cr} (1 + \frac{e}{r} \sec \frac{L}{2K} \sqrt{\frac{\sigma_{cr}}{E}})$ σ_y : Yield stress σ_{cr} : buckling stress E : modulus of direct elasticity K : radius-of-gyration of area L : length r : section modulus/cross section e : eccentricity				
(8) Fuel element hold down part	A6061P	75℃	ditto	1	Bending stress	$\sigma_b = \frac{M}{Z}$	Note 2											

(II)-Table A.4 Design conditions, analytical methods of structural analysis (11/24)

Symbols:
 σ : Principal stress τ_t : Torsional stress
 σ_b : Bending stress F : Load
 σ_c : Compressive stress P : Pressure
 τ : Shear stress A : Cross section

Requirement	Condition	Item	Design condition						Analytical methods		Remark
			Reference figure	Material	Temp.	Design load			Applied formula or element	Standard	
						Type	Loading factor	Element			
B(U) package	Accident test conditions	1.4 Corner drop	(Ⅱ)-Fig. A. 78	SUS630	75℃	Corner drop from 9m height	1	Analyzed for each item of para. 8.1~8.3 above from horizontal and vertical component of impact	$\sigma_{\max} = \sigma_v + \sigma_H$ $\sigma_v = \frac{N_v \cdot W \cdot L_v \cdot \ell_{v\text{MAX}}}{2 \Sigma \ell^2 \cdot A_r}$ $\sigma_H = \frac{N_H \cdot W \cdot L_H \cdot \ell_{H\text{MAX}}}{2 \Sigma \ell^2 \cdot A_r}$	Note 1	Note 1: Analytical standard of each stress component is determined using Sy.
		(1) Inner lid bolt				Corner drop from 9m height (Lid side)	1	Bending stress			
		1.5 Inclined drop	(Ⅱ)-Fig. A. 79~ (Ⅱ)-Fig. A. 82			Inclined drop from 9m height	1	Analyzed for each item of para. 8.1~8.3 above from horizontal and vertical component of impact			

(II)-Table A.4 Design conditions, analytical methods of structural analysis (12/24)

Symbols:

σ : Principal stress τ_t : Torsional stress
 σ_b : Bending stress F : Load
 σ_c : Compressive stress P : Pressure
 τ : Shear stress A : Cross section

Requirement	Condition	Item	Design condition						Analytical methods		Remark	
			Reference figure	Material	Temp.	Design load			Applied formula or element	Standard		
						Type	Loading factor	Element				
B(U) package	Accident test conditions	2. Drop test II										
		2.1 Penetration	(II)-Fig. A. 83									
		(1) Outer lid	(II)-Fig. A. 84	SUS304	75℃	Drop onto a mild bar from 1m height	1	Penetration energy		No Penetration		
		(2) Outer bottom plate		SUS304	75℃	ditto	1	Penetration energy				
		(3) Frame of Outer shell		SUS304	75℃	ditto	1	Penetration energy				
			3. Thermal test									
			3.1 Thermal expansion									
			(1) Gap between inner shell and fuel basket		SUS304	500/225℃	Thermal expansion	1	Compression	Presense of gap between inner shell and basket	free	Note 1: Analytical standard of each stress component is determined using Su.
			3.2 Stress by pressure									
			(1) frame of Inner shell		SUS304	500℃	Internal pressure	1	Combined Stress	Formula for thin cylinder	} Note 1	Note 2: Analytical standard of each stress component is determined using Sy.
			(2) Inner bottom plate		SUS304	500℃	Internal pressure	1	Combined Stress	Formula for fixed disc		
			(3) Inner shell lid		SUS630	225℃	Internal pressure	1	Combined Stress	Formula for simple support disc		
			(4) Inner shell lid bolt		SUS630	225℃	Initial torque	1	Tensile stress	$\sigma_t = \frac{F}{A_i}$	} Note 2	
						225℃	Internal pressure	1	Tensile stress	$\sigma_t = \frac{F}{n \cdot A_i}$		
(5) Displacement of O-ring part of inner lid		SUS630	225℃	Internal pressure	1	Displacement	Formula for displacement of O-ring part	} Note 3	Note 3: Initial margin of tightening is about 1.1mm.			

(II)-Table A.4 Design conditions, analytical methods of structural analysis (13/24)

Symbols:
 σ : Principal stress τ_t : Torsional stress
 σ_b : Bending stress F : Load
 σ_c : Compressive stress P : Pressure
 τ : Shear stress A : Cross section

Requirement	Condition	Item	Design condition						Analytical methods		Remark								
			Reference figure	Material	Temp.	Design load			Applied formula or element	Standard									
						Type	Loading factor	Element											
B(U) package	Accident test conditions	4. <u>Water immersion test</u>	(Ⅱ)-Fig. A. 85								Note 1: Analytical standard of each stress component is determined using Su.								
		4.1 Water immersion (15m depth)																	
		(1) Frame of Inner shell										(Ⅱ)-Fig. A. 88	SUS304	—	External pressure	1	Combined Stress	Formula for thin cylinder	} Note 1
		(2) Inner bottom plate										(Ⅱ)-Fig. A. 89	SUS304	—	External pressure	1	Combined Stress	Formula for fixed disc	
		(3) Inner shell lid										(Ⅱ)-Fig. A. 90	SUS630	—	External pressure	1	Combined Stress	Formula for simply supported disc	} Note 2
		(4) Buckling of inner shell										(Ⅱ)-Fig. A. 86	SUS304	—	External pressure	1	Buckling stress	$P_e = \frac{4B \cdot t}{2D_o}$ B : Buckling factor D ₀ : Outer diameter of inner shell	} Note 1
(5) Displacement of O-ring part of inner lid	(Ⅱ)-Fig. A. 91	SUS630	—	External pressure	1	Displacement	Formula for displacement of O-ring part	} Note 3	Note 3: Initial margin of tightening is about 1.1mm.										

Symbols:

σ : Principal stress τ_t : Torsional stress
 σ_b : Bending stress F : Load
 σ_c : Compressive stress P : Pressure
 τ : Shear stress A : Cross section

(II)-Table A.4 Design conditions, analytical methods of structural analysis (14/24)

Requirement	Condition	Item	Design condition						Analytical methods		Remark
			Reference figure	Material	Temp.	Design load			Applied formula or element	Standard	
						Type	Loading factor	Element			
Fissile package	Normal test conditions	<u>1. Water spray test</u>				Water spray	1	<div><div>Absorption</div><div>Water-repellent</div></div>	Absorption Water-repellent	Nil Good	

(II)-Table A.4 Design conditions, analytical methods of structural analysis (15/24)

Symbols:

σ : Principal stress τ_t : Torsional stress
 σ_b : Bending stress F : Load
 σ_c : Compressive stress P : Pressure
 τ : Shear stress A : Cross section

Requirement	Condition	Item	Design condition						Analytical methods		Remark		
			Reference figure	Material	Temp.	Design load			Applied formula or element	Standard			
						Type	Loading factor	Element					
Fissile package	Normal test conditions	2. Free drop 2.1 Horizontal drop											
		(1) Deformation of shock absorber	(Ⅱ)-Fig. A. 95	—	—	Horizontal drop from 1.2m height	1	Deformation	$\delta = \delta_0 - \delta_H$ δ_0 : Minimum thickness before drop δ_H : Deformation δ : Thickness after drop	Note 1	Note 1: Effect of deformation will be judged in thermal test.		
		(2) Frame of Inner shell	—	SUS304	75℃	ditto	1	Bending stress	$\sigma_b = \frac{M}{Z}$			Note 2	Note 2: Analytical standard of each stress component is determined using Sm.
		(3) Inner shell bottom plate	—	SUS304	75℃	ditto	1	Shear stress	$\tau = \frac{F}{A}$				
		(4) Upper part of inner shell (Inner lid)	—	SUS630	75℃	ditto	1	Shear stress	$\tau = \frac{F}{A}$	Note 3	Note 3: Analysis standard of each stress component is determined using Sy.		
		(5) Inner shell lid bolt	—	SUS630	75℃	ditto	1	Bending stress	$\sigma_b = \frac{M \cdot L_{max}}{I}$				
		(6) Fuel basket	—	SUS304	75℃	ditto	1	Bending stress	$\sigma_b = \frac{M}{Z}$				
		(7) Fuel element/plate	—	AG3NE	75℃	ditto	1	Bending stress	$\sigma_b = \frac{M}{Z}$	Note 4	Note 4: Analysis standard is σ_{cr} .		
							1	Compression stress	$\sigma_c = \frac{W}{a(h_2 - h_1)}$				
							1	Buckling stress	$\sigma_y = \sigma_{cr} \left(1 + \frac{e}{r} \sec \frac{L}{2K} \sqrt{\frac{\sigma_{cr}}{E}} \right)$ σ_y : Yield stress σ_{cr} : buckling stress E : modulus of direct elasticity K : radius-of-gyration of area L : length r : section modulus/cross section e : eccentricity				
											Note 5	Note 5: Analysis standard of each stress component is determined using Sy.	
		(8) Fuel element hold down part	—	A6061P	75℃	ditto	1	Bending stress	$\sigma_b = \frac{M}{Z}$				

(II)-Table A.4 Design conditions, analytical methods of structural analysis (16/24)

Symbols:

σ : Principal stress τ_t : Torsional stress
 σ_b : Bending stress F : Load
 σ_c : Compressive stress P : Pressure
 τ : Shear stress A : Cross section

Requirement	Condition	Item	Design condition						Analytical methods		Remark
			Reference figure	Material	Temp.	Design load			Applied formula or element	Standard	
						Type	Loading factor	Element			
Fissile package	Normal test conditions	2.2 Vertical drop 2.2.1 Vertical drop (Bottom side)									Note 1: Effect of deformation will be judged in thermal test. Note 2: Analytical standard of each stress component is determined using Sm. Note 3: Analysis standard of each stress component is determined using Sy.
		(1) Deformation of shock absorber	(Ⅱ)-Fig. A. 96	—	—	Vertical drop (Bottom side) from 1.2m height	1	Deformation	$\delta = \delta_0 - \delta_v$ δ_0 : Minimum thickness before drop δ_v : Deformation δ : Thickness after drop	Note 1	
		(2) Frame of Inner shell	—	SUS304	75℃	ditto	1	Compression stress	$\sigma_c = \frac{F}{A}$	Note 2	
		(3) Inner shell bottom plate	—	SUS304	75℃	ditto	1	Combined stress	Formula for fixed disc		
		(4) Inner shell lid	—	SUS630	75℃	ditto	1	Combined stress	Formula for simply supported disc	Note 3	
		(5) Inner shell lid bolt	—	SUS630	75℃	ditto	1	—	—		
		(6) Fuel element/plate	—	AG3NE	75℃	ditto	1	Shear stress	$\tau = \frac{F}{2(h_2 - h_1) b}$	Note 3	
							1	Tensile stress	$\sigma_t = \frac{W_o}{A}$		
							1	Compression stress	$\sigma_c = \frac{W}{A}$		
		(7) Fuel element hold down part	—	A6061P	75℃	ditto	1	Compression stress	$\sigma_c = \frac{W}{A}$		

(II)-Table A.4 Design conditions, analytical methods of structural analysis (17/24)

Symbols:

σ : Principal stress τ_t : Torsional stress
 σ_b : Bending stress F : Load
 σ_c : Compressive stress P : Pressure
 τ : Shear stress A : Cross section

Requirement	Condition	Item	Design condition						Analytical methods		Remark
			Reference figure	Material	Temp.	Design load			Applied formula or element	Standard	
						Type	Loading factor	Element			
Fissile package	Normal test condition	2.2.2 Vertical drop (Lid side)									
		(1) Deformation of shock absorber	—	—	—	Vertical drop (Lid side) from 1.2m height	1	Deformation	$\delta = \delta_0 - \delta_v$ δ_0 : Minimum thickness before drop δ_v : Deformation δ : Thickness after drop	Note 1	Note 1: Effect of deformation will be judged in thermal test.
		(2) Frame of Inner shell	—	SUS304	75℃	ditto	1	Compression stress	$\sigma_c = \frac{F}{A}$	Note 2	
		(3) Inner shell bottom plate	—	SUS304	75℃	ditto	1	Combined stress	Formula for fixed disc		
		(4) Inner shell lid	—	SUS630	75℃	ditto	1	Combined stress	Formula for simply supported disc		Note 3: Analysis standard of each stress component is determined using Sy.
		(5) Inner shell lid bolt	—	SUS630	75℃	ditto	1	Tensile stress	$\sigma_t = \frac{R}{n \cdot A_r}$	Note 3	
		(6) Fuel Element/plate	—	AG3NE	75℃	ditto	1	Shear stress	$\tau = \frac{F}{2(h_2 - h_1) b}$		Note 3
							1	Tensile stress	$\sigma_t = \frac{W_o}{A}$		
							1	Compression stress	$\sigma_c = \frac{W}{A}$		
		(7) Fuel element hold down part	—	A6061P	75℃	ditto	1	Compression stress	$\sigma_c = \frac{W}{A}$		
	2.3 Corner drop	—	—	—	Corner drop from 1.2m drop			Analyzed for each item of para. 3.1~3.3 above from horizontal and vertical component of impact			
	(1) Inner lid bolt	—	SUS630	75℃	Corner drop from 1.2m drop (Lid side)	1	Bending stress	$\sigma_{max} = \sigma_v + \sigma_H$ $\sigma_v = \frac{N_v \cdot W \cdot L_v \cdot \ell_{vMAX}}{2\Sigma \ell^2 \cdot A_r}$ $\sigma_H = \frac{N_H \cdot W \cdot L_H \cdot \ell_{HMAX}}{2\Sigma \ell^2 \cdot A_r}$	Note 3		

(II)-Table A.4 Design conditions, analytical methods of structural analysis (18/24)

Symbols:
 σ : Principal stress τ_t : Torsional stress
 σ_b : Bending stress F : Load
 σ_c : Compressive stress P : Pressure
 τ : Shear stress A : Cross section

Requirement	Condition	Item	Design condition						Analytical methods		Remark
			Reference figure	Material	Temp.	Design load			Applied formula or element	Standard	
						Type	Loading factor	Element			
Fissile package	Normal test condition	3. <u>Stacking test</u>									Note 1: Analysis standard of each stress component is determined using Su.
		(1) Frame of Inner shell	—	SUS304	75℃	Mass of package	×5+Self weight	Bending stress	$\sigma_z = \frac{F+m \cdot g}{A}$	}Note 1	
		(2) Inner shell lid	—	SUS630	75℃	Mass of package	×5+Self weight	Combined stress	Formula for simply supported disc	}Note 2	Note 2: Analysis standard of each stress component is determined using Sy.
		4. <u>Penetration test</u>									
		(1) Outer shell	—	SUS304	75℃	Impact on mild steel bar	1	Absorbed energy	$E_2 = \frac{1}{2} \tau_{Cr} \cdot \pi \cdot d \cdot t^2$ (τ_{Cr} : Shear strength)=0.6Su	No penetration	

(II)-Table A.4 Design conditions, analytical methods of structural analysis (19/24)

Symbols:

σ : Principal stress τ_t : Torsional stress
 σ_b : Bending stress F : Load
 σ_c : Compressive stress P : Pressure
 τ : Shear stress A : Cross section

Requirement	Condition	Item	Design condition						Analytical methods		Remark
			Reference figure	Material	Temp.	Design load			Applied formula or element	Standard	
						Type	Loading factor	Element			
Fissile package	Accident test conditions	1. Drop test I									
		1.1 Vertical drop									
		1.1.1 Vertical drop (Bottom side)									
		(1) Deformation of shock absorber	—	—	—	Vertical drop (Bottom side) from 9m height	1	Deformation	$\delta = \delta_o - \delta_v$ δ_o : Minimum thickness before drop δ_v : Deformation δ : Thickness after drop	} Note 1	Note 1: Effect of deformation will be judged in thermal test. Note 2: Analytical standard of each stress component is determined using Su.
		(2) Frame of Inner shell	—	SUS304	75℃	ditto	1	Compression stress	$\sigma_c = \frac{W}{A}$		
		(3) Inner shell bottom plate	—	SUS304	75℃	ditto	1	Combined stress	Formula for fixed disc	} Note 2	Note 3: Analysis standard of each stress component is determined using Sy.
		(4) Inner shell lid	—	SUS630	75℃	ditto	1	Combined stress	Formula for simply supported disc		
		(5) Inner shell lid bolt	—	SUS630	75℃	ditto	1	—	—	} Note 2	
		(6) Fuel element/plate	—	AG3NE	75℃	ditto	1	Shear stress	$\tau = \frac{F}{2(h_2 - h_1) b}$		} Note 2
							1	Tensile stress	$\sigma_t = \frac{W_o}{A}$		
					1	Compression stress	$\sigma_c = \frac{W}{A}$				
		(7) Fuel element hold down part	—	A6061P	75℃	ditto	1	Compression stress	$\sigma_c = \frac{W}{A}$		

(II)-Table A.4 Design conditions, analytical methods of structural analysis (20/24)

Symbols:

σ : Principal stress τ_t : Torsional stress
 σ_b : Bending stress F : Load
 σ_c : Compressive stress P : Pressure
 τ : Shear stress A : Cross section

Requirement	Condition	Item	Design condition						Analytical methods		Remark
			Reference figure	Material	Temp.	Design load			Applied formula or element	Standard	
						Type	Loading factor	Element			
Fissile package	Accident test conditions	1.1.2 Vertical drop (Lid side)									
		(1) Deformation of shock absorber	—	—	—	Vertical drop (Lid side) from 9m height	1	Deformation	$\delta = \delta_0 - \delta_v$ δ_0 : Minimum thickness before drop δ_v : Deformation δ : Thickness after drop	Note 1	Note 1: Effect of deformation will be judged in thermal test.
		(2) Frame of Inner shell	—	SUS304	75℃	ditto	1	Compression stress	$\sigma_c = \frac{F}{A}$	Note 2	
		(3) Inner shell bottom plate	—	SUS304	75℃	ditto	1	Combined stress	Formula for fixed disc		
		(4) Inner shell lid	—	SUS630	75℃	ditto	1	Combined stress	Formula for simply supported disc		
		(5) Inner shell lid bolt	—	SUS630	75℃	ditto	1	Tensile stress	$\sigma_t = \frac{F}{n \cdot Ar}$		Note 3: Analysis standard of each stress component is determined using Sy.
		(6) Fuel element/plate	—	AG3NE	75℃	ditto	1	Shear stress	$\tau = \frac{F}{2(h_2 - h_1) b}$		
							1	Tensile stress	$\sigma_t = \frac{W_o}{A}$		
							1	Compression stress	$\sigma_c = \frac{W}{A}$		
		(7) Fuel element hold down part	—	A6061P	75℃	ditto	1	Compression stress	$\sigma_c = \frac{W}{A}$		

(II)-Table A.4 Design conditions, analytical methods of structural analysis (21/24)

Symbols:

σ : Principal stress τ_t : Torsional stress
 σ_b : Bending stress F : Load
 σ_c : Compressive stress P : Pressure
 τ : Shear stress A : Cross section

Requirement	Condition	Item	Design condition						Analytical methods		Remark	
			Reference figure	Material	Temp.	Design load			Applied formula or element	Standard		
						Type	Loading factor	Element				
Fissile package	Accident test conditions	1.2 Horizontal drop										
		(1) Deformation of shock absorber	—	—	—	Horizontal drop from 9m height	1	Deformation	$\delta = \delta_o - \delta_H$ δ_o : Minimum thickness before drop δ : Thickness after drop δ_H : Deformation	Note 1	Note 1: Effect of deformation will be judged in thermal test.	
		(2) Frame of Inner shell	—	SUS304	75℃	ditto	1	Bending stress	$\sigma_b = \frac{M}{Z}$			Note 2
		(3) Inner shell bottom plate	—	SUS304	75℃	ditto	1	Combined stress	Formula for fixed disc			
		(4) Upper part of inner shell (Inner lid)	—	SUS630	75℃	ditto	1	Shear stress	$\tau = \frac{F}{A}$			
		(5) Inner shell lid bolt	—	SUS630	75℃	ditto	1	Bending stress	$\sigma_b = \frac{M \cdot \ell_{\max}}{I}$	Note 3	Note 3: Analytical standard of each stress component is determined using Sy.	
		(6) Fuel basket	—	SUS304	75℃	ditto	1	Bending stress	$\sigma_b = \frac{M}{Z}$			
		(7) Fuel element/plate	—	AG3NE	75℃	ditto	1	Bending stress	$\sigma_b = \frac{M}{Z}$			
								1	Compression stress	$\sigma_c = \frac{W}{a(h_2 - h_1)}$		
						1	Buckling stress	$\sigma_y = \sigma_{cr} \left(1 + \frac{e}{r} \sec \frac{L}{2K} \sqrt{\frac{\sigma_{cr}}{E}} \right)$ σ_y : Yield stress σ_{cr} : buckling stress E : modulus of direct elasticity K : radius-of-gyration of area L : length r : section modulus/cross section e : eccentricity	Note 4	Note 4: Analytical standard is σ_{cr} .		
		(8) Fuel element hold down part	—	A6061P	75℃	ditto	1	Bending stress	$\sigma_b = \frac{M}{Z}$	Note 3		

(II)-Table A.4 Design conditions, analytical methods of structural analysis (22/24)

Symbols:
 σ : Principal stress τ_t : Torsional stress
 σ_b : Bending stress F : Load
 σ_c : Compressive stress P : Pressure
 τ : Shear stress A : Cross section

Requirement	Condition	Item	Design condition						Analytical methods		Remark
			Reference figure	Material	Temp.	Design load			Applied formula or element	Standard	
						Type	Loading factor	Element			
Fissile package	Accident test conditions	1.3 Corner drop	—	SUS630	75℃	Corner drop from 9m height	1	Analyzed for each item of para.1.1 and 1.2 above from horizontal and vertical component of impact		—	Note 1: Analytical standard of each stress component is determined using Sy.
		(1) Inner shell lid bolt				Corner drop from 9m height (Lid side)	1	Bending stress	$\sigma_{\max} = \sigma_v + \sigma_H$ $\sigma_v = \frac{N_v \cdot W \cdot L_v \cdot \ell_{v\max}}{2 \Sigma \ell^2 \cdot A_i}$ $\sigma_H = \frac{N_H \cdot W \cdot L_H \cdot \ell_{H\max}}{2 \Sigma \ell^2 \cdot A_i}$		

$$\sigma_{\max} = \sigma_v + \sigma_H$$
$$\sigma_v = \frac{N_v \cdot W \cdot L_v \cdot \ell_{v\max}}{2 \Sigma \ell^2 \cdot A_i}$$
$$\sigma_H = \frac{N_H \cdot W \cdot L_H \cdot \ell_{H\max}}{2 \Sigma \ell^2 \cdot A_i}$$

Note 1

(II)-Table A.4 Design conditions, analytical methods of structural analysis (23/24)

Symbols:

σ : Principal stress τ_t : Torsional stress
 σ_b : Bending stress F : Load
 σ_c : Compressive stress P : Pressure
 τ : Shear stress A : Cross section

Requirement	Condition	Item	Design condition						Analytical methods		Remark
			Reference figure	Material	Temp.	Design load			Applied formula or element	Standard	
						Type	Loading factor	Element			
Fissile package	Accident teset conditions	<u>2. Drop test II</u> 2.1 Penetration									
		(1) Outer shell lid	—	SUS304	75℃	Drop onto a mild bar from 1m height	1	Penetration energy		No Penetra- tion	
		(2) Outer shell bottom plate	—	SUS304	75℃	ditto	1	Penetration energy		No Penetra- tion	
		(3) Frame of Outer shell	—	SUS304	75℃	ditto	1	Penetration energy		No Penetra- tion	
		<u>3. Thermal test</u> 3.1 Thermal expansion									
		(1) Gap between inner shell and fuel basket	—	SUS304	500/ 225℃	Thermal expansion	1	Compression	Presence of gap between shell and basket	free	Note 1: Analytical standard of each stress component is determined using Su.
		3.2 Stress by pressure									
		(1) Frame of Inner shell	—	SUS304	500℃	Internal pressure	1	Combined Stress	Formula for thin cylinder	} Note 1	Note 2: Analytical standard of each stress component is determined using Sy.
		(2) Inner shell bottom plate	—	SUS304	500℃	Internal pressure	1	Combined Stress	Formula for fixed disc		
	(3) Inner shell lid		SUS630	225℃	Internal pressure	1	Combined Stress	Formula for simply supported disc			
	(4) Inner shell lid bolt	—	SUS630	225℃	Initial torque	1	Tensile stress	$\sigma_t = \frac{F}{A_i}$	} Note 2	Note 3: Initial margin of tightening is about 1.1mm.	
				225℃	Internal pressure	1	Tensile stress	$\sigma_t = \frac{F}{n \cdot A_i}$			
	(5) Displacement of O-ring part of inner lid	—	SUS630	225℃	Internal pressure	1	Displacement	Formula for displacement of O-ring part	} Note 3		

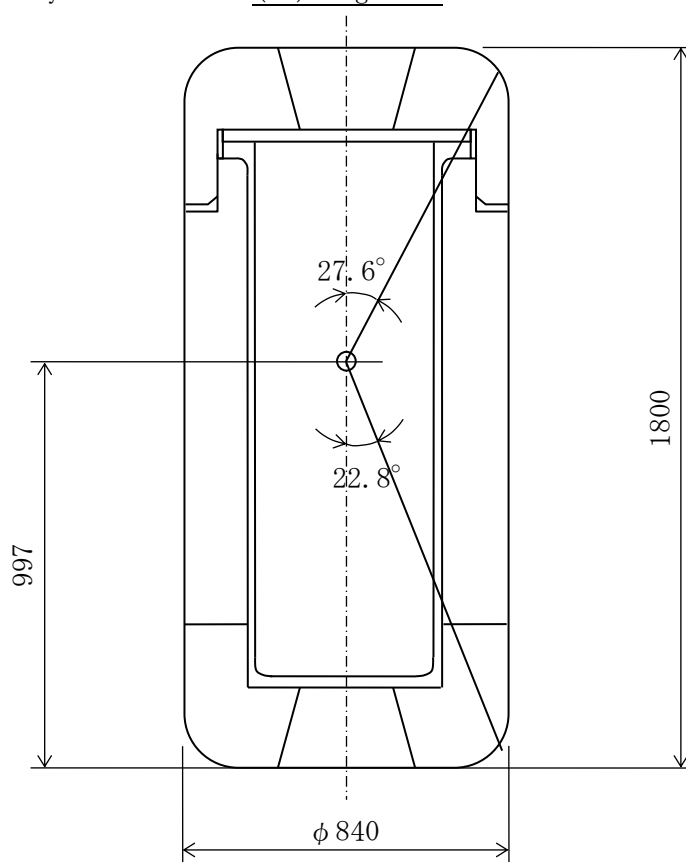
(II)-Table A.4 Design conditions, analytical methods of structural analysis (24/24)

Symbols:
 σ : Principal stress τ_t : Torsional stress
 σ_b : Bending stress F : Load
 σ_c : Compressive stress P : Pressure
 τ : Shear stress A : Cross section

Requirement	Condition	Item	Design condition						Analytical methods		Remark
			Reference figure	Material		Design load			Applied formula or element	Standard	
						Type	Loading factor	Element			
Fissile package	Accident test conditions	4. Water immersion test									
		4.1 Water immersion (0.9m depth)									
		(1) Frame of Inner shell	—	SUS304		External pressure	1	Combined stress	Formula for thin cylinder	} Note 1	Note 1: Analytical standard of each stress component is determined using Su.
		(2) Inner shell bottom plate	—	SUS304		External pressure	1	Combined stress	Formula for fixed disc		
		(3) Inner shell lid		SUS630		External pressure	1	Combined stress	Formula for simply supported disc	} Note 2	
		(4) Buckling of inner shell	—	SUS304		External pressure	1	Buckling stress	$P_e = \frac{4B \cdot t}{2D_o}$ B : Buckling factor D ₀ : Outer diameter of inner shell	} Note 1	Note 2: Analytical standard of each stress component is determined using Su.
(5) Displacement of O-ring part of inner lid	—	SUS630		External pressure	1	Displacement	Formula for displacement of O-ring part	} Note 3	Note 3: Initial margin of tightening is about 1.1mm		

A.2 Weight and center of gravity

As indicated in (I)-Table-C.3, the package weighs 950 kg in maximum. Its center of gravity is shown in (II)-Fig.A.1.



(II)-Fig.A.1 Position of center of gravity

A.3 Mechanical properties of materials

(II)-Table.A.5 is a list of the mechanical properties of the materials used in the analysis.

(II)-Table.A.6 shows the mechanical properties of the materials to be used as analytic references.

In addition, the value based on the current appropriate source is indicated in (). Even in a case where values based on these current, appropriate sources are used for mechanical property of major members etc. of this shipping cask, it is confirmed that the impact on the analysis result will be minimal, and there will be no problem for safety.

Mechanical properties of stainless steel and aluminum alloy versus temperature is indicated in (II)-Fig.A.2, (II)-Fig.A.3, (II)-Fig.A.4, and (II)-Fig.A.5.

(II)-Fig.A.6 and (II)-Fig.A.7 show a design fatigue curve for the analysis.

A stress-strain curve of balsa used as a shock absorber is indicated in (II)-Fig.A.8. The figures are quoted from references shown later.

(II)-Table.A.5 Mechanical properties of materials

Material	Code	Main application parts	Modulus of longitudinal elasticity E [N/mm ²]	Linear expansion factor α [1/°C]	Design tensile strength Su [N/mm ²]	Design yield strength Sy [N/mm ²]	Design stress intensity Sm [N/mm ²]	Poisson's ratio ν	Stress-strain diagram
[2] Stainless steel (austenitic)	SUS304	Main body of inner shell Main body of outer shell and outer lid Fuel basket	(II)-Fig. A. 2 (4/5)	(II)-Fig. A. 2 (5/5)	(II)-Fig. A. 2 (1/5)	(II)-Fig. A. 2 (2/5)	(II)-Fig. A. 2 (3/5)	0.3	—
[2] Stainless steel precipitation hardened type	SUS630 H1150	Inner lid Inner lid clamping bolt Outer lid clamping bolt	(II)-Fig. A. 3 (3/4)	(II)-Fig. A. 3 (4/4)	(II)-Fig. A. 3 (1/4)	(II)-Fig. A. 3 (2/4)	(II)-Fig. A. 4 (1/1)	0.3	—
[14] Aluminum alloy	AG3NE	Fuel element (A) Fuel plate	—	—	—	(II)-Fig. A. 5 (1/1)	—	0.3	—
[4] Balsa	—	Shock absorber	—	—	—	—	—	—	(II)-Fig. A. 8

Stainless steel: see Literature [2]

Aluminum alloy : see Literature [14]

Balsa : see Literature [4]

Numbers shown in brackets ()
indicate the number of the sheets
for the Figure No.

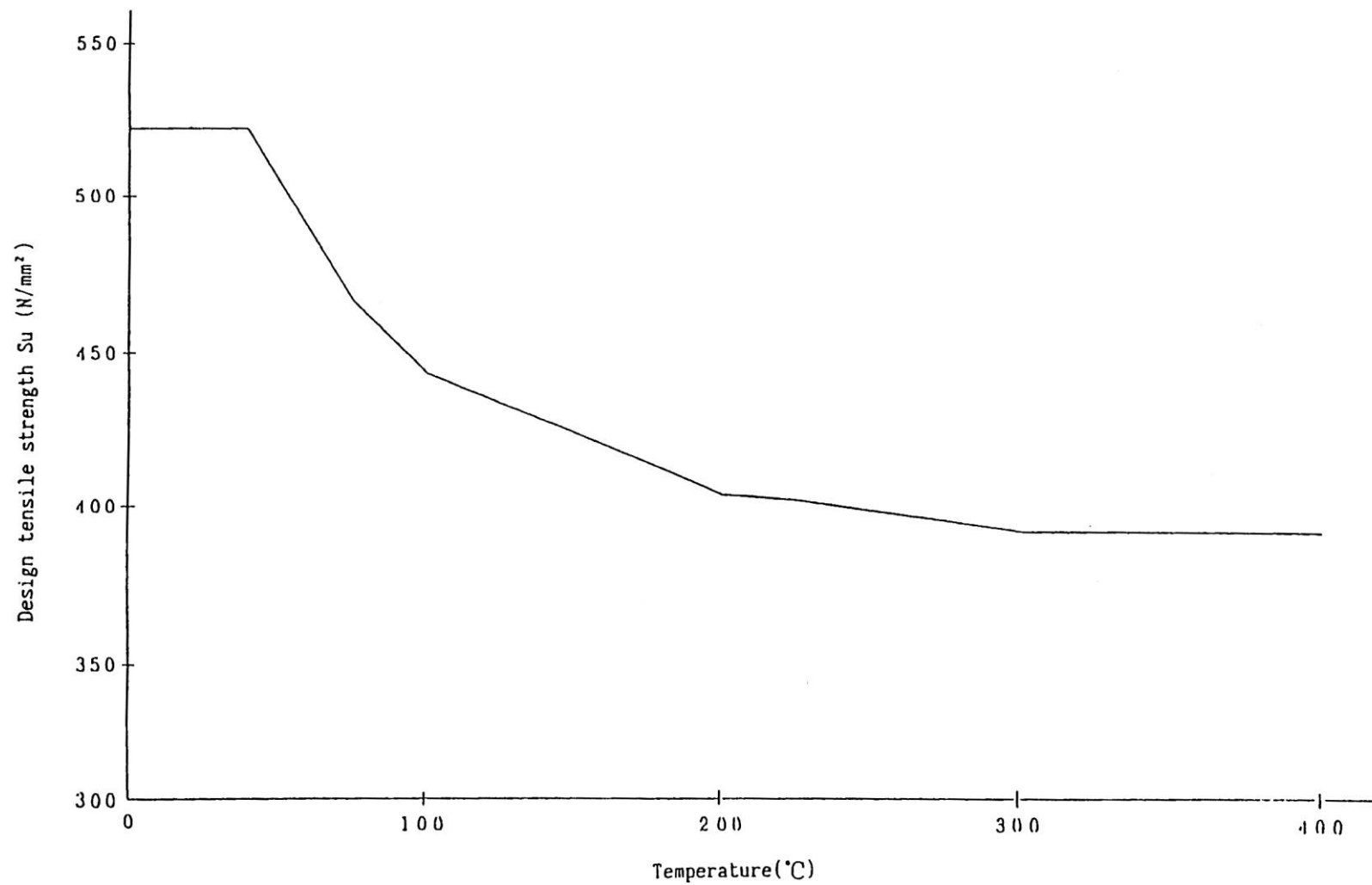
(II)-Table.A.6 Mechanical properties of materials to be used as design standards

No.	Evaluated position	Material	- Normal conditions - Normal test conditions - Accident test conditions (excluding thermal tests)						Accident test conditions (only for thermal tests)					
			T	Sm	Sy	Su	E	α	T	Sm	Sy	Su	E	α
1	Inner shell main body	SUS304	75	137	183 (180)	466	1.92 (1.91)	16.71 (15.9)	500	—	—	387	—	—
2	Inner lid	SUS630	75	311 (310)	688 (687)	847 (846)	1.99 (1.92)	9.38 (11.3)	225	—	612	—	—	—
3	Fuel basket	SUS304	75	137	183 (180)	466	1.92 (1.91)	16.71 (15.9)	—	—	—	—	—	—
4	Outer shell main body	SUS304	75	137	183 (180)	466	1.92 (1.91)	16.71 (15.9)	—	—	—	—	—	—
5	Outer lid	SUS304	75	137	183 (180)	466	1.92 (1.91)	16.71 (15.9)	—	—	—	—	—	—
6	Inner lid clamping bolt	SUS630	75	229	688 (687)	847	1.99 (1.92)	9.38 (11.3)	225	—	612	—	—	—
7	Outer lid clamping bolt	SUS630	75	229	688 (687)	847	1.99 (1.92)	9.38 (11.3)	—	—	—	—	—	—
8	Fuel element (A) Fuel plate	AG3NE	75	—	63.8 63.7	167	0.697	25.7	—	—	—	—	—	—
9	Fuel element (B)	JRR-4B type fuel plate	75	—	63.8	88.3	—	—	—	—	—	—	—	—
10	Fuel element hold down part	A6061P	75	—	245	295	—	—	—	—	—	—	—	—

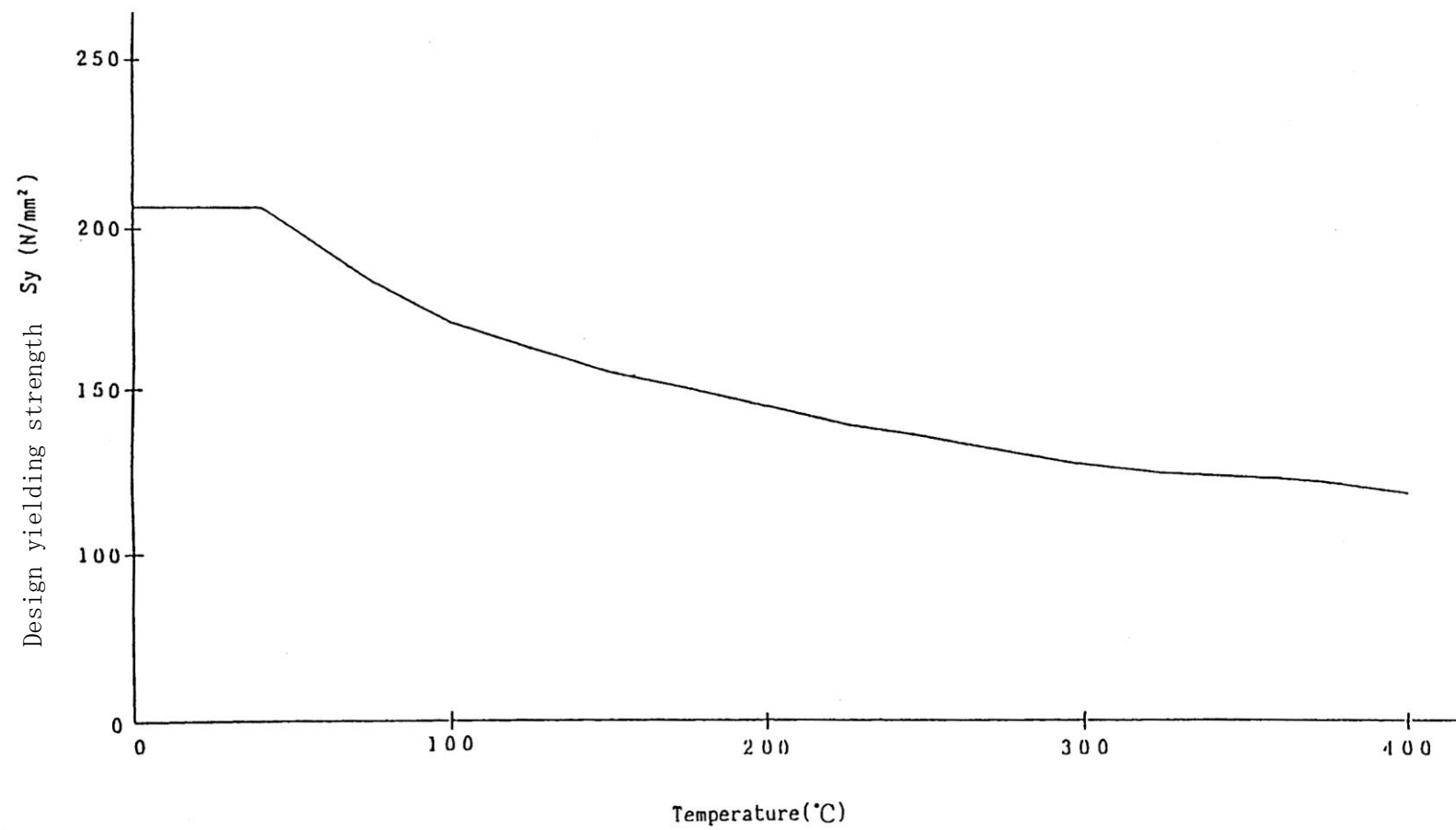
T: Temperature [°C] Sm: Design stress intensity [N/mm²] Sy: Design yield point [N/mm²] Su: Design tensile strength [N/mm²]

E: Modulus of longitudinal elasticity [$\times 10^5$ N/mm²] α : Linear expansion factor [$\times 10^{-6}$ °C⁻¹]

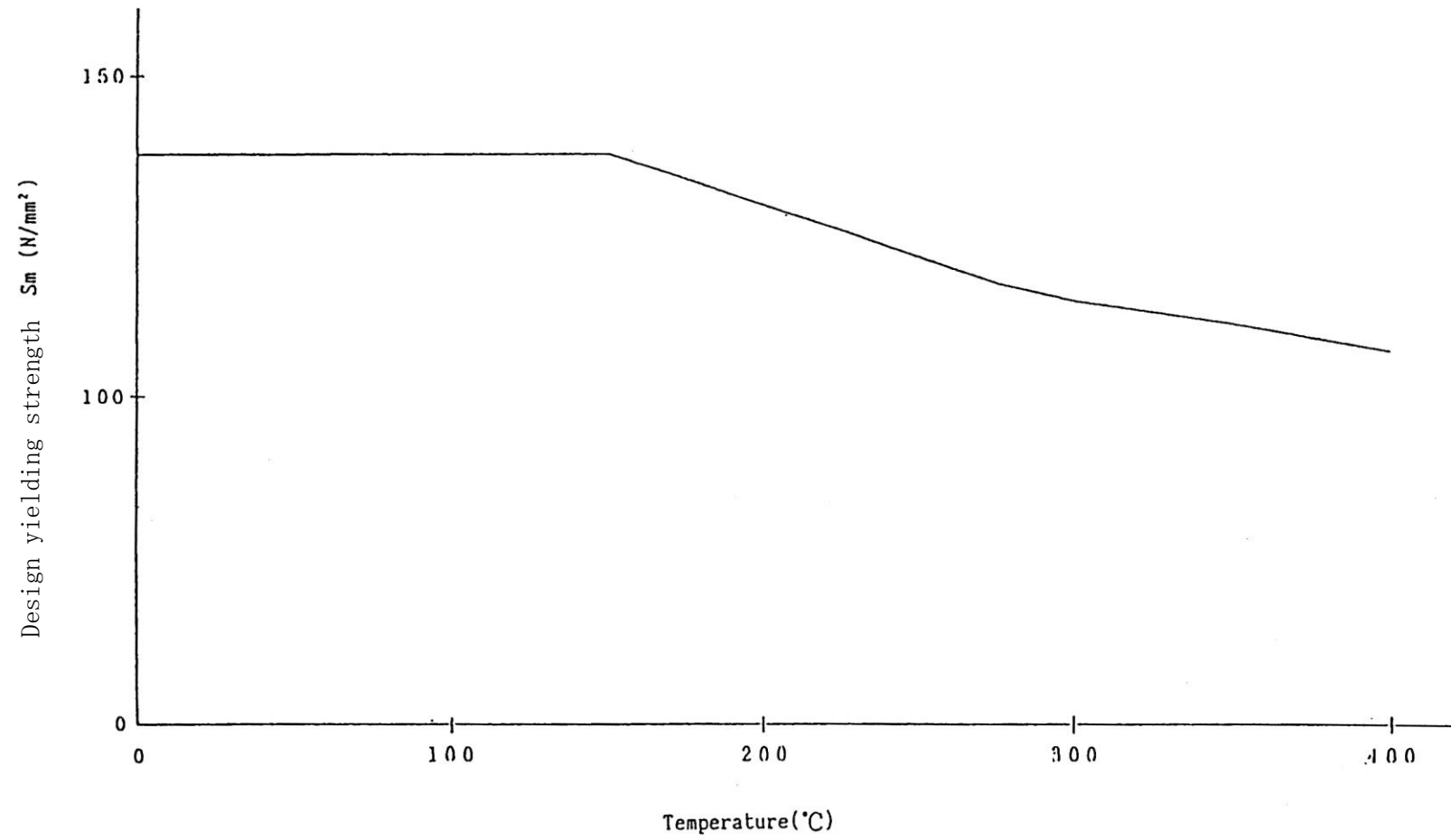
() : Code for Nuclear Power generation Facilities: Rules on of Materials Nuclear Power Plants (2012 edition) of the Japan Society of mechanical Engineers



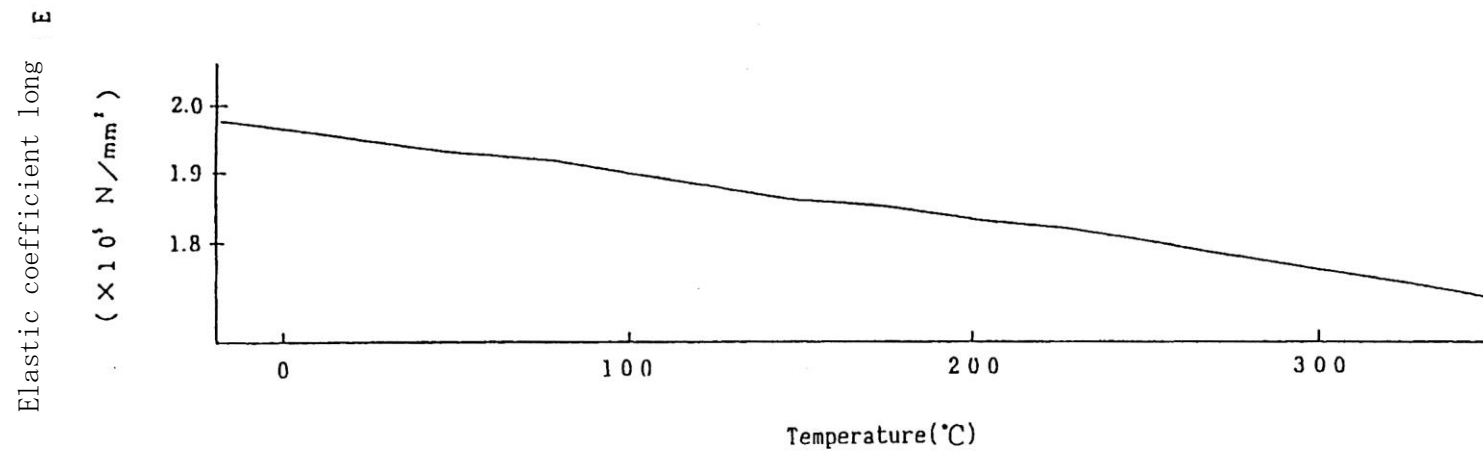
(II)-Fig.A.2 Variations in mechanical properties of SUS304 according to changes in temperature (1/5)



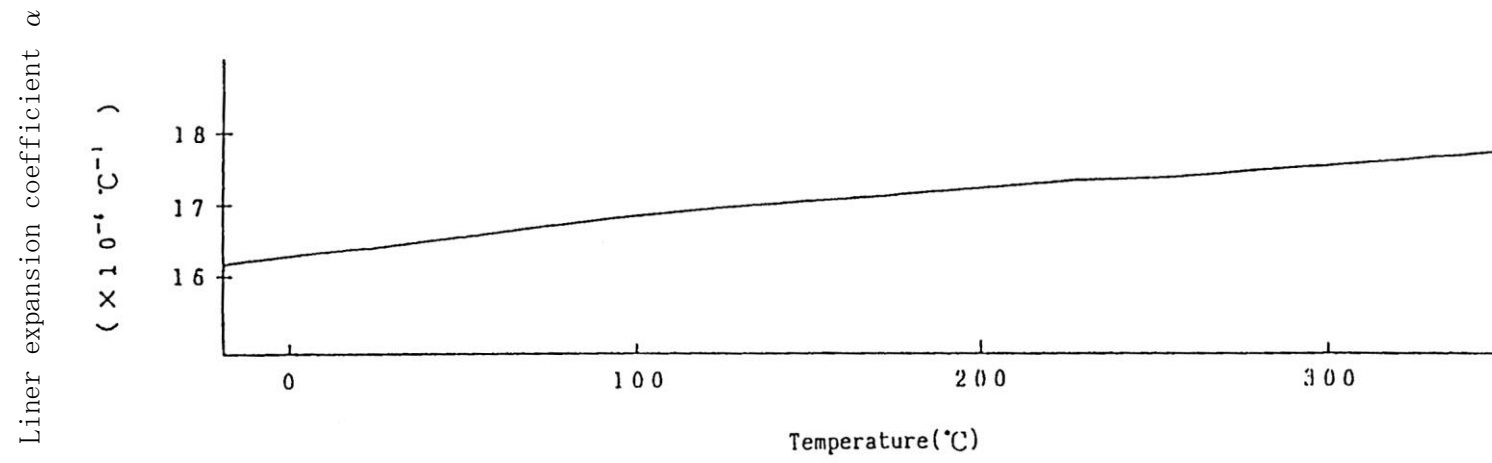
(II)-Fig.A.2 Variations in mechanical properties of SUS304 according to changes in temperature (2/5)



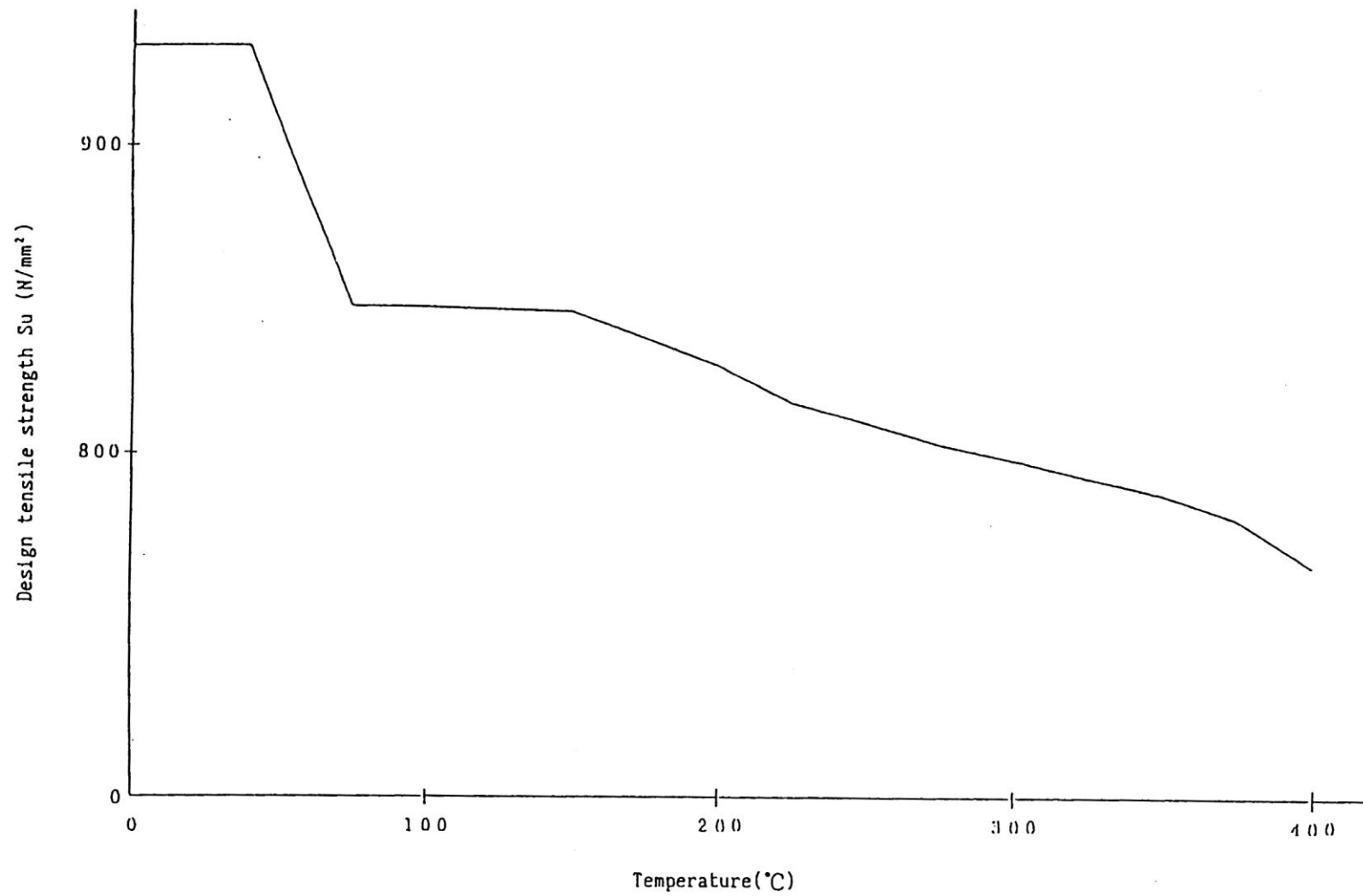
(II)-Fig.A.2 Variations in mechanical properties of SUS304 according to changes in temperature (3/5)



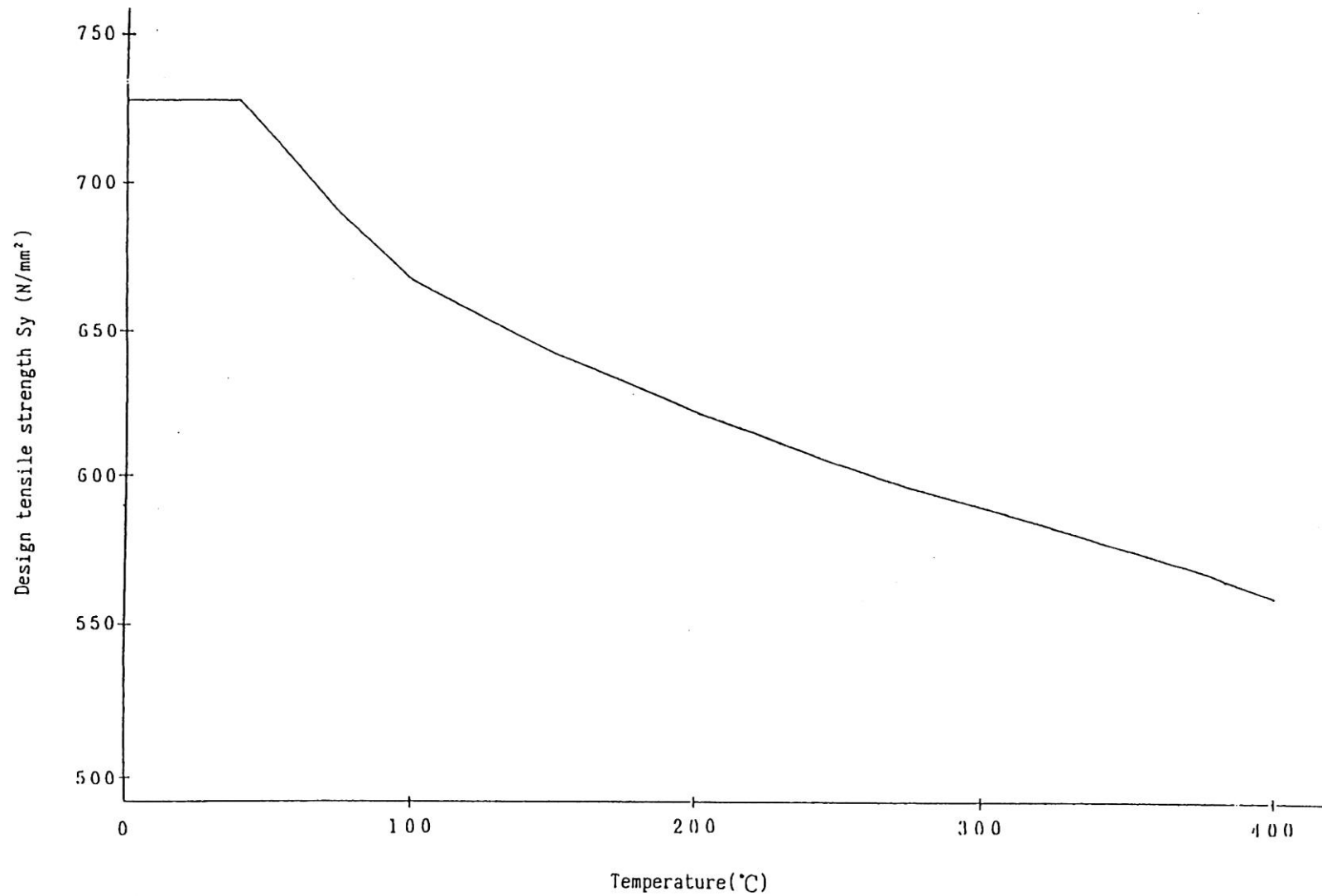
(II)-Fig.A.2 Variations in mechanical properties of SUS304 according to changes in temperature (4/5)



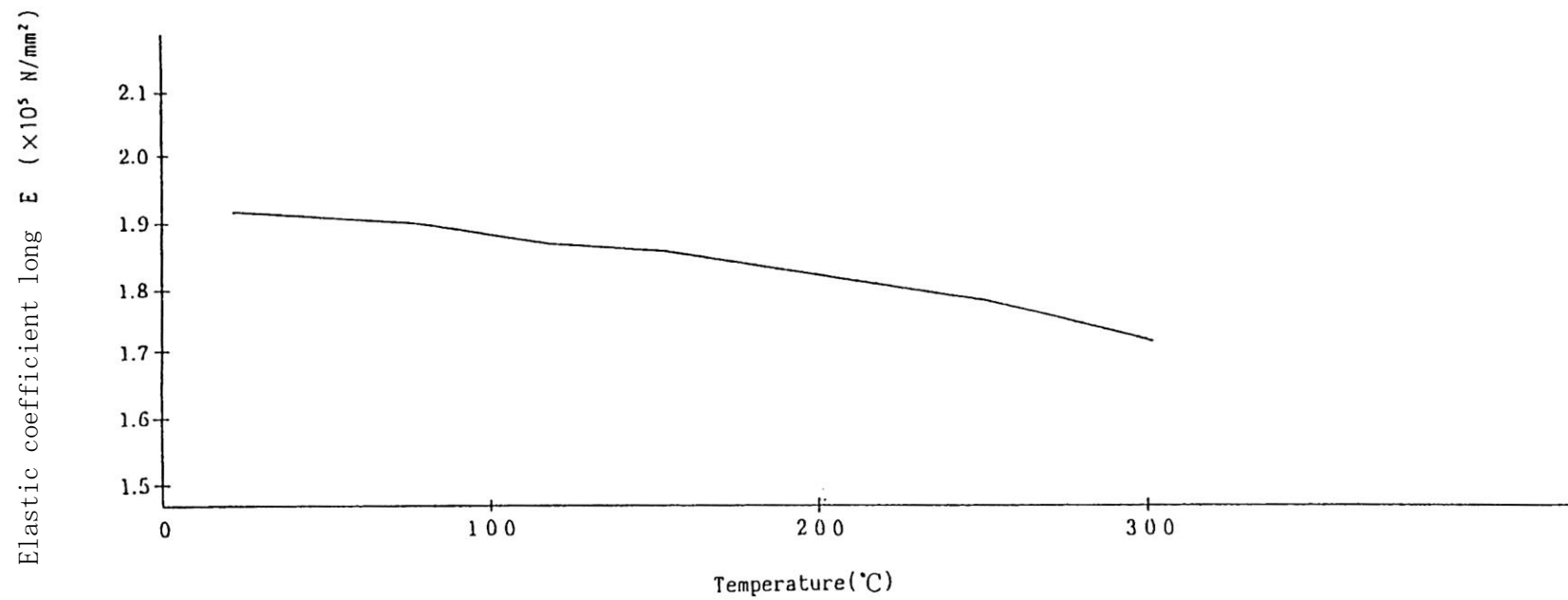
(II)-Fig.A.2 Variations in mechanical properties of SUS304 according to changes in temperature (5/5)



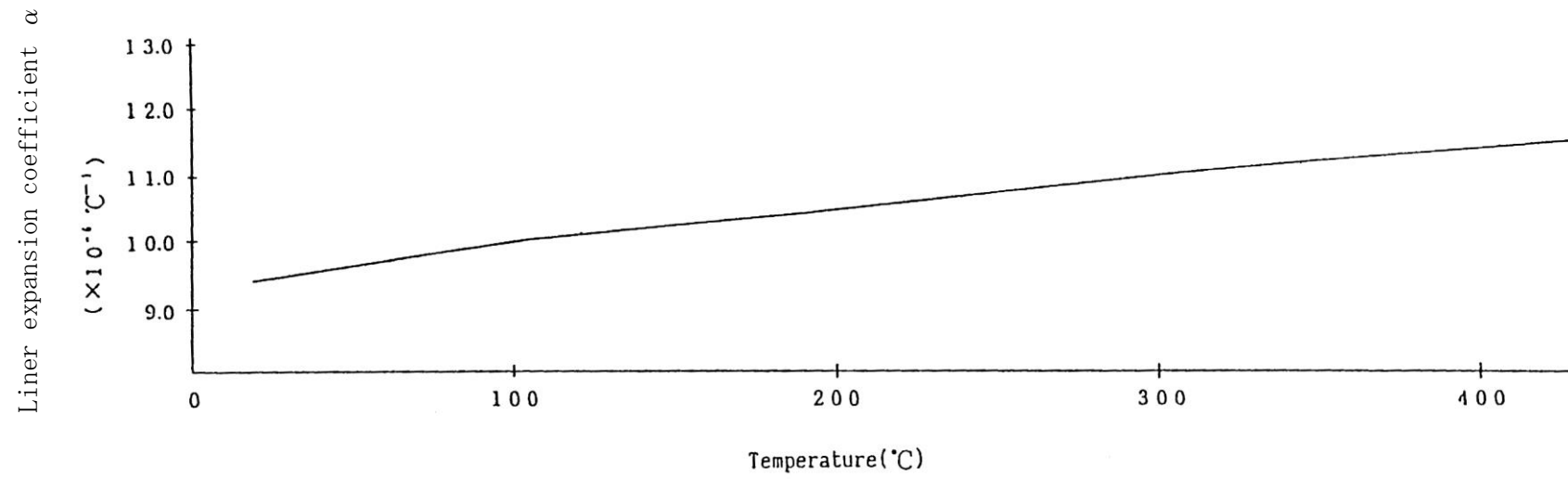
(II)-Fig.A.3 Variations in mechanical properties of SUS630 according to changes in temperature (bolt material) (1/4)



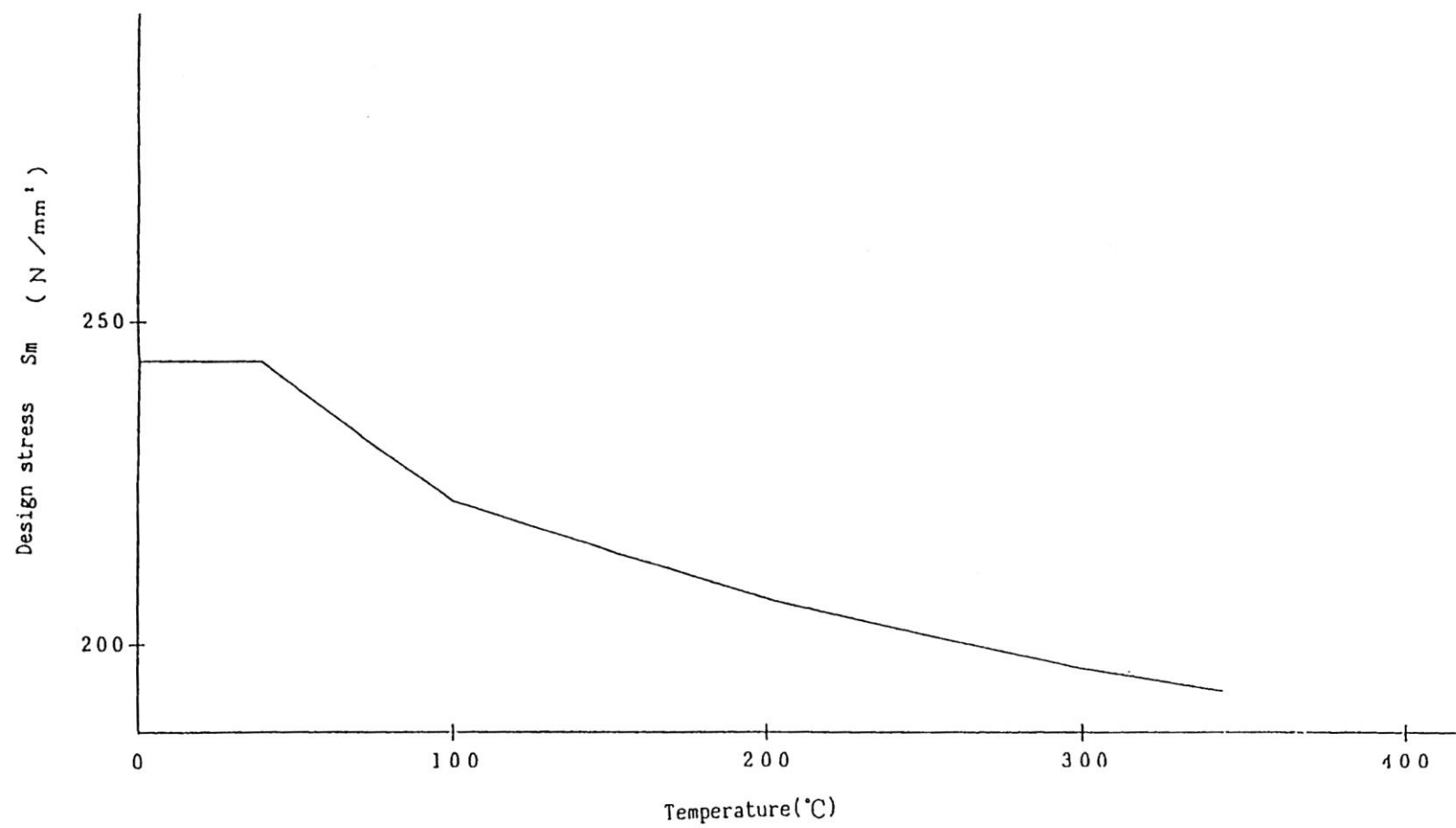
(II)-Fig.A.3 Variations in mechanical properties of SUS630 according to changes in temperature (bolt material) (2/4)



(II)-Fig.A.3 Variations in mechanical properties of SUS630 according to changes in temperature (bolt material) (3/4)

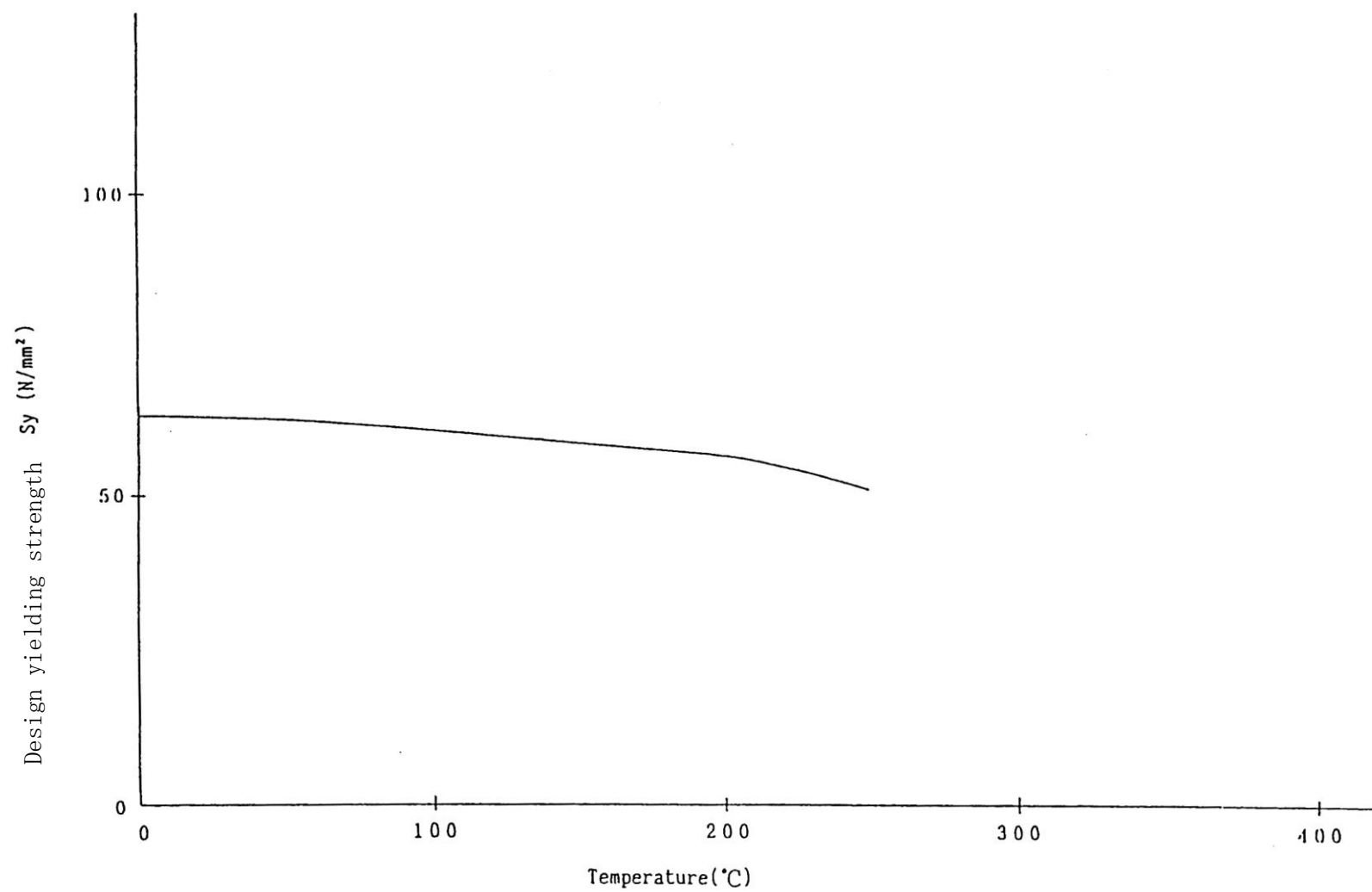


(II)-Fig.A.3 Variations in mechanical properties of SUS630 according to changes in temperature (bolt material) (4/4)



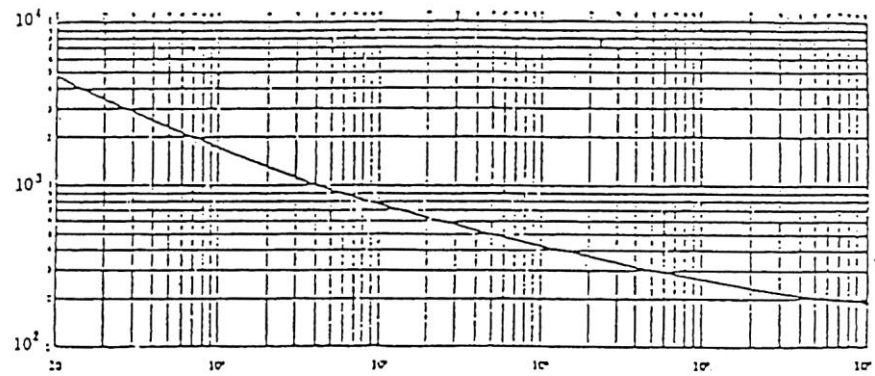
(II)-Fig.A.4 Variations in mechanical properties of SUS630 according to changes in temperature (1/1)

(II) - A-47



(II)-Fig.A.5 Variations in mechanical properties of AG3NE according to changes in temperature (1/1)

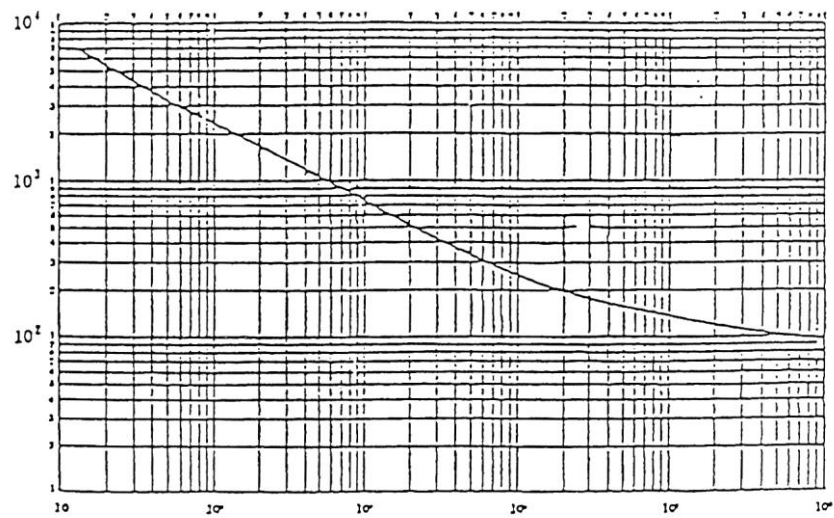
Sa Repetition peak stress strength
Sa (N/mm²)



Na The permission repetition number of times

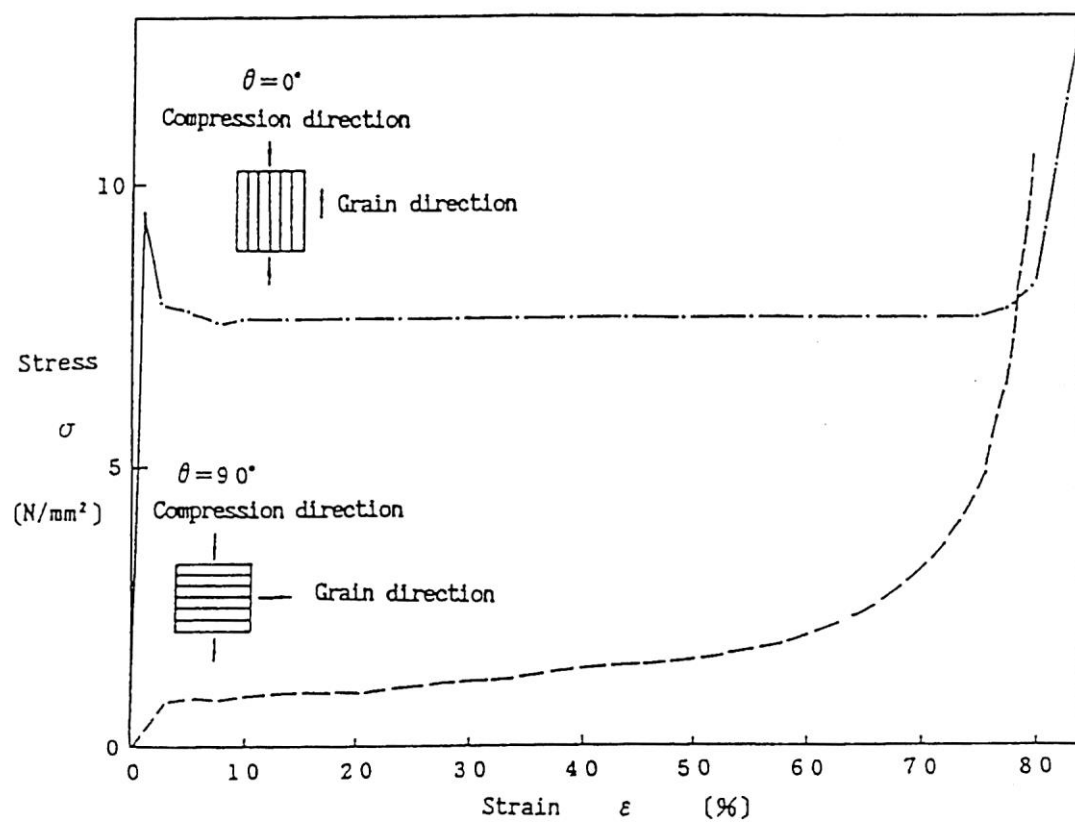
(II)-Fig.A.6 Design fatigue curve (austenitic type stainless steel and high nickel alloy)^[2]

Sa Repetition peak stress strength
Sa (N/mm²)



Na The permission repetition number of times

(II)-Fig.A.7 Design fatigue curve (high tensile strength bolt)^[2]



(II)-Fig.A.8 Stress-strain curve of shock absorber^[4]

A.4 Requirements of the package

A.4.1 Chemical and electrical reactions

(II)-Table A.7 is a list of the different materials that come in contact with each other in this package. The materials used in this package, being chemically stable in air, will not trigger any chemical or electrical reaction when coming in contact with one another.

(II)-Table A.7 List of different materials contacted

Positions		Materials
Inner shell } Outer shell }	— Shock absorber	Stainless steel — Timber
Inner shell } Outer shell }	— Heat insulator	Stainless steel — Hardened polyurethane
Inner shell main body } Inner lid }	— O-ring	Stainless steel — Silicone rubber
Fuel basket } Inner lid }	— Spacer	Stainless steel — Silicone rubber
Protective sheets	— Spacer	Polyethylene — Silicone rubber
Protective sheets	— Fuel basket	Polyethylene — Stainless steel
Protective sheets	— Peripheral shock absorber	Polyethylene — Polyurethane foam
Protective sheets	— Fuel element	Polyethylene — Aluminum alloy
Peripheral shock absorber	— Fuel element	Polyurethane foam — Aluminum alloy
Cushion rubber	— Lower part of the fuel basket	Silicone rubber — Stainless steel
Inner shell } Outer shell }	— Gasket	Stainless steel — Ethylene propylene rubber
Fitting bracket	— Fusible plug	Stainless steel — Solder

A.4.2 Low temperature strength

This package is a BU type package, as is indicated in (I)-B. This section will demonstrate the reliability of the packaging in ambient conditions of -40°C.

The minimum temperatures of each part of the package and the materials involved are shown in (II)-Table A.8.

(II)-Table A.8 Minimum temperatures of parts of package

No.	Evaluated position	Material	Minimum temperature (°C)	Brittleness transition temp./min. service temperature (°C)	Citation, literatures and references
1	Content	Aluminum alloy	-40	No brittle fracture	Aluminum Hand Book ^[20]
2	Inner shell	Austenitic stainless steel	-40	No brittle fracture	JIS B 8270 Stainless Steel Manual ^[16]
3	Outer shell	Austenitic stainless steel	-40	No brittle fracture	
4	Inner lid	Precipitation hardened stainless steel	-40	Below -40	Stainless steel Heat Treatment ^[18]
5	Outer lid	Austenitic stainless steel	-40	No brittle fracture	JIS B 8270 Stainless Steel Manual ^[16]
6	Fuel basket	Austenitic stainless steel	-40	No brittle fracture	
7	Inner lid clamping bolt	Precipitation hardened stainless steel	-40	Below -40	Stainless steel Heat Treatment ^[18]
8	Outer lid clamping bolt	Precipitation hardened stainless steel	-40	Below -40	
9	Inner lid O-ring	Silicone rubber	-40	Below -40	Summary of technology for hybrid materials ^[21]
10	Shock absorber	Balsa	-40	Below -40	Appendices A.10.4
11	Heat insulator	Hardened polyurethane foam	-40	Below -40	Internal data of manufacturers ^[22]

The austenitic stainless steels of the inner and outer shells, as shown in (II)-Fig.A.103 and the precipitation hardened stainless steels of the inner lid and bolts as shown in (II)-Fig.A.104 can maintain adequate value of strength

endurable to impulse at the temperature -40°C , and also the Aluminum alloy used for fuel elements is free from any brittle fracture at the temperature -40°C , as show in (II)-Table.A.8.

The tolerable temperature for the silicone rubber used for the O-ring is lower then -40°C . The O-ring preserves full sealing performance at -40°C .

The Balsa wood used for the shock absorber, as shown in (II)-Fig.A.100, can maintain the function as the shock absorber sufficiently at the temperature -40°C , since the material properties are free of any significant error at each temperatures, at room temperature, -20°C and -40°C .

Therefore, at -40°C , this package is completely functional.

A.4.3 Sealing device

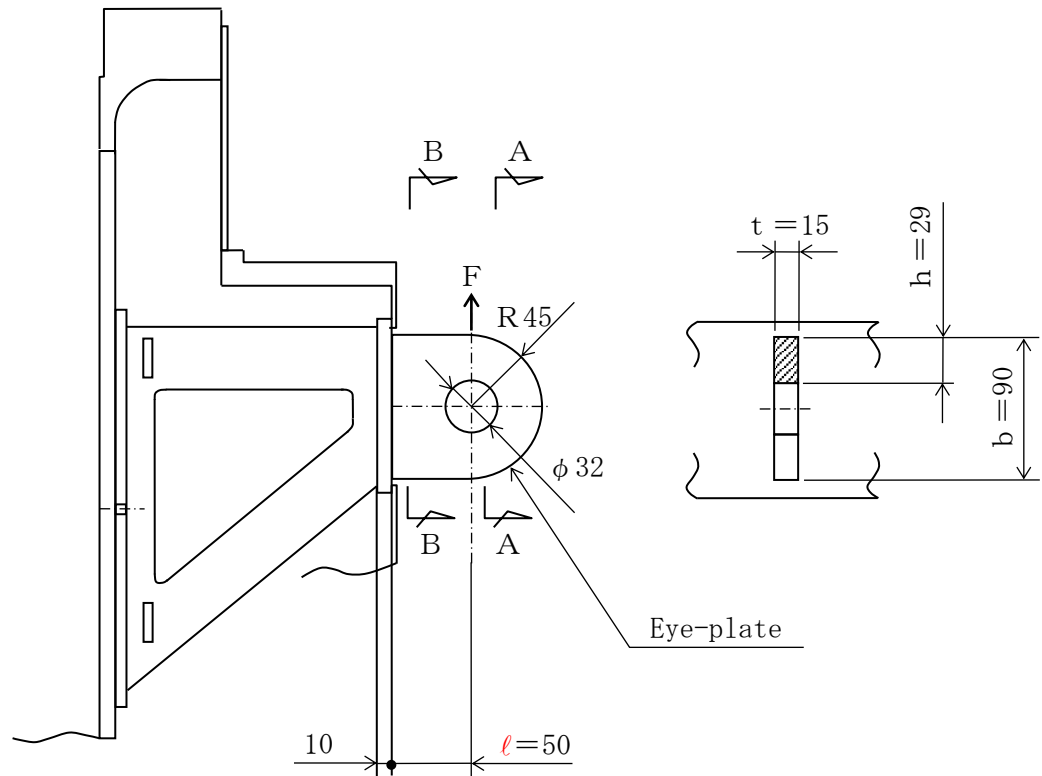
After the fuel elements are stored in the main body of the inner shell, the inner lid is clamped with bolts and then secured with the outer lid. Thus, the inner lid cannot be opened inadvertently. Similarly, the outer lid cannot be easily opened as it is locked and sealed after being fixed to the main body of the outer shell.

If opened, it will easily be detected.

A.4.4 Hoisting accessory

The hoisting accessory described in this section is a hoisting eye-plate fixed to the side of the main body of the outer shell. For design standard of the stress generated at the hoisting accessory, the yield stress S_y at the temperature of 75°C is employed with safety margin, in consideration of 65°C , the maximum temperature at the point of eye-plate on the outer surface of the packaging on normal transportation, obtained by (II) -B Thermal Analysis.

(II)-Fig.A.9 shows an analytical model of an eye-plate of the hoisting accessory for the main body.



(II)-Fig.A.9 Analytical model for eye-plate

The gross weight of a package lifted (m_0) on a hoisting eye-plate of the main body is 950 kg at the maximum, as indicated in (II)-Table C.3.

A maximum load $F(\text{N})$ applied on one of four eye-plates when lifting a package is given by the following equation, with the load factor of 3.

$$F = \frac{1}{n} (3 \times g \times m_0) = \frac{3}{4} \times 9.81 \times 950 = 6.99 \times 10^3 \quad [\text{N}]$$

where

g: gravitational acceleration; $g=9.81 \text{ [m/sec}^2\text{]}$

Therefore, when the upward vertical load , $F=6.99 \times 10^3 \text{ [N]}$ as shown in (II)-Fig.A.9 works on the eye-plate, stress on each cross section is analysed as follows.

(1) Section A-A

The shearing stress $\tau \text{ [N/mm}^2\text{]}$ generated in the shaded portion (section A-A) of the eye-plate shown in (II)-Fig.A.9 is given by the following equation.

$$\tau = \frac{F}{A} = \frac{F}{t \cdot h}$$

where

τ : Shearing stress $\text{[N/mm}^2\text{]}$

F: Maximum load, $F=6.99 \times 10^3 \text{ [N]}$

t: Plate thickness, $t=15 \text{ [mm]}$

h: Height, $h=29 \text{ [mm]}$

Therefore,

$$\tau = \frac{6.99 \times 10^3}{29 \times 15} = 16.1 \text{ [N/mm}^2\text{]}$$

So it is less than the design standard value allowable correspond to shearing stress on the eye-plate material (SUS 304) ($0.6s_y=108 \text{ N/mm}^2$). And the margin of safety (MS) is

$$MS = \frac{0.6S_y}{\tau} - 1 = \frac{108}{16.1} - 1 = 5.70$$

(2) Section B-B

The bending stress $\sigma_b \text{ [N/mm}^2\text{]}$ generated at the fixing point of the eye-plate as indicated in (II)-Fig.A.9 is given by the following equation.

$$\sigma_b = \frac{M}{Z} = \frac{F \cdot l}{t b^2 / 6}$$

where

M: Bending moment $\text{[N/mm}^2\text{]}$

Z: Section modulus [mm³]

l: Moment arm, l=50 [mm]

b: Width of eye-plate, b =90 [mm]

t: Plate thickness, t=15 [mm]

Therefore,

$$\sigma_b = \frac{6.99 \times 10^3 \times 50}{15 \times 90^2 / 6} = 17.3 \quad [\text{N/mm}^2]$$

and it is less than the design yield strength ($S_y=180\text{N/mm}^2$) of the eye-plate material (SUS304).

The margin of safety (MS) turns out

$$\text{MS} = \frac{S_y}{\sigma_b} - 1 = \frac{180}{17.3} - 1 = 9.40$$

And the shearing stress τ generated in the section B-B is given by the following equation.

$$\tau = \frac{F}{A} = \frac{F}{t \times b} = \frac{6.99 \times 10^3}{15 \times 90} = 5.18 \quad [\text{N/mm}^2]$$

It is therefore less than the design standard value allowable correspond to shearing stress on the eye-plate material (SUS304).

The margin of safety (MS) is

$$\text{MS} = \frac{0.6S_y}{\tau} - 1 = \frac{108}{5.18} - 1 = 19.8$$

The composite stress σ [N/mm²] of the above-mentioned bending stress

σ_b and shearing stress τ is given by the following equation.

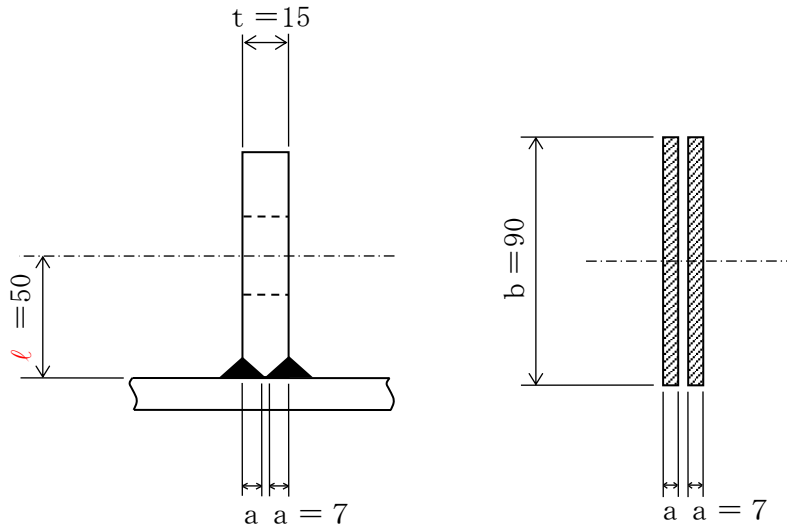
$$\sigma = \sqrt{\sigma_b^2 + 4\tau^2} = \sqrt{17.3^2 + 4 \times 5.18^2} = 20.2 \quad [\text{N/mm}^2]$$

It is less than the yield point of the design of the eye-plate material (SUS304).

The margin of safety (MS) is

$$\text{MS} = \frac{S_y}{\sigma} - 1 = \frac{180}{20.2} - 1 = 7.91$$

(3) Welded part on the section B-B



(II)-Fig.A.10 Analytical model of welded part on eye-plate.

The bending stress σ_b [N/mm²] generated on the welded fixing part of the eye-plate shown in (II)-Fig.A.10 is given by the following equation

$$\sigma_b = \frac{M}{Z} = \frac{F \cdot l}{Z}$$

where

Z: Section modulus of the welded part [mm³]

$$Z = \frac{1}{6} \cdot 2a \cdot b^2$$

a: Weld-throat thickness, a=7 [mm]

b: Width of a plate, b=90 [mm]

Therefore, σ_b will be

$$\sigma_b = \frac{6.99 \times 10^3 \times 50}{\frac{1}{6} \times 2 \times 7 \times 90^2} = 18.5 \quad [\text{N/mm}^2]$$

This is less than the design standard value on the welded part (0.45Sy=81.0N/mm²).

The margin of safety (MS) is

$$MS = \frac{0.45Sy}{\sigma_b} - 1 = \frac{81.0}{18.5} - 1 = 3.37$$

The shearing stress τ generated on the welded part of the section B-B is given by the following equation.

$$\tau = \frac{F}{A} = \frac{F}{2a \cdot b} = \frac{6.99 \times 10^3}{2 \times 7 \times 90} = 5.55 \quad [\text{N/mm}^2]$$

This is less than the design standard value allowable correspond to shearing strength on the welded part ($0.45 \times 0.6 \times S_y = 48.6 \text{ N/mm}^2$).

The margin of safety (MS) is

$$\text{MS} = \frac{0.45 \times 0.6 \times S_y}{\tau} - 1 = \frac{0.45 \times 0.6 \times 180}{5.55} - 1 = 7.75$$

The composite stress σ [N/mm²] of the bending stress mentioned above σ_b and the shearing stress τ is given by the following equation

$$\sigma = \sqrt{\sigma_b^2 + 4 \cdot \tau^2} = \sqrt{18.5^2 + 4 \times 5.55^2} = 21.6 \quad [\text{N/mm}^2]$$

It is less than the design standard value on the welded part ($0.45 S_y = 81.0 \text{ N/mm}^2$).

The margin of safety (MS) is,

$$\text{MS} = \frac{0.45 S_y}{\sigma} - 1 = \frac{81.0}{21.6} - 1 = 2.75$$

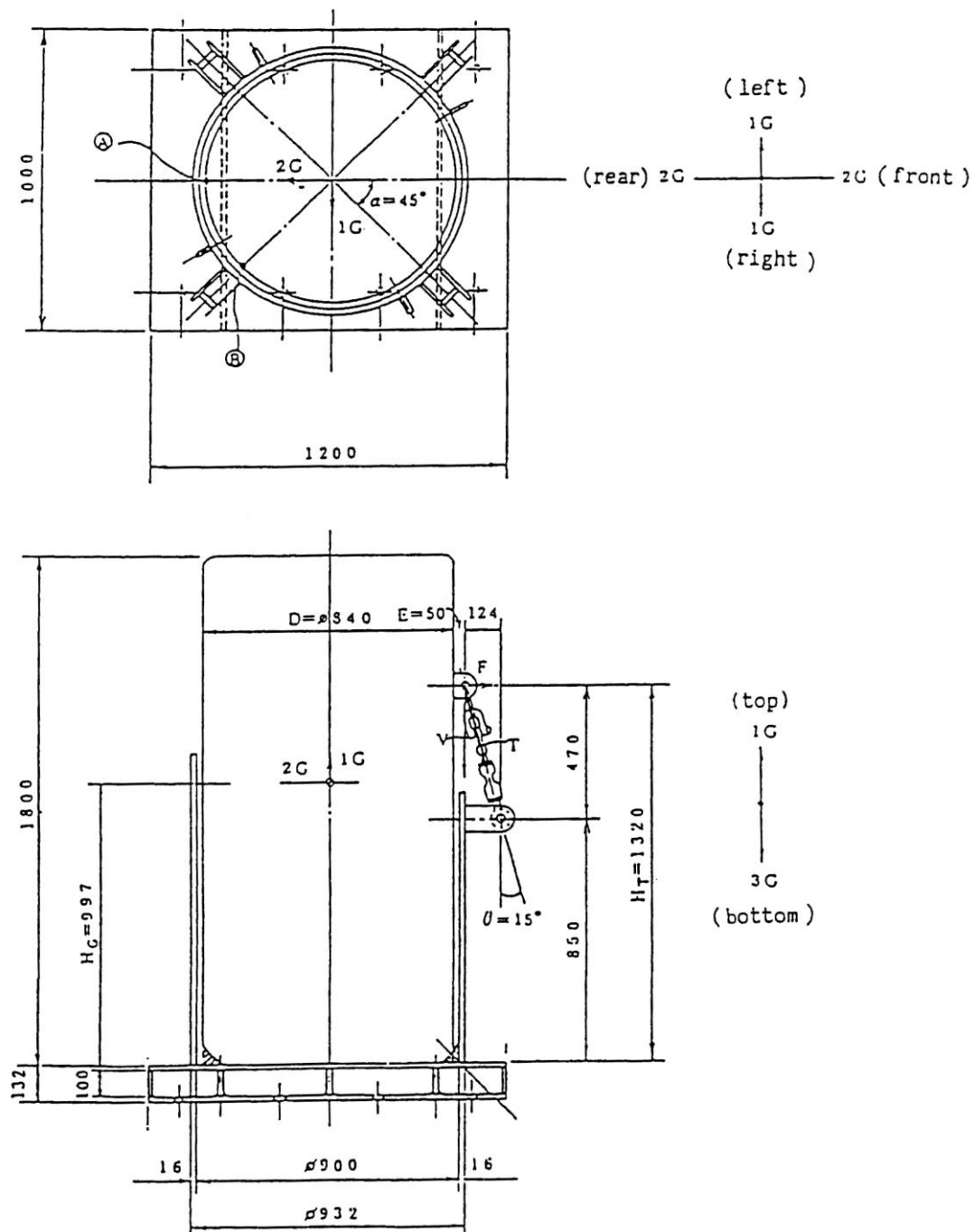
The results of the analysis mentioned above is outlined in (II)-Table A.9.

As indicated in (II)-Table A.9, the margin of safety (MS) in every analysis is positive and the eye-plate is sound during hoisting.

A.4.5 Tightening device

This packaging is transported after being tightened by a device, shown in (II)-Fig.A. 11.

The packaging and the tightening device are secured with an eye-plate and a turnbuckle.



(II)-Fig.A. 11 Acceleration during transportation

The acceleration which occurs during transportation is 2G from front to rear, 1G from left to right, 1G towards the top and 3G towards the bottom, as indicated in (II)-Fig.A.11.

After taking the combined force of these factors into consideration, the tensile strength applied to the turnbuckle due to the overturning moment around the supporting points (A) and (B) as indicated in (II)-Fig.A.11 is as follows:

$$T_A = \frac{2 \cdot H_G + R}{2H_T \sin \theta \cdot \sec \alpha + 2 \cos \theta \{R(1 + \cos \alpha) + E \cos \alpha\}} \times m_o \times g \quad [N]$$

$$T_B = \frac{3 \cdot H_G \cos \alpha + R}{H_T \sin \theta + (2R + E) \cos \theta} \times m_o \times g \quad [N]$$

where

T_A : Tensile force of the turnbuckle taking (A) as the supporting point.

T_B : Tensile force of the turnbuckle taking (B) as the supporting point.

H_G : Gravity height, $H_G = 997$ [mm]

H_T : Height to the center of the eye-plate, $H_T = 1320$ [mm]

R : Outer radius of the packaging, $R = 420$ [mm]

E : Length where the eye-plate is fixed: $E = 50$ [mm]

θ : Angle of the turnbuckle, $\theta = 15^\circ$

α : Direction angle of the eye-plate, $\alpha = 45^\circ$

m_o : Weight of the package, $m_o = 950$ [kg]

g : Gravitational acceleration, $g = 9.81$ [m/s²]

The following equations are given,

$$T_A = \frac{2 \times 997 + 420}{2 \times 1320 \times \sin 15^\circ \cdot \sec 45^\circ + 2 \cos 15^\circ \{420(1 + \cos 45^\circ) + 50 \times \cos 45^\circ\}} \times 950 \times 9.81 = 9.30 \times 10^3 \quad [N]$$

$$T_B = \frac{3 \times 997 \times \cos 45^\circ + 420}{1320 \times \sin 15^\circ + (2 \times 420 + 50) \cos 15^\circ} \times 950 \times 9.81 = 1.97 \times 10^4 \quad [N]$$

Therefore, the tensile force is greater when point (B) is taken as the supporting point

$$T = T_B = 1.97 \times 10^4 \quad [N]$$

Thus, the stress analysis is conducted at this load level.

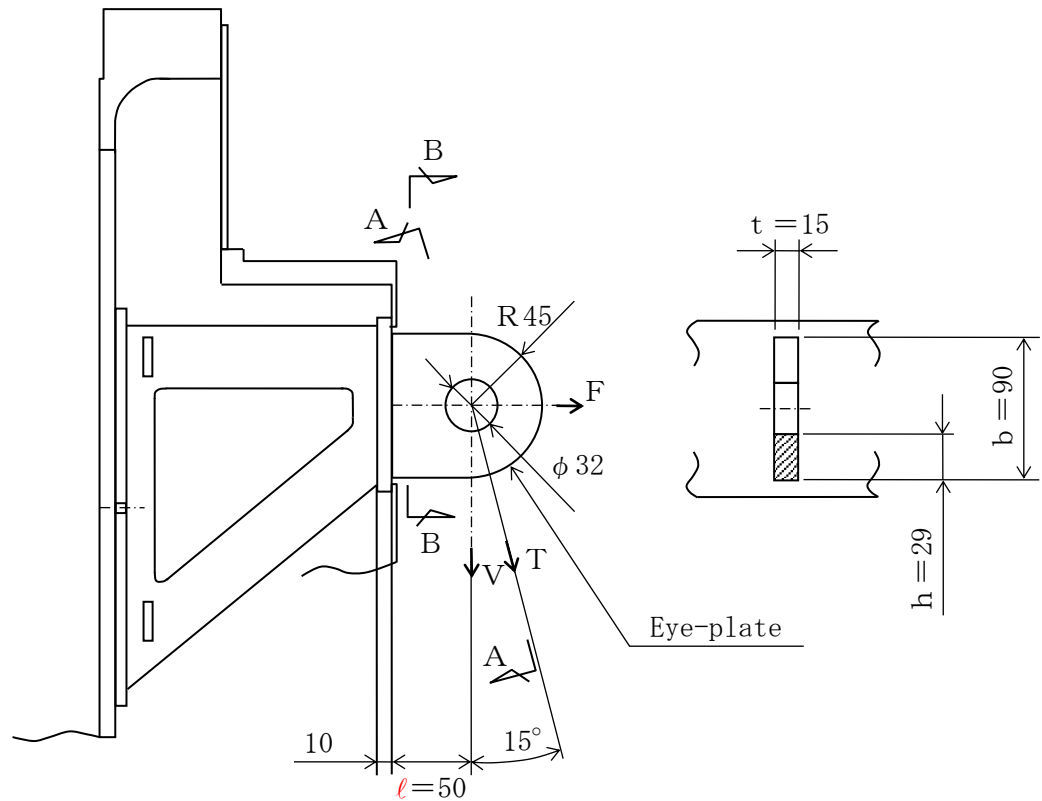
The following equations demonstrate the horizontal and the vertical components of force (F and V) when the eye-plate of the packaging receives the maximum tensile force T from the tie-down turnbuckle during transport.

$$T = 1.97 \times 10^4 \text{ [N]}$$

$$F = T \cdot \sin \theta = 1.97 \times 10^4 \times \sin 15^\circ = 5.10 \times 10^3 \text{ [N]}$$

$$V = T \cdot \cos \theta = 1.97 \times 10^4 \times \cos 15^\circ = 1.90 \times 10^4 \text{ [N]}$$

The analytical model for this case is displayed in (II)-Fig.A.12



(II)-Fig.A.12 Analytical model for eye-plate

The following is an analysis of the stress generated in each cross section when the directional load of the turnbuckle $T = 1.97 \times 10^4$ [N] is applied to the eye-plate as indicated in (II)-Fig. A. 12.

(1) A-A cross section

The following equation demonstrates the shearing stress τ (N/mm²) generated in the shaded portion (A-A cross section) of the eye-plate shown in (II)-Fig. A. 12.

$$\tau = \frac{T}{A} = \frac{T}{t \cdot h}$$

where

τ : shearing stress [N/mm²]

T: maximum load, $T = 1.97 \times 10^4$ [N]

t: board thickness, $t = 15$ [mm]

h: height, $h = 29$ [mm]

Therefore

$$\tau = \frac{1.97 \times 10^4}{29 \times 15} = 45.3 \quad [\text{N/mm}^2]$$

It is less than the design standard value allowable correspond to shearing strength ($0.6S_y = 108 \text{ N/mm}^2$ of the eye-plate material (SUS 304).

The margin of safety MS is

$$MS = \frac{0.6S_y}{\tau} - 1 = \frac{108}{45.3} - 1 = 1.38$$

(2) B-B cross section

The following equation demonstrates the bending stress σ_b (N/mm²) generated in the fixed part (B-B cross section) of the eye-plate shown in (II)-Fig. A. 12.

$$\sigma_b = \frac{M}{Z} = \frac{V \cdot l}{tb^2 / 6}$$

where

M: bending moment [N·mm]

z: section modulus [mm³]

V: vertical component force, $V=1.90 \times 10^4$ [N]

t: eye-plate board thickness, $t=15$ [mm]

l: moment arm, $l=50$ [mm]

b: eye-plate width, $b=90$ [mm]

Therefore,

$$\sigma_b = \frac{1.90 \times 10^4 \times 50}{15 \times 90^2 / 6} = 46.9 \quad [\text{N/mm}^2]$$

is obtained, and it is less than Yield point of the design ($S_y=180\text{N/mm}^2$) of the eye-plate material (SUS 304).

The margin of safety MS is

$$MS = \frac{S_y}{\sigma_b} - 1 = \frac{180}{46.9} - 1 = 2.83$$

The shearing stress τ generated in the B-B cross section is given by the following equation:

$$\tau = \frac{V}{A} = \frac{V}{t \times b} = \frac{1.90 \times 10^4}{15 \times 90} = 14.1 \quad [\text{N/mm}^2]$$

It is less than the design standard value allowable correspond to shearing stress ($0.6S_y=108\text{N/mm}^2$) of the eye-plate material (SUS 304).

The margin of safety (MS) is

$$MS = \frac{0.6S_y}{\tau} - 1 = \frac{108}{14.1} - 1 = 6.65$$

The composite stress σ (N/mm²) of the bending stress σ_b (N/mm²) mentioned above and the shearing stress is given by the following equation

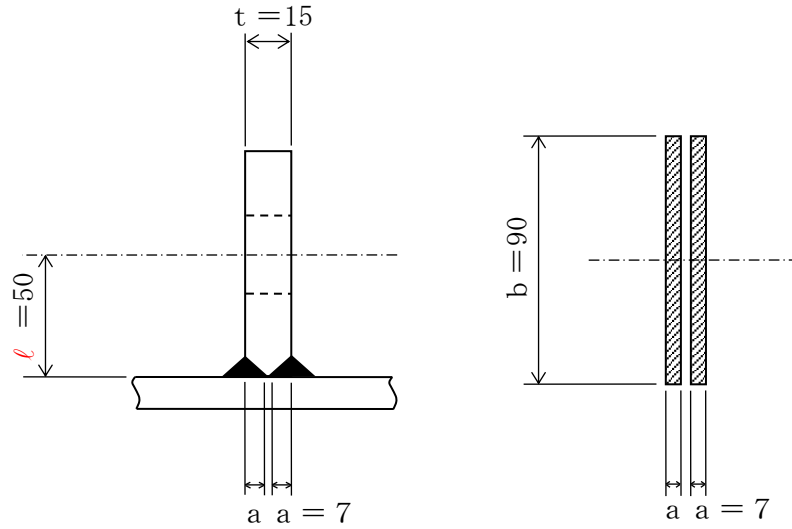
$$\sigma = \sqrt{\sigma_b^2 + 4\tau^2} = \sqrt{46.9^2 + 4 \times 14.1^2} = 54.7 \quad [\text{N/mm}^2]$$

It is less than Yield point of the design ($S_y=180\text{N/mm}^2$) of the eye-plate material (SUS 304).

The margin of safety (MS) is

$$MS = \frac{S_y}{\sigma} - 1 = \frac{180}{54.7} - 1 = 2.29$$

(3) Welded part of B-B cross section



(II)-Fig.A.13 Analytical model for welded part of eye-plate

The following equation demonstrates the bending stress σ_b (N/mm²) generated in the welded part of the fixed part of the eye-plate shown in

(II)-Fig.A.13.

$$\sigma_b = \frac{M}{Z} = \frac{V \cdot l}{Z}$$

where

Z: Section modulus of the welded part,

$$Z = \frac{1}{6} \cdot 2a \cdot b^2 \quad [\text{mm}^3]$$

a: Throat depth, $a = 7$ [mm]

b: Board width, $b = 90$ [mm]

Therefore, σ_b is

$$\sigma_b = \frac{1.90 \times 10^4 \times 50}{\frac{1}{6} \times 2 \times 7 \times 90^2} = 50.3 \quad [\text{N/mm}^2]$$

This is less than the design standard value ($0.45S_y = 81.0 \text{ N/mm}^2$) of the welded part.

The margin of safety (MS) is

$$MS = \frac{0.45S_y}{\sigma_b} - 1 = \frac{0.45 \times 180}{50.3} - 1 = 0.61$$

The shearing stress τ generated at the welded part of the B-B cross section is given by the following equation

$$\tau = \frac{V}{A} = \frac{V}{2a \cdot b} = \frac{1.90 \times 10^4}{2 \times 7 \times 90} = 15.1 \quad [N/mm^2]$$

This is less than the design standard value allowable correspond to shearing stress ($0.45 \times 0.6 \times S_y = 48.6 N/mm^2$) of the welded part.

The margin of safety (MS) is

$$MS = \frac{0.45 \times 0.6 \times S_y}{\tau} - 1 = \frac{0.45 \times 0.6 \times 180}{15.1} - 1 = 2.21$$

The composite stress σ (N/mm^2) of the bending stress σ_b and the shearing stress τ is given by the following equation

$$\sigma = \sqrt{\sigma_b^2 + 4 \cdot \tau^2} = \sqrt{50.3^2 + 4 \times 15.1^2} = 58.7 \quad [N/mm^2]$$

This is less than the design standard value ($0.45S_y = 81.0 N/mm^2$) of the welded part.

The margin of safety (MS) is

$$MS = \frac{0.45S_y}{\sigma} - 1 = \frac{0.45 \times 180}{58.7} - 1 = 0.37$$

A summary of the results of the above-mentioned analyses is given in (II)-Table A.9.

As shown in (II)-Table A.9, the margin of safety (MS) of the results of the analyses being positive in each case, the eye-plate is sound when tied down.

(II)-Table.A.9 Summary of analyses under routine transport

Conditions	Analysis item		Type of load	Design standard	The design standard value [N/mm ²]	Analysis result [N/mm ²]	Margin of safety MS
Routine transport	<u>Hoisting accessory</u>		Weight of the package×3	0.6Sy	108	16.1	5.70
	1.Eye-plate during hoisting						
	A-A cross section	(1)Shearing stress					
	B-B cross section	(1)Bending stress (2)Shearing stress (3)Composite stress		Sy 0.6Sy Sy	180 108 180	17.3 5.18 20.2	9.40 19.8 7.91
	B-B cross section (welded part)	(1)Bending stress (2)Shearing stress (3)Composite stress		0.45Sy 0.27Sy 0.45Sy	81.0 48.6 81.0	18.5 5.55 21.6	3.37 7.75 2.75
	<u>Tightening device</u>		Acceleration	0.6Sy	108	45.3	1.38
	2.Eye-plate in tie-down position						
	A-A Cross section	(1)Shearing stress					
	B-B cross section	(1)Bending stress (2)Shearing stress (3)Composite stress		Sy 0.6Sy Sy	180 108 180	46.9 14.1 54.7	2.83 6.65 2.29
	B-B cross section (welded part)	(1)Bending stress (2)Shearing stress (3)Composite stress		0.45Sy 0.27Sy 0.45Sy	81.0 48.6 81.0	50.3 15.1 58.7	0.61 2.21 0.37

A.4.6 Pressure

We shall analyze the soundness and sealing performance of the packaging in the case where external pressure would decrease to 60 kPa

When external pressure decreases to 60 kPa, the pressure in the inner shell is

$$P_2 = P_0 - P_a = 0.1013 - 0.060 = 0.0413 \text{ [MPa]}$$

where

P_0 : Inner shell initial internal pressure (atmospheric pressure), $P_0 = 0.1013$ [MPa]

P_a : External pressure after pressure decrease, $P_a = 0.060$ [MPa]

For purposes of stress evaluation, in A.5.1.3 Stress Calculation, the internal pressure utilized in the packaging is 9.81×10^{-2} MPa. In this section, we will analyze the internal pressure, utilizing the total of differential pressure

$$P = P_1 + P_2 = 0.0981 + 0.0413 \doteq 0.140 \text{ [MPa]}$$

The stress evaluation parts and the analysis method are the same as in section A.5.1.3 and the results of the stress evaluation are shown in (II)-Table A.10.

(II) -Table A.10 Stresses evaluation under changed pressure

Stress units
;N/mm²

No.	Stress Position to be evaluated		Stress at initial clamping	Stress due to internal pressure	Stress due to thermal expansion	Primary stress						Primary+secondary stress			Fatigue								
						Pm (PL)	Sm	MS	PL+Pb	1. 5Sm	MS	PL+Pb +Q	3Sm	MS	PL+Pb +Q+F	Sa	N	Na	DF	MS			
1	Frame of Inner shell		σ_r	—	-0. 070	—	3. 36	137	39. 7	—	—	—	3. 36	411	121	3. 36	1. 68	500	min 10 ⁶	5×10 ⁻⁴	2×10 ³		
			σ_θ																			3. 29	
			σ_z																			1. 65	
2	Bottom plate of the inner shell		Inner Surface	—	4. 53	—	0. 140	137	977	4. 67	205	42. 8	4. 67	411	87. 0	4. 67	2. 34	500	min 10 ⁶	5×10 ⁻⁴	2×10 ³		
																						σ_θ	1. 36
																						σ_z	-0. 140
			Outer Surface	—	-4. 53	—																	
																						σ_θ	-1. 36
																						σ_z	0
3	Inner shell lid		Inner Surface	—	-4. 66	—	0. 140	2/3Sy 458	3270	4. 66	Sy 687	146	4. 66	Sy 687	146	4. 66	2. 33	500	min 10 ⁶	5×10 ⁻⁴	2×10 ³		
																						σ_θ	-4. 66
																						σ_z	-0. 140
			Outer Surface	—	4. 66	—																	
																						σ_θ	4. 66
																						σ_z	0
4	Inner shell lid clamping bolt	σ_t	174	4. 59	—	180	Sy/1. 5 459	1. 55	—	—	—	180	Sy 688	2. 82	720*	360	500	4000	0. 125	7. 0			
5	Displacement of the inner lid O-ring	(1) Displacement $\mu=1.72\times10^{-2}$ mm (2) Initial clamping value of the O-ring $\delta\approx1.1$ mm (3) Residual margin of tightening of O-ring $\Delta t=\delta-\mu\approx1.082$ mm																					

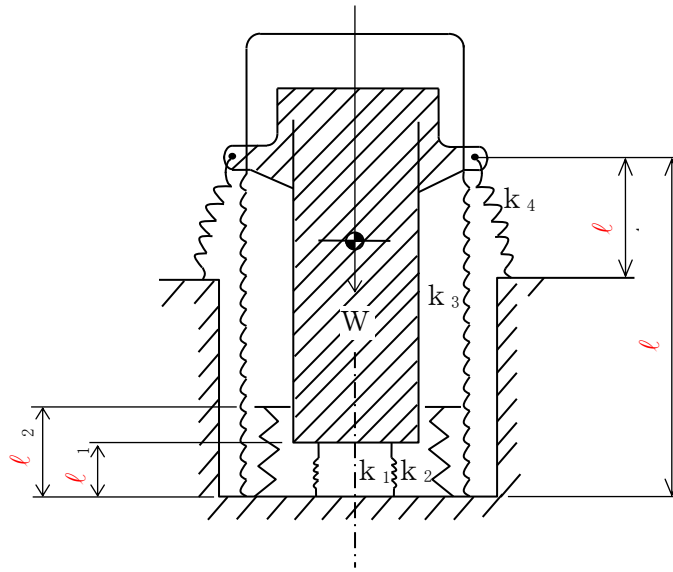
Pm; General primary membrane stress; PL; Local primary membrane stress; Pb; Primary bending stress; Q; Secondary stress; F; Peak stress; Sa; Repeated peak stress;
 N; Number of uses; σ_t ; Ability of bolt stress; Na; Permissible number of repetition; DF; Cumulative fatigue coefficient; Sm; Design stress intensity value;
 Sy; Yield point of the design; MS; Margin of safety; *; Stress concentration factor = 4; σ_r ; Diameter direction stress; σ_θ ; Periphery direction stress; σ_t ; Axial stress;

A. 4. 7 Vibration

This package is secured with a turnbuckle on a tightening device, as indicated in (I)-Fig. C. 2. The turnbuckle is safely secured in order to avoid loosening due to vibration from the transport vehicle. Hence, we shall assume that no vibrations will be caused by this. Below, we shall calculate the natural frequency of the package itself, which will be compared to the vibration caused by the vehicle or ship of transport, and demonstrate that this will not cause the package to resonate during transport.

(1) Vibrations of the packaging

(II)-Fig. A. 14 shows an analytical model for the vibration of the packaging.



(II)-Fig. A. 14 Vibration analytical model of packaging

As is indicated in (II)-Fig.A.14, by assuming that the packaging is a mass system supported by four types of parallel springs, the natural frequency at that time can be given by the following equation ^[8] :

$$\omega_0 = \sqrt{\frac{K}{m}} \times 10^3 \quad [\text{rad/sec}]$$

Therefore,

$$f_0 = \frac{\omega_0}{2\pi} = \frac{1}{2\pi} \sqrt{\frac{K \times 10^3}{m}} \quad [\text{Hz}]$$

where

ω_0 : Natural angular frequency of the packaging $[\text{rad/sec}]$

f_0 : Natural frequency of the packaging $[\text{Hz}]$

m : Package mass, $m=950$ $[\text{kg}]$

K : Parallel spring constant $[\text{kg/mm}]$

$$\begin{aligned} K &= \sum_{i=1}^4 k_i = K_1 + K_2 + K_3 + K_4 \\ &= \sum_{i=1}^4 \frac{A_i E_i}{l_i} = \frac{A_1 E_1}{l_1} + \frac{A_2 E_2}{l_2} + \frac{A_3 E_3}{l_3} + \frac{A_4 E_4}{l_4} \end{aligned}$$

A_1 : Cross section of the reinforcement, $A_1 = 2.83 \times 10^3$ $[\text{mm}^2]$

A_2 : Cross section of the balsa, $A_2 = 4.76 \times 10^5$ $[\text{mm}^2]$

A_3 : Cross section of the outer shell board, $A_3 = 7.92 \times 10^3$ $[\text{mm}^2]$

A_4 : Cross section of the turnbuckle, $A_4 = 2.83 \times 10^3$ $[\text{mm}^2]$

E_1 : Modulus of longitudinal elasticity of the reinforcement;

$$E_1 = 1.92 \times 10^5 \quad [\text{N/mm}^2]$$

E_2 : Modulus of longitudinal elasticity of the balsa, $E_2 = 98.1$ $[\text{N/mm}^2]$

E_3 : Modulus of longitudinal elasticity of the outer shell board,

$$E_3 = 1.92 \times 10^5 \quad [\text{N/mm}^2]$$

E_4 : Modulus of longitudinal elasticity of the turnbuckle,

$$E_4 = 2.04 \times 10^5 \quad [\text{N/mm}^2]$$

l_1 : Length of the reinforcement, $l_1 = 194$ $[\text{mm}]$

l_2 : Length of the balsa, $l_2 = 341$ $[\text{mm}]$

l₃ : Length of the outer shell board, l₃ =1320 [mm]

l₄ : Length of turnbuckle, l₄ =470 [mm]

Therefore,

k₁ : Spring constant of the reinforcement, k₁ =2.79×10⁶ [N/mm]

k₂ : Spring constant of the balsa, k₂ =0.137×10⁶ [N/mm]

k₃ : Spring constant of the inner shell board, k₃ =1.15×10⁶ [N/mm]

k₄ : Spring constant of the turnbuckle, k₄ =1.23×10⁶ [N/mm]

$$K=(2.79+0.14+1.15+1.23) \times 10^6 =5.31 \times 10^6$$

Therefore, the natural frequency is

$$f_0 = \frac{1}{2\pi} \sqrt{\frac{5.31 \times 10^6 \times 10^3}{950}} = 377 \text{ [Hz]}$$

This natural frequency of 377 Hz is outside the vibration range of 0 to 50 Hz which will present in the vehicle or ship during transport. Therefore, there is no possibility of coincidental vibration.

(2) Fuel basket

The fuel basket is supported by a spacer in the inner shell, and will not receive directly any external vibration.

The fuel element is also protected at top and bottom by a silicone foam spacer, and will not receive any vibrations.

(3) Evaluation

The natural frequency of this packaging is higher than the vibration generated by the transport vehicle, and so, coincidental resonance will not occur.

Therefore, the inner lid clamping bolt and other clamping devices will not loosen during transport, and sealing performance will be fully preserved.

In addition, the fuel basket and the fuel element are supported by rubber inside the inner shell, and soundness will be fully preserved despite the vibrations during transport.

A.5 Normal test conditions

This package is a BU type package. Therefore, the normal test conditions defined on the regulation are as follows.

(1) Water spray test

The following tests shall be performed after test (1).

(2) Free drop test

(3) Stacking test

(4) Penetration test

The following test shall be performed after tests (1) to (4).

(5) One week period placed in an environment of -40°C to 38°C .

The following section will analyze the effect to the package caused by the tests mentioned above. The results of this analysis shall demonstrate that the design standards for normal test conditions are satisfied.

A.5.1 Thermal test

A.5.1.1 Outline of temperature and pressure

This section is a summary of the pressure and temperature used for design analysis under normal test conditions.

(1) Design temperature

As determined in (II)-B.4.2 Maximum Temperature, the package temperature may rise to a maximum of 65°C . Therefore, the design temperature under normal test conditions shall be conservatively determined to be 75°C , adopting a margin of safety, as indicated in (II)-Table A.11, for both the inner and outer shells.

(II)-Table A.11 Design temperature under normal test conditions

No.	Part	Design temperature($^{\circ}\text{C}$)
1	Fuel element	75
2	Fuel basket	75
3	Inner shell main body	75
4	Inner lid	75
5	Outer shell	75

(2) Design pressure

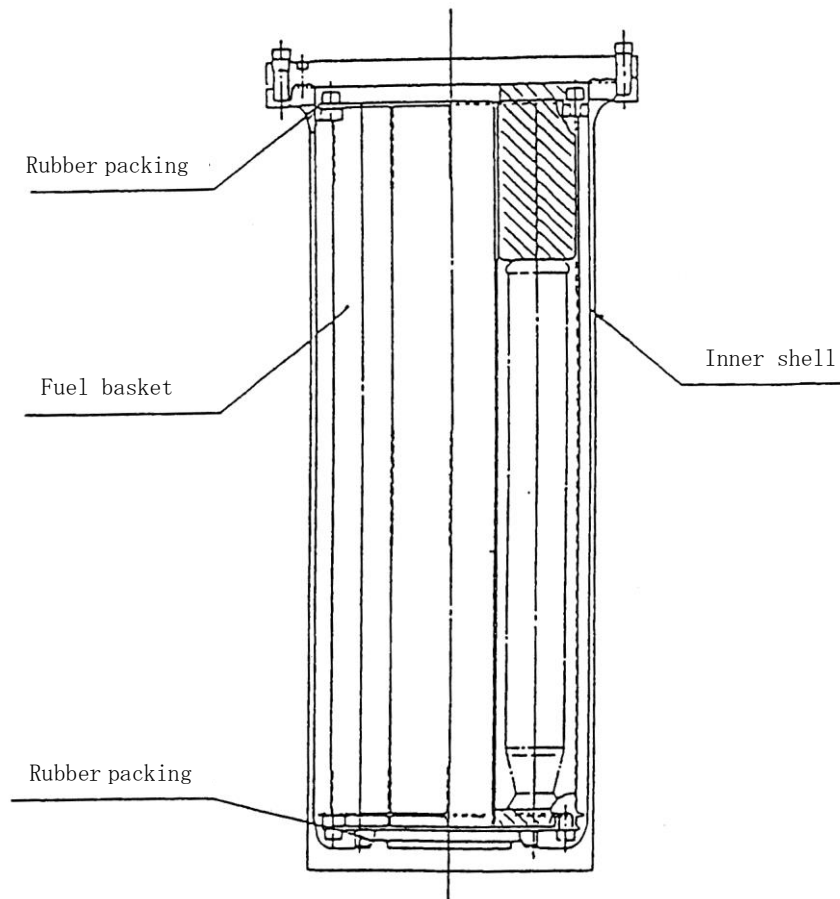
As determined in (II)-B.4.4 Maximum Internal Pressure, the internal pressure of the inner shell may increase up to 0.016 MPa in gauge pressure. Therefore, the design pressure in normal test conditions shall be conservatively determined as 0.0981 MPa, adopting a margin of safety, as indicated in (II)-Table A.12.

(II)-Table A.12 Design pressure under normal test conditions

No.	Portion	Design pressure
1	In the inner shell	$9.81 \times 10^{-2} \text{MPa} \cdot \text{G}$

A.5.1.2 Thermal expansion

This section will assess the stress generated when differential thermal expansion causes the inner shell and fuel basket to come into contact. The analytical model is shown in (II)-Fig.A.15



(II)-Fig.A.15 Analytical model of thermal expansion

The increase in temperature in the fuel basket and the inner shell is 75°C , as indicated in (II)-B Thermal Analysis. There is no temperature difference, where thermal expansion does not occur, since the two parts are made of the same material (SUS 304).

There is also practically no temperature difference between the outer and inner shells. The inner shell will not be influenced by thermal expansion of the outer shell.

Therefore, no stress will be generated by thermal expansion in the fuel basket and inner shell.

A.5.1.3 Stress calculation

Stress calculation shall be conducted in this section.

Temperature gradient, loads from the outside and pressure may generate stress in each part of the package.

The ratio of the inner shell's inner radius to the board thickness is higher than 10 and can be considered as a thin cylinder. Therefore, temperature differences will little occur inside the board thickness of the shell. Also, although the inner lid and the bottom plate of the inner shell are thicker than the other parts, temperature differences will have little possibility of occurring since these parts are protected by heat insulators and shock absorbers, as in the outer lid.

The same applies to the fuel basket, where the board thickness is 3 or 3.4mm. This thinness will make it improbable for temperature differences to occur.

Therefore, since the thermal stress due to temperature differences in the plate thickness of the parts of the packaging is minimal, this stress is not calculated in this section.

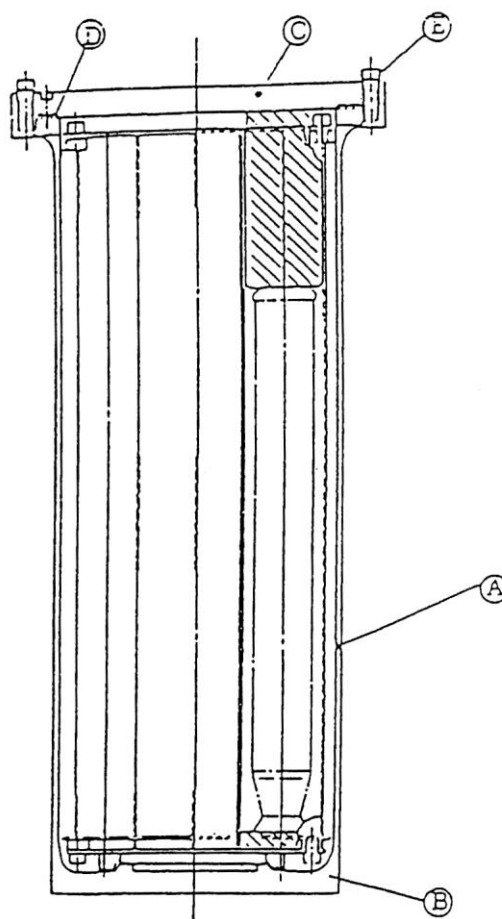
Next, we shall analyze the stress generated in each part by internal pressure, keeping in mind the fact that the internal pressure of the inner shell is the pressure used in the package.

We shall also analyze the inner lid clamping bolt, which is a crucial part in the sealing boundary, after taking into consideration the initial clamping strength and thermal expansion.

(1) Stress evaluation positions

The stress evaluation position of the inner shell under normal test conditions is shown in (II)-Fig. A. 16. In this section, the main stress shall be determined, the different types of stress being shown in (II)-Table A. 13.

A stress evaluation will be conducted in section A. 5. 1. 4.



Code	Evaluation position
Ⓐ	Frame of inner shell
Ⓑ	Bottom plate of inner shell
Ⓒ	Inner lid
Ⓓ	Inner lid O-ring displacement
Ⓔ	Inner lid clamping bolt

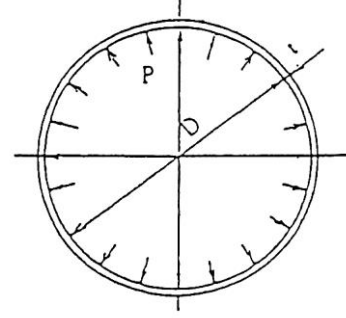
(II)-Fig. A. 16 Stress evaluation position under normal test conditions

Ⓐ Inner shell

In the center of the inner shell, pressure inside the inner shell shall be utilized as internal pressure.

The analytical model of the stress generated in the center of the inner shell which subjected to internal pressure is shown in (II)-Fig.A.17. The stress

(σ_θ , σ_z , σ_r) generated in the center of the shell is given as a thin cylinder by the following equations ^[7]:



(II)-Fig.A.17 Stress analysis model of inner shell center portion

$$\sigma_\theta = \frac{PD_m}{2t}$$

$$\sigma_z = \frac{PD_m}{4t}$$

$$\sigma_r = -\frac{P}{2}$$

where

σ_θ : Circumferential stress [N/mm²]

σ_z : Axial stress [N/mm²]

σ_r : Radial stress [N/mm²]

P: Design pressure inside the inner shell, $P = 9.81 \times 10^{-2}$ [MPa·gauge]

D_m : Frame of inner shell mean diameter, $D_m = D + t = 460 + 10 = 470$ [mm]

t: Frame of inner shell board thickness, $t = 10.0$ [mm]

D: Frame of inner shell bore, $D = 460$ [mm]

Thus, the stresses are

$$\sigma_\theta = \frac{9.81 \times 10^{-2} \times 470}{2 \times 10} = 2.31 \quad [\text{N/mm}^2]$$

$$\sigma_z = \frac{9.81 \times 10^{-2} \times 470}{4 \times 10} = 1.15 \quad [\text{N/mm}^2]$$

$$\sigma_r = -0.0491 \quad [\text{N/mm}^2]$$

Ⓑ Bottom plate of the inner shell

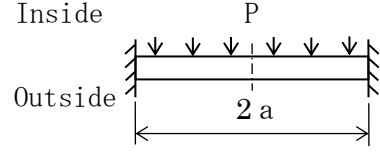
(II)-Fig.A.18 shows an analytical model for the stress on the bottom plate of the inner shell when receiving internal pressure.

The stress σ generated in the fixed part of the peripherally supported disc is,

$$\sigma_{\theta} = \pm 0.225 \frac{P \cdot a^2}{h^2}$$

$$\sigma_r = \pm 0.75 \frac{P \cdot a^2}{h^2}$$

$$\sigma_z = -P \quad (\text{Inner surface})$$



(II)-Fig.A.18 Stress analysis model of inner shell bottom plate

where

$$\sigma_{\theta} : \text{Circumferential stress} \quad [\text{N/mm}^2]$$

$$\sigma_z : \text{Axial stress} \quad [\text{N/mm}^2]$$

$$\sigma_r : \text{Radial stress} \quad [\text{N/mm}^2]$$

P: Design pressure inside the inner shell,

$$P = 9.81 \times 10^{-2} \quad [\text{MPa} \cdot \text{gauge}]$$

a: Radius of inner shell bottom plate, $a = 230$ [mm]

h: Wall thickness of inner shell bottom plate,

$$h = 35 \quad [\text{mm}]$$

Therefore, the stresses are

$$\sigma_{\theta} = \pm 0.225 \frac{9.81 \times 10^{-2} \times 230^2}{35^2} = \pm 0.953 \quad [\text{N/mm}^2]$$

$$\sigma_r = \pm 0.75 \frac{9.81 \times 10^{-2} \times 230^2}{35^2} = \pm 3.18 \quad [\text{N/mm}^2]$$

$$\sigma_z = -0.098 \quad (\text{Inner Surface}) \quad [\text{N/mm}^2]$$

The double signs of the stress values correspond to the inner and outer surface respectively.

© Inner lid

(II)-Fig.A.19 shows an analytical model of the stress on the inner lid when receiving internal pressure.

The stress σ (σ_θ , σ_r , σ_z) generated in the peripherally simply supported disc is maximum at the center

$$\sigma_\theta = \sigma_r = \mp 1.24 \frac{P \cdot a^2}{h^2}$$

$$\sigma_z = -P \quad (\text{Inner surface})$$

where

σ_θ : Circumferential stress [N/mm²]

σ_r : Radial stress [N/mm²]

σ_z : Axial stress [N/mm²]

P: Design pressure inside the inner shell,

$$P = 9.81 \times 10^{-2} \quad [\text{MPa} \cdot \text{gauge}]$$

a: Radius of inner shell bottom plate, a = 285 [mm]

h: Wall thickness of inner shell bottom plate,

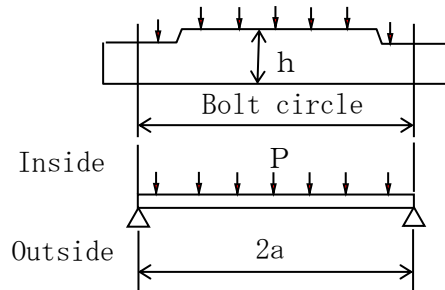
$$h = 55 \quad [\text{mm}]$$

Therefore, the following values are obtained,

$$\sigma_\theta = \sigma_r = \mp 1.24 \frac{9.81 \times 10^{-2} \times 285^2}{55^2} = \mp 3.27 \quad [\text{N/mm}^2]$$

$$\sigma_z = -0.098 \quad (\text{inner surface}) \quad [\text{N/mm}^2]$$

The double sign indicates the inside for the top, the outside for the bottom.



(II)-Fig.A.19 Stress analysis model of inner lid center portion

④ Inner lid O-ring displacement

An analytical model of the inner lid O-ring displacement is shown in (II)-Fig.A.20.

An displacement ω (mm) of the simply supported disc shown in (II)-Fig.A.20 can be determined by the following equations ^[7] :

$$\omega = \frac{P \cdot a^4}{64D} \cdot \left(1 - \frac{r^2}{a^2}\right) \cdot \left(\frac{5+\nu}{1+\nu} - \frac{r^2}{a^2}\right)$$

where

P: Design pressure in the inner shell, $P = 9.81 \times 10^{-2}$ [MPa·gauge]

ν : Poisson's ratio, $\nu = 0.3$

a: Radius of the support points circle of the inner lid, $a = 285$ [mm]

r: Distance from the center to the evaluation point,

ri : radius of inner O-ring groove, $ri = 237.5$ [mm]

D: Inner lid bending stiffness,

$$D = \frac{E \cdot h^3}{12(1-\nu^2)} \quad [N \cdot mm]$$

E: Modulus of longitudinal elasticity

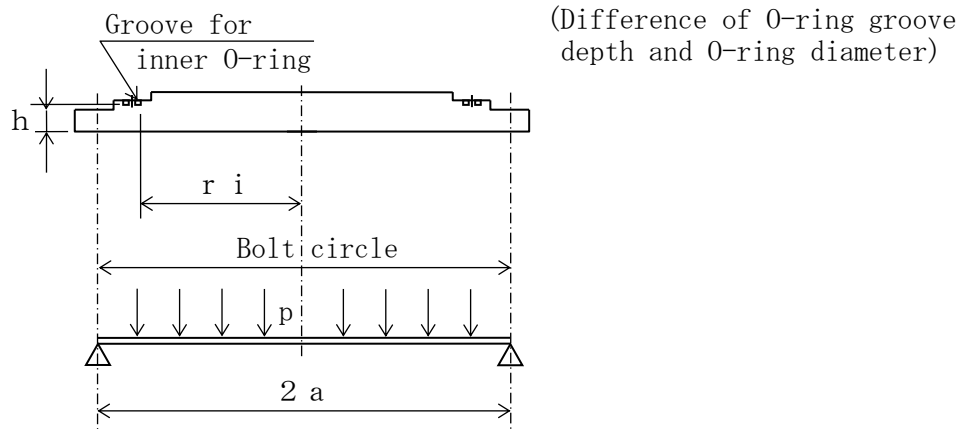
$$E = 1.99 \times 10^5 \quad [N/mm^2]$$

h: Minimum plate thickness of the inner lid, $h = 36.7$ [mm]

Therefore, the displacement ω_i of the groove portion of the inner O-ring is

$$\begin{aligned} \omega_i &= \frac{9.81 \times 10^{-2} \times 285^4 \times 12 \times (1 - 0.3^2)}{64 \times 1.99 \times 10^5 \times 36.7^3} \times \left(1 - \frac{237.5^2}{285^2}\right) \\ &\times \left(\frac{5+0.3}{1+0.3} - \frac{237.5^2}{285^2}\right) = 1.16 \times 10^{-2} \quad [mm] \end{aligned}$$

ω_i is sufficiently smaller than the initial clamping value $\delta \doteq 1.1mm$



(II)-Fig.A.20 Analytical model of inner lid O-ring displacement

⑤ Inner lid clamping bolt

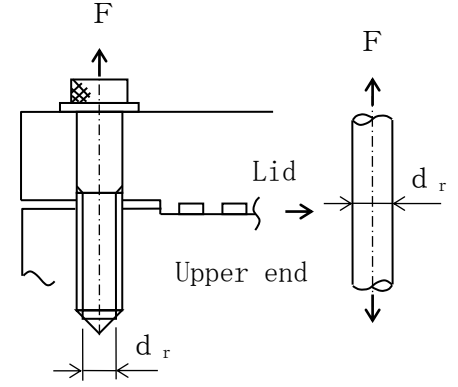
The stress generated by initial clamping stress, internal pressure and thermal expansion shall be analyzed regarding the inner lid clamping bolt (hereinafter referred to as “bolt”).

(a) Initial clamping stress

The analytical model figure of the stress generated by the initial clamping force in the bolt is shown in (II)-Fig.A. 21.

The tensile stress σ_t generated in the bolt as shown in (II)-Fig.A. 21 is given by the equation

$$\sigma_t = \frac{F}{A_i}$$



(II)-Fig.A. 21 Stress analysis model of bolt of inner lid (initial clamping stress)

Where

F : Initial clamping force of the bolt,

$$F = \frac{T}{k \cdot d} = \frac{2.825 \times 10^5}{0.2 \times 24} = 5.89 \times 10^4 \quad [\text{N}]$$

T : Initial clamping torque, $T = 2.825 \times 10^5 \quad [\text{N} \cdot \text{mm}]$

k : Torque coefficient, $k = 0.2$

d : Nominal diameter of the bolt, $d = 24 \quad [\text{mm}]$

A_i : Cross section of the trough radius of the bolt (M24),

$$A_i = \frac{\pi}{4} \cdot d_i^2 = \frac{\pi}{4} \times 20.752^2 = 338.2 \quad [\text{mm}^2]$$

d_i : Minimum diameter of the bolt, $d_i = 20.752 \quad [\text{mm}]$

Therefore, the following value is obtained

$$\sigma_t = \frac{5.89 \times 10^4}{338.2} = 174 \quad [\text{N/mm}^2]$$

(b) Stress due to internal pressure

The analytical model of the stress generated by the internal pressure in the bolt is shown in (II)-Fig A.22.

The tensile stress σ_t generated in the bolt as shown in (II)-Fig.A.22 is given by the following equation

$$\sigma_t = \frac{\pi \cdot r_i^2 \cdot P}{n \cdot A_r}$$

where

r_i : Radius of the surface receiving pressure, $r_i = 237.5$ [mm]

P : Design pressure in the inner shell, $P = 9.81 \times 10^{-2}$ [MPa[gauge]]

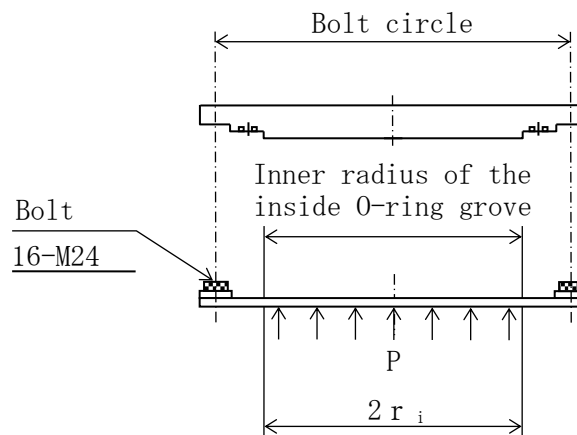
A_r : Cross section of the minimum diameter of the bolt M24,

$A_r = 338.2$ [mm²]

n : Number of bolts, $n = 16$

Therefore, the tensile stress is,

$$\sigma_t = \frac{\pi \times 237.5^2 \times 9.81 \times 10^{-2}}{16 \times 338.2} = 3.21 \text{ [N/mm}^2\text{]}$$

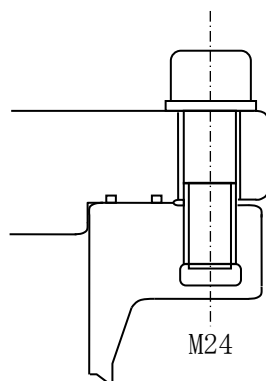


(II)-Fig.A.22 Stress analysis model of bolt of inner lid
(stress due to internal pressure)

(c) Stress due to thermal expansion

The analytical model of the stress generated by thermal expansion in the bolt is shown in (II)-Fig.A. 23.

The temperature of the bolt and of the inner lid is 75°C, in accordance with (II)-B Thermal Analysis, and there is no temperature difference. The material also is the same, the SUS630, Stress due to thermal expansion is negligible.



(II)-Fig.A. 23 Stress analysis model of bolt of inner lid
(stress due to thermal expansion)

A. 5.1.4 Comparison of allowable stress

The results of stress evaluation related to each of the analyses conducted in section (II)-A. 5.1.3 are summarized in (II)-Table A. 13.

As is shown in this table, the margin of safety against the design standard value allocated to each case, whether they are simple or multiple loads, is positive.

Therefore, under normal test conditions (thermal test), the soundness of the package can be maintained.

In addition, in the case where the number of usage of the package is set at 500*, the margin of safety in regard to allowable cycles is, as shown in (II)-Table A. 13, positive. Therefore, the soundness of the packaging will not be lost through repeated loads.

* Times of use $N = 8/\text{year} \times 30 \text{ years} \times \text{tolerance ratio} \doteq 500 \text{ times}$

(II) -Table A.13 Stress evaluation under normal test conditions (thermal test)

Stress units
;N/mm²

No.	Stress Position to be evaluated		Stress at initial clamping	Stress due to internal pressure	Stress due to thermal expansion	Primary stress						Primary+secondary stress			Fatigue																						
						Pm(PL)	Sm	MS	PL+Pb	1.5Sm	MS	PL+Pb +Q	3Sm	MS	PL+Pb +Q+F	Sa	N	Na	DF	MS																	
1	Frame of Inner shell		σ_r	—	-0.0491	—	2.36	137	57.0	—	—	—	2.36	411	173	2.36	1.18	500	min 10 ⁶	5×10 ⁻⁴	2×10 ³																
			σ_θ																			2.31															
			σ_z																			1.15															
2	Bottom plate of the inner shell		Inner Surface	—	3.18	—	0.098	137	1396	3.28	205	61.5	3.28	411	124	3.28	1.64	500	min 10 ⁶	5×10 ⁻⁴	2×10 ³																
					σ_θ																	0.953															
					σ_z																	-0.098															
			Outer Surface	—	-3.18	—																															
					σ_θ																	-0.953															
					σ_z																	0															
			3	Inner shell lid		Inner Surface																—	-3.27	—	0.098	2/3Sy 458	4672	3.27	Sy 687	209	3.27	Sy 687	209	3.27	1.64	500	min 10 ⁶
σ_θ	-3.27																																				
σ_z	-0.098																																				
Outer Surface	—	3.27				—																															
		σ_θ					3.27																														
		σ_z					0																														
4	Inner lid clamping bolt					σ_t	174	3.22	—	177	2/3Sy 458	1.58	—	—	—	177	Sy 687	2.89	708*	354	500	4000	0.125	7.0													
5	Displacement of the inner shell lid O-ring		(1) Displacement $\mu=1.16\times10^{-2}\text{mm}$ (2) Initial clamping value of O-ring $\delta\cong1.1\text{mm}$ (3) Compression depth of O-ring $\Delta t=\delta-\mu\cong1.088\text{mm}$																																		

Pm; General primary membrane stress; PL; Local primary membrane stress; Pb; Primary bending stress; Q; Secondary stress; F; Peak stress; Sa; Repeated peak stress;
 N; Number of uses; σ_t ; Ability of bolt stress Na; Permissible number of repetition; DF; Cumulative fatigue coefficient; Sm; Design stress intensity value;
 Sy; Yield point of deesign; MS; Margin of safety; *; Stress concentration factor = 4 σ_r ; Diameter direction stress σ_θ ; Periphery direction stress

A.5.2 Water spray

The outside surface of this packaging is made of stainless steel, and there is no water absorption. Therefore, there is no possibility of degradation of the material due to the spraying of water.

In addition, the outer lid is secured to the main body with a outer lid clamping bolt using a washer. This is waterproof and presents no risks of water entering inside the packaging.

A.5.3 Free drop

The weight of this package is maximum 950 kg. Since it is below 5000 kg, the free drop height under normal test conditions is determined by regulation standards as 1.2 m.

The free drop posture is analyzed for the following four cases:

- 1) Horizontal drop
- 2) Vertical drop (lid side and bottom side)
- 3) Corner drop (lid side and bottom side)
- 4) Inclined drop (lid side and bottom side)

The purposes of this analysis are,

- 1) To demonstrate that the sealing performance of the inner shell is preserved by demonstrating that the deformation wrought by a free drop do not extend to the inner shell which is the sealing boundary.
- 2) The inner shell will not be damaged by the shock caused by the free drop, and will preserve full leak tightness.
- 3) There is no damage of the contained material.

(1) Analysis method

The following are the analysis conditions for the stress generated in the contained material, the fuel basket, the main body of the packaging and for the deformation of the transport packaging in the case where the package would

be subjected to a free drop test of 1.2m.

(a) Deformation

1) The drop energy of the package will be completely absorbed by the shock absorber in the case where the shock surface is a rigid body. Therefore, the deformation of the outer shell will be the deformation of the shock absorber.

This is conservative assumption ignoring absorption by the steel plate or the heat insulator.

2) The deformation and acceleration caused by the shock absorber shall be calculated on the basis of the shock absorbing function analysis program "CASH-II" indicated in A.10.1.

(b) Stress

1) The drop energy of the package shall be absorbed by the deformation of the steel plate utilized in the shock absorber, the main body of the outer shell and the outer lid.

2) The acceleration utilized in the stress analysis (hereafter referred to as "design acceleration") shall be 1.2 times the calculation value (acceleration generated in the shock absorber) of "CASH-II" (this value was determined through comparison with test results as indicated in section A.10.1) plus the acceleration of the steel plate.

This is a safety evaluation since the shock strength present in the package will be combined to the acceleration of the shock absorber and the acceleration of the steel plate.

Design acceleration = calculation results of CASH-II \times 1.2
+ acceleration due to steel plate.

3) Generated acceleration of the steel plate will be determined using simplified calculations.

(2) Drop energy

The weight of the package utilized in the analysis is 960 kg as indicated in “A.2 Weight and Center of Gravity.” The drop energy is

$$E_a = E_v = m \cdot g \cdot h$$

where

E_a : Energy absorption of the shock absorber [J]

E_v : Drop energy of the package [J]

m : Package mass, $m=950$ [kg]

h : Drop height, $h=1.20$ [m]

g : Gravitational acceleration, $g=9.81$ [m/s²]

Therefore, the following value is obtained

$$\begin{aligned} E_a = E_v &= 960 \times 9.81 \times 1.2 = 1.12 \times 10^4 \quad [\text{J}] \\ &= 1.12 \times 10^7 \quad [\text{N} \cdot \text{mm}] \end{aligned}$$

(3) Performance of the shock absorbers obtained by means of the CASH-Ⅱ analysis program

The results of the deformation in the shock absorber and of the acceleration through the shock absorbers performance analysis program CASH-Ⅱ are shown in (Ⅱ)-Table A.14.

The acceleration which is 1.2 times the results of the CASH-Ⅱ program utilized in the analysis is also shown in the above table.

(II)-Table A.14 Deformation and acceleration of shock
absorber under normal test conditions

Drop posture			Deformation (mm)	Acceleration (×g)	
				Calculation value	× 1.2
Horizontal			20.9	89.3	107.1
Vertical	Lid side		24.1	58.8	70.5
	Bottom side		18.2	78.9	94.6
Corner	Lid side	27.6° *	58.6	16.3	19.6
	Bottom side	22.8°	50.3	17.3	20.8
Inclined	Lid side	5°	21.5	14.1	16.9
		15°	41.5	13.0	15.6
		30°	60.8	17.1	20.5
		45°	65.8	21.7	26.0
		60°	59.3	25.7	30.8
		75°	46.9	34.5	41.4
		85°	27.4	36.5	43.8
	Bottom side	5°	22.2	5.96	7.15
		15°	40.1	16.8	20.2
		30°	56.2	19.5	23.4
		45°	60.4	22.5	27.0
		60°	61.4	24.9	29.9
		75°	44.4	29.0	34.8
		85°	25.0	30.2	36.2

*: This is the angle of the center line of the package to the drop direction.
(same below)

where

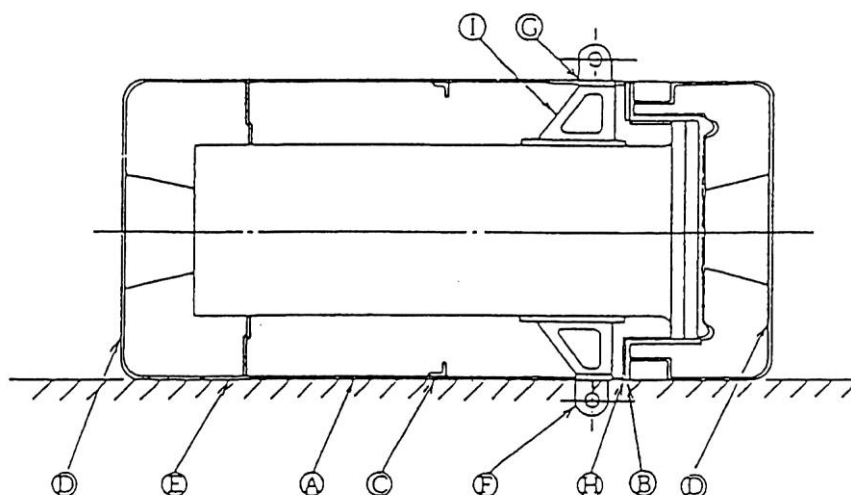
g: Gravitational acceleration, $g = 9.81 \text{ [m/s}^2\text{]}$

(4) Increase in acceleration caused by steel plate

(i) Horizontal drop

We will obtain the increase in acceleration caused by the steel plate during a horizontal drop.

The position of evaluation is shown in (II)-Fig.A.24.

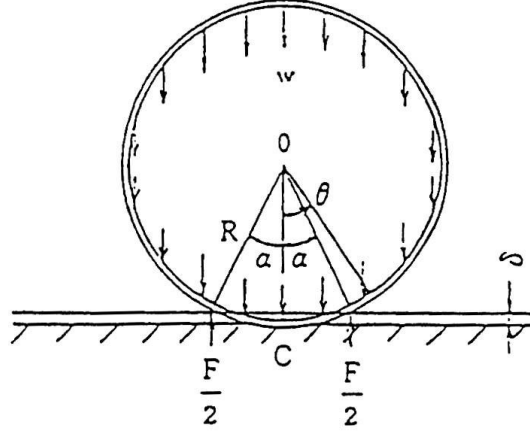


Code	Position of evaluation
Ⓐ	Outside cylinder steel plate
Ⓑ	Outer lid flange
Ⓒ	Stiffening ring
Ⓓ	Outer shell panel
Ⓔ	Partition
Ⓕ	Eye-plate
Ⓖ	Eye-plate fixation plate
Ⓗ	Flange of the main body of the outer shell
Ⓘ	Eye-plate fixation leg

(II)-Fig.A.24 Acceleration evaluation position of steel plate for horizontal drop

① Outside cylinder steel plate

An analytical model of the outside cylinder steel plate as an annulus ring on which the whole weight of the package rests uniformly is shown in (II)-Fig.A. 25.



(II)-Fig.A. 25 Acceleration analysis model of outer shell plate for
horizontal drop

As is indicated in (II)-Fig.A. 25, the bending moment of the annulus ring on which the uniform load w rests, can be given by the following equation.

$$M = wR^2 \left\{ \cos \alpha + \alpha \sin \alpha + \cos \alpha \cdot \sin^2 \alpha + \frac{1}{2} \cos \theta + (\theta - \pi) \sin \theta \right\}$$

In the above equation, M is maximum at $\theta = \alpha$, and the following is obtained,

$$M = wR^2 \left\{ \left(\frac{3}{2} + \sin^2 \alpha \right) \cos \alpha + (2\alpha - \pi) \sin \alpha \right\}$$

When the stress generated by the bending moment becomes equal to the deformation stress σ_s , the maximum resistance force F may be generated.

$$\sigma_s = \frac{M}{Z_p} = \frac{wR^2 \left\{ \left(\frac{3}{2} + \sin^2 \alpha \right) \cos \alpha + (2\alpha - \pi) \sin \alpha \right\}}{Z_p}$$

Therefore, the uniform load w at this time is given by the following

$$W = \frac{\sigma_s \cdot Z_p}{R^2 \left\{ \left(\frac{3}{2} + \sin^2 \alpha \right) \cos \alpha + (2\alpha - \pi) \sin \alpha \right\}}$$

Therefore, the maximum resistance force is the following

$$F = 2\pi wR = \frac{2\pi\sigma_s \cdot Z_p}{R \left\{ \left(\frac{3}{2} + \sin^2 \alpha \right) \cos \alpha + (2\alpha - \pi) \sin \alpha \right\}}$$

where

M: Bending moment of the annulus ring [N·mm]

w: Uniform load [N/mm]

F: Maximum resistance force [N]

R: Radius of the annulus ring, R = 420 [mm]

σ_s : Deformation stress (at ordinary temperatures), $\sigma_s = 520$ [N/mm²]

θ : Arbitrary angle based on OC [rad]

α : Radius of the deformed part,

$$\alpha = \cos^{-1} \left(\frac{R - \delta}{R} \right) = \cos^{-1} \left(\frac{420 - 20.9}{420} \right) = 18.15^\circ = 0.317 \text{ [rad]}$$

δ : Deformation, $\delta = 20.9$ [mm]

Z_p : Plasticity section modulus,

$$Z_p = \frac{1}{4} b h^2 = \frac{1500 \times 3^2}{4} = 3375 \text{ [mm}^3\text{]}$$

b: Annulus ring width, b = 1500 [mm]

h: Annulus ring thickness, h = 3 [mm]

Therefore, the maximum resistance force is,

$$\begin{aligned} F &= \frac{2 \times \pi \times 520 \times 3375}{420 \times \left\{ \left(\frac{3}{2} + \sin^2 18.15^\circ \right) \cos 18.15^\circ + (2 \times 0.317 - \pi) \sin 18.15^\circ \right\}} \\ &= 3.57 \times 10^4 \text{ [N]} \end{aligned}$$

The equation of the increase in acceleration N_{H1} caused by the outside cylindrical steel plate is,

$$N_{H1} = \frac{F}{m} = \frac{3.57 \times 10^4}{950} = 37.6 = 3.83 \cdot g \quad [m/s^2]$$

where

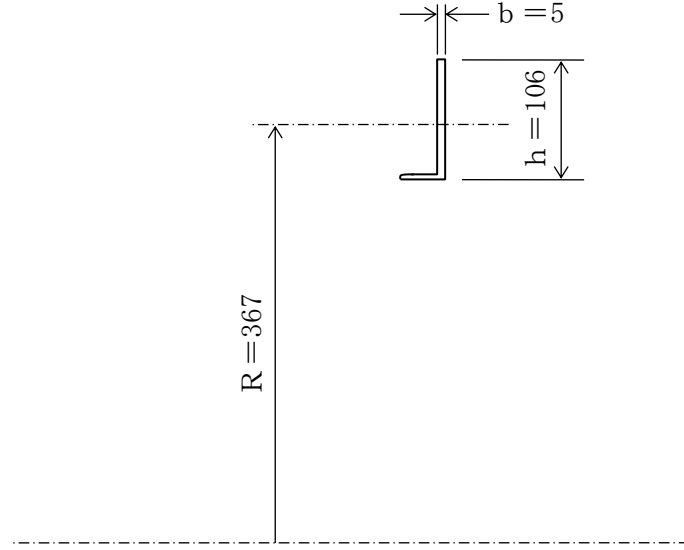
m: Weight of the package, m=950 [kg]

Ⓑ Flange of the outer lid

The analytical model is shown in (II)-Fig.A.25, as with section A.5.3 (4) (i)

Ⓐ . But, since the deformation has not reached the annulus ring, the α in the moment equation is given as 0.

The cross section of the flange of the outer lid is given in (II)-Fig.A.26.



(II)-Fig.A.26 Cross section of outer shell lid flange

The maximum resistance force is given by the following ^[10]

$$F = \frac{4\pi}{3R} \cdot \sigma_s \cdot Z_p = \frac{4 \times \pi}{3 \times 367} \times 520 \times 1.40 \times 10^4 = 8.31 \times 10^4 \quad [\text{N}]$$

where

F: Maximum resistance force [N]

R: Radius of the annulus ring, R = 367 [mm]

σ_s : Deformation stress (at ordinary temperatures), $\sigma_s = 520$ [N/mm²]

Z_p : Section modulus of plasticity,

$$Z_p = \frac{1}{4} b h^2 = \frac{5 \times 106^2}{4} = 1.40 \times 10^4 \quad [\text{mm}^3]$$

b: Annulus ring width, b = 5 [mm]

h: Annulus ring thickness, h = 106 [mm]

Therefore, the increase in acceleration N_{H_2} caused by the flange of the outer

lid is,

$$N_{H_2} = \frac{F}{m} = \frac{8.31 \times 10^4}{950} = 87.5 = 8.92 \cdot g \quad [m/s^2]$$

© Stiffening ring

The analytical model is shown in (II)-Fig.A.25, as with section A.5.3(4)(i)

Ⓐ . The maximum resistance force is given by the following equation ^[10]

$$F = \frac{2\pi\sigma_s \cdot Z_p}{R \left\{ \left(\frac{3}{2} + \sin^2 \alpha \right) \cos \alpha + (2\alpha - \pi) \sin \alpha \right\}}$$

where

F: Maximum resistance force [N]

R: Radius of the annulus ring, R = 406 [mm]

σ_s : Deformation stress (ordinary temperature), $\sigma_s = 520$ [N/mm²]

δ : Deformation amount, $\delta = 6.9$ [mm]

α : Half angle of the deformed part,

$$\alpha = \cos^{-1} \left(\frac{R - \delta}{R} \right) = \cos^{-1} \left(\frac{406 - 6.9}{406} \right) = 10.58^\circ = 0.185 \text{ [rad]}$$

Z_p : section modulus of plasticity [mm³],

$$\begin{aligned} Z_p &= \frac{h}{4} \{ (b-h)^2 + h^2 \} \\ &= \frac{3}{4} \{ (40-3)^2 + 3^2 \} \\ &= 1.03 \times 10^3 \text{ [mm}^3\text{]} \end{aligned}$$

b: Ring width, b = 40 [mm]

h: Ring thickness, h = 3 [mm]

Therefore, F is

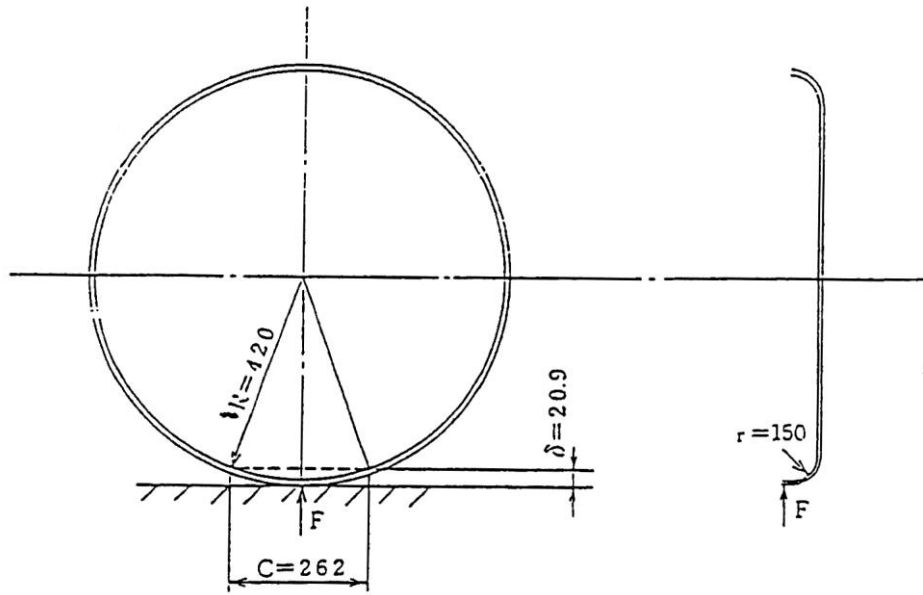
$$\begin{aligned} F &= \frac{2 \times \pi \times 520 \times 1.03 \times 10^3}{406 \times \left\{ \left(\frac{3}{2} + \sin^2 10.58^\circ \right) \cos 10.58^\circ + (2 \times 0.187 - \pi) \times \sin 10.58^\circ \right\}} \\ &= 8.30 \times 10^3 \text{ [N]} \end{aligned}$$

Therefore, the increase in acceleration N_{H3} due to the stiffening ring is

$$N_{H3} = \frac{F}{m} = \frac{8.30 \times 10^3}{950} = 8.74 = 0.891 \cdot g \text{ [m/s}^2\text{]}$$

① Panel of the outer lid

The analytical model is shown in (II)-Fig.A.27.



(II)-Fig.A.27 Acceleration analysis model of outer shell head plate for horizontal drop

As indicated in (II)-Fig.A.27, bending moment is generated by the reaction force of the drop in the outer lid panel at the curved point of the head. When the stress produced by this bending moment becomes equal to the deformation stress σ_s , the maximum resistance force F , assuming that it is generated, is given by the equation

$$F = \frac{\sigma_s}{r} \cdot Z_p = \frac{\sigma_s}{r} \cdot \frac{C \cdot h^2}{4}$$

where

F : Maximum resistance force [N]

σ_s : Deformation stress (room temperature), $\sigma_s = 520$ [N/mm²]

Z_p : Section modulus of plasticity,

$$Z_p = \frac{C \cdot h^2}{4} \quad [\text{mm}^3]$$

C : Shock absorber deformation width, $C = 262$ [mm]

h : Panel thickness, $h = 3$ [mm]

r : Radius of the corner, $r = 150$ [mm]

Therefore, the following equation is given.

$$F = \frac{520}{150} \times \frac{262 \times 3^2}{4} = 2.04 \times 10^3 \quad [\text{N}]$$

Two panels are provided in the packaging, and the increase in acceleration N_{H4} caused by the outer lid panel is

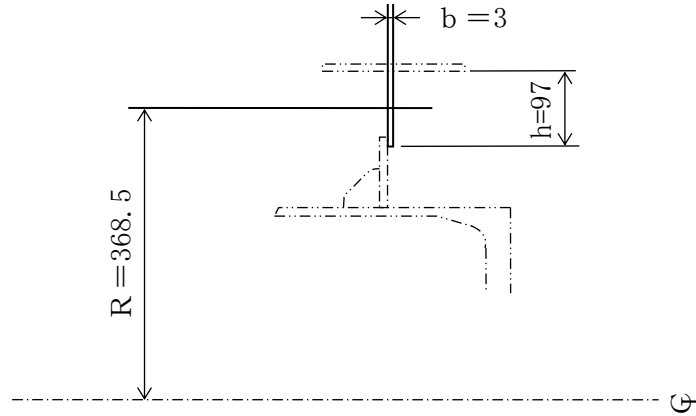
$$N_{H4} = \frac{2 \cdot F}{m} = \frac{2 \times 2.04 \times 10^3}{950} = 4.29 = 0.437 \cdot g \quad [\text{m/s}^2]$$

Ⓔ Partition

The analytical model is shown in (II)-Fig.A.25, as with section A.5.3(4) (i)

Ⓐ .But, since the deformation has not reached the annulus ring, α in the moment equation is given as 0.

The cross section of the partition is given in (II)-Fig.A.28.



(II)-Fig.A.28 Cross section of partition plate

The maximum resistance force is given by the following equation.

$$F = \frac{4\pi}{3R} \cdot \sigma_z \cdot Z_p = \frac{4 \times \pi}{3 \times 368.5} \times 520 \times 7.06 \times 10^3$$

$$= 4.17 \times 10^4 \quad [\text{N}]$$

where

F: Maximum resistance force [N]

R: Radius of the annulus ring, R =368.5 [mm]

σ_z : Deformation stress (at ordinary temperatures), $\sigma_z = 520$ [N/mm²]

Z_p : Plasticity section modulus,

$$Z_p = \frac{1}{4} b \cdot h^2 = \frac{3 \times 97^2}{4} = 7.06 \times 10^3 \quad [\text{mm}^3]$$

b: Annulus ring width, b=3 [mm]

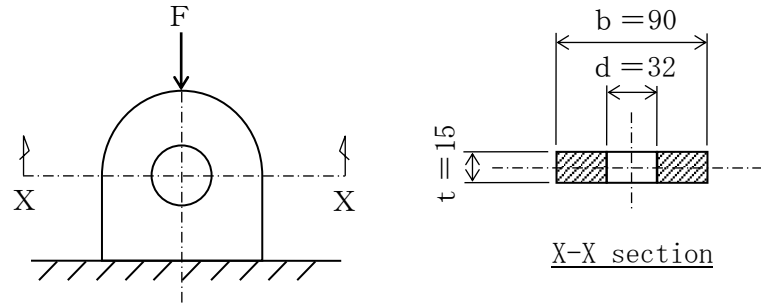
h: Annulus ring thickness, h =97 [mm]

Therefore, the increase in acceleration N_{H5} caused by the partition is obtained by the following.

$$N_{H5} = \frac{F}{m} = \frac{4.17 \times 10^4}{950} = 43.9 = 4.48 \cdot g \quad [m/s^2]$$

⑦ Eye-plate

The analytical model is shown in (II)-Fig.A.29.



(II)-Fig.A.29 Deformation analysis model of eye plate

As is indicated in (II)-Fig.A.29, when the eye-plate is hit by a direct force, maximum compression stress is generated at the cross section X-X. When this stress is equal to the deformation stress σ_s , maximum resistance force F is generated, shown by the following equation

$$F = \sigma_s \cdot A = \sigma_s \cdot (b-d) \cdot t$$

where

F: Maximum resistance force [N]

σ_s : Deformation stress (at room temperatures), $\sigma_s = 520$ [N/mm²]

A: Evaluated cross sectional area [mm²]

b: Eye-plate width, b=90 [mm]

t: Eye-plate board thickness, t=15 [mm]

d: Eye-plate hole radius, d=32 [mm]

Therefore,

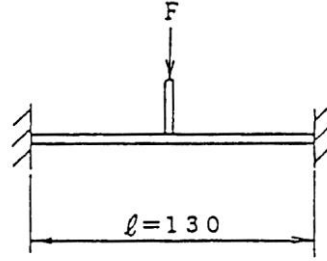
$$F = 520 \times (90 - 32) \times 15 = 4.52 \times 10^5 \quad [N]$$

The increase in acceleration N_{H6} due to the eye-plate is obtained by the following equation.

$$N_{H6} = \frac{F}{m} = \frac{4.52 \times 10^5}{950} = 476 = 48.5 \cdot g \quad [m/s^2]$$

③ Eye-plate fixation plate

The analytical model is shown in (II)-Fig.A. 30.



(Unit: mm)

(II)-Fig.A. 30 Analytical model of eye-plate fixing-plate

As is indicated in (II)-Fig.A. 30, the fixed bridge beams which receive the concentrated load in their center generate maximum bending moments on both extremities.

When this stress is equal to the deformation stress σ_s , maximum resistance force F is generated, shown by the following equation ^[7]

$$F = \frac{8}{1} \cdot \sigma_s \cdot Z_p$$

where

F : Maximum resistance force [N]

σ_s : Deformation stress (at ordinary temperatures), $\sigma_s = 520$ [N/mm²]

Z_p : Plasticity section modulus,

$$Z_p = \frac{1}{4} b \cdot h^2$$

b : Eye-plate width, $b = 110$ [mm]

h : Eye-plate board thickness, $h = 10$ [mm]

l : Distance between fixed points, $l = 130$ [mm]

Therefore,

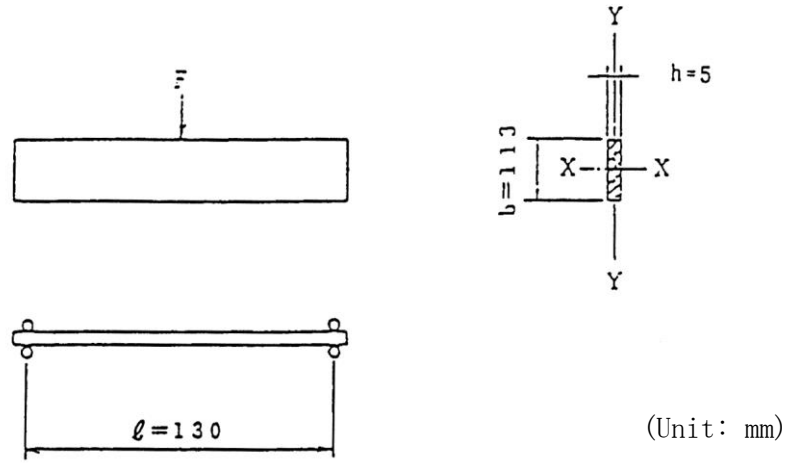
$$F = \frac{8}{130} \times 520 \times \frac{1}{4} \times 110 \times 10^2 = 8.80 \times 10^4 \text{ [N]}$$

The increase in acceleration N_{H7} due to the eye-plate fixation plate is obtained by the following equation

$$N_{H7} = \frac{F}{m} = \frac{8.80 \times 10^4}{950} = 92.6 \text{ [m/s}^2\text{]} = 9.44 \cdot g$$

Ⓗ Flange of the outer shell

The analytical model is shown in (II)-Fig.A. 31.



(II)-Fig.A. 31 Analytical model of flange of outer shell

As indicated in (II)-Fig.A. 31, the fixed beam, having a long thin rectangular cross section, suffers side buckling when receiving the concentrated load on its center. If this buckling load is equal to the maximum resistance force F, it is given by the following equation^[19]

$$F = \frac{16.93 \sqrt{B_y C}}{\ell^2}$$

where

F: Maximum resistance force [N]

ℓ : Distance between supported points, $\ell=130$ [mm]

B_y : Bending rigidity on Y axis,

$$B_y = \frac{1}{12} E b h^3 = \frac{1}{12} \times 1.95 \times 10^5 \times 113 \times 5^3 = 2.30 \times 10^8 \quad [N \cdot mm^2]$$

E: Modulus of longitudinal elasticity (at ordinary temperatures);

$$E = 1.95 \times 10^5 \quad [N/mm^2]$$

h: Flange board thickness, $h=5$ [mm]

b: Flange point width, $b=113$ [mm]

C: Twisting rigidity,

$$\begin{aligned}
C &= \frac{bh^3}{3} \left(1 - 0.630 \frac{h}{b} \right) G \\
&= \frac{113 \times 5^3}{3} \left(1 - 0.630 \times \frac{5}{113} \right) \times 7.51 \times 10^4 \\
&= 3.44 \times 10^8 \quad [N/mm^2]
\end{aligned}$$

G: Modulus of transverse elasticity (at ordinary temperatures);

$$G = 7.51 \times 10^4 \quad [N/mm^2]$$

Therefore, F is

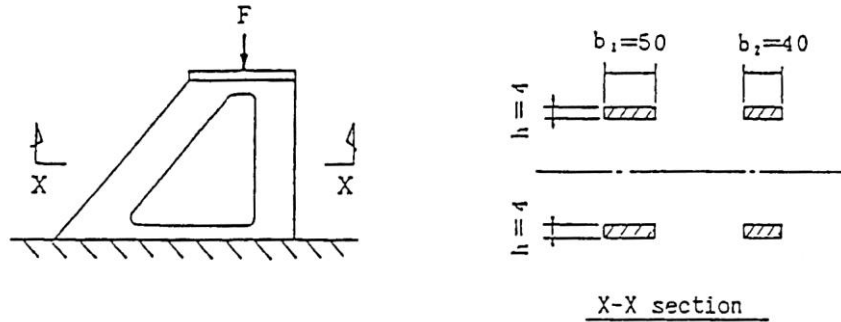
$$F = \frac{16.93 \sqrt{2.30 \times 10^8 \times 3.44 \times 10^8}}{130^2} = 2.82 \times 10^5 \quad [N]$$

The increase in acceleration N_{H8} caused by the flange in the main body of the outer shell is

$$N_{H8} = \frac{F}{m} = \frac{2.82 \times 10^5}{950} = 297 \quad [m/s^2] = 30.3 \cdot g \quad [m/s^2]$$

① Eye-plate fixation lug

The analytical model is shown in (II)-Fig.A.32.



(Unit: mm)

(II)-Fig.A.32 Analytical model of eye-plate fixing lug

As indicated in (II)-Fig.A.32, when the compression stress at the X-X cross section is equal to the deformation stress σ_s , maximum resistance force F is generated and given by

$$F = \sigma_s \cdot A = \sigma_s \cdot 2h \cdot (b_1 + b_2)$$

where

F: Maximum resistance force [N]

σ_s : Deformation stress (at room temperatures); $\sigma_s = 520$ [N/mm²]

A: Evaluated cross sectional area [mm²]

b₁ : Plate width, b₁ = 50 [mm]

b₂ : Plate width, b₂ = 40 [mm]

h: Plate thickness, h = 4 [mm]

Therefore,

$$F = 520 \times 2 \times 4 \times (50 + 40) = 3.74 \times 10^5 \text{ [N]}$$

The increase in acceleration N_{H9} due the eye-plate fixation leg is,

$$N_{H9} = \frac{F}{m} = \frac{3.74 \times 10^5}{950} = 394 = 40.2 \cdot g \text{ [m/s}^2\text{]}$$

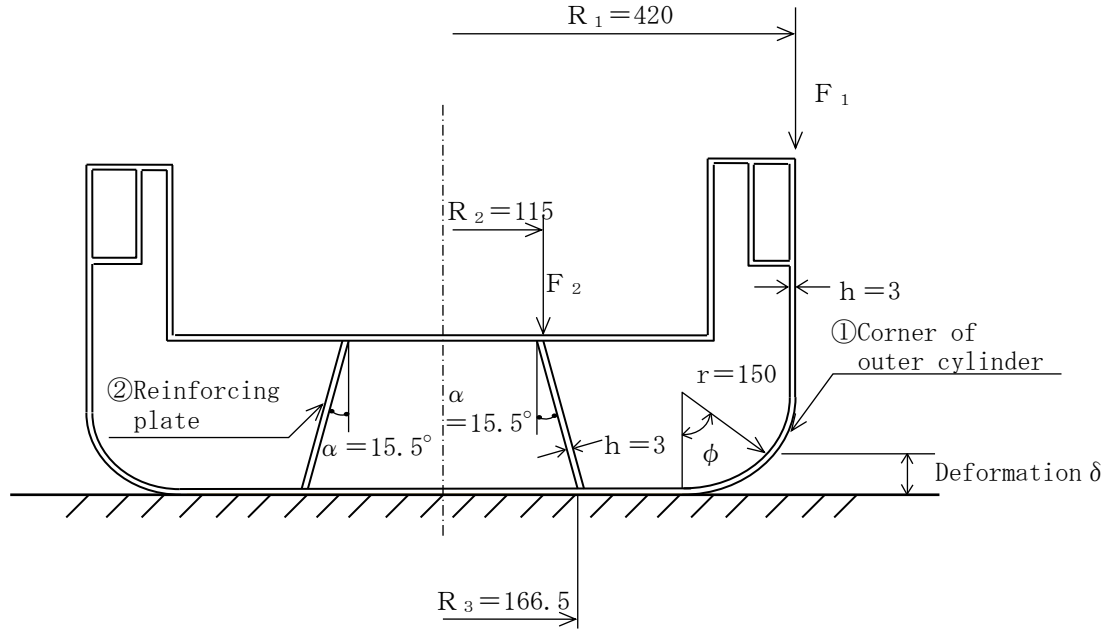
Based on the results mentioned so far, the equation for the total increase in

acceleration caused by the steel plate during the horizontal drop is

$$\begin{aligned}
 N_{\text{H}} &= N_{\text{H1}} + N_{\text{H2}} + N_{\text{H3}} + N_{\text{H4}} + N_{\text{H5}} + N_{\text{H6}} + N_{\text{H7}} + N_{\text{H8}} + N_{\text{H9}} \\
 &= (3.83+8.92+0.891+0.437+4.48+48.5+9.44+30.3+40.2) \times g \\
 &= 147.0 \cdot g \qquad \qquad \qquad [\text{m/s}^2]
 \end{aligned}$$

(ii) Vertical drop

We shall obtain the increase in acceleration caused by the steel plate during a vertical drop. An analytical model is given in (II)-Fig.A. 33.



(II)-Fig.A. 33 Acceleration analysis model of steel plate for vertical drop

As indicated in (II)-Fig.A. 33, the resistance force is the addition of ① the strength F_1 which compresses the outside cylinder corner and ② the strength F_2 which compresses the conical reinforcement plate. The deformation δ of the steel plate is equal to the deformation of the shock absorber indicated in (II)-Table A.14. The resistance forces F_1 and F_2 , which arise when the stress is equal to the deformation stress, can be obtained by the following equations.^[17]

$$F_1 = 2\pi h r \sin 2\phi \cdot \sigma_s$$

$$F_2 = 2\pi h (R_2 + \delta \tan \alpha) \cos \alpha \cdot \sigma_s$$

where

F_1 : Outside cylinder corner resistance force [N]

F_2 : Conical reinforcement plate resistance force [N]

h : Board thickness, h = 3 [mm]

r : Radius of the outside cylinder corner, r = 150 [mm]

ϕ : Angle for deformation σ ,

$$\phi = \cos^{-1} \left(1 - \frac{\delta}{r} \right)$$

δ : deformation, Lid side vertical drop : $\delta_1 = 24.1$ [mm]

Bottom side vertical drop : $\delta_2 = 18.2$ [mm]

$$\phi_1 = \cos^{-1} \left(1 - \frac{24.1}{150} \right) = 32.9^\circ$$

$$\phi_2 = \cos^{-1} \left(1 - \frac{18.2}{150} \right) = 28.5^\circ$$

R_2 : Radius of the upper part of cone,

Lid side vertical drop : $R_2 = 115$ [mm]

Bottom side vertical drop : $R_2 = 113$ [mm]

α : Conical angle, $\alpha = 15.5^\circ$

σ_s : Flow stress (at room temperatures), $\sigma_s = S_u = 520$ [N/mm²]

Therefore, F_1 and F_2 in a lid side vertical drop are as follows,

$$F_1 = 2\pi \times 3 \times 150 \times \sin^2 32.9^\circ \times 520 = 4.34 \times 10^5 \text{ [N]}$$

$$F_2 = 2\pi \times 3 \times (115 + 24.1 \times \tan 15.5^\circ) \times \cos 15.5^\circ \times 520 \\ = 11.49 \times 10^5 \text{ [N]}$$

and in a bottom side vertical drop,

$$F_1 = 2\pi \times 3 \times 150 \times \sin^2 28.5^\circ \times 520 = 3.35 \times 10^5 \text{ [N]}$$

$$F_2 = 2\pi \times 3 \times (113 + 18.2 \times \tan 15.5^\circ) \times \cos 15.5^\circ \times 520 \\ = 11.15 \times 10^5 \text{ [N]}$$

Hence, the acceleration generated by these can be determined by the following equation,

$$N_V = \frac{F}{m} = \frac{F_1 + F_2}{m}$$

In a lid side vertical drop,

$$N_V = \frac{4.34 + 11.49}{950} \times 10^5 = 1.67 \times 10^3 \text{ [m/s}^2\text{]} = 170.2 \cdot g \text{ [m/s}^2\text{]}$$

In a bottom side vertical drop,

$$N_V = \frac{3.35 + 11.15}{950} \times 10^5 = 1.53 \times 10^3 \text{ [m/s}^2\text{]} = 156.0 \cdot g \text{ [m/s}^2\text{]}$$

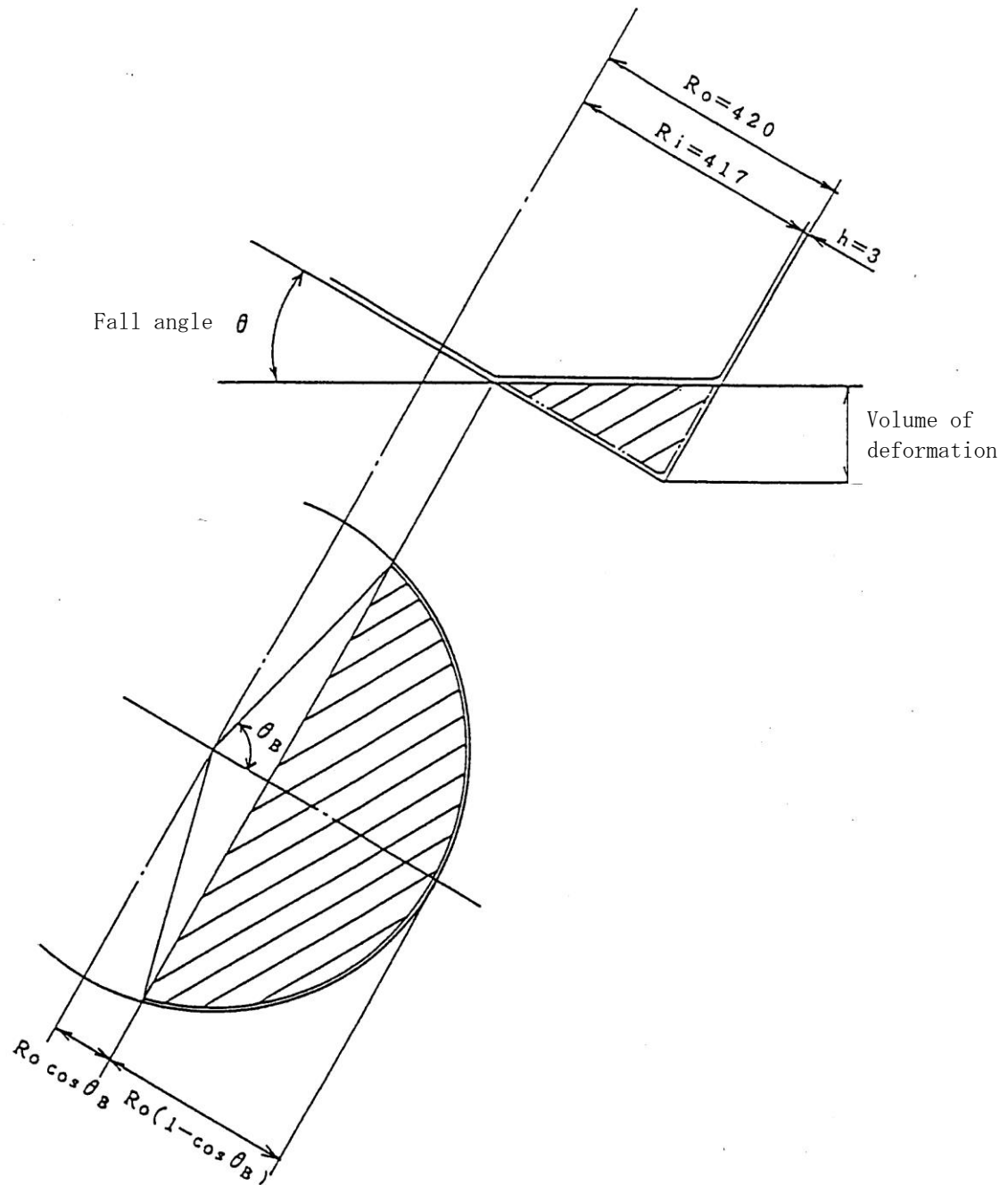
where

g: Gravitational acceleration, $g = 9.81$ [m/s²]

(iii) Corner drop

We shall determine the increase in acceleration caused by the steel plate during a corner drop.

The analytical model is shown in (II)-Fig.A.34.



(II)-Fig.A.34 Acceleration analysis model of steel plate for corner drop.

As indicated in (II)-Fig.A.34, the maximum resistance force caused by the outer steel plate during a corner drop is given by the following^[15]

$$F = \frac{(R_o^3 - R_i^3) \times \tan\theta \times (\theta - \sin\theta_B \cdot \cos\theta_B)}{R_o \times \sin\theta} \times \sigma_s$$

where

F : Maximum resistance force [N]

R_o: Cylindrical steel plate outer radius, R_o = 420 [mm]

R_i: Cylindrical steel plate inner radius, R_i = 417 [mm]

h : Cylindrical steel plate board thickness, h = 3 [mm]

θ : Drop angle

Lid side corner drop: θ = 27.6° = 0.482 [rad]

Bottom side corner drop: θ = 22.8° = 0.398 [rad]

δ : Deformation

Lid side corner drop δ = 58.6 [mm]

Bottom side corner drop δ = 50.3 [mm]

θ_B : Angle

$$\theta_B = \cos^{-1} \left(1 - \frac{\delta}{R_o \sin\theta} \right)$$

Lid side corner drop,

$$\theta_B = \cos^{-1} \left(1 - \frac{58.6}{420 \times \sin 27.6^\circ} \right) = 45.7^\circ = 0.797 \text{ [rad]}$$

Bottom side corner drop,

$$\theta_B = \cos^{-1} \left(1 - \frac{50.3}{420 \times \sin 22.8^\circ} \right) = 46.3^\circ = 0.808 \text{ [rad]}$$

σ_s: Deformation stress (at room temperatures), σ_s = 520 [N/mm²]

Therefore, F is

in the lid side corner drop,

$$F = \frac{(420^3 - 417^3) \times \tan 27.6^\circ \times (0.797 - \sin 45.7^\circ \times \cos 45.7^\circ)}{420 \times \sin 27.6^\circ} \times 520$$

$$= 6.55 \times 10^5 \text{ [N]}$$

and in the bottom side corner drop,

$$F = \frac{(420^3 - 417^3) \times \tan 22.8^\circ \times (0.808 - \sin 46.3^\circ \times \cos 46.3^\circ)}{420 \times \sin 22.8^\circ} \times 520$$

$$= 6.53 \times 10^5 \text{ [N]}$$

Therefore, the acceleration generated by these is given by the following equation.

$$N_c = \frac{F}{m}$$

In the lid side corner drop,

$$N_c = \frac{6.55 \times 10^5}{950} = 689 \text{ [m/s}^2\text{]} = 70.3 \cdot g \text{ [m/s}^2\text{]}$$

and in the bottom side corner drop,

$$N_c = \frac{6.53 \times 10^5}{950} = 687 \text{ [m/s}^2\text{]} = 70.0 \cdot g \text{ [m/s}^2\text{]}$$

(5) Design acceleration

As with the corner drop, we shall determine the acceleration during an inclined drop. This is shown in (II)-Table A.15. In addition, we shall calculate the design acceleration utilized in the drop stress analysis which will be summarized in the same table.

Design acceleration = Calculation results of CASH- II $\times 1.2$ + Acceleration due to steel plate

(II)-Table A.15 Design acceleration under normal test conditions

Drop posture			CASH- II $\times 1.2$	Acceleration due to steel plate ($\times g$)	Design acceleration ($\times g$)
Horizontal			107.1	147.0	254.1
Vertical	Lid side		70.5	170.2	240.7
	Bottom side		94.6	156.0	250.6
Corner	Lid side	27.6°	19.6	70.3	89.9
	Bottom side	22.8°	20.8	70.0	90.8
Inclined	Lid side	5°	16.9	161.7	178.6
		15°	15.6	90.7	106.3
		30°	20.5	67.9	88.4
		45°	26.0	56.3	82.3
		60°	30.8	50.7	81.5
		75°	41.4	58.9	100.3
		85°	43.8	75.6	119.4
	Bottom side	5°	7.15	169.2	176.4
		15°	20.2	86.4	106.6
		30°	23.4	60.5	83.9
		45°	27.0	49.6	76.6
		60°	29.9	53.3	83.2
		75°	34.8	54.3	89.1
		85°	36.2	65.9	101.8

where

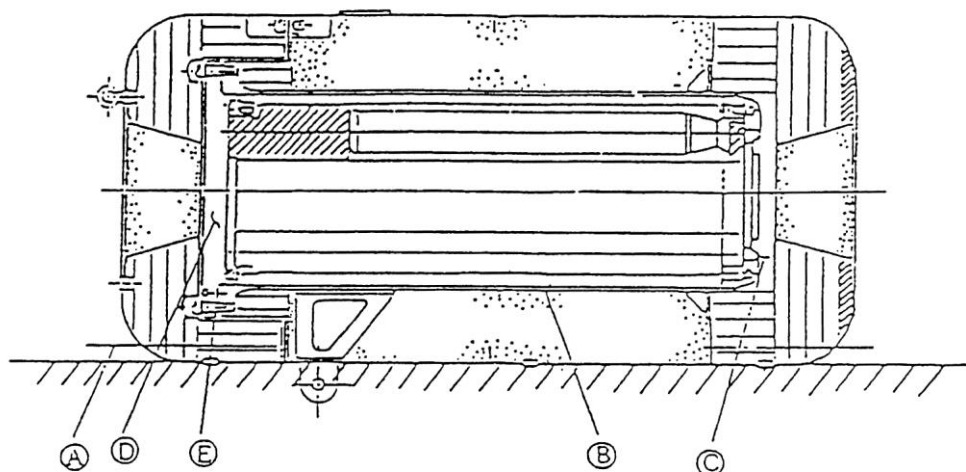
g: Gravitational acceleration, $g = 9.81 \text{ [m/s}^2\text{]}$

(6) Stress analysis of 1.2m horizontal drop

The stress analysis of the 1.2 m horizontal drop are conducted separately with the main body, the fuel basket and the fuel element. In addition, as for the stress analysis in each of these sections, the only principal stress will be determined, the evaluation of the stress intensity and the stress classification shall be conducted in section A.5.3(6) (d).

(a) Main body of the packaging

The stress evaluation positions of the main body of the packaging during the 1.2 m horizontal drop are determined as shown in (II)-Fig.A.35 from a sealing performance preservation.



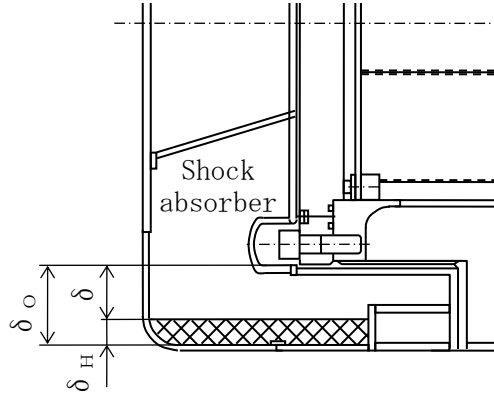
Symbol	Evaluation position
Ⓐ	Shock absorber (deformation quantity)
Ⓑ	Inner shell
Ⓒ	Bottom plate of the inner shell
Ⓓ	Top part of the inner shell (Inner lid)
Ⓔ	Inner lid clamping bolt

(II)-Fig.A.35 Stress evaluation position for 1.2m horizontal drop
(main body of inner shell)

Ⓐ Deformation of the shock absorber

We shall determine that even if the shock absorber is deformed by the 1.2 m horizontal drop, this deformation will not reach the inner shell nor to the inner lid.

The analytical model is shown in (II)-Fig. A. 36.



(II)-Fig. A. 36 Analytical model of interference to inner shell due to shock absorber deformation for 1.2 m horizontal drop

As is indicated in (II)-Fig. A. 36, the remaining thickness δ (mm) of the shock absorber after the 1.2 m horizontal drop can be given by the following equation

$$\delta = \delta_0 - \delta_H$$

where

δ_0 : Minimum thickness of the shock absorber before the test,

$$\delta_0 = 104 \text{ [mm]}$$

δ_H : Deformation of the shock absorber, $\delta_H = 20.9 \text{ [mm]}$

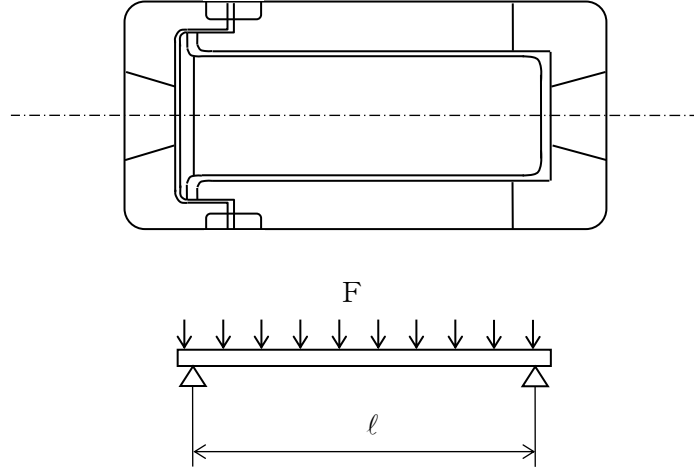
Therefore, the remaining thickness is

$$\delta = 104 - 20.9 = 83.1 \text{ [mm]}$$

This determines that the deformation caused by the 1.2 m horizontal drop will concern the shock absorber only, and will not reach the main body of the inner shell nor to the inner lid.

③ Inner shell

(II)-Fig.A.37 shows an analytical model of the stress on the inner shell for the 1.2 horizontal drop.



(II)-Fig.A.37 Stress analysis model of inner shell for 1.2m horizontal drop

As is indicated in (II)-Fig.A.37, the inner shell is supported at both ends, the beam is assumed to support the uniform load, the bending stress σ_b is at its maximum in the center of the supporting points and can be given by the following equation

$$\sigma_b = \frac{M}{Z}$$

where

M: Bending moment,

$$M = \frac{F \cdot l}{8} = \frac{1}{8} \cdot m \cdot N \cdot l \quad [N \cdot mm]$$

F: Impact load, $F = m \cdot N$ [N]

m: Load between the supporting points of the package, $m = 700$ [kg]

N: Design acceleration, $N = 254.1 \cdot g$ [m/s^2]

l: Length between the supporting points, $l = 1359$ [mm]

$$M = \frac{1}{8} \times 700 \times 254.1 \times 9.81 \times 1359 = 2.96 \times 10^8 \quad [N \cdot mm]$$

Z: section modulus,

$$Z = \frac{\pi}{32} \times \frac{d_2^4 - d_1^4}{d_2} \quad [mm^3]$$

d₂: Outside diameter of the inner shell, d₂ =480 [mm]

d₁: Inside diameter of the inner shell, d₁ =460 [mm]

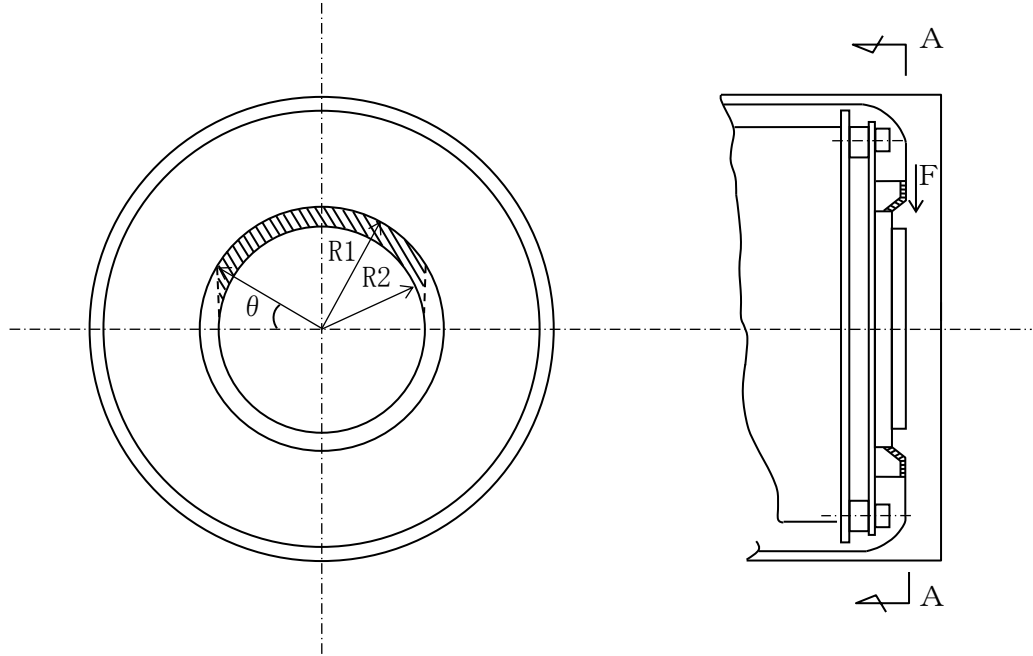
$$Z = \frac{\pi}{32} \times \frac{480^4 - 460^4}{480} = 1.70 \times 10^6 \quad [\text{mm}^3]$$

Therefore, the bending stress is given by the following equation.

$$\sigma_b = \frac{2.96 \times 10^8}{1.70 \times 10^6} = 174 \quad [\text{N/mm}^2]$$

© Bottom plate of the inner shell

An analytical model of the stress on the bottom plate of the inner shell for the 1.2 horizontal drop is shown in (II)-Fig.A. 38.



(II)-Fig.A. 38 Stress analysis model of inner shell bottom plate for 1.2m horizontal drop

As is indicated in (II)-Fig.A. 38, the A-A cross section of the inner shell's bottom plate receives the drop force of the fuel basket for horizontal drop. The stress generated at this time is,

$$\tau = \frac{F}{A}$$

where

F: Impact force,

$$F = \frac{1}{2} (m_B + m_F) \times N \quad [\text{kg}]$$

m_B : Mass of fuel basket, $m_B = 138$ [kg]

m_F : Mass of contents, $m_F = 92$ [kg]

N : Design acceleration, $N = 254.1 \cdot g$ [m/s²]

$$F = \frac{1}{2} (138 + 92) \times 254.1 \times 9.81 = 2.87 \times 10^5 \text{ [N]}$$

A : Cross sectional area of the inner shell's bottom plate
(shaded portion in (II)-Fig.A.38)

$$A = R_1^2 \left(\frac{\pi}{2} - \theta \right) - R_2^2 \left(\frac{\pi}{2} - \tan \theta \right)$$

R_1 : Outside radius of inner shell's bottom plate outside the
protruding section, $R_1 = 130$ [mm]

R_2 : Inside radius of inner shell's bottom plate inside the
protruding section, $R_2 = 105$ [mm]

$$\theta : \text{Angle, } \theta = \cos^{-1} \frac{R_2}{R_1} = 36.1^\circ = 0.631 \text{ [rad]}$$

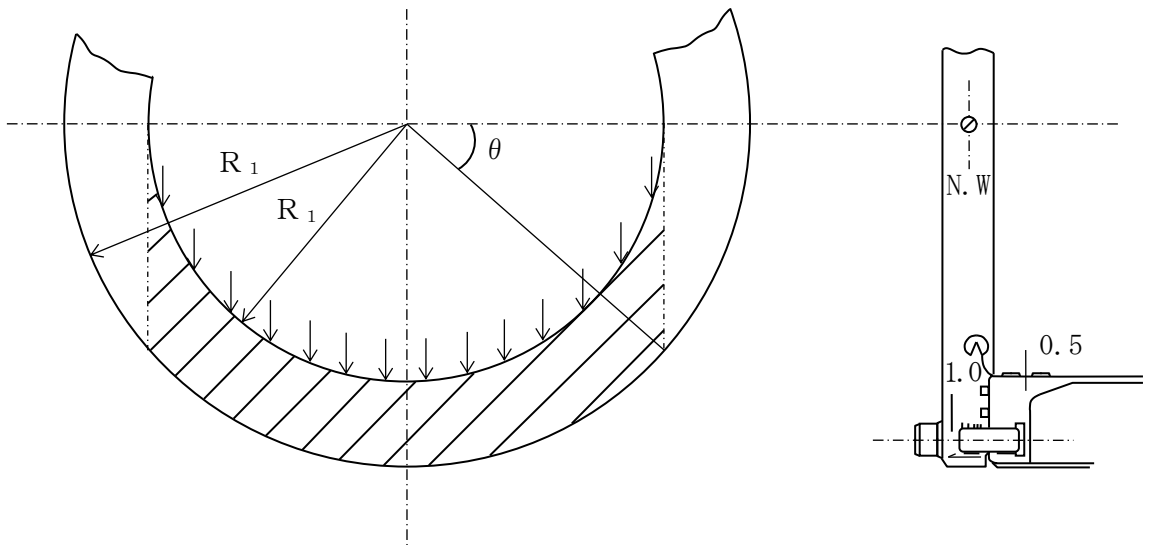
$$A = 130^2 \times \left(\frac{\pi}{2} - 0.631 \right) - 105^2 \times \left(\frac{\pi}{2} - \tan 36.1^\circ \right) \\ = 6.60 \times 10^3 \text{ [mm}^2\text{]}$$

Therefore, the shearing stress τ is,

$$\tau = \frac{2.87 \times 10^5}{6.60 \times 10^3} = 43.5 \text{ [N/mm}^2\text{]}$$

① Upper part of the inner shell

An analytical model of the stress on the upper part of the inner shell for the
1.2 horizontal drop is shown in (II)-Fig.A.39.



(II)-Fig.A.39 Stress analysis model of inner shell upper part
of 1.2m horizontal drop

As indicated in (II)-Fig.A. 39, the inner lid slides to the drop direction and comes in contact with the upper part of the inner shell at point \textcircled{A} .

Shearing stress is generated in the inner lid,

$$\tau = \frac{F}{A}$$

where,

F: Impact strength, $F=N \cdot m$ [N]

m: Weight of the inner lid, $m=120$ [kg]

N: Design acceleration, $N=254.1 \cdot g$ [m/s²]

$F = 254.1 \times 9.81 \times 120 = 2.99 \times 10^5$ [N]

A: Cross sectional area of the inner shell's upper part
(shaded portion in (II)-Fig.A. 39),

$$A=R_1^2 \left(\frac{\pi}{2} - \theta \right) - R_2^2 \left(\frac{\pi}{2} - \tan \theta \right)$$

R₁: Outside radius of the inner shell flange, $R_1=307$ [mm]

R₂: Inside radius of the inner shell, $R_2=230$ [mm]

θ : Angle,

$$\theta = \cos^{-1} \frac{R_2}{R_1} = 41.5^\circ = 0.724 \text{ [rad]}$$

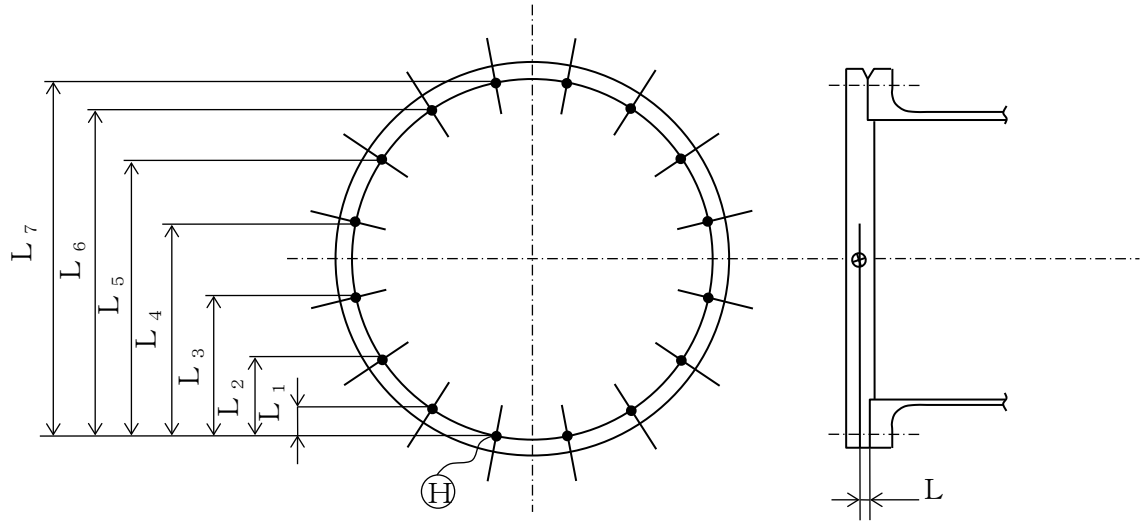
$$\begin{aligned} A &= 307^2 \times \left(\frac{\pi}{2} - 0.724 \right) - 230^2 \times \left(\frac{\pi}{2} - \tan 41.5 \right) \\ &= 4.35 \times 10^4 \text{ [mm}^2\text{]} \end{aligned}$$

Therefore, the shearing stress τ is,

$$\tau = \frac{2.99 \times 10^5}{4.35 \times 10^4} = 6.87 \text{ [N/mm}^2\text{]}$$

Ⓔ Inner lid clamping bolt

An analytical model of the stress on the inner lid clamping bolt for the 1.2 m horizontal drop is shown in (II)-Fig.A. 40.



(II)-Fig.A. 40 Stress analysis model for inner lid clamping bolt
for 1.2m horizontal drop

As indicated in (II)-Fig.A. 40, the momentum of the inner lid acts on the clamping bolts of the inner lid for the 1.2m horizontal drop.

Bending stress σ_b [N/mm²] is thus generated in the clamping bolt, and this is given by the following equation

$$\sigma_b = \frac{M \cdot L_{\max}}{I} = \frac{N \cdot m \cdot L \cdot L_{\max}}{\sum L_i^2 \cdot Ar}$$

where

M: Angular momentum

$M = N \cdot m \cdot L$ [N·mm]

N: Design acceleration, $N=254.1 \cdot g$ [m/s²]

m: Weight of the inner lid, $m=120$ [kg]

L: Moment arm, $L=18.0$ [mm]

L_i : Distance from each bolt to the overturning point Ⓔ [mm]

$L_1 = 42.5$ $L_5 = 437.8$

$L_2 = 121.2$ $L_6 = 516.5$

$L_3 = 223.9$ $L_7 = 559.0$

$L_4 = 335.1$

L_{\max} : Distance from the overturning point to the farthest bolt,

$$L_{\max} = L_7 = 559$$

A_r : Cross section of the groove of the inner lid clamping bolt (M24),

$$A_r = \frac{\pi}{4} \cdot d_r^2 = \frac{\pi}{4} \times 20.752^2 = 338.2 [\text{mm}^2]$$

Therefore, the stress is,

$$\begin{aligned} \sigma_b &= \frac{254.1 \times 9.81 \times 120 \times 18.0 \times 559}{2 \times (42.5^2 + 121.2^2 + 223.9^2 + 335.1^2 + 437.8^2 + 516.5^2 + 559^2) \times 338.2} \\ &= 4.68 [\text{N/mm}^2] \end{aligned}$$

(b) Fuel basket

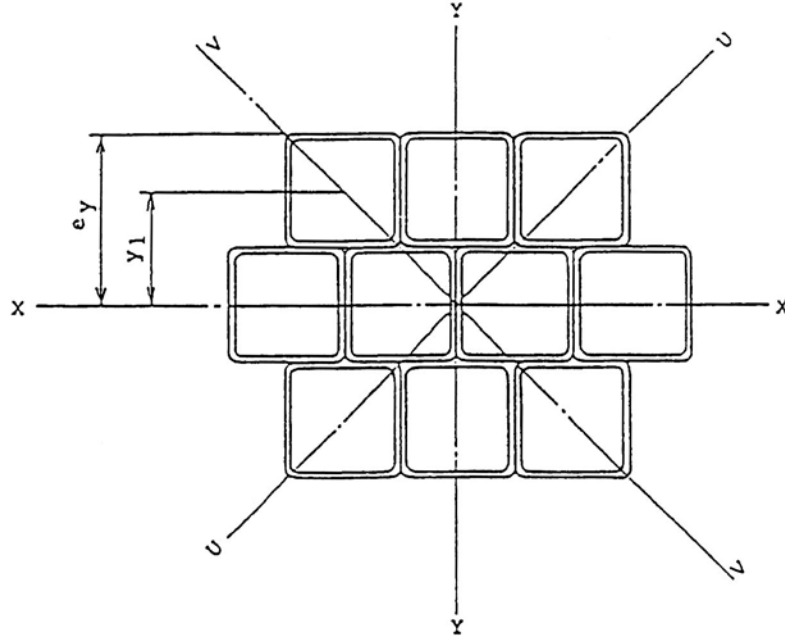
In this section, we shall analyze the stress generated in the fuel basket at the 1.2m horizontal drop. The fuel basket is the rectangular type. We shall determine the section modulus for this type.

The stress shall be evaluated according to the axial strength of the pipe.

(1) Section modulus of square fuel basket

We shall determine the section modulus of the square fuel basket.

The analytical model is shown in (II)-Fig.A.41.



(II)-Fig.A.41 Analytical model of section modulus of rectangular fuel basket

(i) Section modulus regarding X-X axis

As indicated in (II)-Fig.A.41, the section modulus regarding the X-X axis is given by the following equation,

$$Z_x = \frac{10 \cdot I_o + 6A \cdot y_1^2}{e_y}$$

where

Z_x : Section modulus regarding the X-X axis [mm³]

I_o : Second moment of area of a single square pipe,

$$\begin{aligned} I_o &= \frac{1}{12} (h_2^4 - h_1^4) = \frac{1}{12} (100^4 - 94^4) \\ &= 1.83 \times 10^6 \text{ [mm}^4\text{]} \end{aligned}$$

h_1 : Outside dimension of the square pipe, $h_1 = 100$ [mm]

h_2 : Inside dimension of the square pipe, $h_2 = 94$ [mm]

A : Cross sectional area of the square pipe,
 $A = h_1^2 - h_2^2 = 100^2 - 94^2 = 1.16 \times 10^3$ [mm²]

y_1 : Distance to the center of the square pipe, $y_1 = 100$ [mm]

e_y : Distance to the top surface of the fuel basket, $e_y = 150$ [mm]

Therefore, the section modulus is

$$Z_x = \frac{10 \times 1.83 \times 10^6 + 6 \times 1.16 \times 10^3 \times 100^2}{150} = 5.86 \times 10^5 \text{ [mm}^3\text{]}$$

(ii) Section modulus regarding Y-Y axis

As indicated in (II)-Fig.A.41, the section modulus regarding the Y-Y axis is given by the following equation

$$Z_y = \frac{10 \cdot I_o + 2A \cdot (x_1^2 + 2x_2^2 + x_3^2)}{e_x}$$

where

Z_y : Section modulus regarding the Y-Y axis [mm³]

I_o : Secondary moment of the cross section of a single square pipe,
 $I_o = 1.83 \times 10^6$ [mm⁴]

A : Cross sectional area of the square pipe, $A = 1.16 \times 10^3$ [mm²]

x_1 : Distance to the center of the pipe, $x_1 = 50$ [mm]

x_2 : Distance to the center of the pipe, $x_2 = 100$ [mm]

X3 : Distance to the center of the pipe, $x_3 = 150$ [mm]

e_x : Distance to the top part of the fuel basket, $e_x = 200$ [mm]

Therefore, the following equation is obtained.

$$Z_y = \frac{10 \times 1.83 \times 10^6 + 2 \times 1.16 \times 10^3 \times (50^2 + 2 \times 100^2 \times 150^2)}{200}$$
$$= 6.14 \times 10^5 \text{ [mm}^3\text{]}$$

(iii) Section modulus regarding U-U axis

As indicated in (II)-Fig.A.41, the section modulus regarding the U-U axis is given by the following equation.

$$Z_u = \frac{10 \cdot I_o + 2A \cdot (v_1^2 + v_2^2 + v_3^2 + v_4^2)}{e_v}$$

where

Z_u : Section modulus regarding the U-U axis [mm³]

I_o : Second moment of area for a single square pipe,

$$I_o = 1.83 \times 10^6 \text{ [mm}^4\text{]}$$

A : Cross sectional area of the square pipe, $A = 1.16 \times 10^3$ [mm²]

V_1 : Distance to the center of the pipe, $v_1 = 25\sqrt{2} = 35.4$ [mm]

V_2 : Distance to the center of the pipe, $v_2 = 50\sqrt{2} = 70.7$ [mm]

V_3 : Distance to the center of the pipe, $v_3 = 75\sqrt{2} = 106$ [mm]

V_4 : Distance to the center of the pipe, $v_4 = 100\sqrt{2} = 141$ [mm]

e_v : Distance to the top of the fuel basket, $e_v = 150\sqrt{2} = 212$ [mm]

Therefore, the sectional modulus is

$$Z_u = \frac{10 \times 1.83 \times 10^6 + 2 \times 1.16 \times 10^3 \times (35.4^2 + 70.7^2 + 106^2 + 141^2)}{212}$$
$$= 4.95 \times 10^5 \text{ [mm}^3\text{]}$$

Of the values mentioned above, the smallest shall be adopted

$$Z_{\min} \{Z_x, Z_y, Z_u\} = 4.95 \times 10^5 \text{ [mm}^3\text{]}$$

(2) Axial strength of square fuel basket

The analytical model is the same as in (II)-Fig.A.41.

The bending stress generated in the fuel basket reaches its maximum in the center and is given by the following equation.

$$\sigma_b = \frac{M}{Z} = \frac{(W_f + W_p) \cdot N \cdot L^2}{8Z}$$

where

σ_b : Bending stress [N/mm²]

M: Maximum bending moment [N·mm]

$$M = \frac{(W_f + W_p) \cdot N \cdot L^2}{8}$$

W_f : Uniform weight due to the fuel element

(This uniform load should be of the maximum weight per unit length among all square fuel elements (JRR-3 Standard type))

$$W_f = \frac{m_f}{l} = \frac{92}{1150} = 0.08 \quad [\text{kg/mm}]$$

m_f : Weight of the fuel element, $m_f = 92$ [kg]

l : Length of the fuel element, $l = 1150$ [mm]

W_p : Uniform weight due to the individual weight of the fuel basket,

$$W_p = \frac{m_p}{L} = \frac{138}{1200} = 0.115 \quad [\text{kg/mm}]$$

m_p : Weight of the fuel basket, $m_p = 138$ [kg]

L : Length of the supporting point, $L = 1200$ [mm]

N : Acceleration, $N = 254.1 \cdot g$ [m/s²]

Z : Section modulus of the fuel basket, $Z = 4.95 \times 10^5$ [mm³]

Therefore, the bending stress is,

$$\sigma_b = \frac{(0.08 + 0.115) \times 254.1 \times 9.81 \times 1200^2}{8 \times 4.95 \times 10^5} = 177 \quad [\text{N/mm}^2]$$

(c) Fuel elements and fuel plate

(c)-1. Fuel elements

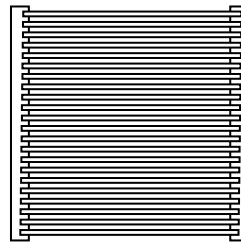
In this paragraph, an analysis of stress is performed on fuel elements for the 1.2 m horizontal drop. As indicated in (I)-D, specifications of the rectangular fuel elements.

(1) Evaluation of the fuel elements for a drop case

Fuel elements are evaluated for two cases of horizontal drop as shown in

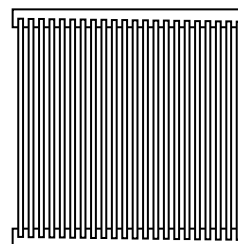
(II)-Fig.A. 42.

① Horizontal drop to the direction perpendicular to the fuel plate



Rectangular fuel elements

② Horizontal drop to the direction parallel to the fuel plate



Rectangular fuel elements

(II)-Fig.A. 42 Evaluation of fuel elements for 1.2 m horizontal drop

(2) Fuel elements

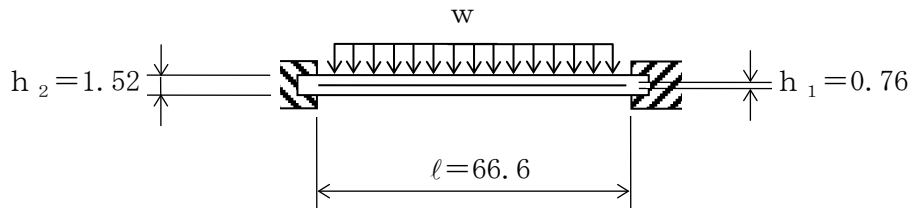
(i) Fuel plate

As shown in (I)-D with regard to the rectangular fuel element, there are 11 types of fresh fuel elements including 3 KUR fuel elements, and there are 9 types of lowly irradiated fuel elements. In this section, horizontal drop to the direction perpendicular to fuel plate and to the direction parallel to the fuel plate are treated separately. Furthermore, it is assumed that uranium aluminum alloy has the same strength as the covering material.

① Horizontal drop to the direction perpendicular to fuel plate

In this section, the analysis method for JRR-3 standard type is shown and the analysis result for the other 19 types, using the same analysis method, is shown in (II)-Table A.16.

The analytical model is shown in (II)-Fig.A.43.



(II)-Fig.A.43 Analytical model of rectangular fuel elements for 1.2 m horizontal drop perpendicular to fuel plate.

As indicated in (II)-Fig.A.43, a beam with both ends fixed and receiving uniform load due to dead load will receive maximum bending moment at its fixed end. The bending stress σ_b is,

$$\sigma_b = \frac{M}{Z}$$

where M: Bending moment per unit [N·mm/mm]

$$M = \frac{w \cdot l^2}{12}$$

w: Uniform load [N/mm²]

$$w = \frac{m}{b \cdot a} \cdot N = \frac{0.279}{66.6 \times 770} \times 254.1 \times 9.81 = 1.36 \times 10^{-2}$$

m: Weight of the fuel plate, m=0.279 [kg]

N: Design acceleration, $N=254.1 \cdot g$ $[m/s^2]$

a: Length of the fuel plate, $a=770$ $[mm]$

l: Distance between fixed points, $l=66.6$ $[mm]$

Z: Cross sectional area per unit width,

$$Z = \frac{1}{6} \cdot \frac{h_2^3 - h_1^3}{h_2} = \frac{1}{6} \times \frac{1.27^3 - 0.51^3}{1.27} = 0.251 \quad [mm^3/mm]$$

h_2 : Fuel plate thickness, $h_2 = 1.27$ $[mm]$

h_1 . Fuel plate core thickness, $h_1 = 0.51$ $[mm]$

Therefore, the bending stress is,

$$\sigma_b = \frac{1.36 \times 10^{-2} \times 66.6^2}{12 \times 0.251} = 20.0 \quad [N/mm^2]$$

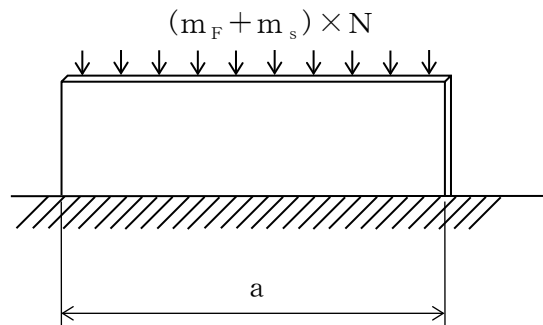
② Horizontal drop to the direction parallel to the fuel plate

As shown in (I)-D with regard to the fuel elements, the KUR fuel elements consists of curved fuel plates, so the inertial force of the fuel plates and side plates may cause both compressive and buckling stress. Therefore, buckling stress analysis is performed for KUR fuel elements.

For the KUR special fuel element, the two middle plates of 3.1mm thickness placed in parallel to the fuel plates receive the inertial force of the side plates. Therefore, for the fuel plates of the KUR special element, stress analysis of the middle plates will be performed, followed by stress analysis of the fuel plates.

For the fuel elements of other reactor types, the analysis method for JRR-3 standard type is shown in the following and the analysis result for the other 16 types, using the same analysis method, is shown in (II)-Table A.16.

The analytical model is shown in (II)-Fig.A.44.



(II)-Fig.A.44 Analytical model of rectangular fuel element
for 1.2m horizontal drop parallel to fuel plate

As indicated in (II)-Fig.A. 44, the rectangular plate which receives its dead load and the partial weight of the side plate generates compressive stress σ_c .

$$\sigma_c = \frac{W}{A} = \frac{(m_F + m_S) \times N}{a (h_2 - h_1)} \quad [N/mm^2]$$

where

N: Design acceleration, $N = 254.1 \cdot g \quad [m/s^2]$

mF: Weight of the fuel plate, $m_F = 0.279 \quad [kg]$

ms: Partial weight of the side plate, $m_S = 0.038 \quad [kg]$

a: Length of the fuel plate, $a = 770 \quad [mm]$

h2: Fuel plate thickness, $h_2 = 1.27 \quad [mm]$

h1: Fuel plate core thickness, $h_1 = 0.51 \quad [mm]$

Therefore, the compressive stress is,

$$\sigma_c = \frac{(0.279 + 0.038) \times 254.1 \times 9.81}{770 \times (1.27 - 0.51)} = 1.35 \quad [N/mm^2]$$

Next, the analysis for the KUR fuel elements are summarized as following.

Firstly, KUR standard and half-loaded fuel elements are analyzed. Here, the analysis method for KUR standard type is shown, and the half-loaded fuel elements are analyzed using the same method.

For a curved beam subject to compressive axial load, the maximum bending moment occurs at the concave surface of the beam. Here, the buckling stress is analyzed based on the following formula by Southwell [23], where the combined compressive stress and yield stress are correlated;

$$\sigma_y = \sigma_{cr} \left(1 + \frac{e}{r} \sec \frac{L}{2k} \sqrt{\frac{\sigma_{cr}}{E}} \right) \text{-----} \textcircled{1}$$

where

σ_{cr} : bucking stress of the beam (averaged axial compressive stress), $\frac{P}{A} \quad [N/mm^2]$

P : compressive load of the beam $[N]$

A : cross section of the beam $[mm^2]$

σ_y : yield stress $[N/mm^2]$

E : modulus of direct elasticity $[N/mm^2]$

L : beam length $[mm]$

e : eccentricity of the beam $[mm]$

k : radius-of-gyration of area $\sqrt{\frac{I}{A}} \quad [mm]$

I : geometrical moment of inertia $[mm^4]$

Z : modulus of section $[mm^3]$

$$r = \frac{Z}{A} \quad [\text{mm}]$$

The corresponding values for KUR standard elements are as follows;

modulus of direct elasticity at 75°C : $E = 6.97 \times 10^4$ [N/mm²]

yield stress at 75°C : $\sigma_y = 63.7$ [N/mm²]

cross section per fuel plate unit width :

$$A = (1.52 - 0.5) \times 1 = 1.02 \quad [\text{mm}^2 / \text{mm}]$$

geometrical moment of inertia per fuel plate unit width :

$$I = 0.282 \quad [\text{mm}^4 / \text{mm}]$$

modulus of section per fuel plate unit width :

$$Z = 0.371 \quad [\text{mm}^3 / \text{mm}]$$

eccentricity : $e = 4$ [mm]

width : $L = 66$ [mm]

Then we obtain;

$$\begin{aligned} k &= \sqrt{\frac{I}{A}} \\ &= \sqrt{\frac{0.282}{1.02}} \\ &= 0.526 \quad [\text{mm}] \\ r &= \frac{Z}{A} \\ &= \frac{0.371}{1.02} \\ &= 0.364 \quad [\text{mm}]. \end{aligned}$$

By substituting the above values to RHS of Eq. ①, σ_{cr} could be obtained

as

$$\sigma_{cr} = 4.67 \quad [\text{N/mm}^2].$$

The compressive stress σ_c is obtained using the following formula

as in the case of JRR-3 standard fuel element;

$$\sigma_c = \frac{W}{A} = \frac{(m_f + m_s) \cdot N}{a \cdot (h_2 - h_1)} \quad [\text{N/mm}^2]$$

where

N : Design acceleration, $N = 254.1 \cdot g$ [m/s²]

m_f : Weight of the fuel plate, $m_f = 0.235$ [kg]

m_s : Partial weight of the side plate, $m_s = \frac{M_s}{n}$

M_s : weight of side plate 0.650 [kg]

n : number of fuel plates 18 [plates]

$$m_s = \frac{0.650}{18} = 0.036 \quad [\text{kg}]$$

a : Length of the fuel plate a = 625 [mm]

h_2 : Fuel plate thickness $h_2 = 1.52$ [mm]

h_1 : Fuel plate core thickness $h_1 = 0.50$ [mm]

Therefore, compressive stress is

$$\begin{aligned} \sigma_c &= \frac{(0.235+0.036) \times 254.1 \times 9.81}{625 \times (1.52 - 0.50)} \\ &= 1.07 \quad [\text{N/mm}^2]. \end{aligned}$$

This gives

$$\sigma_c = 1.07 \text{ [N/mm}^2] < \sigma_{cr} = 4.67 \text{ [N/mm}^2],$$

which shows that the integrity of fuel plates of KUR standard fuel elements are maintained under the horizontal drop condition to the direction perpendicular to the fuel plate.

Next, the KUR special elements will be analyzed as follows.

The KUR special fuel elements have two middle plates (thickness 3.18mm) placed in parallel to the fuel plates. In the analysis, we first assume that the inertial force of the side plates are totally received by these two middle plates and verify the integrity of the middle plates. Then, the integrity of the fuel plates will be analyzed.

The compressive stress of the middle plates σ_c are given as follows;

$$\sigma_c = \frac{W}{A} = \frac{(m_m + m_s) \cdot N}{a \cdot t} \quad [\text{N/mm}^2]$$

where

N : Design acceleration, $N = 254.1 \cdot g$ [m/s²]

m_m : weight of middle plate, $m_m = a \cdot t \cdot \ell \cdot \rho$ [kg]

a : length of middle plate, a = 721 [mm]

t : thickness of middle plate, t = 3.18 [mm]

ℓ : distance between fixed edge, $\ell = 66$ [mm]

ρ : density, $\rho = 2.7 \times 10^{-6}$ [kg/mm³]

$$m_m = 721 \times 3.18 \times 66 \times 2.7 \times 10^{-6}$$

$$= 0.409 \quad [\text{kg}]$$

m_s : weight of side plate section, $m_s = \frac{M_s}{n}$

M_s : weight of side plate, 0.650 [kg]

n : number of middle plates, 2 [plates]

$$m_s = \frac{0.650}{2} = 0.325 \quad [\text{kg}]$$

Therefore, the compressive stress is

$$\begin{aligned}\sigma_c &= \frac{(0.409+0.325) \times 254.1 \times 9.81}{721 \times 3.18} \\ &= 0.80 \quad [\text{N/mm}^2],\end{aligned}$$

which is less than the design yield strength of the material at 75°C (63.7 (N/mm²)). Thus the integrity of the middle plates are maintained.

The integrity of the fuel plates are analyzed as follows. As the fuel plates of the KUR special type elements are identical to those of the KUR standard fuel elements, the buckling stress σ_{cr} is identical to that of KUR standard fuel element, i.e.

$$\sigma_{cr} = 4.67 \quad [\text{N/mm}^2].$$

The compressive stress σ_c is given as follows;

$$\sigma_c = \frac{W}{A} = \frac{m_f \cdot N}{a \cdot (h_2 - h_1)} \quad [\text{N/mm}^2]$$

where,

$$\begin{aligned}N &: \text{Design acceleration, } N = 254.1 \cdot g \quad [\text{m/s}^2] \\ m_f &: \text{Weight of the fuel plate, } m_f = 0.235 \quad [\text{kg}] \\ a &: \text{Length of the fuel plate } a = 625 \quad [\text{mm}] \\ h_2 &: \text{Fuel plate thickness } h_2 = 1.52 \quad [\text{mm}] \\ h_1 &: \text{Fuel plate core thickness } h_1 = 0.50 \quad [\text{mm}].\end{aligned}$$

Therefore,

$$\begin{aligned}\sigma_c &= \frac{0.235 \times 254.1 \times 9.81}{625 \times (1.52 - 0.5)} \\ &= 0.92 \quad [\text{N/mm}^2],\end{aligned}$$

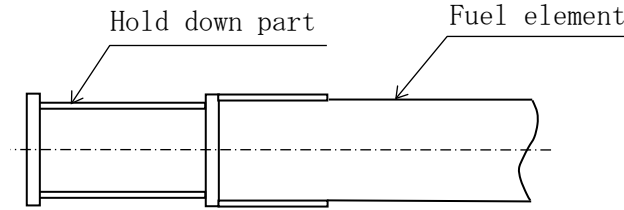
This gives

$$\sigma_c = 0.92 \quad [\text{N/mm}^2] < \sigma_{cr} = 4.67 \quad [\text{N/mm}^2],$$

which shows that the integrity of fuel plates of KUR special fuel elements are maintained under the horizontal drop condition to the direction perpendicular to the fuel plate.

(ii) Fuel element hold down part

The lowly irradiated fuel element, as shown in section I-D, is cut at the portion of the lower adapter and the upper holder in order to reduce the weight. Therefore, since the total length becomes short, a hold-down part is provided to adjust the length. In this section, the stress analysis method and the stress generated at the hold-down part are shown, the result is described in (II)-Table A.16, and the stress analysis model is described in (II)-Fig.A.45.



(II)-Fig.A.45 Analytical model of holder

As shown (II)-Fig.A.45, the hold-down part is considered to be a beam supported at the both end, subjected to the uniform load of its own weight, the maximum bending moment occurs at the center of the beam, and the stress is given as follows.

$$\sigma_b = \frac{M}{Z}$$

where M: Bending moment per unit length [N·mm]

$$M = \frac{w \cdot l^2}{8}$$

w: Uniform load [N/mm²]

$$w = \frac{m_z}{l} \times N$$

$$= \frac{1.4}{204} \times 254.1 \times 9.81 = 17.1$$

$$M = \frac{1}{8} \times 17.1 \times 204^2 = 8.90 \times 10^4 \text{ [N} \cdot \text{mm]}$$

m_z: Mass of the hold down part, m_z=1.4 [kg]

N : Design acceleration, N=254.1·g [m/s²]

l : Length of hold down part, l=204 [mm]

z : Modulus of elasticity

$$Z = \frac{\pi}{32} \cdot \frac{h_o^4 - h_i^4}{h_o}$$

$$= 9.242 \times 10^3 \text{ [mm}^3\text{]}$$

h_o: Outside diameter of hold down part; h_o=60 [mm]

h_i: Inside diameter of hold down part; h_i=52 [mm]

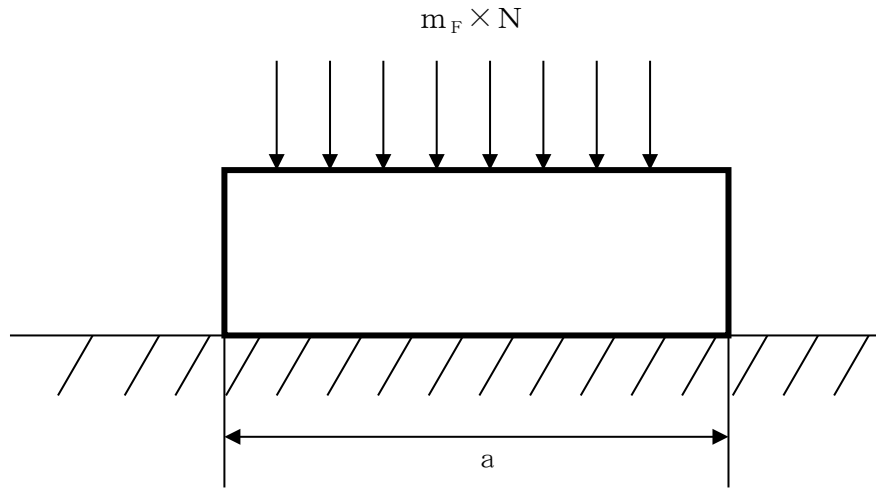
Therefore,

$$\sigma_b = \frac{8.90 \times 10^4}{9.242 \times 10^3} = 9.63 \text{ [N/mm}^2\text{]}$$

(c)-2. Fuel plate (for Critical Assembly fuel (KUCA fuel))

In this paragraph, an analysis of stress is performed on KUCA fuel for the 1.2 m horizontal drop. As indicated in (I)-D, specifications of the rectangular fuel plate.

The analytical model is shown in (II)-Fig.A.46.



(II)-Fig.A.46 Analytical model of the fuel plate
for 1.2m horizontal drop parallel to fuel plate

As indicated in (II)-Fig.A.46, the fuel plate which receives its dead load generates compressive stress σ_c .

$$\sigma_c = \frac{W}{A} = \frac{(m_F + m_S) \times N}{a (h_2 - h_1)} \quad [\text{N/mm}^2]$$

where

m_F : Weight of the fuel plate [kg]

a : Length of the fuel plate [mm]

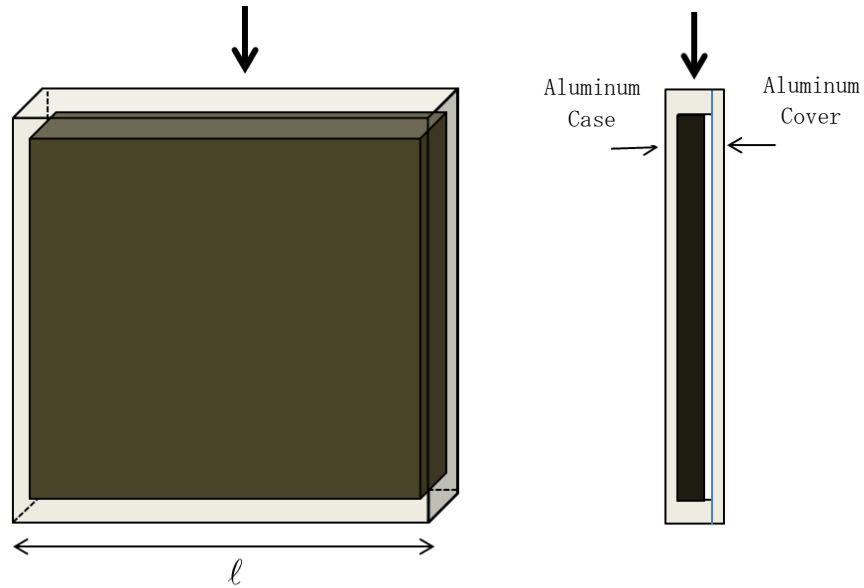
h_2 : Fuel plate thickness [mm]

h_1 : Fuel plate core thickness [mm]

$h_2 - h_1$: Cladding thickness [mm]

N : Design acceleration [m/s^2]

In the case of horizontal drop, the design acceleration is applied to coupon fuel in the direction shown in (II)-Fig.A.47



(II)-Fig.A.47 Analytical model of the coupon fuel for 1.2m horizontal drop

In this case, the total thickness of cladding is 0.8 mm, which is the total of the bottom plate of aluminum case (thickness 0.4 mm) and the aluminum cover (thickness 0.4mm).

m_f : Weight of the fuel plate	$m_f=0.036$ [kg]
l : Length of the fuel plate	$l=50.8$ [mm]
h_2-h_1 :Cladding thickness	$h_2-h_1= 0.8$ [mm]
N : Design acceleration	$N=254.1 \cdot g$ [m/s ²]

Therefore, the compressive stress σ_c are given as follows.

$$\begin{aligned}\sigma_c &= (0.036 \times 254.1 \times g) / (50.8 \times 0.8) \\ &= 2.21 \quad [\text{N/mm}^2]\end{aligned}$$

Regarding flat fuel plate, two cases are conceivable: one is horizontal drop in the plane direction of the fuel plate and the other horizontal drop in the

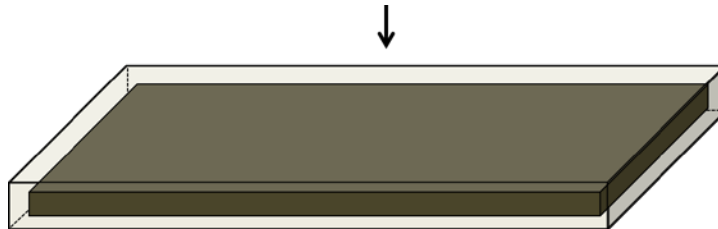
direction parallel to the fuel plate.

In the case of horizontal drop in the plane direction of the fuel plate ((II)-Fig.A.48), the compressive stress σ_c is obtained by the fuel plate width (62 mm) , fuel core width (56 mm) and as follows.

m_f : Weight of the fuel plate	$m_f=0.23$ [kg]
l : Length of the fuel plate	$l=600$ [mm]
h_2 : Fuel plate thickness	$h_2=62$ [mm]
h_1 : Fuel plate core thickness	$h_1=56$ [mm]
N : Design acceleration	$N=254.1 \cdot g$ [m/s ²]

Therefore, the compressive stress σ_c are given as follows.

$$\begin{aligned}\sigma_c &= (0.23 \times 254.1 \times g) / (600 \times (62-56)) \\ &= 0.16 \quad [\text{N/mm}^2]\end{aligned}$$



((II)-Fig.A.48 Analytical model of the flat fuel plate for 1.2m
horizontal drop in the plane direction of the fuel plate

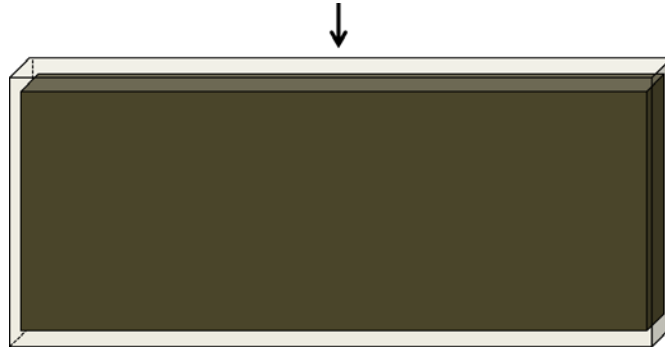
In the case of horizontal drop in the direction parallel to the fuel plate ((II)-Fig.A.49),

m_f : Weight of the fuel plate	$m_f=0.23$ [kg]
l : Length of the fuel plate	$l=600$ [mm]

h_2 : Fuel plate thickness	$h_2 = 1.5 \text{ [mm]}$
h_1 : Fuel plate core thickness	$h_1 = 0.5 \text{ [mm]}$
N : Design acceleration	$N = 254.1 \cdot g \text{ [m/s}^2\text{]}$

Therefore, the compressive stress σ_c are given as follows.

$$\begin{aligned}\sigma_c &= (0.23 \times 254.1 \times g) / (600 \times (1.5 - 0.5)) \\ &= 0.96 \text{ [N/mm}^2\text{]}\end{aligned}$$



(II)-Fig.A.49 Analytical model of the flat fuel plate for 1.2m horizontal drop in the direction parallel to the fuel plate

(d) Comparison of the allowable stress

A summary of the stress evaluation results obtained for each analysis in section (II)-A.5.3(6) is given in (II)-Table A.16.

As demonstrated in this table, the margin of safety in regard to the design standard value is positive for individual or multiple loads.

Therefore, the soundness of this package is maintained under test conditions of the 1.2m horizontal drop.

(II) -Table A.16 Stress evaluation for 1.2 m horizontal drop (1/6)

Stress units
;N/mm²

No.	Stress Position to be evaluated		Stress at initial clamping	Stress due to internal pressure	Stress due to thermal expansion	Impact stress	Primary stress						Primary+secondary stress			Fatigue					
							Pm(PL)	Sm	MS	PL+Pb	1.5Sm	MS	PL+Pb +Q	3Sm	MS	PL+Pb +Q+F	Sa	N	Na	DF	MS
1	Frame of Inner shell	σ_r	—	-0.0491	—	—	2.36	137	57.0	175	205	0.171	—	—	—	—	—	—	—	—	—
		σ_θ		2.31		—															
		σ_z		1.15		174															
2	Bottom plate of the inner shell	σ_r	—	3.18	—	—	0.098	137	1396	87.1	205	1.35	—	—	—	—	—	—	—	—	—
		σ_θ		0.953		—															
		σ_z		-0.098		—															
		τ		—		43.5															
3	Upper part of the inner shell (Inner lid)	σ_r	—	-0.0491	—	—	2.36	137	57.0	13.9	205	13.7	—	—	—	—	—	—	—	—	—
		σ_θ		2.31		—															
		σ_z		1.15		—															
		τ		—		6.87															
4	Inner shell lid clamping bolt	σ_t	174	3.20	—	—	177	2/3Sy 458	1.58	182	Sy 687	2.77	182	Sy 687	2.77	—	—	—	—	—	—
		σ_b	—	—	—	4.68															
		τ	—	—	—	—															
5	Square fuel basket	σ_b	—	—	—	177	—	—	—	177	205	0.158	—	—	—	—	—	—	—	—	—

Pm; General primary membrane stress; PL; Local primary membrane stress; Pb; Primary bending stress; Q; Secondary stress; F; Peak stress;

Sa; Repeated peak stress; N; Number of uses; Na; Permissible number of repetition; DF; Cumulative fatigue coefficient;

Sm; Design stress intensity value; Sy; Yield point of the design; MS; Margin of safety σ_r ; Diameter direction stress σ_θ ; Periphery direction stress σ_z ; Axial stress σ_b ; Bending stress τ ; Shear stress σ_t ; Ability of bolt stress

(II) -Table A.16 Stress evaluation for 1.2 m horizontal drop (2/6)

Stress units
;N/mm²

No.	Stress Position to be evaluated		Stress at initial clamping	Stress due to internal pressure	Stress due to thermal expansion	Impact stress	Primary stress						Primary+secondary stress			Fatigue					
							Pm(PL)	2/3Sy	MS	PL+Pb	Sy	MS	PL+Pb +Q	Sy	MS	PL+Pb +Q+F	Sa	N	Na	DF	MS
1	JRR-3 standard element (Uranium silicon aluminum dispersion alloy)	Surface direction	σ_b	—	—	—	20.0	—	—	—	20.0	63.8	2.19	—	—	—	—	—	—	—	—
		Axial direction	σ_c	—	—	—	1.35	—	—	—	1.35	63.8	46.2	—	—	—	—	—	—	—	—
2	JRR-3 follower element (Uranium silicon aluminum dispersion alloy)	Surface direction	σ_b	—	—	—	13.2	—	—	—	13.2	63.8	3.83	—	—	—	—	—	—	—	—
		Axial direction	σ_c	—	—	—	1.13	—	—	—	1.13	63.8	55.4	—	—	—	—	—	—	—	—
3	JRR-4 B type element	Surface direction	σ_b	—	—	—	16.0	—	—	—	16.0	63.8	2.98	—	—	—	—	—	—	—	—
		Axial direction	σ_c	—	—	—	1.17	—	—	—	1.17	63.8	53.5	—	—	—	—	—	—	—	—
4	JRR-4 L type element	Surface direction	σ_b	—	—	—	16.4	—	—	—	16.4	63.8	2.89	—	—	—	—	—	—	—	—
		Axial direction	σ_c	—	—	—	1.62	—	—	—	1.62	63.8	38.3	—	—	—	—	—	—	—	—
5	JRR-4 (Uranium silicon aluminum dispersion alloy)	Surface direction	σ_b	—	—	—	22.0	—	—	—	22.0	63.8	1.90	—	—	—	—	—	—	—	—
		Axial direction	σ_c	—	—	—	1.50	—	—	—	1.50	63.8	41.5	—	—	—	—	—	—	—	—
6	JMTR standard element	Surface direction	σ_b	—	—	—	20.3	—	—	—	20.3	63.8	2.14	—	—	—	—	—	—	—	—
		Axial direction	σ_c	—	—	—	1.37	—	—	—	1.37	63.8	45.5	—	—	—	—	—	—	—	—
7	JMTR follower element	Surface direction	σ_b	—	—	—	13.9	—	—	—	13.9	63.8	3.58	—	—	—	—	—	—	—	—
		Axial direction	σ_c	—	—	—	1.18	—	—	—	1.18	63.8	53.0	—	—	—	—	—	—	—	—

Pm; General primary membrane stress; PL; Local primary membrane stress; Pb; Primary bending stress; Q; Secondary stress; F; Peak stress;

Sa; Repeated peak stress; N; Number of uses; Na; Permissible number of repetition; DF; Cumulative fatigue coefficient;

Sm; Design stress intensity value; Sy; Yield point of design; MS; Margin of safety σ_b ; Bending stress σ_c ; Compression stress

(II) -Table A.16 Stress evaluation for 1.2 m horizontal drop (3/6)

Stress units
;N/mm²

No.	Stress Position to be evaluated		Stress at initial clamping	Stress due to internal pressure	Stress due to thermal expansion	Impact stress	Primary stress						Primary+secondary stress			Fatigue					
							Pm(PL)	2/3Sy	MS	PL+Pb	Sy	MS	PL+Pb +Q	Sy	MS	PL+Pb +Q+F	Sa	N	Na	DF	MS
1	KUR standard element (Uranium silicon aluminum dispersion alloy)	Surface direction	σ_b	—	—	—	13.9	—	—	—	13.9	63.7	3.58	—	—	—	—	—	—	—	—
		Axial direction	σ_c	—	—	—	1.06*1	1.06	4.67	3.40	—	—	—	—	—	—	—	—	—	—	—
2	KUR Special element (Uranium silicon aluminum dispersion alloy)	Surface direction	σ_b	—	—	—	13.9	—	—	—	13.9	63.7	3.58	—	—	—	—	—	—	—	—
		Axial direction	σ_c	—	—	—	1.06*1	1.06	4.67	3.40	—	—	—	—	—	—	—	—	—	—	—
3	KUR half-loaded element (Uranium silicon aluminum dispersion alloy)	Surface direction	σ_b	—	—	—	13.9	—	—	—	13.9	63.7	3.58	—	—	—	—	—	—	—	—
		Axial direction	σ_c	—	—	—	0.92*1	0.92	4.67	4.07	—	—	—	—	—	—	—	—	—	—	—

Pm; General primary membrane stress; PL; Local primary membrane stress; Pb; Primary bending stress; Q; Secondary stress; F; Peak stress;

Sa; Repeated peak stress; N; Number of uses; Na; Permissible number of repetition; DF; Cumulative fatigue coefficient;

Sm; Design stress intensity value; Sy; Yield point of design; MS; Margin of safety σ_b ; Bending stress σ_c ; Compression stress

*1: axial compression stress

(II) -Table A.16 Stress evaluation for 1.2 m horizontal drop (4/6)

Stress units
:N/mm²

No.	Stress Position to be evaluated		Stress at initial clamping	Stress due to internal pressure	Stress due to thermal expansion	Impact stress	Primary stress						Primary+secondary stress			Fatigue					
							Pm(PL)	2/3Sy	MS	PL+Pb	Sy	MS	PL+Pb +Q	Sy	MS	PL+Pb +Q+F	Sa	N	Na	DF	MS
1	JMTRC Standard fuel element (A, B, C type)	Surface direction	σ_b	—	—	—	15.5	—	—	—	15.5	63.8	3.11	—	—	—	—	—	—	—	—
		Axial direction	σ_c	—	—	—	1.10	—	—	—	1.10	63.8	57.0	—	—	—	—	—	—	—	—
2	JMTRC Standard fuel element ($\phi 2.2$ pin, fix type) (B, C type)	Surface direction	σ_b	—	—	—	15.4	—	—	—	15.4	63.8	3.14	—	—	—	—	—	—	—	—
		Axial direction	σ_c	—	—	—	1.09	—	—	—	1.09	63.8	57.5	—	—	—	—	—	—	—	—
3	JMTRC Special fuel element (Special A type)	Surface direction	σ_b	—	—	—	23.2	—	—	—	23.2	63.8	1.75	—	—	—	—	—	—	—	—
		Axial direction	σ_c	—	—	—	1.10	—	—	—	1.10	63.8	57.0	—	—	—	—	—	—	—	—
4	JMTRC Special fuel element (Special B type)	Surface direction	σ_b	—	—	—	15.9	—	—	—	15.9	63.8	3.01	—	—	—	—	—	—	—	—
		Axial direction	σ_c	—	—	—	1.37	—	—	—	1.37	63.8	45.5	—	—	—	—	—	—	—	—
5	JMTRC Special fuel element (Special C, Special D type)	Surface direction	σ_b	—	—	—	23.1	—	—	—	23.1	63.8	1.76	—	—	—	—	—	—	—	—
		Axial direction	σ_c	—	—	—	1.65	—	—	—	1.65	63.8	37.6	—	—	—	—	—	—	—	—
6	JMTRC fuel follower (HF type)	Surface direction	σ_b	—	—	—	9.92	—	—	—	9.92	63.8	5.43	—	—	—	—	—	—	—	—
		Axial direction	σ_c	—	—	—	0.89	—	—	—	0.89	63.8	70.6	—	—	—	—	—	—	—	—
7	JMTRC Standard fuel element (MA, MB, MC type)	Surface direction	σ_b	—	—	—	15.4	—	—	—	15.4	63.8	3.14	—	—	—	—	—	—	—	—
		Axial direction	σ_c	—	—	—	1.09	—	—	—	1.09	63.8	57.5	—	—	—	—	—	—	—	—
8	JMTRC Special fuel element (Special MB, Special MC type)	Surface direction	σ_b	—	—	—	23.0	—	—	—	23.0	63.8	1.77	—	—	—	—	—	—	—	—
		Axial direction	σ_c	—	—	—	1.08	—	—	—	1.08	63.8	58.0	—	—	—	—	—	—	—	—
9	JMTRC fuel follower (MF type)	Surface direction	σ_b	—	—	—	10.0	—	—	—	10.0	63.8	5.38	—	—	—	—	—	—	—	—
		Axial direction	σ_c	—	—	—	0.91	—	—	—	0.91	63.8	69.1	—	—	—	—	—	—	—	—

Pm; General primary membrane stress; PL; Local primary membrane stress; Pb; Primary bending stress; Q; Secondary stress; F; Peak stress;

Sa; Repeated peak stress; N; Number of uses; Na; Permissible number of repetition; DF; Cumulative fatigue coefficient;

Sy; Yield point of design; MS; Margin of safety σ_b ; Bending stress σ_c ; Compression stress

(II) -Table A.16 Stress evaluation for 1.2 m horizontal drop (5/6)

Stress units
;N/mm²

No.	Stress Position to be evaluated	Stress at initial clamping	Stress due to internal pressure	Stress due to thermal expansion	Impact stress	Primary stress						Primary+secondary stress			Fatigue					
						Pm(PL)	2/3Sy	MS	PL+Pb	Sy	MS	PL+Pb +Q	Sy	MS	PL+Pb +Q+F	Sa	N	Na	DF	MS
1	JMTRC Special fuel element hold down part (Special A type)	σ_b	—	—	—	9.63	—	—	—	9.63	245	24.4	—	—	—	—	—	—	—	—
2	JMTRC Special fuel element hold down part (Special B type)	σ_c	—	—	—	15.6	—	—	—	15.6	245	14.7	—	—	—	—	—	—	—	—
3	JMTRC Special fuel element hold down part (Special C, Special D type)	σ_c	—	—	—	9.63	—	—	—	9.63	245	24.4	—	—	—	—	—	—	—	—
4	JMTRC Special fuel element hold down part (Special MB, Special MC type)	σ_c	—	—	—	9.63	—	—	—	9.63	245	24.4	—	—	—	—	—	—	—	—

Pm; General primary membrane stress; PL; Local primary membrane stress; Pb; Primary bending stress; Q; Secondary stress; F; Peak stress;

Sa; Repeated peak stress; N; Number of uses; Na; Permissible number of repetition; DF; Cumulative fatigue coefficient;

Sy; Yield point of design; MS; Margin of safety σ_b ; Bending stress σ_c ; Compression stress

(II) -Table A.16 Stress evaluation for 1.2 m horizontal drop (6/6)

Stress units
;N/mm²

No.	Stress Position to be evaluated		Stress at initial clamping	Stress due to internal pressure	Stress due to thermal expansion	Impact stress	Primary stress						Primary+secondary stress			Fatigue					
							Pm(PL)	2/3Sy	MS	PL+Pb	Sy	MS	PL+Pb +Q	Sy	MS	PL+Pb +Q+F	Sa	N	Na	DF	MS
1	KUCA coupon		σ_c	—	—	—	2.21	—	—	—	2.21	63.7	28.8	—	—	—	—	—	—	—	—
2	KUCA flat plate	Surface direction	σ_b	—	—	—	0.16	—	—	—	0.16	63.7	398	—	—	—	—	—	—	—	—
		Axial direction	σ_c	—	—	—	0.96	—	—	—	0.96	63.7	66.4	—	—	—	—	—	—	—	—

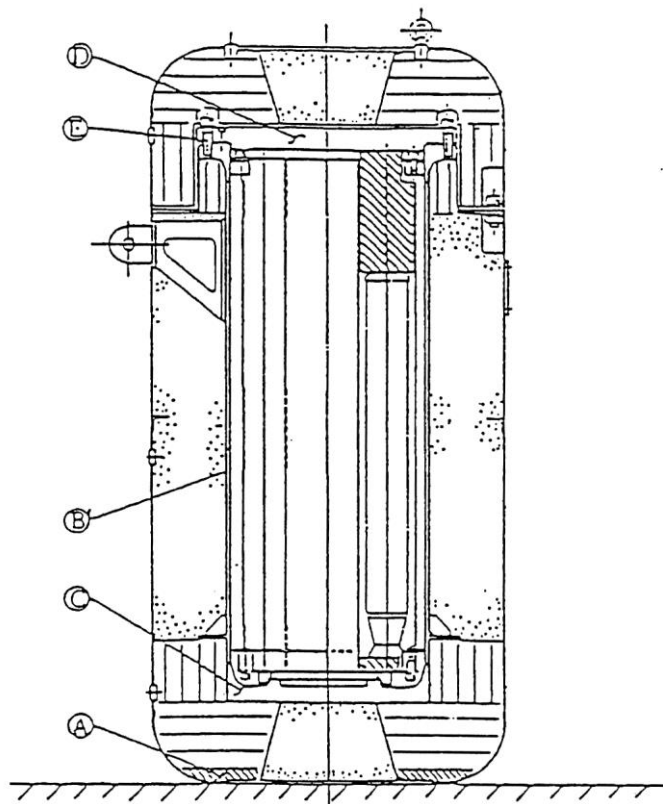
Pm; General primary membrane stress; PL; Local primary membrane stress; Pb; Primary bending stress; Q; Secondary stress; F; Peak stress;
Sa; Repeated peak stress; N; Number of uses; Na; Permissible number of repetition; DF; Cumulative fatigue coefficient;
Sy; Yield point of design; MS; Margin of safety σ_b ; Bending stress σ_c ; Compression stress

(7) Analysis of stress for 1.2 m bottom side vertical drop

Analysis of stress for 1.2 m bottom side vertical drop is separately performed for the main body of the packaging and fuel elements. Stress analysis in each portion should be performed in order to determine the principal stress. Classification of stress and evaluation of stress intensity are conducted in A.5.3 (7) (c).

(a) Main body of the packaging

The positions for stress evaluation of the main body of the packaging for 1.2 m bottom side vertical drop are given as in (II)-Fig.A.50 from the standpoint of maintaining sealing performance.



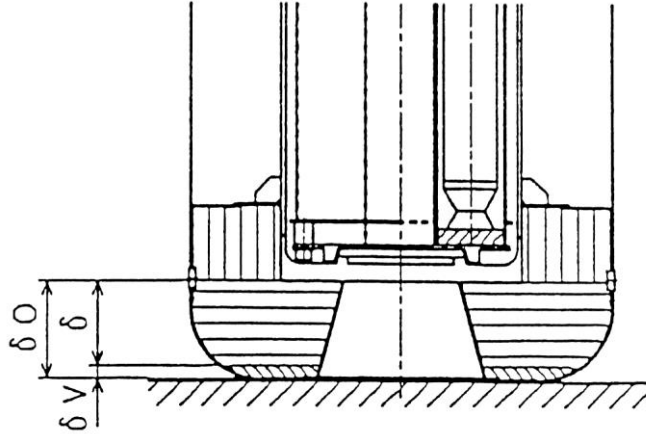
Symbol	Evaluation position
(A)	Shock absorber (for quantity of deformation)
(B)	Barrel of the inner shell
(C)	Bottom plate of the inner shell
(D)	Inner lid
(E)	Inner lid clamping bolt

(II)-Fig.A.50 Stress evaluation position for 1.2m lower side vertical drop
(main body of packaging)

Ⓐ Deformation of the shock absorber

Even if the shock absorber is deformed for 1.2 m bottom side vertical drop, the deformation should not reach the bottom of the inner shell.

An analytical model is shown in (II)-Fig.A. 51.



(II)-Fig.A. 51 Analytical model of interference to inner shell
due to shock absorber deformation for 1.2 m
lower side vertical drop

As is indicated in (II)-Fig.A. 51, residual quantity δ (mm) of the shock absorber for 1.2 m bottom side vertical drop is,

$$\delta = \delta_0 - \delta_v$$

where

δ_0 : Minimum thickness of the shock absorber before deformation,

$$\delta_0 = 194 \quad [\text{mm}]$$

δ_v : Deformation of the shock absorber,

$$\delta_v = 18.2 \quad [\text{mm}]$$

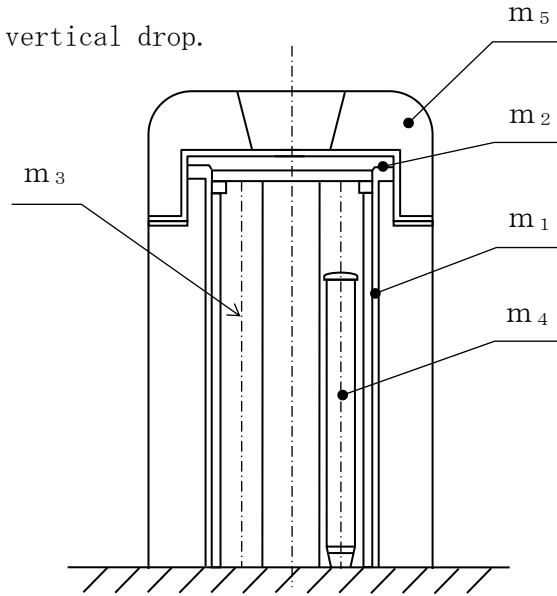
Therefore, the deformation is

$$\delta = 194 - 18.2 = 175.8 \quad [\text{mm}]$$

Thus, for 1.2 m bottom side vertical drop, deformation suffered by the shock absorber does not reach the bottom of the inner shell.

Ⓑ Frame of Inner shell

(II)-Fig. A. 52 shows an analytical model for the stress on the frame of inner shell for 1.2 m bottom side vertical drop.



(II)-Fig. A. 52 Stress analysis model of inner shell for 1.2m lower side vertical drop

As shown in (II)-Fig. A. 52, compression force, due to dead weight and the weight of the peripheral part of the inner lid, acts on the inner shell.

The stress resulting from the compression is,

$$\sigma_c = \frac{F}{A}$$

where F: Compressive force acting on the side of inner shell,

$$F = (m_1 + m_2 + m_3 + m_4 + m_5) \cdot N \quad [N]$$

m_1 : Weight of the inner shell (side and flange), $m_1 = 200 \quad [kg]$

m_2 : Weight of the inner lid $m_2 = 120 \quad [kg]$

m_3 : Weight of the fuel basket $m_3 = 138 \quad [kg]$

m_4 : Weight of the content $m_4 = 92 \quad [kg]$

m_5 : Weight of the outer lid $m_5 = 120 \quad [kg]$

N : Design acceleration, $N = 250.6 \cdot g [m/s^2]$

$$F = (200 + 120 + 138 + 92 + 120) \times 250.6 \times 9.81 = 1.65 \times 10^6 \quad [N]$$

A: Cross sectional area of the inner shell

$$A = \frac{\pi}{4} (d_2^2 - d_1^2) \quad [\text{mm}^2]$$

d_2 : Outer diameter of the inner shell, $d_2=480$ [mm]

d_1 : Inner diameter of the inner shell, $d_1=460$ [mm]

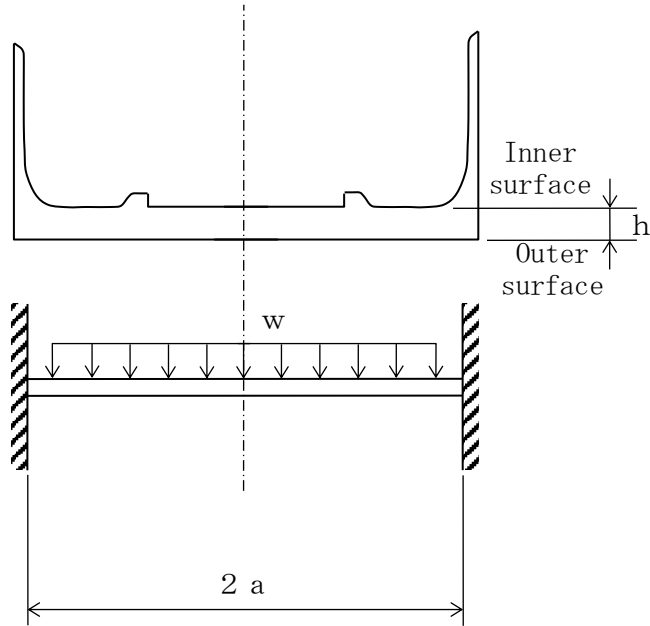
$$A = \frac{\pi}{4} (480^2 - 460^2) = 1.48 \times 10^4 \quad [\text{mm}^2]$$

Therefore, σ_c due to compression is,

$$\sigma_c = \frac{1.65 \times 10^6}{1.48 \times 10^4} = 111 \quad [\text{N/mm}^2]$$

© Bottom plate of the inner shell

(II)-Fig. A. 53 shows the stress analysis model of the inner shell's bottom plate for 1.2 m bottom side vertical drop.



(II)-Fig. A. 53 Stress analysis model of inner shell bottom plate for 1.2m lower side vertical drop

As indicated in (II)-Fig. A. 53, the weight of the fuel baskets contents and the dead weight of the inner shell's bottom plate act uniformly on the bottom of the inner shell. The stress, generated on the disc which receives uniform load, reaches its maximum at the fixing point of the circumferentially fixed disc.

The stress is

$$\sigma_{\theta} = \pm 0.225 \frac{w \cdot a^2}{h^2}$$

$$\sigma_r = \pm 0.75 \frac{w \cdot a^2}{h^2}$$

$$\sigma_z = -w \text{ (inner surface)}$$

where

σ_{θ} : Circumferential stress [N/mm²]

σ_r : Radial stress [N/mm²]

σ_z : Axial stress [N/mm²]

a : Inner radius of inner shell's bottom plate, a=230 [mm]

h : Thickness of the inner shell's bottom plate, h= 35 [mm]

w : Uniform load,

$$w = \frac{(m_3 + m_4 + m_7) \cdot N}{\pi a^2}$$

m3 : Weight of the fuel basket, m3 =138 [kg]

m4 : Weight of the content m4 = 92 [kg]

m7 : Weight of the inner shell's bottom plate, m7 =55 [kg]

N : Design acceleration, N=250.6 · g [m/s²]

$$w = \frac{(138+92+55) \times 250.6 \times 9.81}{\pi \times 230^2} = 4.22 \text{ [N/mm}^2\text{]}$$

Therefore,

$$\sigma_{\theta} = \pm 0.225 \times \frac{4.22 \times 230^2}{35^2} = \pm 41.0 \text{ [N/mm}^2\text{]}$$

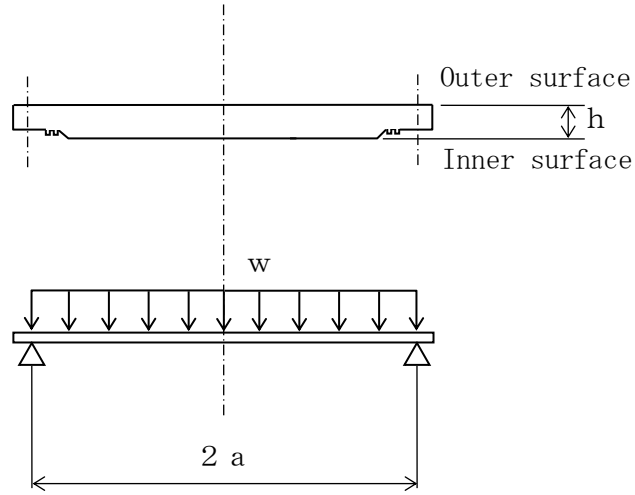
$$\sigma_r = \pm 0.75 \times \frac{4.22 \times 230^2}{35^2} = \pm 137 \text{ [N/mm}^2\text{]}$$

$$\sigma_z = -4.22 \text{ (inner surface) [N/mm}^2\text{]}$$

For the double signs of the stress values, the upper sign (+) corresponds to the inner surface and the lower sign (−) to the outer surface

① Inner lid

(II)-Fig. A. 54 shows the stress analytical model of the inner lid for 1.2 m bottom side vertical drop.



(II)-Fig. A. 54 Stress analysis model of inner lid for 1.2m lower side vertical drop

As indicated in (II)-Fig. A. 54, the dead weight acts uniformly on the inner lid. The stress, generated in the disc which receives uniform load, reaches its maximum in the center of the disc.

The stress is,

$$\sigma_r = \sigma_\theta = \mp 1.24 \frac{w \cdot a^2}{h^2}$$

$$\sigma_z = -w \text{ (outer surface)}$$

where

σ_r : Radial stress [N/mm²]

σ_θ : Circumferential stress [N/mm²]

σ_z : Axial stress [N/mm²]

a: Radius of the circle of the inner lid supporting points,

a=285 [mm]

h: Thickness of the inner lid, h=55 [mm]

w: Uniform load resulting from dead weight of the lid,

$$w = \gamma \cdot h \cdot N = 7.93 \times 10^{-6} \times 55 \times 250.6 \times 9.81 = 1.07 \text{ [N/mm}^2\text{]}$$

N: Design acceleration, $N = 250.6 \cdot g$ [m/s²]

γ : Density of the inner lid, $\gamma = 7.93 \times 10^{-6}$ [kg/mm³]

Hence,

$$\sigma_r = \sigma_\theta = \mp 1.24 \frac{1.07 \times 285^2}{55^2} = \mp 35.6 \text{ [N/mm}^2\text{]}$$

$$\sigma_z = -1.07 \text{ (outer surface) [N/mm}^2\text{]}$$

For the double signs of the stress values, the upper sign (−) corresponds to the outer surface and the lower sign (+) to the inner surface.

Ⓔ Inner lid clamping bolt

In a bottom side vertical drop, no load is received by the inner lid clamping bolt.

Therefore, no stress is generated.

(b) Fuel elements and fuel plate

(b)-1. Fuel elements

(1) Fuel plate

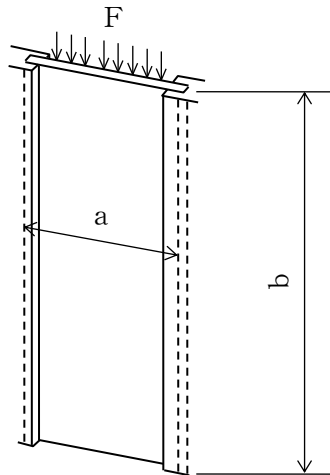
This section analyzes the stress generated on the rectangular fuel element for 1.2 m bottom side vertical drop.

(i) In case of calking both ends of fuel plate

With regard to the rectangular fuel element, there are 11 types of fresh fuel elements including the follower type, and there are 9 types of lowly irradiated fuel elements. In this section the analysis method is described for the JRR-3 standard, the same analysis was conducted for the other 11 types, and the result is shown in the (II)-Table A.17.

However, analysis is performed on the assumption that uranium-aluminum alloy has the same strength as the covering material.

(II)-Fig.A.55 shows an analytical model.



(II)-Fig.A.55 Stress analysis model of rectangular fuel element for 1.2m lower side vertical drop.

As indicated in (II)-Fig.A.55, the fuel plate is caulked and fixed at both extremities. Its sustaining force is,

$$F_H = f \cdot 2b$$

where

F_H : Strength to sustain the fuel plate [N]

f : Sustaining force per unit length; $f=26.5$ [N/mm]

b: Length of the fuel plate; b=770 [mm]

Therefore,

$$F_H = 26.5 \times 2 \times 770 = 4.08 \times 10^4 \text{ [N]}$$

Thus, the force for dropping of the fuel plate is

$$F = m \cdot N$$

where

F: Force for dropping [N]

m: Weight of the fuel plate, m=0.279 [kg]

N: Design acceleration, N=250.6 · g [m/s²]

Therefore,

$$F = 0.279 \times 250.6 \times 9.81 = 686 \text{ [N]}$$

Thus, the fuel plate does not slip down since the force to sustain the fuel plate exceeds the force for dropping of the plate.

As shown above, when a force for dropping due to the dead weight of the fuel plate which is fixed on its extremities acts on it, the shearing stress τ occurs. This stress is,

$$\tau = \frac{F}{2(h_2 - h_1) b}$$

where

τ : Shearing stress [N/mm²]

F: Force for dropping of the fuel plate, F=686 [N]

h₂: Thickness of the fuel plate, h₂=1.27 [mm]

h₁: Thickness of fuel plate core, h₁=0.51 [mm]

b: Length of the fuel plate, b=770 [mm]

Thus, the shearing stress is

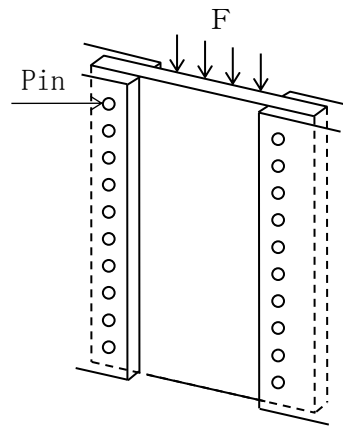
$$\tau = \frac{686}{2 \times (1.27 - 0.51) \times 770} = 0.586 \text{ [N/mm}^2\text{]}$$

(ii) In case of fuel plate fixed by pin

The stress of the pin fixing of the fuel plate of the lowly irradiated fuel element, generated at 1.2m vertical drop, is analyzed. There are 6 types of lowly irradiated fuel elements including follower types, in this section, the stress analysis method for the pin fixing type fuel element is described and its result is shown in the (II)-Table A.17.

The uranium aluminum alloy is treated to have the same strength as the clad material in the analysis.

The analytical model is shown in (II)-Fig. A. 56.



(II)-Fig. A. 56 Analytical model of 1.2m lower portion vertical drop of lowly irradiated fuel element

As shown in (II)-Fig. A. 56, the fuel plate is fixed with pin at the side plate.

This retaining force is given as follows.

$$F_H = \tau_a \times A \quad [\text{N}]$$

Where,

F_H : Force for retaining fuel plate [N]

τ_a : Allowable shear stress of pin = 36.8 [N/mm²]

A : Sectional area of pin [mm²]

$$= \frac{\pi}{4} \times d^2 \times n$$

d : Pin diameter = 2.2 [mm]

n : No. of pin = 62 [-]

$$F_H = \tau_a \times \frac{\pi}{4} \times d^2 \times n$$

$$= 36.8 \times \frac{\pi}{4} \times 2.2^2 \times 62 = 8.67 \times 10^3 \quad [\text{N}]$$

The force acting on the fuel plate due to the acceleration is given as follows,

$$F = m \cdot N$$

Where,

F : Force acts on fuel plate when dropping [N]

m : Weight of the fuel plate = 0.217 [kg]

N : Design acceleration = 250.6 [m/s²]

Therefore the following value is obtained.

$$F = 0.217 \times 250.6 \times 9.81 = 533 \quad [\text{N}]$$

From the above, the retaining force of the pin is larger than the dropping force of the fuel plate by the acceleration. The fuel plate does not slide from fixing.

When the fuel plate, fixed with pin at the both ends, is freely dropped, the tensile force occurs at the pin portion of the fuel plate and is given as follows,

$$\sigma_t = \frac{W_o}{A}$$

Where,

$$W_o = \frac{W \times N}{n/2}$$

$$W_o = \frac{0.217 \times 250.6 \times 9.81}{62/2} = 17.2$$

σ_t : Stress of fuel plate pin [N/mm²]

W_o : Load acting on fuel pin portion [kg]

n : No. of pin, n = 62

N : Design acceleration, N = 250.6g [m/sec²]

A : Effective sectional area of pin [mm²]

$$A = ((L_1 - L_2)/2 - d) \times t_1$$

L₁ : Width of fuel plate, L₁ = 70.6 [mm]

L₂ : Width of fuel plate core, L₂ = 61.8 [mm]

t₁ : Thickness of fuel plate, t =1.27 [mm]

d : Pin diameter, d =2.35 [mm]

$$A = ((70.8 - 60.4)/2 - 2.35) \times 1.27 = 2.60 \text{ [mm}^2\text{]}$$

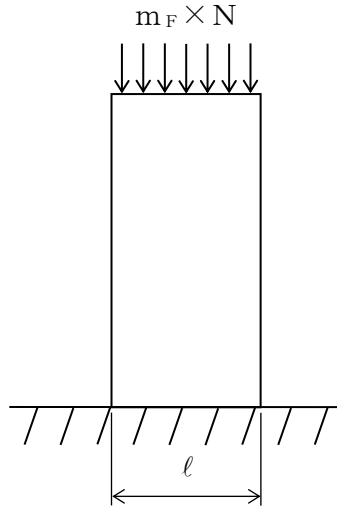
Therefor the following value of stress is obtained.

$$\sigma_t = \frac{17.2}{2.60} = 6.61 \text{ [N/mm}^2\text{]}$$

(iii) In case of fuel plate not fixed by the side plate

The stress of the lowly irradiated fuel element, when dropped vertically from 1.2m height, is analyzed. There are five types of lowly irradiated fuel elements including follower types, in this section. The fuel element not fixed by the side plate is analyzed and the result is shown in (II)-Table A.17.

The uranium aluminum alloy is treated to have the same strength as the clad material in this analysis. The analytical model is shown in [\(II\)-Fig.A.57](#).



[\(II\)-Fig.A.57](#) Analytical model of 1.2m lower portion vertical drop of lowly irradiated fuel element

As shown in [\(II\)-Fig.A.57](#), the compressive stress is generated in the rectangular plate subjected to its own weight of the fuel element, and is given as follows,

$$\sigma_c = \frac{W}{A} = \frac{m_F \times N}{l(h_2 - h_1)}$$

Where,

m_F : Fuel plate mass, m_F = 0.223 [kg]

l : Width of fuel plate, l =66.6 [mm]

h2 : Thickness of fuel plate, h2 =1.27 [mm]

h1 : Thickness of fuel plate core, h1 =0.51 [mm]

N : Design acceleration, N =250.6g [m/s²]

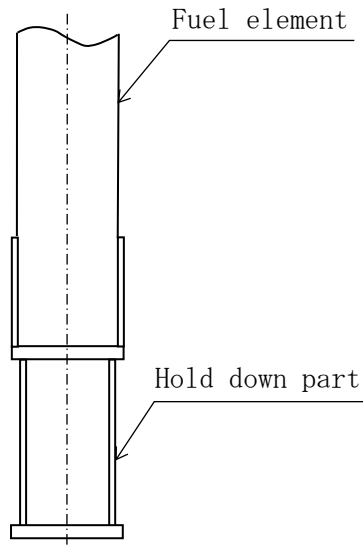
Therefore, the following value of stress is obtained.

$$\sigma_c = \frac{0.223 \times 250.6g}{66.6 \times (1.27 - 0.51)} = 10.8 \text{ [N/mm}^2\text{]}$$

(2) Fuel element hold-down part

As shown in (I)-D section, the lowly irradiated fuel elements are cut at the lower adapter portion and the upper holder portion in order to reduce the weight, therefore the total length becomes short, A hold-down part is provided to adjust the length. In this section, the stress analysis method for the stress occurs in the hold down part is shown and the result is summarized in (II)-Table A.17.

The analysis model is shown in [\(II\)-Fig. A. 58.](#)



[\(II\)-Fig. A. 58](#) Analytical model of hold down part

As shown in [\(II\)-Fig. A. 58](#), the hold-down part is subjected to the own weight and the fuel element weight, and the compressive stress σ_c is generated as follows,

$$\sigma_c = \frac{W}{A} = \frac{(m_z + m_f) \times N}{\frac{1}{4} (h_o^2 - h_i^2)}$$

Where,

m_z : Mass of hold down part, $m_z = 1.3 \times 2$ [kg]

m_f : Mass of hold element, $m_f = 2.0$ [mm]

N : Design acceleration, $N = 250.6g$ [m/s^2]

h_o : Outside diameter of hold down part, $h_o = 60$ [mm]

h_i : Inside diameter of hold down part, $h_i = 52$ [mm]

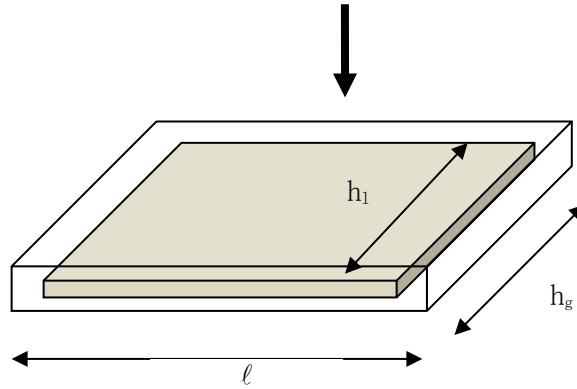
Therefore, following is obtained.

$$\sigma_c = \frac{(2.6 + 2.0) \times 250.6 \cdot g}{\frac{1}{4} \times (60^2 - 52^2)} = 16.1 \text{ [N/mm}^2\text{]}$$

(b)-2. Fuel plate for the critical assembly fuel (KUCA fuel)

This section analyzes the stress generated in the fuel plate for the critical assembly at the time of 1.2 m vertical drop. The analysis model is the same as the lowly irradiated fuel elements shown in (II)-Fig.A.57 (when the fuel plate and side plate are not fixed).

For the coupon fuel in vertical drop, the design acceleration is applied to the perpendicular direction to the plane of the fuel as shown in (II)-Fig.A.59.



(II)-Fig.A.59 Analytical model of 1.2m vertical drop: coupon fuel

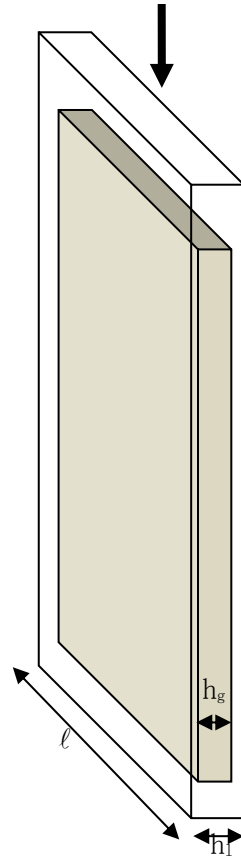
In the case, the total thickness of cladding is 6 mm, which is the twice width of aluminum case.

m_F : Weight of the fuel plate	$m_F=0.036$ [kg]
l : Length of the fuel plate	$l=50.8$ [mm]
h_2-h_1 :Cladding thickness	$h_2-h_1= 6$ [mm]
N : Design acceleration	$N=250.6 \cdot g$ [m/s ²]

Therefore, the compressive stress σ_c are given as follows.

$$\begin{aligned}\sigma_c &= (0.036 \times 250.6 \times g) / (50.8 \times 6) \\ &= 0.30 \quad [\text{N/mm}^2]\end{aligned}$$

For the flat fuel in vertical drop, the design acceleration is applied to the parallel direction to the plane of the fuel plate as shown in (II)-Fig.A. 60.



(II)-Fig.A. 60 Analytical model of 1.2m vertical drop: flat fuel

In the case,

m_F : Weight of the fuel plate	$m_F=0.23$ [kg]
l : Length of the fuel plate	$l=62$ [mm]
h_2 : Fuel plate thickness	$h_2=1.5$ [mm]
h_1 : Fuel plate core thickness	$h_1=0.5$ [mm]
N : Design acceleration	$N=250.6 \cdot g$ [m/s ²]

Therefore, the compressive stress σ_c are given as follows.

$$\begin{aligned}\sigma_c &= (0.23 \times 250.6 \times g) / (62 \times (1.5 - 0.5)) \\ &= 9.12 \quad [\text{N/mm}^2]\end{aligned}$$

(c) Comparison of allowable stress

Results of the stress evaluation in each analysis item in (II)-5.3 (7) are shown together in (II)-Table A.17.

As shown in this table, the margin of safety in regard to analysis reference is positive even if each or combined load is applied.

Therefore, the integrity of this package is maintained under the condition of the 1.2 m bottom side vertical drop test.

(II) -Table A.17 Stress evaluation for 1.2 m bottom side vertical drop (1/6)

Stress units
;N/mm²

No.	Stress Position to be evaluated		Stress at initial clamping	Stress due to internal pressure	Stress due to thermal expansion	Impact stress	Primary stress						Primary+secondary stress			Fatigue					
							Pm(PL)	Sm	MS	PL+Pb	1.5Sm	MS	PL+Pb +Q	3Sm	MS	PL+Pb +Q+F	Sa	N	Na	DF	MS
1	Frame of Inner shell		σ_r	—	−0.0491	—	112	137	0.223	—	—	—	—	—	—	—	—	—	—	—	
			σ_θ	2.31	—	—															
			σ_z	1.15	−111																
2	Bottom plate of the inner shell		Inner Surface	σ_r	3.18	137	4.32	137	30.7	144.5	205	0.418	—	—	—	—	—	—	—	—	
				σ_θ	0.953	41.0															
				σ_z	−0.098	−4.22															
			Outer Surface	σ_r	−3.18	−137	0	137	—	140	205	0.464	—	—	—	—	—	—	—	—	
				σ_θ	−0.953	−41.0															
				σ_z	0	0															
3	Upper part of the inner shell (Inner lid)		Inner Surface	σ_r	−3.27	35.6	0.098	2/3Sy 458	4672	32.4	Sy 687	20.2	—	—	—	—	—	—	—	—	
				σ_θ	−3.27	35.6															
				σ_z	−0.098	0															
			Outer Surface	σ_r	3.27	−35.6	1.07	2/3Sy 458	427	31.3	Sy 687	20.9	—	—	—	—	—	—	—	—	
				σ_θ	3.27	−35.6															
				σ_z	0	−1.07															
4	Inner shell lid clamping bolt		σ_t	174	3.20	—	177	2/3Sy 458	1.58	—	—	—	—	—	—	—	—	—	—	—	
			σ_b	—	—	—															
			τ	—	—	—															

Pm; General primary membrane stress; PL; Local primary membrane stress; Pb; Primary bending stress; Q; Secondary stress; F; Peak stress;

Sa; Repeated peak stress; N; Number of uses; Na; Permissible number of repetition; DF; Cumulative fatigue coefficient;

Sm; Design stress intensity value; Sy; Yield point of the design; MS; Margin of safety σ_r ; Diameter direction stress σ_θ ; Periphery direction stress σ_z ; Axial stress σ_b ; Bending stress τ ; Shear stress σ_t ; Ability of bolt stress

(II) -Table A.17 Stress evaluation for 1.2 m bottom side vertical drop (2/6)

Stress units
;N/mm²

No.	Stress Position to be evaluated	Stress at initial clamping	Stress due to internal pressure	Stress due to thermal expansion	Impact stress	Primary stress						Primary+secondary stress			Fatigue					
						Pm(PL)	2/3Sy	MS	PL+Pb	Sy	MS	PL+Pb +Q	Sy	MS	PL+Pb +Q+F	Sa	N	Na	DF	MS
1	JRR-3 standard (Uranium silicon aluminum dispersion alloy)	τ	—	—	—	0.586	—	—	—	0.586	63.8	107	—	—	—	—	—	—	—	—
2	JRR-3 follower element (Uranium silicon aluminum dispersion alloy)	τ	—	—	—	0.479	—	—	—	0.479	63.8	132	—	—	—	—	—	—	—	—
3	JRR-4 B type element	τ	—	—	—	0.439	—	—	—	0.439	63.8	144	—	—	—	—	—	—	—	—
4	JRR-4 L type element	τ	—	—	—	0.693	—	—	—	0.693	63.8	91.0	—	—	—	—	—	—	—	—
5	JRR-4 (Uranium silicon aluminum dispersion alloy)	τ	—	—	—	0.603	—	—	—	0.603	63.8	104	—	—	—	—	—	—	—	—
6	JMTR standard element	τ	—	—	—	0.595	—	—	—	0.595	63.8	106	—	—	—	—	—	—	—	—
7	JMTR follower element	τ	—	—	—	0.498	—	—	—	0.498	63.8	127	—	—	—	—	—	—	—	—

Pm; General primary membrane stress; PL; Local primary membrane stress; Pb; Primary bending stress; Q; Secondary stress; F; Peak stress;

Sa; Repeated peak stress; N; Number of uses; Na; Permissible number of repetition; DF; Cumulative fatigue coefficient;

Sy; Yield point of design; MS; Margin of safety τ ; Shear stress

Stress units

;N/mm²

(II) -Table A.17 Stress evaluation for 1.2 m bottom side vertical drop (3/6)

No.	Stress Position to be evaluated	Stress at initial clamping	Stress due to internal pressure	Stress due to thermal expansion	Impact stress	Primary stress						Primary+secondary stress			Fatigue					
						Pm(PL)	2/3Sy	MS	PL+Pb	Sy	MS	PL+Pb +Q	Sy	MS	PL+Pb +Q+F	Sa	N	Na	DF	MS
1	KUR standard (Uranium silicon aluminum dispersion alloy)	τ	—	—	—	0.454	—	—	—	0.454	63.7	139	—	—	—	—	—	—	—	—
2	KUR Special element (Uranium silicon aluminum dispersion alloy)	τ	—	—	—	0.454	—	—	—	0.454	63.7	139	—	—	—	—	—	—	—	—
3	KUR half-loaded element (Uranium silicon aluminum dispersion alloy)	τ	—	—	—	0.454	—	—	—	0.454	63.7	139	—	—	—	—	—	—	—	—

Pm; General primary membrane stress; PL; Local primary membrane stress; Pb; Primary bending stress; Q; Secondary stress; F; Peak stress;
Sa; Repeated peak stress; N; Number of uses; Na; Permissible number of repetition; DF; Cumulative fatigue coefficient;
Sy; Yield point of design; MS; Margin of safety τ ; Shear stress

(II) -Table A.17 Stress evaluation for 1.2 m bottom side vertical drop (4/6)

No.	Stress Position to be evaluated	Stress at initial clamping	Stress due to internal pressure	Stress due to thermal expansion	Impact stress	Primary stress						Primary+secondary stress			Fatigue					
						Pm(PL)	2/3Sy	MS	PL+Pb	Sy	MS	PL+Pb +Q	Sy	MS	PL+Pb +Q+F	Sa	N	Na	DF	MS
1	JMTRC Standard fuel element (A, B, C type)	τ	—	—	—	0.45	—	—	—	0.45	63.8	140	—	—	—	—	—	—	—	—
2	JMTRC Standard fuel element ($\phi 2.2$ pin, fix type) (B, C type)	σ_t	—	—	—	6.61	—	—	—	6.61	63.8	8.65	—	—	—	—	—	—	—	—
3	JMTRC Special fuel element (Special A type)	σ_c	—	—	—	10.8	—	—	—	10.8	63.8	4.90	—	—	—	—	—	—	—	—
4	JMTRC Special fuel element (Special B type)	σ_c	—	—	—	0.38	—	—	—	0.38	63.8	166	—	—	—	—	—	—	—	—
5	JMTRC Special fuel element (Special C, Special D type)	σ_c	—	—	—	11.0	—	—	—	11.0	63.8	4.80	—	—	—	—	—	—	—	—
6	JMTRC fuel follower (HF type)	τ	—	—	—	0.36	—	—	—	0.36	63.8	176	—	—	—	—	—	—	—	—
7	JMTRC Standard fuel element (MA, MB, MC type)	τ	—	—	—	0.45	—	—	—	0.45	63.8	140	—	—	—	—	—	—	—	—
8	JMTRC Special fuel element (Special MB, Special MC type)	σ_c	—	—	—	10.7	—	—	—	10.7	63.8	4.96	—	—	—	—	—	—	—	—
9	JMTRC fuel follower (MF type)	τ	—	—	—	0.36	—	—	—	0.36	63.8	176	—	—	—	—	—	—	—	—

Pm; General primary membrane stress; PL; Local primary membrane stress; Pb; Primary bending stress; Q; Secondary stress; F; Peak stress;

Sa; Repeated peak stress; N; Number of uses; Na; Permissible number of repetition; DF; Cumulative fatigue coefficient;

Sy; Yield point of the design; MS; Margin of safety σ_c ; Compression stress τ ; Shear stress σ_t ; Stress of the part of fuel plate pin

(II) -Table A.17 Stress evaluation for 1.2 m bottom side vertical drop (5/6)

No.	Stress Position to be evaluated		Stress at initial clamping	Stress due to internal pressure	Stress due to thermal expansion	Impact stress	Primary stress						Primary+secondary stress			Fatigue					
							Pm(PL)	2/3Sy	MS	PL+Pb	Sy	MS	PL+Pb +Q	Sy	MS	PL+Pb +Q+F	Sa	N	Na	DF	MS
1	JMTRC Special fuel element hold down part (Special B type)	σ_c	—	—	—	16.1	—	—	—	16.1	245	14.2	—	—	—	—	—	—	—	—	—

Pm ; General primary membrane stress; PL ; Local primary membrane stress; Pb ; Primary bending stress; Q ; Secondary stress; F ; Peak stress;

Sa ; Repeated peak stress; N ; Number of uses; Na ; Permissible number of repetition; DF ; Fatigue accumulation coefficient;

Sy ; Yield point of the design; MS ; Margin of safety σ_c ; Compression stress

(II) -Table A.17 Stress evaluation for 1.2 m bottom side vertical drop (6/6)

No.	Position to be evaluated	Stress	Stress at initial clamping	Stress due to internal pressure	Stress due to thermal expansion	Impact stress	Primary stress						Primary+secondary stress			Fatigue					
							Pm(PL)	2/3Sy	MS	PL+Pb	Sy	MS	PL+Pb +Q	Sy	MS	PL+Pb +Q+F	Sa	N	Na	DF	MS
1	KUCA Coupon type	σ_b	—	—	—	0.30	—	—	—	0.30	63.7	212	—	—	—	—	—	—	—	—	—
2	KUCA Flat type	σ_b	—	—	—	9.12	—	—	—	9.12	63.7	7.0	—	—	—	—	—	—	—	—	—

Pm; General primary membrane stress; PL; Local primary membrane stress; Pb; Primary bending stress; Q ; Secondary stress; F ; Peak stress;
Sa; Repeated peak stress; N ; Number of uses; Na; Permissible number of repetition; DF; Fatigue accumulation coefficient;
Sy; Yield point of the design; MS; Margin of safety σ_b ; Bending stress σ_c ; Compression stress

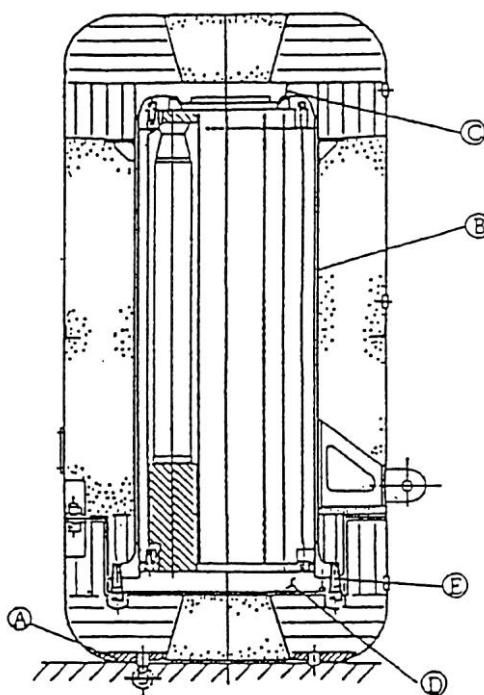
(8) Stress analysis for 1.2m lid side vertical drop

This section analyzes the stress for 1.2 m lid side vertical drop separately for the main body of the packaging and fuel basket. Stress analysis in each item is performed for the purpose of determining the principal stress.

Classification of stress and evaluation of stress intensity are conducted in A.5.3(8)(c).

(a) Main body of the packaging

Stress evaluation positions of the main body of the packaging for 1.2 m lid side vertical drop are determined as shown in [\(II\)-Fig.A.61](#) from the viewpoint of maintaining the containment.



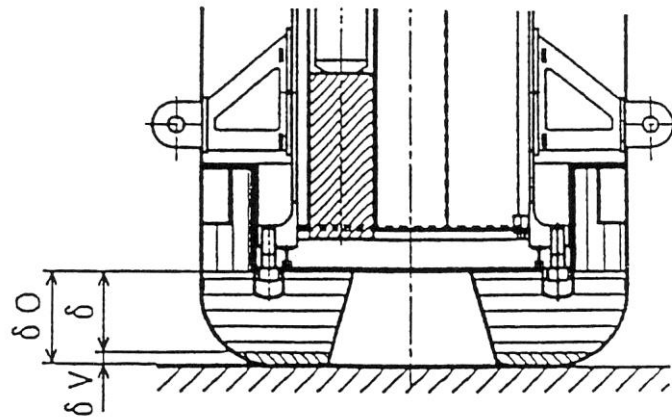
Symbol	Evaluation position
Ⓐ	Shock absorber (Quantity of deformation)
Ⓑ	Barrel of an inner shell
Ⓒ	Bottom plate of an inner shell
Ⓓ	Inner lid
Ⓔ	Inner lid clamping bolt

[\(II\)-Fig.A.61](#) Stress evaluation position for 1.2m lid side vertical drop
(main body of a packaging)

Ⓐ Deformation of the shock absorber

Even if the shock absorber is deformed for 1.2 m lid side vertical drop, the deformation should not reach the bottom of the inner shell.

An analytical model is shown in (II)-Fig. A. 62.



(II)-Fig. A. 62 Analytical model of interference to inner shell due to shock absorber deformation for 1.2m lid side vertical drop

As is indicated in (II)-Fig. A. 62, the remaining quantity δ (mm) of the shock absorber in the 1.2 m lid side vertical drop is,

$$\delta = \delta_0 - \delta_v$$

where

δ_0 : Minimum thickness of shock absorber before deformation,

$$\delta_0 = 186 \text{ [mm]}$$

δ_v : Deformation of the shock absorber, $\delta_v = 24.1 \text{ [mm]}$

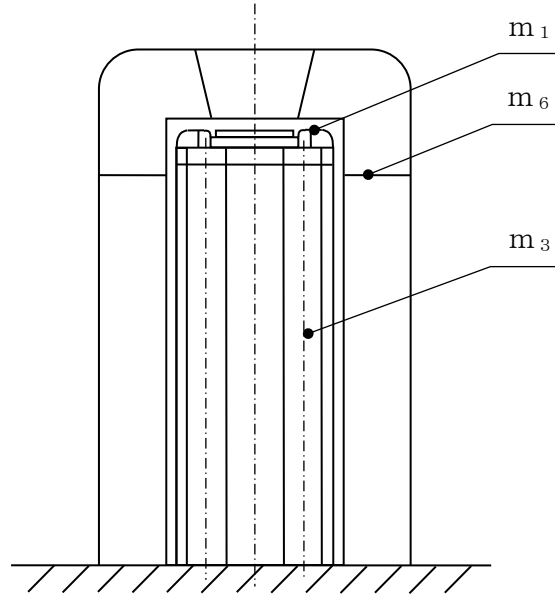
Hence, the remaining thickness is,

$$\delta = 186 - 24.1 = 161.9 \text{ [mm]}$$

Therefore, for 1.2 m lid side vertical drop, it is only the shock absorber that suffers deformation and the deformation does not attain the inner lid.

③ Frame of Inner shell

(II)-Fig.A. 63 is a stress analysis model of the frame of inner shell for 1.2 m lid side vertical drop.



(II)-Fig.A. 63 Stress analysis model of inner shell for 1.2m lid side vertical drop

As shown in (II)-Fig.A. 63, compression, due to dead weight and the weight of the peripheral part of the inner lid, acts on the frame of inner shell.

The stress generated from the compression is given by the following equation.

$$\sigma_c = \frac{F}{A}$$

where

F: Compression force acting on the inner shell

$$F = (m_1 + m_3 + m_6) \cdot N \quad [N]$$

m₁ : Weight of the inner shell (side and flange), m₁=210 [kg]

m₃ : Weight of the fuel basket, m₃=138 [kg]

m₆ : Weight of the outer shell, m₆=225 [kg]

N : Acceleration, N=240.7 · g [m/s²]

$$F = (210 + 138 + 225) \times 240.7 \times 9.81 = 1.35 \times 10^6 \quad [N]$$

A: Cross sectional area of the frame of inner shell,

$$A = \frac{\pi}{4} (d_2^2 - d_1^2) \quad [mm^2]$$

d_2 : Outer diameter of the inner shell, $d_2 = 480$ [mm]

d_1 : Inner diameter of the inner shell, $d_1 = 460$ [mm]

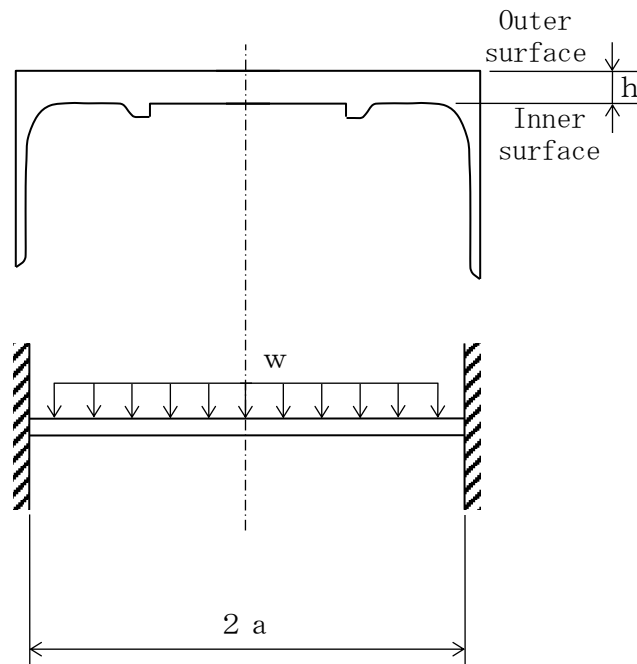
$$A = \frac{\pi}{4} (480^2 - 460^2) = 1.48 \times 10^4 \text{ [mm}^2\text{]}$$

Therefore,

$$\sigma_c = \frac{1.35 \times 10^6}{1.48 \times 10^4} = 91.2 \text{ [N/mm}^2\text{]}$$

© Bottom plate of the inner shell

(II)-Fig. A. 64 shows the stress analysis model of the inner shell's bottom plate for 1.2 m lid side vertical drop.



(II)-Fig. A. 64 Stress analysis model of inner shell bottom plate for 1.2m lid side vertical drop

As indicated in (II)-Fig. A. 64, the dead weight of both the bottom of the outer shell and the bottom plate of the inner shell act uniformly on the bottom of the inner shell. Stress generated in the disc which receives the uniform load reaches its maximum at the fixed end.

The stress is

$$\sigma_{\theta} = \pm 0.225 \frac{w \cdot a^2}{h^2}$$

$$\sigma_r = \pm 0.75 \frac{w \cdot a^2}{h^2}$$

$$\sigma_z = -w \text{ (Outer surface)}$$

where

σ_θ : Circumferential stress [N/mm²]

σ_r : Radial stress [N/mm²]

σ_z : Axial stress [N/mm²]

a: Inner radius of the inner shell's bottom plate, a= 230 [mm]

h: Plate thickness of the inner shell's bottom plate, h=35 [mm]

w: Uniform load,

$$w = \frac{(m_7 + m_8) \cdot N}{\pi a^2}$$

m_7 : Weight of the inner shell's bottom plate, $m_7 = 55$ [kg]

m_8 : Weight of the bottom of the outer shell, $m_8 = 120$ [kg]

N: Acceleration, $N = 240.7 \cdot g$ [m/s²]

$$w = \frac{(55+120) \times 240.7 \times 9.81}{\pi \times 230^2} = 2.49 \text{ [N/mm}^2\text{]}$$

Therefore,

$$\sigma_\theta = \pm 0.225 \times \frac{2.49 \times 230^2}{35^2} = \pm 24.2 \text{ [N/mm}^2\text{]}$$

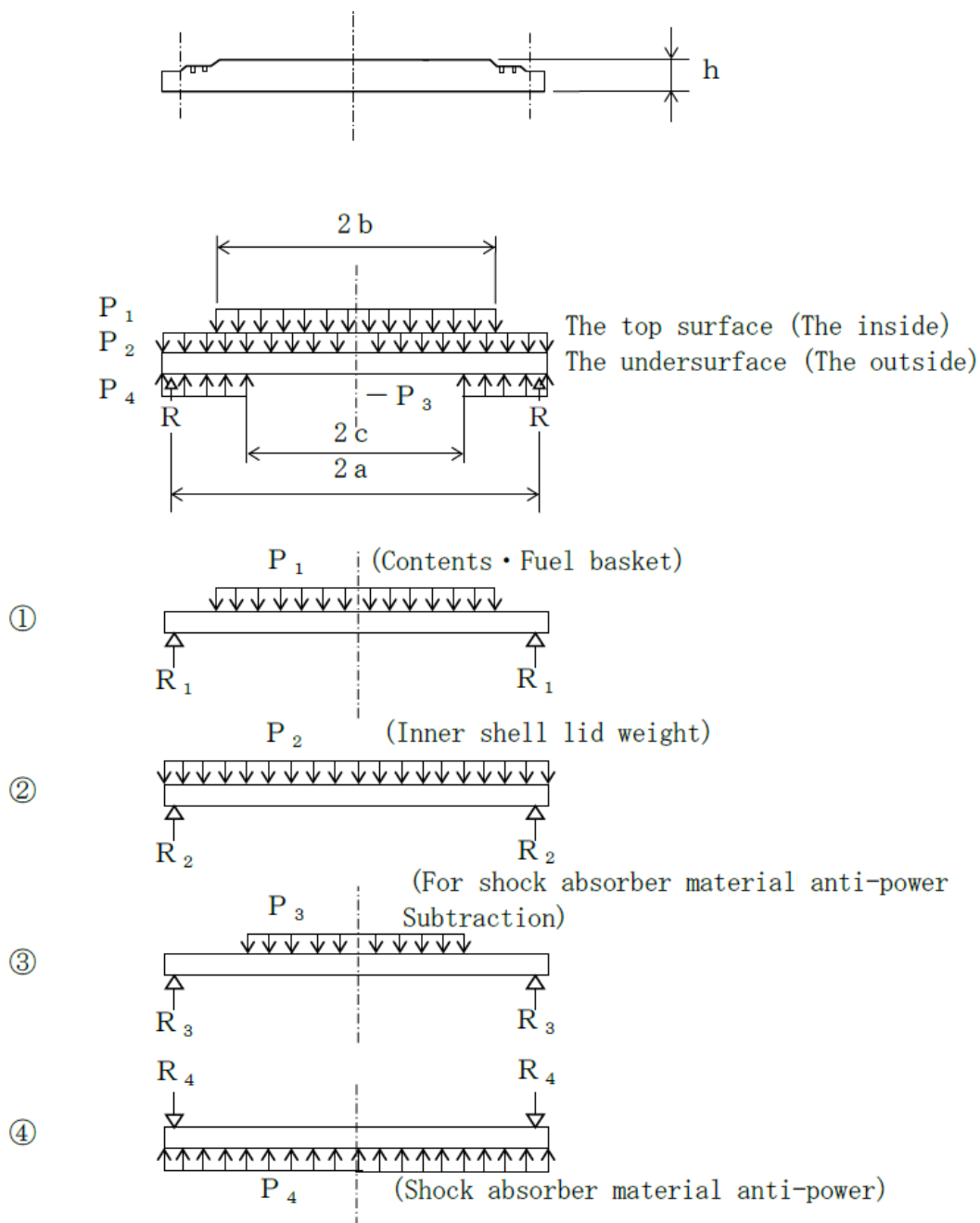
$$\sigma_r = \pm 0.75 \times \frac{2.49 \times 230^2}{35^2} = \pm 80.6 \text{ [N/mm}^2\text{]}$$

$$\sigma_z = -2.49 \text{ (outer surface)}$$

For the double signs of the stress values, the plus sign corresponds to the outer surface and the minus sign to the inner surface.

① Inner lid

(II)-Fig.A.65 shows a stress analysis model of the inner lid for 1.2 m lid side vertical drop.



(II)-Fig.A.65 Stress analysis model of inner lid for 1.2m lid side vertical drop

As indicated in (II)-Fig. A. 65, the weight of the contents and the fuel basket act uniformly on the center of the inner lid, and the dead weight of the inner lid also acts uniformly, while the latter is being supported by the circular reaction of the shock absorber and the inner lid clamping bolt.

The stress, generated on the circumferentially supported disc under these loads, reaches its maximum in the disc center. It can be given by superposing the analysis results of each of the models (1), (2), (3) and (4) shown in (II)-Fig. A. 65.

① Contents and fuel basket

As shown in (II)-Fig. A. 65-(1), the stress, generated within the concentric circle of the circumferentially supported disc under uniform load, reaches its maximum in the disc center. It is given by the following equation^[7]

$$\sigma_r = \sigma_\theta = \mp \frac{3P_1 \cdot b^2}{8h^2} \left\{ 4(1+\nu) \ln \frac{a}{b} + 4 - (1-\nu) \frac{b^2}{a^2} \right\}$$

$$\sigma_z = -P_1 \text{ (inner surface)}$$

where

σ_r : Radial stress [N/mm²]

σ_θ : Circumferential stress [N/mm²]

σ_z : Axial stress [N/mm²]

a: Radius of supporting points circle on inner lid, a=285 [mm]

b: Radius of load, b=230 [mm]

h: Plate thickness of the inner lid, h=55 [mm]

P₁: Uniform load resulting from content and fuel basket,

$$P_1 = \frac{(m_3 + m_4)}{\pi b^2} \cdot N \quad [\text{N/mm}^2]$$

m₃: Weight of the fuel basket, m₃=138 [kg]

m₄: Weight of the bottom of the outer shell, m₄=92 [kg]

N: Acceleration, N=240.7 · g [m/s²]

$$P_1 = \frac{(138+92)}{\pi \times 230^2} \times 240.7 \times 9.81 = 3.27 \quad [\text{N/mm}^2]$$

ν : Poisson's ratio, $\nu = 0.3$

Therefore,

$$\sigma_r = \sigma_\theta = \mp \frac{3 \times 3.27 \times 230^2}{8 \times 55^2} \left\{ 4(1+0.3) \ln \frac{285}{230} + 4 - (1-0.3) \frac{230^2}{285^2} \right\}$$

$$= \mp 99.9 \quad [\text{N/mm}^2]$$

$$\sigma_z = -3.27 \quad (\text{inner surface})$$

For the double sign of the stress value, the upper sign (−) corresponds to the inner surface and the lower sign (+) to the outer surface.

The supporting point reaction R_1 in this case is,

$$R_1 = (m_3 + m_4) \cdot N$$

$$= (138 + 92) \times 240.7 \times 9.81 = 5.43 \times 10^5 \quad [\text{N}]$$

② Dead weight of inner lid

As indicated in (II)-Fig. A.65-(2), the stress, generated on the circumferentially supported disc under the uniform load resulting from the disc's dead weight, reaches its maximum at the disc center. It is given by the following equation

$$\sigma_r = \sigma_\theta = \mp 1.24 \frac{P_2 \cdot a^2}{h^2}$$

$$\sigma_z = -P_2 \quad (\text{inner surface})$$

where

σ_r : Radial stress $[\text{N/mm}^2]$

σ_θ : Circumferential stress $[\text{N/mm}^2]$

σ_z : Axial stress $[\text{N/mm}^2]$

a : Radius of supporting points circle on inner lid, $a = 285 \quad [\text{mm}]$

h : Plate thickness of the inner lid, $h = 55 \quad [\text{mm}]$

N : Acceleration, $N = 240.7 \cdot g \quad [\text{m/s}^2]$

γ : Density of the inner lid, $\gamma = 7.93 \times 10^{-6} \quad [\text{kg/mm}^3]$

P_2 : Uniform load resulting from the lid's dead weight,

$$P_2 = \gamma \cdot h \cdot N = 7.93 \times 10^{-6} \times 55 \times 240.7 \times 9.81 = 1.03 \quad [\text{N/mm}^2]$$

Hence, the stress on the lid is

$$\sigma_r = \sigma_\theta = \mp 1.24 \frac{1.03 \times 285^2}{55^2} = \mp 34.3 \quad [\text{N/mm}^2]$$

$$\sigma_z = -1.03 \quad (\text{inner surface})$$

The upper sign (−) of the stress value corresponds to the inner surface and the lower sign (+) to the outer surface.

The supporting points' reaction force R_2 in this case is as follows.

$$R_2 = P_2 \cdot \pi \cdot a^2 = 1.03 \times \pi \times 285^2 = 2.63 \times 10^5 \quad [\text{N}]$$

③ Deduction of the shock absorber's reaction

As shown in (II)-Fig. A. 65-(3), the stress, generated within the concentric circle of the circumferentially supported disc under uniform load, reaches its maximum at the disc center. It is given by the following equation^[7]

$$\sigma_r = \sigma_\theta = \mp \frac{3P_3 \cdot c^2}{8h^2} \left\{ 4(1+\nu) \ln \frac{a}{c} + 4 - (1-\nu) \frac{c^2}{a^2} \right\}$$

$$\sigma_z = -P_3 \quad (\text{inner surface})$$

where

σ_r : Radial stress $[\text{N/mm}^2]$

σ_θ : Circumferential stress $[\text{N/mm}^2]$

σ_z : Axial stress $[\text{N/mm}^2]$

a : Radius of supporting points circle on inner lid, $a = 285 \quad [\text{mm}]$

c : Radius of load;

$$c = c_0 + \delta \cdot \tan \alpha = 115 + 24.1 \times \tan 15.5^\circ = 122 \quad [\text{mm}]$$

c_0 : Upper radius of the circular cone, $c_0 = 115 \quad [\text{mm}]$

α : Circular cone angle, $\alpha = 15.5^\circ$

δ : Deformation thickness in the shock absorber, $\delta = 24.1 \quad [\text{mm}]$

h : Plate thickness of the inner lid, $h = 55 \quad [\text{mm}]$

ν : Poisson's ratio, $\nu = 0.3$

P_3 : Compressive stress on the shock absorber, $P_3 = 0.932 \quad [\text{N/mm}^2]$

Therefore,

$$\sigma_r = \sigma_\theta = \mp \frac{3 \times 0.932 \times 122^2}{8 \times 55^2} \left\{ 4(1+0.3) \ln \frac{285}{122} + 4 - (1-0.3) \frac{122^2}{285^2} \right\}$$

$$= \mp 14.2 \quad [\text{N/mm}^2]$$

$$\sigma_z = -0.932 \quad (\text{inner surface}) \quad [\text{N/mm}^2]$$

For the double sign of the stress value, the upper sign (−) corresponds to the inner surface and the lower sign (+) to the outer surface.

The supporting points' reaction in this case is

$$R_3 = P_3 \pi c^2 = 0.932 \times \pi \times 122^2 = 4.36 \times 10^4 \quad [\text{N}]$$

④ Reaction of the shock absorber

As shown in (II)-Fig. A. 65-(4), the stress, generated in the circumferentially supported disc under uniform load of the shock absorber's reaction, reaches its maximum at the disc center, and it is given by the following equation.

$$\sigma_r = \sigma_\theta = \mp 1.24 \frac{P_4 \cdot a^2}{h^2}$$

$$\sigma_z = -P_4 \text{ (outer surface)}$$

where

$$\begin{aligned} \sigma_r &: \text{Radial stress} && [\text{N/mm}^2] \\ \sigma_\theta &: \text{Circumferential stress} && [\text{N/mm}^2] \\ \sigma_z &: \text{Axial stress} && [\text{N/mm}^2] \\ a &: \text{Radius of supporting points circle on inner lid, } a=285 \text{ [mm]} \\ h &: \text{Plate thickness of the inner lid, } h=55 \text{ [mm]} \\ P_4 &: \text{Compressive stress on the shock absorber, } P_4=0.932 \text{ [N/mm}^2] \end{aligned}$$

Hence, the stress on the lid is

$$\sigma_r = \sigma_\theta = \mp 1.24 \frac{0.932 \times 285^2}{55^2} = \mp 31.0 \quad [\text{N/mm}^2]$$

$$\sigma_z = -0.932 \text{ (outer surface)} \quad [\text{N/mm}^2]$$

For the double sign of the stress value, the upper sign (+) corresponds to the inner surface and the lower sign (−) to the outer surface.

The supporting points' reaction force R_4 in this case is,

$$R_4 = P_4 \cdot \pi \cdot a^2 = -0.932 \times \pi \times 285^2 = -2.38 \times 10^5 \quad [\text{N}]$$

On the basis of the results mentioned above, the superposed reaction is,

$$\begin{aligned} \sigma_r = \sigma_\theta &= \mp 99.9 \mp 34.3 \mp 14.2 \pm 31.0 = \mp 117 \quad [\text{N/mm}^2] \\ \sigma_z &= -3.27 - 1.03 - 0.932 = -5.23 \text{ (inner surface)} \quad [\text{N/mm}^2] \end{aligned}$$

The upper signs of these terms correspond to the inner surface and the lower signs to the outer surface.

The combined reaction of the supporting points is,

$$R = (5.43 + 2.63 + 0.44 - 2.38) \times 10^5 = 6.12 \times 10^5 \quad [\text{N}]$$

Ⓔ Inner lid clamping bolt

As indicated in A.5.3 (8) (a) (D), the dead weight of the contents, the fuel basket and the inner lid act on the inner lid. On the other hand, the inner lid is supported by the reaction of the shock absorber, the reaction of the conical reinforcing plate and the inner lid clamping bolt.

The supporting point reaction R works on the inner lid clamping bolts.

Therefore, the tensile stress arising in these bolts is,

$$\sigma_t = \frac{R}{n \cdot A_r}$$

where

σ_t : Tensile stress [N/mm²]

R: Supporting points reaction, $R = 6.12 \times 10^5$ [N]

n: Number of inner lid clamping bolts, $n = 16$

A_r : Root thread area of the clamping bolt M 24,

$$A_r = \frac{\pi}{4} \cdot d_r^2 = \frac{\pi}{4} \times 20.752^2 = 338.2 \text{ [mm}^2\text{]}$$

d_r : Minimum diameter of the clamping bolt, $d_r = 20.752$ [mm]

Therefore,

$$\sigma_t = \frac{6.12 \times 10^5}{16 \times 338.2} = 113 \text{ [N/mm}^2\text{]}$$

(b) Fuel elements, fuel plate

(b)-1. Fuel element

(I) Fuel plate

In this section, the stresses of the rectangular fuel elements are analyzed for 1.2 m lid side vertical drop.

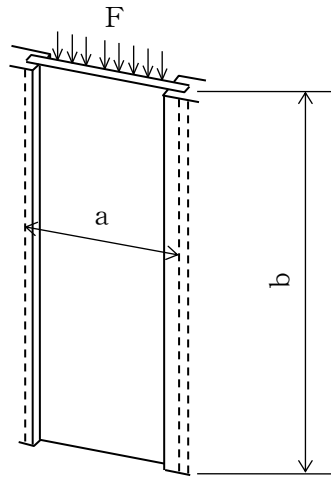
(i) In case of calking both ends of fuel plate

With regard to the rectangular fuel element, there are 7 types of fresh fuel elements including the follower type, and there are 9 types of lowly irradiated fuel elements. In this section, the analysis method is described for the JRR-3 standard, the same analysis was conducted for the other 8 types and the result is shown in the

(II)-Table A.18.

However, the analysis is performed on the assumption that uranium-aluminum alloy has the same strength as the covering material.

(II)-Fig.A.66 shows an analytical model.



(II)-Fig.A.66 Stress analysis model of rectangular fuel element for 1.2m lid side vertical drop

As indicated in (II)-Fig.A.66, the fuel plate is caulked and fixed at both ends and its retaining strength is,

$$F_H = f \cdot 2 \cdot b$$

where

F_H : Strength to sustain the fuel plate [N]

f : Sustaining strength per unit length, $f=26.5$ [N/mm]

b : Length of the fuel plate, $b=770$ [mm]

Therefore,

$$F_H = 26.5 \times 2 \times 770 = 4.08 \times 10^4 \text{ [N]}$$

On the other hand, the force for dropping of the fuel plate is

$$F = m \cdot N$$

where

F : Dropping force of the fuel plate [N]

m : Weight of the fuel plate, $m=0.279$ [kg]

N : Design acceleration, $N=240.7 \cdot g$ [m/s^2]

Therefore,

$$F = 0.279 \times 240.7 \times 9.81 = 659 \text{ [N]}$$

Thus, the fuel plate does not slip down since the strength to sustain the fuel plate exceeds the dropping force.

As shown above, when the fuel plate which is fixed at its both ends suffers a dropping force due to its own dead weight, a shearing stress τ arises.

$$\tau = \frac{F}{2(h_2 - h_1) b}$$

where

τ : Shearing stress [N/mm²]

F : Dropping force of the fuel plate, $F=659$ [N]

h_2 : Thickness of the fuel plate, $h_2=1.27$ [mm]

h_1 : Thickness of the core of the fuel plate, $h_1=0.51$ [mm]

b : Length of the fuel plate, $b=770$ [mm]

Therefore, the shearing stress is,

$$\tau = \frac{659}{2 \times (1.27 - 0.51) \times 770} = 0.563 \text{ [N/mm}^2\text{]}$$

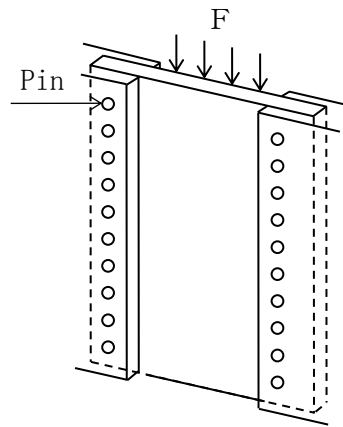
(ii) In case of fuel plate fixed by pin

The stress of the pin-fixing the fuel plate of the lowly irradiated fuel element, generated at 1.2m vertical drop, is analyzed.

There are 6 types of lowly irradiated fuel elements including follower types, in this section, the stress analysis method for the pin fixing type fuel element is shown and it's result is shown in (II)-Table A.18.

The uranium aluminum alloy is treated to have the same strength as the clad material in the analysis.

The analytical model is shown in (II)-Fig.A.67.



(II)-Fig.A.67 Analytical model of 1.2m upper portion vertical drop of lowly irradiated fuel element

As shown in (II)-Fig.A.67, the fuel plate is fixed with pin at the side plate.

This retaining force is given as follows.

$$F_H = \tau_a \times A \quad [N]$$

Where,

F_H : Force for retaining fuel plate [N]

τ_a : Allowable shear stress of pin = 36.8 [N/mm²]

A : Sectional area of pin [mm²]

$$= \frac{\pi}{4} \times d^2 \times n$$

d : Pin diameter = 2.2 [mm]

n : No. of pin = 62

Therefore, the following value is obtained.

$$F_H = \tau_a \times \frac{\pi}{4} \times d^2 \times n$$

$$= 36.8 \times \frac{\pi}{4} \times 2.2^2 \times 62 = 8.67 \times 10^3 \quad [\text{N}]$$

The force acting on the fuel plate due to the acceleration is given as follows,

$$F = mN$$

Where,

F : Force acts on fuel plate when dropping [N]

m : Weight of the fuel plate = 0.217 [kg]

N : Design acceleration = 240.7g [m/s²]

Therefore the following value is obtained.

$$F = 0.217 \times 240.7 \times 9.81 = 512 \quad [\text{N}]$$

From the above, the retaining force of the pin is larger than the dropping force of the fuel plate by the acceleration, the fuel plate does not slide from fixing.

When the fuel plate, fixed with pin at the both ends, is freely dropped, the tensile force occurs at the pin portion of the fuel plate and is given as follows,

$$\sigma_t = \frac{W_o}{A}$$

Where,

$$W_o = \frac{W \times N}{n/2}$$

$$W_o = \frac{0.217 \times 240.7 \times 9.81}{62/2} = 16.5 \quad [\text{N}]$$

σ_t : Stress of fuel plate pin [N/mm²]

W_o : Load acting on fuel pin portion [kg]

n : No. of pin, n = 62

N : Design acceleration, N = 240.7g [m/sec²]

A : Effective sectional area of pin [mm²]

$$A = ((L1 - L2)/2 - d) \times t1$$

L1 : Width of fuel plate, L1 =70.6 [mm]

L2 : Width of fuel plate core, L2 =61.8 [mm]

t1 : Thickness of fuel plate, t =1.27 [mm]

d : Pin diameter, d =2.35 [mm]

$$A = ((70.6 - 61.8)/2 - 2.35) \times 1.27 = 2.60 \text{ [mm}^2\text{]}$$

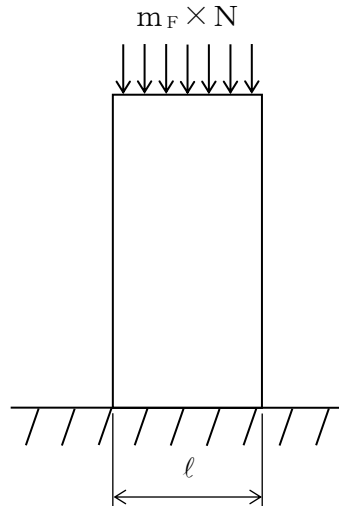
Therefore, the following value of stress is obtained.

$$\sigma_t = \frac{16.5}{2.60} = 6.35 \text{ [N/mm}^2\text{]}$$

(iii) In case of fuel plate not fixed by the side plate

The stress of the lowly irradiated fuel element, when dropped vertically from 1.2m height, is analyzed. Among five types of lowly irradiated fuel element including follower types, in this section, the fuel element not fixed by the side plate is analyzed and the result is shown in (II)-Table A.18.

The uranium aluminum alloy is treated to have the same strength as the clad material in this analysis. The analytical model is shown in (II)-Fig. A. 68.



(II)-Fig. A. 68 Analytical model for 1.2m upper portion vertical drop of lowly irradiated fuel element

As shown in (II)-Fig. A. 68, the compressive stress is generated in the rectangular plate subjected to the fuel element own weight, and is shown as follows,

$$\sigma_c = \frac{W}{A} = \frac{m_F \times N}{l (h_2 - h_1)}$$

Where,

m_F : Fuel plate mass, $m_F = 0.223$ [kg]

l : Width of fuel plate, $l = 66.6$ [mm]

h_2 : Thickness of fuel plate, $h_2 = 1.27$ [mm]

h_1 : Thickness of fuel plate core, $h_1 = 0.51$ [mm]

N : Design acceleration, $N = 240.7g$ [m/s^2]

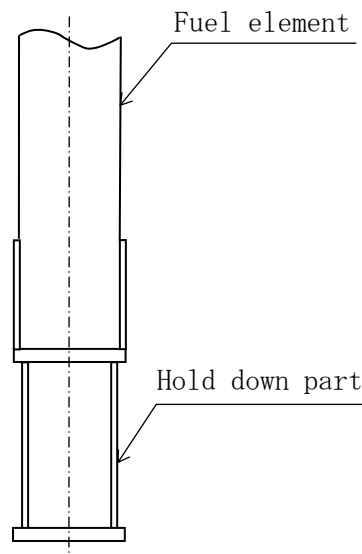
Therefore, the following value of stress is obtained.

$$\sigma_c = \frac{0.223 \times 240.7g}{66.6 \times (1.27 - 0.51)} = 10.4 \text{ [N/mm}^2\text{]}$$

(ii) Fuel element hold down part

As shown in (I)-D section, the lowly irradiated fuel elements are cut at the lower adapter portion and the upper holder portion in order to reduce the weight, Therefore the total length becomes short. A hold-down part is provided to adjust the length. In this section, the stress analysis method for the stress occurs in the hold-down part is shown and the result is summarized in (II)-Table A. 18.

The analysis model is shown in (II)-Fig. A. 69.



(II)-Fig. A. 69 Analytical model of hold down part

As shown in (II)-Fig. A. 69, the hold down part is subjected to the own weight and the fuel element weight, and the following compressive stress is generated.

$$\sigma_c = \frac{W}{A} = \frac{(m_z + m_f) \times N}{\frac{\pi}{4}(h_o^2 - h_i^2)}$$

Where,

m_z : Weight of the hold down part = 1.4 [kg]

m_f : Weight of the fuel element = 6.6 [kg]

N : Design acceleration = 240.7g [m/sec²]

h_o : Outer diameter of the hold down part = 60 [mm]

h_i : Inner diameter of the hold down part = 52 [mm]

Therefore,

$$\sigma_c = \frac{(1.4 + 6.6) \times 240.7g}{\frac{\pi}{4}(60^2 - 52^2)} = 26.8 \quad [N/mm^2]$$

(b)-2. Fuel plate for the critical assembly fuel (KUCA fuel)

This section analyzes the stress generated in the fuel plate for the critical assembly at the time of 1.2 m vertical drop. The analysis model is the same as the lowly irradiated fuel elements shown in (II)-Fig.A.68 (when the fuel plate and side plate are not fixed).

For the coupon fuel in vertical drop, the design acceleration is applied to the perpendicular direction to the plane of the fuel as shown in (II)-Fig.A.59 and the total thickness of cladding is 6 mm, which is the twice width of aluminum case.

m_F : Weight of the fuel plate	$m_F=0.036$ [kg]
l : Length of the fuel plate	$l=50.8$ [mm]
h_2-h_1 :Cladding thickness	$h_2-h_1= 6$ [mm]
N : Design acceleration	$N=240.7 \cdot g$ [m/s ²]

Therefore, the compressive stress σ_c are given as follows.

$$\begin{aligned}\sigma_c &= (0.036 \times 240.7 \times g) / (50.8 \times 6) \\ &= 0.28 \quad [\text{N/mm}^2]\end{aligned}$$

For the flat fuel in vertical drop, the design acceleration is applied to the parallel direction to the plane of the fuel plate as shown in (II)-Fig.A.60.

In the case,

m_F : Weight of the fuel plate	$m_F=0.23$ [kg]
l : Length of the fuel plate	$l=62$ [mm]
h_2 : Fuel plate thickness	$h_2 =1.5$ [mm]
h_1 : Fuel plate core thickness	$h_1= 0.5$ [mm]
N : Design acceleration	$N=240.7 \cdot g$ [m/s ²]

Therefore, the compressive stress σ_c are given as follows.

$$\begin{aligned}\sigma_c &= (0.23 \times 240.7 \times g) / (62 \times (1.5 - 0.5)) \\ &= 8.76 \quad [\text{N/mm}^2]\end{aligned}$$

(c) Comparison of the allowable stresses

The results of the stress evaluation concerning each analyzed item in (II)-5.3(8) are shown together in (II)-Table A.18.

As shown in this table, the margin of safety in regard to the analysis reference is positive for individual and combined loads.

Therefore, the integrity of this package is maintained under the 1.2 m lid side vertical drop test conditions.

(II) -Table A.18 Stress evaluation for 1.2 m lid side vertical drop (1/6)

Stress units
;N/mm²

No.	Stress Position to be evaluated		Stress at initial clamping	Stress due to internal pressure	Stress due to thermal expansion	Impact stress	Primary stress						Primary+secondary stress			Fatigue						
							Pm(PL)	Sm	MS	PL+Pb	1.5Sm	MS	PL+Pb +Q	3Sm	MS	PL+Pb +Q+F	Sa	N	Na	DF	MS	
1	Frame of Inner shell		σ_r	—	-0.0491	—	92.4	137	0.482	—	—	—	—	—	—	—	—	—	—	—	—	
			σ_θ		2.31																	—
			σ_z		1.15																	-91.2
2	Bottom plate of inner shell		Inner Surface	—	3.18	—	-80.6	0.098	137	1396	77.3	205	1.65	—	—	—	—	—	—	—	—	
					0.953		-24.2															
					-0.098		0															
			Outer Surface	—	-3.18	—	80.6	2.49	137	54.0	79.9	205	1.56	—	—	—	—	—	—	—	—	
					-0.953		24.2															
					0		-2.49															
3	Inner shell lid		Inner Surface	—	-3.27	—	-117	5.33	2/3Sy 458	84.9	115	Sy 687	4.97	—	—	—	—	—	—	—	—	
					-3.27		-117															
					-0.098		-5.23															
			Outer Surface	—	3.27	—	117	0.932	2/3Sy 458	490	121	Sy 687	4.67	—	—	—	—	—	—	—	—	
					3.27		117															
					0		-0.932															
4	Clamping bolt of inner shell lid		σ_r	174	3.20	—	113	290	2/3Sy 458	0.579	—	—	—	—	—	—	—	—	—	—	—	
			σ_θ	—			—															
			σ_z				—															

Pm; General primary membrane stress; PL; Local primary membrane stress; Pb; Primary bending stress; Q; Secondary stress; F; Peak stress;

Sa; Repeated peak stress; N; Number of uses; Na; Permissible number of repetition; DF; Cumulative fatigue coefficient;

Sm; Design stress intensity value; Sy; Yield point of the design; MS; Margin of safety σ_t ; Ability of bolt stress σ_r ; Diameter direction stress σ_θ ; Periphery direction stress σ_z ; Axial stress σ_b ; Bending stress τ ; Shear stress

(II) -Table A.18 Stress evaluation for 1.2 m lid side vertical drop (2/6)

Stress units
;N/mm²

No.	Stress Position to be evaluated	Stress at initial clamping	Stress due to internal pressure	Stress due to thermal expansion	Impact stress	Primary stress						Primary+secondary stress			Fatigue					
						Pm(PL)	2/3Sy	MS	PL+Pb	Sy	MS	PL+Pb +Q	Sy	MS	PL+Pb +Q+F	Sa	N	Na	DF	MS
1	JRR-3 standard element (Uranium silicon aluminum dispersion alloy)	τ	—	—	—	0.563	—	—	—	0.563	63.8	112	—	—	—	—	—	—	—	—
2	JRR-3 follower element (Uranium silicon aluminum dispersion alloy)	τ	—	—	—	0.460	—	—	—	0.460	63.8	137	—	—	—	—	—	—	—	—
3	JRR-4 B type element	τ	—	—	—	0.422	—	—	—	0.422	63.8	150	—	—	—	—	—	—	—	—
4	JRR-4 L type element	τ	—	—	—	0.666	—	—	—	0.666	63.8	94.7	—	—	—	—	—	—	—	—
5	JRR-4 (Uranium silicon aluminum dispersion alloy)	τ	—	—	—	0.579	—	—	—	0.579	63.8	109	—	—	—	—	—	—	—	—
6	JMTR standard element	τ	—	—	—	0.572	—	—	—	0.572	63.8	110	—	—	—	—	—	—	—	—
7	JMTR follower element	τ	—	—	—	0.479	—	—	—	0.479	63.8	132	—	—	—	—	—	—	—	—

Pm; General primary membrane stress; PL; Local primary membrane stress; Pb; Primary bending stress; Q; Secondary stress; F; Peak stress;

Sa; Repeated peak stress; N; Number of uses; Na; Permissible number of repetition; DF; Cumulative fatigue coefficient;

Sy; Yield point of the design; MS; Margin of safety τ ; Shear stress

Stress units
;N/mm²

(II) -Table A.18 Stress evaluation for 1.2 m lid side vertical drop (3/6)

No.	Position to be evaluated	Stress	Stress at initial clamping	Stress due to internal pressure	Stress due to thermal expansion	Impact stress	Primary stress						Primary+secondary stress			Fatigue					
							Pm(PL)	2/3Sy	MS	PL+Pb	Sy	MS	PL+Pb +Q	Sy	MS	PL+Pb +Q+F	Sa	N	Na	DF	MS
1	KUR standard (Uranium silicon aluminum dispersion alloy)	τ	—	—	—	0.436	—	—	—	0.436	63.7	145		—	—	—	—	—	—	—	—
2	KUR Special element (Uranium silicon aluminum dispersion alloy)	τ	—	—	—	0.436	—	—	—	0.436	63.7	145		—	—	—	—	—	—	—	—
3	KUR half-loaded element (Uranium silicon aluminum dispersion alloy)	τ	—	—	—	0.436	—	—	—	0.436	63.7	145	—	—	—	—	—	—	—	—	—

Pm ; General primary membrane stress; PL ; Local primary membrane stress; Pb ; Primary bending stress; Q ; Secondary stress; F ; Peak stress;
Sa ; Repeated peak stress; N ; Number of uses; Na ; Permissible number of repetition; DF ; Cumulative fatigue coefficient;
Sy ; Yield point of the design; MS ; Margin of safety τ ; Shear stress

(II) -Table A.18 Stress evaluation for 1.2 m lid side vertical drop (4/6)

No.	Stress Position to be evaluated	Stress at initial clamping	Stress due to internal pressure	Stress due to thermal expansion	Impact stress	Primary stress						Primary+secondary stress			Fatigue					
						Pm(PL)	2/3Sy	MS	PL+Pb	Sy	MS	PL+Pb +Q	Sy	MS	PL+Pb +Q+F	Sa	N	Na	DF	MS
1	JMTRC Standard fuel element (A,B,C type)	τ	—	—	—	0.44	—	—	—	0.44	63.8	144	—	—	—	—	—	—	—	—
2	JMTRC Standard fuel element ($\phi 2.2$ pin, fix type) (B,C type)	σ_t	—	—	—	6.35	—	—	—	6.35	63.8	9.04	—	—	—	—	—	—	—	—
3	JMTRC Special fuel element (Special A type)	σ_c	—	—	—	10.4	—	—	—	10.4	63.8	5.13	—	—	—	—	—	—	—	—
4	JMTRC Special fuel element (Special B type)	σ_c	—	—	—	0.37	—	—	—	0.37	63.8	171	—	—	—	—	—	—	—	—
5	JMTRC Special fuel element (Special C, Special D type)	σ_c	—	—	—	10.4	—	—	—	10.4	63.8	5.13	—	—	—	—	—	—	—	—
6	JMTRC fuel follower (HF type)	τ	—	—	—	0.34	—	—	—	0.34	63.8	186	—	—	—	—	—	—	—	—
7	JMTRC Standard fuel element (MA, MB, MC type)	τ	—	—	—	0.43	—	—	—	0.43	63.8	147	—	—	—	—	—	—	—	—
8	JMTRC Special fuel element (Special MB, Special MC type)	σ_c	—	—	—	10.3	—	—	—	10.3	63.8	5.19	—	—	—	—	—	—	—	—
9	JMTRC fuel follower (MF type)	τ	—	—	—	0.35	—	—	—	0.35	63.8	181	—	—	—	—	—	—	—	—

Pm; General primary membrane stress; PL; Local primary membrane stress; Pb; Primary bending stress; Q; Secondary stress; F; Peak stress;

Sa; Repeated peak stress; N; Number of uses; Na; Permissible number of repetition; DF; Cumulative fatigue coefficient;

Sy; Yield point of the design; MS; Margin of safety τ ; Shear stress σ_c ; Compression stress σ_t ; Stress of the part of fuel pin

(II) -Table A.18 Stress evaluation for 1.2 m lid side vertical drop (5/6)

No.	Stress Position to be evaluated	Stress at initial clamping	Stress due to internal pressure	Stress due to thermal expansion	Impact stress	Primary stress						Primary+secondary stress			Fatigue					
						Pm(PL)	2/3Sy	MS	PL+Pb	Sy	MS	PL+Pb +Q	Sy	MS	PL+Pb +Q+F	Sa	N	Na	DF	MS
1	JMTRC Special fuel element hold down part (Special A type)	σ_c	—	—	—	26.8	—	—	—	26.8	245	8.14	—	—	—	—	—	—	—	—
2	JMTRC Special fuel element hold down part (Special B type)	σ_c	—	—	—	15.4	—	—	—	15.4	245	14.9	—	—	—	—	—	—	—	—
3	JMTRC Special fuel element hold down part (Special C, Special D type)	σ_c	—	—	—	27.9	—	—	—	27.9	245	7.78	—	—	—	—	—	—	—	—
4	JMTRC Special fuel element hold down part (Special MB, Special MC type)	σ_c	—	—	—	27.9	—	—	—	27.9	245	7.78	—	—	—	—	—	—	—	—

Pm; General primary membrane stress; PL; Local primary membrane stress; Pb; Primary bending stress; Q; Secondary stress; F; Peak stress;

Sa; Repeated peak stress; N; Number of uses; Na; Permissible number of repetition; DF; Cumulative fatigue coefficient;

Sy; Yield point of the design; MS; Margin of safety σ_c ; Compression stress

(II) -Table A.18 Stress evaluation for 1.2 m lid side vertical drop (6/6)

No.	Position to be evaluated	Stress	Stress at initial clamping	Stress due to internal pressure	Stress due to thermal expansion	Impact stress	Primary stress						Primary+secondary stress			Fatigue					
							Pm(PL)	2/3Sy	MS	PL+Pb	Sy	MS	PL+Pb +Q	Sy	MS	PL+Pb +Q+F	Sa	N	Na	DF	MS
1	KUCA coupon type	σ_b	—	—	—	0.28	—	—	—	0.28	63.7	227	—	—	—	—	—	—	—	—	—
2	KUCA Flat type	σ_b	—	—	—	8.76	—	—	—	8.76	63.7	7.3	—	—	—	—	—	—	—	—	—

Pm ;General primary membrane stress; PL ;Local primary membrane stress; Pb ;Primary bending stress; Q ;Secondary stress; F ;Peak stress;
Sa ;Repeated peak stress; N ;Number of uses; Na ;Permissible number of repetition; DF ;Cumulative fatigue coefficient;
Sy ;Yield point of the design; MS ;Margin of safety σ_b ; Bending stress σ_c ; Compression stress

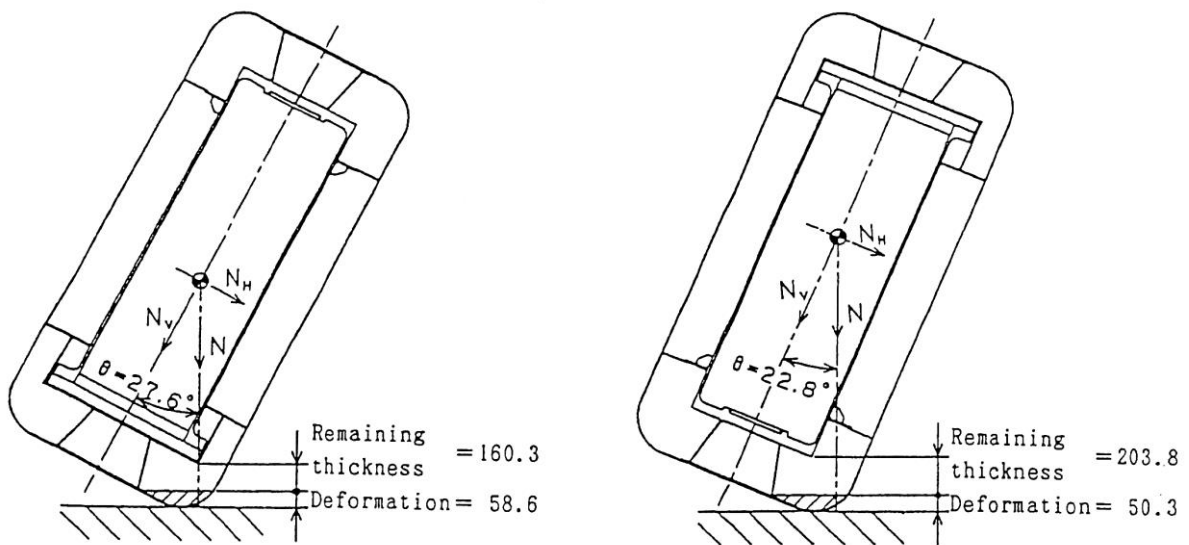
(9) Corner drop

A corner drop is a special case of inclining drops. The package is made to drop with its corner directed downwards, as shown in [\(II\)-Fig. A. 70](#), where the line drawn from the center of gravity to the point which first touches the ground meets at a right angle to the solid plane.

(a) Deformation of shock absorber

[\(II\)-Fig. A. 70](#) shows the relationship between the deformation of the shock absorber and its remaining thickness.

This figure shows that deformation only occurs in parts of the shock absorber and does not reach the inner shell.



[\(II\)-Fig. A. 70](#) Analytical model of interference to inner shell due to shock absorber deformation for 1.2 m corner drop

(b) Stresses on the packaging and content

(II)-Table A. 19 shows the horizontal and vertical components of the design acceleration for the corner drops (see (II)-Table A. 15).

(II)-Table A. 19 Design acceleration for corner drops

		(×g)		
Drop type for specimen		Total acceleration (N)	Vertical component ($N_V = N \cos \theta$)	Horizontal component ($N_H = N \sin \theta$)
Corner	Lid side	89.9	79.7	41.7
	Bottom side	90.8	83.7	35.2

(II)-Table A. 19 shows that each accelerating component is smaller than the acceleration recorded in the vertical and horizontal drop. Hence, stress is not analyzed here.

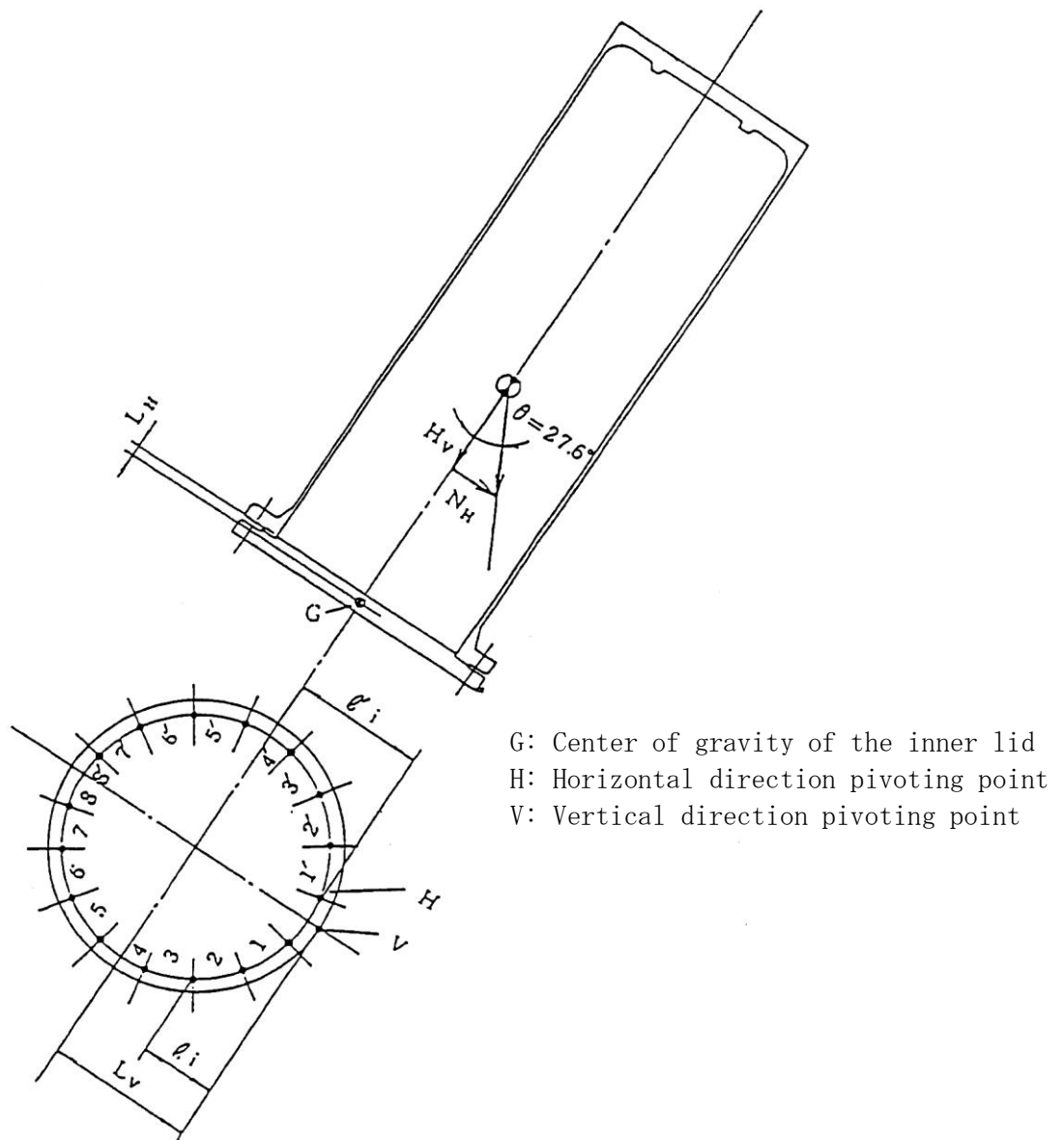
The analyses of the inner lid clamping bolts of different kinds other than those shown in section A. 5.3(6) to (8) are described in the following paragraphs.

(c) Stress on the inner lid clamping bolts for corner drop

During the drop of the bottom side corner, the acceleration of the vertical component is far greater than that of the horizontal component. For this reason, the stress due to momentum on the bolts of the lid can be neglected.

During the drop of the upper corner, stress occurs on the bolts due to momentum of the inner lid. The stress is analyzed in this section.

(II)-Fig. A. 71 shows an analytical model of the stress.



(II)-Fig. A. 71 Analytical model of stress on inner lid clamping bolts for lid side corner drop

Bending stress occurs on the inner lid clamping bolts due to the momentum of the inner lid when the package is made to fall with its lid side corner facing downwards (see (II)-Fig.A.71).

The maximum bending stress that occurs on the bolt (8) and (8') during this drop is obtained as follows:

$$\sigma_{\max} = \sigma_V + \sigma_H$$

$$\sigma_V = \frac{N_V \cdot m \cdot L_V \cdot l_8}{2 \times (l_1^2 + l_2^2 + l_3^2 + l_4^2 + l_5^2 + l_6^2 + l_7^2 + l_8^2) \cdot Ar}$$

$$\sigma_H = \frac{N_H \cdot m \cdot L_H \cdot l'_8}{2 \times (l'_2{}^2 + l'_3{}^2 + l'_4{}^2 + l'_5{}^2 + l'_6{}^2 + l'_7{}^2 + l'_8{}^2) \cdot Ar}$$

where

σ_{\max} : Maximum bending stress on bolts 8 and 8' [N/mm²]

σ_V : Stress due to vertical acceleration component [N/mm²]

σ_H : Stress due to horizontal acceleration component [N/mm²]

N_V : Vertical acceleration component $N_V = 79.7 \cdot g$ [m/s²]

N_H : Horizontal acceleration component $N_H = 41.7 \cdot g$ [m/s²]

m : Load applied on the inner lid $m = 350$ [kg]

L_V : Vertical momentum arm $L_V = 310$ [mm]

L_H : Horizontal momentum arm $L_H = 18.6$ [mm]

l_i : Distance from pivoting point V to a bolt [mm]

l'_i : Distance from pivoting point H to a bolt [mm]

$$l_1 = 30.5$$

$$l_2 = 73.0 \quad l'_2 = 42.5$$

$$l_3 = 151.7 \quad l'_3 = 121.2$$

$$l_4 = 254.4 \quad l'_4 = 223.9$$

$$l_5 = 365.6 \quad l'_5 = 335.1$$

$$l_6 = 468.3 \quad l'_6 = 437.8$$

$$l_7 = 547.0 \quad l'_7 = 516.5$$

$$l_8 = 589.5 \quad l'_8 = 559.0$$

Ar : Area of core section of bolt (M24);

$$Ar = \frac{\pi}{4} \cdot d^2 = \frac{\pi}{4} \times 20.752^2 = 338.2 \quad [\text{mm}^2]$$

Hence, the stresses are obtained as follows:

$$\begin{aligned}\sigma_v &= \frac{79.7 \times 9.81 \times 350 \times 310 \times 589.5}{2 \times (30.5^2 + 73.0^2 + 151.7^2 + 254.4^2 + 365.6^2 + 468.3^2 + 547.0^2 + 589.5^2) \times 338.2} \\ &= 67.6 \quad [\text{N/mm}^2] \\ \sigma_H &= \frac{41.7 \times 9.81 \times 350 \times 18.6 \times 559.0}{2 \times (42.5^2 + 121.2^2 + 223.9^2 + 335.1^2 + 437.8^2 + 516.5^2 + 559^2) \times 338.2} \\ &= 2.32 \quad [\text{N/mm}^2]\end{aligned}$$

(II)-Table A.20 shows an evaluation of the stresses on the inner lid clamping bolts for lid side corner drop.

(II) —Table A.20 Stress evaluation for 1.2 m lid side corner drop

Stress units
;N/mm²

No.	Position to be evaluated	Stress	Stress at initial clamping	Stress due to internal pressure	Stress due to thermal expansion	Impact stress		Primary stress						Primary+secondary stress			Fatigue					
						Horizontal Component	Vertical Component	Pm (PL)	Sm	MS	PL+Pb	1.5Sm	MS	PL+Pb +Q	3Sm	MS	PL+Pb +Q+F	Sa	N	Na	DF	MS
1	Inner lid clamping bolt	σ_t	174	3.20	—	—	—	177	2/3Sy 458	1.58	247	Sy 687	1.78	—	—	—	—	—	—	—	—	—
		σ_b	—	—	—	2.32	67.6															
		τ				—	—															

Pm ; General primary membrane stress; PL ; Local primary membrane stress; Pb ; Primary bending stress; Q ; Secondary stress; F ; Peak stress;

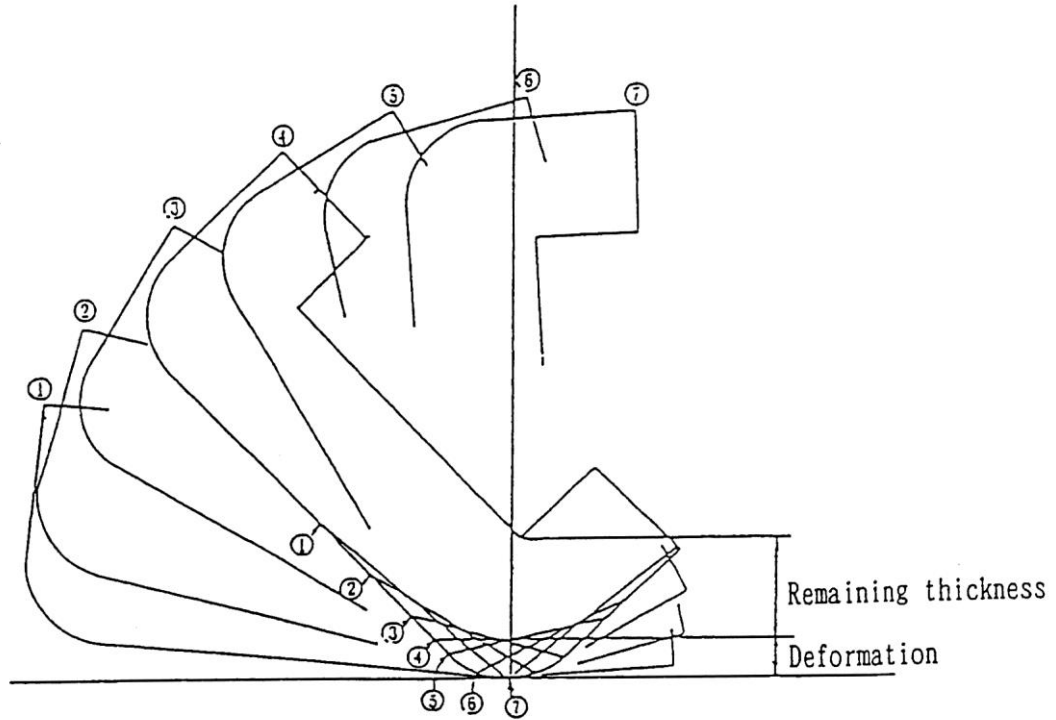
Sa ; Repeated peak stress; N ; Number of uses; Na ; Permissible number of repetition; DF ; Cumulative fatigue coefficient; Sm ; Design stress intensity value;

Sy ; Yield point of the design; σ_c ; Compression stress MS ; Margin of safety σ_t ; Ability of bolt stress σ_b ; Bending stress, τ ; Shear stress

(10) Bottom side inclined drop

(a) Deformation in shock absorber

(II)-Fig.A. 72 shows the relationship between the angle of dropping and the deformation for various types of bottom side inclined drop.



No.	Angle of dropping θ	Minimum thickness of shock absorber before deformation	Deformation of shock absorber	Remaining thickness of shock absorber
①	5°	211.9	22.2	189.7
②	15°	236.8	40.1	196.7
③	30°	260.2	56.2	204.0
④	45°	265.7	60.4	205.3
⑤	60°	252.9	61.4	191.5
⑥	75°	222.6	44.4	178.2
⑦	85°	193.7	25.0	168.7

(II)-Fig.A. 72 Analytical model of interference with inner shell due to shock absorber deformation for 1.2 m lower side inclined drop

(II)-Fig.A. 72 shows that at the drop, deformation only occurs in parts of the shock absorber and does not reach the inner shell.

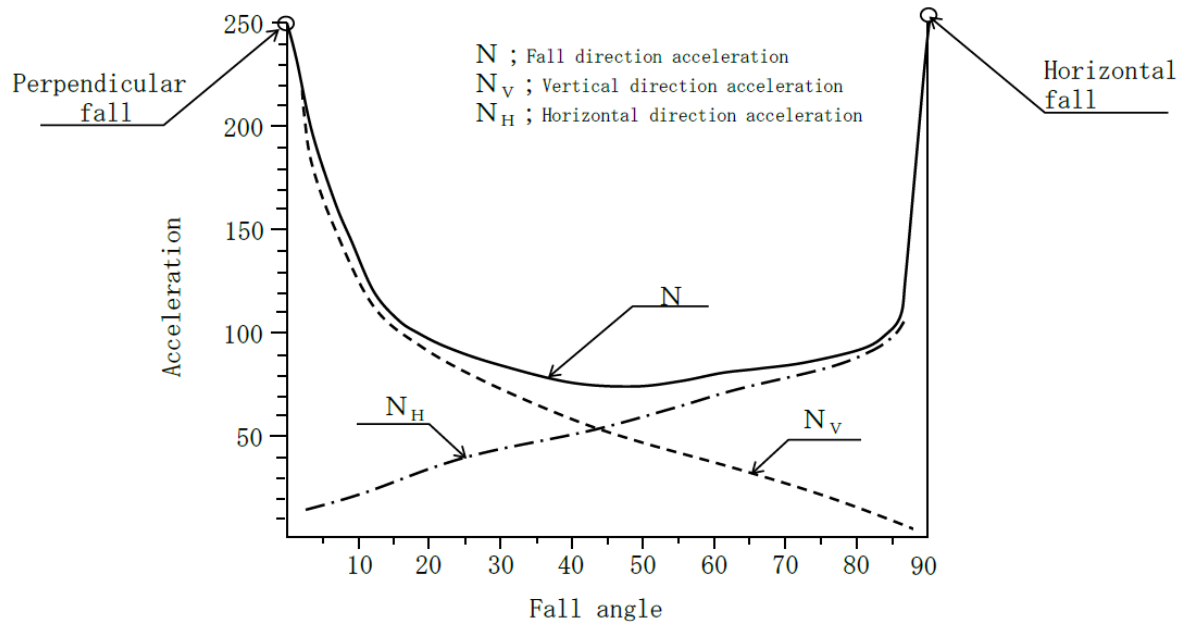
(b) Stresses on packaging and content

(II)-Table A. 21 shows the horizontal and vertical components of the design acceleration at the bottom side inclined drop ((II)-Table A.15).

(II)-Fig. A. 73 shows the relationships between the angle of dropping and the acceleration.

(II)-Table A. 21 Relationship between drop angle and acceleration

Angle at dropping θ (degrees)	Acceleration (G)		
	Acceleration (N)	Vertical component ($N \cdot \cos \theta$)	Horizontal component ($N \cdot \sin \theta$)
5	176.4	175.7	15.4
15	106.6	103.0	27.6
30	83.9	72.7	42.0
45	76.6	54.2	54.2
60	83.2	41.6	72.1
75	89.1	23.1	86.1
85	101.8	8.9	101.4



(II)-Fig. A. 73 Relationship between acceleration and drop angle for 1.2 m lower side inclined drop

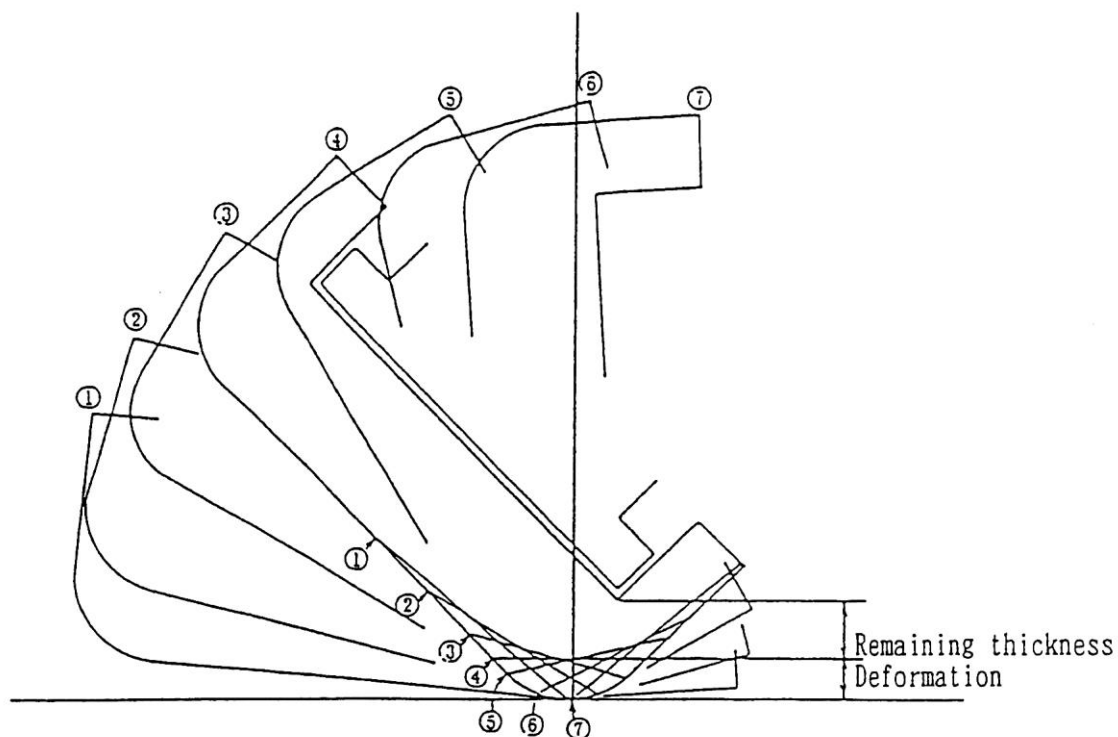
(II)-Table A. 21 shows that each acceleration component is smaller than the acceleration recorded in the horizontal and vertical drop.

Hence, stress is not analyzed here.

(11) Lid side inclined drop

(a) Deformation of the shock absorber

(II)-Fig.A. 74 shows the relationship between the dropping angle and the deformation.



No.	Angle at dropping (θ)	Minimum thickness of shock absorber before deformation	Deformation in shock absorber	Remaining thickness of shock absorber
①	5°	201.1	21.5	179.6
②	15°	210.5	41.5	169.0
③	30°	212.2	60.8	151.4
④	45°	199.1	65.8	133.3
⑤	60°	171.9	59.3	112.6
⑥	75°	132.7	46.9	85.8
⑦	85°	101.1	27.4	73.7

(II)-Fig.A. 74 Analytical model of interference with inner shell due to shock absorber deformation for 1.2 m upper side inclined drop

(II)-Fig.A. 74 shows that deformation only occurs in parts of the shock absorber and does not reach the inner shell.

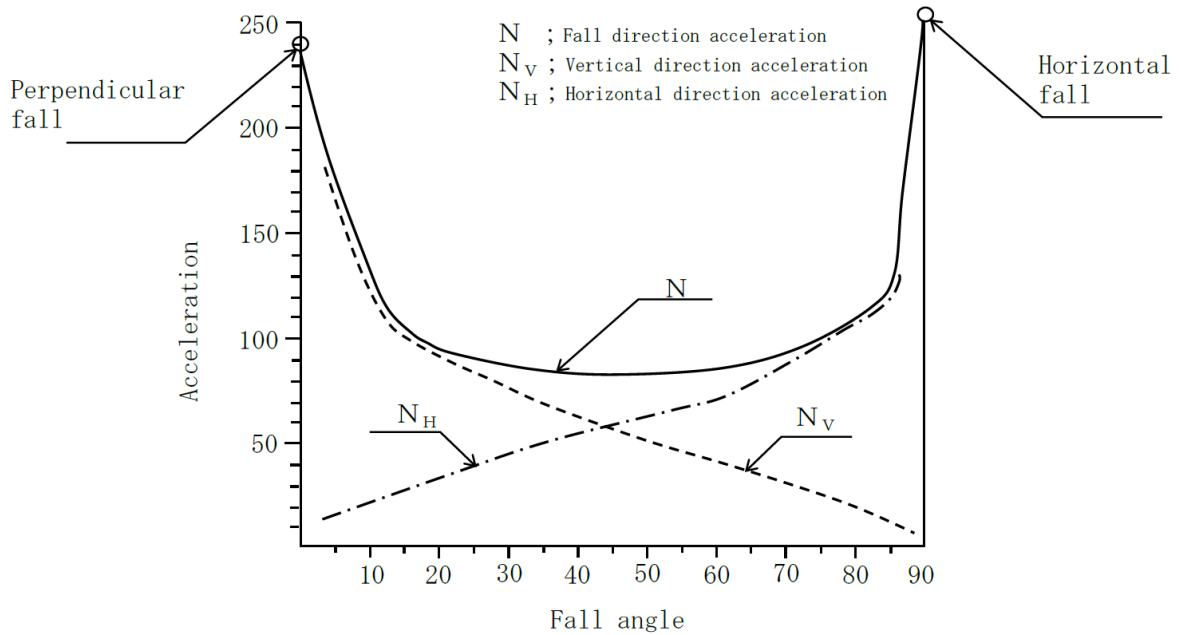
(b) Stresses on the packaging and content

(II)-Table A. 22 shows the vertical and horizontal components of the design acceleration for lid side inclined drop (see (II)-Table A.15).

(II)-Fig. A. 75 shows the relationships between the angle of drop and the acceleration.

(II)-Table A. 22 Relationship between drop angle and acceleration

Angle at dropping θ (degrees)	Acceleration (G)		
	Acceleration (N)	Vertical component ($N \cdot \cos \theta$)	Horizontal component ($N \cdot \sin \theta$)
5	178.6	177.9	15.6
15	106.3	102.7	27.5
30	88.4	76.6	44.2
45	82.3	58.2	58.2
60	81.5	40.8	70.6
75	100.3	26.0	96.6
85	119.4	10.4	118.9



(II)-Fig. A. 75 Relationship between acceleration and drop angle for 1.2 m upper side inclined drop

(II)-Table A. 22 shows that each acceleration component is smaller than the acceleration recorded in the horizontal and vertical drop. Hence, stress is not analyzed here.

A.5.4 Stacking test

We will analyze here the stresses that may occur on the package when a compressive load on technical standards is applied on it.

In the analysis of the stresses, the principal stress is obtained. The stress classifications and stress intensity evaluations are shown in section A.5.4(3).

(1) Compressive load

The specified load to be applied to the specimen under the test condition is ; the greater of the two, the compressive load W_1 five times as high as the weight of the package, or the load W_2 obtained by multiplying the projected area A of the package by the pressure of 0.013 [MPa] (any which is larger).

For the package in question, these loads are respectively

$$W_1 = 5 \cdot m_o \cdot g \text{ [N]}$$

$$W_2 = 0.013 \cdot A \text{ [N]}$$

Where,

m_o : Weight of the package, $m_o = 950$ [kg]

A : Projected area of the package,

$$A = \frac{\pi}{4} \cdot D^2 = \frac{\pi}{4} \times 840^2 = 5.54 \times 10^5 \text{ [mm}^2\text{]}$$

D : Outer diameter of the package, $D = 840$ [mm]

g : Gravitational acceleration, $g = 9.81$ [m/s²]

Thus,

$$W_1 = 5 \times 950 \times 9.81 = 4.66 \times 10^4 \text{ [N]}$$

$$W_2 = 0.013 \times 5.54 \times 10^5 = 7.20 \times 10^3 \text{ [N]}$$

and $W_1 > W_2$.

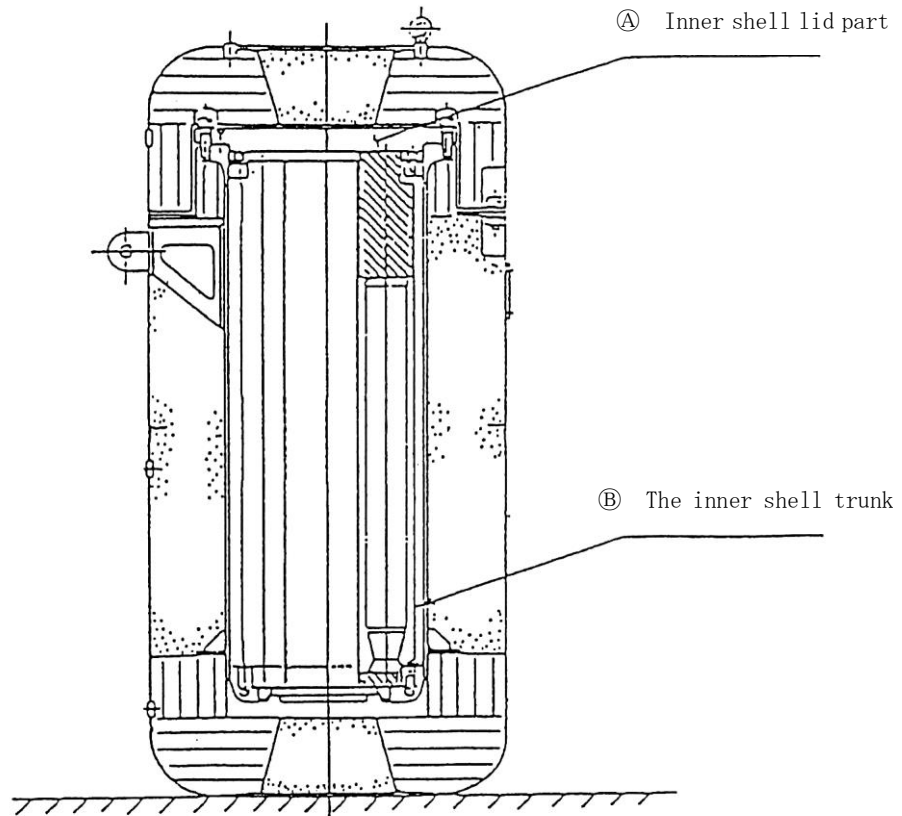
The compressive load F is defined.

$$F = W_1 = 4.66 \times 10^4 \text{ [N]}$$

(2) Analysis of the stresses

We will analyze stresses that may be generated when a compressive load is applied for a period of twenty-four hours to different parts of the packaging.

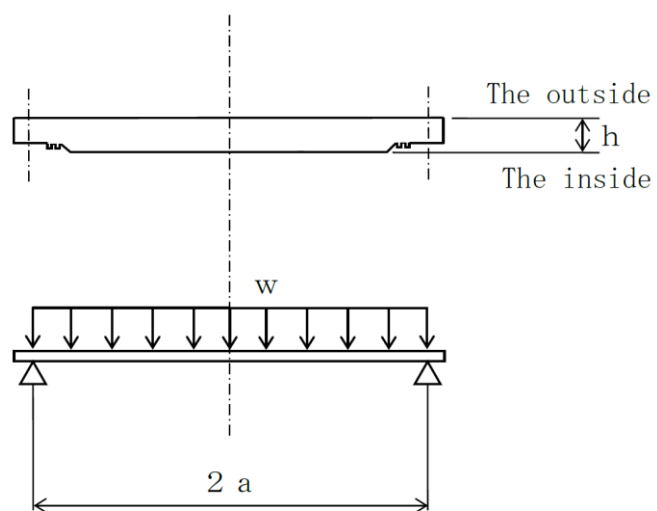
(II)-Fig. A. 76 shows the positions where stresses under the compressive load are to be evaluated.



(II)-Fig.A. 76 Stress evaluation position for compressive load

(A) Inner lid

(II)-Fig.A. 77 shows an analytical model of the inner lid.



(II)-Fig.A. 77 Analytical model of inner lid under compressive load

(II)-Fig. A. 77 shows that both its own weight and the compressive load act uniformly on the inner lid which, supported on its circumference, suffers the maximum stress at the center. The stress results are as follows.

$$\sigma_r = \sigma_\theta = \mp 1.24 \cdot \frac{w \cdot a^2}{h^2}$$

$$\sigma_z = -w \text{ (outer surface)}$$

where

σ_r : Radial stress [N/mm²]

σ_θ : Circumferential stress [N/mm²]

σ_z : Axial stress [N/mm²]

a: Diameter of inner lid supporting points, a = 285 [mm]

h: Thickness of inner lid, h = 55 [mm]

w: Uniform load,

$$w = \frac{(m_2 + m_5) \cdot g + F}{\pi a^2} \quad [\text{N/mm}^2]$$

m₂: Weight of inner lid, m₂ = 120 [kg]

m₅: Weight of outer lid, m₅ = 120 [kg]

F : Compressive load, F = 4.66 × 10⁴ [N/mm²]

$$W = \frac{(120 + 120) \times 9.81 + 4.66 \times 10^4}{\pi \times 285^2} = 0.192 \quad [\text{N/mm}^2]$$

Thus, the stress to be obtained is,

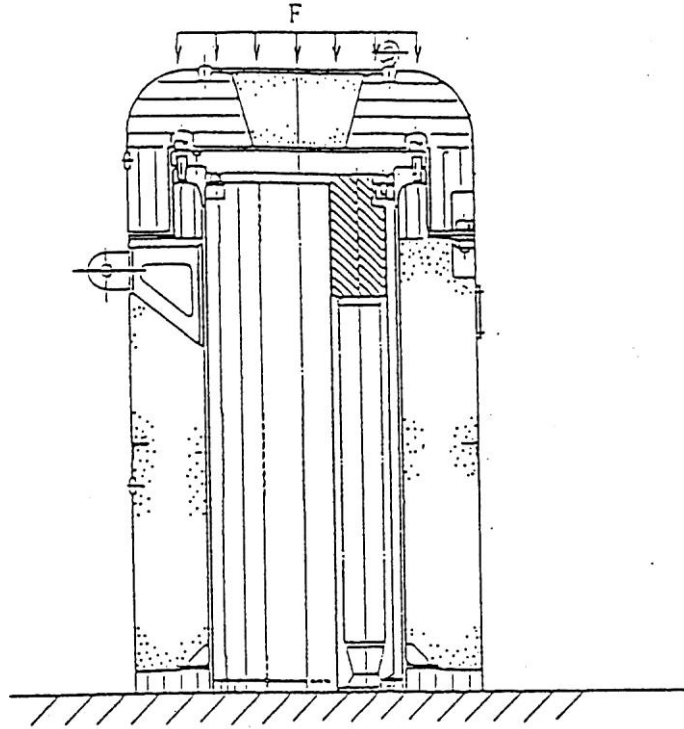
$$\sigma_r = \sigma_\theta = \mp 1.24 \times \frac{0.192 \times 285^2}{55^2} = \mp 6.39 \quad [\text{N/mm}^2]$$

$$\sigma_z = -0.192 \text{ (outer surface)} \quad [\text{N/mm}^2]$$

The upper and lower parts of the double sign correspond to the outer and inner surfaces respectively.

(B) Inner shell

(II)-Fig. A. 78 shows an analytical model of the inner shell.



(II)-Fig. A. 78 Analytical model of inner shell under compressive load

(II)-Fig. A. 78 shows that both the weight of the inner shell and compressive load act on the inner shell. The stress σ_z which is generated by this compressive force is,

$$\sigma_z = \frac{F + m \cdot g}{A}$$

where

σ_z : Compressive load [N/mm²]

F : Compressive force [N] $F = 4.66 \times 10^4$ [N]

m : Weight of the inner shell

$$m = m_1 + m_2 + m_3 + m_4 + m_5 + m_6$$

m_1 : Weight of inner shell (barrel and flanges), $m_1 = 200$ [kg]

m_2 : Weight of inner lid, $m_2 = 120$ [kg]

m_3 : Weight of fuel basket, $m_3 = 138$ [kg]

m_4 : Weight of content, $m_4 = 92$ [kg]

m_5 : Weight of outer shell, $m_5 = 120$ [kg]

m_6 : Weight of outer lid, $m_6 = 120$ [kg]

$m = 200 + 120 + 138 + 92 + 120 + 120 = 790$ [kg]

g : Gravitational acceleration, $g = 9.81$ [m/s²]

A : Cross section of inner shell,

$$A = \frac{\pi}{4} \cdot (d_2^2 - d_1^2)$$

d_2 : Outer diameter of inner shell, $d_2 = 480$ [mm]

d_1 : Inner diameter of inner shell, $d_1 = 460$ [mm]

$$A = \frac{\pi}{4} (480^2 - 460^2) = 1.48 \times 10^4 \text{ [mm}^2\text{]}$$

Thus, the stress to be obtained is,

$$\sigma_z = \frac{4.66 \times 10^4 + 895 \times 9.81}{1.48 \times 10^4} = 3.74 \text{ [N/mm}^2\text{]}$$

(3) Comparison of allowable stress

The results of the stress evaluation from the analyzed items defined in section A.5.4 are put together in (II)-Table A.23.

This table shows that in relation to the reference values, a positive margin of safety can be achieved when single or superposed loads are generated.

Therefore, the soundness of the package can be maintained under normal test conditions (compression).

(II) -Table A.23 Stress evaluation for stacking test

Stress units

;N/mm²

No.	Position to be evaluated		Stress at initial clamping	Stress due to internal pressure	Stress due to thermal expansion	Impact stress	Primary stress						Primary+secondary stress			Fatigue					
							Pm(PL)	Sm	MS	PL+Pb	1.5Sm	MS	PL+Pb +Q	3Sm	MS	PL+Pb +Q+F	Sa	N	Na	DF	MS
1	Inner shell lid	Inner Surface	σ_r	—	—	6.39	0.098	2/3Sy 458	4672	3.22	Sy 687	212	—	—	—	—	—	—	—	—	—
			σ_θ			6.39															
			σ_z			0															
		Outer Surface	σ_r	—	—	-6.39	0.192	2/3Sy 458	2384	2.93	Sy 687	233	—	—	—	—	—	—	—	—	—
			σ_θ			-6.39															
			σ_z			-0.192															
2	Frame of Inner shell		σ_r	—	—	—	4.83	137	27.3	—	—	—	—	—	—	—	—	—	—	—	—
			σ_θ			—															
			σ_z			-3.74															

Pm; General primary membrane stress; PL; Local primary membrane stress; Pb; Primary bending stress; Q; Secondary stress; F; Peak stress;

Sa; Repeated peak stress; N; Number of uses; Na; Permissible number of repetition; DF; Cumulative fatigue coefficient;

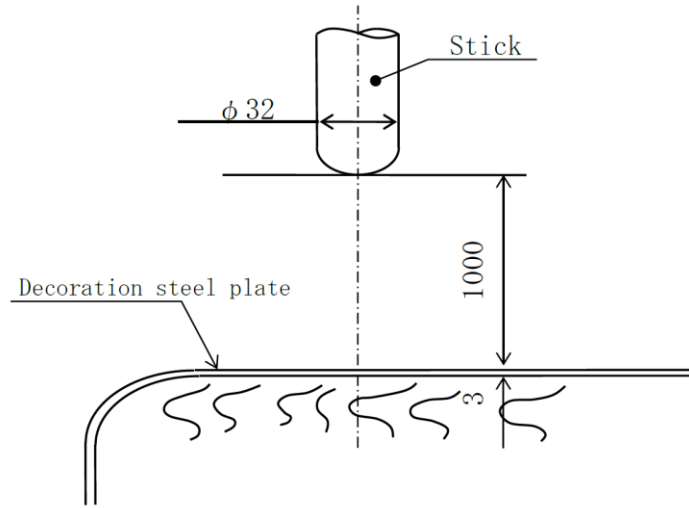
Sm; Design stress intensity value; Sy; Yield point of the design; MS; Margin of safety σ_r ; Diameter direction stress σ_θ ; Periphery direction stress σ_z ; Axial stress

A.5.5 Penetration

The penetration test is carried out to demonstrate that a bar of 32 mm in diameter and 6kg in weight dropped vertically from a height of 1 meter with its hemispherical end downwards does not penetrate the weakest part of the package.

In the analyses, the contributions from the shock absorber and heat insulator under the outer shell is neglected on the assumption that the entire energy will be consumed in the deformation of the outer steel plate of the outer shell. Thus, the evaluation will ensure the maximum in safety.

The inner shell and lid that form the main structure of the containment system is covered with an outer shell and lid. The thickness of the outer steel sheet is 3 mm. [\(II\)-Fig. A.79](#) shows an analytical model of the package.



[\(II\)-Fig. A.79](#) Penetration model

We will describe below the case where the testing bar drops and reaches the object in such an orientation that the outer steel sheet is penetrated with the greatest of ease (see [\(II\)-Fig. A.79](#)).

The potential energy E_1 [N·mm] of the bar before the drop is obtained as follows.

$$E_1 = m \cdot g \cdot h$$

where

m : Weight of the bar, $m = 6$ [kg]

h : Drop height, $h = 1000$ [mm]

g : Gravitational acceleration, $g = 9.81$ [m/s²].

Thus,

$$E_1 = 6 \times 9.81 \times 1000 = 5.89 \times 10^4 \text{ [N}\cdot\text{mm]}$$

The energy E_2 which is necessary to permit the bar to penetrate the 3 mm steel sheet is obtained as follows.

$$E_2 = \int_0^t \tau_{cr} \cdot \pi \cdot d \cdot (t-y) \cdot dy$$

Where,

τ_{cr} : Shearing strength of the outer steel sheet,

$$\tau_{cr} = 0.6 \times Su = 0.6 \times 466 = 280 \text{ [N/mm}^2\text{]}$$

Su: Design tensile strength, $Su = 466 \text{ [N/mm}^2\text{]}$

d: Diameter of the bar, $d = 32 \text{ [mm]}$

t: Thickness of the outer steel sheet, $t = 3 \text{ [mm]}$.

When the equation is integrated with the above values,

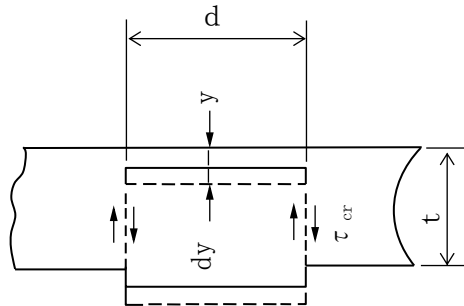
$$E_2 = \tau_{cr} \cdot \pi \cdot d \times \frac{1}{2} \times t^2$$

$$= 280 \times \pi \times 32 \times \frac{1}{2} \times 3^2 = 1.27 \times 10^5 \text{ [N}\cdot\text{mm]}$$

$$E_1 = 5.89 \times 10^4 \text{ [N}\cdot\text{mm}] < E_2 = 1.27 \times 10^5 \text{ [N}\cdot\text{mm]}$$

Therefore, the dropping bar does not penetrate the outer steel sheet.

(II)-Fig. A. 80 shows an analytical model for this test.



(II)-Fig. A. 80 Shearing model

This concludes that the dropping bar does not adversely affect the containment system or the soundness of the package.

A.5.6 Corner or edge drop

These requirements should be applied for the wooden or fiber plate made rectangular parallels piped shapes weighting less than 50kg and the cylindrical objects made of fiber plate weight less than 100kg. This packages, weighting 950kg, will be excluded from those requirements.

A.5.7 Summary of results and evaluation

An outline of the test results for the package under normal test conditions is given below.

(1) 1.2 m drop

As shown in section A.5.3, deformations in the shock absorber in different cases of 1.2 m drop come within the range from 18.2 mm (vertical drop) to 58.6 mm (corner drop). Hence, deformation in each orientation does not affect the inner shell.

The impact accelerations occurring come within the range from 89.9•G to 254.1•G. Stresses occurring are lower than the analytical reference values. Hence, the package retains its soundness and containment.

(2) Other analyses

The tests concerning the pressures at drop, vibration, water spraying, stacking test, and the analyses for penetration, prove that the inner shell constituting the containment barrier retains its sound containment and leaktightness.

(3) Comparison with the allowable stresses

The analyses conducted in consideration of the composite effect of different loads described in section A.1.2-(2) show that the package conforms with all the items of the design reference in section A.1.2-(1).

The package retains its sound containment and leaktightness.

A.6 Accident test conditions

This package is classified as B(U) type, and has the following test conditions set out in the relevant technical standards.

(1) Drop test I

After the drop test I, package must be exposed to the following conditions.

(2) Drop test II

(3) Thermal test

(4) Water immersion test

After these tests (1) to (4) the package must be exposed to the following test conditions.

This section analyzes the effects that the preceding test conditions have on the package and shows how test results satisfy the design standards for the accident test conditions.

A.6.1 Mechanical test – Drop test I (9 m drop) or mechanical test-Drop test III (dynamic pressure pickles)

This section describes the effects at 9 m drop that has on the package and covers the following four types of drop, which shows this package can maintain its soundness at 9m drops.

1) Vertical drop (lid side, bottom side)

2) Horizontal drop

3) Corner drop (lid side, bottom side)

4) Inclined drop (lid side, bottom side)

(a) Analysis model

Analysis illustrates the stresses generated in these drop tests.

The energy generated by a 9 m drop is absorbed by the deformation of the shock absorber installed at the top and bottom sections of the outer shell.

This section evaluates the shock force applied to the package and analyzes its effects.

(b) Prototype test

The details are given in the accompanying document.

(c) Model test

Not applicable.

This analysis is intended to ensure ;

- 1) The deformation in outer shell, caused by the 9 m drop, is not transmitted to the sealed inner shell, thus precluding breaking of the containment
- 2) The impact of the 9 m drop does not damage the inner shell and break the seal.
- 3) No damage to package content.

(1) Analysis methods

The following characteristics of deformation and stress generated in the packaging, fuel baskets and content are analyzed when the 9 m drop tests performed on the package.

(a) Deformation

- 1) It is assumed that impact is with a rigid surface and the drop energy of the package is absorbed only by the shock absorber. This means the volume of outer shell deformation is equivalent to the extent of shock absorber deformation. It ignores absorption by the metal plating and heat insulator, and leads to the higher deformation values, safety evaluation.
- 2) The acceleration and volume of deformation caused by the shock absorbing material are calculated using the CASH-II absorption performance program described in section A.10.1.

(b) Stress

- 1) The drop energy of the package is absorbed by the deformation of the shock absorber and the metal plating that constitutes the outer shell body and outer lid.
- 2) The design acceleration used for analyzing stress is a summation of the acceleration of the metal plating and the CASH-II value

(acceleration generated in the external shock absorber) multiplied by 1.2 (factor established through comparisons with test results shown in section A.10.1.)

As this acceleration combines the acceleration factors of both the shock absorbing material and metal plating, it is used for safety evaluations of impact generated in the package.

Design accelerations = CASH-II result \times 1.2 + metal plating acceleration

3) The acceleration generated in the metal plating is obtained by simple calculations.

(2) Drop force

As indicated in section [A.2 Weight and Center of Gravity], the weight of the package used for analysis is 950kg and drop force is calculated using the following equation:

$$U_a = U_v = m \cdot g \cdot h$$

where

U_a : Energy absorbed by shock absorber [J]

U_v : Drop energy of the package [J]

m : Mass of transportation packaging, $m = 950$ [kg]

h : Height of drop, $h = 9$ [m]

g : Gravitational acceleration $g = 9.81$ [m/s²]

And drop energy is、

$$\begin{aligned} U_a = U_v &= 950 \times 9.81 \times 9 = 8.39 \times 10^4 \text{ [J]} \\ &= 8.39 \times 10^7 \text{ [N} \cdot \text{mm]} \end{aligned}$$

(3) Results of CASH-II shock absorber analysis program

(II)-Table A.24 shows the results of CASH-II program calculations of the values for acceleration and deformation generated in the shock absorbing material.

The table also lists the acceleration of the CASH-II values multiplied by 1.2, which are used in stress analysis.

(4) Design acceleration

(II)-Table A.25 lists the CASH-II calculation code values multiplied by 1.2, shown in (II)-Table A.24, and the acceleration factors for identical metal plating described in section A.5.3(4) and calculated using identical procedures.

The design acceleration factors, used for drop stress analysis, are calculated according to the following equation and are also listed in the table.

Design acceleration = CASH-II result \times 1.2 + metal plating acceleration.

(II)-Table A.24 Deformation and acceleration of shock absorber
under accident test conditions

Drop posture			Volume of Deformation [mm]	Acceleration [$\times g$]	
				Calculated value	$\times 1.2$
Horizontal			81.6	162.6	195.1
Vertical	Lid side		126.7	110.4	132.5
	Bottom side		106.3	102.4	122.9
Corner	Lid side	27.6°	128.6	61.8	74.2
	Bottom side	22.8°	111.3	65.1	78.1
Inclined	Lid side	5°	35.7	34.6	41.5
		15°	85.2	50.2	60.2
		30°	133.9	62.6	75.1
		45°	145.2	76.5	91.8
		60°	129.6	81.3	97.6
		75°	98.4	81.5	97.8
		85°	49.5	61.0	73.2
	Bottom side	5°	36.0	21.4	25.7
		15°	84.6	60.3	72.4
		30°	127.1	65.2	78.2
		45°	135.6	74.8	89.8
		60°	133.5	76.5	91.8
		75°	93.7	67.7	81.2
		85°	44.8	45.9	55.1

where

g: Gravitational acceleration, $g=9.81 \text{ [m/s}^2\text{]}$

(II)-Table A.25 Design acceleration under accident test conditions

Drop posture			CASH- II $\times 1.2$	Acceleration due to steel plate [$\times g$]	Design acceleration [$\times g$]
Horizontal			195.1	171.9	367.0
Vertical	Lid side		132.5	277.3	409.8
	Bottom side		122.9	265.5	388.4
Corner	Lid side	27.6°	74.2	225.6	299.8
	Bottom side	22.8°	78.1	232.8	310.9
Inclined	Lid side	5°	41.5	342.8	384.3
		15°	60.2	296.1	356.3
		30°	75.1	214.8	289.9
		45°	91.8	176.2	268.0
		60°	97.6	158.7	256.3
		75°	97.8	175.5	273.3
		85°	73.2	181.1	254.3
	Bottom side	5°	25.7	349.2	374.9
		15°	72.4	291.7	364.1
		30°	78.2	194.9	273.1
		45°	89.8	160.0	249.8
		60°	91.8	165.6	257.4
		75°	81.2	163.3	244.5
		85°	55.1	156.1	211.2

where

g: Gravitational acceleration, $g=9.81 \text{ [m/s}^2\text{]}$

A.6.1.1 Vertical drop

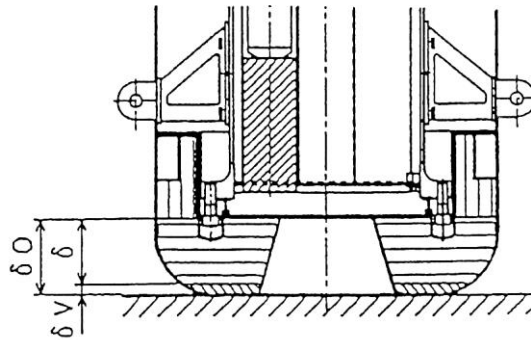
(1) Bottom side vertical drop

Shock absorber deformation is 106.3 mm as shown in (II)-Table A.24 and acceleration is 388.4·g as shown in (II)-Table A.25 when package is dropped 9 m vertically onto its bottom.

(a) Deformation in shock absorber

This shows that deformation in the shock absorber caused by at 9 m vertical drop onto its bottom is not transmitted to the bottom of the inner shell.

(II)-Fig. A.81 shows an analytical model.



(II)-Fig. A.81 Analytical model of interference to inner shell due to shock absorber deformation for 9 m lower side vertical drop

As shown in (II)-Fig. A.81, the remaining δ mm of shock absorber after the package is dropped vertically 9 m onto its bottom is calculated using the following equation.

$$\delta = \delta_o - \delta_v$$

where

δ_o : Minimum thickness of shock absorber prior to deformation,

$$\delta_o = 194 \text{ [mm]}$$

δ_v : Deformation of shock absorber, $\delta_v = 106.3 \text{ [mm]}$

The remained thickness is,

$$\delta = 194 - 106.3 = 87.7 \text{ [mm]}$$

The deformation produced by dropping the package vertically 9 m onto its bottom is limited to the shock absorber and is not transmitted to the bottom of the inner shell.

(b) Stress generated in various parts of package

The analysis procedures and evaluation positions described in section (II) A.5.3 (7) are used and the analysis and evaluation results are both listed in (II)-Table A.26.

(II) -Table A.26 Stress evaluation for 9 m lower side vertical drop (1/6)

Stress units
;N/mm²

No.	Stress Position to be evaluated		Stress at initial clamping	Stress due to internal pressure	Impact stress	Primary stress							
						Pm(PL)	2/3 Su	MS	PL+Pb	Su	MS		
1	Frame of Inner shell		σ_r	—	-0.0491	—	173	310	0.791	—	—	—	
			σ_θ		2.31	—							
			σ_z		1.15	-172							
2	Bottom plate of inner shell		Inner Surface	—	3.18	211	6.63	310	45.7	221	466	1.10	
					σ_θ	0.953							63.4
					σ_z	-0.098							-6.53
			Outer Surface	—	-3.18	-211	0	310	—	214	466	1.17	
					σ_θ	-0.953							-63.4
					σ_z	0							0
3	Inner shell lid		Inner Surface	—	-3.27	55.3	0.098	2/3 Sy 458	4672	52.1	Sy 687	12.1	
					σ_θ	-3.27							55.3
					σ_z	-0.098							0
			Outer Surface	—	3.27	-55.3	1.66	2/3 Sy 458	274	50.4	Sy 687	12.6	
					σ_θ	3.27							-55.3
					σ_z	0							-1.66
4	Inner shell lid clamping bolt		σ_t	174	3.20	—	177	2/3 Sy 458	1.58	—	—	—	
			σ_b	—	—	—							
			τ		—								

Pm; General primary membrane stress; PL; Local primary membrane stress; Pb; Primary bending stress;

Sy; Yield point of the design; Su; Design tensile strength; MS; Margin of safety σ_r ; Diameter direction stress σ_ϕ ; Periphery direction stress σ_2 ; Axial stress σ_b ; Bending stress τ ; Shear stress σ_t ; Ability of bolt stress

(II) -Table A.26 Stress evaluation for 9 m lower side vertical drop (2/6)

Stress units
;N/mm²

No.	Position to be evaluated	Stress	Stress at initial clamping	Stress due to internal pressure	Impact stress	Primary stress					
						P _m (PL)	2/3 S _y	MS	PL+P _b	S _y	MS
1	JRR-3 standard element (Uranium silicon aluminum dispersion alloy)	τ	—	—	0.908	—	—	—	0.908	63.8	69.2
2	JRR-3 follower element (Uranium silicon aluminum dispersion alloy)	τ	—	—	0.742	—	—	—	0.742	63.8	84.9
3	JRR-4 B type element	τ	—	—	0.680	—	—	—	0.680	63.8	92.8
4	JRR-4 L type element	τ	—	—	1.074	—	—	—	1.074	63.8	58.4
5	JRR-4 (Uranium silicon aluminum dispersion alloy)	τ	—	—	0.935	—	—	—	0.935	63.8	67.2
6	JMTR standard element	τ	—	—	0.922	—	—	—	0.922	63.8	68.1
7	JMTR follower	τ	—	—	0.772	—	—	—	0.772	63.8	81.6

P_m; General primary membrane stress; PL; Local primary membrane stress; P_b; Primary bending stress;
 S_y; Yield point of the design; MS; Margin of safety τ ; Shear stress

(II) -Table A.26 Stress evaluation for 9 m lower side vertical drop (3/6)

Stress units
;N/mm²

No.	Position to be evaluated	Stress	Stress at initial clamping	Stress due to internal pressure	Impact stress	Primary stress					
						P _m (PL)	2/3 S _y	MS	PL+Pb	S _y	MS
1	KUR standard (Uranium silicon aluminum dispersion alloy)	τ	—	—	0.703	—	—	—	0.703	63.7	89.6
2	KUR Special element (Uranium silicon aluminum dispersion alloy)	τ	—	—	0.703	—	—	—	0.703	63.7	89.6
3	KUR half-loaded element (Uranium silicon aluminum dispersion alloy)	τ	—	—	0.703	—	—	—	0.703	63.7	89.6

P_m; General primary membrane stress; PL; Local primary membrane stress; Pb; Primary bending stress;
S_y; Yield point of the design; MS; Margin of safety τ; Shear stress

(II) -Table A.26 Stress evaluation for 9 m lower side vertical drop (4/6)

Stress units
;N/mm²

No.	Position to be evaluated	Stress	Stress at initial clamping	Stress due to internal pressure	Impact stress	Primary stress					
						Pm(PL)	2/3 Sy	MS	PL+Pb	Sy	MS
1	JMTRC Standard fuel element (A, B, C type)	τ	—	—	0.71	—	—	—	0.71	63.8	88.8
2	JMTRC Standard fuel element ($\phi 2.2$ pin, fix type) (B, C type)	σ_t	—	—	10.2	—	—	—	10.2	63.8	5.25
3	JMTRC Special fuel element (Special A type)	σ_c	—	—	16.8	—	—	—	16.8	63.8	2.79
4	JMTRC Special fuel element (Special B type)	σ_c	—	—	0.59	—	—	—	0.59	63.8	107
5	JMTRC Special fuel element (Special C, Special D type)	σ_c	—	—	17.1	—	—	—	17.1	63.8	2.73
6	JMTRC fuel follower (HF type)	τ	—	—	0.56	—	—	—	0.56	63.8	112
7	JMTRC Standard fuel element (MA, MB, MC type)	τ	—	—	0.70	—	—	—	0.70	63.8	90.1
8	JMTRC Special fuel element (Special MB, Special MC type)	σ_c	—	—	16.6	—	—	—	16.6	63.8	2.84
9	JMTRC fuel follower (MF type)	τ	—	—	0.56	—	—	—	0.56	63.8	112

Pm ; General primary membrane stress; PL ; Local primary membrane stress; Pb ; Primary bending stress;

Sy ; Yield point of the design; MS ; Margin of safety σ_t ; Ability of bolt stress σ_c ; Compression stress τ ; Shear stress

(II) -Table A.26 Stress evaluation for 9 m lower side vertical drop (5/6)

Stress units
;N/mm²

No.	Position to be evaluated	Stress	Stress at initial clamping	Stress due to internal pressure	Impact stress	Primary stress					
						P _m (PL)	2/3 S _y	MS	PL+P _b	S _y	MS
1	JMTRC Special fuel element hold down part (Special B type)	σ_c	—	—	24.9	—	—	—	24.9	245	8.83

P_m ;General primary membrane stress; PL ;Local primary membrane stress; P_b ;Primary bending stress;
S_y ;Yield point of the design; MS ;Margin of safety σ_2 ;Axial stress

(II) -Table A.26 Stress evaluation for 9 m lower side vertical drop (6/6)

Stress units
;N/mm²

No.	Position to be evaluated	Stress	Stress at initial clamping	Stress due to internal pressure	Impact stress	Primary stress					
						P _m (P _L)	2/3 S _y	MS	P _L +P _b	S _y	MS
1	KUCA coupon type	τ	—	—	0.46	—	—	—	0.46	63.7	138
	KUCA flat type	τ	—	—	14.2	—	—	—	14.2	63.7	4.5

P_m;General primary membrane stress; P_L;Local primary membrane stress; P_b;Primary bending stress;
S_y;Yield point of the design; MS;Margin of safety τ; Shear stress

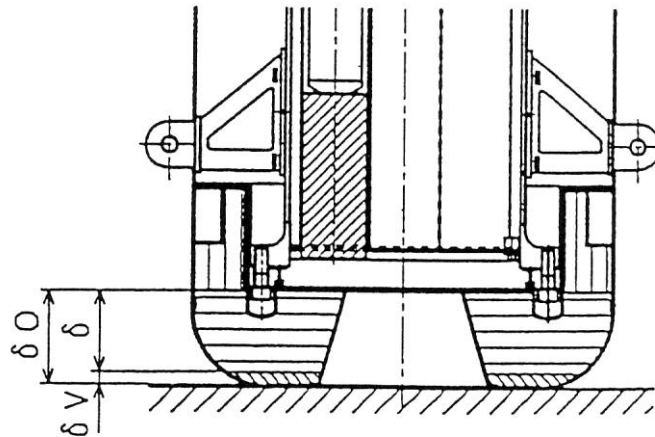
(2) Lid side vertical drop

Shock absorber deformation is 126.7 mm as shown in (II)-Table A. 24 and acceleration is 409.8•g as shown in (II)-Table A. 25 when the package is dropped 9 m vertically onto its top.

(a) Deformation in shock absorber

This shows that deformation in the shock absorber caused by a 9 m vertical drop onto its top is not transmitted to the top area of the inner shell.

(II)-Fig. A. 82 shows an analytical model.



(II)-Fig. A. 82 Analytical model of interference to inner shell due to shock absorber deformation for 9 m upper side vertical drop

As shown in (II)-Fig. A. 82, the remaining δ mm of shock absorber after the package is dropped vertically 9 m onto its top is calculated using the following equation.

$$\delta = \delta_o - \delta_v$$

where

δ_o : Minimum thickness of shock absorber prior to deformation,

$$\delta_o = 186 \text{ [mm]}$$

δ_v : Deformation of shock absorber, $\delta_v = 126.7 \text{ [mm]}$

The remained thickness is,

$$\delta = 186 - 126.7 = 59.3 \text{ [mm]}$$

This shows that deformation in the shock absorber caused by a 9 m vertical drop onto its top is not transmitted to the inner shell lid.

(b) Stress generated in various parts of package

The analysis procedures and evaluation positions described in section (II)A. 5. 3(8) are used and the analysis and evaluation results are both listed in (II)-Table A. 27.

(II) -Table A.27 Stress evaluation for 9 m upper side vertical drop (1/6)

Stress units
;N/mm²

No.	Position to be evaluated	Stress	Stress at initial clamping	Stress due to internal pressure	Impact stress	Primary stress					
						Pm(PL)	2/3 Su	MS	PL+Pb	Su	MS
1	Frame of Inner shell	σ_r	—	-0.0491	—	156	310	0.987	—	—	—
		σ_θ		2.31	—						
		σ_z		1.15	-155						
2	Bottom plate of inner shell	Inner Surface	—	3.18	-137	0.098	310	3162	134	466	2.47
				0.953	-41.1						
				-0.098	0						
		Outer Surface	—	-3.18	137	4.23	310	72.2	138	466	2.37
				-0.953	41.1						
				0	-4.23						
3	Inner shell lid	Inner Surface	—	-3.27	-193	10.1	2/3 Sy 458	44.3	186	Sy 687	2.69
				-3.27	-193						
				-0.098	-10.0						
		Outer Surface	—	3.27	193	—	—	—	196	Sy 687	2.50
				3.27	193						
				0	0						
4	Inner shell lid clamping bolt	σ_t	174	3.20	150	327	2/3 Sy 458	0.400	—	—	—
		σ_b	—	—	—						
		τ			—						

Pm; General primary membrane stress; PL; Local primary membrane stress; Pb; Primary bending stress;

Sy; Yield point of the design; Su; Design tensile strength; MS; Margin of safety σ_r ; Diameter direction stress σ_θ ; Periphery direction stress σ_z ; Axial stress σ_b ; Bending stress σ_t ; Stress of the part fuel plater pin

(II) -Table A.27 Stress evaluation for 9 m upper side vertical drop (2/6)

Stress units
;N/mm²

No.	Position to be evaluated	Stress	Stress at initial clamping	Stress due to internal pressure	Impact stress	Primary stress					
						Pm(PL)	2/3 Sy	MS	PL+Pb	Sy	MS
1	JRR-3 standard element (Uranium silicon aluminum dispersion alloy)	τ	—	—	0.958	—	—	—	0.958	63.8	65.5
2	JRR-3 follower element (Uranium silicon aluminum dispersion alloy)	τ	—	—	0.783	—	—	—	0.783	63.8	80.4
3	JRR-4 B type element	τ	—	—	0.718	—	—	—	0.718	63.8	87.9
4	JRR-4 L type element	τ	—	—	1.133	—	—	—	1.133	63.8	55.3
5	JRR-4 (Uranium silicon aluminum dispersion alloy)	τ	—	—	0.987	—	—	—	0.987	63.8	63.6
6	JMTR standard element	τ	—	—	0.973	—	—	—	0.973	63.8	64.5
7	JMTR follower	τ	—	—	0.815	—	—	—	0.815	63.8	77.2

Pm; General primary membrane stress; PL; Local primary membrane stress; Pb; Primary bending stress;

Sy; Yield point of the design; MS; Margin of safety τ ; Shear stress

(II) -Table A.27 Stress evaluation for 9 m upper side vertical drop (3/6)

Stress units
;N/mm²

No.	Position to be evaluated	Stress	Stress at initial clamping	Stress due to internal pressure	Impact stress	Primary stress					
						Pm(PL)	2/3 Sy	MS	PL+Pb	Sy	MS
1	KUR standard (Uranium silicon aluminum dispersion alloy)	τ	—	—	0.741	—	—	—	0.741	63.7	84.9
2	KUR Special element (Uranium silicon aluminum dispersion alloy)	τ	—	—	0.741	—	—	—	0.741	63.7	84.9
3	KUR half-loaded element (Uranium silicon aluminum dispersion alloy)	τ	—	—	0.741	—	—	—	0.741	63.7	84.9

Pm; General primary membrane stress; PL; Local primary membrane stress; Pb; Primary bending stress;

Sy; Yield point of the design; MS; Margin of safety τ ; Shear stress

(II) -Table A.27 Stress evaluation for 9 m upper side vertical drop (4/6)

Stress units
;N/mm²

No.	Position to be evaluated	Stress	Stress at initial clamping	Stress due to internal pressure	Impact stress	Primary stress					
						Pm(PL)	2/3 Sy	MS	PL+Pb	Sy	MS
1	JMTRC Standard fuel element (A, B, C type)	τ	—	—	0.74	—	—	—	0.74	63.8	85.2
2	JMTRC Standard fuel element ($\phi 2.2$ pin, fix type) (B, C type)	σ_t	—	—	10.8	—	—	—	10.8	63.8	4.90
3	JMTRC Special fuel element (Special A type)	σ_c	—	—	17.7	—	—	—	17.7	63.8	2.60
4	JMTRC Special fuel element (Special B type)	σ_c	—	—	0.63	—	—	—	0.63	63.8	100
5	JMTRC Special fuel element (Special C, Special D type)	σ_c	—	—	18.1	—	—	—	18.1	63.8	2.52
6	JMTRC fuel follower (HF type)	τ	—	—	0.59	—	—	—	0.59	63.8	107
7	JMTRC Standard fuel element (MA, MB, MC type)	τ	—	—	0.73	—	—	—	0.73	63.8	86.3
8	JMTRC Special fuel element (Special MB, Special MC type)	σ_c	—	—	17.6	—	—	—	17.6	63.8	2.62
9	JMTRC fuel follower (MF type)	τ	—	—	0.59	—	—	—	0.59	63.8	107

Pm ; General primary membrane stress; PL ; Local primary membrane stress; Pb ; Primary bending stress;

Sy ; Yield point of the design; MS ; Margin of safety σ_t ; Stress of the part fuel plater pin τ ; Shear stress σ_c ; Compression stress

(II) -Table A.27 Stress evaluation for 9 m upper side vertical drop (5/6)

Stress units

;N/mm²

No.	Position to be evaluated	Stress	Stress at initial clamping	Stress due to internal pressure	Impact stress	Primary stress					
						Pm(PL)	2/3 Sy	MS	PL+Pb	Sy	MS
1	JMTRC Special fuel element hold down part (Special A type)	σ_c	—	—	45.7	—	—	—	45.7	245	4.36
2	JMTRC Special fuel element hold down part (Special B type)	σ_c	—	—	26.3	—	—	—	26.3	245	8.31
3	JMTRC Special fuel element hold down part (Special C, Special D type)	σ_c	—	—	47.4	—	—	—	47.4	245	4.16
4	JMTRC Special fuel element hold down part (Special MB, Special MC type)	σ_c	—	—	47.4	—	—	—	47.4	245	4.16

Pm ; General primary membrane stress; PL ; Local primary membrane stress; Pb ; Primary bending stress;

Sy ; Yield point of the design; MS ; Margin of safety σ_c ; Compression stress

Stress units
;N/mm²

(II) -Table A.27 Stress evaluation for 9 m upper side vertical drop (6/6)

No.	Position to be evaluated	Stress	Stress at initial clamping	Stress due to internal pressure	Impact stress	Primary stress					
						Pm(PL)	2/3 Sy	MS	PL+Pb	Sy	MS
1	KUCA coupon type	τ	—	—	0.50	—	—	—	0.50	63.7	127
2	KUCA flat type	τ	—	—	15.0	—	—	—	15.0	63.7	4.2

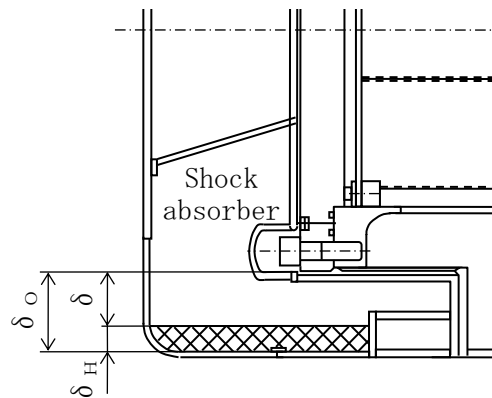
Pm ;General primary membrane stress; PL ;Local primary membrane stress; Pb ;Primary bending stress;
Sy ;Yield point of the design; MS ;Margin of safety τ ; Shear stress

A. 6. 1. 2 Horizontal drop

The deformation of 81.6 mm as shown in (II)-Table A. 24 and acceleration of 367.0·g as shown in (II)-Table A. 25 are generated in the shock absorber when horizontal drop is 9 m.

(1) Deformation in shock absorber

This shows that the deformation generated in the shock absorber by a 9 m horizontal drop is not transmitted to the inner shell. [\(II\)-Fig. A. 83](#) shows an analytical model.



[\(II\)-Fig. A. 83](#) Analytical model of interference to inner shell due to shock absorber deformation for 9 m horizontal drop

As shown in [\(II\)-Fig. A. 83](#), the remaining δ mm of shock absorber after a 9 m horizontal drop is calculated by the following equation,

$$\delta = \delta_o - \delta_H$$

where

δ_o : Minimum thickness of shock absorber prior to deformation,

$$\delta_o = 104 \text{ [mm]}$$

δ_H : Deformation of shock absorber, $\delta_H = 81.6 \text{ [mm]}$

The remaining thickness is,

$$\delta = 104 - 81.6 = 22.4 \text{ [mm]}$$

The deformation produced by a 9 m horizontal drop is limited to the shock absorber and is not transmitted to the inner shell.

(2) Stress generated in package and content

The analysis procedures and evaluation positions described in section (II) A. 5. 3(6) are used and both the analysis and evaluation results are listed in [\(II\)-Table A. 28.](#)

(II) -Table A.28 Stress evaluation for 9 m horizontal drop (1/6)

Stress units
;N/mm²

No.	Position to be evaluated	Stress	Stress at initial clamping	Stress due to internal pressure	Impact stress	Primary stress					
						Pm(PL)	2/3Su	MS	PL+Pb	Su	MS
1	Frame of Inner shell	σ_r	—	-0.0491	—	2.36	310	130	253	466	0.841
		σ_θ		2.31	—						
		σ_z		1.15	252						
2	Bottom area of inner shell	σ_r	—	3.18	—	0.098	310	3162	125	466	2.72
		σ_θ		0.953	—						
		σ_z		-0.098	—						
		τ		—	62.6						
3	Top area of inner shell	σ_r	—	-0.0491	—	2.36	2/3 Sy 120	50.6	20.0	Sy 180	8.00
		σ_θ		2.31	—						
		σ_z		1.15	—						
		τ		—	9.93						
4	Inner shell lid clamping bolt	σ_t	174	3.20	—	177	2/3 Sy 458	1.58	184	Sy 687	2.73
		σ_b	—	—	6.78						
		τ	—	—	—						
5	Rectangular fuel basket	σ_x	—	—	255	—	—	—	255	466	0.827
		σ_y									
		σ_z									

Pm; General primary membrane stress; PL; Local primary membrane stress; Pb; Primary bending stress;

Sy; Yield point of the design; Su; Design tensile strength; MS; Margin of safety σ_r ; Diameter direction stress σ_θ ; Periphery direction stress σ_z ; Axial stress σ_b ; Bending stress σ_t ; Stress of the part fuel plater pin τ ; Shear stress

(II) -Table A.28 Stress evaluation for 9 m horizontal drop (2/6)

Stress units

;N/mm²

No.	Stress Position to be evaluated			Stress at initial clamping	Stress due to internal pressure	Impact stress	Primary stress					
							Pm(PL)	2/3 Sy	MS	PL+Pb	Sy	MS
1	JRR-3 standard element (Uranium silicon aluminum dispersion alloy)	Surface directio	σ_b	—	—	28.8	—	—	—	28.8	63.8	1.21
		Axial directio	σ_c	—	—	1.94	—	—	—	1.94	63.8	31.8
2	JRR-3 follower element (Uranium silicon aluminum dispersion alloy)	Surface directio	σ_b	—	—	19.0	—	—	—	19.0	63.8	2.35
		Axial directio	σ_c	—	—	1.63	—	—	—	1.63	63.8	38.1
3	JRR-4 B type element	Surface directio	σ_b	—	—	23.1	—	—	—	23.1	63.8	1.76
		Axial directio	σ_c	—	—	1.68	—	—	—	1.68	63.8	36.9
4	JRR-4 L type element	Surface directio	σ_b	—	—	24.6	—	—	—	24.6	63.8	1.59
		Axial directio	σ_c	—	—	2.34	—	—	—	2.34	63.8	26.2
5	JRR-4 (Uranium silicon aluminum dispersion alloy)	Surface directio	σ_b	—	—	31.8	—	—	—	31.8	63.8	1.00
		Axial directio	σ_c	—	—	2.17	—	—	—	2.17	63.8	28.4
6	JMTR standard element	Surface directio	σ_b	—	—	29.6	—	—	—	29.6	63.8	1.15
		Axial directio	σ_c	—	—	1.99	—	—	—	1.99	63.8	31.0
7	JMTR follower	Surface directio	σ_b	—	—	20.1	—	—	—	20.1	63.8	2.17
		Axial directio	σ_c	—	—	1.71	—	—	—	1.71	63.8	36.3

Pm; General primary membrane stress; PL; Local primary membrane stress; Pb; Primary bending stress;

Sy; Yield point of the design; MS; Margin of safety σ_b ; Bending stress σ_c ; Compression stress

Stress units

;N/mm²

(II) -Table A.28 Stress evaluation for 9 m horizontal drop (3/6)

No.	Stress Position to be evaluated			Stress at initial clamping	Stress due to internal pressure	Impact stress	Primary stress					
							Pm(PL)	2/3 Sy	MS	PL+Pb	Sy	MS
1	KUR standard (Uranium silicon aluminum dispersion alloy)	Surface directio	σ_b	—	—	20.1	—	—	—	20.1	63.7	2.16
		Axial directio	σ_c	—	—	1.54 *1	1.54	4.67	2.03	—	—	—
2	KUR half-loaded element (Uranium silicon aluminum)	Surface directio	σ_b	—	—	20.1	—	—	—	20.1	63.7	2.16
		Axial directio	σ_c	—	—	1.54 *1	1.54	4.67	2.03	—	—	—
3	KUR Special element (Uranium silicon aluminum dispersion alloy)	Surface directio	σ_b	—	—	20.1	—	—	—	20.1	63.7	2.16
		Axial directio	σ_c	—	—	1.33 *1	1.33	4.67	2.51	—	—	—

Pm ; General primary membrane stress; PL ; Local primary membrane stress; Pb ; Primary bending stress;

Sy ; Yield point of the design; Su ; Design tensile strength; MS ; Margin of safety σ_b ; Bending stress σ_c ; Compression stress

*1 ; axial compression stress

(II) -Table A.28 Stress evaluation for 9 m horizontal drop (4/6)

Stress units

;N/mm²

No.	Stress Position to be evaluated			Stress at initial clamping	Stress due to internal pressure	Impact stress	Primary stress					
							Pm(PL)	2/3 Sy	MS	PL+Pb	Sy	MS
1	JMTRC Standard fuel element (A, B, C type)	Surface directio	σ_b	—	—	22.4	—	—	—	22.4	63.8	1.84
		Axial directio	σ_c	—	—	1.59	—	—	—	1.59	63.8	39.1
2	JMTRC Standard fuel element ($\phi 2.2$ pin, fix type) (B, C type)	Surface directio	σ_b	—	—	22.2	—	—	—	22.2	63.8	1.87
		Axial directio	σ_c	—	—	1.58	—	—	—	1.58	63.8	39.3
3	JMTRC Special fuel element (Special A type)	Surface directio	σ_b	—	—	33.4	—	—	—	33.4	63.8	0.91
		Axial directio	σ_c	—	—	1.59	—	—	—	1.59	63.8	39.1
4	JMTRC Special fuel element (Special B type)	Surface directio	σ_b	—	—	22.9	—	—	—	22.9	63.8	1.78
		Axial directio	σ_c	—	—	1.98	—	—	—	1.98	63.8	31.2
5	JMTRC Special fuel element (Special C, Special D type)	Surface directio	σ_b	—	—	33.4	—	—	—	33.4	63.8	0.91
		Axial directio	σ_c	—	—	2.39	—	—	—	2.39	63.8	25.6
6	JMTRC fuel follower (HF type)	Surface directio	σ_b	—	—	14.3	—	—	—	14.3	63.8	3.46
		Axial directio	σ_c	—	—	1.29	—	—	—	1.29	63.8	48.4
7	JMTRC Standard fuel element (MA, MB, MC type)	Surface directio	σ_b	—	—	22.3	—	—	—	22.3	63.8	1.86
		Axial directio	σ_c	—	—	1.57	—	—	—	1.57	63.8	39.6
8	JMTRC Special fuel element (Special MB, Special MC type)	Surface directio	σ_b	—	—	33.2	—	—	—	33.2	63.8	0.92
		Axial directio	σ_c	—	—	1.56	—	—	—	1.56	63.8	39.8
9	JMTRC fuel follower (MF type)	Surface directio	σ_b	—	—	14.4	—	—	—	14.4	63.8	3.43
		Axial directio	σ_c	—	—	1.31	—	—	—	1.31	63.8	47.7

Pm; General primary membrane stress; PL; Local primary membrane stress; Pb; Primary bending stress;

Sy; Yield point of the design; MS; Margin of safety σ_b ; Bending stress σ_c ; Compression stress

Stress units
;N/mm²

(II) -Table A.28 Stress evaluation for 9 m horizontal drop (5/6)

No.	Position to be evaluated	Stress	Stress at initial clamping	Stress due to internal pressure	Impact stress	Primary stress					
						Pm(PL)	2/3 Sy	MS	PL+Pb	Sy	MS
1	JMTRC Special fuel element hold down part (Special A type)	σ_b	—	—	13.9	—	—	—	13.9	245	16.6
2	JMTRC Special fuel element hold down part (Special B type)	σ_b	—	—	22.5	—	—	—	22.5	245	9.88
3	JMTRC Special fuel element hold down part (Special C, Special D type)	σ_b	—	—	13.9	—	—	—	13.9	245	16.6
4	JMTRC Special fuel element hold down part (Special MB, Special MC type)	σ_b	—	—	1.39	—	—	—	1.39	245	16.6

Pm ; General primary membrane stress; PL ; Local primary membrane stress; Pb ; Primary bending stress;

Sy ; Yield point of the design; MS ; Margin of safety σ_b ; Bending stress

Stress units
;N/mm²

(II) -Table A.28 Stress evaluation for 9 m horizontal drop (6/6)

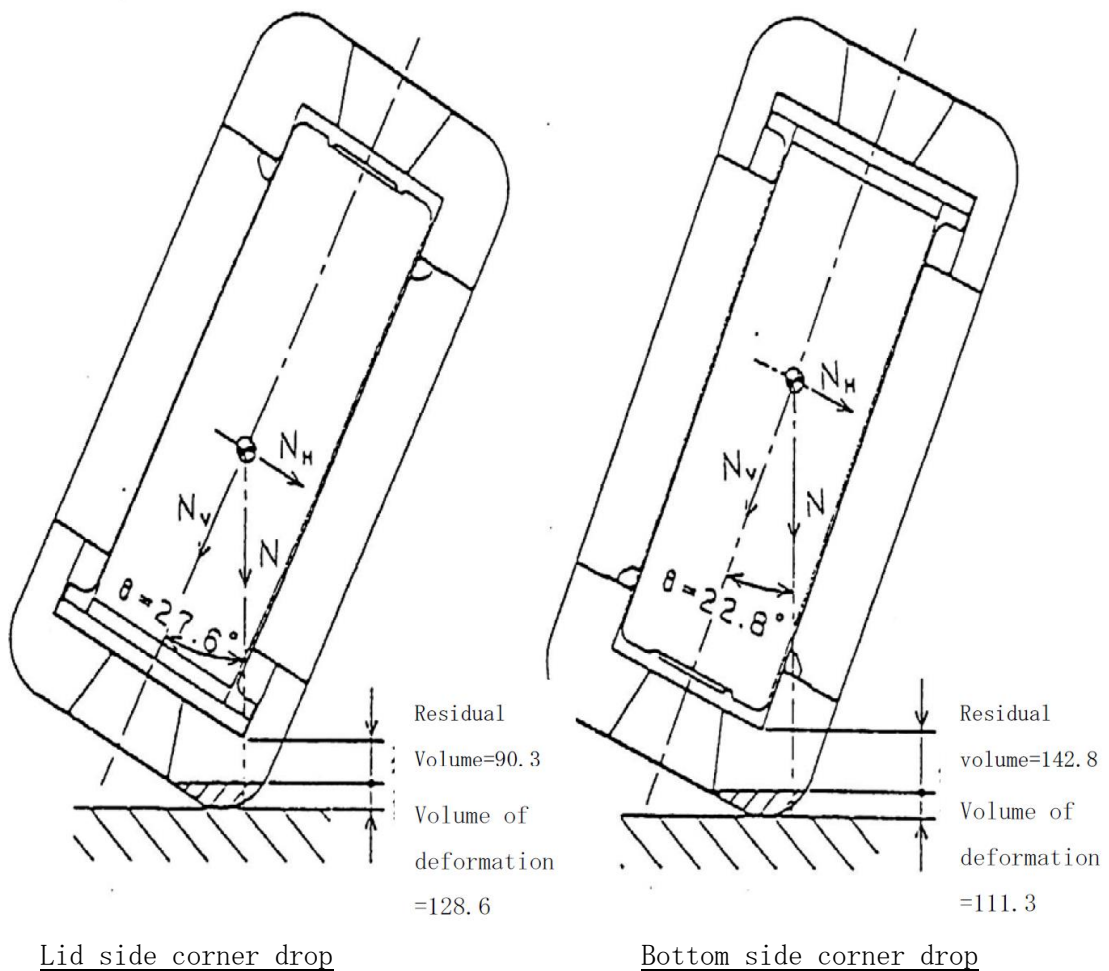
No.	Stress Position to be evaluated		Stress at initial clamping	Stress due to internal pressure	Impact stress	Primary stress						
						Pm(PL)	2/3 Sy	MS	PL+Pb	Sy	MS	
1	KUCA coupon type		σ_c	—	—	3.19	—	—	—	3.19	63.7	20.0
2	KUCA flat type	Surface direction	σ_b	—	—	0.24	—	—	—	0.24	63.7	265
		Axial direction	σ_c	—	—	1.39	—	—	—	1.39	63.7	45.8

Pm ;General primary membrane stress; PL ;Local primary membrane stress; Pb ;Primary bending stress;
Sy ;Yield point of the design; MS ;Margin of safety σ_b ; Bending stress σ_c ; Compression stress

A. 6. 1. 3 Corner drop

(1) Deformation of shock absorber

(II)-Fig. A. 84 shows the deformation and the remaining thickness of the shock absorber. Deformation affects only the external shock absorber and is not transmitted to the inner shell.



(II)-Fig. A. 84 Analytical model of interference to inner shell
due to shock absorber deformation for 9m corner drop

(2) Stresses of packaging and content

(II)-Table A.29 shows the design acceleration factors for the corner drop, listed in (II)-Table A.25, separated into vertical and horizontal elements.

(II)-Table A.29 Design acceleration for corner drop

(×g)			
Drop type	Acceleration (N)	Vertical acceleration ($N_v = N \cos \theta$)	Horizontal acceleration ($N_h = N \sin \theta$)
Corner			
Lid side	299.8	265.7	138.9
Bottom side	310.9	286.6	120.5

As (II)-Table A.29 shows, acceleration components for all directions are smaller than those for vertical and horizontal drop. For this reason stress analysis is omitted.

The procedures described in section (II) A.5.3 (9) are used for the inner lid clamping bolts and the analysis and evaluation results are both listed in (II)-Table A.30.

(II) -Table A.30 Stress evaluation for 9 m upper corner drop

Stress units
;N/mm²

No.	Position to be evaluated	Stress	Stress at initial clamping	Stress due to internal pressure	Impact stress		Primary stress					
					Horizontal Component	Vertical Component	Pm(PL)	2/3 Sy	MS	PL+Pb	Sy	MS
1	Inner lid clamping bolt	σ_t	174	3.20			177	459	1.58	411	687	0.671
		σ_b	—	—	7.73	226						
		τ										

Pm ; General primary membrane stress; PL ; Local primary membrane stress; Pb ; Primary bending stress;

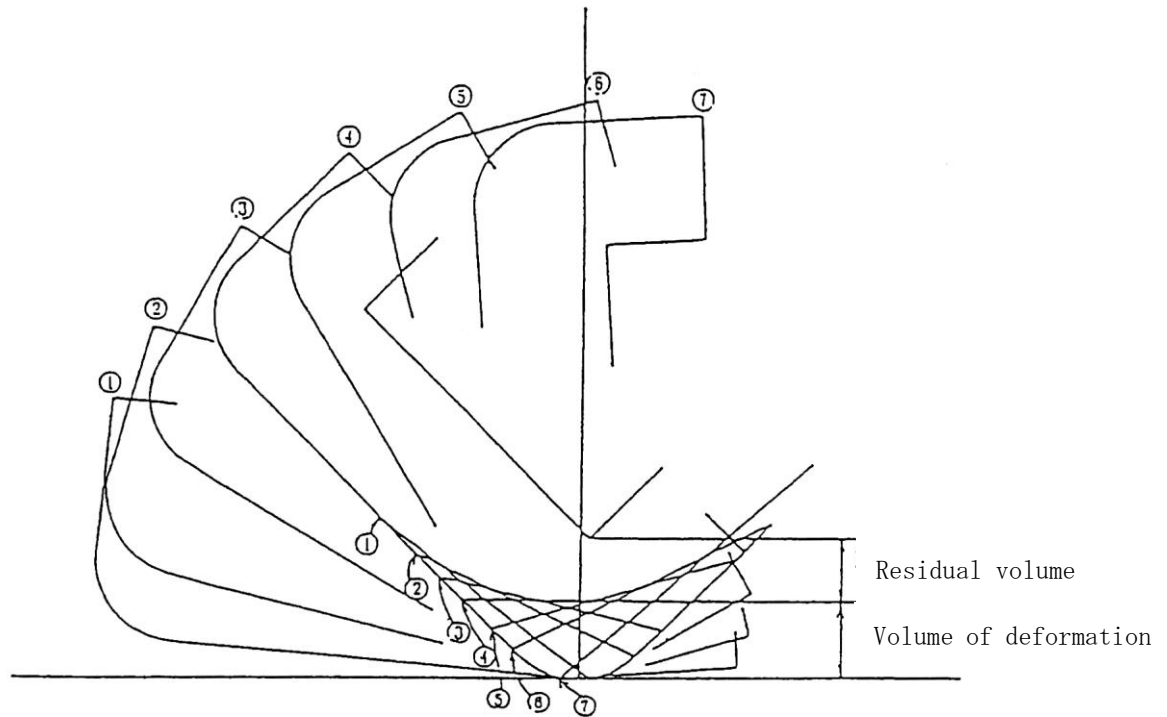
Sy ; Yield point of the design; MS ; Margin of safety σ_t ; Ability of bolt stress σ_b ; Bending stress τ ; Shear stress

A.6.1.4 Inclined drop

(1) Bottom side inclined drop

(a) Deformation of shock absorber

(II)-Fig. A.85 shows the relationship between the angle at dropping and the deformation.



No.	Angle at dropping θ	Minimum thickness of shock absorber before deformation (mm)	Deformation of shock absorber (mm)	Remaining thickness of shock absorber (mm)
①	5°	211.9	36.0	175.9
②	15°	236.8	84.6	152.2
③	30°	260.2	127.1	133.1
④	45°	265.7	135.6	130.1
⑤	60°	252.9	133.5	119.4
⑥	75°	222.6	93.7	128.9
⑦	85°	193.7	44.8	148.9

(II)-Fig. A.85 Analytical model of interference to inner shell due to shock absorber deformation for 9m lower side inclined drop

(II)-Fig. A. 85 shows that in the drop, deformation occurs only in parts of the shock absorber and does not reach the inner shell.

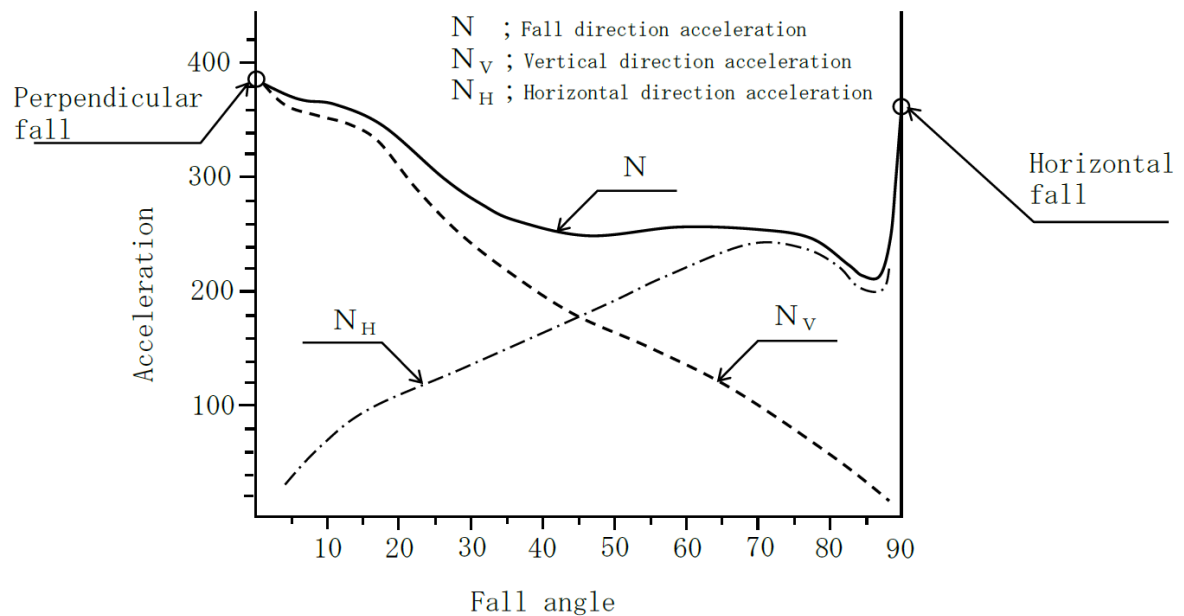
(b) Stresses of packaging and content

(II)-Table A. 31 shows the horizontal and vertical components of the design acceleration for the bottom side corner drop (II)-Table A. 25.

(II)-Fig. A. 86 shows the relationships between the angle of drop and the acceleration.

(II)-Table A. 31 Relationship between drop angle and acceleration

Angle at dropping θ	Acceleration (G)		
	Acceleration (N)	Vertical component ($N \cdot \cos \theta$)	Horizontal component ($N \cdot \sin \theta$)
5	374.9	373.5	32.7
15	364.1	351.7	94.2
30	273.1	236.5	136.6
45	249.8	176.6	176.6
60	257.4	128.7	222.9
75	244.5	63.3	236.2
85	211.2	18.4	210.4



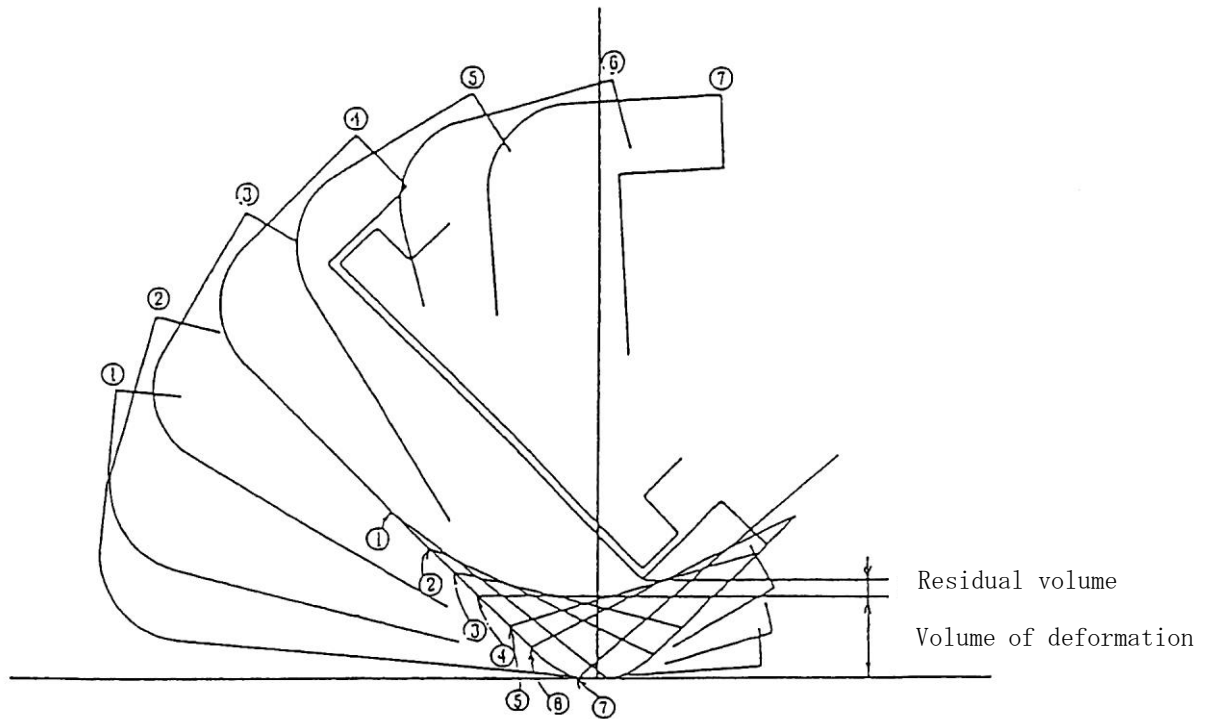
(II)-Fig. A. 86 Relationship between acceleration and drop angle for 9m lower side inclined drop

(II)-Table A. 31 shows that each accelerating component is smaller than the acceleration recorded for the vertical and horizontal drop. Hence, stress is not analyzed here.

(2) Lid side inclined drop

(a) Deformation of the shock absorber

(II)-Fig. A. 87 shows the relationship between the angle at dropping and the deformation.



No.	Angle at dropping θ	Minimum thickness of shock absorber before deformation (mm)	Deformation in shock absorber (mm)	Remaining thickness of shock absorber (mm)
①	5°	201.1	35.7	165.4
②	15°	210.5	85.2	125.3
③	30°	212.2	133.9	78.3
④	45°	199.1	145.2	53.9
⑤	60°	171.9	129.6	42.3
⑥	75°	132.7	98.4	34.3
⑦	85°	101.1	49.5	51.6

(II)-Fig. A. 87 Analytical model of interference to inner shell due to shock absorber deformation for 9 m upper side inclined drop

(II)-Fig. A. 87 shows that deformation only occurs in parts of the shock absorber and does not reach the inner shell.

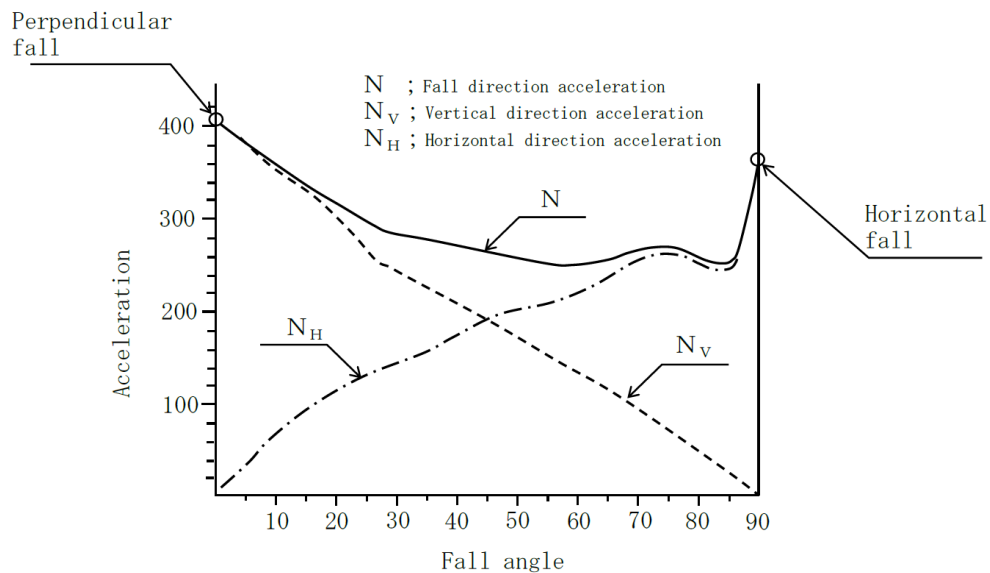
(b) Stresses on the packaging and content

(II)-Table A. 32 shows the horizontal and vertical components of the design acceleration when dropped on the lid side corner (II)-Table A. 25.

(II)-Fig. A. 88 shows the relationships between the angle of dropping and the acceleration.

(II)-Table A. 32 Relationship between drop angle and acceleration for drop test I

Angle at dropping θ	Acceleration (G)		
	Acceleration (N)	Vertical component ($N \cdot \cos \theta$)	Horizontal component ($N \cdot \sin \theta$)
5	384.3	382.8	33.5
15	356.3	344.2	92.2
30	289.9	251.1	145.0
45	268.0	189.5	189.5
60	256.3	128.2	222.0
75	273.3	70.7	264.0
85	254.3	22.2	253.3



(II)-Fig. A. 88 Relationship between acceleration and drop angle for 9 m upper side inclined drop

(II)-Table A. 32 shows that each acceleration component is smaller than the acceleration recorded for the horizontal and vertical drop. Hence, stress is not analyzed here

A.6.1.5 Summary of the results

We will describe here what deformations occur on the package observed in the mechanical test (drop I). The analysis will evaluate the possibility of the inner shell being damaged.

(II)-Table A.33 shows the deformations in various drop tests.

(II)-Table A.33 Relationship between drop angle and acceleration for drop test II

Item Drop type		Analyzed part of shock absorber	Minimum thickness of shock absorber before deformation (mm)	Deformation in shock absorber (mm)	Remaining thickness of shock absorber (mm)	Design acceleration $\times g (m/s^2)$
Vertical drop		Lid side end	186	126.7	59.3	409.8
		Bottom side end	194	106.3	87.7	388.4
Horizontal drop		Cylindrical part	104	81.6	22.4	367.0
Corner drop		Lid side end	218.9	128.6	90.3	299.8
		Bottom side end	254.1	111.3	142.8	310.9
Inclined drop	5°	Lid side end	201.1	35.7	165.4	384.3
		Bottom side end	211.9	36.0	175.9	374.9
	15°	Lid side end	210.5	85.2	125.3	356.3
		Bottom side end	236.8	84.6	152.2	364.1
	30°	Lid side end	212.2	133.9	78.3	289.9
		Bottom side end	260.2	127.1	133.1	273.1
	45°	Lid side end	199.1	145.2	53.9	268.0
		Bottom side end	265.7	135.6	130.1	249.8
	60°	Lid side end	171.9	129.6	42.3	256.3
		Bottom side end	252.9	133.5	119.4	257.4
	75°	Lid side end	132.7	98.4	34.3	273.3
		Bottom side end	222.6	93.7	128.9	244.5
	85°	Lid side end	101.1	49.5	51.6	254.3
		Bottom side end	193.7	44.8	148.9	211.2

(II)-Table A.33 shows that deformation occurs only in parts of the shock absorber and does not reach the inner shell in a bottom side corner drop.

(II)-Tables A.26, A.27, A.28 and A.30 show that stress occurring on the packaging and content for each drop does not exceed the standard value, and therefore does not cause any damage to them.

Thus, the package do not affect the containments and shielding performance of the packaging.

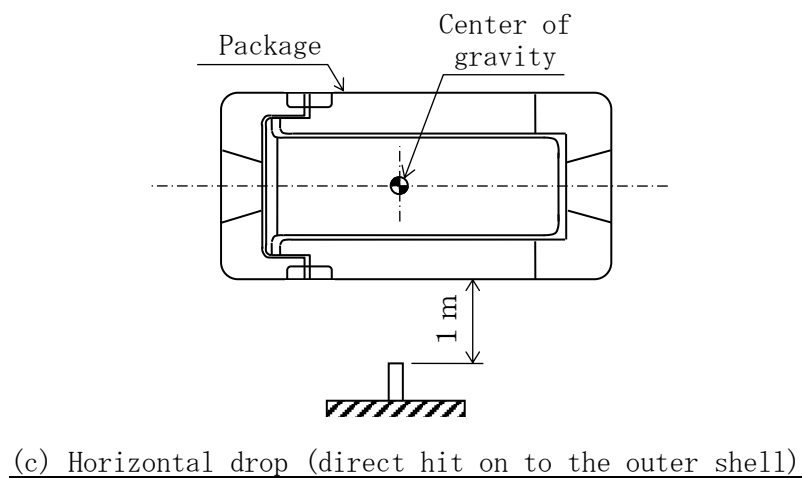
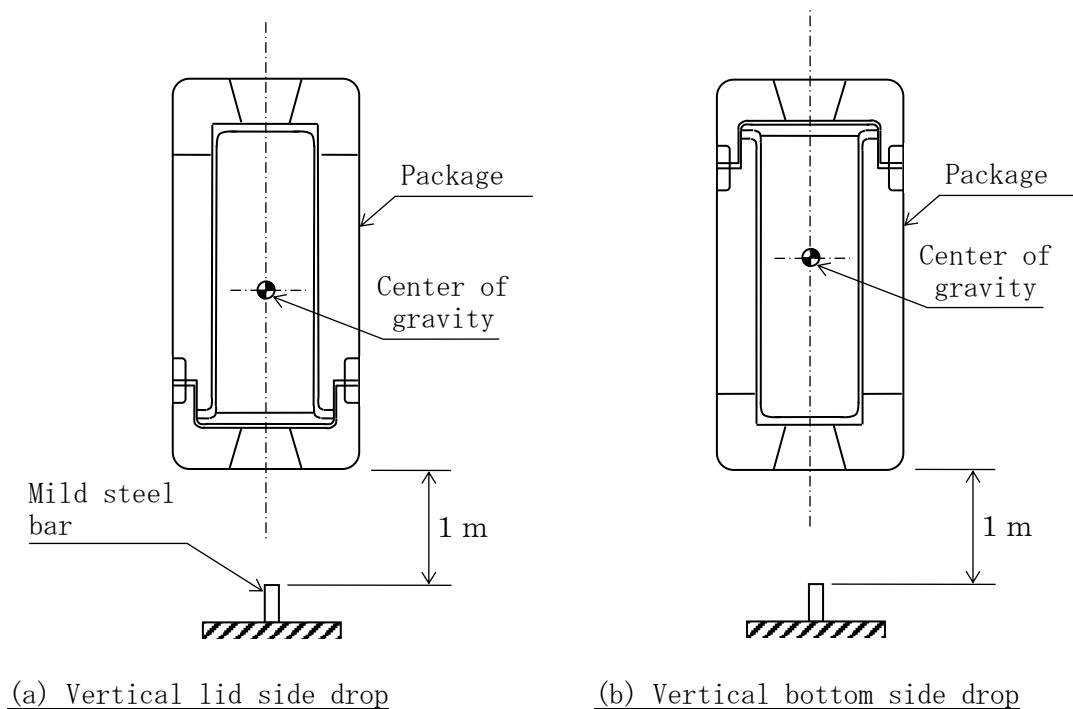
A.6.2 Mechanical test --- Drop test II (1 m drop)

In this section we will analyze the package on the assumption that drop test II is carried out after drop test I.

We will examine here how the package is affected when it is dropped from the height of one meter onto a mild steel cylinder with a diameter of 150 mm.

(II)-Fig.A.89 shows the package to be examined in this section for three different drops:

- (a) Vertical lid side drop (direct hit on to the outer lid)
- (b) Vertical bottom side drop (direct hit on to the outer shell bottom plate)
- (c) Horizontal drop (direct hit on to the outer shell).



(II)-Fig.A.89 Analytical model for drop test II

(1) Penetration

We will demonstrate in this section that the evaluated portions shown in (II)-Fig. A. 89 are not penetrated.

In the analyses, the contributions from the shock absorber and heat insulator under the outer shell is neglected on the assumption that the entire energy will be consumed in the transformation of the outer steel plate of the outer shell. Thus, the evaluation will ensure the maximum of safety.

(a) Direct hit of outer lid onto test cylinder (vertical drop) with the lid side end directed downwards.

(II)-Fig.A.82(a) shows the case of a direct hit of the outer lid onto the mild steel test cylinder, the dropping energy U_o of the package is obtained by the equation.

$$U_o = m \cdot g \cdot H$$

where

m : Weight of the package, $m = 950$ [kg]

H : Height from which the package is dropped, $H = 1000$ [mm]

g : Gravitational acceleration, $g = 9.81$ [m/s²]

Thus, U_o is,

$$U_o = 950 \times 9.81 \times 1000 = 9.32 \times 10^6 \text{ [N} \cdot \text{mm]}$$

The deformation (U) is obtained on the assumption that the dropping energy U_o is equal to the deforming energy U .

$$U = \sigma_s \cdot V$$

where

σ_s : Stress on the panel, $\sigma_s = 466$ [N/mm²]

V : Volume of panel deformed,

$$V = \{ \pi (d + t) t \} \delta \text{ [mm}^3\text{]}$$

d : Diameter of mild steel cylinder, $d = 150$ [mm]

t : Thickness of the panel, $t = 6$ [mm]

δ : Deformation [mm]

On the assumption that U_o is equal to U ,

$$9.32 \times 10^6 = 466 \times \{ \pi \cdot (150 + 6) \cdot 6 \} \cdot \delta$$

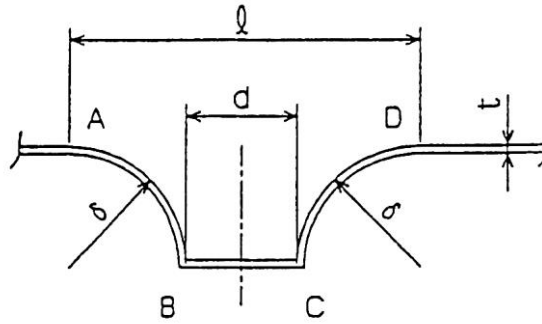
Hence,

$$\delta = 6.8 \text{ [mm]}$$

When the deformation of 126.7 mm caused in drop test I is added to the above value, we obtain 133.5 mm. As the minimum thickness before deformation of the heat insulator is 186 mm, its remaining thickness after deformation is 52.5 mm. Therefore, deformation does not reach the inner shell.

The strength of the outer lid panel is evaluated on the assumption that the deformational strain is smaller than the specified elongation of the material. Drop test II will not cause any penetration in the panel.

(II)-Fig. A. 90 shows an analytical model of the panel.



(II)-Fig. A. 90 Analytical model for penetration strength under conditions of drop test II

As (II)-Fig. A. 90 shows, the elongation (Δl) of the outer lid panel under the conditions of drop test II is obtained by the equation

$$\Delta l = l' - l$$

where

l' : Length of the panel after deformation,

$$l' = \left(2 \times \frac{\pi}{2} \delta + d \right) \text{ [mm]}$$

l : Length of the panel before deformation, $l = 2 \times \delta + d \text{ [mm]}$

δ : Deformation, $\delta = 6.8 \text{ [mm]}$

d : Diameter of the mild steel bar, $d = 150 \text{ [mm]}$

Therefore,

$$\Delta l = \left(2 \times \frac{\pi}{2} \cdot \delta + d \right) - (2 \cdot \delta + d) = 1.14 \cdot \delta$$

The strain ε in the case of such an elongation is

$$\varepsilon = \frac{\Delta l}{l} = \frac{1.14\delta}{2\delta + d} = \frac{1.14 \times 6.8}{2 \times 6.8 + 150} = 0.047$$

The strain in head plate is 4.7 (%). Because the outer lid head plate of type SUS 304 has a specified elongation of more than 40 % before penetration, no real penetration can occur.

(b) Direct hit of the outer shell bottom plate onto the mild steel bar
(Vertical drop, bottom side down)

As shown in (II)-Fig. A. 89 (b), the deformation δ produced when the bottom plate of the outer shell directly hits the mild steel bar, is 6.8mm because the thickness and materials of the bottom plate and head plate are the same as those described in the preceding section.

When the above value is added to the deformation value of 106.3 mm obtained in drop test I, 113.1 mm is obtained. As the minimum thickness of the heat insulator before deformation is 194 mm, its remaining thickness after deformation is 80.9 mm. Therefore, deformation does not reach the inner shell.

The strain is 4.7 %, the same as that described in the preceding section, and likewise, the elongation before penetration is 40 %. Therefore, no penetration occurs in the outer shell bottom plate.

(c) Direct hit of the outer shell on to mild steel bar (horizontal drop)

As (II)-Fig. A. 89(c) shows, the deformation δ which occurs when the outer shell directly hits the mild steel bar is obtained by the equation

$$U_o = \sigma_s \cdot \{ \pi (d + t) \cdot t \} \delta$$

Where

U_o : Dropping energy, $U_o = 9.32 \times 10^6$ [N/mm]

d : Diameter of the mild steel bar, $d = 150$ [mm]

t : Thickness of shell plate, $t = 3$ [mm]

σ_s : Deforming stress on the shell, $\sigma_s = 466$ [N/mm²]

Hence,

$$9.32 \times 10^6 = 466 \times \{ \pi (150 + 3) \times 3 \} \times \delta$$

$$\delta = 13.9 \text{ [mm]}$$

When the above value is added to the value of deformation 81.6 mm obtained in drop test I, 95.5 mm is obtained. As the remaining thickness of the heat insulator before deformation is 177 mm, its remaining thickness after deformation is 81.5 mm. Therefore, deformation does not reach the inner shell.

As in the preceding cases, the strain ε is obtained by the following equation.

$$\varepsilon = \frac{\Delta l}{l} = \frac{1.14\delta}{2\delta + d}$$

where

Δl : Elongation [mm]

l : Length before deformation [mm]

δ : Deformation, $\delta = 13.9$ [mm]

d : Diameter of the mild steel bar, $d = 150$ [mm]

Hence,

$$\varepsilon = \frac{1.14 \times 13.9}{2 \times 13.9 + 150} = 0.089$$

The strain in the shell sheet is 8.9 %. Because the outer lid head plate of type SUS304 has an elongation of more than 40 % before penetration, no real penetration can occur.

(2) Study of the packaging

The packages acceleration which occurs at the 1m drop will be obtained in this section.

(a) Lid side vertical drop

The acceleration, N , of the package which occurs when the outer lid directly hits the mild steel bar (see (II)-Fig. A. 89(a)) is obtained by using the analytical model (see (II)-Fig. A. 90) and the following equation,

$$N = \frac{F}{m} \quad [\text{m/s}^2]$$

where

F : Reaction force in the deformation of the panel,

$$F = \sigma_s \cdot \pi \cdot (d + t) \cdot t \quad [\text{N}]$$

σ_s : Deforming stress in the panel, $\sigma_s = 466 \text{ [N/mm}^2\text{]}$

d : Diameter of the mild steel bar, $d = 150 \text{ [mm]}$

t : Thickness of the panel, $t = 6 \text{ [mm]}$

m : Weight of the package, $m = 950 \text{ [kg]}$

Therefore, N is,

$$N = \frac{466 \times \pi \times (150 + 6) \times 6}{950} = 1442 = 147.0 \cdot g \text{ [m/s}^2\text{]}$$

(b) Bottom side vertical drop

The acceleration, N , of the package which occurs when the outer lids bottom plate directly hits the mild steel bar (see (II)-Fig. A. 89(b)) is $147.0 \cdot g$ because the thickness and material of the head plate is the same as those described in the preceding section.

(c) Horizontal drop

The acceleration, N , of the package which occurs when the outer shell directly hits the mild steel bar (see (II)-Fig. A. 89(c)) is obtained by using the analytical model (see (II)-Fig. A. 90) and the following equation,

$$N = \frac{F}{m} \text{ [m/s}^2\text{]}$$

where

F : Reaction force in the deformation of the panel,

$$F = \sigma_s \cdot \pi \cdot (d + t) \cdot t \text{ [N]}$$

σ_s : Deforming stress in the panel, $\sigma_s = 466 \text{ [N/mm}^2\text{]}$

d : Diameter of the mild steel bar, $d = 150 \text{ [mm]}$

t : Thickness of the panel, $t = 3 \text{ [mm]}$

m : Weight of the package, $m = 950 \text{ [kg]}$

Hence, N is

$$N = \frac{466 \times \pi \times (150 + 3) \times 3}{950} = 707 = 72.1 \cdot g \text{ [m/s}^2\text{]}$$

This result of the analysis is smaller than the design acceleration obtained in drop test I ((II)-Table A. 33 shows horizontal: $367.0 \cdot g$, vertical/lid side end: $409.8 \cdot g$; vertical/bottom side end: $388.4 \cdot g$). For this reason, stresses are not analyzed in this section.

A.6.2.1 Summary of the results

(II)-Table A.34 shows the results of the analyses and evaluation of drop test II/mechanical test.

(II)-Table A.34 Evaluation of penetration for drop test II

(1) Deformation

No.	Evaluated position	Minimum insulator thickness before deformation (mm)	Deformation in drop test I (mm)	Deformation in drop test II (mm)	Remaining thickness (mm)
1	Outer shell lid	186	126.7	6.8	52.5
2	Outer shell bottom plate	194	106.3	6.8	80.9
3	Frame of outer shell	177	81.6	13.9	81.5

(2) Deformed strain

No.	Evaluated position	Reference in analysis	Reference value in analysis	Result	Margin of safety
1	Outer shell lid	Rupture strain	40 %	4.7 %	7.51
2	Outer shell bottom plate	Rupture strain	40 %	4.7 %	7.51
3	Frame of outer shell	Rupture strain	40 %	8.9 %	3.49

(3) Acceleration

No.	Evaluated position	Reference in analysis	Reference value in analysis	Result	Margin of safety
1	Outer shell lid	Acceleration in drop test I	409.8 · g	147.0 · g	1.79
2	Outer shell bottom plate	Acceleration in drop test I	388.4 · g	147.0 · g	1.64
3	Frame of outer shell	Acceleration in drop test I	367.0 · g	72.1 · g	4.09

(II)- of the packaging and contents are not damaged because the acceleration Table A.34 shows that the deformed strain of different parts observed in drop test II is smaller than the reference elongation of SUS304. Therefore, no penetration occurs and the damage in this case does not reach the inner shell.

The acceleration occurring at drop test II is lower than that which occurs at drop test I.

Thus, dropping conditions that may cause maximum damage to the package do not affect the containment and shielding performance of the packaging.

The main body on is lower than that at drop test I.

A.6.3 Thermal test

A.6.3.1 Summary of temperatures and pressure

In this section, we will describe the outline of the temperatures and pressures to be used in the designing and analysis of the behavior of the package under accident test conditions.

(1) Design temperatures

The evaluation of (II)-B.5.3 revealed that the temperature rises up to 209.9°C in the fuel basket, 483.2°C in the inner shell and 187.8°C in the inner lid. Therefore, the design temperature under accident conditions is evaluated in the manner that contributes to ensuring the maximum safety as shown in (II)-Table A.35.

(II)-Table A.35 Design temperatures used for accident test condition

No.	Position	Temperature (°C)
1	Fuel basket	225
2	Inner shell	500
3	Inner lid	225

(2) Design pressure

As was evaluated in the section (II)-B.5.4, the pressure in the inner shell can rise up to 0.065 MPa (measured at the gauge). Hence, the design pressure in the package under accident test conditions is evaluated to achieve maximum safety on the assumption that a pressure difference of 0.0981 MPa·G occurs (see (II)-Table A.36).

(II)-Table A.36 Design pressure of package under accident condition

No.	Position	Design pressure
1	Inner shell inside	9.81×10^{-2} MPa

A.6.3.2 Thermal expansion

Stress due to the difference of thermal expansion between the inner surface of the inner shell and the outer surface of the fuel basket will be described here.

The temperature of fuel basket and the inner shell may rise to 225°C and 500°C respectively (see (II)-Table A.35).

However, stress is generated by difference of thermal expansion because the fuel basket is not fixed to the inner shell.

A.6.3.3 Comparison of allowable stresses

(1) Stress calculation

Stress generated on different parts of the package due to the design pressure will be analyzed for the same parts as those described in section A.5.1.3, using the same method.

In this analysis, the temperatures shown in (II)-Table A.35 will be used on the parts of the package.

(2) Displacement of the O-rings of inner lid

Displacement that can be generated at the O-rings due to the design pressure will be analyzed for the same parts as those described in section A.5.1.3(1) D , using the same method.

(3) Stress analysis and evaluation

(II)-Table A.37 shows the results of the stress analyses.

These results demonstrate that the integrity of the package can be maintained under accident test conditions (thermal test).

(II) -Table A.37 Stress analysis and evaluation under accident test conditions (thermal test)

Stress units
;N/mm²

No.	Position to be evaluated	Stress	Stress at initial clamping	Stress due to internal pressure	Stress due to thermal expansion	Primary stress					
						Pm(PL)	2/3Su	MS	PL+Pb	Su	MS
1	Frame of Inner shell	σ_r	—	-0.0491	—	2.36	258	108	—	—	—
		σ_θ		2.31	—						
		σ_z		1.15	—						
2	Bottom plate of inner shell	Inner Surface	—	3.18	—	0.098	258	2631	3.28	387	116
				0.953	—						
				-0.098	—						
		Outer Surface	—	-3.18	—	0	258	—	3.18	387	120
				-0.953	—						
				0	—						
3	Inner shell lid	Inner Surface	—	-3.27	—	0.098	2/3 Sy 408	4162	3.17	Sy 612	192
				-3.27	—						
				-0.098	—						
		Outer Surface	—	3.27	—	0	2/3 Sy 408	—	3.27	Sy 612	186
				3.27	—						
				0	—						
4	Inner shell lid clamping bolt	σ_t	174	3.22		177	2/3 Sy 408	1.30	—	—	—
5	Displacement of the inner lid O-ring	Interior : 1) Displacement $\mu = 1.29 \times 10^{-2}$ mm 2) Initial clamping value of the O-ring $\delta = 1.1$ mm 3) Remaining height of O-rings $\Delta l = \delta - \mu \approx 1.087$ mm									

Pm; General primary membrane stress; PL; Local primary membrane stress; Pb; Primary bending stress;

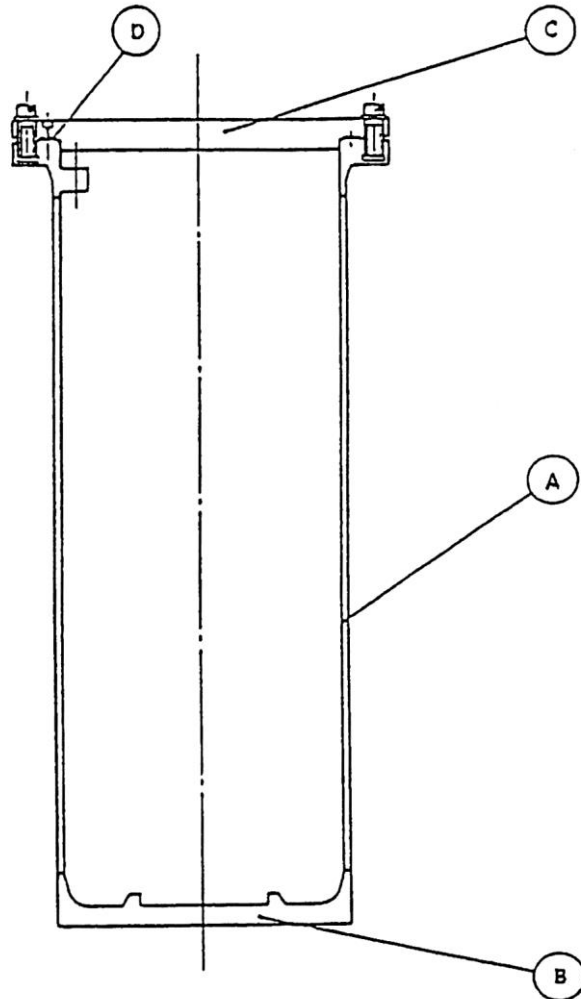
Sy; Yield point of the design; Su; Design tensile strength; MS; Margin of safety σ_r ; Diameter direction stress σ_θ ; Periphery direction stress σ_z ; Axial stress σ_t ; Ability of bolt stress

A.6.4 Water immersion

In this section we will demonstrate that when immersed 15 m under water, the package can sufficiently endure the external pressure of 147 kPa.

We supposed here that the inner shell is subjected to this pressure. (II)-Fig A.91 shows the parts evaluated for stress.

Since the radioactivity of this package will not exceed 10^5 times A_2 , then water immersion test is not required.



Symbol	Evaluated position
Ⓐ	Frame of inner shell
Ⓑ	Bottom plate of inner shell
Ⓒ	Inner shell lid
Ⓓ	Displacement of O-rings on inner shell lid

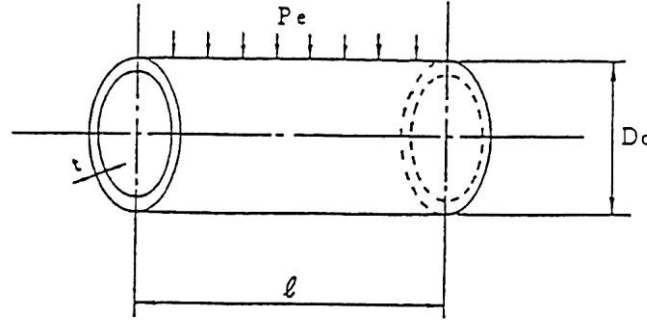
(II)-Fig A.91 Stress evaluation position of inner shell for 15 m immersion test

Ⓐ Frame of inner shell

The frame of inner shell suffering external pressure is evaluated for its buckling and for the stress that may occur at its center.

(a) Buckling

(II)-Fig. A. 92 Analytical model shows the permissible buckling pressure for the frame of inner shell under external pressure.



(II)-Fig. A. 92 Analytical model of allowable buckling pressure for frame of inner shell

The allowable buckling pressure P_e ((II)-Fig. A. 92) for the frame of inner shell is obtained by the following equation ^[1]

The formula and figure for finding the respective allowable buckling stress P_e are applied also to the current, appropriate source.

$$P_e = \frac{4B \cdot t}{2D_o}$$

where

P_e : Allowable buckling pressure [MPa]

D_o : Outer diameter of inner shell, $D_o = 480$ [mm]

t : Wall thickness of frame of inner shell, $t = 10$ [mm]

B : Factor obtained from (II)-Fig. A. 93, $B = 650$

l : Length of the inner shell, $l = 1324$ [mm]

Hence,

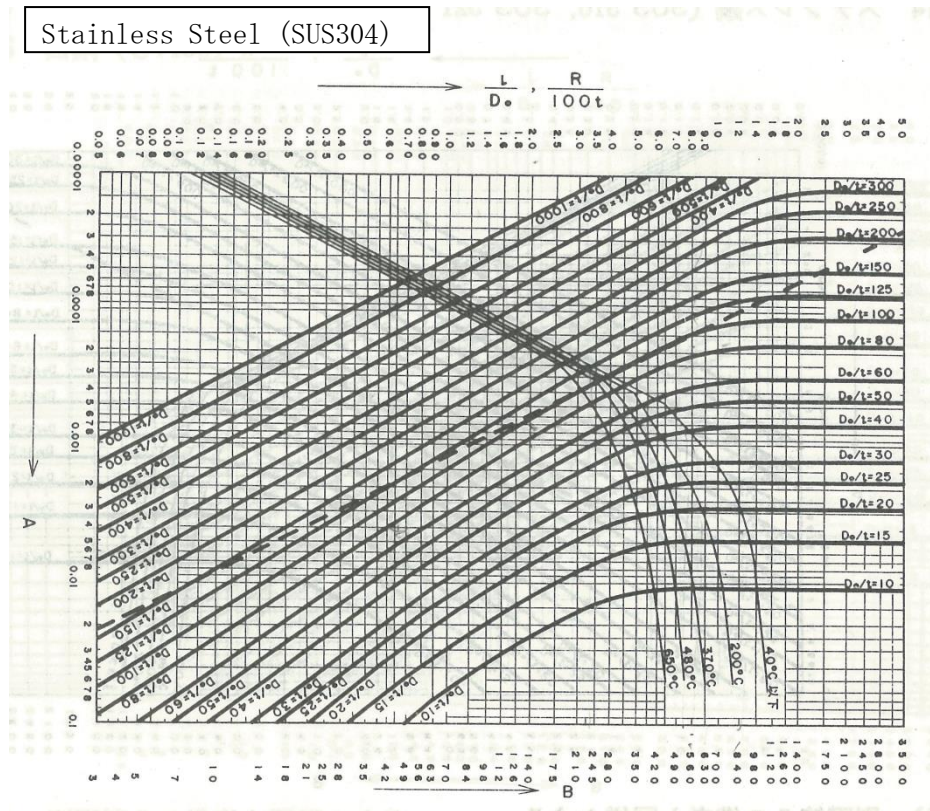
$$P_e = \frac{4 \times 650 \times 10 \times 9.81}{3 \times 480 \times 100} = 1.17 \text{ [MPa]}$$

$$= 2.86 \text{ [MPa]}$$

Therefore, the margin of safety MS for the external pressure $P = 0.147$ MPa which the frame of inner shell suffers is,

$$MS = \frac{P_e}{P} - 1 = \frac{1.77}{0.147} - 1 = 11.0$$

Hence, the inner shell does not buckle under external pressure.



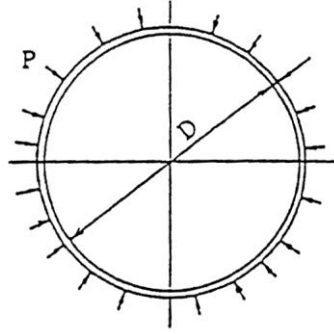
(Remarks)

1. The intermediate value shall be obtained by proportional calculation.
2. The way of application of this figure shall be given in the following,
 «In case of the cylinder shape subjected to a pressure on the outer surface»
 - (1) Take a value, $1/D_o$, on the axis of ordinates.
 - (2) Calculate the value, D_o/t , assuming the thickness, t , of the plate to be used.
 - (3) Draw a horizontal line from the point responding to $1/D_o$ and obtain the crossing point of the horizontal line with the curve responding to D_o/t .
 - (4) Draw a vertical line through the crossing point obtained in (c), and obtain the crossing point of the vertical line with the curve corresponding to the operating temperature.
 - (5) Draw a horizontal line from the crossing point obtain in (d), obtaining B which is the crossing point of the said horizontal line with the axis of ordinates.

(II)-Fig.A. 93 Curve representing buckling behavior factor of inner shell under external pressure

(b) Center of inner shell

(II)-Fig. A. 94 shows an analytical model for the stresses occurring at the center of the inner shell under external pressure. The stress σ that may occur at the center of the inner shell is supposed to be a thin cylindrical wall and is obtained by the following equation.



(II)-Fig. A. 94 Stress analysis model of center of inner shell

$$\sigma_{\theta} = - \frac{P \cdot D_m}{2t}$$

$$\sigma_z = - \frac{P \cdot D_m}{4t}$$

$$\sigma_r = - \frac{P}{2}$$

where

σ_{θ} : Circumferential stress [N/mm²]

σ_z : Axial stress [N/mm²]

σ_r : Radial stress [N/mm²]

P: External pressure, P = 0.147 [MPa]

D_m: Average diameter of frame of inner shell,

$$D_m = D + t = 460 + 10 = 470 \text{ [mm]}$$

t: Wall thickness of frame of inner shell, t = 10.0 [mm]

D: Inner diameter of frame of inner shell, D = 460 [mm]

Hence, the following values are obtained.

$$\sigma_{\theta} = - \frac{0.147 \times 470}{2 \times 10} = -3.45 \text{ [N/mm}^2\text{]}$$

$$\sigma_z = - \frac{0.147 \times 470}{4 \times 10} = -1.73 \text{ [N/mm}^2\text{]}$$

$$\sigma_r = -0.0735 \text{ [N/mm}^2\text{]}$$

Ⓑ Bottom plate of inner shell

(II)-Fig.A.95 Analytical model shows the stresses on the bottom plate of the inner shell under external pressure.

Assuming that the bottom plate of the inner shell is a disk fixed on its circumference, the stress σ on this fixed part is,

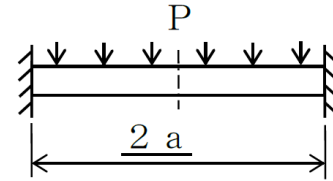
$$\sigma_\theta = \pm 0.225 \frac{P \cdot a^2}{h^2}$$

$$\sigma_r = \pm 0.75 \frac{P \cdot a^2}{h^2}$$

$$\sigma_z = -P \text{ (outer surface)}$$

The outside

The inside



(II)-Fig.A.95 Stress analysis model of bottom plate of inner shell

where

σ_θ : Circumferential stress [N/mm²]

σ_r : Radial stress [N/mm²]

σ_z : Axial stress [N/mm²]

P: External pressure, P = 0.147 [MPa]

a: Diameter of the bottom plate of inner shell, a = 230 [mm]

h: Wall thickness of the bottom plate of inner shell, h = 35 [mm]

Hence,

$$\sigma_\theta = \pm 0.225 \frac{0.147 \times 230^2}{35^2} = \pm 1.428 \text{ [N/mm}^2\text{]}$$

$$\sigma_r = \pm 0.75 \frac{0.147 \times 230^2}{35^2} = \pm 4.76 \text{ [N/mm}^2\text{]}$$

$$\sigma_z = -0.147 \text{ (outer surface) [N/mm}^2\text{]}$$

For the double sign of the stress value, the upper sign (-) corresponds to the inner surface and the lower sign (+) to the outer surface respectively.

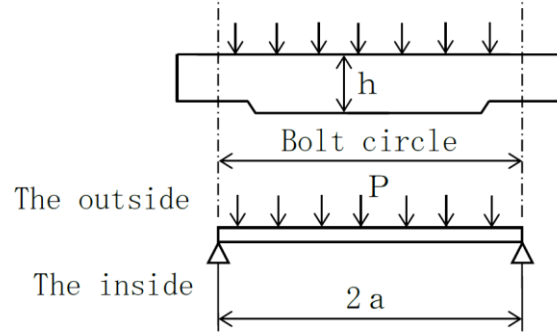
© Inner lid

(II)-Fig.A. 96 Analytical model shows the stresses that may occur on the inner lid under external pressure.

The stress σ [N/mm²] that may occur on the disk supported on its circumference is at a maximum in the center (see (II)-Fig.A. 96) and is obtained as follows.

$$\sigma_{\theta} = \sigma_r = \mp 1.24 \frac{P \cdot a^2}{h^2}$$

$$\sigma_z = -P \text{ (outer surface)}$$



(II)-Fig.A. 96 Stress analysis model of center of inner lid

where

σ_{θ} : Circumferential stress [N/mm²]

σ_r : Radial stress [N/mm²]

σ_z : Axial stress [N/mm²]

P: External pressure, P = 0.147 [MPa]

a: Diameter of the bottom plate of inner shell, a = 285 [mm]

h: Wall thickness of the bottom plate of inner shell, h = 55 [mm]

Hence,

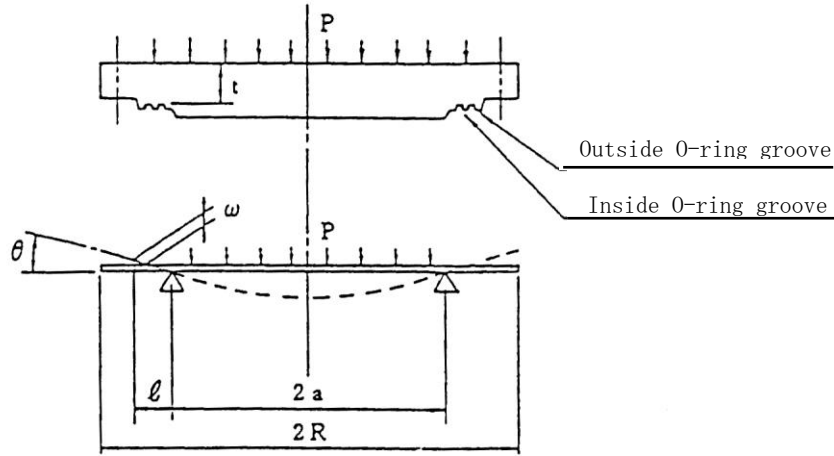
$$\sigma_{\theta} = \sigma_r = \mp 1.24 \frac{0.147 \times 285^2}{55^2} = \mp 4.89 \text{ [N/mm}^2\text{]}$$

$$\sigma_z = -0.147 \text{ (outer surface) [N/mm}^2\text{]}$$

For the double sign of the stress value, the upper sign (-) corresponds to the inner surface and lower sign (+) to the outer surface respectively.

① Displacement of the O-rings of inner lid

(II)-Fig.A. 97 Analytical model shows the displacement of the O-rings on the inner lid under external pressure.



(II)-Fig.A. 97 Displacement analysis model of O-rings of inner lid under external pressure

The outer O-ring is at a distance of l from the supporting point of the disk suffering the uniform load. Its displacement ω is obtained as follows:

$$\omega = \theta \cdot l = \frac{P \cdot \alpha \cdot a^3}{8D \cdot (1 + \nu)} \times l \quad [\text{mm}]$$

where

ω : Displacement of the outer O-ring [mm]

θ : Angle of deflection at supporting point [rad];

$$\theta = \frac{P \cdot \alpha \cdot a^3}{8D \cdot (1 + \nu)}$$

P: External pressure, $P = 0.147$ [MPa]

α : Factor of safety, $\alpha = (R/a)^2$

a : Distance from the center of inner lid to the supporting point,

$a = 230$ [mm]

R : Radius of the inner lid, $R = 310$ [mm]

D : Bending stiffness,

$$D = \frac{E \cdot t^3}{12(1 - \nu^2)} \quad [\text{N} \cdot \text{mm}]$$

E : Longitudinal elastic modulus of the inner lid, $E = 1.92 \times 10^5$ [N/mm²]

t : Minimum wall thickness of the inner lid, $t = 36.7$ [mm]

ν : Poisson's ratio, $\nu = 0.3$

l : Distance from the supporting point to the outer O-ring, $l = 30.1$ [mm]

Hence, the displacement of the outer O-ring is

$$\begin{aligned}\omega &= \frac{0.147 \times (310/230)^2 \times 230^3 \times 12 \times (1 - 0.3^2)}{8 \times 1.92 \times 10^5 \times 36.7^3 \times (1 + 0.3)} \times 30.1 \\ &= 0.0108 \quad [\text{mm}]\end{aligned}$$

This value is far smaller than the initial clamping value of the O-ring ($\delta = 1.1 \text{ mm}$). For this reason, the packaging cannot be adversely affected when exposed to external pressure.

(II)-Table A.38 shows the test results of items (A) to (D).

(II)-Table A.38 Stresses evaluated for 15 m water immersion test

Stress Position		Stress	Primary stress						
			P _m (PL)	2/3 S _u	M _s	P _l +P _b	S _u	M _s	
Center of inner shell		σ_r	-0.0735	3.38	310	91.7	—	—	—
		σ_θ	-3.45						
		σ_z	-1.73						
Bottom plate of inner shell	Inner Surface	σ_r	0.147	310	2107	4.91	466	93.9	
		σ_θ							-1.428
		σ_z							0
	Outer Surface	σ_r							4.76
		σ_θ							1.428
		σ_z							-0.147
Inner lid	Inner Surface	σ_r	0.147	2/3 S _y 458	3114	4.89	S _y 687	139	
		σ_θ							4.89
		σ_z							0
	Outer Surface	σ_r							-4.89
		σ_θ							-4.89
		σ_z							-0.147
									Buckling of the inner shell
Displacement of O-rings on inner lid		—	-Displacement of outer O-ring ω = 0.0108 mm -Initial clamping value of O-rings δ = 1.1mm						

Note. Stress and stress intensity units: N/mm^2

These figures show that the package can maintain the integrity for its containment.

A.6.5 Summary of result and evaluation

The tests under accident conditions were examined by analytical methods. The results of the mechanical test (drop test I) revealed that only the outer shell suffered deformation.

The results of the mechanical test (drop test II) revealed that only the outer shell suffered local deformation.

In addition, the stress that occurs on each part of the inner shell does not exceed the allowable value, so the containment interface, suffering no damage, is not adversely affected.

In the thermal test, the stress that occurs on each part of the inner shell does not exceed the allowable value, so the containment interface, suffering no damage, is not adversely affected.

In the water immersion test, the inner shell can endure an external pressure of 147 KPa and maintain its soundness. Further, the fuel elements will never get fractured in the strength test, and the stress generated is not more than the allowable value.

The results of the evaluation of the outer shell, inner shell and content will be used for

(B) Thermal analysis, (C) Containment analysis, (D) Shielding analysis, and (E) Criticality analysis.

In the (B) Thermal analysis, (C) Containment analysis, (D) Shielding analysis, and (E) Criticality analysis, the results of the (A) Structural analysis were taken into consideration as follows.

(1) Thermal analysis

Those parts of the packaging which are essential to the thermal analysis are represented by the inner shell and inner lid.

The inner lid is covered with the outer lid.

In the structural analysis, the deformation of the lid side shock absorber is 126.7 mm at the vertical drop and 81.6 mm at the horizontal drop, while the thickness before deformation of the material is respectively 186 mm and 104 mm. So the deformation does not occur in the inner shell.

No penetration occurs in the outer shell at drop test II.

The outer lid does not come off, sufficiently maintaining its functions as

a heat insulator.

We therefore suppose that in the thermal analysis, the inner shell is not damaged, and that the remaining thickness of the heat insulator and the shock absorber are determined to ensure the maximum in safety.

(2) Containment analysis

In the structural analysis, both the containment system of the packaging and the fuel elements suffer no damage and maintain their integrity.

In the containment analysis, the results are used to evaluate the leakage of radioactive material.

(3) Shielding analysis

In the shielding analysis, damage of either the outer shell, inner shell or fuel elements will influence the results.

In the structural analysis, the thickness of the lid side and bottom side shock absorber is 186 mm in the axial direction and 104 mm in the radial direction. Thus, deformation does not reach the inner shell and the packaging maintains its integrity.

In drop test II, the outer shell is locally deformed, but the inner shell is not deformed.

Thus, in the shielding analysis we supposed that the inner shell would not be deformed, and, in order to ensure the maximum in safety, that the package has no outer shell, no heat insulator, and no shock absorbers.

(4) Criticality analysis

As in the case of the shielding analysis, we supposed here that the inner shell would not be deformed, and, in order to ensure the maximum in safety, that the package has no outer shell, no heat insulator, and no shock absorbers.

A.7 Reinforced immersion test

The maximum quantity of radioactivity of these transported articles is less than 100,000 times of the A2 level, which is not considered relevant.

A.8 Radioactive content

The fuel element, the radioactive content in the package consists of laminated fuel plates supported by the side plates on its ends (see (I)-Fig.D.1). The fuel is located between aluminum alloy plates.

The specifications of the fuel element are shown in (I)-Table D.

Structural analyses of the fuel elements are carried out under normal and accident test conditions on the assumption that they will suffer the same impact acceleration as that in the transport packaging. Therefore, the stress generated in any of the fuel elements is not more than the allowable stress under general and specific testing conditions, so that the fuel element are free from getting fractured.

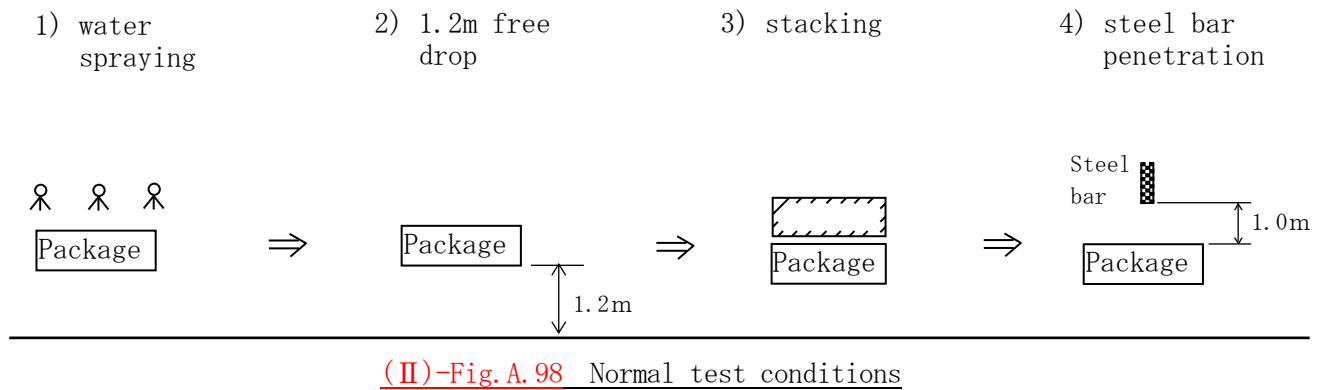
A.9 Fissile package

This package, under the category of the fissile package in the Regulations, is used at an ambient temperature of more than -40°C . It is very unlikely that the package, as described in A.4.2, will be damaged or cracked at operating temperatures between -40°C and 38°C .

Therefore, here is analyzed the damage of the package under the following test conditions, which is assumed for criticality analysis in (II)-E Criticality Analysis.

A.9.1 Normal test conditions

In consideration of (II) E Criticality Analysis, damage of the package is analyzed on the results of A.5 and A.9.2 as show in (II)-Fig.A.98.



A 9.1.1 Continuous test

(1) Water spray

The same as A 5.2, there is no damage to the package.

(2) 1.2m free drop(1.2m drop)

The same as the normal test conditions for the B(U) type package, there is no damage to the inner cell of criticality system as described in A 5.3

A 9.1.2 Stacking test

The same as A 5.4 there is no damage to the inner cell of criticality model.

A9.1.3 Penetration test

The same as A 5.5, there is no damage to the inner cell of criticality model. With the results above, the damages of the package are summarized as shown in (II)-Table A.39. This package, as shown in (II)-Table A40, meets the requirements for the fissile package under the normal tests conditions stipulated by the regulation and the notification.

(II)-Table A 39 Damages of the fissile package under the normal test conditions

Test conditions	Damage to the package	Note
Water spray	No damage	=====
1.2m drop	Deformation of outer shell, shock absorber and heat insulator	Outer shell, shock absorber and heat insulator are neglected in criticality analysis. Eye-plate has possibility to be deformed, but it is neglected in criticality analysis. Acceleration, stress at each part of the package, etc. do not exceed the value of 9m drop test respectively.
Stacking	No damage	=====
6kg penetration	No damage	=====

(II)-Table A40 Compliance with requirements for fissile package under normal test conditions

Requirements for fissile package	Evaluation
The structure should not be made a dent which contains a cube of 10cm.	The outer shell, shock absorber and heat insulator are deformed, but the deformation of inner shell, constituting criticality system, is not deformed with a dent which contains a cube of 10cm.
The package shall preserve the minimum overall outside dimensions of the package to at least 10cm.	The external dimensions of the inner shell, which is a system subject to criticality assessment, are 48 cm in outer diameter and 140 cm in length, and each side of the circumscribed rectangular solid is 10 cm or more.

A.9.2 Special test conditions for fissionable transported articles

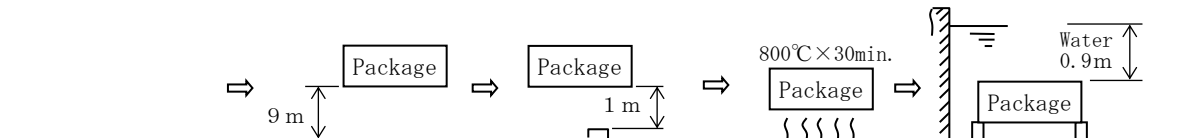
The accident test conditions for the fissile packages are given as the testing procedures shown in (II)-Fig. A. 99, as A and B, i.e.,

- | | |
|---|--|
| { | <p>A The damage incurred under normal test conditions and composite effect caused by the different tests including 9 m drop, 1 m penetration, fire test (800°C for 30 minutes) and 0.9 m immersion.</p> <p>B The damage incurred under normal test conditions and 15 m immersion test.</p> |
|---|--|

Among the above given A and B, the safety evaluation is to be executed under the condition A, in which the composite effect is taken into account considering 9 m drop test which is presumed having significant effect on the critical system and the fire test where the shock absorber burns out and adjacent packages come to be placed closer to each other.

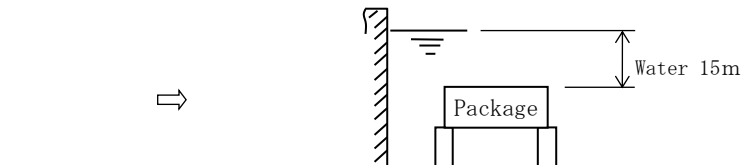
[a]

- | | | | | |
|--|-----------------------|------------------------|---------------------|--------------------------------|
| <p>1) Normal test conditions
(A. 9. 1)</p> | <p>2) Drop test I</p> | <p>3) Drop test II</p> | <p>4) Fire test</p> | <p>5) Water immersion test</p> |
|--|-----------------------|------------------------|---------------------|--------------------------------|



[b]

- | | |
|--|--------------------------|
| <p>1) Normal test conditions
(A. 9. 1)</p> | <p>2) Immersion test</p> |
|--|--------------------------|



(II)-Fig. A. 99 Accident test condition

Here is employed as normal test conditions a continuous test accompanying damage, as shown in (II)-Table A 39.

In consideration of criticality analysis in (II) E, damage affected package is evaluated as follows.

1. Continuous test of normal test conditions

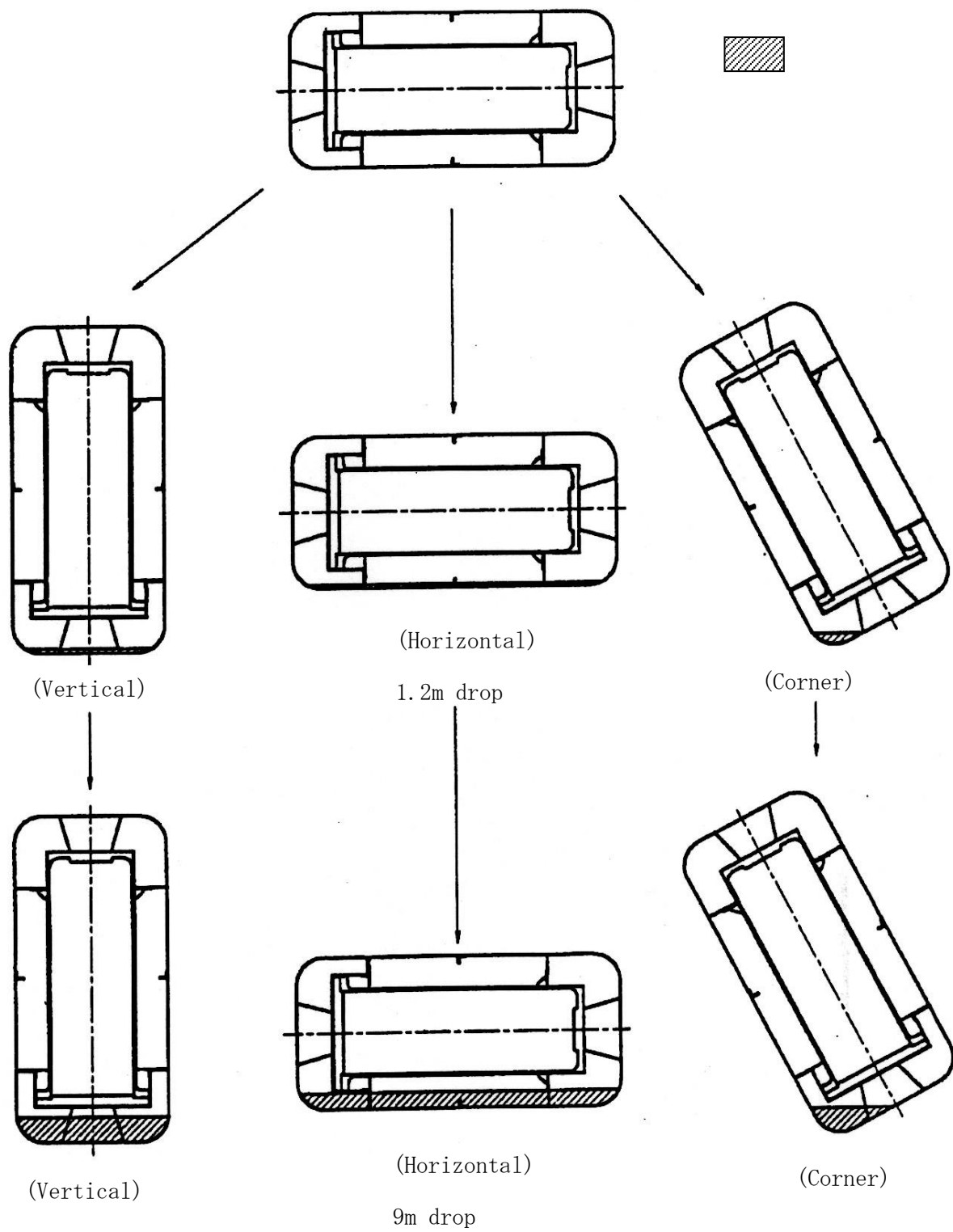
Damage of the package under the mentioned test conditions is as shown in (II)-Table 39.

2. drop test(9m)

- (1) Dropping attitude and the order of the drop test

Dropping attitude and the order of the drop test are given in (II)-Fig. A. 100.

In case the dropping directions of 1.2m drop and 9m drop test are the same, deformation of the shock absorber will be considered the greatest, and thus here is considered that case.



(II)-Fig. A.100 Drop attitude and test order

(2) Deformations and design accelerations

Deformations and design accelerations of the fissile package produced in the drop test I (1.2m drop test and the consecutive 9m drop test) for fissile package are analyzed by the method described in section A.5.3.

(II)-Table A.41 shows the results of the analyses.

(II)-Table A.41 Deformations and design accelerations of shock absorber under accident test conditions (combined evaluation)

Drop height	Acceleration and Deformation Drop attitude		Acceleration (g)			Deformation (mm)	Rate of acceleration to design acceleration due to drop test I (9m drop only)
			CASH- II $\times 1.2$	Steel plate acceleration	Design acceleration		
*9m	Horizontal		206.2	172.8	379.0	88.8	1.033
	Vertical	Upper Portion	161.8	284.4	446.2	136.6	1.089
		Lower portion	131.4	276.2	407.6	117.6	1.049
	Corner	Upper Portion	85.6	238.2	323.8	133.9	1.080
		Lower Portion	87.1	245.2	332.3	115.7	1.069

*1: 9 m drop is evaluated by considering the deformation by 1.2 m drop.

(3) Evaluation of damages of the package

Design acceleration of the drop test for the fissile package, as shown in (II)-Table A.41, increases by 9% at the maximum in comparison with that of the drop test 1 for the B(U) fissile package. Among the structural evaluation results of drop test 1 of the fissile package, the part of the smallest safety margin is an inner shell lid fastening bolt on the vertical drop, as shown in (II)-Table A. 27. The safety margin is 0.404 or 40.4%.

In structural evaluation of the package, the increasing rate of acceleration is the same as that of the generated stress. Even when the design acceleration and the generated stress increases by 9%, the smallest safety margin is 0.348, which shows that the structural integrity of the packaging and its contents is maintained.

3. 1m penetration test

In the drop test of A 9.2.1 and A 9.2.2 above, the outer shell, shock absorber and heat insulator are deformed, but these are not related to evaluation of 1m penetration test, as shown in A 6.2. Therefore, the damage of the package on the present test will be the same as the results in A 6.2(See the summary A 6.2).

4. Thermal test

In the thermal test, deformation of outer shell, shock absorber and heat insulator is taken into account, but effect of their deformation is considered negligible. Thus, damage evaluation of the package under this test will be the same as A 6.3.3(3).

5. Immersion test(0.9m)

As proved by 15m immersion test, the package damage in 0.9m immersion test will not expand.

6. Summary of the package damage

Summary of damage to the package under special test conditions is described here.

(II)-Table A. 42 Damage of the fissile package under special test conditions

Conditions	Damage of the package	Notes
drop(9m)	Deformation of outer shell, shock absorber and heat insulator	Outer shell, shock absorber and heat insulator are neglected in criticality analysis.
Penetration(1m)	Deformation of outer shell, shock absorber and heat insulator	Outer shell, shock absorber and heat insulator are neglected in criticality analysis.
Thermal test(fire)	Partly damaged by a fire Rise in temperature for each part	In criticality analysis, heat insulator is neglected and water density is set at 1.0g/cm ³
Immersion(0.9m)	No damage	In criticality analysis, assessed for the package filled with water

A.10 Appendix

A.10.1	Analysis program for absorbing performance of shock Absorber : CASH-II”	(II)-A-276
A.10.2	Validity of the free drop analyses of JRF-90Y-950K package	(II)-A-282
A.10.3	Displacement of inner lid O-rings	(II)-A-283
A.10.4	Stress/strain characteristics of the shock absorber at low temperatures	(II)-A-288
A.10.5	Stress/strain characteristics of hard polyurethane foam	(II)-A-289
A.10.6	Low temperatures strength of SUS 304	(II)-A-290
A.10.7	Low temperature impact value of SUS 304	(II)-A-291
A.10.8	Low temperature impact value of SUS 630/H1150	(II)-A-292
A.10.9	Method for calculating the torque of inner lid clamping bolt	(II)-A-293
A.10.10	Mechanical characteristics of JRR-4B fuel plate	(II)-A-299
A.10.11	Literature	(II)-A-301

A.10.1 Analysis program for the absorbing performance of shock absorber :

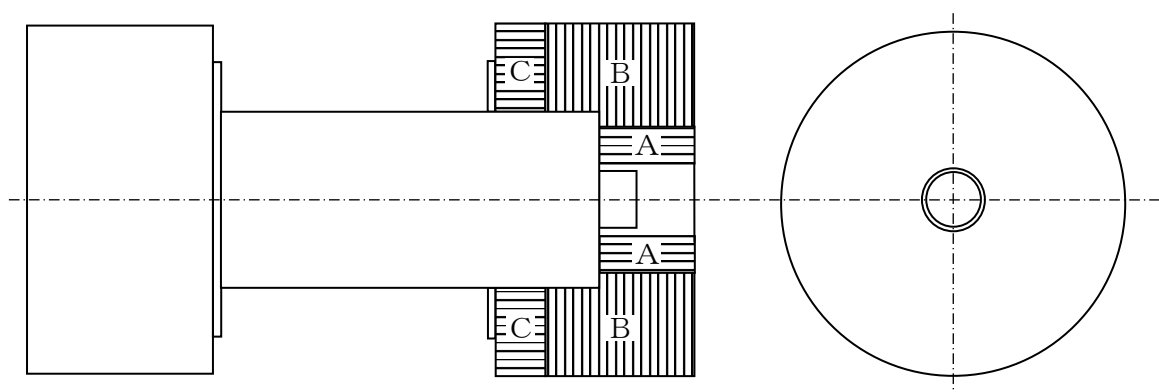
“CASH- II”

(1) General

“CASH- II” is a calculation code which is used to analyze the shock absorber by an uniaxial displacement method (U.D.M) when the package equipped with shock absorber on its top and bottom is dropped.

The deformation, the energy absorbed, and the impact force (acceleration and g value) occurring in the package when dropped with various postures (vertical, horizontal, and inclined).

As shown in [\(II\)-Fig.A.101](#), this code can be applied to shock absorbers consisting of areas (called “material areas”) of different mechanical characteristics (stress/strain relationships).



A, B, and C represent material areas.

[\(II\)-Fig.A.101](#) Analytical model of shock absorber

(2) Analysis theory

The “CASH- II” code is a program for analyzing the impact performance of the packages shock absorber in various inclined drop tests (inclination $\theta = 0$ degrees: vertical drop, inclination $\theta = 90$ degrees: horizontal drop) in a uniaxial displacement method (U.D.M.) which is based on the following two basic principles.

- a) Energy absorbing characteristics are analyzed by a U.D.M. ;

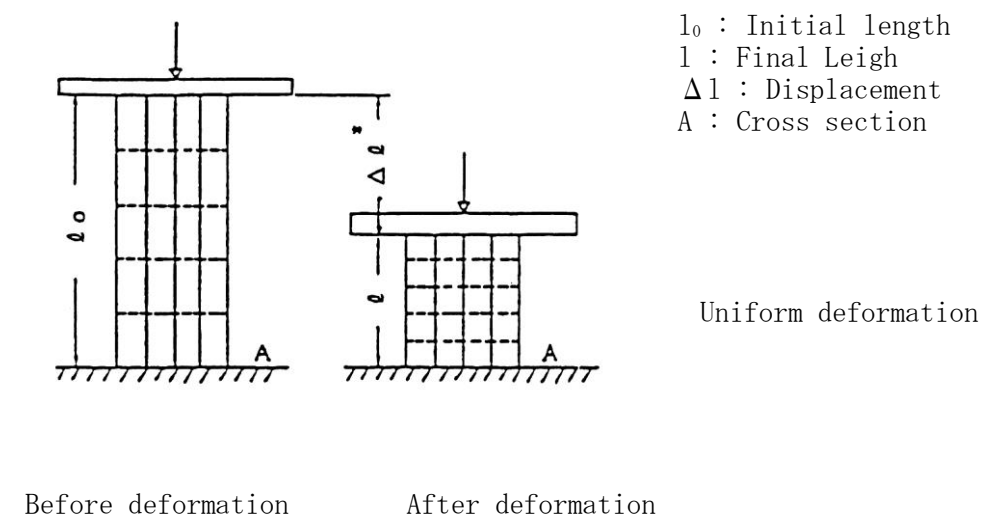
b) Uniaxial bars with inclined orientation is replaced with an equivalent couple of uniaxial bars of horizontal and vertical orientation.

The analysis theory of the “CASH-II” code based on these principles is described below.

a) Uniaxial displacement method (U.D.M.)

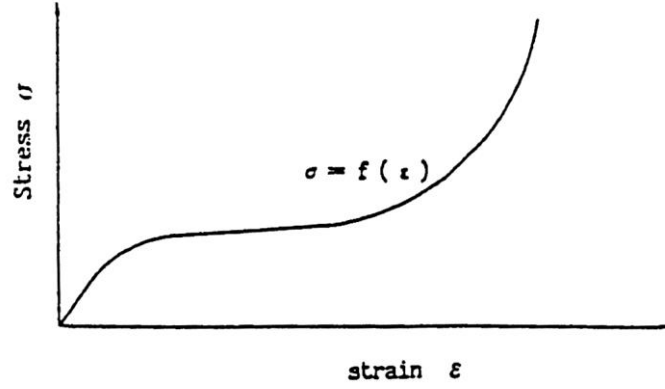
This is a theory which assumes that each area subject to deformation absorbs the deforming energy in a uniform and uniaxial manner. Areas subject to deformation such as shock absorber are replaced with a number of uniaxial bars. The energy absorbing characteristics of the entire shock absorber is evaluated on the basis of the energy absorbing characteristics of the uniaxial bars.

We will consider here a case where a mass which weighs W and has an energy E_0 hits the structure shown in (II)-Fig. A. 102.



(II)-Fig. A. 102 Analytical model by uniaxial displacement method

The compressive stress/strain relationship of the structure is supposed to appear as shown in [\(II\)-Fig. A. 103](#)



[\(II\)-Fig. A. 103](#) Compressive stress/strain relationship of material

The deformation Δl of the structure and the acceleration a which occurs in the mass are obtained as follows.

The strain ε that is generated when a structure suffers a Δl deformation is,

$$\varepsilon = \Delta l / l_0 \quad (\text{A. 10-1})$$

The stress σ is,

$$\sigma = f(\varepsilon) = f(\Delta l / l_0) \quad (\text{A. 10-2})$$

Hence, the force F that occurs when the structure suffers a Δl deformation is,

$$F = A \sigma = A \times f(\Delta l / l_0) \quad (\text{A. 10-3})$$

The energy E that is absorbed by the structure when it suffers a Δl deformation is,

$$E = \int_0^{\Delta l} F dl = l_0 \cdot \int_0^{\Delta l / l_0} A \sigma(\varepsilon) d\varepsilon \quad (\text{A. 10-4})$$

When the energy E_0 that the structure has to absorb is given, the final deformation Δl^* is determined using formula A. 10-4,

$$E_0 = l_0 \cdot \int_0^{\Delta l^* / l_0} A \sigma(\varepsilon) d\varepsilon \quad (\text{A. 10-5})$$

When Δl^* is substituted in formula(A.10-3), we obtain as follows,

$$F^* = A f(\Delta l^* / l_0) \quad (\text{A. 10-6})$$

Therefore, the acceleration a^* is,

$$a^* = F^* / W \quad (\text{A. 10-7})$$

b) Uniaxial bar with inclined orientation

We will describe in this section how to handle the uniaxial bars inclined orientation based on a uniaxial displacement method.

Calling θ the inclined drop angle, we suppose that the following equation is valid among the stresses with inclined direction σ_θ , vertical σ_z and horizontal direction σ_x for the same strain ε ,

$$\sigma_\theta(\varepsilon) = \sigma_z(\varepsilon) \cos^m \theta + \sigma_x(\varepsilon) \sin^m \theta \quad (\text{A.10-8})$$

Where m is the constant for inclination of the material.

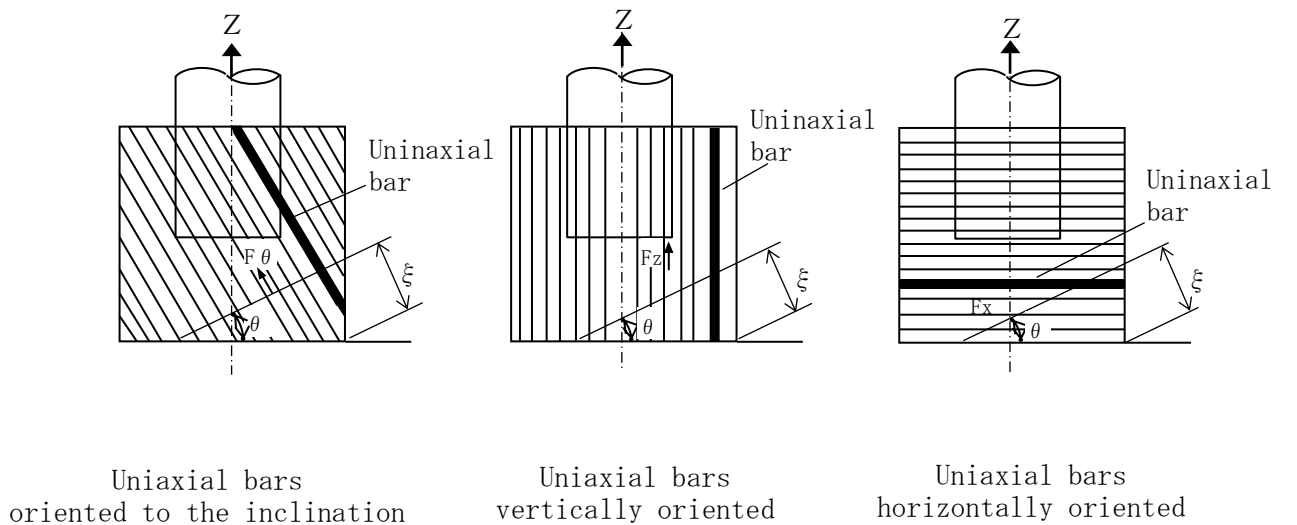
In this case, there is approximately the following relationship between E_θ , E_z , and E_x ,

$$E_\theta = E_z \cos^{m-2} \theta + E_x \sin^{m-2} \theta \quad (\text{A.10-9})$$

also, approximately the relationship between F_θ , F_z , and F_x ,

$$F_\theta = F_z \cos^{m-1} \theta + F_x \sin^{m-1} \theta \quad (\text{A.10-10})$$

where E_θ and F_θ are respectively the energy and force generated when the uniaxial bars oriented to the inclination θ suffer ε , while the energy and force generated in E_z and F_z when the uniaxial bars are vertically oriented suffer ε , and the energy and force generated in E_x and F_x when the uniaxial bars are horizontally oriented suffer ε (see the following charts).



(3) Demonstration of “CASH- II” code

To demonstrate the validity of the “CASH- II”, drop tests carried out for four kinds of casks were analyzed. The comparison of the analytical and experimental values are shown in (II)-Table A.43.

(II)-Table A.43 shows that,

a) The deformation of the shock absorber was found to be greater in the analytical values based on the “CASH- II” code than in the experimental values, thus ensuring the maximum safety.

b) The design value of the acceleration based on the “CASH- II” was found to be equal to, or greater than, the experimental value, thus ensuring valid results.

The weight of the package is 950 kg which remains within the weight range of the four different casks.

(II)-Fig. A.104 shows that the shock absorber used in the package is in the same proportion as those of other packagings and cause no problems in applying the analysis code.

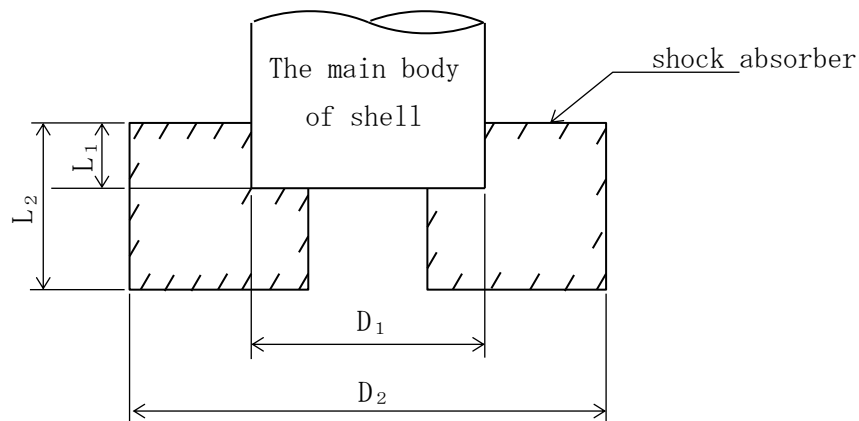
These results permit us to suppose that evaluation of the shock absorber performance based on the “CASH- II” code will lead to justifiable results. However, in the designing of the shock absorber, the following points are taken into account,

- i) A design acceleration + 20 % of the value based on the “CASH- II” code is adopted as the acceleration that can occur.
- ii) Calculated values are adopted as the deformation of the shock absorber because the “CASH- II” code leads to higher values.

(II)-Table A.43 Comparisons of analytical values by “CASH-II” and experimental values

Type of cask		TYPE 1		TYPE 2			TYPE 3		TYPE 4		
Weight (kg)		62, 000		43, 500			710		9, 600		
Outer dimensions (mm)		$6,080 \times \phi 2,400$		$6,220 \times \phi 1,800$			$3,960 \times \phi 566$		$3,290 \times \phi 1,080$		
Posture at dropping		Verti- cal	Hori- zontal	Verti- cal	Hori- zontal	Corner	Verti- cal	Hori- zontal	Verti- cal	Hori- zontal	Corner
Acceleration	Analytical value (g)	78.2	90.8	95.4	112.4	115.4	131.4	274.9	167	128	73.3
	Design value (g)	93.8	109.0	115	135	138.4	158	330	201	152	88.0
	Experimental value (g)	70	67	114	117	73	135	320	200	150	51.5
Deformation	Analytical value (mm)	172	190.3	187	156	383	189.4	50.0	63.4	120	310.1
	Experimental value (mm)	131	117	88	73	155	68.5	16.3	50.0	73.7	22.4

*The design values which are equal to the values of the analytical value multiplied by a factor of 1.2 are used in the designing, taking possible variations of test results into account.



	TYPE 1	TYPE 2	TYPE 3	TYPE 4	Package
L_1/L_2	0.42	0.53	0.56	0.68	0.43
D_1/D_2	0.52	0.67	0.56	0.57	0.57
Shock absorber	Plywood	Plywood	Balsa	Balsa +Redwood	Balsa

(II)-Fig A.104 Proportion of shock absorbers

A.10.2 Validity of the free drop analyses of the JRF-90Y-950K package

(II)-Table A.44 compares the results of a drop tests and the analytical results obtained from a prototype packaging.

Generally, the analytical results were obtained so as to ensure the maximum in safety.

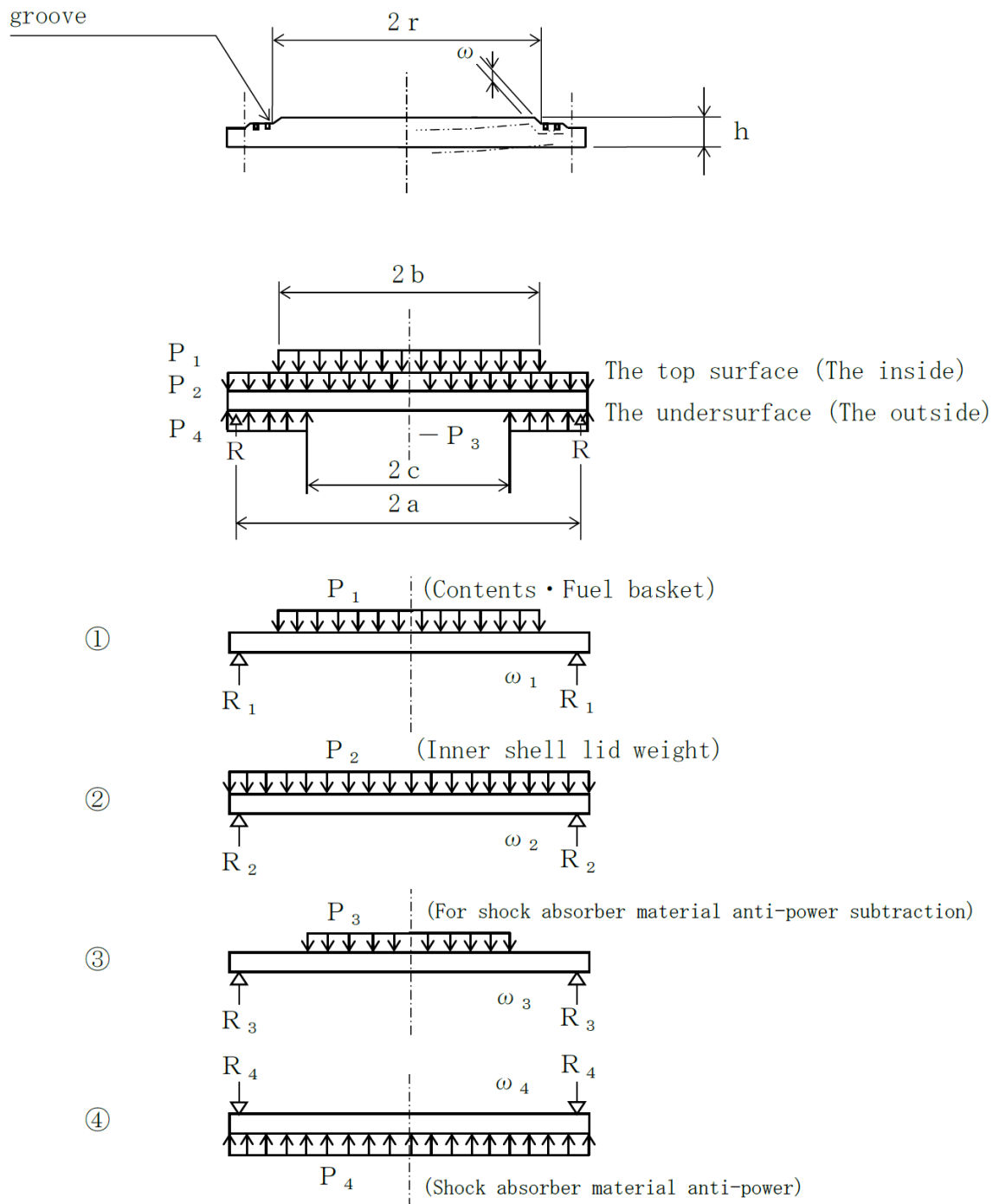
(II)-Table A.44 Comparison of analytical and experimental results

Item		Analytical results	Test results	Ratio of analyses/ test	Remarks
Acceleration (G)	Drop test I	367.0	366	1.003	
	Drop test II	80.4	18.3	4.393	
Deformation (mm)	Drop test I + II	94.0	46	2.043	

A.10.3 Displacement of inner lid O-rings

(II)-Fig.A.105 shows an analytical model showing the displacement of the O-rings in the 1.2 m lid side vertical drop of the package.

Inside O-ring



(II)-Fig.A.105 Analytical model of inner lid for 1.2 m lid side vertical drop

(II)-Fig. A. 105 shows that the uniform load consisting of the weight of the content and that of the fuel basket act at the center of the inner lid, and that the uniform load due to the dead weight of the inner lid acts on the lid.

On the other hand, the inner lid is supported by inner lid clamping bolt and the shock absorber which has a circular reaction force.

Displacement of the O-rings fixed on the inner lid which suffer these loads can be calculated by combining the results of the analyses using the ①, ②, ③ and ④ models (see (II)-Fig. A. 99).

① Contents + fuel basket

The displacement that can occur in the disk suffering a uniform load on its concentric circle(see (II)-Fig. A. 105①) is,

$$\omega_1 = \frac{P_1 b^4}{16 D} \left\{ \frac{r^4}{4b^4} - \frac{4a^2 - (1-\nu)b^2}{2(1+\nu)a^2} \cdot \frac{r^2}{b^2} - \left[2 \cdot \frac{r^2}{b^2} + 1 \right] \cdot 1_n \frac{a}{b} + \frac{4(3+\nu)a^2 - (7+3\nu)b^2}{4(1+\nu)b^2} \right\}$$

where

ω_1 : Displacement of the inner O-ring [mm]

ν : Poisson's ratio, $\nu = 0.3$

a : Radius of the supported points of the inner lid, $a = 285$ [mm]

b : Radius of the loads, $b = 230$ [mm]

r : Radius of the inner O-ring groove, $r = 237.5$ [mm]

m_3 : Weight of the fuel basket, $m_3 = 138$ [kg]

m_4 : Weight of the content, $m_4 = 92$ [kg]

N : Acceleration, $N = 240.7 \cdot g$ [m/s^2]

h : Minimum wall thickness of the inner lid, $h = 36.7$ [mm]

E : Longitudinal modulus of elasticity, $E = 1.99 \times 10^5$ [N/mm^2]

P_1 : uniform load of the content/fuel basket,

$$P_1 = \frac{(m^3 + m^4)}{\pi b^2} \cdot N = \frac{(138 + 92)}{\pi \times 230^2} \times 240.7 \times 9.81 = 3.27 \text{ [N/mm}^2\text{]}$$

D : Bending stiffness of the inner lid,

$$D = \frac{E \cdot h^3}{12(1-\nu^2)} = \frac{1.99 \times 10^5 \times 36.7^3}{12(1-0.3^2)} = 9.01 \times 10^8 \text{ [N} \cdot \text{mm]}$$

Hence the displacement ω_1 due to the content + fuel basket is,

$$\omega_1 = \frac{3.27 \times 230^4}{16 \times 9.01 \times 10^8} \left\{ \frac{237.5^4}{4 \times 230^4} - \frac{4 \times 285^2 - (1 - 0.3) \times 230^2}{2 \times (1 + 0.3) 285^2} \times \frac{237.5^2}{230^2} - \left[2 \cdot \frac{237.5^2}{230^2} + 1 \right] \ln \frac{285}{230} + \frac{4(3 + 0.3) 285^2 - (7 + 3 \times 0.3) 230^2}{4(1 + 0.3) 230^2} \right\}$$

$$= 0.341 \text{ [mm]}$$

② Weight of the inner lid

The displacement ω_2 (mm) that can occur in the disk suffering a uniform load (see (II)-Fig. A. 105 ②) is,

$$\omega_2 = \frac{P_2 a^4}{64D} \left[1 - \frac{r^2}{a^2} \right] \left[\frac{5 + \nu}{1 + \nu} - \frac{r^2}{a^2} \right]$$

where

ω_2 : Displacement of the inner O-ring [mm]

ν : Poisson's ratio, $\nu = 0.3$

a : Radius of the supported points of the inner lid, $a = 285$ [mm]

r : Radius of the inner O-ring groove, $r = 237.5$ [mm]

h : Wall thickness of the inner O-ring groove, $h = 55$ [mm]

N : Acceleration, $N = 240.7 \cdot g$ [m/s²]

γ : Density of the inner lid, $\gamma = 7.93 \times 10^{-6}$ [kg/mm³]

D : Bending rigidity of the inner lid, $D = 9.01 \times 10^8$ [N·mm]

P_2 : Uniform load due to the dead weight of the inner lid,

$$P_2 = \gamma h N = 7.93 \times 10^{-6} \times 55 \times 240.7 \times 9.81 = 1.03 \text{ [N/mm}^2\text{]}$$

Hence the displacement ω_2 due to the weight of the inner lid is,

$$\omega_2 = \frac{1.03 \times 285^4}{64 \times 9.01 \times 10^8} \left[1 - \frac{237.5^2}{285^2} \right] \left[\frac{5 + 0.3}{1 + 0.3} - \frac{237.5^2}{285^2} \right] = 0.122 \text{ [mm]}$$

③ Reaction force of the shock absorber to be subtracted

The displacement ω_3 (mm) that can occur in the disk suffering a uniform load on its concentric circle (see (II)-Fig. A. 105 ③) is,

$$\omega_3 = \frac{P_3 C^4}{16 D} \left\{ \frac{r^4}{4C^4} - \frac{4a^2 - (1 - \nu)C^2}{2(1 + \nu)^2} \cdot \frac{r^2}{C^2} - \left[2 \frac{r^2}{C^2} + 1 \right] \frac{1}{C} + \frac{4(3 + \nu)a^2 - (7 + 3\nu)C^2}{4(1 + \nu)C^2} \right\}$$

where

ω_3 : Displacement of the inner O-ring [mm]

ν : Poisson's ratio, $\nu = 0.3$

a : Radius of the supported points of the inner lid, $a = 285$ [mm]

C: Radius of the load,

$$C = C_0 + \delta \tan \alpha = 115 + 24.1 \tan 15.5^\circ = 122 \text{ [mm]}$$

C₀: Upper radius of the circular cone, C₀ = 115 [mm]

α : Circular cone angle, $\alpha = 15.5^\circ$ [degrees]

δ : Deformation of the shock absorber, $\delta = 24.1$ [mm]

D: Bending rigidity of the inner lid, D = 9.01×10^8 [N • mm]

P₃: Compressive stress on the shock absorber, P₃ = 0.932 [N/mm²]

r: Radius of the inner O-ring groove, r = 237.5 [mm]

Hence, ω_3 is,

$$\begin{aligned} \omega_3 = & \frac{0.932 \times 122^4}{16 \times 9.01 \times 10^8} \left\{ \frac{237.5^4}{4 \times 122^4} - \frac{4 \times 285^2 - (1 - 0.3) \times 122^2}{2 \times (1 + 0.3) 285^2} \times \frac{237.5^2}{122^2} - \right. \\ & \left. \left[2 \frac{237.5^2}{122^2} + 1 \right] \ln \frac{285}{122} + \frac{4(3 + 0.3) 285^2 - (7 + 3 \times 0.3) 122^2}{4(1 + 0.3) 122^2} \right\} \\ & = 0.0370 \text{ [mm]} \end{aligned}$$

④ Reaction force of the shock absorber

The displacement ω_4 (mm) that can occur in the disk which suffers a uniform load on its concentric circle (see (II)-Fig. A.105 ④) is,

$$\omega_4 = \frac{P_4 a^4}{64D} \left[1 - \frac{r^2}{a^2} \right] \left[\frac{5 + \nu}{1 + \nu} - \frac{r^2}{a^2} \right]$$

where,

ω_4 : Displacement in the inner O-ring [mm]

ν : Poisson's ratio, $\nu = 0.3$

a: Radius of the supported points of the inner lid, a = 285 [mm]

r: Radius of the inner O-ring groove, r = 237.5 [mm]

D: Bending rigidity of the inner lid, D = 9.01×10^8 [N • mm]

P₄: Compressive stress on the shock absorber, P₄ = 0.932 [N/mm²]

Hence the displacement ω_4 due to the reaction force of the shock absorber is,

$$\omega_2 = \frac{0.932 \times 285^4}{64 \times 9.01 \times 10^8} \left[1 - \frac{237.5^2}{285^2} \right] \left[\frac{5 + 0.3}{1 + 0.3} - \frac{237.5^2}{285^2} \right] = 0.110 \text{ [mm]}$$

Thus, the total displacement ω is,

$$\omega = \omega_1 + \omega_2 + \omega_3 - \omega_4 = 0.341 + 0.122 + 0.0370 - 0.110 = 0.390 \text{ [mm]}$$

Incidentally, as for the 9 m lid side vertical drop test replacing the values of acceleration, (409.8g), compressive stress of shock absorber, (2.66N/mm²) and displacement, (127mm), with the corresponding value for 1.2 m lid side vertical drop test, the same analysis is conducted and the results of evaluation are given in (II)-Table A.45.

(II)-Table A.45 Analysis results of displacement of inner
O-rings of inner lid

No.	Analysis condition	Name of displacement	Displacement	Total displacement	Remaining height *
1	Normal condition (internal pressure)	ω_0	0.0116	0.402	0.698
	1.2 m lid side vertical drop	ω_1	0.341		
		ω_2	0.122		
		ω_3	0.0370		
		$-\omega_4$	-0.110		
2	Normal condition (internal pressure)	ω_0	0.0116	0.636	0.464
	9 m lid side vertical drop	ω_1	0.581		
		ω_2	0.207		
		ω_3	0.151		
		$-\omega_4$	-0.315		

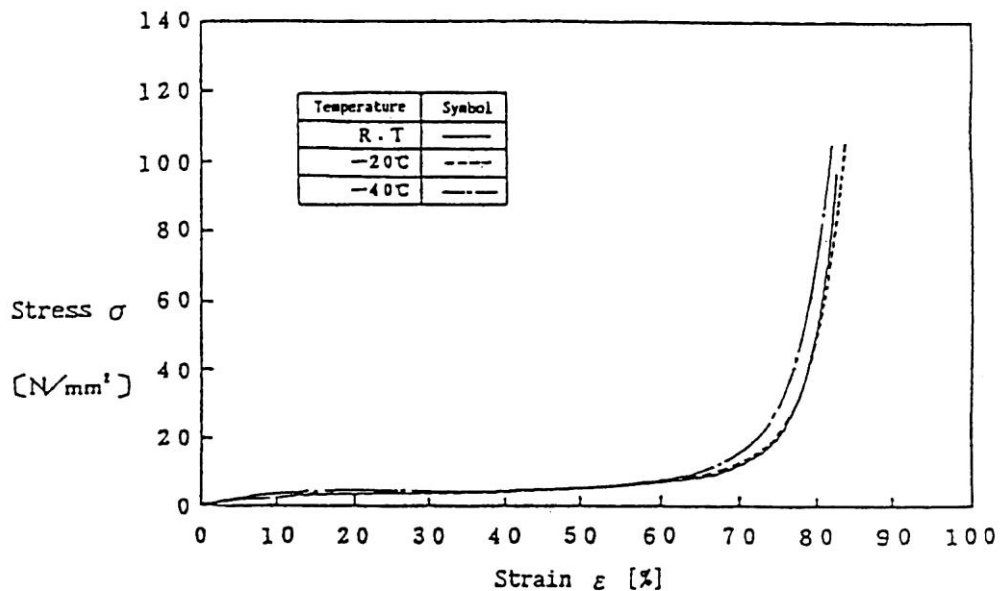
*Note: Residual tightening interference = Initial clamping value (1.1 mm) - Total displacement

As shown in (II)-Table A.45, remaining height of the inner O-ring in each of the cases of 1.2 m and 9 m lid side vertical drop tests is always positive so that it can be granted that the containment of packages will be duly maintained.

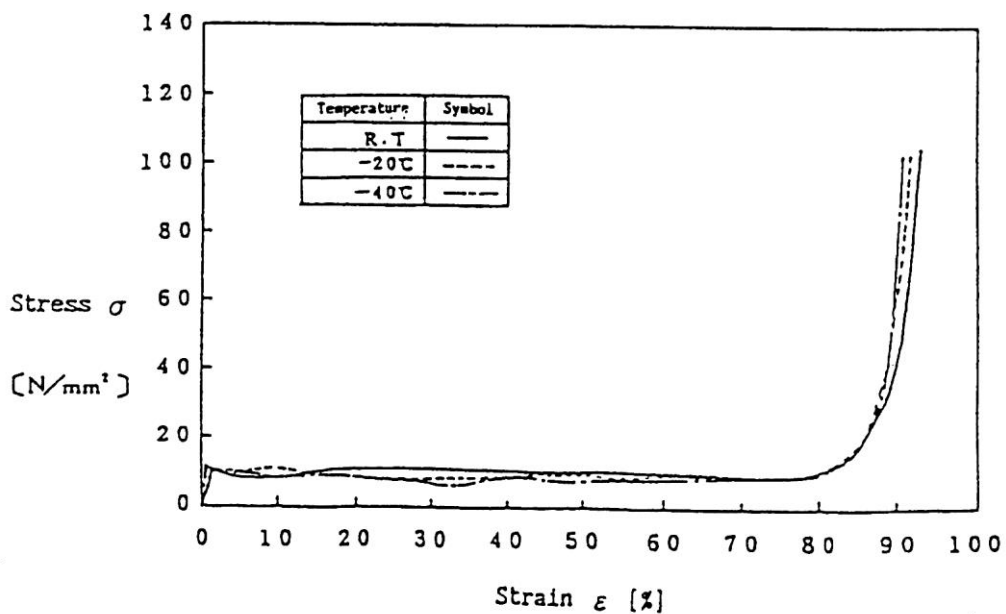
A.10.4 Stress/strain characteristics of the shock absorber at low temperatures

(II)-Fig. A.106 shows the stress/strain characteristics of the shock absorber at low temperatures.

(1) Direction perpendicular to the wood grain of the shock absorber



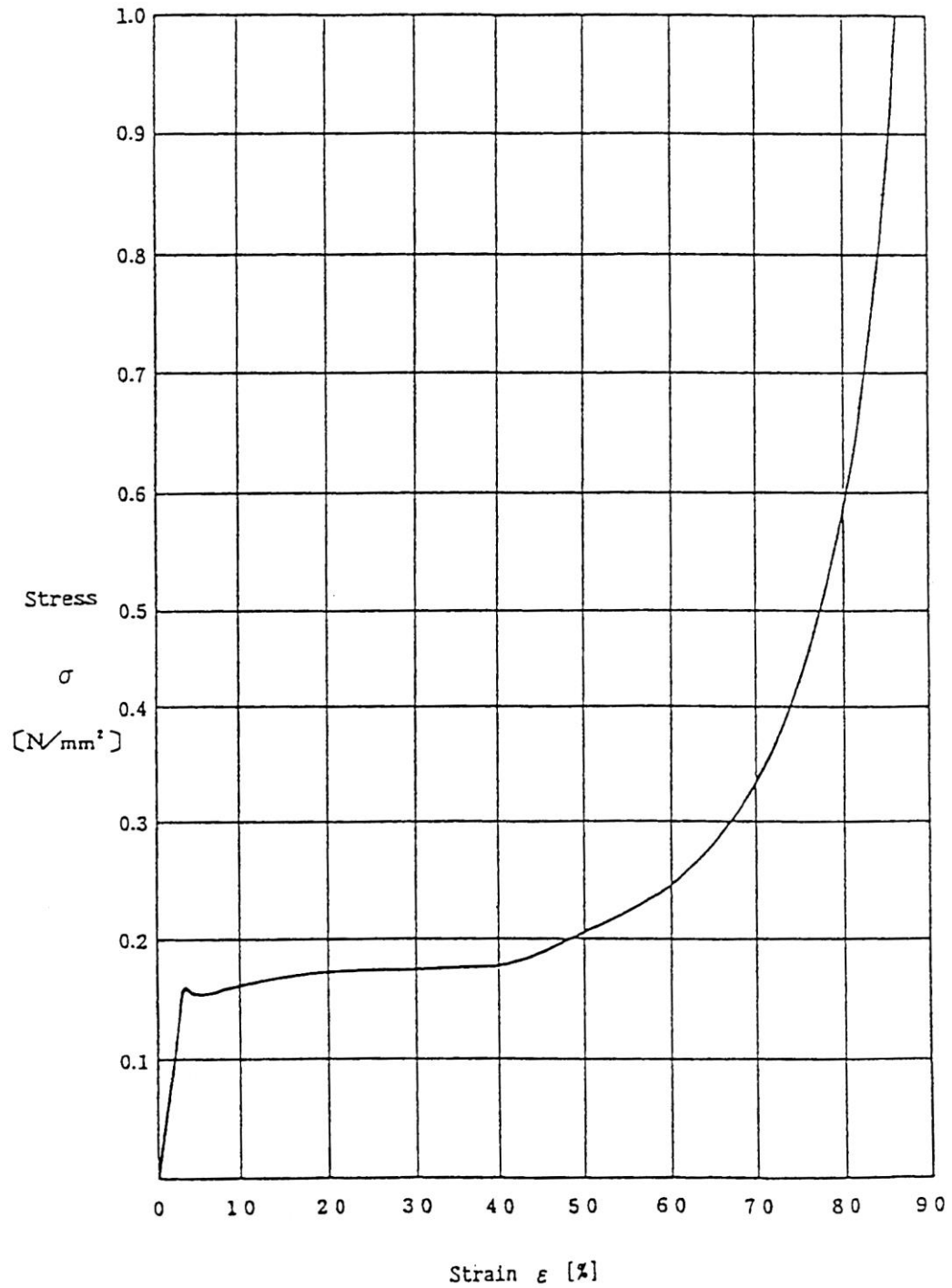
(2) Direction parallel to the wood grain of the shock absorber



(II)-Fig. A.106 Stress/strain characteristics curves for shock absorber at low temperatures ^[4]

A.10.5 Stress/strain characteristics of hard polyurethane foam

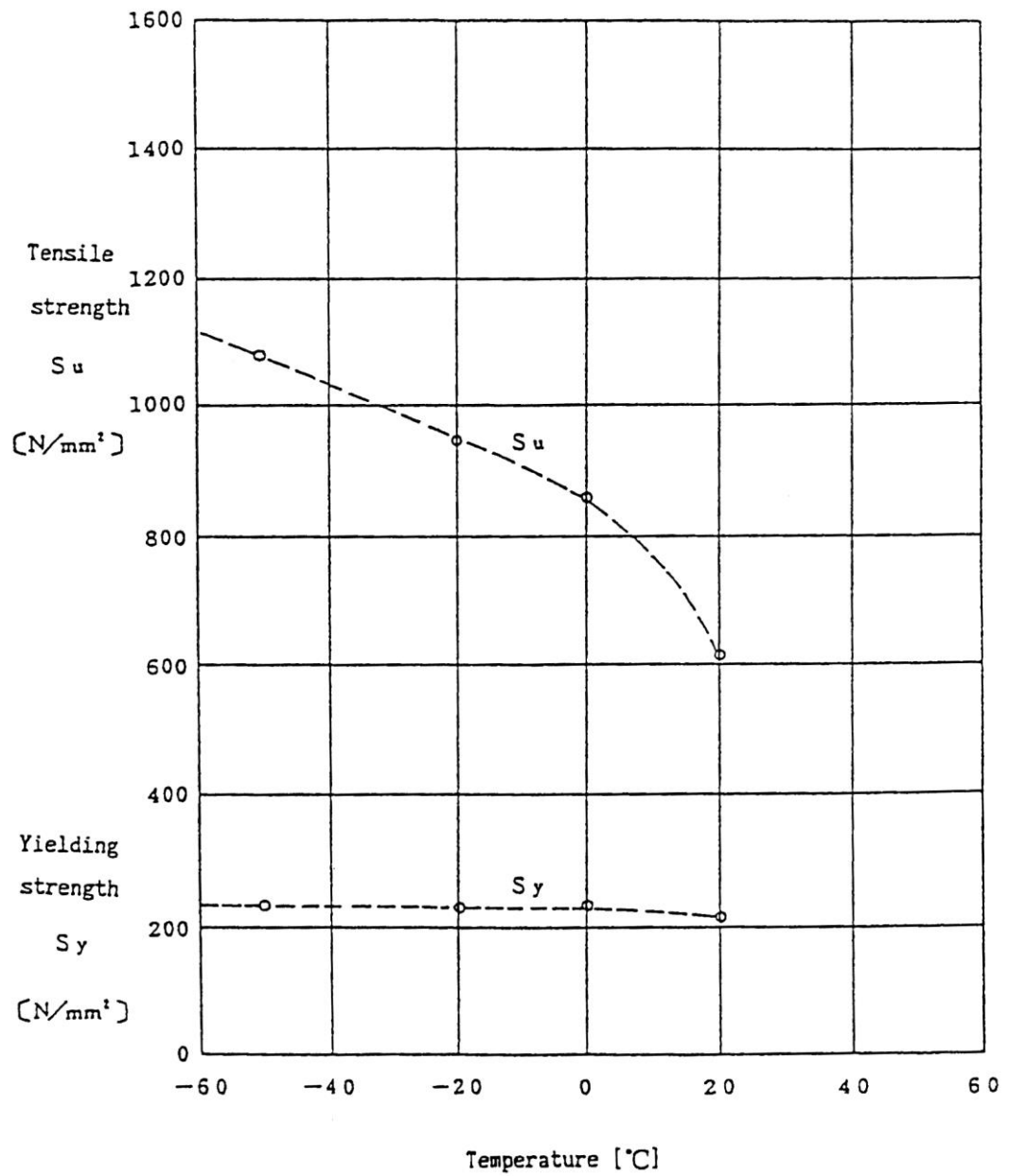
(II)-Fig.A.107 shows the stress/strain characteristics of the hard polyurethane foam.



(II)-Fig.A.107 Stress/strain curves for hard polyurethane foam^[4]

A.10.6 Low temperature strength of SUS 304

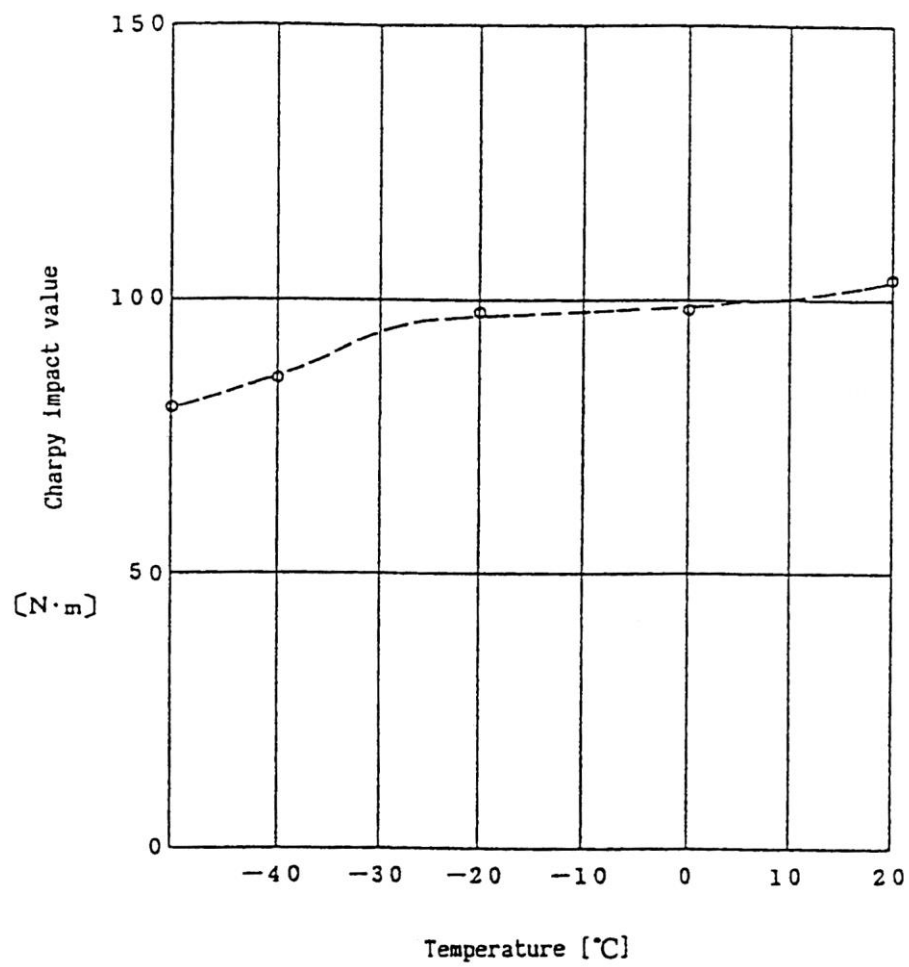
(II)-Fig. A. 108 shows the mechanical characteristics of the material SUS 304 at low temperatures.



(II)-Fig. A. 108 Low temperature strength of SUS 304 ^[16]

A.10.7 Low temperature impact values of SUS 304

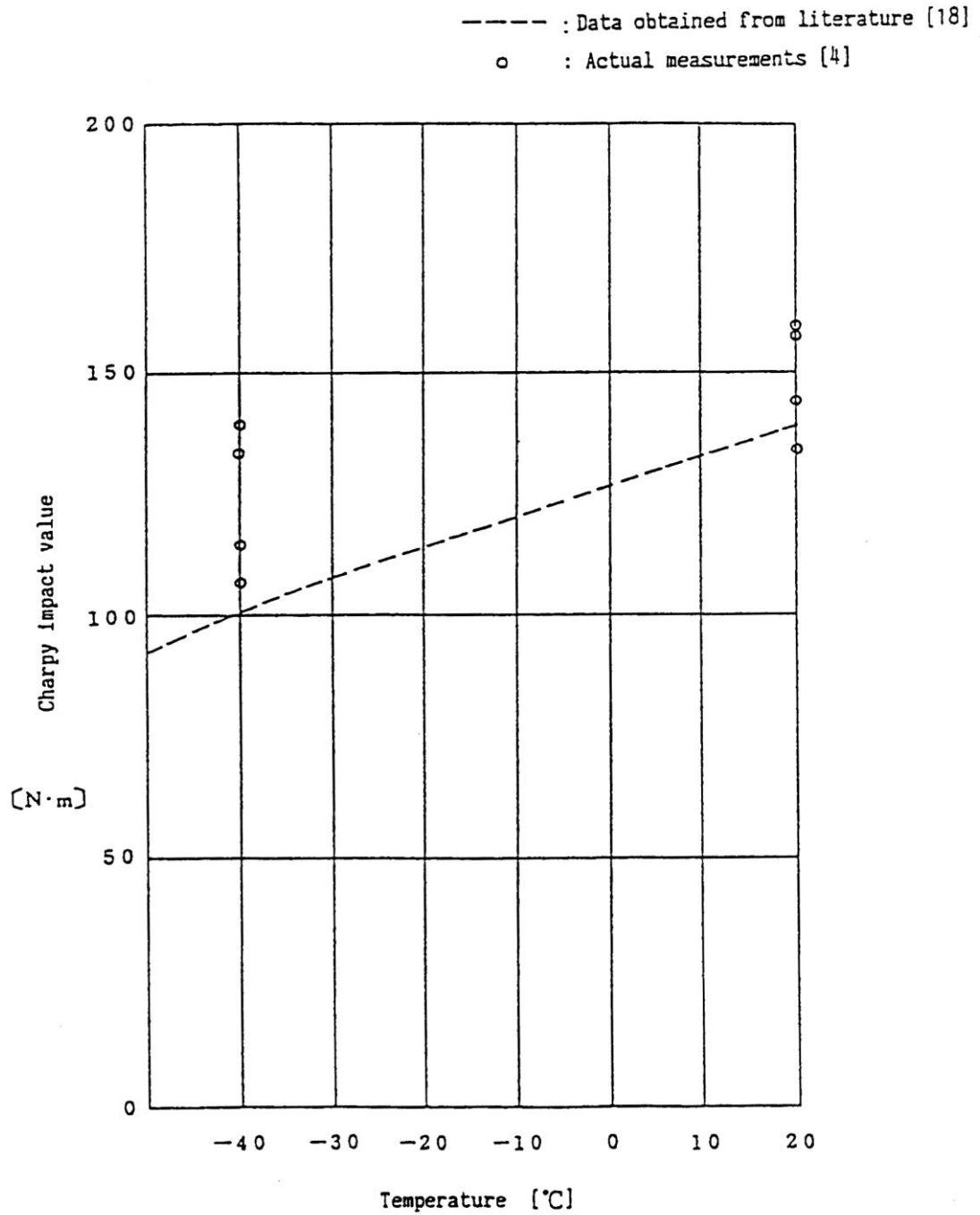
(II)-Fig. A.109 shows the low temperature impact values of the material SUS 304.



(II)-Fig. A.109 Low temperature impact value of SUS 304 ^[16]

A.10.8 Low temperature impact Value of SUS 630/H1150

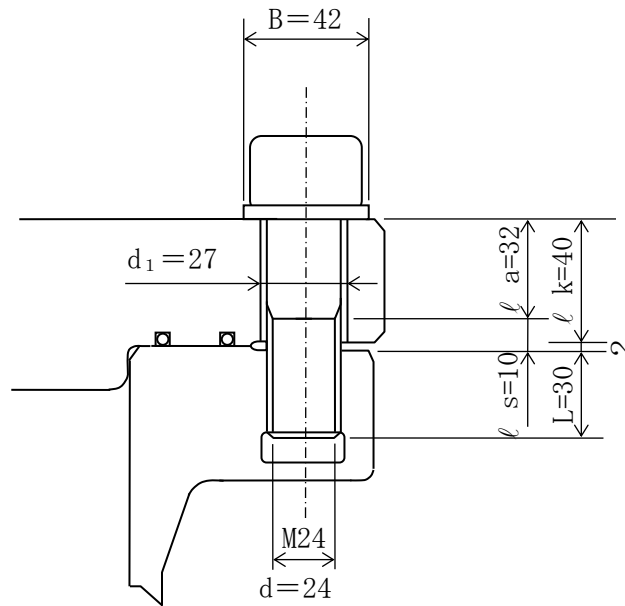
(II)-Fig.A.110 shows the low temperature impact values of the material.



(II)-Fig.A.110 Low temperature impact value of SUS 630·H1150 [18]

A.10.9 Method for calculating torque of inner lid clamping bolts

In this section, we will analyze the initial clamping force of the inner lid clamping bolt (called “the bolt” below).



(II)-Fig.A.111 Analytical model for initial clamping force of inner lid clamping bolts

The minimum required clamping force for the bolt shown in (II)-Fig.A.111 is,

$$F_{\min} = F_C + F_G + F_H$$

where

F_{\min} : Minimum force required for tightening the bolt [N]

F_C : Loss of compressive force in the inner lid when external force is applied [N]

F_G : Clamping force assured by the O-rings [N]

F_H : Decrease of clamping force due to differential thermal expansion [N]

These three values will be analyzed below.

(1) F_c , the loss of compressive force in the inner lid when external force is applied is

$$F_c = (1 - \phi) W_a = (1 - \phi) (W_1 + W_2) / n$$

where

$$\begin{aligned} W_a : \text{Axial external force, } W_a &= (W_1 + W_2) / n \\ &= (0.309 + 8.13) \times 105 / 16 = 5.27 \times 10^4 \quad [\text{N}] \end{aligned}$$

W_1 : Load due to internal pressure,

$$W_1 = P \cdot \frac{\pi}{4} G_1^2 = 0.175 \times \frac{\pi}{4} \times 474^2 = 3.09 \times 10^4 \quad [\text{N}]$$

where

P : Maximum internal pressure, $P = 0.175$ [MPa]

G_1 : Inner O-ring diameter, $G_1 = 474$ [mm]

W_2 : Load occurring at 9 m lid side vertical drop, $W_2 = 8.13 \times 10^5$ [N]

n : Number of bolts, $n = 16$

ϕ : Internal force factor of the bolt,

$$\phi = \frac{F_t}{W_a} = \frac{K_t}{K_t + K_c} = \frac{1.50 \times 10^6}{(1.50 + 6.92) \times 10^6} = 0.178 \quad [-]$$

where

K_t : Tension spring constant of the bolt,

$$K_t = E_b / \left(\frac{l_a}{A_b} + \frac{l_s + l\delta}{A_s} \right) = 1.45 \times 10^6 \quad [\text{N/mm}]$$

where

l_a : Length of the bolt cylinder, $l_a = 32$ [mm]

l_s : Length of the thin bolt cylinder, $l_s = 10$ [mm]

A_b : Cross section of the bolt cylinder,

$$A_b = \frac{\pi}{4} d^2 = \frac{\pi}{4} 24^2 = 452 \quad [\text{mm}^2]$$

A_s : Effective cross section,

$$A_s = \frac{\pi}{4} d_2^2 = \frac{\pi}{4} 22.051^2 = 382 \quad [\text{mm}^2]$$

Where

d_2 : Core diameter of the bolt, $d_2 = 22.051$ [mm]

E_b : Longitudinal modulus of elasticity of the bolt,

$$E_b = 1.99 \times 10^5 \text{ [N/mm}^2\text{]}$$

l_δ : Length equivalent to the elastic displacement in the fitting parts of the nut, $l_\delta = 0.57d = 13.7$ [mm]

K_C : Compression spring constant of the inner lid,

$$K_C = \frac{E_C}{l_K} \cdot \frac{\pi}{4} [d_m^2 - d_i^2] = 6.68 \times 10^6 \text{ [N/mm}^2\text{]}$$

Where

l_K : Tightening length, $l_K = 40$ [mm]

d_1 : Diameter of bolt hole, $d_1 = 27$ [mm]

B : Diameter of the contact surface of the bolt head, $B = 42$ [mm]

d_m : Diameter of equivalent cylinder,

$$d_m = B + \frac{l_K}{5} = 42 + \frac{40}{5} = 50 \text{ [mm]}$$

E_C : Longitudinal modulus of elasticity of the inner lid,

$$E_C = 1.92 \times 10^5 \text{ [N/mm}^2\text{]}$$

Hence,

$$F_c = (1 - \phi) W_a = (1 - 0.178) \times 5.27 \times 10^4 = 4.33 \times 10^4 \text{ [N]}$$

The tensile force F_t in the bolt due to external force is,

$$F_t = \phi W_a = 0.178 \times 5.27 \times 10^4 = 9.38 \times 10^3 \text{ [N]}$$

(2) Clamping force for the O-rings

The clamping force F_G for the O-rings is,

$$F_G = \pi (G_1 + G_2) \times q / n$$

where

G_1 : Diameter of the inner O-ring, $G_1 = 474$ [mm]

G_2 : Diameter of the outer O-ring, $G_2 = 514$ [mm]

q : Linear load of the O-rings, $q = 14.3$ [N/mm]

Hence,

$$F_G = \pi \times (474 + 514) \times 14.3 / 16 = 2.77 \times 10^3 \text{ [N]}$$

(3) Decrease of clamping force F_H due to differential thermal extension

F_H is 0 because the material of the inner lid is the same as that used for the bolts.

Thus, the minimum required clamping force is,

$$F_{\min} = F_C + F_G + F_H = (4.33 + 0.277 + 0) \times 10^4 = 4.61 \times 10^4 \text{ [N]}$$

(4) The initial clamping force for the bolt

The initial clamping force F_0 of the bolt is a little more than the minimum required force.

$$F_0 = 5.89 \times 10^4 \text{ [N]} = 6.0 \times 10^3 \text{ [kgf]}$$

(5) Initial torque for the bolt

The initial torque for the bolt is,

$$\begin{aligned} T &= k \cdot d \cdot F_0 = 0.2 \times 24 \times 5.89 \times 10^4 = 2.83 \times 10^5 \text{ [N}\cdot\text{mm]} \\ &= 28.8 \text{ [kgf}\cdot\text{m]} \end{aligned}$$

where k is the torque coefficient ($k = 0.2$).

(6) Bolt clamping triangle

The above analysis results are shown in the bolt clamping triangle (see [\(II\)-Fig. A.112](#)).

The following is the symbols used in [\(II\)-Fig. A.112](#).

F_0 : Initial clamping force of bolt, $F_0 = 5.89 \times 10^4 \text{ [N]}$

F_{\min} : Minimum required force for clamping the bolt, $F_{\min} = 4.61 \times 10^4 \text{ [N]}$

W_a : Axial external force, $W_a = 5.27 \times 10^4 \text{ [N]}$

F_t : Increment of the bolts tensile force when external force is applied,
 $F_t = 0.94 \times 10^4 \text{ [N]}$

F_C : Loss in the lids compressive force when external force is applied,
 $F_C = 4.33 \times 10^4 \text{ [N]}$

F_C' : Residual compressive force in the inner lid, $F_C' = 1.56 \times 10^4 \text{ [N]}$

F_H : Decrease of clamping force due to differential thermal extension,

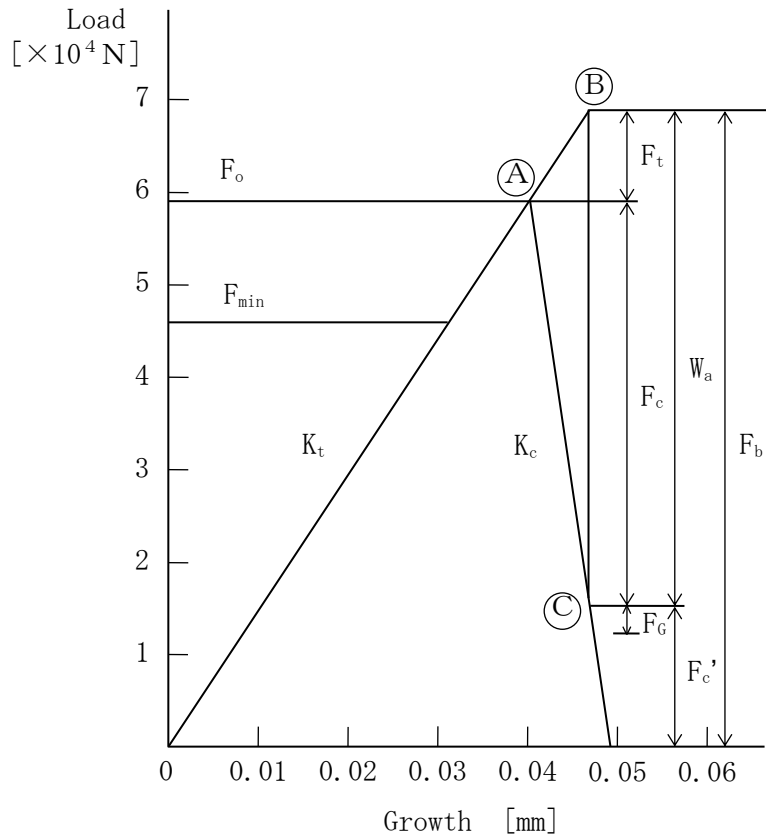
$$F_H = 0 \text{ [N]}$$

F_b : Bolt tensile force, $F_b = 6.83 \times 10^4 \text{ [N]}$

F_G : O-rings clamping force, $F_G = 0.28 \times 10^4 \text{ [N]}$

(II)-Fig. A. 112 shows that the residual compressive force F_c' on the inner lid is higher than the O-ring's clamping force F_G .

Therefore, the containment of the O-rings can be maintained by the initial clamping force F_0 .



(II)-Fig. A. 112 Triangle diagram for inner lid clamping bolt

Explanation of (II)-Fig. A. 112

- (1) This illustration shows that even if axial external force W_a acts from the initial clamp force of bolt F_0 , the residual compressive force in the inner lid F_c would be larger than O-ring clamping force F_c .
- (2) On the axial part of the bolts a tensile force F_0 will be imposed by the initial clamping, and on the body to be clamped, (that is the lid part), a compressive force F_0 will be generated, two forces being in balance with each other at point A, the status of which is shown in the illustration.
- (3) When axial external force W_a , acts on any of the bolts in axial direction, the status of the bolt and lid will be moved to point B and point C.

Point B will be removed from Point A by means of elongation δ being generated, by a tensile force F_t acting on the bolt axial part, and point C will be removed from point A to point C by means of clamping length being extended as much as δ according to the compressive force, F_c , being lost from

the body to be clamped, (that is the lid part).

- (4) That is to say, on the bolt a tensile force F_t is added, from the body to be clamped, (the lid part) a compressive force F_c being removed, and the clamping length will be extended as much as δ where the compressive force remaining on the body to be clamped (The lid part).

A.10.10 Mechanical characteristics of JRR-4B fuel plate

In order to define the analysis criteria by which the plastic deformation will never be generated in the analysis of fuel plate, the proof stress is taken as the analysis standard value.

The proof stress of the JRR-4B fuel plate which is the material for the fuel element (B) shall be specified as given below,

- (1) The mechanical property of AG3NE, which is the material of fuel element (A) is shown in IAEA Guide Book, Vol.2 (referential document [14]), in which it is specified that the design yielding point (S_y) is not less than 63.8 N/mm^2 at the evaluating temperature 75°C .
- (2) JRR-4B fuel has been subjected to a tensile strength test on the basis of a tensile strength test piece which is manufactured from a sheet of fuel plate sampled from each roll badge, the criteria of the test being $88.3 \text{ (N/mm}^2\text{)}$ in the tensile strength; that is $\langle 9\text{kgf/mm}^2 \rangle$.

This test is considered as one of the subjects of precommissioning test of the nuclear reactor facility.

- (3) Besides the above, the results of measurements on 20 pieces of samples in the tensile strength test cited in the proceeding articles (2) are as follows.

	Results of measurements		
	Minimum	Maximum	Average
Proof stress (0.2%) (N/mm^2)	97.1	135	114
Tensile strength (N/mm^2)	108	143	122

(4) H12 materials of JIS 1100P and A1200P, which are the raw materials of JRR-4B type fuel plate cladding material, are deemed to have the strength more than those figures shown in the table given below.

	JIS A 1100P H12 A 1200P H12
Proof stress (N/mm ²)	73.6
Tensile strength (N/mm ²)	93.2~128

(5) Looking from the above, it can be deemed as the safety side estimation that the proof stress for the fuel plate having the tensile strength of 88.3N/mm² as previously cited in the article (2) as the proof stress of the mechanical property of JRR-4B type fuel may be adopted as 63.8N/mm² (yield point of the design) which is equal proof stress mentioned in proceeding article (1).

A.10.11 Literature

- [1] ASME Sec. III Subsec. NB (1974).
- [2] Technical Standards for Atomic Energy Installation for Power Generation Including Standards for Structure, ministerial Notice No.501, 1980.
- [3] Commentary on Standards for the Structure of Boilers and Pressure Vessels, Japan Boiler Association, 1980.
- [4] In-house data of Mitsubishi Heavy Industries. Ltd.
- [5] Roark, J.R., Formulas for Stress and Strain (4th edition), Mc'Graw-Hill International Book Company, 1965.
- [6] Timoshenko, S.P., Theory of Plate and Shell (I); Japanese translation version by Hasegawa, T.
- [7] Manual for Mechanical Engineering, 6th revised edition, Japan Society of Mechanical Engineering, 1977.
- [8] Den Hartog, J.P., Mechanical Vibrations, Mc'Graw-Hill Book Co.
- [9] Mizuhara, A. et al., Handbook for Structural Calculation, Sangyo Tosho Publishing, 1965.
- [10] Formulas Used in Structural Dynamics, compiled by Japan Society of Civil Engineering.
- [11] Sekiyu, T. et al., Handbook for Flat Structure Strength, Asakura Shorten.
- [12] Handbook for Elastic Stability, Long Column Research Committee, Corona.
- [13] Report on Development and Arrangement of Structural Analysis of Transport Packaging for Used Nuclear Fuel II, Japan
- [14] IAEA Guide Book Vol.2: Research Reactor Core Conversion Safety Analysis and Licensing Issues Fuels.
- [15] On the Prediction of Deformation and Deceleration of a Composite Cylindrical Body for the Corner Drop Case, CONF-710801 (Vol.2), 1971, pp. 733-776.

- [16] Hasegawa, M., Manual for Stainless Steel, Nikkan Kogyo Shinbun.
- [17] Data Book for Strength Designing, compiled by Editorial Committee for data book for strength designing.
- [18] Fujita, T., Thermal Processing for Stainless Steel, Nikkan Kogyo Shinbun.
- [19] Timoshenko, S.P., Buckling Theory; Japanese translation version by Naka, I. et al., Corona.
- [20] Aluminum Hand Book (4th edition), Light Metal Society, (1990)
- [21] Summary of Technology for Hybrid Materials, Industrial Technology Center, 1990
- [22] In-house data of Nichias Co.,Ltd
- [23] Code for Nuclear Power Generation Facilities: Rules on Materials Nuclear Power Plants (2012 edition) of The Japan Society of Mechanical Engineers
- [24] Code for Nuclear Power Generation Facilities: Rules on Design and Construction for Nuclear Power Plants (2012 edition) of The Japan Society of Mechanical Engineers

(II)-B Thermal analysis

(II)-B Thermal analysis

B.1 General description

This analysis shows that this package maintains the integrity and satisfies the thermal performance under normal and accident conditions specified in IAEA Regulation.

This packaging is dry type. The package is transported by vertically fixed on the tie-down device. Consequently, the thermal analysis is carried out as the package is located as vertically.

B.1.1 Thermal design

The configuration of this packaging is shown in (II)-Fig.B.1. As shown in this figure, this packaging consists of the main body, inner lid, fuel basket, and outer lid.

The design features of this packaging are described below.

(1) There are 22 types of fuel elements as shown in the paragraph D of section (I). The heat generation from the radioactive contents is ignored in this analysis, since the decay heat generated from unirradiated fuel elements are negligibly small.

(2) Heat transmission (Refer to (II)-Fig.B.2)

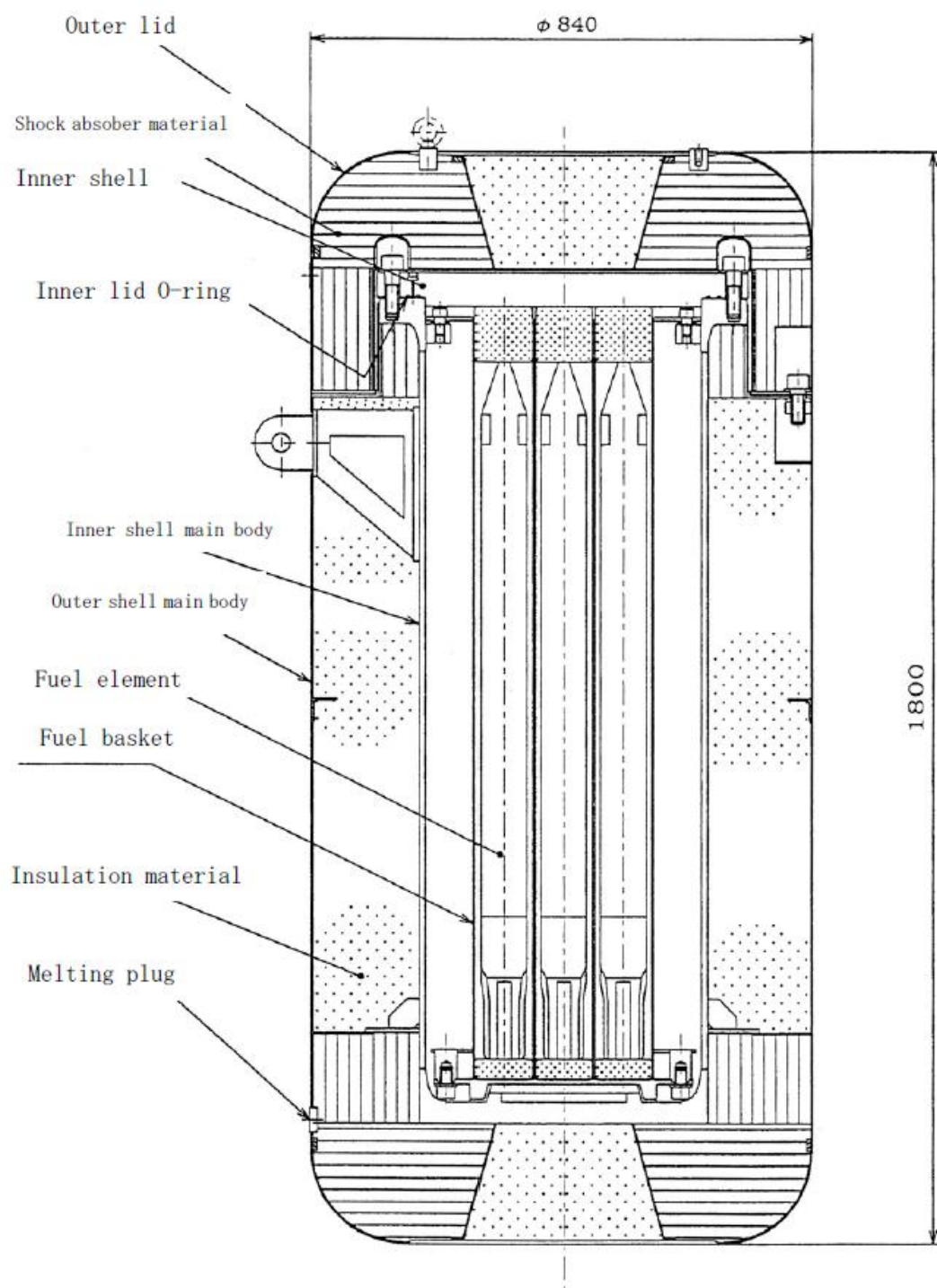
(a) Heat gain from the surface of package consists of solar insulation and heat during fire under accident conditions.

(b) The heat on the external surface of package is transmitted into the internal surface of inner shell or inner lid by conduction.

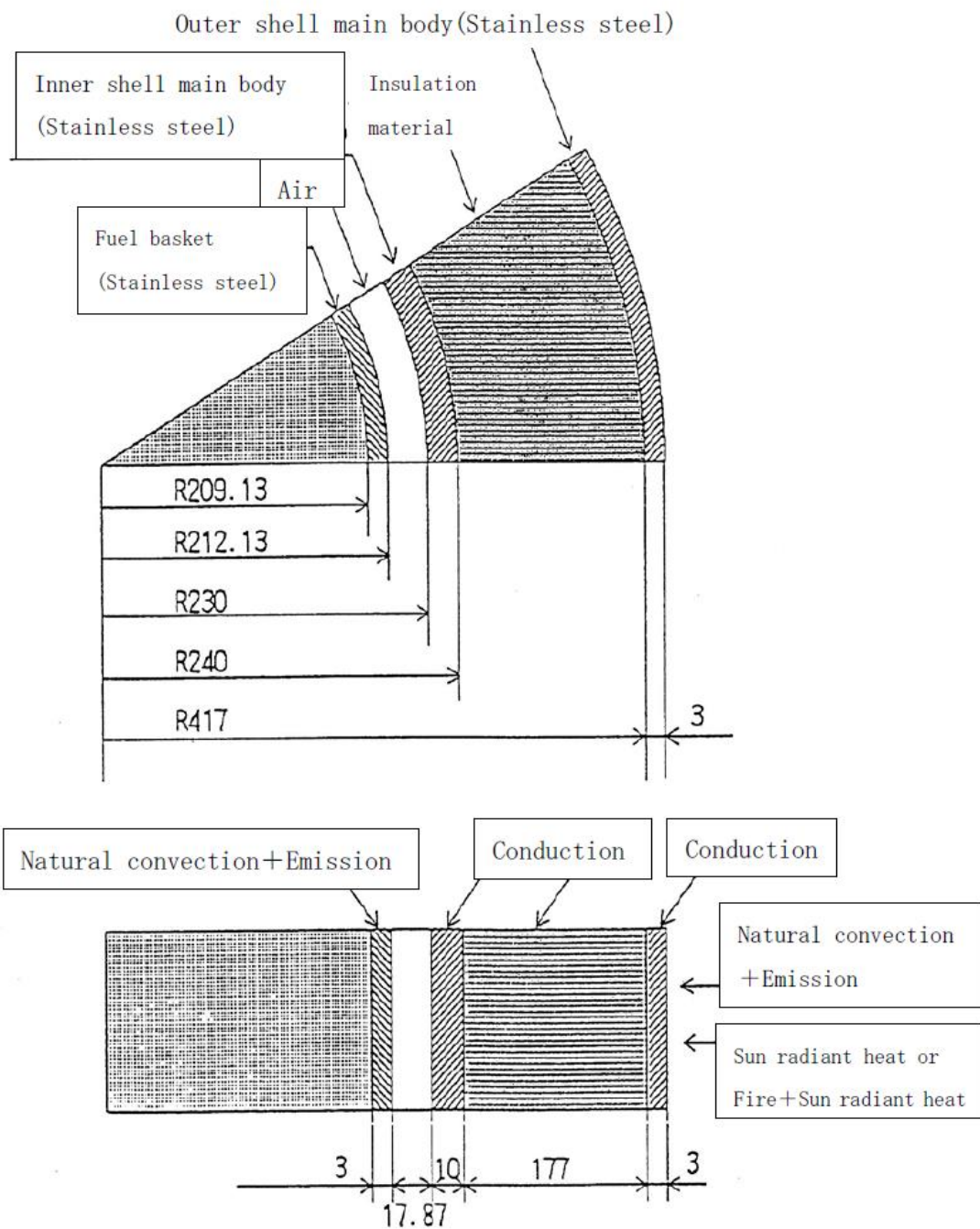
(c) The heat on the internal surface of inner shell or inner lid is transmitted to the external surface of fuel basket by natural convection and conduction.

(d) The interior of the basket is not taken into account in the thermal analytical model, the temperature on the outer surface of the basket represents the temperature on the fuel elements and basket on the assumption that insulation is effective.

- i) No temperature gradient occurs since minimal heat is generated in the basket under normal test conditions.
 - ii) Only external heat affects the package under accident test conditions, rendering the external maximum temperature higher than the internal maximum temperature.
- (3) The balsa used as shock absorber maintains its insulating characteristics even under accident test conditions.
- (4) the outer shell and the external sheet have fusible plugs through which any vapor or gases emitted by the shock absorber and heat insulator under accident test conditions are discharged, preventing the inner pressure from rising.
- (5) The O-ring provided on the inner lid to maintain the leaktightness of the packaging is protected from the heat resulting from fire under accident test conditions by the heat insulation effect of the heat insulator and shock absorber.



(II)-Fig.B.1 Component of packaging



Unit (mm)

(II)-Fig.B.2 Concept of thermal transmission

B.1.2 Conditions and methods of thermal analyses

(1) Conditions of thermal analyses

(II)-Table B.1 shows the thermal conditions used for the normal and accident test conditions.

(II)-Table B.1 Conditions of thermal analyses

Condition Item		Normal test conditions			Accident test conditions		
					Before fire	During fire	After fire
Decay heat		0	0	0	0	0	0
Environmental conditions	Ambient temp.	38°C Stagnant air	38°C Stagnant air	-40°C Stagnant air	38°C Stagnant air	800°C 30min	38°C Stagnant air
	Solar rad. heat	No	Yes	No	Yes	Yes	Yes
	Ambient rad. factor	1.0	1.0	1.0	1.0	0.9	1.0
Radiation factor for packaging surface		0.4	0.4	0.4	0.4 ^{a)}	0.8 ^{b)}	0.6 ^{c)}

a): Surface radiation factor for steel (SUS304) not exposed to fire.

b): Surface radiation factor for steel (SUS304) being exposed to fire.

c): Surface radiation factor for steel (SUS304) exposed to fire.

2) Methods of thermal analyses

(II)-Table B.2 shows the methods by which thermal analyses are performed.

(II)-Table B.2 Methods of thermal analyses

Item		Description
Specifications of contents		See Section D of Chapter (I) of fuel elements
Maximum decay heat (W)		0
Calculation model	Packaging	Axially symmetric two-dimensional model
	Contents	—
Temperature calculation		Simplified analyses*
		TRUMP, non-steady state thermal analysis code** (see B.6.2)
Physical properties used (thermal properties)		See Section B.2 “Thermal Properties of the Materials.”

* :Under normal test conditions.

** :Under accident test conditions.

B.2 Thermal properties of the materials

The materials used for the package are described in Chapter I.

Of these, the materials shown below were used in the thermal analyses.

- Stainless steel
- Air
- Shock absorber (balsa)
- Heat insulator (hard polyurethane foam).

This section will describe the thermal properties of these materials.

(1) Stainless steel

The thermal properties of the stainless steel used are shown in

(II)-Table B.3 ⁽¹⁾

Stainless steel is used as the main structural material for the principal elements of the packaging.

(II)-Table B.3 Thermal properties of stainless steel

Specific weight	7.875g/cm ³	
Temperature (°C)	Specific heat (kJ/kg·K)	Thermal conductivity (mW/m·K)
50	0.469	1.477×10^4
100	0.490	1.558×10^4
200	0.519	1.697×10^4
400	0.561	1.953×10^4
600	0.594	2.232×10^4
800	0.640	2.488×10^4

(2) Air

(II)-Table B.4 ⁽²⁾ shows the thermal properties of the air used.

(II)-Table B.4 Thermal properties of air

Specific weight	9.16×10^{-4} g/cm ³	
Temperature (°C)	Specific heat (kJ/kg·K)	Thermal conductivity (mW/m·K)
0	1.005	24.07
40	1.009	27.21
100	1.013	31.63
140	1.017	34.54
200	1.026	38.61
500	1.093	56.17
800	1.156	70.94

(3) Shock absorber (balsa)

(II)-Table B.5 ⁶⁾ shows the thermal properties of the shock absorber (balsa).

This material, which is used as the shock absorber in the upper and lower part of the packaging, has a heat insulation capability.

(II)-Table B.5 Thermal properties of shock absorber (balsa)

Specific weight	0.16 g/cm ³	
Temperature (°C)	Specific heat (kJ/kg·K)	Thermal conductivity (mW/m·K)
0	1.750	187.2
50	1.695	187.2
100	1.796	175.6
150	1.988	—
200	1.905	195.5
250	1.955	—
275	1.867	255.8
320	1.453	255.8
350	0.917	255.8
500	0.130	255.8
900	0.071	255.8

(4) Heat insulator (hard polyurethane foam)

(II)-Table B.6⁽³⁾ shows the thermal properties of the heat insulator (hard polyurethane foam).

(II)-Table B.6 Thermal properties of heat insulator
(hard polyurethane foam)

Specific weight	0.04 g/cm ³	
Temperature (°C)	Specific heat (kJ/kg·K)	Thermal conductivity (W/m·K)
20	1.193	0.535
50	1.402	0.581
100	1.645	0.675
250	1.859	0.937
300	1.344	0.937
400	0.193	0.937
800	0.151	0.937

B.3 Specifications of components

The following components are taken into account in the thermal analyses.

(1) Silicone rubber O-ring

(II)-Table B.7⁽⁴⁾ shows the specifications of the silicone rubber O-ring.

(II)-Table B.7 Specifications of silicone rubber O-ring

Item	Specifications
Material	Silicone rubber
Hardness	Shore hardness: 70
Normal service temperature	-47°C to 150°C
Service temperature and period under accident conditions	250°C, 5 hours

(2) Fusible plug

(II)-Table B.8 shows the specifications of the fusible plugs.

(II)-Table B.8 Specifications of fusible plug

Item	Specifications
Material	Solder (JIS Z 3282 H63A)
Melting point	183°C to 184°C

B.4 Normal test conditions

The following sections will show how the package meets the requirements of the technical standards under normal test conditions.

B.4.1 Thermal analytical model

Since the decay heat of fuel elements is minimal, the heat emitted by the contents is not taken into account in the analyses.

No heat is generated by the contents of the package and no solar radiation enters, in the shade with a 38°C ambient temperature, the temperature on the outer surface does not exceed 38°C.

Increase in temperature of the package under normal test conditions is caused by entry of solar radiation heat with a 38°C ambient temperature.

This analysis uses a vertically positioned package model. Solar radiation heat enters it and is transmitted by natural convection and radiation.

In this analysis, simplified calculation methods are used (B.6.1, APPENDIX).

B.4.1.1 Analytical model

This section will describe the following items related to the calculations.

- Geometrical model
- Conditions for analyses
- Heat transfer in the package.

(1) Geometrical model

The geometrical model for thermal analyses under normal test conditions supposes that no deformation occurs in the cylindrical packaging that is 840 mm in diameter and 1,800 mm in height.

(2) Conditions for analyses

(II)-Table B.9 shows the thermal conditions under normal test conditions.

(II)-Table B.9 Thermal conditions under normal test conditions

Item		Conditions		
Decay heat (W)		0	0	0
Environmental conditions	Ambient temp. (°C)	Stagnant air 38	Stagnant air 38	Stagnant air -40
	Solar rad. heat (W/m ²)	0	400*, 800**	0
	Ambient rad. factor	1.0	1.0	1.0
Radiation factor for packaging surface		0.4	0.4	0.4

*:Although the radiant heat on the surface of an article that is vertically transported is 200 w/m2, 400 W/m2 shall be conservatively set as the value for “other surfaces.”

**:“The surface of an article that is horizontally transported” and “the surface turned upward”

(3) Heat transfer in the package (see (II)-Fig.B.2)

With regard to heat transfer in the package, the following conditions apply,

- (a) Deformation is not taken into account since deformation under normal test conditions is minimal.
- (b) Steady state thermal calculations are performed for the package surface of the model in which heat entry (solar radiation heat) and heat emission (natural convection to the atmosphere and radiation) are in equilibrium.
- (c) The maximum temperature on the package surface (paragraph b) represents the maximum temperature in the package.

- (d) Only solar radiation heat enters the package. This heat is transferred to the outer surface of the package by natural convection and radiation.
- (e) Heat reaching the outer surface of the package is transferred to the inner surface of the inner shell by thermal conduction.

Based on these conditions, steady state thermal calculations were performed by simplified methods.

The details of the results are given in B.6.1, APPENDIX.

B.4.1.2 Test model

An analytical model is used, and a test model is not used.

B.4.2 Maximum temperatures

(II)-Table B.10 shows the maximum temperatures on the main parts of the package under normal test conditions.

(II)-Table B.10 Maximum temperatures of each part of package

<div> <div>Item</div> <div>Parts</div> </div>	Normal test conditions		
	No solar rad. heat Ambient temp.: 38°C	Solar rad. heat Ambient temp.: 38°C	No solar rad. heat Ambient temp.: -40°C
Ext. surface of basket	38°C	65°C	-40°C
Inner lid O-ring	38°C	65°C	-40°C
Inner surface of inner shell	38°C	65°C	-40°C
Outer surface of main body	38°C	65°C	-40°C

The maximum temperature of the package under normal test conditions is uniformly 62.1°C at these parts as shown in section B.6.1 Appendix. The value of 65°C is adopted here as a conservative figure.

B.4.3 Minimum temperatures

Since the small amount of decay heat of the contents is not taken into account, temperatures at various parts of the package are uniformly -40 °C under the conditions of no solar radiation heat and -40°C stagnant air. Under this thermal condition, the packaging maintains its capabilities, since the value -40 °C lies within the normal service temperature range of the silicone rubber O-ring (-47°C to 150°C). The structural material is stainless steel and does not embattle.

Hence, the packaging maintains its integrity.

B.4.4 Maximum internal pressure

As described in Section B.4.2, the maximum temperature of the package is 65°C under normal test conditions. In the evaluation of the maximum inner pressure under normal test conditions, pressures due to thermal expansion of the air contained in the packaging are taken into account on the supposition that the temperature of each part of the package is uniformly 65°C, as shown in Section B.6.4., APPENDIX.

The inner pressure in the packaging is thus 0.016 MPa•G. Since this value is far lower than the design pressure of 0.0981 MPa•G, the package maintains its integrity.

B.4.5 Maximum thermal stress

Thermal stresses under normal test conditions do not adversely affect the structural strength of the package as shown in Section A.5.1, Chapter (II).

B.4.6 Summary of the results and evaluation

We confirmed that the structural strength and containment of the package are not adversely affected by the normal test conditions, as shown by the following evaluations of the thermal analyses.

(1) Surface temperature of package

The surface temperature of the package is 65°C, lower than the allowable reference value 85°C.

(2) Structural strength

The various parts of the package were analyzed for their maximum inner pressure, thermal stress and maximum temperature, which constitute the main factors for structural strength. For the maximum internal pressure, the internal pressure rises by 0.016 MPa·G in the packaging, far lower than the design pressure of 0.0981 MPa·G and does not adversely affect the structural strength.

Thermal stresses do not adversely affect the structural strength of the packaging, as described in Section A.5.1, Chapter (II).

(3) Containment

The inner lid O-ring, functioning as containment border and thus constituting the most important part for containment, was evaluated for its temperature, deformation and maximum internal pressure.

The temperatures of the O-ring, containment border, are within the range from -40°C to 65°C. Since this range is within its normal service temperature range (-47°C to 150°C), the O-ring does not deteriorate.

No deformation occurs that might adversely affect the containment border.

B.5 Accident test conditions

This section will describe how the package meets the technical standards under accident test conditions.

B.5.1 Thermal analytical model

Thermal evaluations were conducted for accident test conditions, using the three-dimensional, non-steady state thermal analysis code "TRUMP."

B.5.1.1 Analytical model

The section concerns the following items used in the calculation by "TRUMP".

- Geometrical model
- Conditions for analyses
- Heat transfer in the package.

(1) Geometrical model

As shown in Section A (Structural Analyses), Chapter (II), the packaging maintains its integrity in spite of small local deformations in the drop tests under accident test conditions, as required for Type B(U) packages.

Since the drop test I showed the deformation imposed was 126.7mm in vertical direction, being 81.6mm in horizontal direction, the thermal analysis under the specific testing conditions adopted the dimensions of shock absorber and heat insulating material reduced up to 51mm (deformation;135mm) despite 186mm before the deformation imposed in the former in axial direction and up to 82mm (deformation:95mm) despite 177mm before the deformation imposed in the latter in radial direction respectively.

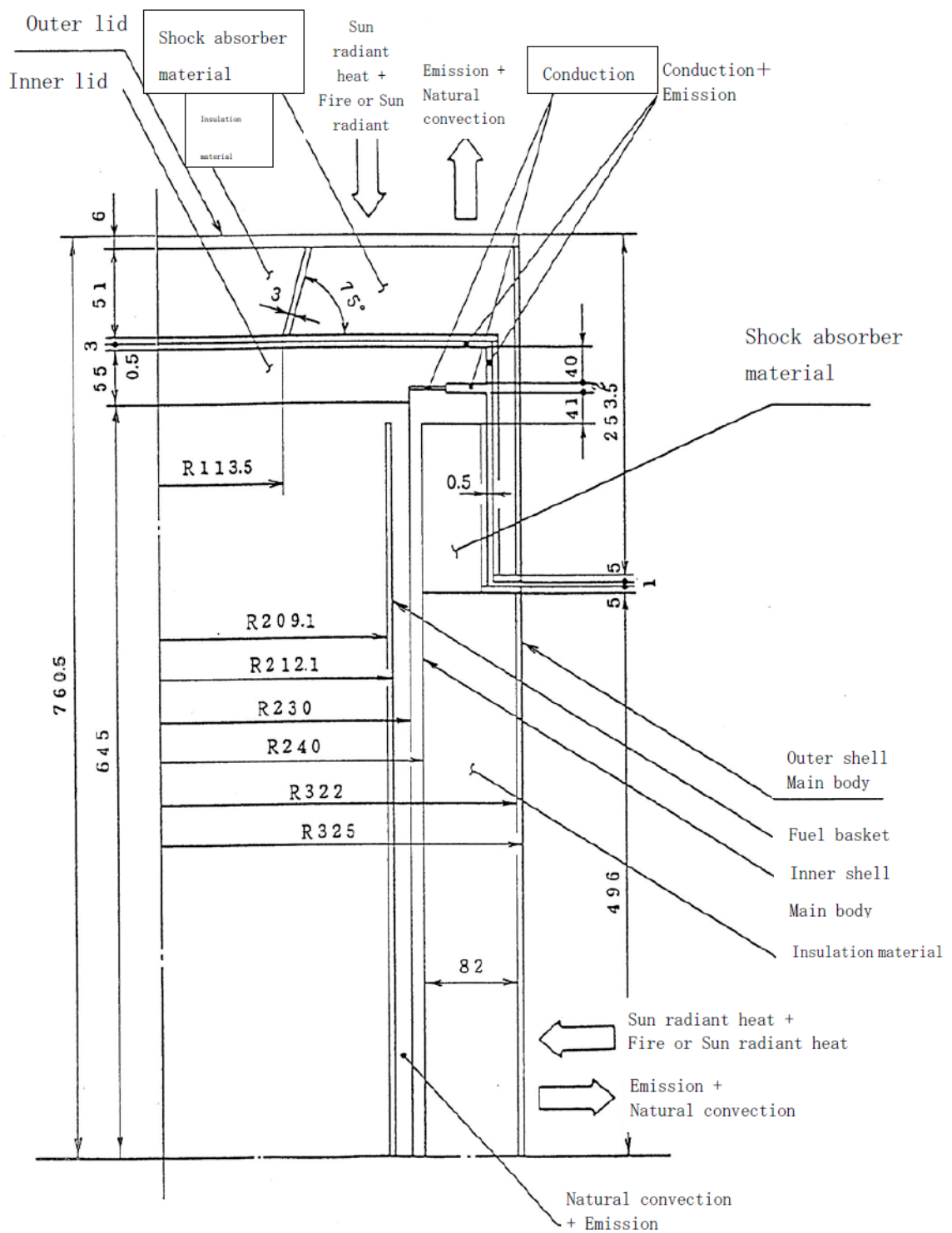
However, the drop test II showed the deformation rather localized and it seemed there were no significant effects considered thermally, so that no particular modeling was considered.

(II)-Fig.B.3 shows the geometrical model (axially symmetrical, two-dimensional model) under the accident test conditions.

In this geometrical model, a circular section was adopted despite the actual angular section, as shown in B.6.3.

The following parts were evaluated.

- Fuel basket
- Inner surface of the inner shell
- Inner lid O-ring
- Outer surface of the main body.



(II)-Fig.B.3 Two dimensional axis symmetrical model

(2) Conditions for analyses

The following thermal conditions were used in the analyses.

The decay heat of the contents is minimal and is not considered. The thermal analyses for the accident test conditions suppose that the package is placed under fire accident conditions subsequently to the mechanical test conditions under accident test conditions. The temperature distribution for the normal test conditions is used for the packaging which has not undergone the fire conditions.

The thermal conditions during fire accident are, ambient temperature of 800 °C, period of 30 minutes, fire radiation factor of 0.9, and radiation factor for the package surface of 0.8. The package is supposed to suffer solar radiation heat. Both radiation and convection are taken into account with regard to the heat transfer from the ambient environment to the packaging.

The thermal conditions after fire accident are, ambient temperature of 38 °C, radiation factor for outer surface of the main body as packaging surface of 0.6, and radiation factor for ambient environment of 1.0. Natural convection and radiation are taken into account with regard to the heat diffusion from the outer surface of the packaging. Solar radiation heat is also taken into account.

(II)-Table B.11 shows the above conditions for analyses.

The evaluation takes into account any entry of heat due to a fire resulting from combustion of the heat decomposition gas from hard polyurethane foam.

(II)-Table B.11 Thermal conditions under accident test conditions

Item		Initial conditions	During fire accident	After fire accident
Decay heat (W)		0	0	0
Environmental Conditions	Ambient temp. (°C)	Stagnant air 38	30 minutes 800	Stagnant air 38
	Solar rad. heat (W/m ²)	400 ^(d) , 800 ^(e)	400 ^(d) , 800 ^(e)	400 ^(d) , 800 ^(e)
	Ambient rad. factor	1.0	0.9	1.0
Radiation factor for packaging surface		0.4 ^(a)	0.8 ^(b)	0.6 ^(c)

- (a): Surface radiation factor for steel (SUS304) not exposed to fire.
(b): Surface radiation factor for steel (SUS304) being exposed to fire.
(c): Surface radiation factor for steel (SUS304) exposed to fire.
(d): Although the radiant heat on the surface of an article that is vertically transported is 200 w/m², 400 W/m² shall be conservatively set as the value for "other surfaces."
(e): "The surface of an article that is horizontally transported" and "the surface turned upward"

(3) Heat transfer for package (see (II)-Fig.B.2)

For the heat transfer for the package, the evaluation supposes that,

- (a) External heat is transferred to the outer surface of the package through natural convection and radiation.
(b) The heat on the outer surface of the package is transferred to the inner surface of the inner shell through thermal conduction.
(c) The heat on the inner surface of the package is transferred to the outer surface of the fuel basket by radiation and thermal conduction.
(d) The interior of the basket maintains its heat insulating capability as under the normal test conditions.

The relational expressions used in the analyses of these heat transfers are shown in Section B.6.3, APPENDIX.

(4) Thermal analyses of fissile packages

As shown below, the deformation of the fissile package which suffers composite effect of different drops under normal test conditions plus a 9 m drop is smaller than that obtained for this thermal analytical model((II)-Fig.B.3) except in the case of the vertical drop, in which deformation slightly exceeds 1.6 mm.

Item	Vertical		Horizontal
	Lid side	Bottom side	
Minimum thickness before deformation (mm)	186	199	177
Deformation at 9m drop as BU package (mm)	126.7 (59.3)	106.3 (87.7)	81.6 (95.4)
Deformation at 9m drop as Fissile package (combination) (mm)	136.6 (49.4)	117.6 (76.4)	88.8 (88.2)
Deformation of thermal analytical model (mm)	135 (51)		95 (82)

Numbers given in brackets() indicate remaining thickness.

In addition, a combination of drops test I and II causes no deformation in the inner shell, and deformations are local.

There supposed to be no significant difference between the thermal analytical model taking into account the composite effect of various conditions on fissile packages and the thermal analytical model, for this reason, the package is not analyzed here for thermal conditions under the accident test conditions.

B.5.1.2 Test model

An analytical model is used, and a test model is not used.

B.5.2 Evaluation conditions for packages

In the evaluation, the conditions shown in (II)-Fig.B.3, which take into account deformations resulting from drop tests under accident test conditions, were used.

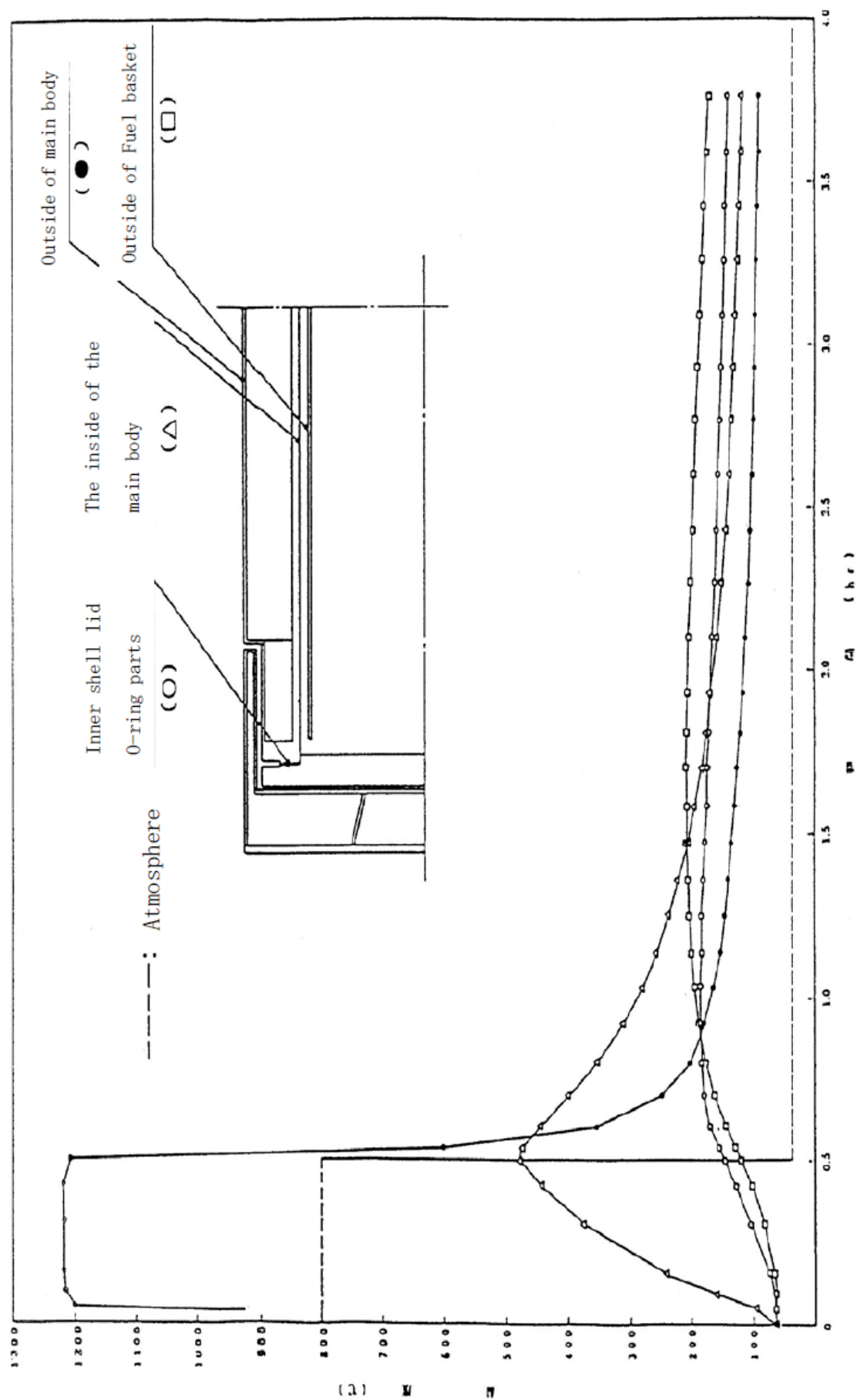
B.5.3 Temperatures of packages

(II)-Fig.B.4 shows the results of the calculations using the analytical model described in Section B.5.1.1. Temperature evolutions for various parts of the package under accident test conditions are plotted here in relation to time. (II)-Table B.12 shows the maximum temperature of each part and the period of time required from the occurrence of fire to the attainment of the maximum temperature.

(II)-Table B.12 Maximum temperatures of package
under accident test conditions

<div>Item</div> <div>Parts</div>	Accident test conditions	
	Maximum temp.	Time required from fire occurrence of fire to attainment of maximum temp.
Fuel basket	209.9°C	Approx. 1.6 hours
Inner lid O-ring	187.8°C	Approx. 0.9 hours
Inner surface of inner shell	483.2°C	Approx. 0.5 hours
Outer surface of main body	1,226.6°C	Approx. 0.4 hours

Note: The fact that the maximum temperature of the outer surface of the main body exceeds the ambient temperature of 800°C is explained by the combustion of the gases generated from the heat insulator passing through fusible plugs.



(II)-Fig. B. 4 Temperature time history under accident test conditions

B.5.4 Maximum internal pressure

The evaluation of the maximum internal pressure under accident test conditions takes into account the pressure due to thermal expansion of the air contained in the packaging. The calculation methods shown in Section B.6.4, APPENDIX, were used.

The value 0.065 MPa•G was obtained for the internal pressure in the packaging. Since this value is lower than the design value, the packaging maintains its integrity at its different parts.

B.5.5 Maximum thermal stresses

Thermal stresses occurring in the package under accident test conditions do not adversely affect its structural strength, as shown in Section A.6.3, Chapter (II).

B.5.6 Summary of results and evaluation

We confirmed that the structural strength and containment of the package are not adversely affected by the accident test conditions, as shown by the following evaluations of the thermal analyses.

(1) Temperatures

(II)-Table B.12 shows the maximum temperatures of various parts of the package under accident test conditions, and (II)-Fig.B.4 shows the recorded temperatures of various parts under accident test conditions.

The fuel basket under accident test conditions reaches its maximum temperature of 209.9°C 1.6 hours after the occurrence of fire. Since this evaluation supposes maintenance of heat insulation in the basket, the temperature of plate-shaped fuel elements to be actually contained does not exceed 209.9°C.

This value is lower than the temperature of occurrence of blistering (“allowable temperature for fuel”) of 400°C for plate-shaped fuel elements used in the experiment and research reactors of the Japan Atomic Energy Research Institute and Institute for Integrated Radiation and Nuclear Science, Kyoto University. Therefore, the contents maintain their soundness.

The inner lid O-ring reaches its maximum temperature of 187.8°C, 0.9 hours after the occurrence of fire. This value is lower than the service temperature 250°C for the silicone rubber O-rings under accident. Thus, the O-ring maintains its integrity even under the accident test conditions, and the packaging retains its containment.

(2) Pressure

As described in the preceding section, the temperature of the parts of the package rises under the accident test conditions. This rise in temperature causes the air in the packaging to thermally expand, raising the internal pressure.

The packaging is evaluated for its internal pressure, supposing the maximum temperature of the outer surface of the basket to be 209.9°C. (II)-Table B.13

shows the maximum pressure in the packaging under accident test conditions.

(II)-Table B.13 Maximum pressure in packaging under
accident test conditions

Position \ Conditions	Maximum pressure under accident test conditions (MPa • [gauge])
Inside the packaging	0.065

The pressure 0.065 MPa • [gauge] is lower than the design pressure for the packaging, 0.0981 MPa • [gauge].

Thus, the packaging maintains its integrity.

(3) Structural strength

This section concerns the maximum inner pressure, thermal stresses and maximum temperature in the packaging, which are to be examined for structural strength of the packaging.

As far as the maximum inner pressure is concerned, the pressure rise in the packaging 0.065 MPa • [gauge] is lower than the design pressure 0.0981 MPa • [gauge] and does not adversely affect the structural strength of the packaging.

As shown in Section A.5, Chapter (II), thermal stresses do not adversely affect the structural strength of the packaging.

(4) Containment

The maximum temperature of the O-ring provided on the inner lid, which constitutes the containment border, is 187.8°C. This value is lower than the service temperature 250°C of silicone rubber O-ring under accident conditions, and the package thus maintains its containment.

B. 6 Appendix

B. 6.1 Maximum temperature of package under normal test conditions

..... (II)-B-26

B. 6.2 Outline of “TRUMP” -- General purpose program for heat transfer

..... (II)-B-29

B. 6.3 Input data for “TRUMP” used for temperature calculations for

accident test conditions (II)-B-35

B. 6.4 Internal pressure of the package (II)-B-40

B. 6.5 Validity Justification of thermal analysis methods (II)-B-41

B. 6.6 Bibliography (II)-B-44

B. 6.1 Maximum temperature of package under normal test conditions

The maximum temperature is obtained, using the thermal balance for a steady state, as follows.

The quantity of entering heat Q_{in} [kcal/h] only consists of solar radiation heat, and the quantity of emitted heat Q_{out} [kcal/h] is the sum of radiation heat Q_1 [kcal/h] and emitted heat due to natural convection Q_2 [kcal/h]. The packaging reaches its maximum temperature, when $Q_{in} = Q_{out}$.

It is obtained with the outer surface temperature of the packaging t [°C], supposing,

t_o : Ambient temperature, $t_o = 38$ [°C]

A_v : Vertical area to which heat is transferred,

$$A_v = \pi \times 0.84 \times 1.8 = 4.750 \text{ [m}^2\text{]}$$

A_h : Upper horizontal area to which heat is transferred,

$$A_h = 0.84^2 \times \pi / 4 \text{ [m}^2\text{]} = 0.554 \text{ [m}^2\text{]}$$

(1) Radiation heat from solar heat Q_{in}

$$Q_{in} = 400 \text{ [W/m}^2] \times \epsilon \times A_v + 800 \text{ [W/m}^2] \times \epsilon \times A_h$$

$$= 344 \text{ [kcal/m}^2 \cdot \text{h]} \times \epsilon \times A_v + 688 \text{ [kcal/m}^2 \cdot \text{h]} \times \epsilon \times A_h \dots (6.1-1)$$

where ϵ : radiation factor for the packaging outer surface,

$$\epsilon = 0.4$$

(2) Radiation heat from package Q_1

$$Q_1 = (A_v + A_h) \times \epsilon \times \sigma \times (T^4 - T_o^4)$$

$$= (4.75 + 0.554) \times 0.4 \times 4.88 \times 10^{-8} \times \{(t + 273)^4 - (38 + 273)^4\}$$

$$= 10.353 \times 10^{-8} \times \{(t + 273)^4 - 311^4\} \dots \dots \dots (6.1-2)$$

$$T = t + 273$$

where T: Absolute temperature [K]

t: Outer surface temperature for the package [°C]

σ : Stefan -Boltzmann constant [kcal/m² · h · K⁴]

(3) Emitted heat due to natural convection Q_2

Heat transfer of natural convection of vertical cylindrical surface is given by Mc Adam's formula as follows. ⁽⁵⁾

$$Nuv = 0.13 (Gr \cdot Pr)^{1/3(5)} [10^9 < Gr \cdot Pr < 10^{12}] \dots \dots (6.1-3)$$

$$Nuv: \text{Nusselt number, } Nuv = h_v \cdot L / K \dots \dots (6.1-4)$$

$$Gr: \text{Grashof number, } Gr = g \cdot \beta \cdot L^3 \cdot \Delta t / \nu^2 \dots \dots (6.1-5)$$

$$Pr: \text{Prandtl number, } Pr = C_p \cdot \mu / K \dots \dots (6.1-6)$$

where h_v : Heat transfer coefficient for vertical,

cylindrical surface [kcal/m²h°C]

L : Representative length [m]

K : Heat transfer coefficient for air [kcal/mh°C]

g : Gravitational acceleration,

$$9.8 \text{ [m/sec}^2] = 1.27 \times 10^8 \text{ [m/h}^2]$$

β : Coefficient of cubical expansion for air [1/K]

Δt : Difference of temperatures ($t-t_o$) [$^{\circ}\text{C}$]

ν : Coefficient of kinematic viscosity for air [m^2/h]

C_p : Isopiestic specific heat for air [kcal/kg $^{\circ}\text{C}$]

μ : Viscosity of air [kg/mh]

The Nusselt number Nu is obtained by Equations (6.1-3), (6.1-5), and (6.1-6), and the heat transfer coefficient for vertical, cylindrical surface h_v by Equation (6.1-4). The heat transfer coefficient for horizontal surface h_h is similarly obtained by Equations (6.1-7) and (6.1-8).

$$Nu = 0.14 \cdot (Gr \cdot Pr)^{1/3} \quad [2 \times 10^7 < Gr \cdot Pr < 3 \times 10^{10}] \quad \dots\dots\dots (6.1-7)$$

$$Nu = h_h \cdot L / k \quad \dots\dots\dots (6.1-8)$$

The emitted Heat due to Natural Convection Q_2 is

$$Q_2 = (h_v \cdot A_v + h_h \cdot A_h) \cdot (t - t_o) \quad \dots\dots\dots (6.1-9)$$

(4) Calculation of the maximum temperature t_{\max}

When the air temperature is 38°C , each value is,

$$\begin{aligned} L &= 1.8 & [\text{m}] \\ g &= 1.27 \times 10^8 & [\text{m}/\text{h}^2] \\ k &= 0.0271 & [\text{kcal}/\text{mh}^{\circ}\text{C}] \\ \beta &= 1/(273+38) = 3.22 \times 10^{-3} & [1/\text{K}] \\ \Delta t &= t_{\max} - t_o & [^{\circ}\text{C}] \\ \nu &= 0.0623 & [\text{m}^2/\text{h}] \\ a &= 0.0882 & [\text{m}^2/\text{h}] \end{aligned}$$

Hence, by equations (6.1-6), (6.1-5), and (6.1-3),

$$Pr = \nu / a = 0.0623 / 0.0882 = 0.706$$

$$\begin{aligned} Gr &= g \cdot \beta \cdot L^3 \cdot \Delta t / \nu^2 \\ &= 1.27 \times 10^8 \times 3.22 \times 10^{-3} \times 1.8^3 \times \Delta t / 0.0623^2 \\ &= 6.14 \times 10^8 \times \Delta t \end{aligned}$$

$$\text{Nu} = 0.13 \cdot (\text{Gr} \cdot \text{Pr})^{1/3} = 98.4 \times \Delta t^{1/3}$$

Thus, using equation (6.1-4),

$$h_v = \frac{\text{Nu}_v \cdot k}{L} = 1.481 \times \Delta t^{1/3} \quad [\text{W}/\text{m}^2 \cdot \text{K}]$$

and

$$h_h = \frac{\text{Nu}_h \cdot k}{L} = 1.595 \times \Delta t^{1/3} \quad [\text{W}/\text{m}^2 \cdot \text{K}]$$

The thermal balance in the steady state is $Q_{\text{in}} = Q_{\text{out}}$. The convergence calculation for the difference of temperatures Δt , using Equations (6.1-1), (6.1-2), (6.1-9) and the heat transfer coefficient h , leads to the maximum temperature t_{max} .

$$t_{\text{max}} = 62 \text{ } [^{\circ}\text{C}]$$

The value of 65°C is adopted here as a conservative figure.

B.6.2 Outline of “TRUMP” --General purpose program for heat transfer

(1) General

“TRUMP” is a program developed in 1968 by the Lawrence Livermore Laboratory for heat transfer calculations based on a node method.

(2) Functions

The program “TRUMP” is designed to handle heat generation, chemical reactions, phase changes, and heat transfer. This program can cover 3-dimensional objects by dividing them into elements by means of rectangular, cylindrical, rotating body or polar coordinates.

Material properties such as heat transfer coefficient and specific heat are given as functions of temperature or time.

The program can handle heat transfer between elements resulting from thermal conduction, natural convection, forced convection, and radiation as well as that resulting from natural or forced convection and radiation as boundary condition. In this program, boundary temperatures can be expressed as functions of time. Initial temperature can vary with position in the space.

“TRUMP” outputs can be obtained, such as temperature distribution for determined time points and thermal balance for each element.

(3) Calculation methods (see (II)-Fig. B. 5)

The “TRUMP” solves simultaneous partial differential equations that have four independent variables regarding space coordinates and time as well as a total of three dependent variables, temperature and two densities of reactant. In case of normal three dimensions, the equations for heat generation, thermal conduction accompanied by chemical reactions and mass transfer are given in the form of normal vector operations:

$$\begin{aligned}\frac{DT}{Dt} &= \frac{\delta T}{\delta t} + \mathbf{v} \cdot \nabla T \\ &= \frac{1}{\rho C} \cdot \nabla \cdot \mathbf{K} \nabla T + G - \frac{Q_a}{C} \cdot \frac{\delta a}{\delta t} - \frac{Q_b}{C} \cdot \frac{\delta b}{\delta t}\end{aligned}$$

$$\begin{aligned}\frac{Da}{Dt} &= \frac{\delta a}{\delta t} + \mathbf{v} \cdot \nabla a \\ &= -a \cdot \exp \left(Z_a - \frac{E_a}{R \cdot T} \right)\end{aligned}$$

$$\begin{aligned}\frac{Db}{Dt} &= \frac{\delta b}{\delta t} + \mathbf{v} \cdot \nabla b \\ &= -b \cdot \exp \left(Z_b - \frac{E_b}{R \cdot T} \right)\end{aligned}$$

$$K_1 \cdot \left(\frac{\delta T_1}{\delta r} \right)_i = h_i \cdot (T_{2i} - T_{1i}) = K_2 \cdot \left(\frac{\delta T_2}{\delta r} \right)_i$$

$$h_i = h_{i0} + h_{ic} [(T_{2i} - T_{1i})^2]^{Pi/2} + \rho \cdot F_i (T_{1i} + T_{2i}) \cdot (T_{1i}^2 - T_{2i}^2)$$

The conductance h_i for the boundary surface is expressed in a common form that takes into account contact conductance, natural convection, forced convection, and radiation. ρ is the Stefan-Boltzmann constant and F is the overall radiation morphological coefficient.

$$K \cdot \left(\frac{\delta T}{\delta r} \right)_s = U_{sb} \cdot (T_b - T_s)$$

where T_b : external temperature

U_{sb} : surface conductance.

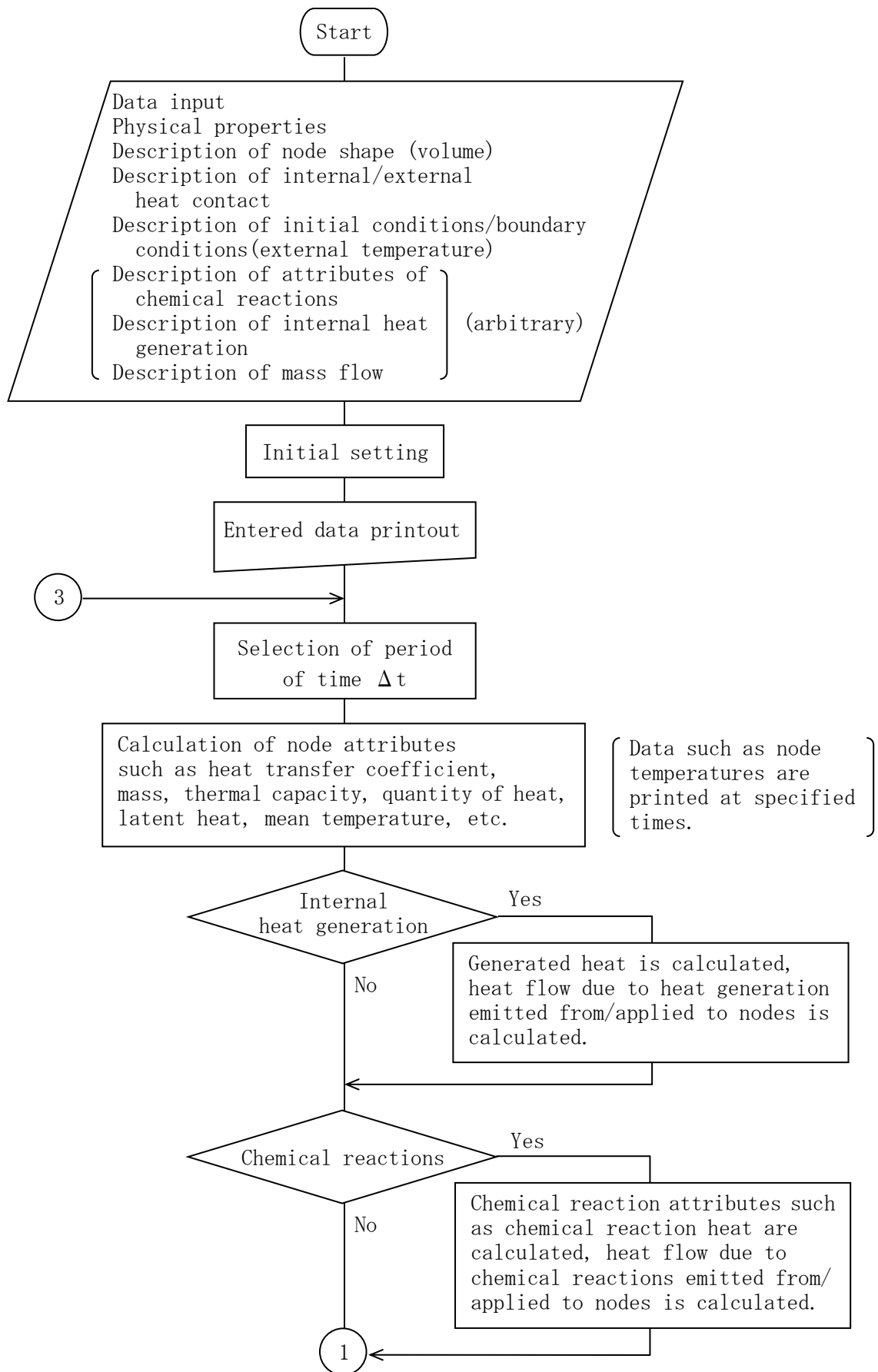
As in the case of mass phase, U_{sb} is

$$U_{sb} = h_{so} + h_{sc} \cdot [(T_b - T_s)^2]^{Pi/2} \\ + \rho \cdot F_b \cdot (T_s + T_b) \cdot (T_s^2 + T_b^2)$$

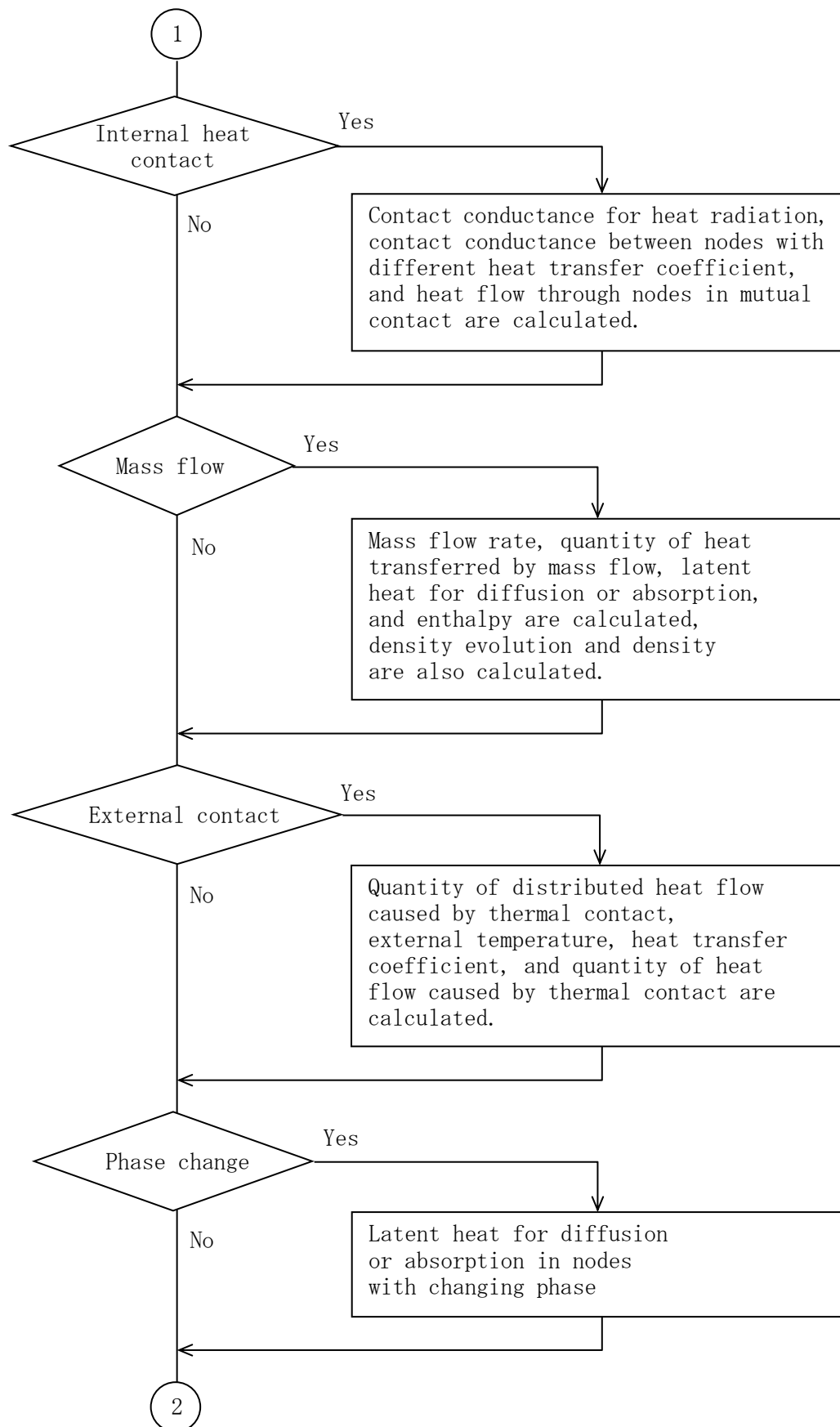
The “TRUMP” solves actual equations in relation to minute periods of time. In fact, the time differential $\delta u / \delta t$ should be replaced by $(u' - u) / \Delta t$ in the preceding equation. U' and U are the initial and final value of the period of time Δt .

(4) Utilization of “TRUMP”

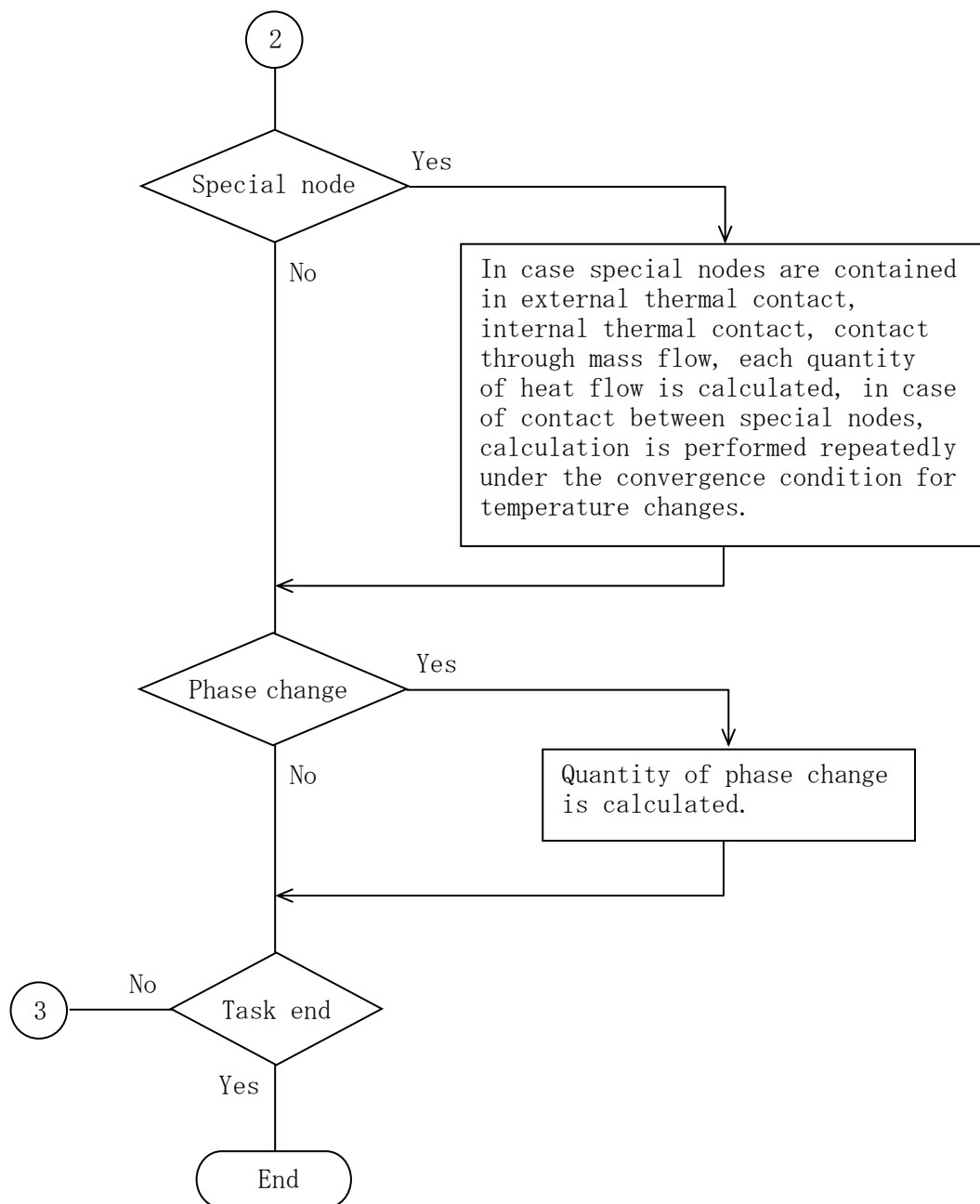
The “TRUMP” program, developed by the Lawrence **Livermore** Laboratory, has been and is being used in many laboratories in the United States.



(II)-Fig. B. 5 "TRUMP" flowchart (1/3)



(II)-Fig. B. 5 "TRUMP" flowchart (2/3)



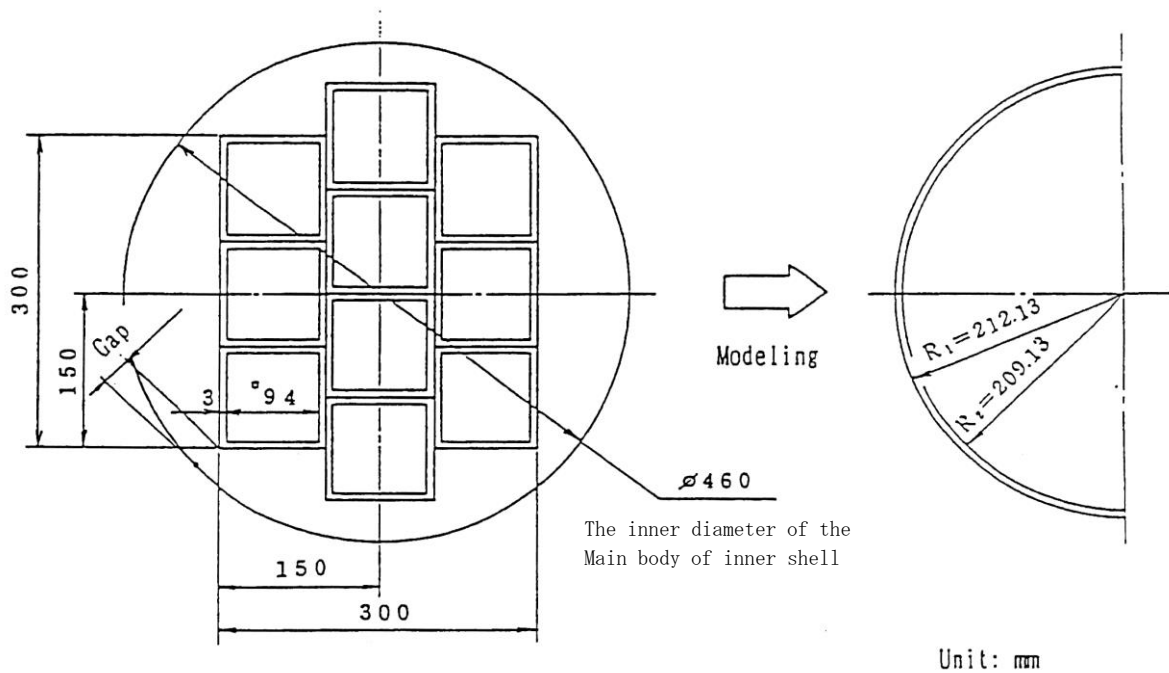
(II)-Fig. B. 5 “TRUMP” flowchart (3/3)

B.6.3 Input data for “TRUMP” used for temperature calculations for accident test conditions

(1) Modeling of fuel basket (see (II)-Fig.B.6)

The fuel basket was modeled to a cylindrical shape the wall thickness of which is equal to the smallest gap between the inner shell and the fuel basket.

The heat capacity of the fuel basket was corrected to be equivalent by compensating the specific weight.



(II)-Fig.B.6 Fuel basket model

(a) The outside radius R_1 of the cylindrical model R_1 is,

$$R_1 = R - G$$

where R : Inside radius of inner shell, $R = 230$ [mm]

$$G: \text{Gap (minimum)}, G = 230 - 150 \times \sqrt{2} \\ = 17.87 \text{ [mm]}$$

$$R_1 = 230 - 17.87 \\ = 212.13 \text{ [mm]}$$

(2) Heat transfer between package outer surface and ambient environment

(a) Convection heat transfer coefficient

The heat transfer coefficient for natural convection on the outer surface of the package is obtained by McAdams equation⁵⁾,

(i) Outer surface of vertical cylinder

$$Gr = \frac{g \cdot \beta \cdot L^3 \cdot \Delta t}{\nu^2} \quad \dots (6.3-1)$$

$$Nuv = 0.13 \cdot (Gr \cdot Pr)^{1/3} \quad [10^9 < Gr \cdot Pr < 10^{12}] \quad \dots (6.3-2)$$

$$h = \frac{Nuv \cdot k}{L} \quad \dots (6.3-3)$$

(ii) Upper horizontal, flat surface

$$Gr = \frac{g \cdot \beta \cdot L^3 \cdot \Delta t}{\nu^2}$$

$$Nuh = 0.14 \cdot (Gr \cdot Pr)^{1/3} \quad [2 \times 10^7 \cdot < Gr \cdot Pr < 3 \times 10^{10}] \quad \dots (6.3-4)$$

$$h = \frac{Nuh \cdot k}{L}$$

Where

h : Convection heat transfer coefficient [cal/cm² s°C]

k : Heat transfer coefficient of air [cal/cm s°C]

During fire: 7.094×10^{-4} (at 800°C)

After fire: 2.706×10^{-5} (at 38°C)

L : Representative length [cm]

Vertical surface: 152 [cm]

Horizontal surface: 65 [cm]

g : Gravitational acceleration;

$$g = 980 \quad [\text{cm/s}^2]$$

β : Coefficient of cubical expansion [1/K]

$$\text{During fire: } 1/(273+800) = 9.23 \times 10^{-4}$$

$$\text{After fire: } 1/(273+38) = 3.22 \times 10^{-3}$$

ν : Coefficient of kinematic viscosity [cm²/s]

$$\text{During fire: } 1.37$$

After fire: 0.173

Gr: Grashof number

Pr: Prandtl number; Pr = 0.706

Nu: Nusselt number

(II)-Table B.14 shows the results of a calculation in which the preceding values were substituted for the corresponding letters of Equations (6.3-1) to (6.3-4)

(II)-Table B.14 Convection heat transfer coefficient
between package surface and ambient environment

Position Condition	Vertical cylindrical surface	Upper horizontal surface
During fire	$6.459 \times 10^{-5} \cdot \Delta t^{1/3}$	$6.956 \times 10^{-5} \cdot \Delta t^{1/3}$
After fire	$1.480 \times 10^{-4} \cdot \Delta t^{1/3}$	$1.594 \times 10^{-4} \cdot \Delta t^{1/3}$

(b) Radiation heat transfer

The radiation morphological coefficient is

$$F_{12} = \frac{1}{1/\epsilon_1 + 1/\epsilon_2 - 1} \quad \dots (6.3-5)$$

Where F_{12} : Radiation morphological coefficient

ϵ_1 : Radiation factor for surface No. 1

ϵ_2 : Radiation factor for surface No. 2

(II)-Table B.15 shows the radiation factors for both surfaces and the radiation morphological coefficient obtained using Equation (6.3-5).

(II)-Table B.15 Radiation factor and radiation
morphological coefficient

Condition		During fire	After fire
Item			
Radiation factor	Package Surface	0.8	0.6
	Ambient environment	0.9	0.1
Radiation morphological coefficient		0.735	0.6

(3) Heat transfer between basket and inner cylinder

(a) Convection heat transfer coefficient

The heat transfer coefficient for the closed fluid layer between vertical, concentric cylinders²⁾ is obtained by means of the following equations.

$$\text{Nu} = 1.0 \quad [\text{Ra} < 10^3] \quad \dots\dots\dots (6.3-6)$$

$$\text{Nu} = 0.28 \cdot \text{Ra}^{1/4} \cdot (\text{L}/\text{D})^{1/4} \quad [10^3 < \text{Ra} < 10^7] \quad \dots\dots\dots (6.3-7)$$

$$\text{Ra} = \frac{g \cdot \beta \cdot \text{D}^3 \cdot \Delta t}{a \cdot \nu} \quad \dots\dots\dots (6.3-8)$$

$$h = \frac{\text{Nu} \cdot k}{\text{D}} \quad \dots\dots\dots (6.3-9)$$

where

Nu : Nusselt number

Ra : Raleigh number

g : Gravitational acceleration,

$$g = 980 \text{ [cm/s}^2\text{]}$$

β : Coefficient of cubical expansion,

$$\beta = 1/(273+250) = 1.912 \times 10^{-3} \text{ [1/K]}$$

D : Thickness of fluid layer,

$$D = 23 - 21.213 = 1.787 \text{ [cm]}$$

Δt : Temperature difference between inner and outer cylinder [$^{\circ}\text{C}$]

a : Thermal diffusivity, $a = 6.194 \times 10^{-1} \text{ [cm}^2\text{/s]}$

ν : Coefficient of kinematic viscosity,

$$\nu = 0.426 \text{ [cm}^2\text{/s]}$$

L : Length of fuel basket [cm]

k : Heat transfer coefficient,

$$k = 4.175 \times 10^{-4} \text{ [cal/cm s}^{\circ}\text{C]}$$

h : Heat transfer coefficient for natural convection,

$$\text{[cal/cm s}^{\circ}\text{C]}$$

$$\text{Ra} = \frac{980 \times 1.912 \times 10^{-3} \times 1.787^3}{6.194 \times 10^{-1} \times 0.426} \Delta t$$

$$= 40.52 \times \Delta t$$

When 200 [°C] is substituted for Δt the Reynolds number Ra is,

$$Ra = 40.52 \times 200 = 8.104 \times 10^3 \quad [10^3 < Ra < 10^7]$$

Nu is obtained by Equation (6.3-7)

$$\begin{aligned} Nu &= 0.28 \cdot Ra^{1/4} \cdot (L/D)^{-1/4} \\ &= 0.28 \times (8.104 \times 10^3)^{1/4} \times (125.6/1.787)^{-1/4} \\ &= 0.918 \end{aligned}$$

Thus, using Equation (6.3-9), the heat transfer coefficient for natural convection h is

$$\begin{aligned} h &= \frac{Nu \cdot K}{D} = \frac{0.918 \times 4.175 \times 10^{-4}}{1.787} \\ &= 2.145 \times 10^{-4} \quad [\text{cal/cm}^2 \cdot \text{s} \cdot ^\circ\text{C}] \end{aligned}$$

(b) Radiation heat transfer

The radiation morphological coefficient for the gas layer between concentric cylinders is obtained using the following equation:

$$F_{12} = \frac{1}{1/\epsilon_1 + (A_1/A_2)(1/\epsilon_2 - 1)} \quad \dots\dots\dots (6.3-10)$$

$$A_1 / A_2 = r_1 / r_2 \quad \dots\dots\dots (6.3-11)$$

where

F_{12} : Radiation morphological coefficient

ϵ_1 : Radiation factor for surface No.1; $\epsilon_1 = 0.4$

ϵ_2 : Radiation factor for surface No.2; $\epsilon_2 = 0.4$

r_1 : Inside radius of external cylinder; $r_1 = 230$ [mm]

r_2 : Outside radius of internal cylinder; $r_2 = 212.13$ [mm]

$$\begin{aligned} F_{12} &= \frac{1}{1/0.4 + (230/212.13)(1/0.4 - 1)} \\ &= 0.242 \end{aligned}$$

(4) Entry of Heat due to Fire Resulting from Combustion of Hard Polyurethane Foam

The package was analyzed on the assumption that the heat resulting from combustion of hard polyurethane foam (23.45 kJ/g) exists on the outer surface of the package in the form of fire.

B.6.4 Internal pressure of the package

The internal pressures of the package under normal and accident test conditions are calculated.

(1) Operating pressures

The operating pressure of the air in the packaging is obtained.

(a) Initial pressure

The initial pressure in the packaging is equal to the atmospheric pressure (=0.101 MPa ·abs).

(b) P_1

The pressure resulting from air expansion P_1 is obtained using the following equation based on the Boyle-Charles law.

$$P_1 = P_0 \frac{T_1}{T_0} \dots\dots\dots (6.5-1)$$

where

P_0 : initial pressure (at 20°C);

$P_0 = 0.101$ [MPa]

T_0 : Initial temperature; $T_0 = 273 + 20 = 293$ [K]

T_1 : Air temperature under specific conditions [K]

(II)-Table B.16 shows the results of this calculation.

(II)-Table B.16 Calculation result for packaging internal pressure

Position	Air in the packaging	
Test conditions	Normal	Accident
Pressure (MPa· [gauge])	0.016	0.065
Temperature(°C)	65	209.9

(2) Design pressures

The conservative design pressures shown in (II)-Table B.17 are used for the various parts of the package evaluation.

(II)-Table B.17 Design pressures for specific test conditions

	Inside the packaging
Normal test conditions	0.0981 MPa•[gauge]
Accident test conditions	0.0981 MPa•[gauge]

B.6.5 Validity Justification of thermal analysis methods

This section describes the examination of the analyses simulating the fire test (herein referred to as “analyses”) on the basis of the results of the fire test on a prototype packaging, analyses carried out to verify the justifiability of the thermal analysis methods described in this section.

(1) Prototype Packaging and Test Methods

- Prototype packaging: see (II)-Fig.G.1.
- Test methods: see (II)-G-6

(2) Examination of analysis results

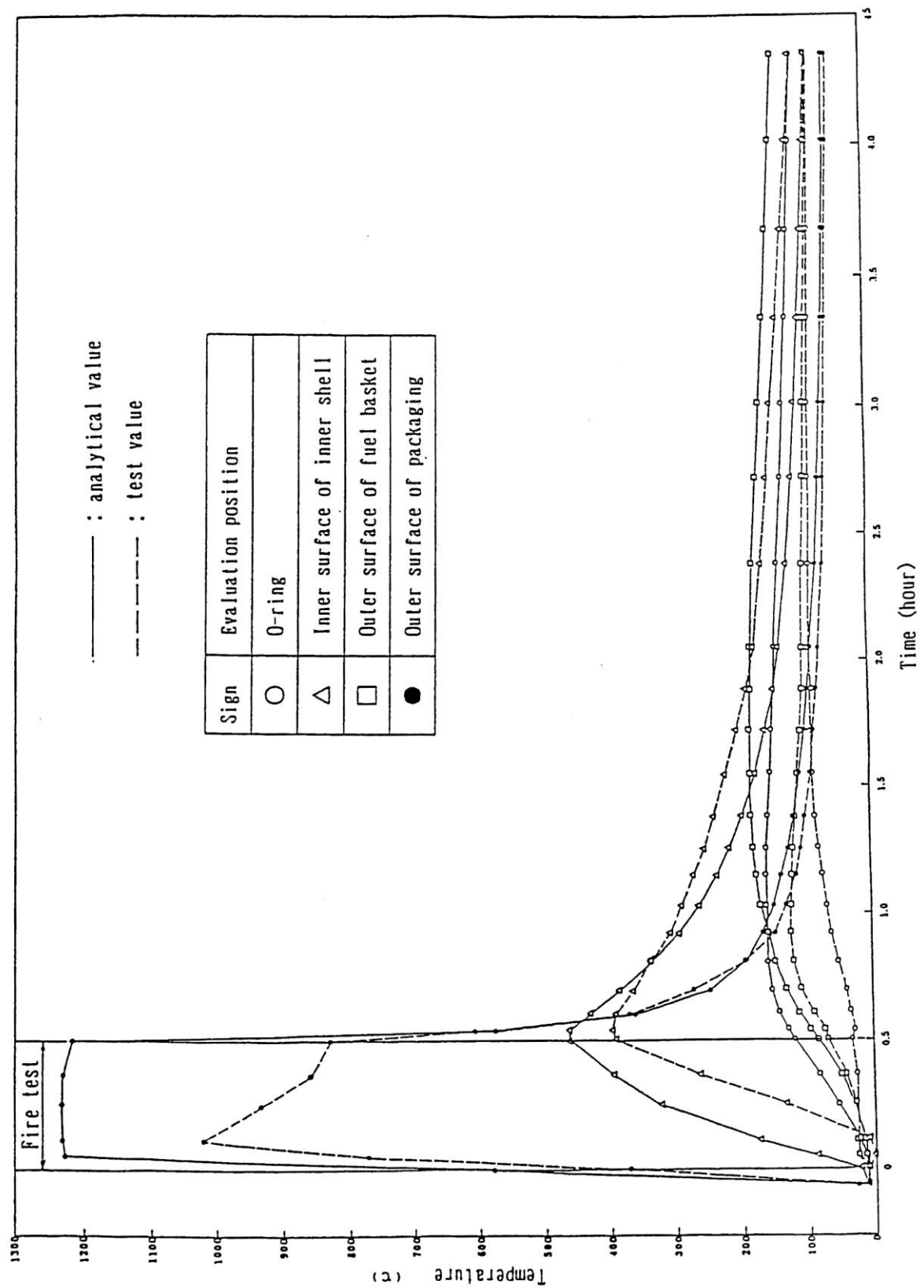
(II)-Table B.18 and (II)-Fig.B.7 show the test and analysis results.

Analyses were performed using the conditions described in Section B.6.3. The measurements recorded in the tests of prototype packaging were used as input data for the initial temperature and the temperatures in furnace in order to simulate actual test conditions. This indoor test does not take into account solar radiation heat.

As shown in (II)-Table B.18 and (II)-Fig.B.7, the analytical values are conservative and the thermal analysis methods shown in Sections B.5 and B.6.3 are valid.

(II)-Table B.18 Comparison of prototype packaging test results
with analysis results

Conditions Evaluation position	Maximum temperature (°C)		Time required before the maximum temperature hour(h)	
	Test	Analysis	Test	Analysis
Near O-ring	88.6	161.0	2.0	1.0
Inner surface of inner shell	396.2	464.1	0.6	0.5
Outer surface of fuel basket	123.3	182.5	1.0	1.6
Outer surface of packaging	1051.6	1229.7	0.1	0.1



(II)-Fig.B.7 Comparison of prototype packaging test results with analysis results

B. 6. 6 Bibliography

- (1) “Study on an application of inelastic structures analyzing methods (I),” a report at Section Meeting for Application of Inelastic Structures Analyzing Methods (EPIOC), Mechanical Engineering society of Japan, 1977.
- (2) “Material for Heat Transfer Engineering, III Edition,” Mechanical Engineering Society of Japan, 1975.
- (3) In-house data of Nihon Asbestos Co., Ltd.
- (4) In-house data of Nippon Valqua Industries, Ltd.
- (5) McAdams, “Heat transmission.”
- (6) In-house data of Mitsubishi Heavy Industries, Ltd.

(II)-C Containment analysis

(II)-C. Containment analysis

C.1 General

The following part relates to the sealing performances of this packaging tested under normal and accident test conditions. The containment system is considered as the part which ensures the sealing of the packaging. The containment system of this packaging consists of an inner shell comprising a main body and a lid, and the contact between the main body and the lid is sealed by a silicon rubber O-ring (inner shell lid O-ring).

The leakage rate of the containment system is checked by leak tightness test and must meet the reference value during the manufacturing process and the maintenance period. The leakage rate of the O-ring of the inner shell lid is checked by a leak tightness test carried out before shipment of the package and must be confirmed meet the reference value.

C.2 Containment system

C.2.1 Containment system

(1) Structure

The containment system of this packaging is composed, as shown in (II)-Fig. C.1, of an inner shell main body and an inner shell lid.

(2) Materials

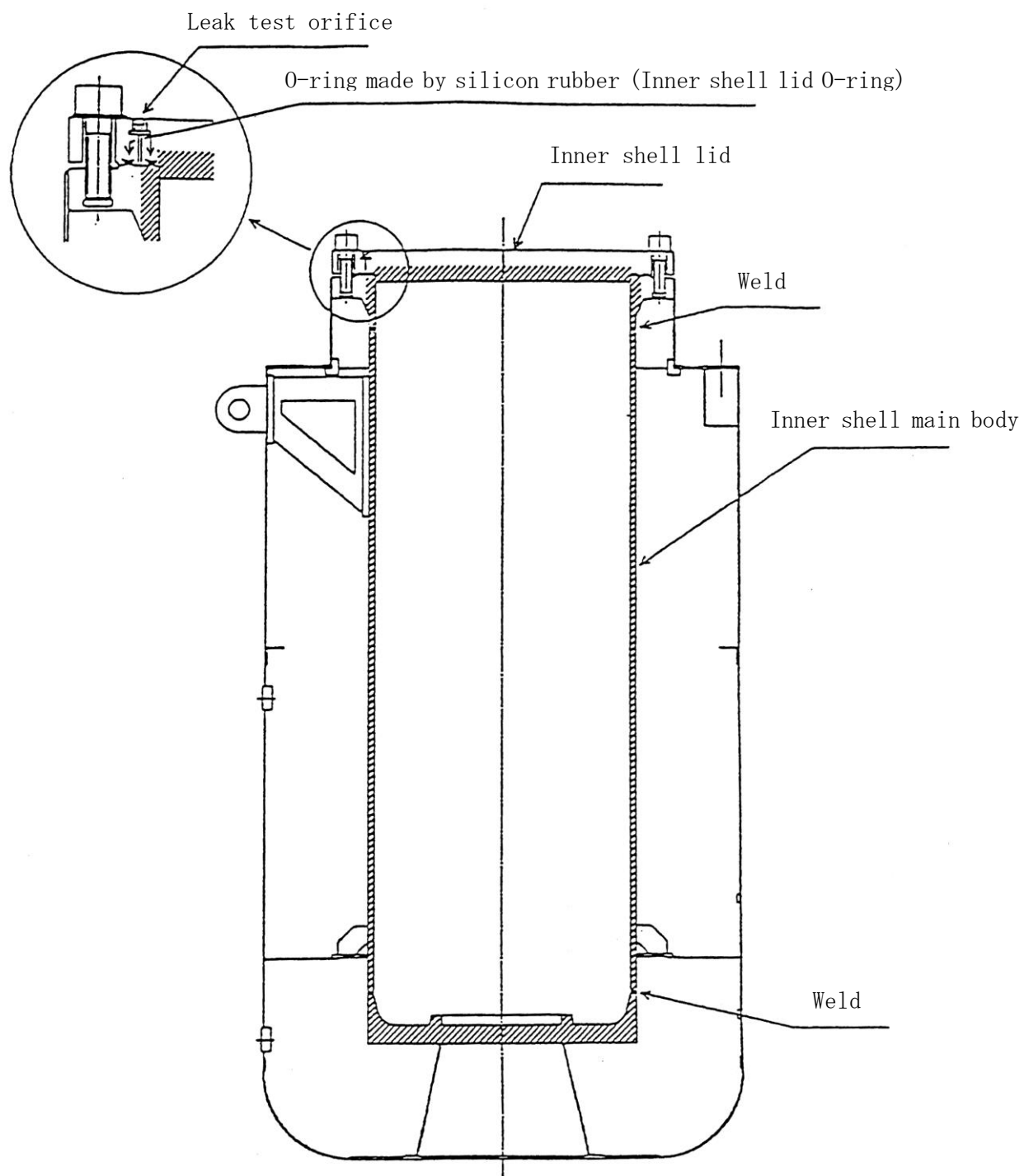
The material used for the fabrication of the main body and the lid of the inner shell is stainless steel, and the sealing part of the inner shell lid is a silicon rubber O-ring.


(3) Design pressure and design temperature

As shown in the (II)-Table C.1, the leakage rate is evaluated according to the design pressure and design temperature.

(II)-Table C.1 Design pressure and design temperature
of containment system

Conditions	Item	Containment System
Normal test conditions	Design pressure (MPa[gauge])	0.0981
	Design temperature (°C)	65
Accident test conditions	Design pressure (MPa[gauge])	0.0981
	Design temperature (°C)	209.9



 : The range that the surrounded with a slanted line shows a seal border.

(II)-Fig.C.1 Containment boundary of packaging

(4) Seal

Since the inner shell lid is covered by the outer shell lid, there is no possibility of the clamping bolts being removed inadvertently.

Moreover, after installation of the clamping bolts to fix the lid to the main body of the inner shell, the lid is sealed and locked.

(5) Manufacture and checking

Manufacture and checking of the structural parts of the containment system are conducted by a suitable method which ensures sealing performances.

C.2.2 Penetration of the containment system

Since the only opening of this packaging is the inner shell lid, this item is not applicable.

C.2.3 Gasket and weldings of the containment system

(1) Containment system gasket

For a gasket of the containment system gasket a silicon rubber O-ring is used. With this O-ring no chemical or electrical reaction should occur, as explained in (II)-A.4.1. Moreover, this ring shows excellent sealing performances under the pressures and temperatures in normal and accident test conditions.

(2) Specifications of the gasket (C-4) (C-3)

The dimensions and material of the gasket are shown in (II)-Table C.2

The silicon rubber O-ring can maintain the sealing performance of the inner shell lid under the normal and special test conditions and at the lowest temperature of use, with its heat-resistant property (See B.3 Specifications of components) and cold-resistant property (See A.4.2 Low temperature strength).

(II)-Table C.2 The dimensions and material of the gasket

Positions		dimensions	material	Note
Inner shell lid	Inner side	$\phi 5.4 \times \text{I.D. } 473$	silicone	O-ring
	Outer side	$\phi 5.4 \times \text{I.D. } 513$	rubber	

(3) Weldings

The weldings of the flange, of the barrel, and of the bottom plate are performed as explained in Chapter (III)-A. Weldings are subjected to a non-destructive test during the fabrication process, as explained in Chapter (III)-B, the integrity of the weldings is checked and a pressure resistance test is carried out to check the absence of leakage.

C.2.4 Lid

The inner shell lid is equipped with 2 drains for the 2 silicon rubber O-rings, as shown in the (II)-Fig.C.1. Moreover, the inner shell lid has been designed to be resistant under normal and accident test conditions and to maintain its performances. To preserve the sealing performances of the packaging, the inner shell clamping bolts are tightened to an appropriate torque as shown in (II)-Table C.3.

(II)-Table C.3 Inner shell clamping bolt

Designation	Size	Number	Tightening torque (N•m)
Inner shell clamping bolts	M24	16	Approx. 280

C.3 Normal test conditions

The integrity of the containment system of this package remains unchanged after an impact under normal test conditions as required for all type B(U) packages, and as shown in the results of structural analyses in (II) – A. Moreover, the results of thermal analyses in (II) – B show that variations in pressure or temperature under normal test conditions do not affect the integrity of the containment system.

Therefore, as the sealing performances of the containment system remain unchanged under normal test conditions, in these analyses, the evaluation of the sealing performances based on the leak tightness test of the O-ring of the inner shell lid which must meet the reference value, conducted before shipment of the package, shows that the leakage rate of radioactive substances under normal test conditions is lower than the IAEA regulation standard value.

C.3.1 Leakage of radioactive materials

C.3.1.1 Volume of Leakage from the Inner Shell

The containment system is checked against leakage by a leak tightness test carried out during the manufacturing process and the maintenance period.

For sealing performance, it is confirmed, further, on each shipment that the leakage rate of the package is lower than the reference value.

The leakage rate of radioactive materials is analyzed, on the assumption that, regarding the air supplied to the seal of inner shell lid on a leak tightness test, the pressure change corresponding to the maximum permissible leakage rate is detected in a certain time.

Radioactive materials exist in the gas of containment system and its leakage rate is different from that obtained from the air leakage rate.

Therefore, leakage rate of the gas under normal test conditions is first determined from the maximum permissible air leakage rate and then the obtained

leakage rate is applied to acquire leakage rate of the radioactive materials from concentration of radioactive materials in the gas. It is finally confirmed that the leakage rate of the radioactive materials is below the reference values specified by the regulation and notification.

(1) Maximum permissible leakage rate of the air

The maximum permissible leakage rate of the air L_a specified in design criteria for containment analysis is given as the leakage rate of the air in (II)-Table C.4

(II)-Table C.4 Maximum permissible leakage rate of the air

Item	Containment boundary (inner shell lid O-ring)
L_a : maximum permissible leakage rate of the air(std cm ³ /s)	1.08×10^{-1}

(2) Leakage rate at leak tightness test and the test conditions

(a) Leakage rate at leak tightness test

Leakage rate at leak tightness test by pressure drop is given by the following formula.

$$L_R = \frac{VT_s}{60HP_s} \left(\frac{P_1}{T_1} - \frac{P_2}{T_2} \right)^{1)} \dots\dots\dots (C.3-1)$$

where,

L_R : Leakage rate(std cm³/s) under normal condition at 25°C, 0.101MPa(1 atm abs.)

V: Volume of the testing system(100m³)

H: Testing time

T_s : Reference temperature 298(K)

T_1 : Air temperature at the beginning of the test(K)

T_2 : Air temperature at the end of the test(K)

P_s : eference pressure(0.101MPa, (1 atm abs.))

P_1 : Air pressure at the beginning of the test(MPa)

P_2 : Air pressure at the end of the test (MPa)

The formula (C-31) above will determine the air leakage rate with the following leak tightness test conditions, and the deduced value will be confirmed to be lower than the maximum permissible leakage rate, the reference value.

(b) Leak tightness test conditions

(i) Air pressure at the beginning of the test is fixed at 0.493 (MPa)

(ii) Air pressure at the end of the test is fixed at 0.297 (MPa)

(iii) Testing time is fixed at 30 min.

(iv) In calculation the temperature is set $T_1=T_2=T_S=298$ (K) (25°C).

These conditions are applied to the formula (C-31) to obtain the maximum permissible air leakage rate. The results of calculation is given in (II)-Table C.4.

(v) In consideration of the conditions (i) to (iv) above and the volume of the testing system, the testing time H and pressure drop $\Delta P(P_1-P_2)$ is fixed to confirm that the air leakage rate $L_R(L_R=\sum L_{Ri})$ at O-ring of inner shell lid is lower than the maximum permissible air leakage rate $L_{R(}L_R=2.21 \times 10^{-2} \text{ cm}^3/\text{s}$ at 0.493 MPa (1.08 std cm^3/s), 298K).

(3) The maximum gas leakage rate under normal test conditions

The maximum gas leakage rate under normal test conditions is obtained on the basis of the maximum permissible air leakage rate L_{Rt} as follows.

(a) Diameter of leak

The leak is assumed to be a round hole which crosses the sealing part along the shortest path. Fluid is considered to pass through the leak in the form of free molecular flow or continuous flow and its leakage rate is given by the following formula.

$$L=(F_c+F_a)(P_u-P_d)^{2/3} \dots\dots\dots (C.3-2)$$

where,

L : Volume leakage rate at pressure P_a (cm^3/s at P_a, T_a)

P_a: Average pressure of flow (M Pa)

$$P_a = \frac{1}{2}(P_u + P_d) \dots\dots\dots (C. 3-3)$$

T_a: Average temperature of fluid

P_u: Pressure on upstream side

P_d: Pressure on downstream side

F_c: Flow heat conduction coefficient for continuous flow(cm³/MPa • s)

F_m: Flow heat conduction coefficient for free molecular flow(cm³/MPa. s)

$$F_c = 2.49 \times 10^{-2} \times \frac{D^4}{a\mu} \dots\dots\dots (C. 3-4)$$

$$F_m = 3.81 \times 10^3 \times \frac{D^3 \sqrt{\frac{T}{M}}}{aPa} \dots\dots\dots (C. 3-5)$$

Where,

D: Diameter of leak (cm)

a: length of leak (cm)

μ : Viscosity coefficient of the air(MPa. s)

T: Temperature of fluid(K)

M: Molecular weight(g/mol)

Diameter of leak hole is obtained by the following formula and the formula (C-3-2)

$$L = L_R i \cdot \frac{P_s}{P_a} \cdot \frac{T_a}{T_s} \dots\dots\dots (C. 3-6)$$

Where,

L_R i: Air leakage rate at containment boundary(std cm³/s)

T_a: Average temperature(=T^s) (K)

The maximum diameter of leak of inner shell lid on leakage rate test is given in (II)-Table C.5.

Note: the formula ANSI 4.5 is converted into SI unit.

(II)-Table C.5 The maximum radius of leak hole on leakage rate test

Items	Positions	0-ring parts
L_R i: Air leakage rate at containment boundary(std cm^3/s)		1.08×10^{-1}
P_u : Pressure on upstream side (M P_a)		0.493
P_d : Pressure on downstream side (M P_a)		0.101
P_a : Average pressure of flow (M P_a)		0.297
T_a . T: Temperature of the air(K)		298
L: Air leakage rate on leak tightness test(cm^3/s at P_a , T_a)		3.673×10^{-2}
μ : Viscosity coefficient of the air(MPa.s)		1.85×10^{-11} at 25°C^{*1}
a: length of leak hole(cm)		0.54 ^(note)
M: Molecular weight(g/mol)		29.0
F_c : Thermal conductivity coeffim $^3/\text{MPa} \cdot \text{s}$)		$2.49 \times 10^9 D^4$
F_m : Thermal conductivity coefficient for free molecular flow		$7.61 \times 10^4 D^3$
D: Diameter of leak (cm)		2.490×10^{-3}

Note: Diameter of cross section of 0-ring is employed.

*1 : Since viscosity coefficient of the air increases with temperature, it is conservative to employ the low temperature.

(b) The maximum gas leakage rate under normal test conditions

The maximum gas leakage rate under normal test conditions is obtained by substituting the values of pressure, gas and the maximum diameter of leak under normal test conditions into the formula (C.3.2) to (C.3.5).

Gas leakage rate L_x calculated from (C.3.2) is converted to leakage rate $L_{s,x}$ under normal test conditions, at 25°C, 0.101MP abs (1 atm abs), by the following formula.

$$L_{s,x} = L_x \times \left(\frac{P_{a,x}}{0.101} \times \frac{298}{T_{a,x}} \right) \dots\dots\dots (C.3-7)$$

where,

Subscript x: Normal test conditions

but it is assumed that $T_{a,x} = T_{u,x}$

Gas leakage rate under normal test conditions is provided in (II)-Table

C. 6. The maximum gas leakage rate at O-ring is employed for calculation.

(II)-Table C.6 The maximum gas leakage rate under normal test conditions

Item	Position	Containment boundary (O-ring of inner shell lid)
D: Diameter of leak (cm)		2.490×10^{-3}
a: Length of leak (cm)		0.54
μ : Viscosity coefficient of the gas (MPa.s)		1.85×10^{-11} at 25°C*1
$P_{u,x}$: Pressure of containment system under normal test conditions (MPa abs)		0.199
$P_{d,x}$: External pressure under normal test conditions (MPa abs)		0.060
$T_{u,x}$: Gas temperature under normal test conditions (K)		338
M: Molecular weight (g/mol)		29
L_x : Leakage rate under normal test conditions (cm ³ /s at $P_{a,x}$ $T_{a,x}$)		1.38×10^{-2}
$L_{s,x}$: Leakage rate under normal test conditions (cm ³ /s at 25°C 0.10MPa)		1.55×10^{-2} (5.58×10^1 cm ³ /h)

*1 : Since viscosity coefficient of the air increases with temperature, it is conservative to employ the low temperature

C.3.1.2 Evaluation of the volume of leakage radioactive substances

- (1) In transporting the fresh fuel elements and critical assembly fuel
 - (a) Evaluation of the radioactive substances contained in the inner shell concerning the leakage.

Since there is no possibility of degradation of the fuel plates under normal test conditions, as described in part (II)-A, it is considered that there is no leakage of the enriched uranium contained in the fuel plates. It is supposed that the only radioactive substances that may have leaked are the uranium particles which adhere to the surface of the fuel elements during the manufacturing process, in other words, uranium surface contamination. It is supposed that the level of contamination is 8.00×10^{-2} Bq/100cm²[²³⁵U] ($1 \mu\text{g} \cdot ^{235}\text{U}/100\text{cm}^2$) for the whole surface of the fuel elements, which is the reference value of the surface contamination test during manufacturing process.

It is supposed that the contaminated surface uranium are 93% enriched uranium, 45% enriched uranium, 20% enriched uranium and 93% enriched uranium of the degraded uranium for which the rate of $^{234}\text{U}/^{235}\text{U}$ is at its maximum level.

The weight of radioactive nuclides of 93% enriched uranium adhering to one fuel element is calculated according to the usual method as follows.

- (i) Quantity of ^{235}U : This quantity is calculated by using the level of 8.00×10^{-2} Bq/100cm² and of the whole surface of the fuel element ($1 \mu\text{g} \cdot ^{235}\text{U}/100\text{cm}^2$).
- (ii) Quantity of ^{238}U : The quantity of ^{234}U and ^{236}U being considered as nil, the quantity of ^{238}U is calculated by using the lower limit of the tolerance of the enrichment (93.15 ± 0.15 wt%) of ^{235}U calculated in (i).
- (iii) Quantity of ^{234}U and ^{236}U : No weight limit has been fixed for ^{234}U and ^{236}U , because these are decided during the fuel manufacturing.

The quantity of ^{234}U and ^{236}U is calculated using the maximum weight proportion recorded in the past material record and in rounding off these figures (x 2) according to the usual method.

Moreover, the total weight of uranium needed for these calculations is obtained by adding the quantity of ^{235}U calculated in (i) and the quantity of ^{238}U calculated in (ii). The weight proportions of ^{234}U and ^{236}U used for the calculations are shown in the (II)-Table C.7.

The Surface contamination level is shown in (II)-Table C.8.

(II)-Table C.7 Weight proportions of ^{234}U and ^{236}U
used for calculations

Enrichment (wt%)	Isotope	Maximum weight proportions in the mill sheets (wt%)	Weight proportions used for calculations (wt%)
93.15 ± 0.15	^{234}U	1.08	2.2
	^{236}U	0.47	0.94

(II)-Table C.8 Surface contamination level per fuel element

Fuel element	Radioactivity (Bq)				
	^{234}U	^{235}U	^{236}U	^{238}U	Total
JRR-3 Standard Type (Uranium silicon aluminum dispersion type alloy)	1.58×10^3	2.31×10^1	7.00	2.71×10^{-1}	1.61×10^3
JRR-3 Follower Type (Uranium silicon aluminum dispersion type alloy)	8.80×10^2	1.29×10^1	3.90	1.51×10^{-1}	8.97×10^2
JRR 4B Type	9.34×10^2	1.37×10^1	4.14	1.60×10^{-1}	9.52×10^2
JRR 4L Type (Uranium aluminum dispersion type alloy)	9.34×10^2	1.37×10^1	4.14	1.60×10^{-1}	9.52×10^2
JRR-4 (Uranium silicon aluminum dispersion type alloy)	9.34×10^2	1.37×10^1	4.14	1.60×10^{-1}	9.52×10^2
JMTR Standard	1.22×10^3	1.78×10^1	5.41	2.09×10^{-1}	1.24×10^3
JMTR Follower Fuel	8.74×10^2	1.28×10^1	3.88	1.50×10^{-1}	8.91×10^2
KUR Standard & Half Loaded	1.12×10^3	1.64×10^1	4.97	1.93×10^{-1}	1.14×10^3
KUR Special	8.01×10^2	1.17×10^1	3.56	1.38×10^{-1}	8.17×10^2
KUCA Coupon (120 coupons as one fuel element)	3.69×10^2	5.40	1.64	6.35×10^{-2}	3.76×10^2
KUCA Flat (30 plates as one fuel element)	1.25×10^2	1.83×10^1	5.56	2.16×10^{-1}	1.28×10^3

(b) Evaluation of the leakage volume of radioactive substances under normal test conditions.

The uranium responsible for the surface contamination which adheres to the surface of the elements is assumed to be powder. For the evaluation of the leakage rate, this uranium is supposed to be completely separated and uniformly dispersed in the cavity of the inner shell.

The leakage rate under normal test conditions is calculated by multiplying the concentration of each radioactive nuclide existed in the cavity of the inner shell by the leakage rate calculated in C.3.1.13 (b). By using the JRR-3 standard fuel element, (Uranium silicon aluminum dispersion type alloy) which is highest surface uranium contamination fuel, and by calculating the leakage rate of radioactive substances, the results are obtained as shown in (II)-Table C.9.

As shown in the (II)-Table C.6, the level of the leakage rate of radioactive substances under normal test conditions is lower than the standard value.

(II)-Table C.9 Leakage rate of radioactive substances
under normal test conditions

Nuclide	Radioactivity (TBq/cm ³)	Leakage rate (TBq/h)	Standard Value (A ₂ × 10 ⁻⁶) (TBq/h)	Rate
²³⁴ U	1.07 × 10 ⁻¹³	5.97 × 10 ⁻¹²	6 × 10 ⁻⁹	9.96 × 10 ⁻⁴
²³⁵ U	1.56 × 10 ⁻¹⁵	8.71 × 10 ⁻¹⁴	∞	0
²³⁶ U	4.73 × 10 ⁻¹⁶	2.64 × 10 ⁻¹⁴	6 × 10 ⁻⁹	4.40 × 10 ⁻⁶
²³⁸ U	1.83 × 10 ⁻¹⁷	1.02 × 10 ⁻¹⁵	∞	0
Total				1.00 × 10 ⁻³

* : Use 1.48 × 10⁵ cm³ for the inner air volume.

(2) In transporting of lowly irradiated fuel element

(a) Evaluation of radioactive material in the inner shell concerning leak.

As shown in (II)-A, the fuel plate does not failure under the normal test condition, the enriched uranium contained in the fuel plate does not leak.

The radioactive material concerning leak, the surface contaminated uranium, adheres when the fuel element is produced, is similarly assumed as the previous section of C.3.1.2(1), (a).

The water in the reactor is assumed to adhere in a thickness of 1 mm on the all surface of the lowly irradiated fuel element.

Therefore, the radioactive material to be considered in studying the seal function is the radioactive nuclide contained in the water of the reactor.

The leak of the radioactive material is evaluated by assuming that the radioactive concentration of the water in the reactor is $12\text{Bq}/\text{cm}^3$, which is two times of the maximum value of the measured data of the No.1 canal water, obtained for past twenty years.

The radioactive concentration of the water adheres on the fuel element surface is $12\text{Bq}/\text{cm}^3$, the nuclide is ^{60}Co and shown in (II)-Table C.10.

The surface radioactivity per one lowly irradiated fuel element is shown in (II)-Table C.11.

(II)-Table C.10 Nuclide of JMTRC fuel surface water and
radioactive concentration

Nuclide	Radioactive concentration (Bq/cm^3)
^{60}Co	12

(II)-Table C.11 Surface activity per one fuel element of lowly irradiated fuel
element

	Activity (Bq)				
	^{234}U	^{235}U	^{236}U	^{238}U	Total
JMTRC Standard fuel element (Uranium aluminum alloy) (A, B, C type)	1.19×10^3	1.74×10^1	5.28×10^0	2.04×10^{-1}	1.21×10^3
JMTRC Standard fuel element (Uranium aluminum alloy) (B, C type)	1.19×10^3	1.74×10^1	5.28×10^0	2.04×10^{-1}	1.21×10^3
JMTRC Special fuel element (Special A type) (Uranium aluminum alloy)	1.24×10^3	1.82×10^1	5.50×10^0	2.13×10^{-1}	1.26×10^3
JMTRC Special fuel element (Special B type) (Uranium aluminum alloy)	4.65×10^2	6.82×10^0	2.06×10^0	7.98×10^{-2}	4.74×10^2
JMTRC Special fuel element (Special C, Special D type) (Uranium aluminum alloy)	1.27×10^3	1.86×10^1	5.62×10^0	2.17×10^{-1}	1.29×10^3
JMTRC Control rod fuel Follower (HF type) (Uranium aluminum alloy)	8.41×10^2	1.23×10^1	3.73×10^0	1.44×10^{-1}	8.57×10^2
JMTRC Standard fuel element (MA, MB, MC type) (Uranium aluminum dispersion type alloy)	1.19×10^3	1.74×10^1	5.28×10^0	2.04×10^{-1}	1.21×10^3
JMTRC Special fuel element (Special MB, Special MC type) (Uranium aluminum dispersion type alloy)	1.25×10^3	1.83×10^1	5.55×10^0	2.14×10^{-1}	1.27×10^3
JMTRC Fuel follower (MF type) (Uranium aluminum dispersion type alloy)	8.41×10^2	1.23×10^1	3.73×10^0	1.44×10^{-1}	8.57×10^2

(b) Radioactive material leak evaluation under normal test condition

It is similarly assumed as the previous section of C.3.1.2(1), (a) that the all surface contaminated uranium adheres on the fuel surface is separated and uniformly dispersed in the air in the inner container.

The radioactive concentration of the water adheres on the fuel element surface is 12Bq/cm^3 , and the nuclide is ^{60}Co .

The leak rate of the radioactive material under the general test condition is obtained by multiplying the concentration of the nuclide existing in the air of the inner shell by the leak rate obtained in the section of C.3.1.1(2).

The radioactive concentration on the surface of the fuel for the HEU special fuel element (Special C,D types), which has the largest surface area, is shown in (II)-Table C.12.

The leak rate of the radioactive material is obtained by assuming that the radioactive material is uniformly dispersed in the air of the inner container of seal boundary, and is shown in (II)-Table C.12.

As shown in (II)-Table C.12, the leak rate of the radioactive material is smaller than the allowable value under the normal test condition.

(II)-Table C.12 Leak rate of the radioactivity under normal test condition

Nuclide	Radioactive concentration (TBq/cm ³)	Leak rate (TBq/h)	Allowable Value ($A2 \times 10^{-6}$) (TBq/h)	Rate
^{60}Co	1.89×10^{-12}	1.06×10^{-10}	4.0×10^{-7}	2.64×10^{-4}
^{234}U	8.64×10^{-14}	4.82×10^{-12}	6.0×10^{-9}	8.04×10^{-4}
^{235}U	1.27×10^{-15}	7.09×10^{-14}	∞	0
^{236}U	3.83×10^{-16}	2.14×10^{-14}	6.0×10^{-9}	3.56×10^{-6}
^{238}U	1.48×10^{-17}	8.26×10^{-16}	∞	0
Total				1.07×10^{-3}

C.3.2 Pressurization of the containment system

Since this package is transported in 'dry' condition, it does not contain any water which becomes a cause of pressurization by the effects of radiation or heat. Therefore, the only cause of pressurization in the inside part of the package is expansion of the air caused by a temperature rise. This case is explained in (II)-Table B.16.

Concerning the analyses of the pressure resistance of the containment system, a safe margin has been taken from the results of internal pressure of the (II)-Table B.16 and these analyses have been conducted against the design pressure of the (II)-Table B.17.

C.3.3 Coolant contamination

Since coolant is not used for this package, this item is not applicable.

C.3.4 Loss of coolant

Since coolant is not used for this package, this item is not applicable.

C.4 Accident test conditions

The integrity of the containment system of this package remains unchanged after an impact under accident test conditions, as required for all types of B(u) packages and the results of structural analyses is shown in (II)-A.

Moreover, the results of thermal analyses in (II)-B show that variations in pressure or temperature under accident test conditions have no effect on the integrity of the containment system.

Therefore, as the sealing performances of the containment system remain unchanged under accident test conditions, in these analyses, the evaluation of the sealing performances based on the leak tightness test of the O-ring of the inner shell lid which must meet the reference value, conducted before shipment of the package, shows that the leakage rate of radioactive substances under accident test conditions is lower than the legally established standard value.

C.4.1 Fissile gas

(1) In transporting fresh fuel element

Since the contents are composed of non-irradiated fuel elements, no fissile gas will appear.

(2) In transporting lowly irradiated fuel elements

Under the accident test condition, as described in the section (II)A.6, since the failure of the fuel element does not occur and the fissile gas contained in the fuel plate does not leak, the enrichment of the fissile gas in the sealed shell is the same value as for the normal test condition, shown in the (II)-Table C.10 and in the (II)-Table C.11.

C.4.2 Leakage of radioactive materials

C.4.2.1 Leakage from the inner shell

The maximum gas leakage rate under the accident test conditions

The maximum gas leakage rate under the accident test conditions can be obtained by substituting the relevant values of pressure, gas and the maximum leak hole diameter under the same test conditions into the formula(C3-2) to (C.3-5) and (C. 3-7).

Gas leakage rate under the accident test conditions is shown in (II)-Table C. 13. The maximum gas leakage rate is calculated concerning the inner shell lid.

(II)-Table C. 13 The maximum gas leakage rate under the accident test conditions

Item	Position	Containment boundary (O-ring of inner shell lid)
D: Diameter of leak (cm)		2.490×10^{-3}
a: Length of leak (cm)		0.54
μ : Viscosity coefficient of the gas(MPa.s)		1.85×10^{-11} at 25°C^{*1}
$P_{u,x}$: Pressure of containment system under normal test conditions (MPa abs)		0.199
$P_{d,x}$: External pressure under normal test conditions (MPa abs)		0.060
$T_{u,x}$: Gas temperature under normal test conditions(K)		482.9
M: Molecular weight(g/mol)		29
L_x : Leakage rate under normal test conditions (cm ³ /s at $P_{a,x}$ $T_{a,x}$)		1.38×10^{-2}
$L_{s,x}$: Leakage rate under normal test conditions (cm ³ /s at 25°C 0.10MPa)		1.09×10^{-2} ($6.59 \times 10^3 \text{ cm}^3/\text{week}$)

*1: Since the viscosity coefficient of air increases as the temperature rises, it is conservative to use the low temperature.

C.4.2.2 Evaluation of the volume of leakage of radioactive materials

(1) In transporting the fresh fuel element and critical assembly fuel

As described in Chapter (II)-A, since no deterioration of the fuel Plates occurs under accident test conditions, it can be supposed, as in the case of normal test conditions, that the only radioactive substances affected by the leakage are the uranium particles which adhere to surface of the fuel elements

during the manufacturing process, i. e. uranium surface contamination.

Surface contamination level per fuel element is shown in the (II)-Table C. 8.

The leakage rate of radioactive substances under accident test conditions is calculated by multiplying the concentration of each nuclide present in the cavity of the inner shell by the leakage rate calculated in C. 4. 2. 1.

(II)-Table C. 14 gives the leakage rate for radioactive substances for the JRR-3 standard fuel element (Uranium silicon aluminum dispersion type alloy), which is the highest uranium surface contamination element.

As shown in (II)-Table C. 14, the leakage rate of radioactive substances under accident test conditions is lower than the standard value.

(2) In transporting the lowly irradiated fuel elements

As described in the section (II)-A, under the accident condition, since the failure of the fuel plate does not occur, the leakage of the enriched uranium contained in the fuel plate is similarly assumed not to occur as for the normal test condition.

The surface radio activity per one fuel element is shown in (II)-Table C. 10 and in (II)-Table C. 11.

The leakage rate of the radioactive substance under the accident condition is obtained by multiplying the enrichment of the nuclide existed in the shell by the leakage rate obtained in the paragraph C. 4. 2. 1.

The radioactive enrichment on the fuel element surface for the HEU special fuel element C, D type, having the maximum surface, is obtained by the same method in the paragraph C. 3. 1. 2. (2) and is shown in the (II)-Table C. 15. As shown in the (II)-Table C. 15, the leakage rate of the radioactive substance under the accident condition is less than the reference value.

(II)-Table C.14 Leakage rate of radioactive substances

under normal test conditions

Nuclide	Radioactive substance concentration (TBq/cm ³)	Leakage rate (TBq/week)	Standard value (TBq/week)	Rate
²³⁴ U	1.07×10^{-13}	7.05×10^{-10}	6×10^{-2}	1.18×10^{-7}
²³⁵ U	1.56×10^{-15}	1.03×10^{-11}	∞	0
²³⁶ U	4.73×10^{-16}	3.12×10^{-12}	6×10^{-2}	5.20×10^{-10}
²³⁸ U	1.83×10^{-17}	1.21×10^{-13}	∞	0
Total				1.18×10^{-7}

(II)-Table C.15 Leak rate of radioactive substances

under accident test condition

Nuclide	Radioactive concentration (TBq/cm ³)	Leakage rate (TBq/week)	Allowable value (TBq/week)	Rate
⁶⁰ Co	1.89×10^{-12}	1.25×10^{-8}	4.0×10^{-1}	3.11×10^{-8}
²³⁴ U	8.64×10^{-14}	5.69×10^{-10}	6.0×10^{-3}	9.49×10^{-8}
²³⁵ U	1.27×10^{-15}	8.37×10^{-12}	∞	0
²³⁶ U	3.83×10^{-16}	2.52×10^{-12}	6.0×10^{-3}	4.21×10^{-10}
²³⁸ U	1.48×10^{-17}	9.75×10^{-14}	∞	0
Total				1.26×10^{-7}

C.5 Summary of the results and the evaluation

(1) In transporting the fresh fuel element and critical assembly fuel

Concerning the leakage of radioactive substances, it may be supposed to all the particles of uranium responsible for the surface contamination which adhere to the surface of the elements during the manufacturing process are completely separated, and that these particles are dispersed uniformly in the air in the inner shell. If the concentration of each radioactive substance is multiplied by the leakage rate to evaluate the leakage rate under normal and accidental test conditions, it can be seen, as shown in (II)-Table C.9 and in (II)-Table C.14, that the leakage rate for radioactive substances is lower than the standard value.

(2) In transporting lowly irradiated fuel element

The leak rate is evaluated under general and special test conditions, by multiplying each radioactive concentration by leak rate, by assuming that the all surface contaminated uranium, adheres when the fuel element is produced, is separated and is uniformly dispersed in the air of the inner shell and also by assuming that the all pool water adheres on the surface of the fuel element is evaporated and uniformly dispersed in the air of the inner shell, the leak rates for both test conditions are smaller than the allowable value, as shown in (II)-Table C.12 and (II)-Table C.15.

C.6 Appendix

C.6.1 Design temperature for containment analyses

The design temperature for the containment analyses is used for the calculation of the internal pressure of the inner shell, and this pressure is calculated from the average temperature of the air contained in the inner shell.

The volume of the air contained in the fuel basket constitutes the largest proportion (77%) of the total air volume contained in the inner shell, and since there is no emission of heat from the fuel, the temperature of the air contained in the fuel basket is lower than the temperature of the fuel basket.

For greater safety, the temperature of the air contained in the fuel basket is regarded as equivalent to the average temperature of the fuel basket (180.7°C)* and the temperature of the air contained in the space between the fuel basket and the main body of the inner shell is regarded as equivalent to the average of the average temperature of the fuel basket and the average temperature of the main body of the inner shell (403.4°C)*, namely a temperature of 292.1°C , proceeding in this way, the average temperature of the air inside the inner shell can be calculated as 206.3°C , which is lower than the maximum temperature of the fuel basket (209.9°C).

As explained above, if the maximum temperature of the fuel basket (209.9°C) is used as the average temperature of the air contained in the inner shell, the internal pressure of the inner shell is overestimated. Therefore, the maximum temperature of the fuel basket is used as the design temperature for the containment analyses.

*: Value obtained by the calculation of the average of the TRUMP CODE

C.6.2 Reference documents

- (1) ANSI-N 14.5 American National Standard for Leakage Tests on Packages for Shipment of Radioactive Materials (1977)

American national Standards Institute, Inc.

American national Standards for radioactive materials

Leakage test on packages for shipment (1997)

ANS N14.5 - 1997

- (2) “Document for Heat Transfer Engineering, III Edition” Mechanical Engineering Society of Japan.

(II)-D Shield analysis

(II)-D. Shield analysis

D.1 Outline

In the case where the package contents consist of fresh fuel elements (including KUCA fuel), ^{235}U and ^{238}U are considered as a gamma radiation source, and neutrons emitted by the uranium spontaneous fission is considered as a neutron source.

In case of the lowly irradiated fuel elements, ^{235}U , ^{238}U and the radioactive nuclides are considered as a gamma radiation source, and the uranium spontaneous fission is considered as the neutron source.

Regarding the gamma radiation source calculation, we have to consider that under normal test conditions and accident test conditions, the outer shell is subjected to a transformation and that, under normal transport conditions, with normal test conditions and accident test conditions, the dose-equivalent rate is evaluated by assimilation of the inner shell surface to the package surface.

The neutron dose-equivalent rate is calculated by assimilating the uranium content to the point radiation source. There, the content are distributed inside the cavity, but their position is calculated in such a way that the distance between the point radiation source and the inner shell surface is as small as possible. In the same way, the gamma radiation source calculation is evaluated by considering the inner shell surface to be equivalent to the package surface and for safety reasons, by ignoring the inner shell shield effect and considering only the distance attenuation effect.

D.2 Radiation source specification

There are unirradiated fresh fuel element and lowly irradiated fuel element in the package.

For unirradiated uranium, the radioactive nuclide such as ^{235}U and ^{238}U etc. are considered as the gamma radiation source.

The neutron emitted by uranium spontaneous fission is considered as the neutron source.

In case of the lowly irradiated fuel element, the radioactive element such as the ^{235}U , ^{238}U etc. are considered as the gamma radiation source, and the neutrons emitted by spontaneous fission of uranium etc. are considered as the neutron source.

D.2.1 Gamma radiation source

(1) In loading the fresh fuel element

The uranium isotope contained in the fuel packaged are ^{234}U , ^{235}U , ^{236}U and ^{238}U , and these gamma ray emitting rates are shown in (II)-Table D.1.⁽¹⁾

The gamma radiation source intensity per one fuel element of the JRR-3 standard type (Uranium silicon aluminum dispersion alloy) (Enrichment $19.75 \pm 0.2\text{wt}\%$), which has highest radioactivity, is shown in (II)-Table D.2.

The gamma radiation source intensity is obtained as follows.

$$S_E = C \cdot W \cdot R_E$$

Where,

S_E : Gamma radiation source intensity (Photons/s) of energy E

C : Specific activity (Bq/g), shown in (II)-Table D.3⁽²⁾

W : Uranium isotope weight (g)

R_E : Gamma ray emission rate of energy E (photons/decay)

The weight of the uranium isotope is conservatively obtained as follows.

(a) ^{235}U :Maximum ^{235}U contained quantity in the fuel element.

(b) ^{238}U :By assuming the quantities of ^{234}U and ^{236}U are to be zero, the quantity of ^{238}U is obtained by using the quantity of the ^{235}U obtained above and the lower limit of the enrich tolerance.

(c) ^{234}U , ^{236}U :As the quantities of ^{234}U and ^{236}U are determined when the fuel element is produced, the weight limit is not determined. Therefore the maximum weight rate is selected from the past material record sheet, by using the conservatively rounded up weight rate, the quantities of ^{235}U and ^{236}U are obtained. In this case, the necessary total uranium quantity is the sum of the ^{235}U obtained in (a) and ^{238}U obtained in (b).

The weight rates of ^{234}U and ^{236}U used in the calculation are shown in (II)-Table D.4.

The uranium isotope weight for one element used in calculation is shown in (II)-Table D.5.

(II)-Table D.1 Gamma radiation emission rate of uranium isotope

Uranium isotope	Gamma radiation energy (MeV)	Gamma radiation emission rate (photons/decay)
^{234}U	0.05322	0.00119
	0.12090	0.000405
^{235}U	0.10914	0.015
	0.14376	0.105
	0.16335	0.047
	0.18572	0.54
	0.20212	0.010
	0.20531	0.047
^{236}U	0.04937	0.00079
	0.11275	0.00019
^{238}U	0.04955	0.0032

(II)-Table D.2 Gamma radiation source intensity for one fuel element

Energy (MeV)	Gamma radiation Source intensity (photons/s)
0.04937	4.716×10^4
0.04955	7.948×10^4
0.05322	3.434×10^6
0.10914	5.820×10^5
0.11275	1.134×10^4
0.12090	1.169×10^6
0.14376	4.074×10^6
0.16335	1.824×10^6
0.18572	2.095×10^7
0.20212	3.880×10^5
0.20531	1.824×10^6

(II)-Table D.3 Specific activity used for calculation

Uranium isotope	Specific activity (Bq/g)
^{234}U	2.309×10^8
^{235}U	8.001×10^4
^{236}U	2.397×10^6
^{238}U	1.244×10^4

(II)-Table D.4 ^{234}U and ^{236}U weight rate used for calculation

Isotope	Weight rate (wt%)	
	Mill sheet maximum value	Value used for calculation
^{234}U	0.13	0.5
^{236}U	0.21	1.0

(II)-Table D.5 Radioactive nuclide weight per one element used in calculation

Uranium isotope	Weight (g)
^{234}U	12.41
^{235}U	485
^{236}U	24.81
^{238}U	1996

(2) In loading lowly irradiated fuel element

(a) Gamma radiation source by the isotope from uranium

The uranium isotope contained in the package fuel are mainly ^{234}U , ^{235}U , ^{236}U and ^{238}U etc., and these gamma ray emission rates are shown in (II)-Table D.6.⁽¹⁾

The gamma radiation source intensity of the one equivalent fuel element (mixed fuel elements) of the JMTRC HEU fuel element, which has the highest radioactivity and the MEU fuel element, by assuming these fuel elements are packaged together, is shown in (II)-Table D.7.

The gamma radiation source intensity is obtained as follows.

$$S_E = C \cdot W \cdot R_E$$

Where,

S_E : Gamma radiation source intensity of energy E (Photons/s)

C : Specific activity (Bq/g), shown in (II)-Table D.8⁽²⁾

W : Weight of Uranium isotope (g)

R_E : Gamma ray emission rate of energy E (Photons/decay)

The weight of the uranium isotope is conservatively obtained as follows.

(i) ^{235}U :Maximum contained quantity in the fuel element.

(ii) ^{238}U :The quantity of ^{238}U is obtained, by assuming the quantities of ^{234}U and ^{236}U are to be zero, by using the quantity of ^{235}U obtained in (1) and the lower limit of the enrichment tolerance.

(iii) ^{234}U , ^{236}U :The quantities of ^{234}U and ^{236}U are determined when the fuel element is produced, the limit of the weight is not determined. Therefore the maximum weight rate is selected from the past material record sheet, and the weights of ^{234}U and ^{236}U are obtained by using the conservatively rounded up weight rate.

In this case, the necessary total uranium weight is the sum of the weight of ^{235}U obtained in (1) and the weight of ^{238}U obtained (ii). The weight rate of ^{234}U and ^{236}U used in the calculation are shown in (II)-Table D.9.

The weight of uranium isotope per one fuel element used in the calculation is shown in (II)-Table D.10.

(II)-Table D.6 Gamma radiation emission rate of uranium isotope

Uranium isotope	Gamma radiation energy (MeV)	Gamma radiation emission rate (photons/decay)
^{234}U	0.05322	0.00119
	0.12090	0.000405
^{235}U	0.10914	0.015
	0.14376	0.105
	0.16335	0.047
	0.18572	0.54
	0.20212	0.010
	0.20531	0.047
^{236}U	0.04937	0.00079
	0.11275	0.00019
^{238}U	0.04955	0.0032

(II)-Table D.7 Gamma radiation source intensity per one mixed
fuel element (actinoids)

Energy (MeV)	Gamma radiation source intensity (photons/s)
0.04937	2.321×10^4
0.04955	1.609×10^4
0.05322	1.923×10^6
0.10914	3.804×10^5
0.11275	5.583×10^3
0.12090	6.545×10^5
0.14376	2.663×10^6
0.16335	1.192×10^6
0.18572	1.369×10^7
0.20212	2.536×10^5
0.20531	1.192×10^6

(II)-Table D.8 Specific activity used for calculation

Uranium isotope	Specific activity (Bq/g)
^{234}U	2.309×10^8
^{235}U	8.001×10^4
^{236}U	2.397×10^6
^{238}U	1.244×10^4

(II)-Table D.9 ^{234}U and ^{236}U weight rate used for calculation

Uranium isotope	Weight rate (wt%)	
	HEU fuel element	MEU fuel element
^{234}U	2.2 (2 times of the actual contained substance weight)	0.47 (1.5 times of the actual contained substance weight)
^{236}U	0.94 (2 times of the actual contained substance weight)	1.7 (1.5 times of the actual contained substance weight)

(II)-Table D.10 Radioactive nuclide weight per one element used in calculation

Uranium isotope	Weight (g)
^{234}U	7.00
^{235}U	317
^{236}U	12.26
^{238}U	404

(b) Gamma ray from the fission product

The irradiation time and the cooling time of the JMTRC fuel element is as follows.

- (i) HEU fuel: 302h irradiation (100W equivalence) (0.0013MWd) 15 years cooling
- (ii) MEU fuel: 100h irradiation (100W equivalence) (0.0005MWd) 4 years cooling

The fission products are calculated by using ORIGEN for the above 2 types of fuel elements with the following assumption.

- ① The peaking factor of the fuel element during operation is 2.00.
- ② The effect of the radioactivity except the main nuclide is considered by scaling the radioactivity of the main nuclide to be 100%.

The radioactivity of the fission product of the mixed fuel elements is determined from the fuel element which has the higher radioactivity.

The radioactivity and the gamma radiation source intensity of the main nuclides are shown in (II)-Table D.11.

(II)-Table D.11 Radioactivity rate of the fission products obtained by ORIGEN

Main nuclide	Gamma ray energy (MeV)	Emission rate (%)	Radioactivity by ORIGEN (Bq)	Scaling factor*	Photons/s
Cs-137	0.662	85.1	1.261×10^7	1.0391	1.11×10^7
	0.0364	1.3			1.70×10^5
	0.0322	5.6			7.33×10^5
Kr-85	0.514	0.43	1.072×10^6		4.78×10^3
Rh-106	1.05	1.6	1.050×10^3		1.74×10^1
	0.662	9.9			1.08×10^2
	0.512	20.4			2.22×10^2
Sb-125	0.671	1.8	1.452×10^4		2.71×10^2
	0.636	11.3			1.70×10^3
	0.607	5			7.54×10^2
	0.601	17.9			2.70×10^3
	0.463	10.5			1.58×10^3
	0.428	29.6			4.46×10^3
	0.176	6.8			1.03×10^3
	0.0355	4.3			6.48×10^2
Sr-90	—	—	1.234×10^7		—
Y-90	1.7608	0.012	1.234×10^7		1.54×10^3
Ba-137m	—	—	1.179×10^7		—
Total	—	—	5.017×10^7	—	1.21×10^7

* Ratio of total radioactivity ($5.213 \times 10^7 \text{Bq}$) by ORIGEN versus radioactivity ($5.017 \times 10^7 \text{Bq}$) of main nuclide.

D.2.2 Neutron source

(1) In loading fresh fuel element

As the contents are non-irradiated uranium, it is necessary to take into consideration that, the neutron emission, occurs by spontaneous fission of uranium is considered as a neutron source.

The uranium isotope spontaneous fission speed is shown in (II)-Table D.12⁽³⁾.

(II)-Table D.12 Uranium isotope spontaneous fission speed

Isotope	²³⁴ U	²³⁵ U	²³⁶ U	²³⁸ U
Spontaneous fission speed (unit/g·s)	3.5×10^{-3}	3.1×10^{-4}	2.8×10^{-3}	7.0×10^{-3}

Since among uranium isotope, the spontaneous fission speed of ²³⁸U is the largest, the intensity of the neutron source for one JRR-3 fuel element (Uranium Silicon Aluminum Dispersion Type Alloy) in which uranium content is largest, reaches maximum. This value is 35.6 (n/s). The neutron source intensity by spontaneous fission is calculated by the following formula.

$$S_n = \sum W_i \cdot f_i \cdot n$$

In this formula

S_n : Neutron source intensity for one fuel element (n/s)

W_i : Uranium isotope weight for one element (g)

((II)-Table D.5)

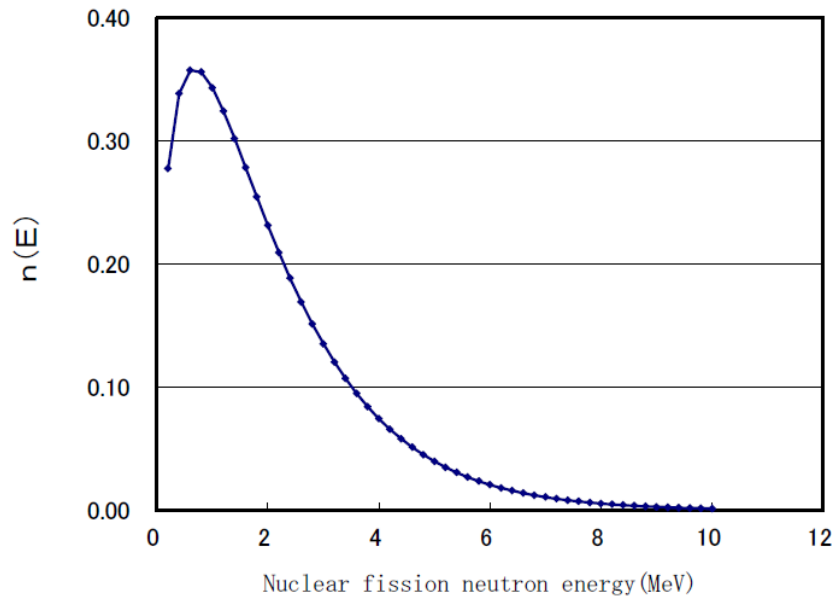
f_i : Spontaneous fission speed of uranium isotope (unit/g·s)

((II)-Table D.12)

n : No. of neutrons emitted by one core fission⁽⁴⁾ (2.5)

The energy spectrum of neutrons emitted by fission is shown in (II)-Fig. D.1⁽⁴⁾. The higher the neutron energy, the bigger the calculation factor becomes consequently, to evaluate a dose-equivalent factor in a safe way, the neutron total energy emitted should be 10 MeV.

From the result of criticality analysis, the k_{eff} effective multiplication factor of one package containing 10 JRR-3 standard elements (Uranium Silicon Aluminum Dispersion Type Alloy) of 20 wt% enrichment without water whose ^{235}U content reaches a maximum, and is 0.032 by considering 3σ . By the same calculation method, if for safety reasons the effective multiplication rate is fixed to 0.1, it is necessary to consider the multiplication effect of neutrons ($1/(1-k_{\text{eff}}) = 1.11$) on the intensity of neutrons radiation.



(II)-Fig. D.1 Neutron fission energy spectrum

(2) In loading lowly irradiated fuel element

It is neutron emission by the spontaneous fission of uranium etc. that is necessary to be considered as the neutron source.

The emission rate of the spontaneous fission of these isotopes is shown in (II)-Table D.13.⁽³⁾

(II)-Table D.13 Emission rate of spontaneous fission of uranium isotope

Uranium isotope	^{234}U	^{235}U	^{236}U	^{238}U
Emission rate of Spontaneous fission (Unit/g·s)	3.5×10^{-3}	3.1×10^{-4}	2.8×10^{-3}	7.0×10^{-3}

The neutron source intensity per one mixed fuel element having the highest radioactivity is maximum of 7.46(n/s)

The neutron source intensity by the spontaneous fission is calculated by the same method as the paragraph D.2.3(1).

D.3 Model specification

D.3.1 Analysis model

(1) Gamma radiation dose-equivalent rate

The ANISN code⁽⁵⁾ is used for calculation of the gamma radiation shield. The evaluation of the dose-equivalent rate is performed by considering that both under normal test conditions and accident test conditions, the outer shell is subjected to a deformation, and that under routine transport conditions, both under normal and accident test conditions, the inner shell surface is assumed to be the content surface. The gamma radiation shield calculation model is shown (II)-Fig.D.2.

The Intensity of gamma radiation is identical to 19.75 wt % enriched JRR-3 standard fuel (Uranium Silicon Aluminum Dispersion Type Alloy), but in order to reduce fuel self shielding, the data of JRR-4L type fuel for which aluminum weight is limited is used, and it is supposed that the source area, for one fuel element, is a 6.8 cm long, 8.0 cm wide and 61.0 cm high rectangular solid. For the lateral part of the radiation source area model, 10 cylindrical fuel elements with equivalent cross section are evenly distributed. At this time, the shielding effect of the basket is ignored, but as shown in (II)-Table B.6, the gap between the fuel basket and the inner shell barrel represents, for the lateral model, a 1.8 cm empty space. In view of this space thickness, the model was realized in order that the source area surface could be as close as possible to the detection point.

Since the detection point is one meter from the packaging surface, and for safety reasons, the dose-equivalent rate is evaluated by the ANISN calculation code, we have to proceed with empty space attenuation effect by the following formula.

Supposing that the angles flux of the packaging surface obtained by the ANISN code shield calculation is $4\pi \phi(\vec{r}_s, E, \vec{\Omega})$, it calculates the source flux $\phi(\vec{r}_p, E)$ and the source volume rate D at rp calculation point of space shown in (II)-Fig.D.3 by the following formula.

$$\phi(\vec{r}_p, E) = \int \vec{\Omega}' \int_s \phi(\vec{r}_s, E, \vec{\Omega}') \delta(\vec{\Omega}', \vec{\Omega}) \cos \varphi \frac{d_s}{r^2} d\vec{\Omega} \quad (D.3-1)$$

$$D = \int_E K(E) \phi(\vec{r}_p, E) dE \quad (D.3-2)$$

In this formula,

d_s : Surface element of the packaging surface

r : Distance between surface element d_s and calculation point

$$r = \left| \vec{r}_p - \vec{r}_s \right|$$

$K(E)$: Dose rate conversion factor

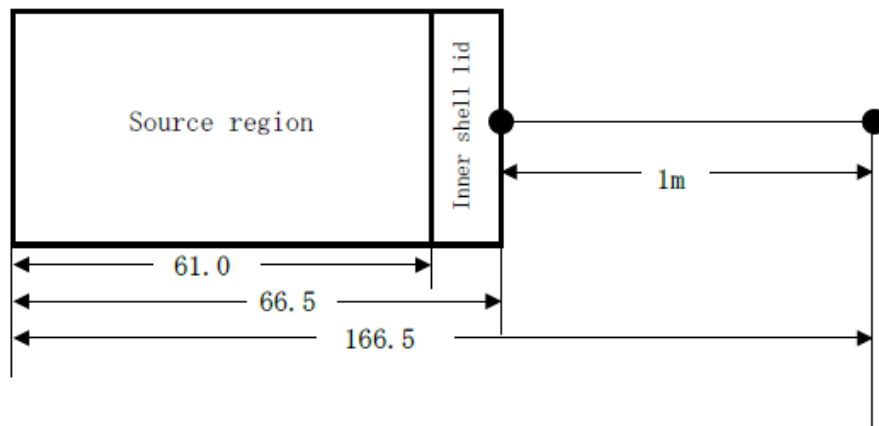
ϕ : Angle between $\vec{\Omega}$ and n, normal vector of d_s

$\vec{\Omega}$: Unit vector which indicates the angle between d_s and calculation point

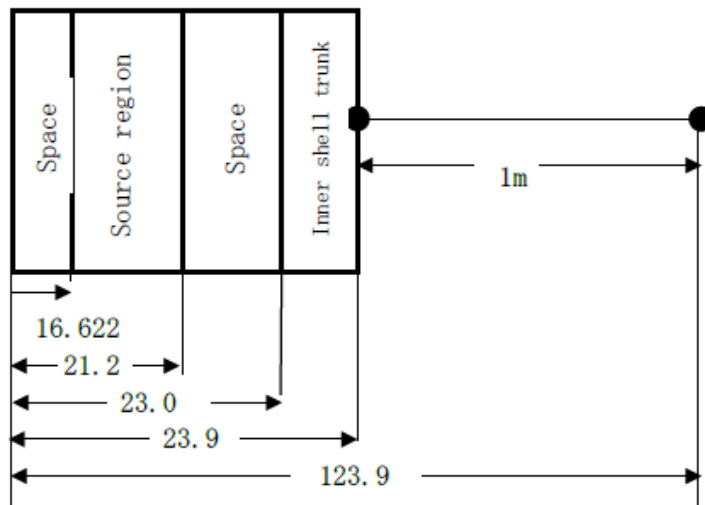
$\vec{\Omega}'$: Unit vector which indicates the arbitrary angle direction from d_s

E : Energy

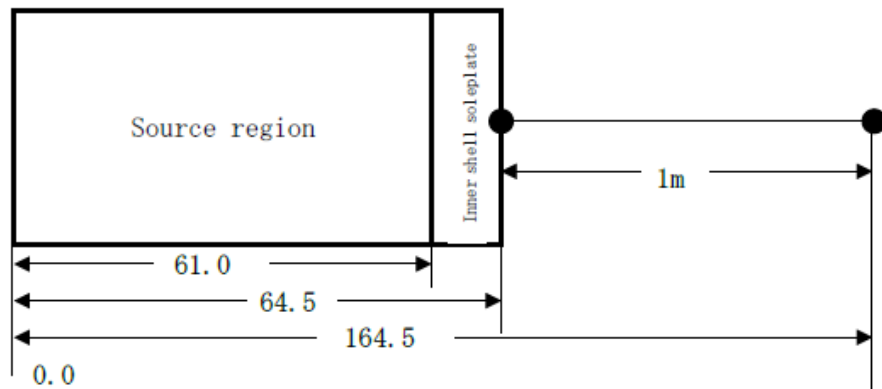
(1) Upper portion



(2) Middle portion

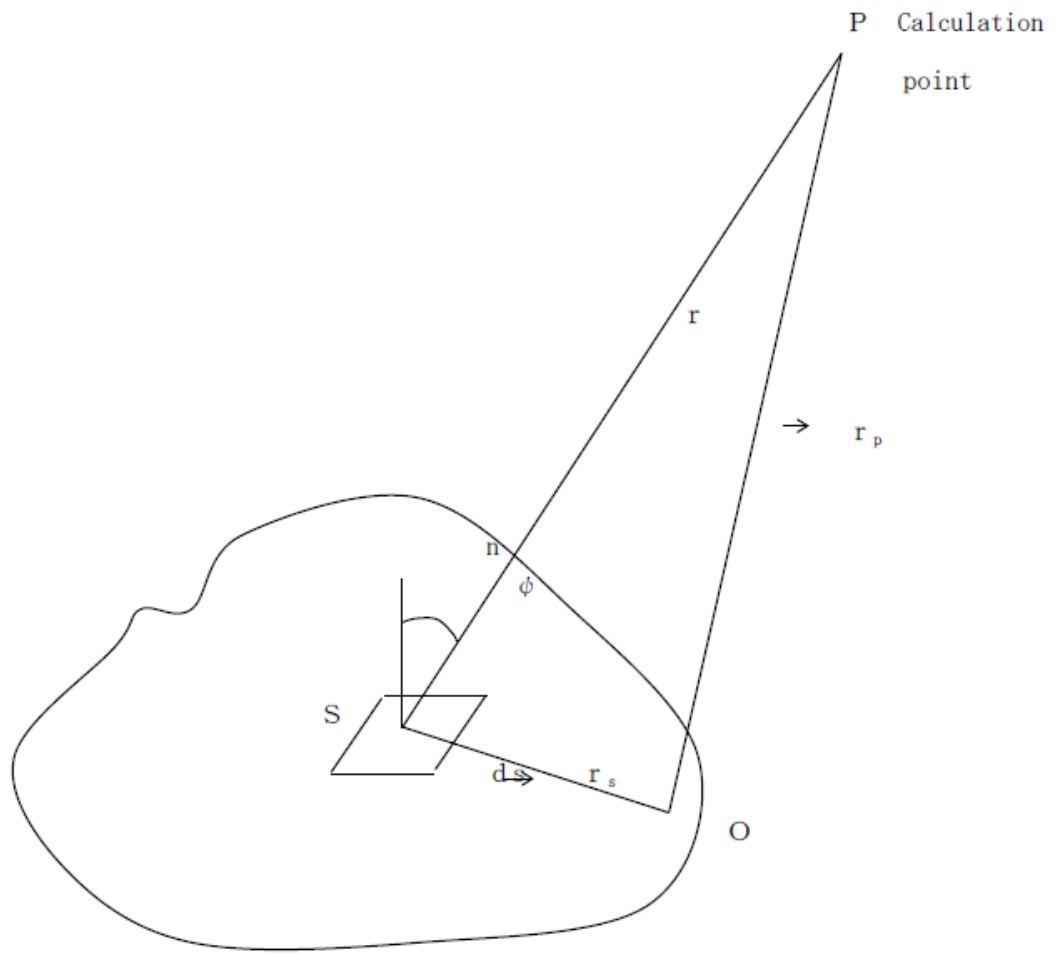


(3) Lower portion



Explanatory notes
 ● Detection point
 Unit : cm

(II)-Fig.D.2 Gamma radiation shield calculation model

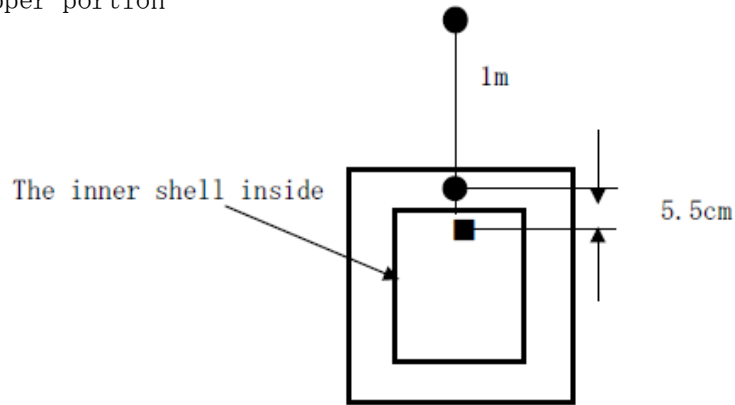


(II)-Fig. D.3 Relationship between packaging surface angles flux
and calculation point of packaging surface

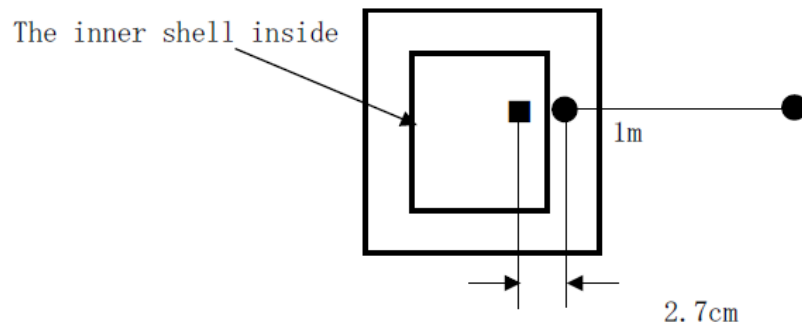
(2) Neutron dose-equivalent rate

Neutron dose-equivalent rate, as it is shown in (II)-Fig.D.4, is calculated by considering the content of uranium as the point radiation source. The content is distributed in the cavity, but its position is evaluated so that the distance between the radiation source point and inner shell surface is as small as possible. For safety reasons, the evaluation of the neutron shield calculation is performed considering the surface of the inner shell to be equivalent to the surface of the package. Then, proceeding with the evaluation, for more safety, the shielding effect of the inner shell lid, bottom and barrel parts should be ignored, and only the distance attenuation effect should be taken into consideration.

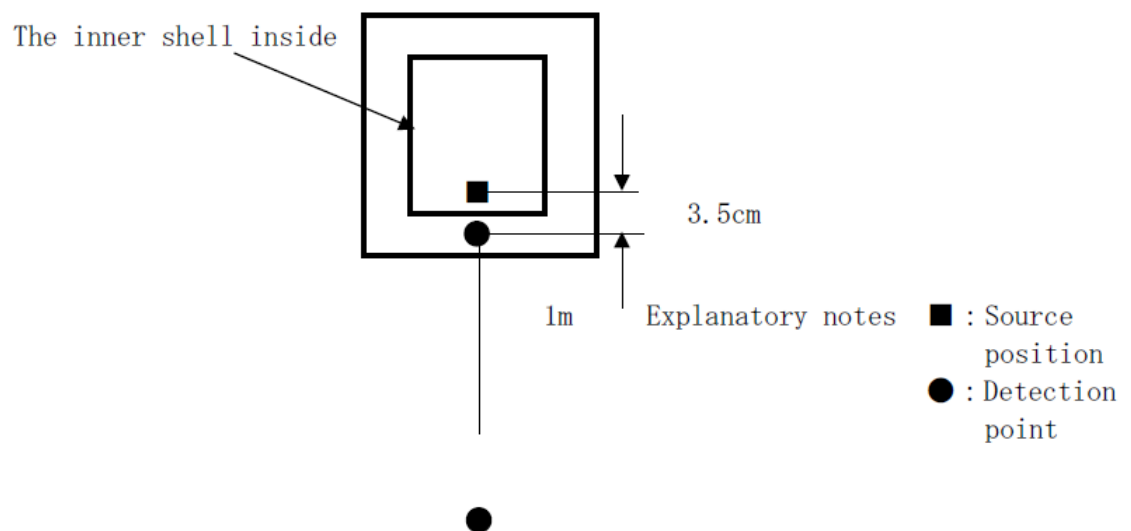
(1) Upper portion



(2) Middle portion



(3) Lower portion



(II)-Fig. D.4 Neutron shield calculation model

D.3.2 Numeric density of atoms in each area of analysis model

Density and material for each zone used for calculation of the gamma radiation shield are shown in (II)-Table D.14 and the volumetric rate of shield material for each area is shown in (II)-Table D.15. The numeric density of atoms for each shield material is shown in (II)-Table D.16.

For neutron dose-equivalent rate, the material of the structure is not taken into consideration and then the following tables are not applicable.

(II)-Table D.14 Material and density

Part name	Material	Density (g/cm ³)
Inner shell lid	SUS 630	7.85
Inner shell barrel	SUS 304	7.85
Inner shell bottom plate	SUS 304	7.85

(II)-Table D.15 Volumetric rate of shield material for each area used
in shield calculation

Area	Shield material	Volumetric rate (%)
Radiation source area (lateral part evaluation)	Fuel core	16.7
	Cladding	14.3
	Cavity	69.0
Radiation source area (lid and bottom part evaluation)	Fuel core	6.43
	Cladding	5.51
	Cavity	88.06
Inner shell lid	Stainless steel (SUS 630)	100
Inner shell barrel	Stainless steel (SUS 304)	100
Inner shell bottom plate	Stainless steel (SUS 304)	100

(II)-Table D.16 Atom density for each material

(atoms/barn · cm)

Nuclide	Radiation source area (lateral part evaluation)	Radiation source area (lid and bottom parts evaluation)	SUS 304	SUS 630
C	—	—	1.18×10^{-4}	2.76×10^{-4}
Al	1.7985×10^{-4}	6.9293×10^{-5}	—	—
Si	—	—	1.68×10^{-3}	1.68×10^{-3}
Cr	—	—	1.73×10^{-2}	1.50×10^{-2}
Mn	—	—	1.72×10^{-3}	8.60×10^{-4}
Fe	—	—	5.66×10^{-2}	6.22×10^{-2}
Ni	—	—	8.86×10^{-3}	3.22×10^{-3}
Cu	—	—	—	2.98×10^{-3}
^{235}U	7.0793×10^{-6}	2.7275×10^{-6}	—	—
^{238}U	7.0793×10^{-6}	2.7275×10^{-6}	—	—

D.4 Shield evaluation

(1) Dose equivalent rate by gamma radiation

(a) In loading fresh fuel element

The ANISN code is used for the shield calculation for fresh fuel loading.

The cross section of the energy group structure (group 18) of the DLC-23E/CASK library⁽⁶⁾ is used as the cross section for the gamma ray.

This energy group structure is shown in (II)-Table D.17.

The dose equivalent rate calculation factor for the gamma ray to obtain the dose equivalent rate⁽⁷⁾ is shown in (II)-Table D.17.

The calculation result is shown in (II)-Table D.18.

As for the increasing rate of the dose equivalent rate under the normal test condition, by considering the deformation of the outer shell, the surface of the inner shell is considered to be the package surface in the analysis under the usual transport condition, normal test condition and accident condition, so, the dose equivalent rate does not increase and is within the allowable value.

(II)-Table D.17 Gamma radiation energy group structure
and dose-equivalent rate calculation factor

Energy groups	Upper limit energy (eV)	Dose-equivalent rate calculation factor $((\text{mSv/h})/(\gamma/\text{cm}^2 \cdot \text{s}))$
1	1.00×10^7	8.4944×10^{-5}
2	8.00×10^6	7.2388×10^{-5}
3	6.50×10^6	6.1456×10^{-5}
4	5.00×10^6	5.2036×10^{-5}
5	4.00×10^6	4.4163×10^{-5}
6	3.00×10^6	3.7842×10^{-5}
7	2.50×10^6	3.3385×10^{-5}
8	2.00×10^6	2.8967×10^{-5}
9	1.66×10^6	2.4817×10^{-5}
10	1.33×10^6	2.0800×10^{-5}
11	1.00×10^6	1.7275×10^{-5}
12	8.00×10^5	1.4112×10^{-5}
13	6.00×10^5	1.0523×10^{-5}
14	4.00×10^5	7.5325×10^{-6}
15	3.00×10^5	5.4060×10^{-6}
16	2.00×10^5	3.2205×10^{-6}
17	1.00×10^5	1.9332×10^{-6}
18	5.00×10^4 1.00×10^4	2.6973×10^{-6}

(II)-Table D.18 Dose-equivalent rate by gamma radiation
(fresh fuel elements loading)

Evaluated position		Dose-equivalent rate (mSv/h)
Package surface	Lid	<0.001
	Side	0.033
	Bottom	0.003
1m apart from package surface	Lid	<0.001
	Side	0.004
	Bottom	<0.001

(2) In loading lowly irradiated fuel element

The shield analysis of the gamma radiation for the case where the lowly irradiated fuels are loaded, is conducted by the same method described in the section of previous (1)(a). The result of the analysis is shown in (II)-Table D.19.

As for the increase rate of the dose-equivalent rate under the general test condition, the surface of the inner shell is evaluated as the surface of the package under the usual transport condition, the normal test condition and the accident test condition, by considering that the outer shell is deformed under the normal test condition, therefore the increase of the dose-equivalent rate does not occur and satisfies the criteria.

(II)-Table D.19 Dose-equivalent rate by gamma radiation
(lowly irradiated fuel elements loading)

Evaluated position		Dose-equivalent (mSv/h)		Total (mSv/h)
		Actinides	FP	
Package surface	Lid	<0.001	0.025	0.026
	Side	0.022	0.145	0.167
	Bottom	0.002	0.069	0.071
1m apart from package surface	Lid	<0.001	0.005	0.006
	Side	0.003	0.015	0.018
	Bottom	<0.001	0.013	0.014

(3) Neutron dose-equivalent rate

(a) In loading fresh fuel element

Neutrons dose-equivalent rate is calculated by following formula.

$$D_n = A \times \frac{S_n \cdot n}{4 \pi r^2} \times k$$

In this formula,

D_n : Dose-equivalent rate (mSv/h)

S_n : Neutron source intensity for one fuel element 35.6 (n/s)

n : Number of fuel elements for one packaging 10

r : Distance from point radiation source to evaluation point (cm)

k : Neutron multiplication effect 1.11

A : Conversion factor of Dose-equivalent rate of 10 MeV energy

neutron flux⁽⁷⁾

0.00159 ((mSv/h)/(n/cm²·s))

The calculation result of neutron dose-equivalent rate is shown in

(II)-Table D.20

(II)-Table D.20 Neutron dose-equivalent rate

Calculation result		Dose-equivalent rate
Evaluated position		(mSv/h)
Package surface	Lid part	0.002
	Middle part	0.007
	Bottom part	0.005
Position at one meter from container surface	Lid part	<0.001
	Middle part	<0.001
	Bottom part	<0.001

(b) In loading the lowly irradiated fuel element

The does-equivalent rate of the lowly irradiated fuel element loading is calculated by the same method in the previous section of (2) (a).

The analysis result of the does-equivalent rate of the lowly irradiated fuel element loading is shown in (II)-Table D.21.

(II)-Table D.21 Dose-equivalent rate of neutron irradiation
(lowly irradiated fuel elements loading)

Evaluated position		Dose-equivalent rate (mSv/h)
Package surface	Lid	<0.001
	Middle	0.002
	Bottom	<0.001
1m apart from package surface	Lid	<0.001
	Middle	<0.001
	Bottom	<0.001

D.5 Summary of the results and evaluation

Dose-equivalent rate results obtained with the present package shield analysis for the fresh fuel element and the lowly irradiated fuel element are shown in (II)-Table D.22. and in (II)-Table D.23. Gamma radiation dose-equivalent rate is calculated with the one dimensional discrete ordinates transport code ANISN, neutron dose-equivalent rate is easily calculated by using the model of point radiation source.

As shown in (II)-Table D.22, and in (II)-Table D.23, the result of calculation always satisfies the standard values.

(II)-Table D.22 Package dose-equivalent rate

Evaluated position Item		(fresh fuel element loading)			(unit: mSv/h)		
		Package surface			Position at one meter from the packaging surface		
		Middle	Lid	Bottom	Middle	Lid	Bottom
Routine transport condition	Gamma radiation	0.033	<0.001	0.003	0.004	<0.001	<0.001
	Neutron	0.007	0.002	0.005	<0.001	<0.001	<0.001
	Total	0.040	0.003	0.007	0.005	0.002	0.002
	Standard value	2 or less			0.1 or less		
Normal test condition	Gamma radiation	0.033	<0.001	0.003			
	Neutron	0.007	0.002	0.005			
	Total	0.040	0.003	0.008			
	Standard value	2 or less			—		
Accident test condition	Gamma radiation				0.004	<0.001	<0.001
	Neutron				<0.001	<0.001	<0.001
	Total				0.005	0.002	0.002
	Standard value	—			10 or less		

(II)-Table D.23 Package Dose-equivalent Rate

(lowly irradiated fuel element loading) (unit: mSv/h)

Evaluation point Item		Package surface			Position at one meter from the packaging surface		
		Middle	Lid	Bottom	Middle	Lid	Bottom
Routine transport condition	Gamma radiation	0.167	0.026	0.071	0.018	0.006	0.014
	Neutron	0.002	<0.001	<0.001	<0.001	<0.001	<0.001
	Total	0.169	0.027	0.072	0.019	0.007	0.015
	Standard value	2 or less			0.1 or less		
Normal test condition	Gamma radiation	0.167	0.026	0.071			
	Neutron	0.002	<0.001	<0.001			
	Total	0.169	0.027	0.072			
	Standard value	2 or less			—		
Accident test condition	Gamma radiation				0.018	0.006	0.014
	Neutron				<0.001	<0.001	<0.001
	Total				0.019	0.007	0.015
	Standard value	—			10 or less		

D.6 Appendix

D.6.1	Explanations of ANISN code	(II)-D-30
D.6.2	Reference literature	(II)-D-33

D.6.1 Explanations of ANISN code

The ANISN code developed by ORNL in the USA, is a numerical calculation of the one dimensional Boltzmann transport equation based upon Discrete Ordinates Sn.

The transport equation is a mathematical representation of the balance between formation and disintegration of particles inside a volume element phase space resulting from position, energy and the direction of progression, the equation is given by the following formula.

$$\begin{aligned} & \Omega \cdot \nabla \phi(r, E, \Omega) + \sigma_t(r, E) \phi(r, E, \Omega) \\ &= \iint \phi(r, E', \Omega') \sigma_s(r, E' \rightarrow E, \Omega' \rightarrow \Omega) dE', d\Omega' + S(r, E, \Omega) \dots \dots \dots (D.6-1) \end{aligned}$$

where,

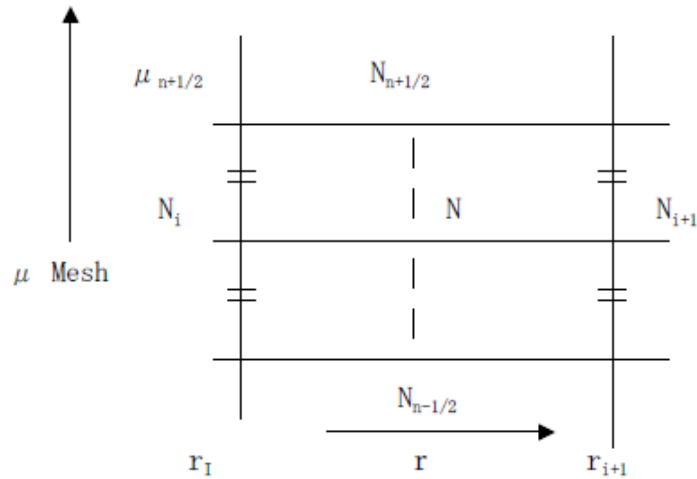
$\phi(r, E, \Omega)$: Angle neutron flux (number of particles passing per unit time through the surface perpendicular to the unit vector Ω and per unit solid angle in the direction of unit vector Ω at position r)
$\sigma_t(r, E)$: Total macro cross section
$\sigma_s(r, E \rightarrow E, \Omega \rightarrow \Omega)$: Dispersion macro cross section or creation of a macro cross section of secondary gamma radiation from neutrons
$S(r, E, \Omega)$: External radiation source

The Sn method is a numeric evaluation of the transport equation discretely dealing with position, energy and direction of progression. It is called the Sn method because of the special way evaluating the angle division point(Sn division point).

This technique uses the fundamental cell to express the transport equation for the direction of progression of each energy group, then calculates until convergence, by iterations of the difference equation.

To express the primary transport equation $(r_i, r_{i+1}), (\mu_{n-1/2}, \mu_{n+1/2})$ with the adjacent mesh that determines the fundamental cell (see (II)-Fig.D.5 below)

$$W \cdot \mu \cdot (A_{i+1}N_{i+1} - A_iN_i) + \alpha_{n+1/2} \cdot N_{n+1/2} - \alpha_{n-1/2} \cdot N_{n-1/2} \\ = V \cdot (S - \Sigma t) \cdot N \cdot W \dots \dots \dots (D.6-2)$$



(II)-Fig.D.5 Mesh distribution drawing

Where,

N : Neutron flux (including angles distribution)
(for each energy group)

μ : Cosine

A : Surface factor

$$\begin{cases} \text{for flat plate shape: } 1.0 \\ \text{for cylindrical shape: } 2\pi r \\ \text{for circular shape: } 4\pi r^2 \end{cases}$$

W : Weight coefficient of direction cosines $\mu \quad \sum_n W = 1.0$

V : Volume factor

$$\begin{aligned} \text{for flat plate shape} & : r_{i+1} - r_i \\ \text{for cylindrical shape} & : \pi (r_{i+1}^2 - r_i^2) \\ \text{for circular shape} & : 4/3 \pi (r_{i+1}^3 - r_i^3) \end{aligned}$$

Σt : Total cross section

S : Radiation source term (external radiation source + dispersion integral term)

α : Value given by the following formula

$$\begin{aligned} \alpha_{n+1/2} &= \alpha_{n-1/2} - W \cdot \mu (A_{i+1} + A_i) \\ \alpha_{1/2} &= 0.0 \end{aligned}$$

The formula (D.6-2) is obtained by multiplying the phase space to (D.6-1) formula, integrating it and substituting the differential value to difference value.

The formula (D.6-2) includes 5 unknown variables (N , N_i , N_{i+1} , $N_{n-1/2}$, $N_{n+1/2}$). To reduce the number of unknown variables, diamond difference calculation method or approximation step function can be used.

Diamond difference calculation: Linear approximation at adjacent meshes
intermediate point.

$$N = 1/2 (N_{i+1} + N_i) = 1/2 (N_{n-1/2} + N_{n+1/2})$$

Step function approximation : $N = N_i = N_{n+1/2}$ for $\mu < 0$

$N = N_{i+1} = N_{n+1/2}$ for $\mu > 0$

For the diamond difference calculation, in case $\mu > 0$

$$N = \frac{2\mu AN_i + \frac{2\alpha}{W} N_{N-1/2} + SV}{2\mu A + \frac{2\alpha}{W} + \Sigma tV} \quad (D.6-3)$$

Then,

$$\alpha = 1/2(\alpha_{n+1/2} - \alpha_{n-1/2})$$

$$A = 1/2(A_{i+1} + A_i)$$

To calculate this difference equation, an initial value is assigned, then the equation calculated iteratively until it converges. This gives the basic solution.

D.6.2 Reference literature

- (1) Murakami Yukio: "Radioactivity Data Book" Chijinshokan (1982).
- (2) IAEA Safety Guides : "Advisory Material for the IAEA Regulations for the Safe Transport of Redioactive Material" (1985) IAEA Safety Series No. 37 (1985)
- (3) Ethesington : "Nuclear Engineering Handbook" (1965)
- (4) Nuclear Handbook. Glaston (1965)
- (5) ORNL/RSIC Computer Code Collection ANISN-W "A One Dimensional Discrete Ordinates Transport Code" CCC-82
- (6) RSIC Data Library Collection DLC-23 "Cask 40 Group Coupled Neutron and Gamma-Ray Cross Section Data"
- (7) Japan Isotope Association: "Conversion factor for use in Radiological Protection against External Radiation " ICRP Publication 74 (1998)

(II)-E Criticality analysis

(II)-E. Criticality analysis

E.1 General

The criticality analysis on the present package is performed to demonstrate compliance of the package with the technical standards in accordance with the following Regulations:

(a) The Regulations Regarding the Transporting of the Nuclear Fuel Material etc. Outside of the Factory or Workshop (Ordinance No. 57 dated on Dec. 28, 1978 of the Prime Minister's Office, Ordinance No.1 dated on June 15, 2001 of Ministry of Education, Culture, Sports, Science and Technology, Ministry of Economy, Trade and Industry and Ministry of Land, Infrastructure and Transport) (hereinafter referred to as 'Ordinance') and

(b) The Notification Stipulating the Particulars Concerning the Technical Standards for the Transportation of Nuclear Fuel Materials etc. Outside of the Factory or Workshop (Notification No. 11 dated on Dec. 18, 1978 of Science and Technology Agency, Notification No.1 dated on June 15, 2001 of Ministry of Education, Culture, Sports, Science and Technology, Ministry of Economy, Trade and Industry and Ministry of Land, Infrastructure and Transport) (hereinafter referred to as 'Notification')

20 types of fuel elements are contained in this package. The numbers of the fuel elements contained in one package is 10. For KUCA fuel, the coupon type has a maximum of 120 plates as one fuel element, and the flat type has a maximum of 30 plates as one fuel element, and the numbers of the fuel elements contained in one package is 10. In this analysis, the criticality analysis is conducted for the case where the nine types of fuel elements, excluding the fuel follower, special fuel and half-loaded fuel element, are contained. The weight of contained ^{235}U per one fuel follower, special fuel and half-loaded fuel element is equal or less than the standard fuel element, therefore, the effective multiplication constant for the package becomes small, and the analysis is not conducted. For the criticality analysis of KUCA fuel, the coupon type is treated a maximum of 120 plates as one fuel element, and the flat type is treated a maximum of 30 plates as one fuel element. As for the JMTRC fuel elements, two types of fuels of different enrichment (MEU, HEU fuels), are contained and

transported. In this analysis, the subcriticality is also confirmed for containing MEU fuel elements and ten HEU fuel elements, and in addition, for containing five HEU fuel elements and five MEU fuel elements as the case of mixed sample.

E.2 Parts to be analyzed

E.2.1 Content

The package is designed to contain ten box-type fuel elements maximum as shown in (II)-Table E.1. All fuel elements to be loaded have the same enrichment. The maximum mass of ^{235}U loaded in a package is 4.85 kg, which corresponds to the JRR-3 standard type fuel element (Uranium Silicon Aluminum Dispersion Type Alloy). The fuel element is composed of the fuel plate which has a fuel meat made of an uranium-aluminum-silicon dispersion alloy. The uranium-aluminum dispersion alloy, the uranium-aluminum-silicon dispersion alloy or the uranium-molybdenum-aluminum dispersion alloy is covered with the aluminum alloy cladding. The specifications of fuel plate are shown in (II)-Table E.2.

E.2.2 Packaging

As described in (I)-A.9, a part of shock absorber and heat insulator of outer shell is deformed under normal test conditions concerning fissile package, but there is no deformation of inner shell, affecting criticality analysis.

Fuel elements or inner shell is not damaged while a part of shock absorber and heat insulator is deformed, under the accident test conditions concerning fissile package.

Therefore, this analysis model, excluding conservatively shock absorber and heat insulator as mentioned in (II)-E. 3.1, can be applied to the undamaged package during transport and the damaged package under the normal test conditions as well as the accident test conditions concerning the fissile package.

(II)-Table E.3 shows the deformation and remaining thickness of the shock absorber under normal transport conditions as well as under normal and accident test conditions of the fissile package.

(II)-Table E.1 Specification of fuel element

Item		Total Length	Cross Section	²³⁵ U Enrichment (wt%)	Mass of ²³⁵ U (g/one fuel element)	Maximum Number of Fuel Elements Loaded in a Package	Remark
Fuel element		(mm)	(mm)				
JRR-3 standard type (Uranium silicon aluminum dispersion type alloy)		1150	76.2×76.2	19.95	485	10	
JRR-3 follower type (Uranium silicon aluminum dispersion type alloy)		880	63.6×63.6	19.95	310	10	
JRR-4 B type fuel element		1025	80.0×80.0	93.3	170	10	
JRR-4 L type fuel element		1025	80.0×80.0	19.95	230	10	
JRR-4 (Uranium silicon aluminum dispersion type alloy)		1025	80.0×80.0	19.95	210	10	
JMTR standard fuel element		1200	77.0×77.0	46.0	320	10	MEU
				19.95	425	10	LEU
JMTR fuel follower		890	64.0×64.0	19.95	280	10	LEU
JMTRC standard fuel element	A	800	77.0×77.0	90.0	285	10	HEU
	B				242		
	C				199		
	A	800		46.0	317	10	MEU
	B				286		
	C				255		
JMTRC fuel follower		800	64.0×64.0	90.0	199	10	HEU
				46.0	210	10	MEU
JMTRC special fuel element	A	970	77.0×77.0	90.0	199	10	HEU
	B	435	65.7×65.7		67		
	C	970	77.0×77.0		242		
	D			46.0	285		MEU
	B				286		
	C				255		
KUR Standard fuel element		873.1	75.40×79.18	19.95	218	10	LEU
KUR Half-loaded fuel element		952.5	75.40×79.18	19.95	109	10	LEU
KUR Special fuel element		873.1	75.40×79.18	19.95	109	10	LEU
KUCA coupon fuel		—	—	—	—	1200	LEU
KUCA flat fuel		—	—	—	—	300	LEU

(II)-Table E.2 Specification of fuel plate (1/2)

Item Name of fuel elements		Fuel plate total length (mm)	Fuel plate width (mm)	Fuel plate thickness (mm)	Clad thickness (mm)	Weight per one fuel plate (g)	Remark
JRR-3 standard fuel element (Uranium silicon aluminum dispersion type alloy)		770	71.4	1.27	0.38	279	
JRR-3 follower type fuel element (Uranium silicon aluminum dispersion alloy)		770	59.4	1.27	0.38	228	
JRR-4B type fuel element		734	74.5	1.26	0.38	189	Outer fuel plate
		630	74.5	1.26	0.38	171	Inner fuel plate
JRR-4L type fuel element		734	74.5	1.65	0.38	270	Outer fuel plate
		630	74.5	1.65	0.38	266	Inner fuel plate
JRR-4 type fuel element (Uranium silicon aluminum dispersion alloy)		734	74.5	1.26	0.38	262	Outer fuel plate
		630	74.5	1.26	0.38	235	Inner fuel plate
JMTR-standard fuel element		778	70.8	1.27	0.385	271	MEU
						287	LEU
JMTR-fuel follower		769	58.9	1.27	0.385	235	LEU
JMTRC-standard fuel element	A	775	70.8	1.27	0.380	204	HEU
	B					201	
	C					199	
	A	778			0.385	212	MEU
	B					209	
	C					206	
JMTRC-fuel follower		780	58.5	1.27	0.380	171	HEU
		750	57.9		0.385	168	MEU
JMTRC-special fuel element	A	778	70.8	1.27	0.38	199	HEU
	B	385	58.5			71	
	C	800	70.6			201	
	D					204	
	B	800	70.8	1.27	0.385	209	MEU
	C					205	
KUR Standard fuel element		676.3 max	69.93	1.52	0.51	235	LEU
KUR Half-loaded fuel element		676.3 max	69.93	1.52	0.51	235	LEU
KUR Special fuel element		676.3 max	69.93	1.52	0.51	235	LEU
KUCA coupon fuel		50.8	50.8	2.3	0.4	30	LEU
KUCA flat fuel		600	62	1.5	0.5	190	LEU

(II)-Table E.2 Specification of fuel plate (2/2)

Item		Weight of ²³⁵ U per one fuel plate (g)	Fuel plate core length (mm)	Fuel plate core width (mm)	Fuel plate core thickness (mm)	Fuel plate core material	Remark
Name of fuel element							
JRR-3 standard fuel Element (Uranium silicon aluminum dispersion alloy)		23.1	750	62.0	0.51	Uranium silicon aluminum dispersion alloy	
JRR-3 follower type fuel element (Uranium silicon aluminum dispersion alloy)		18.2	750	49.0	0.51	Uranium silicon aluminum dispersion alloy	
JRR-4B type fuel element		6.0	600	68.0	0.50	Uranium aluminum alloy	Outer fuel plate
		11.9					Inner fuel plate
JRR-4L type fuel element		7.4	600	65.4	0.89	Uranium aluminum dispersion alloy	Outer fuel plate
		14.8					Inner fuel plate
JRR-4 type fuel element (Uranium silicon aluminum dispersion alloy)		7.5	600	65.4	0.50	Uranium silicon aluminum dispersion alloy	Outer fuel plate
		15.0					Inner fuel plate
JMTR-standard fuel element		16.8	759	61.6	0.50	Uranium aluminum dispersion type alloy	MEU
		22.4			0.51	Uranium silicon aluminum dispersion alloy	LEU
JMTR-fuel follower		17.5	750	49.7	0.50	Uranium silicon aluminum dispersion alloy	LEU
JMTRC-standard fuel element	A	15.0	750	58.0	0.508	Uranium aluminum alloy	HEU
	B	12.7					
	C	10.5					
	A	16.7	759	61.6	0.50	Uranium aluminum dispersion alloy	MEU
	B	15.1					
	C	13.4					
JMTRC-fuel follower		12.4	762	45.5	0.51	Uranium aluminum alloy	HEU
		13.1	730	49.7	0.50	Uranium aluminum dispersion alloy	MEU
JMTRC-special fuel element	A	10.5	750	61.8	0.51	Uranium aluminum alloy	HEU
	B	4.2	375	49.9			
	C	12.7	750	61.8			
	D	15.0					
	B	15.1	759	61.6			
	C	13.4					
KUR Standard fuel element		11.83	594.0	63.0	0.50	Uranium silicon aluminum dispersion alloy	LEU
KUR Half-loaded fuel element		11.83	594.0	63.0	0.50	Uranium silicon aluminum dispersion alloy	LEU
KUR Special fuel element		11.83	594.0	63.0	0.50	Uranium silicon aluminum dispersion alloy	LEU
KUCA coupon fuel		4	44.8	44.8	1.45	Uranium molybdenum aluminum dispersion alloy	LEU
KUCA flat fuel		15	570	56	0.5	Uranium silicon aluminum dispersion alloy	LEU

(II)-Table E.3 Distance from the surface of the inner shell
to the surface of the packaging

(Unit : mm)

Conditions Item	Normal transport condition (undamaged package)	Normal test condition for fissile packages	Accident test condition for fissile packages
Distance from the surface of the inner shell to that of the packaging	180	180	180
Deformation	0	34.8	102.7
Remained thickness	180	145.2 ^{*1}	77.3 ^{*1}

*1 In the damage system, it suppose distance from the pestle surface to the transportation container surface to be zero.

E.2.3 Neutron absorbing materials

The packaging is designed to use no neutron absorbing materials.

E.3 Model specification

E.3.1 Calculation model

This packaging is designed to contain fifteen types of rectangular fuel elements. The fuel follower contains less U235 per fuel element, compared with the standard type fuel element, so that the effective multiplication factor of the packaging will become smaller, and consequently we will analyze, here, 9 kinds of fuel elements, excluding the fuel follower and the special fuel element. The KUCA coupon and flat fuel are included in the analysis.

In the evaluation of subcriticality, under the assumption that all of the gap existing inside and outside of the packaging are filled with water, investigation will be conducted to select the package under severest condition among the damaged package and undamaged package in isolation and in arrays so that the analysis is to be executed under the severest conditions.

(1) Package in isolation (damaged package vs. undamaged package)

As for the packages in isolation, the zone surrounding the packaging of undamaged package consists of insulating material and the damaged packages are assumed as those having insulation taken out, to be replaced by water.

In this context, the neutron reflecting effect and neutron moderating effect of the water are greater than those of insulating material so that the conditions to which the damaged packages to be subjected will be severer since they have larger neutron reflecting effect and moderating effect.

(2) Arrays of packages (damaged package vs. undamaged package)

In the arrays of packages, the damaged packages which have no insulating material will be subjected to the severer conditions, compared with the undamaged packages, because the distances between the adjacent packaging in the arrays of packages are smaller and the neutron mutual interference effect is larger.

(3) Damaged packages in isolation vs. damaged packages in array

As for the damaged packages in isolation and in array, in case of packaging being filled by water, the neutrons will be sufficiently moderated in this model, and the extent of neutron moderation will be almost same in both of the cases, and the arrays of packages of perfect reflection with no leaks of neutrons at all will be subjected to severer results than the packages in isolation in which the neutrons leaks are considered smaller, taking the reflecting effect into account.

Consequently in this analysis the arrays of packages in radial direction will be taken, as shown in (II)-Fig.E.1 and (II)-Fig.E.2, as a triangular lattice type having the most densely arranged infinitive arrays composed of packaging having external shock absorber and insulating materials removed completely. In the axial direction, the evaluation will be conducted on the analysis model of damaged packages in array placed under the severest condition having infinite length of fuel part.

Therefore, the moderation of neutrons is at the same level in packages in isolation and those in array.

Packages in array in which no leakage of neutrons is supposed to occur may be subjected to more severe conditions than those in isolation in which less leakage of neutrons is supposed to occur because of the reflecting effect of the water.

Requirements defined in the regulation and analysis conditions is shown in (II)-Table E.4

(II)-Fig.E. 3 (box type fuel element) shows the model of the fuel element loaded in the inner shell. The inner shell is filled and surrounded with water, the density of which is 1.0g/cm^3 . Any structure materials except fuel baskets in inner shell are replaced by water to neglect neutron absorption by these materials.

As for the JMTRC fuels, two kinds of fuels of different enrichment are mixed in the package, as a sample of this case, (II)-Fig.E. 4 shows the criticality analysis model for mixed fuels.

Calculation model of 9-types fuel elements used in these analyses are shown in (II)-Fig.E. 5 to (II)-Fig.E. 14. The model of both JMTR standard fuel elements (LEU and MEU) is the same except for fuel meat compositions. JRR-4 B, JRR-4 L type fuel elements and JRR-4 fuel elements (Uranium Silicon Aluminum Dispersion Type Alloy) have the outer fuel plates which contain less amount of fissile than inner plates.

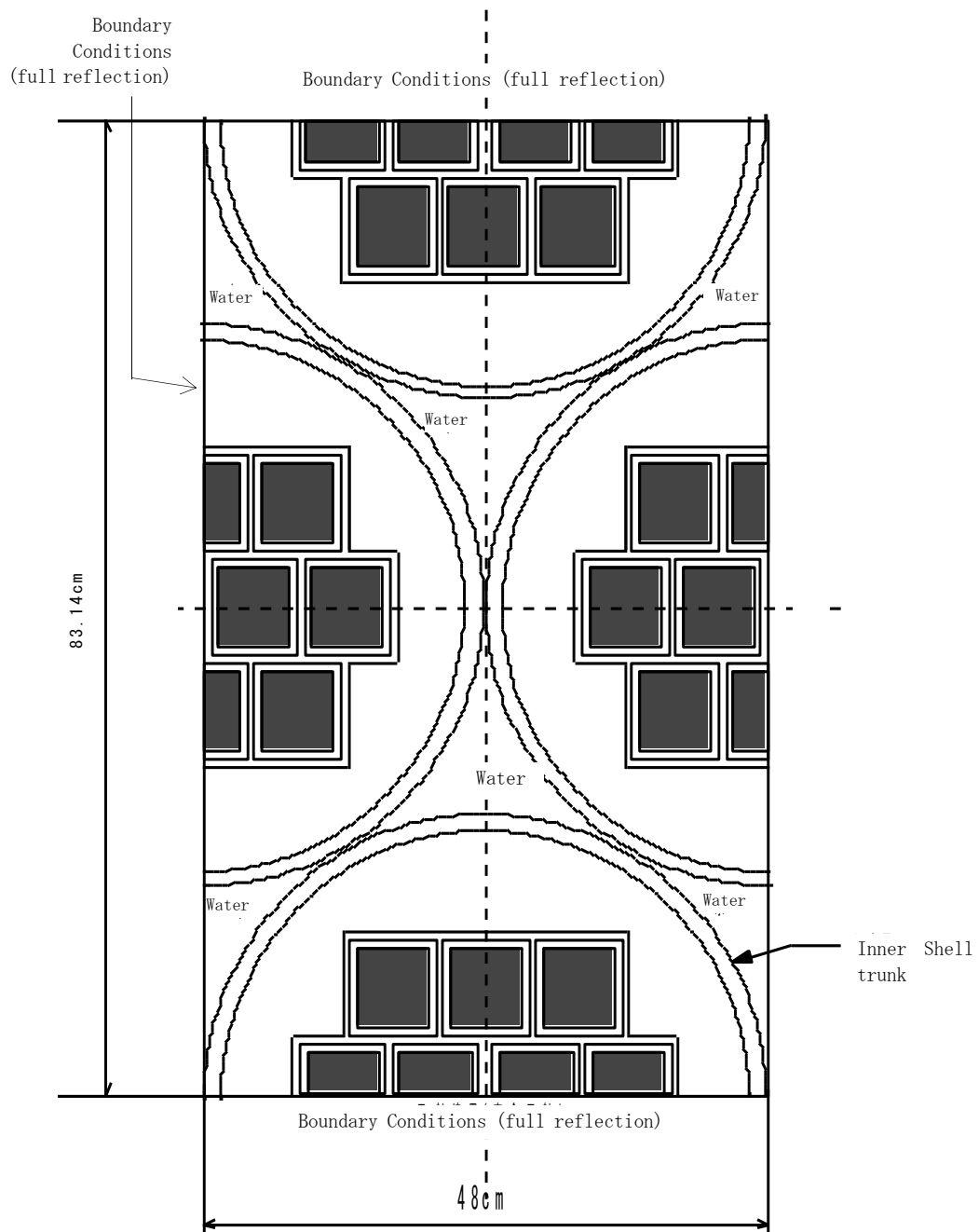
These outer plates are conservatively assumed to be the same with inner plates.

For the KUCA fuels, the analysis was conducted assuming the fuel core part and the aluminum cladding part were homogenized and the fuel plate was spread evenly throughout the square pipe of the basket. The coupon fuel was evenly arranged in the vertical direction in the square pipe, and the flat fuel was arranged in the horizontal direction in the square pipe.

E.3.2 Regional densities for each analyzed model region

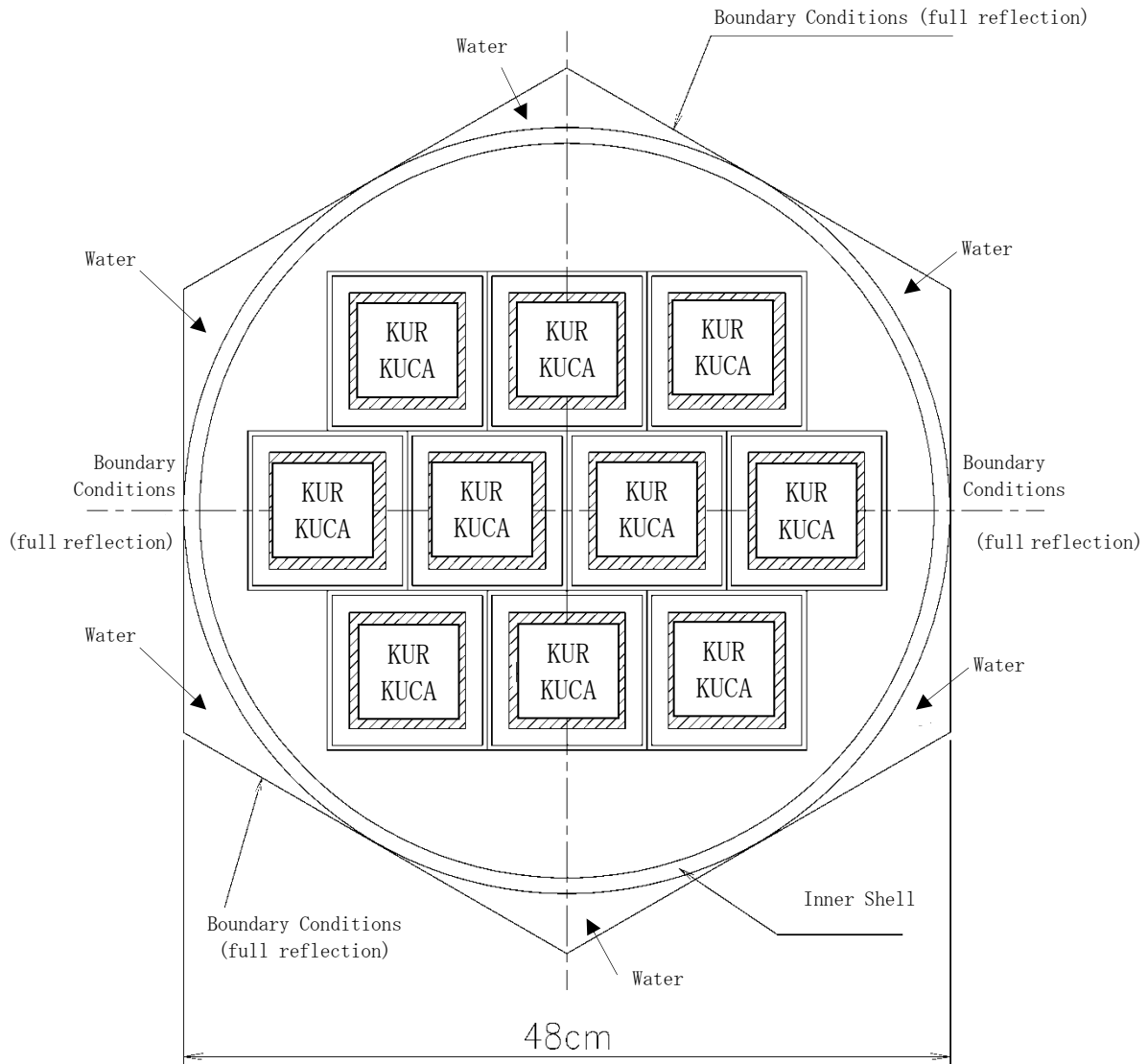
Atomic number density used in the calculation models of the package and the fuel elements are shown in (II)-Table E.5 and (II)-Table E.6 respectively.

Conservatively, the maximum value of enrichment of ^{235}U considering the tolerance is assumed for each fuel element.



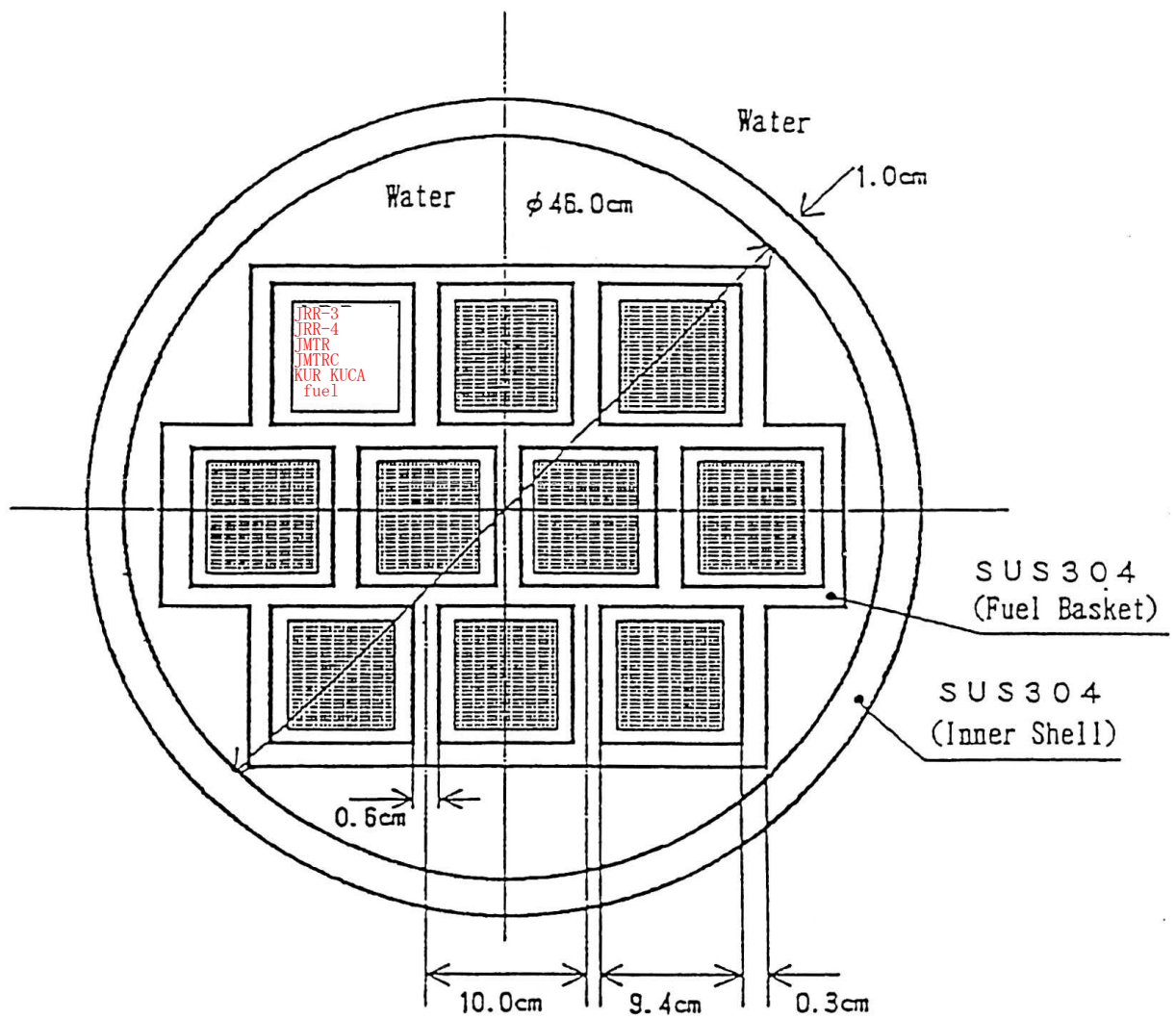
In this model of criticality, 60cm is chosen for the axial length and full reflection is supposed for the boundary conditions.

(II)-Fig.E.1 Calculation model of arrayed packages for criticality with 10 box type fuel elements (except KUR)

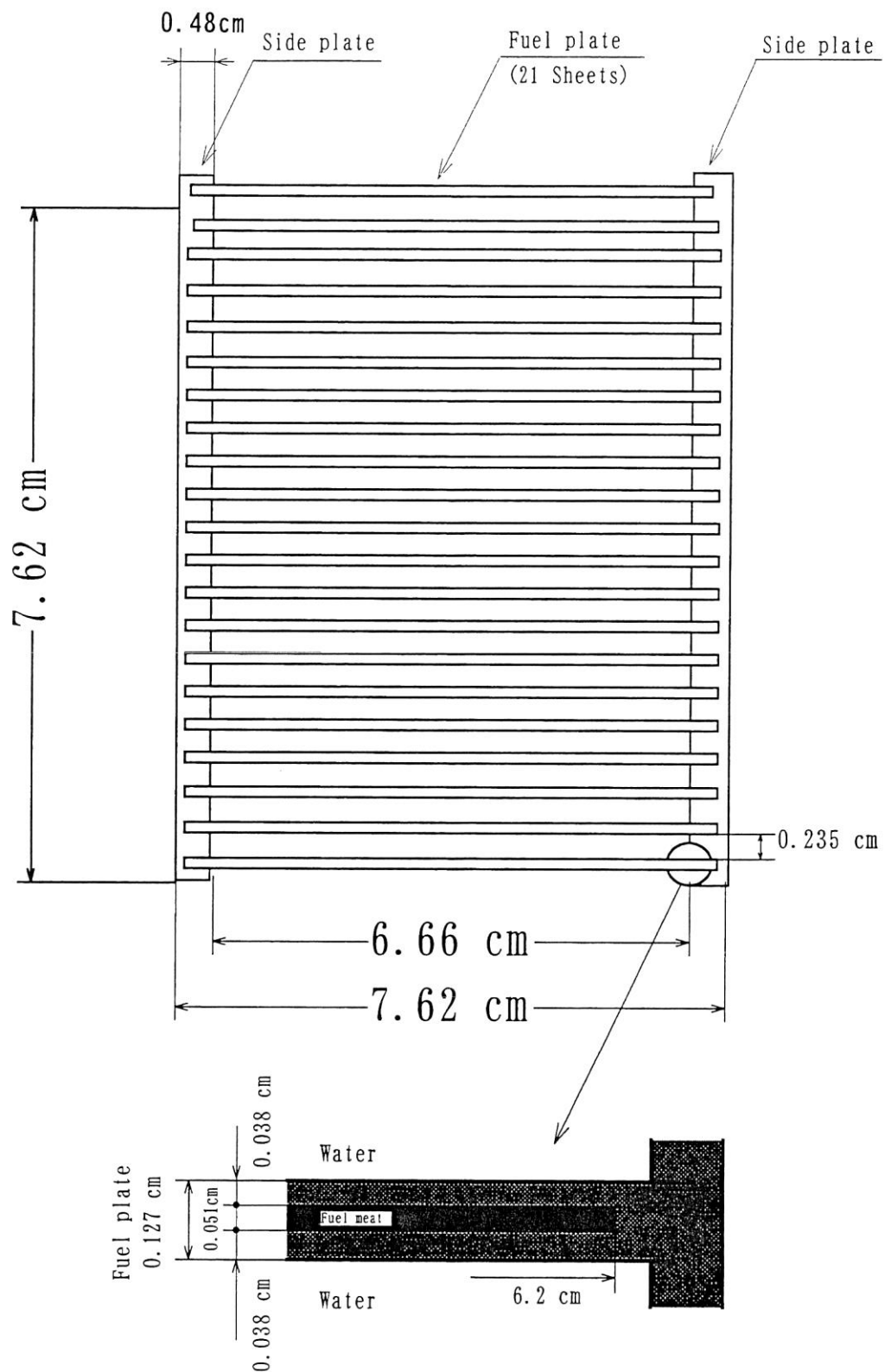


In this model of criticality, 60cm in the axial length is chosen for KUR and KUCA flat fuel, 120cm in the axial length is chosen for KUCA coupon fuel and full reflection is supposed for the boundary conditions. In the calculation, metal spacer was not included.

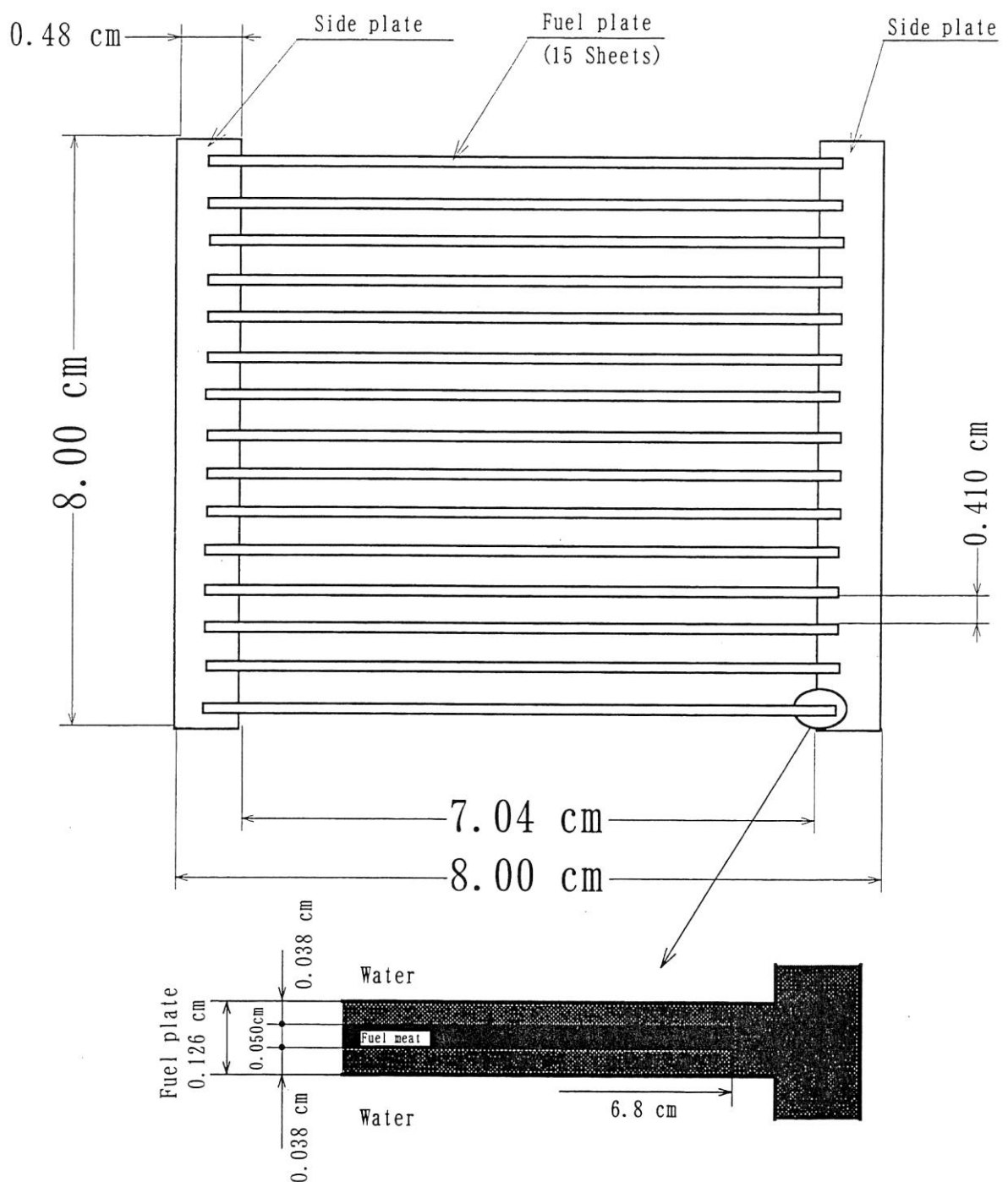
(II)-Fig.E.2 Calculation model of arrayed packages for criticality with 10 box type fuel elements (KUR and KUCA fuels)



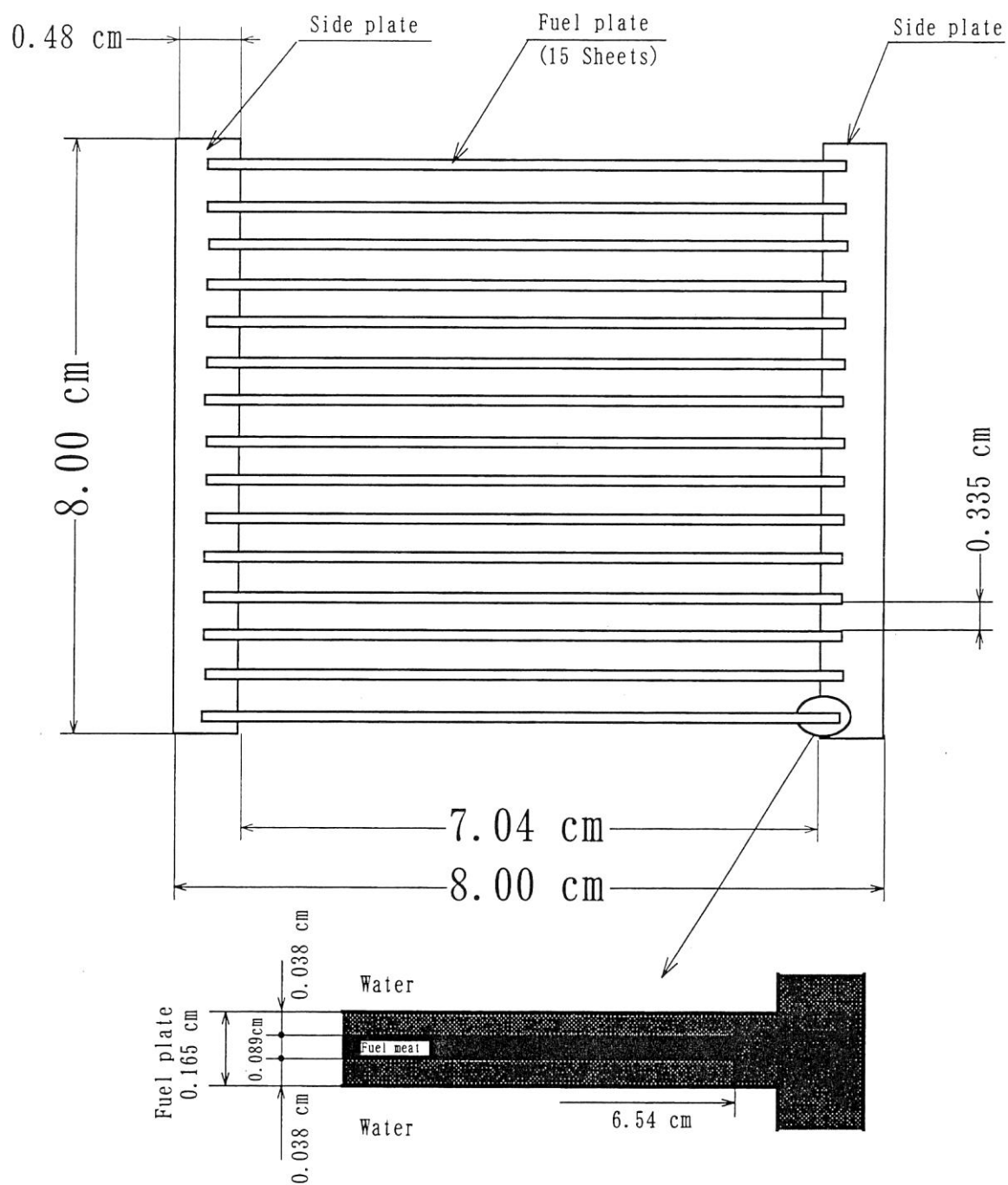
(II)-Fig.E.3 Calculation model of package for criticality
with 10 box type fuel elements



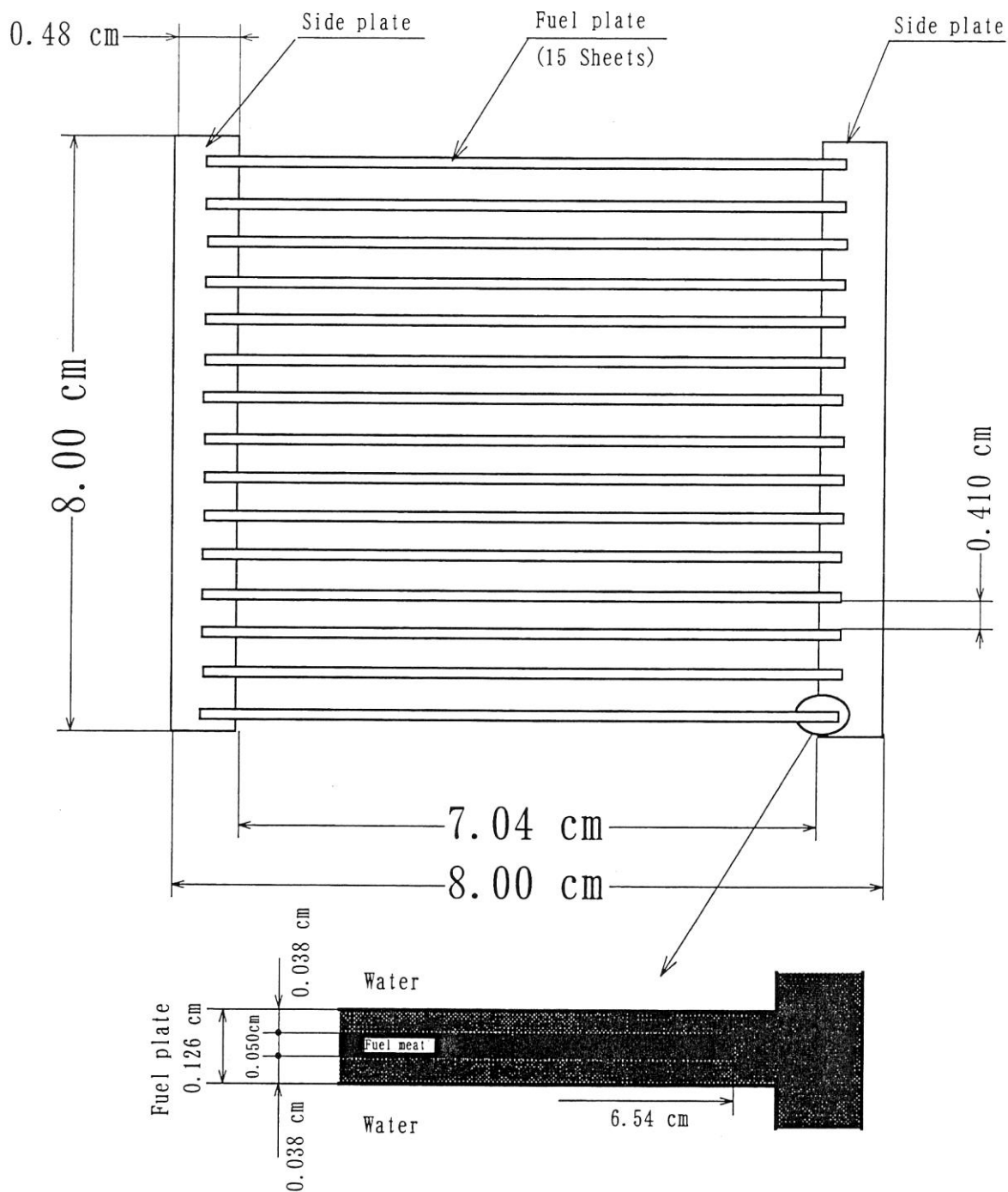
(II)-Fig.E.5 Criticality calculation model of JRR-3 standard fuel element



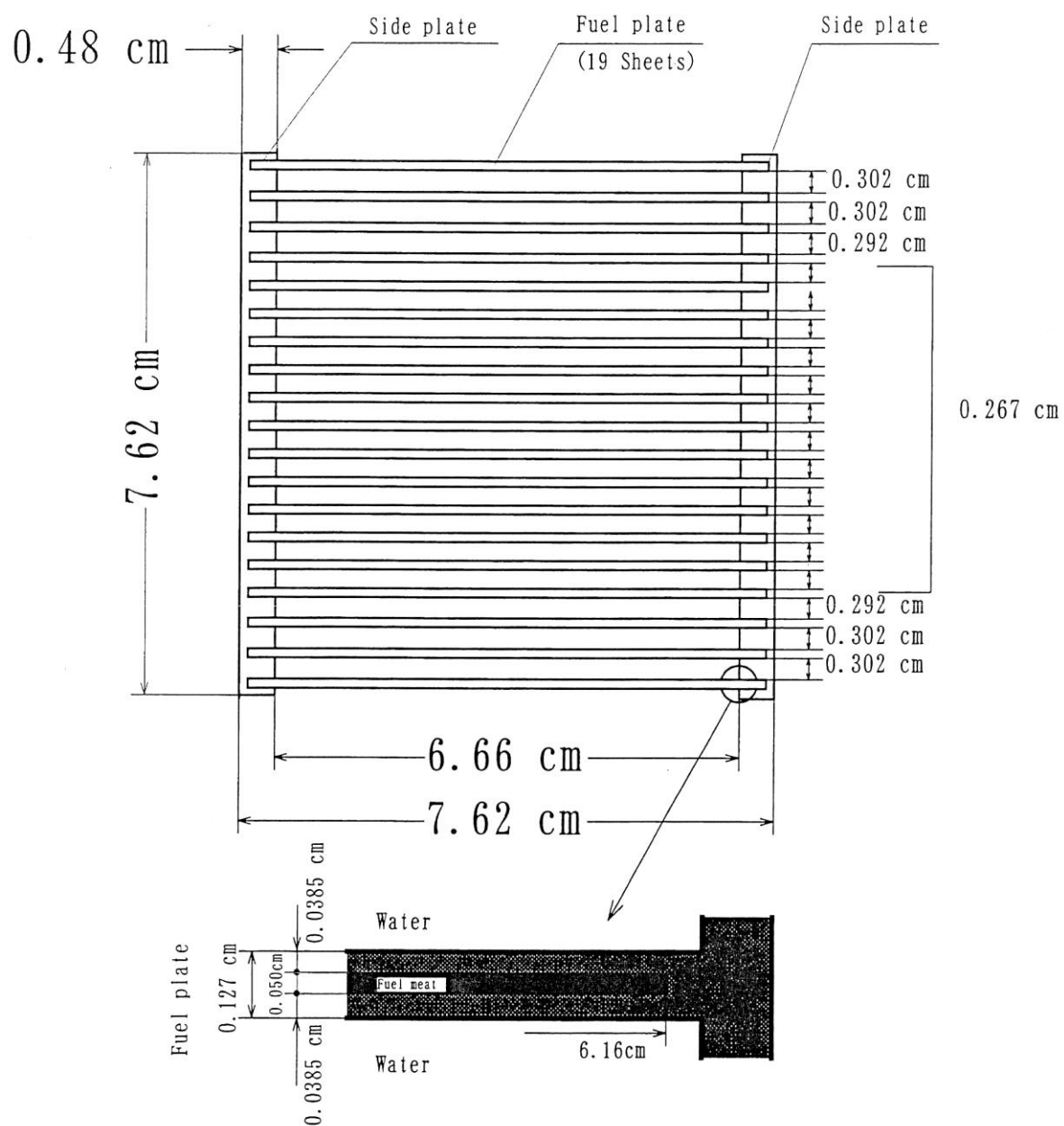
(II)-Fig.E.6 Criticality calculation model of JRR-4B type fuel element



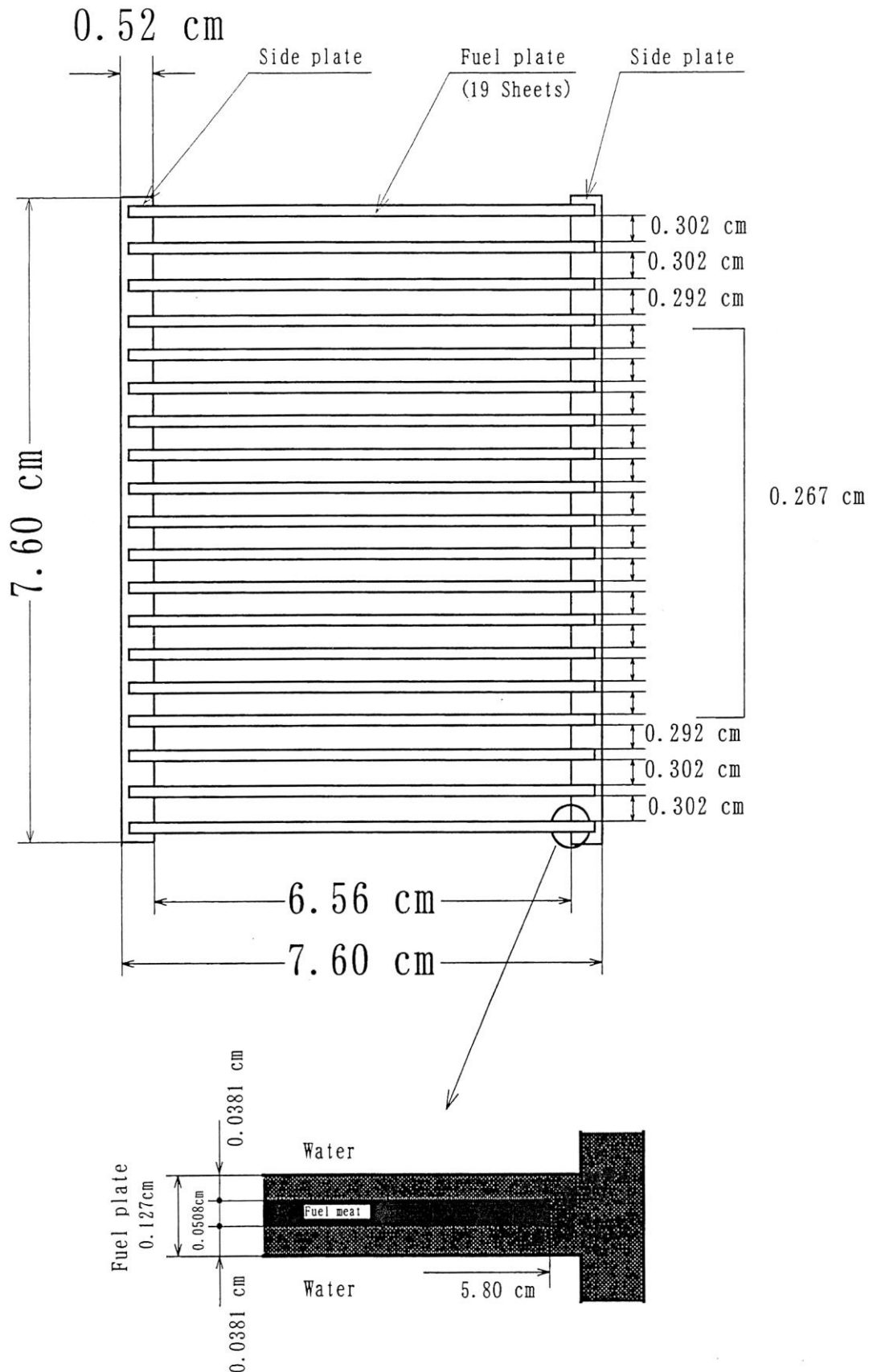
(II)-Fig.E.7 Criticality calculation model of JRR-4L type fuel element



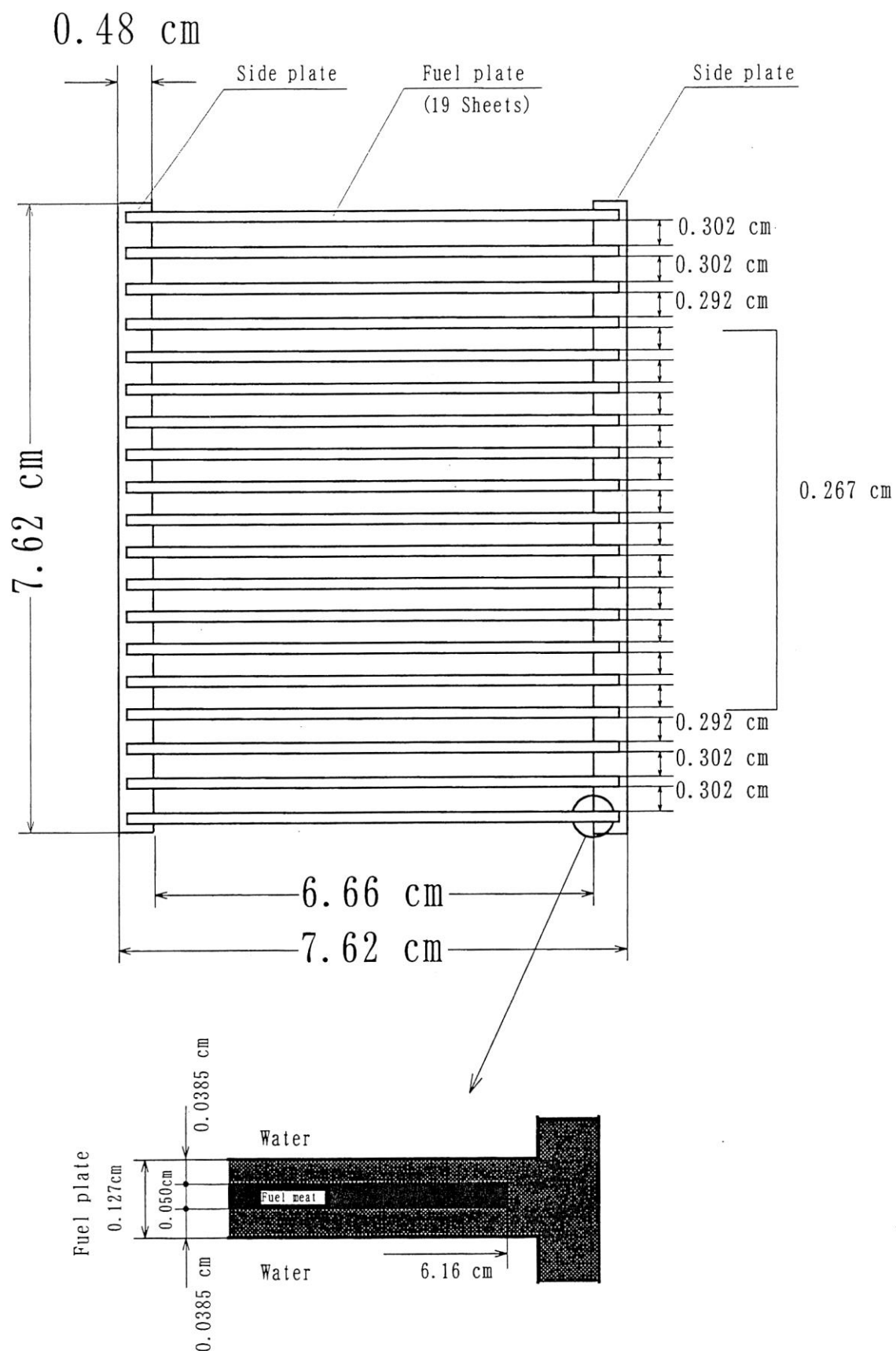
(II)-Fig.E.8 Criticality calculation model JRR-4 type fuel element



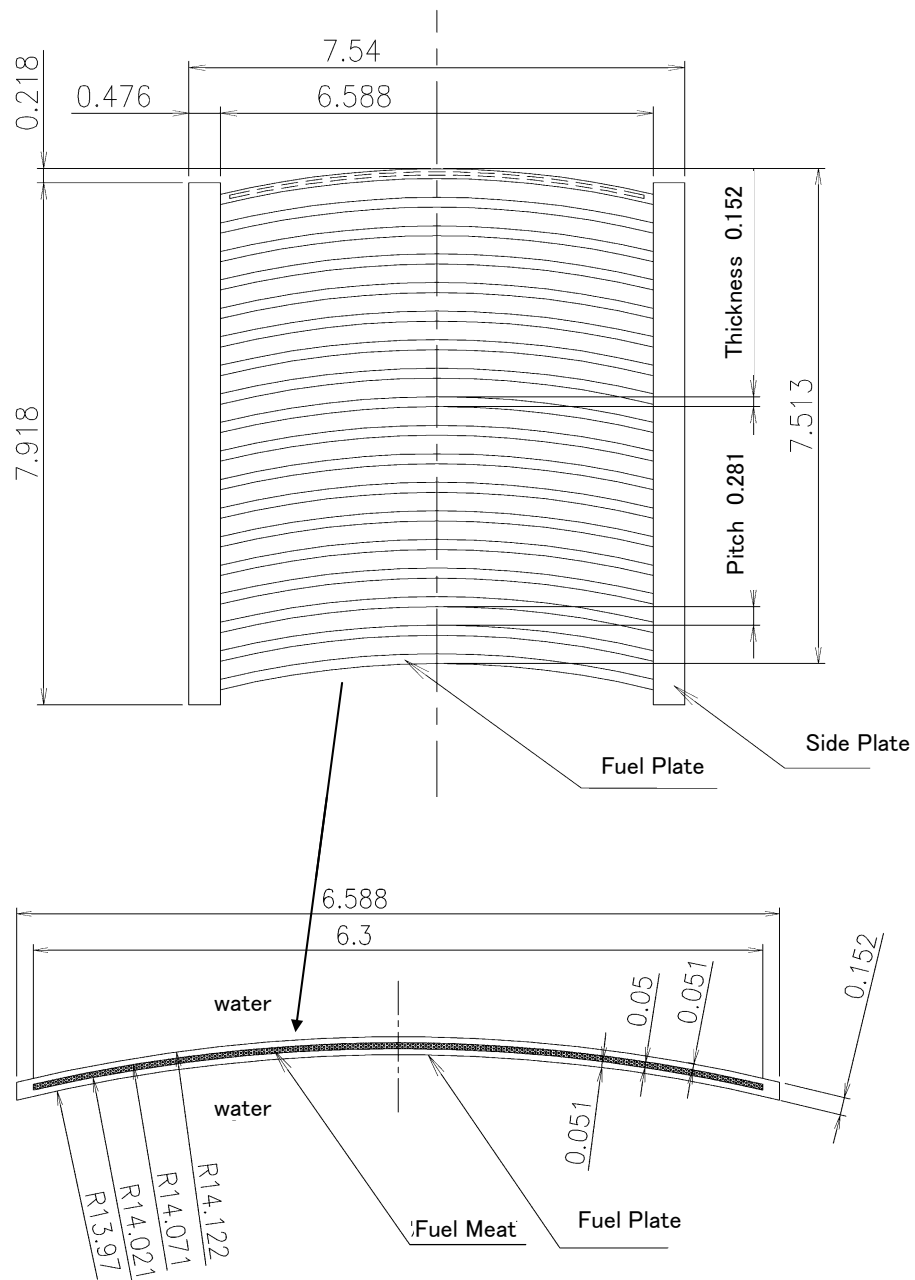
(II)-Fig.E.9 Criticality calculation model of JMTR standard type fuel element



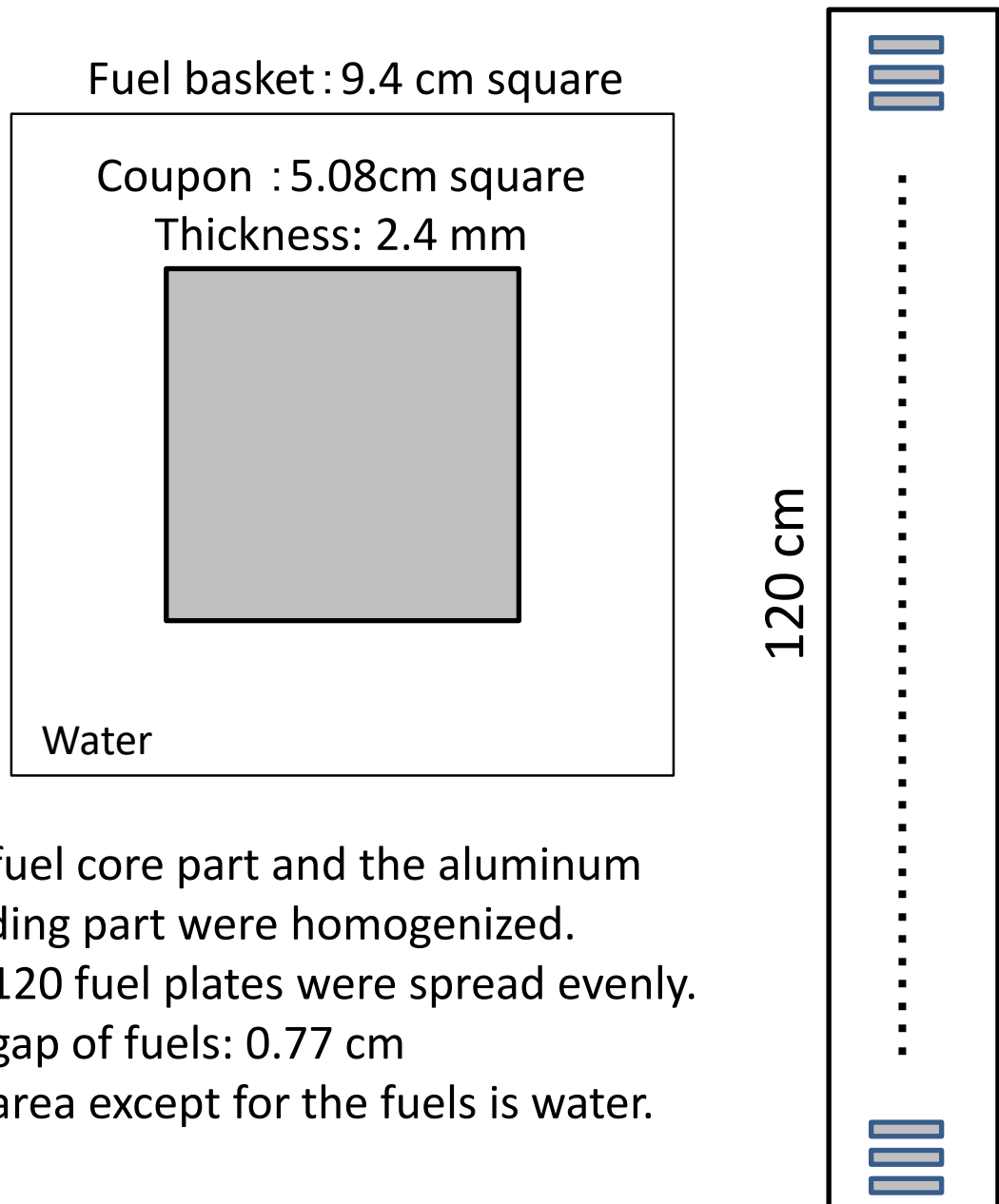
(II)-Fig.E.10 Criticality calculation model of JMTRC standard type
fuel element (HEU)



(II)-Fig.E.11 Criticality calculation model of JMTRC standard type
fuel element (MEU)

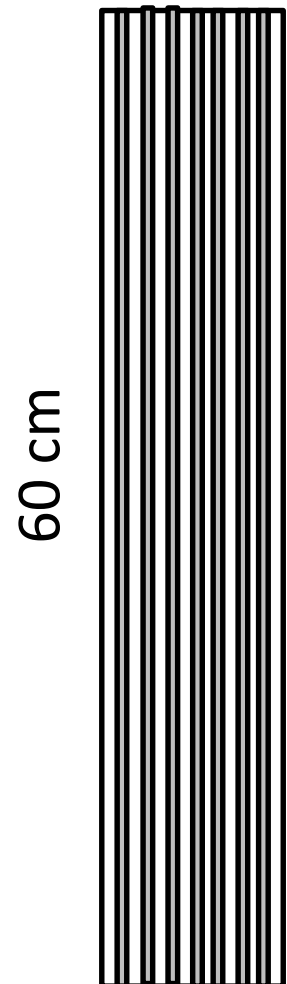
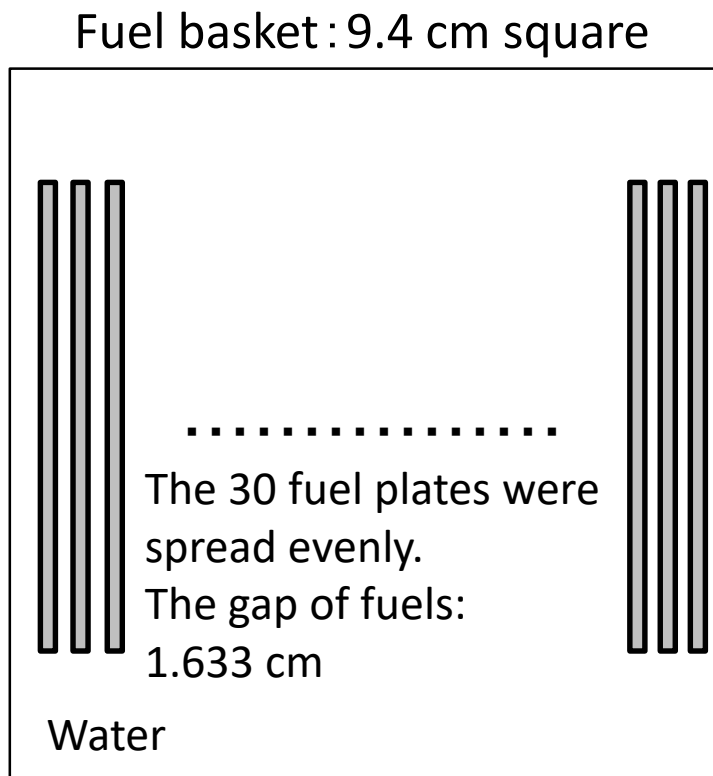


(II)-Fig.E.12 Criticality calculation model of KUR standard type fuel element



The fuel core part and the aluminum cladding part were homogenized.
 The 120 fuel plates were spread evenly.
 The gap of fuels: 0.77 cm
 The area except for the fuels is water.

(II)-Fig.E.13 Criticality calculation model of KUCA coupon type fuel



The fuel core part and the aluminum cladding part were homogenized.

(II)-Fig.E.14 Criticality calculation model of KUCA flat type fuel

(II)-Table E.4 Requirements defined in the regulation and analysis conditions

Requirement defined in the regulation				Analysis condition		
Conditions	Transport product	Infiltration of water into the transported articles	Approach of water reflection	Placement of the transported materials	Infiltration of water into the transported articles	Approach of water reflection
1. Normal Transportation Conditions		None	None	A triangular-lattice type model, in which inner shells are infinitely most densely-arranged, was adopted	Available	This is assessed with an infinite number, which is stricter than proximity/reflection of water.
2. Independent	1 pc	Available	Available			
3. General test condition	1 pc (Isolation)	Available	Available			
4. Special test condition	1 pc (Isolation)	Available	Available			
5. General test condition	5N pc* (Array)	要件なし	Available			
6. Special test condition	2N pc* (Array)	要件なし	Available			

* : N is Transport limited number. In this transport shell N=Infinite

(II)-Table E.5 Atom density of regions used in criticality calculation

(atoms/barn·cm)		
Nuclide	Inner shell and pipe of fuel basket	Water (1.0g/cm ³)
H	—	6.686×10^{-2}
O	—	3.343×10^{-2}
Cr	1.727×10^{-2}	—
Mn	1.721×10^{-3}	—
Fe	5.905×10^{-2}	—
Ni	7.449×10^{-3}	—

(II)-Table E.6 Atom density of fuel element used in criticality calculation

(atoms/barn·cm)

Nuc- lide	JRR-3 Standard Type (Uranium Silicon Aluminum Dispersion Alloy)	JRR-4 B Type Fuel Element	JRR-4 L Type Fuel Element (Uranium Aluminum Dispersion Alloy)	JRR-4 Fuel Element (Uranium Silicon Aluminum Dispersion Alloy)	JMTR (MEU) Standard Fuel Element	JMTR (LEU) Standard Fuel Element	JMTRC (HEU) Standard Fuel Element	JMTRC (MEU) Standard Fuel Element	KUR (LEU) Standard Fuel Element	Cladd- ing
Al	3. 0820 × 10 ⁻²	5. 6159 × 10 ⁻²	4. 7729 × 10 ⁻²	3. 8562 × 10 ⁻²	5. 2434 × 10 ⁻²	3. 3440 × 10 ⁻²	6. 0614 × 10 ⁻²	5. 0660 × 10 ⁻²	4. 353 × 10 ⁻²	5. 9922 × 10 ⁻²
Si	8. 6527 × 10 ⁻³	0	0	6. 4118 × 10 ⁻³	0	8. 2830 × 10 ⁻³	0	0	4. 932 × 10 ⁻³	5. 7890 × 10 ⁻⁵
Fe	0	0	0	0	0	0	0	0	0	1. 3387 × 10 ⁻⁴
²³⁵ U	2. 4952 × 10 ⁻³	1. 5415 × 10 ⁻³	1. 1563 × 10 ⁻³	1. 8490 × 10 ⁻³	1. 8459 × 10 ⁻³	2. 4515 × 10 ⁻³	1. 7397 × 10 ⁻³	1. 8511 × 10 ⁻³	1. 661 × 10 ⁻³	0
²³⁸ U	9. 8853 × 10 ⁻³	1. 0930 × 10 ⁻³	4. 5811 × 10 ⁻³	7. 3249 × 10 ⁻³	2. 1395 × 10 ⁻³	9. 7126 × 10 ⁻³	1. 9890 × 10 ⁻⁴	2. 3294 × 10 ⁻³	6. 741 × 10 ⁻³	0
Nuc- lide	KUCA Coupon		Nuc -lide	KUCA flat						
Al	6. 0262 × 10 ⁻²		Al	6. 0262 × 10 ⁻²						
Mo	1. 5956 × 10 ⁻³		Si	2. 3213 × 10 ⁻²						
²³⁵ U	1. 7266 × 10 ⁻³		²³⁵ U	7. 0175 × 10 ⁻⁴						
²³⁸ U	6. 8407 × 10 ⁻³		²³⁸ U	2. 7802 × 10 ⁻³						

E.4 Evaluation for subcriticality

E.4.1 Calculation conditions

(1) Content

(Ⅱ)-Table E.7 shows the 11 kinds of fuel elements, the content of packaging to be analyzed.

(Ⅱ)-Table E.7 Fuel elements to be analyzed

Fuel element \ Item	Enrichment of U235 (wt%)*	Maximum number of elements per package
JRR-3 standard type fuel element (Uranium Silicon Aluminum Dispersion Type Alloy)	20	10
JRR-4 B type fuel element	93	10
JRR-4 L type fuel element	20	10
JRR-4 fuel element (Uranium Silicon Aluminum Dispersion Type Alloy)	20	10
JMTR standard type fuel element	46	10
JMTR standard type fuel element	20	10
JMTRC standard type fuel element	90	10
JMTRC standard type fuel element	46	10
KUR standard type fuel element	20	10
KUCA coupon fuel	20	1200
KUCA flat fuel	20	300

* Nominal value

(2) Packaging

We evaluated the packaging on the assumption that the surface of the inner shell is the surface of the packaging (see (Ⅱ)-Fig.E.3)

E.4.2 Water Immersion into package

The Keff calculations when varying the density of water within and surrounding package are performed assuming that water enter into the package. The maximum Keff is observed at the density of water about 0.02g/cm^3 , and even in this case, the package is maintained subcritical.

In this calculation the displacement of package or temperature change due to water immersion is ignored.

The evaluation of Optimum Moderating Water Density is shown in E.7.1. Appendix.

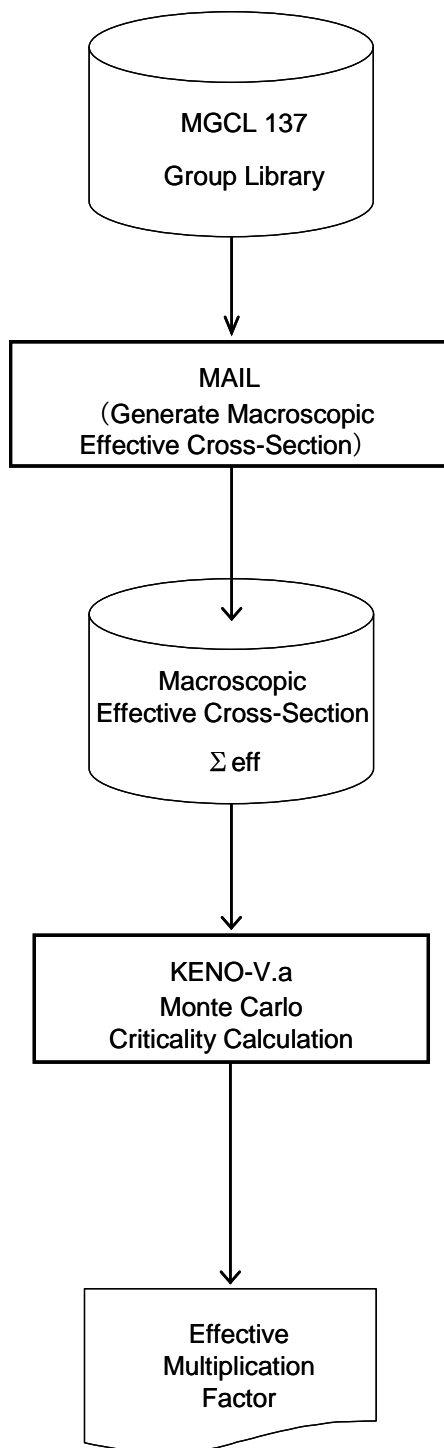
E.4.3 Calculation method

Criticality calculations are performed using a combination of the KENO-V.a Monte Carlo computer code[1] with the 137-energy group MGCL neutron cross-section library⁽²⁾. The explanations of KENO-V.a and MGCL is shown in E.6.2 and E.6.3. The slab geometry Dancoff-Ginsberg correction factor is considered in calculating the resonance self-shielding effects with MAIL code⁽¹⁾ included in the MGCL.

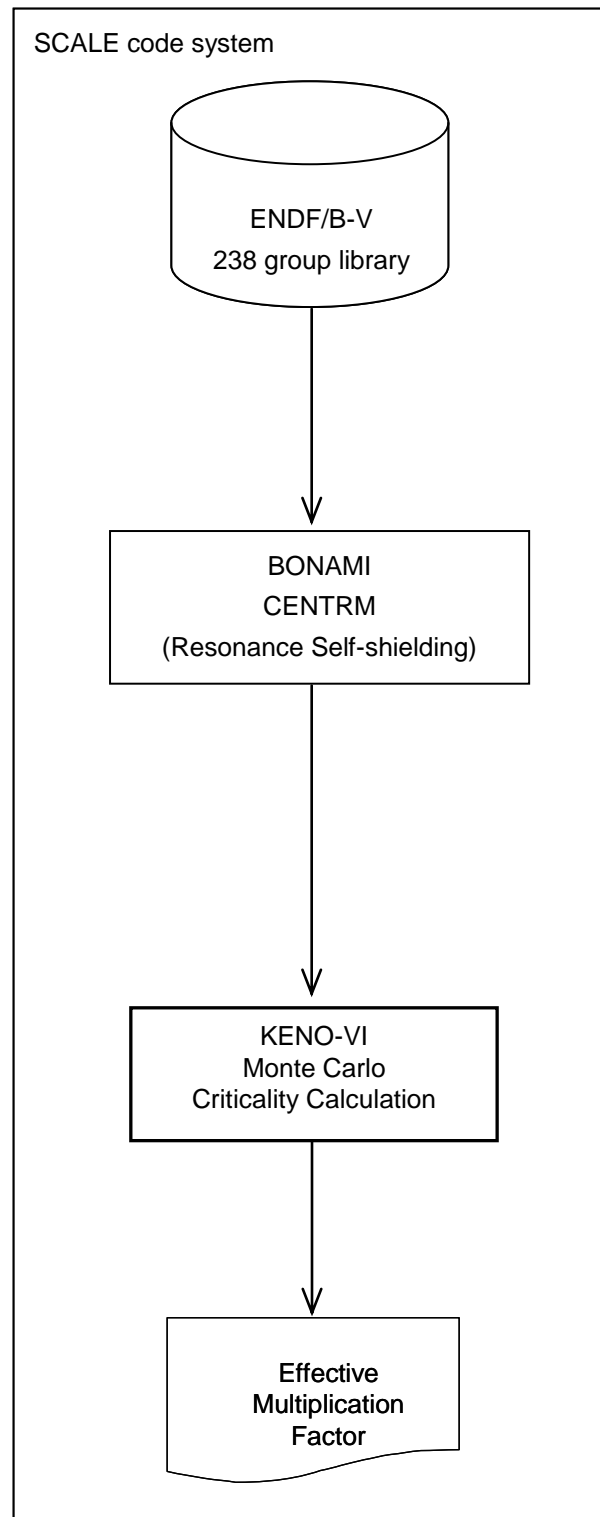
For the KUR fuel element (including KUCA fuel), criticality calculations were performed using the SCALE code system(3). KENO-VI Monte Carlo module together with the 238-energy group ENDF/B-V neutron cross section library of the SCALE code system was used for the calculation of keff. The resonance self-shielding effects were treated using the BONAMI and CENTRM modules of the SCALE code system. The explanation of KENO-VI code is shown in E.6.2.

(II)-Fig.E.15 shows the procedure of the calculation.

For Fuel elements except
KUR and KUCA fuel



For KUR and KUCA fuel



(II)-Fig.E. 15 Schematic flow of criticality analysis

E. 4. 4 Results

In the evaluation of subcriticality, arrays of damaged packages were analyzed which could be subjected to the most severe conditions (Section E. 3. 1).

(II)-Table E. 8 shows the calculation results of the effective multiplication factor in arrays of damaged packages under submergence.

The maximum $K_{eff} \pm \sigma$ is 0.902 ± 0.005 (standard deviation of the Monte Carlo calculation) with JRR-3 standard type fuel elements (Uranium Silicon Aluminum Dispersion Type Alloy) in a package. The maximum K_{eff} at a 99% confidence level of this result $K_{eff} + 3\sigma$ is 0.917, which is less than the standard value of 0.95.

For KUCA coupon fuel, when 1200 KUCA coupon fuels in a package (120 coupons are inserted into one grid of rectangular pipe) and the coupon gaps were 0.4 cm, and the fuel in each grid is at the center of the basket, the maximum $K_{eff} \pm \sigma$ is 0.8080 ± 0.0026 . The maximum K_{eff} at a 99% confidence level of this result $K_{eff} + 3\sigma$ is 0.8158, which is less than the standard value of 0.95.

For KUCA flat fuel, when 300 KUCA flat fuels in a package (30 flat plates are inserted into one grid of rectangular pipe) and the fuel plates gaps are evenly spread most, and the fuel in each grid is at the center of each grid, the maximum $K_{eff} \pm \sigma$ is 0.9055 ± 0.003 . The maximum K_{eff} at a 99% confidence level of this result $K_{eff} + 3\sigma$ is 0.9145, which is less than the standard value of 0.95.

The effect of optimum moderation by water is considered by varying the density of water within and surrounding the inner shell from 1.0 g/cm^3 to 0.0 g/cm^3 . The calculations are performed for the JRR-3 standard type fuel element (Uranium Silicon Aluminum Dispersion Type Alloy) which shows the highest effective multiplication factor of the 11 types of fuel elements at Max density of water 1.0 g/cm^3 . The results show that the optimum moderation occurs at a water density of 0.02 g/cm^3 , and it is subcritical

($k_{eff}+3\sigma=0.939$).

For KUCA fuel, the effect of optimum moderation by water is considered by varying the density of water within and surrounding the inner shell from 1.0g/cm³ to 0.0g/cm³. The calculations are performed for the flat fuel which shows the highest effective multiplication factor at Max density of water 1.0 g/cm³. The results show that the optimum moderation occurs at a water density of 0.001 g/cm³, and it is subcritical ($k_{eff}+3\sigma=0.9325$).

As for JMTRC fuel, there is a case in which two kinds of fuel of different enrichment (MEU, HEU fuels) are mixed in the package and transported.

In this case, the quantity of ²³⁵U loaded is less than the case where the MEU fuels are loaded, and the effective multiplication factor becomes smaller than the case of MEU fuels loading.

(II)-Table E.8 Results of criticality analysis when immersed

Fuel Element	Meat Material	Enrichment of $^{235}\text{U}^{*1}$ (wt%)	Mass of $^{235}\text{U}^{*1}$ (g/element)	Number of Fuels *2 (Unit/package)	$K_{\text{eff}} \pm \sigma$	$K_{\text{eff}} \pm 3\sigma$
JRR-3 Standard Type	Uranium-Silicon-Aluminum dispersion Alloy	19.95	485	10	0.902 ± 0.005	0.917
						0.939 *3
JRR-4 B Type	Uranium-Aluminum Alloy	93.3	182	10	0.811 ± 0.006	0.829
JRR-4 L Type	Uranium-Aluminum dispersion Alloy	19.95	245.3	10	0.801 ± 0.007	0.822
JRR-4	Uranium-Silicon-Aluminum dispersion Alloy	19.95	210	10	0.799 ± 0.004	0.811
JMTR Standard Type (MEU)	Uranium-Aluminum dispersion Alloy	46.0	320	10	0.827 ± 0.006	0.845
JMTR Standard Type (LEU)	Uranium-Silicon-Aluminum dispersion Alloy	19.95	425	10	0.893 ± 0.004	0.905
JMTRC Standard Type (HEU)	Uranium-Aluminum Alloy	90.0	285	10	0.783 ± 0.004	0.796
JMTRC Standard Type (MEU)	Uranium-Aluminum dispersion Alloy	46.0	317	10	0.812 ± 0.004	0.825
JMTRC Standard Type (HEU, MEU)	Uranium-Aluminum Alloy	90.0	285	5	0.796 ± 0.004	0.809
	Uranium-Aluminum dispersion Alloy	46.0	317	5		
KUR Standard Type	Uranium-Silicon-Aluminum dispersion Alloy	19.95	218	10	0.771 ± 0.001	0.774
KUCA Coupon fuel	Uranium-Molybdenum-Aluminum dispersion Alloy	19.95	4	1200 (120/grid)	0.8080 ± 0.0026	0.8158 *4
KUCA Flat fuel	Uranium-Silicon-Aluminum dispersion Alloy	19.95	15	300 (30/grid)	0.9055 ± 0.003	0.9145
						0.9325 *5

*1 : The value utilized in calculation

*2 : Number of fuel elements loaded in a package

*3 : Water density 0.02g/cm³

*4 : Fuels was slide at the center of basket

*5 : Water density 0.001g/cm³ which is outside of basket

E.5 Benchmark test

(1) Benchmark test

To verify the validity of the criticality analysis method by using a combination of the KENO-Va code and the 137 energy group MGCL Library which is used in this chapter, the analysis is conducted for the following experiments, and the result is evaluated.

- (a) The criticality test (TCA criticality test)⁽³⁾ conducted in National institute of Japan Atomic Energy Agency (JAEA), in which the lowly enriched UO₂ fuel rods clad by Aluminum are arrayed.
- (b) The criticality test (International benchmark test)⁽⁴⁾ conducted in ORNL using the SPERT-D fuel (Uranium Aluminum alloy, 93.17% ²³⁵U enrichment)
- (c) The criticality test⁽⁵⁾ conducted for JRR-4
(20% enrichment, U₃Si₂, plate type fuel)

(2) Description of benchmark experiment

(a) TCA criticality test

The benchmark experiment was performed at Tank-type Critical Assembly (TCA) of JAEA. The critical water heights were measured by the experiment. The experiment was performed varying fuel type, rod lattice pattern, lattice pitch and fixed poisons. The fuel material is uranium or uranium-plutonium oxide.

The experimental configuration of TCA facility and the dimension of uranium oxide rod are shown in [\(II\)-Fig. E. 16.](#)

The fuel rods are arrayed on a square pitch in the tank and four kind of lattice pitch, which correspond to the water-to-fuel volume ratio are 1.50, 1.83, 2.48 and 3.00. The number of fuel rods in a tank is changed according to the lattice pitch.

The calculations are performed for five cases of above experiment with low enriched (2.6% ²³⁵U) uranium oxide fuel.

(b) International benchmark test

OECD/NEA planned ICSBEP (International Criticality Safety Benchmark Evaluation Project) in 1994 to verify the criticality safety analysis code, and produced the International Handbook of Evaluation Criticality Safety Benchmark Experiments. In this handbook, the criticality test conducted in ORNL (23 tests) to determine the specification of fuel storage, transport and reprocessing by using SPERT-D fuel (Uranium aluminum alloy, 93.17% ^{235}U enrichment, shown in [\(II\)-Fig.E.17](#), [\(II\)-Fig.E.18](#)) is described.

The three cases of criticality data, which are close to the JRR-4, are selected from the above test data as the international benchmark test data, are analyzed by using MGCL library and KENO-V a code. The above three cases are described as follows.

(i) CASE3 (SPART3)

Shape of lattice	: 4×3.09
No. of criticality fuel	: 12.36 ± 0.17
Criticality mass (^{235}U)	: $3.79 \pm 0.05\text{kg}$
Lattice array	: Refer to (II)-Fig.E.19 (The figure shows the No. of the fuel plate)

(ii) CASE15 (SPART15)

Shape of lattice	: 16×3
No. of criticality fuel	: 48
Criticality mass (^{235}U)	: 19.62kg
Lattice array	: Refer to (II)-Fig.E.19 (The figure shows the No. of the fuel plates)

(iii) CASE23 (SPART23)

Shape of lattice	: 6×5.55
No. of criticality fuel	: 33.12 ± 0.10
Critical mass (^{235}U)	: $10.15 \pm 0.03\text{kg}$
^{235}U enrichment	: $3.99\text{g}/\ell$
Boron enrichment	: $0.871\text{g}/\ell$
Lattice array	: (II)-Fig. E. 19 (The figure shows the No. of fuel plates)

(c) JRR-4 critical test

JRR-4 is a swimming pool type research reactor of maximum 3.5MW output, and the fuel is lowly enriched uranium silicon aluminum dispersion type fuel.

The fuel elements are arrayed in the 4×5 lattice, and the graphite reflector (Lid tank side, the large reflector is made of Aluminum), irradiation shell and the neutron source are arranged outside the fuels. The plate shape 5 control rods and back up safety control rod are located between the fuel elements and the reflector. The moderator and the coolant are light water.

The fuel elements and the core arrangement are shown in (II)-Fig. E. 20 and (II)-Fig. E. 21 respectively. The minimum core and total core criticality tests are conducted in July in 1998.

As for the minimum core, the 12 fuel elements are arranged on the cross lines, and the graphite reflector is located outside the fuel elements, and the control rods of C_1 , C_2 and C_3 are being withdrawn by full stroke, and the C_4 control rod and the C_5 control rod are being withdrawn by 369mm and 292mm respectively. The core temperature during the experiment is approximately 20°C .

The criticality analysis for these minimum core criticality and for the maximum core criticality are conducted by combining the MGCL library and KENO-V a code.

(3) The result of the benchmark test

In order to verify the accuracy of the criticality analysis by combining the MGCL library and the KENO-V.a code used in this analysis, the effective multiplication factors by using MGCL and KENO-V.a are obtained for the following conditions, and the result is shown in (II)-Table E.9.

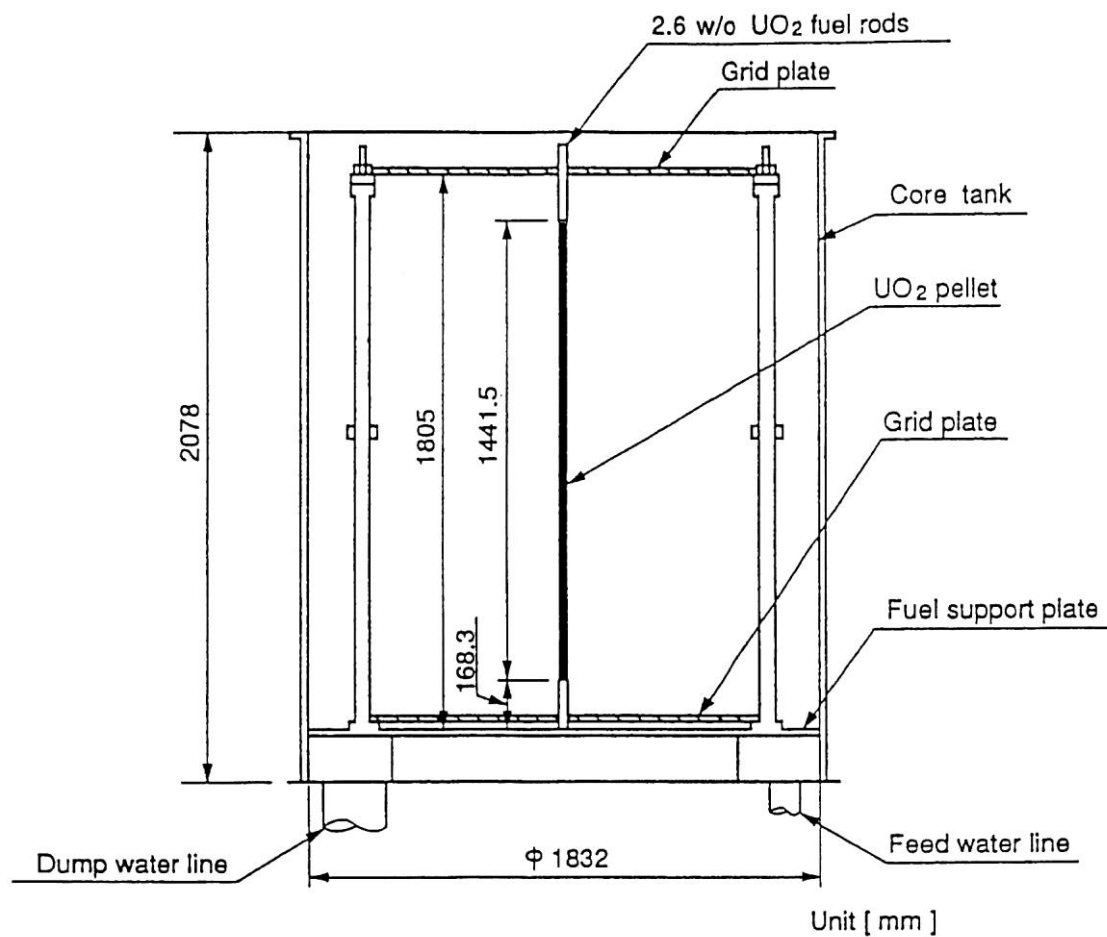
- (a) The criticality experiment (TCA criticality experiment) in which the lowly enriched UO_2 fuel rod with the Aluminum clad, conducted in JAEA.
- (b) The criticality experiment (International benchmark experiment) conducted in ORNL using SPERT-D fuel (Uranium Aluminum alloy, ^{235}U enrichment of 93.17%)
- (c) The maximum and minimum core criticality experiment conducted in JRR-4 (20% enrichment, U_3Si_2 , plate fuel)

From these results, the analytical procedure and the nuclear data is judged to bring the valid result.

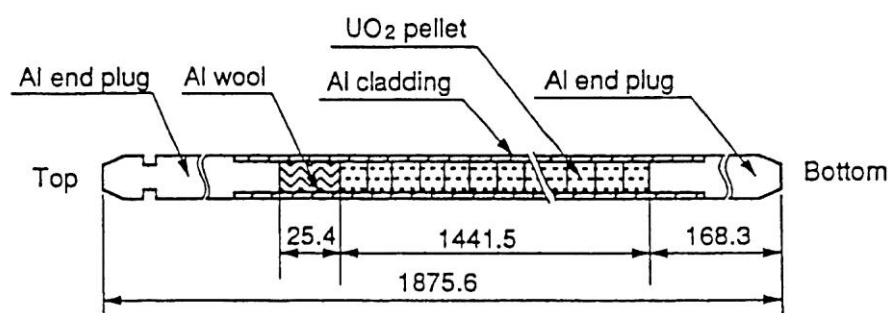
(II)-Table E.9 Analysis result of benchmark criticality test

Test name	Fuel rod (Plate) (Element) array	Keff	1σ	Keff+3 σ
TCA criticality experiment	$17 \times 17 - 1.83^*$	0.9926	0.0042	1.0052
	$21 \times 21 - 1.83$	0.9911	0.0043	1.0040
	$20 \times 20 - 1.50$	0.9883	0.0040	1.0003
	$18 \times 18 - 2.48$	0.9859	0.0041	0.9982
	$17 \times 17 - 3.00$	0.9981	0.0041	1.0104
International benchmark test	$(88 \times 68 + 1 \times 2)$	0.98896	0.00174	0.99418
	(352×88)	0.98865	0.00141	0.99288
	$(132 \times 110 + 11 + 12 + 11 + 12 + 12 + 11)$	0.99110	0.00138	0.99524
JRR-4 criticality test	$(2 \times 4 + 4)$	0.98901	0.00138	0.99315
	(4×5)	0.98319	0.00116	0.98667

* : Volumetric ratio of fuel and water

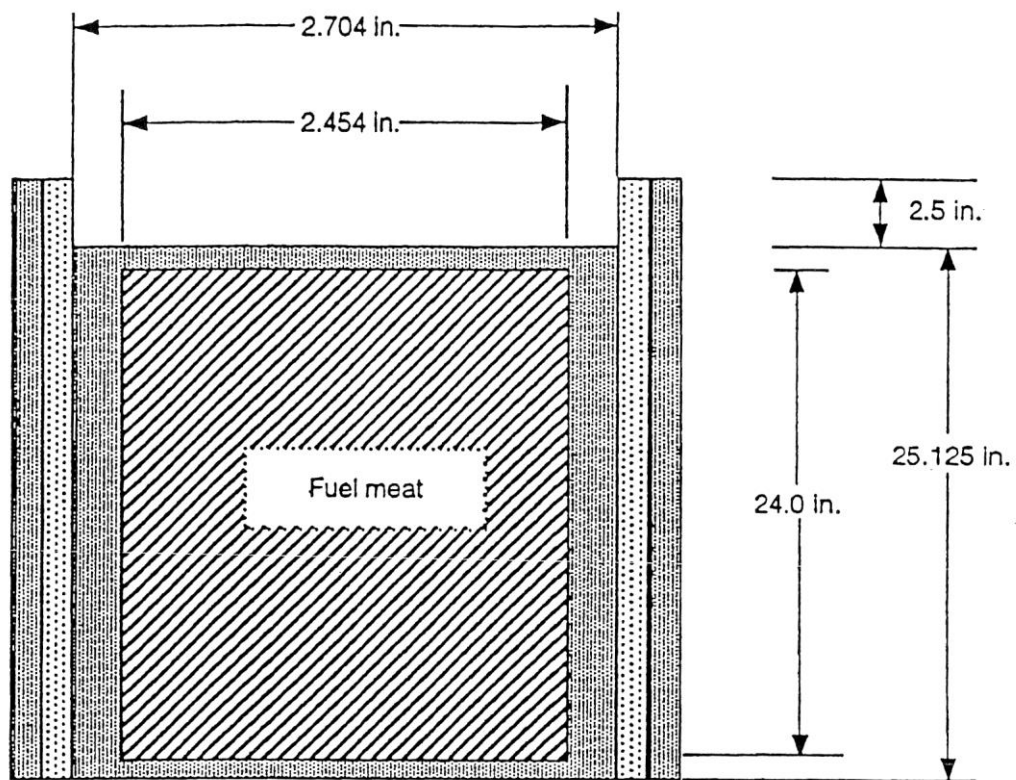


Vertical cross-sectional view of core tank



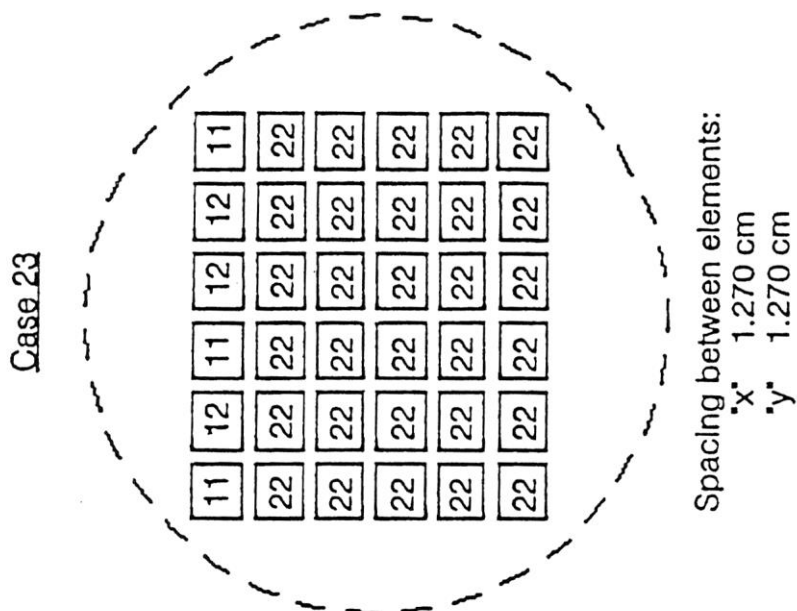
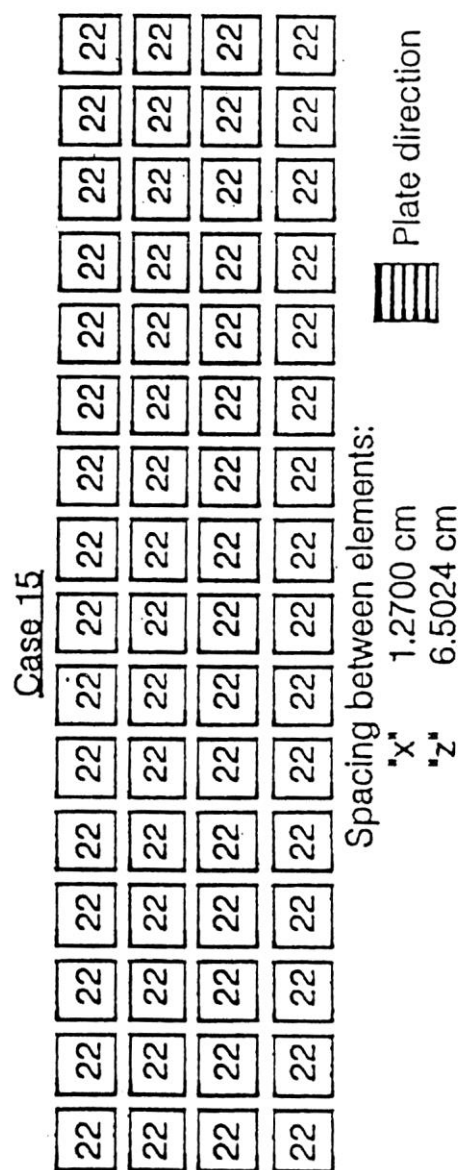
2.6 w/o UO_2 fuel rods

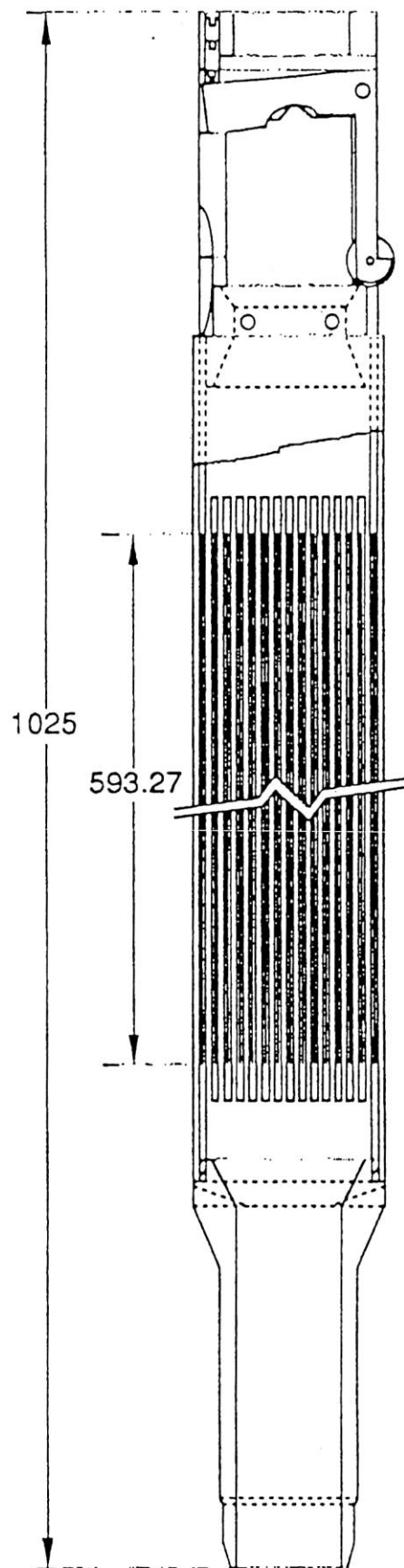
(II)-Fig. E. 16 Configuration of TCA criticality experiments



Section A - A

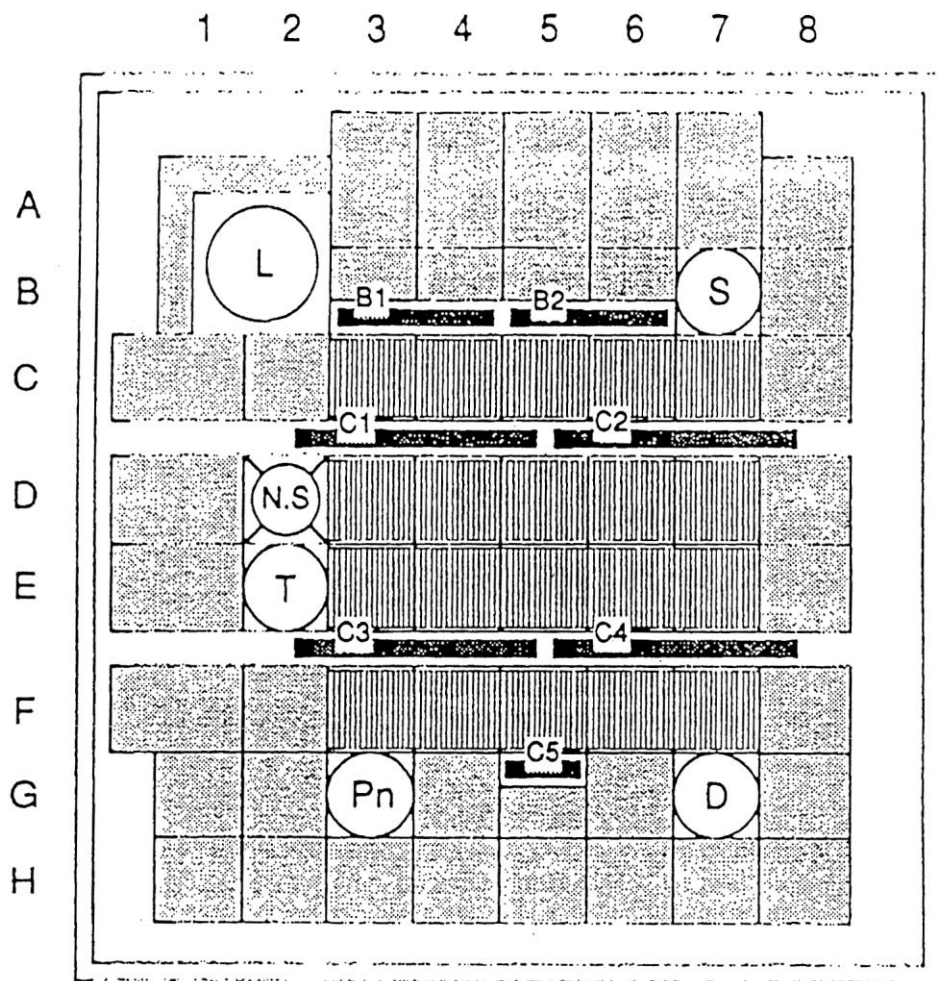
(II)-Fig. E. 18 SPERT-D fuel (continued)





(dimensions in mm)

(II)-Fig. E. 20 Fuel element



Fuel



Graphite Reflector



Irradiation Pipe



Neutron Source



Control Rod (C1~C5, B1,B2)

(II)-Fig. E. 21 Core arrangement

E.6 Summary of results and evaluation

If it is assumed that the article is under the general test conditions for fissionable transported articles, the deformation of the shipping casket is the deformation of the outer shell, which is outside a system subject to criticality assessment (surface of the transported article with the state of damage considered). No dent containing a cube measuring 10 cm on a side would occur in the inner shell that is a system subject to criticality assessment, and each side of a circumscribed rectangular solid would not be below 10 cm.

The maximum effective multiplication factor was obtained when one package contained ten JRR-3 standard type fuel elements (Uranium Silicon Aluminum Dispersion Type Alloy) as shown in (II)-Table E. 7.

$$K_{eff} + 3\sigma = 0.917$$

and the packaging is in subcriticality.

E.7 Appendix

E.7.1 Evaluation of optimum moderating water density

E.7.2 Description of KENO-V a code and KENO-VI code

E.7.3 Explanation of MGCL neutron cross section library and MAIL code

E.7.5 References

E.7.1 Evaluation of optimum moderating water density

The effect of water density change to the subcriticality of the package is evaluated under the condition of water immersion in the package.

The water density at optimum moderation depends on the distance and the neutron absorbing materials between fuel elements. In case of this package, there is no considerable difference in the pitch of steel pipe enveloping a fuel element.

Therefore, the evaluation of multiplication factor under the optimum moderation is performed for the case where the most reactive fuel element in the water of 1.0g/cm^3 is loaded to the package.

As the JRR-3 standard type fuel element (Uranium Silicon Aluminum Dispersion Type Alloy) is the most reactive in the water of 1.0g/cm^3 , the critical calculation is performed for JRR-3 standard type fuel elements (Uranium Silicon Aluminum Dispersion Type Alloy) by varying the water density from 0.0 to 1.0g/cm^3 . In addition, KUCA flat fuel case was investigated by varying the water density from 0.0 to 1.0g/cm^3 . The calculation model and material compositions except water composition is same as the water density of 1.0g/cm^3 .

(II)-Table E.10 and (II)-Fig.E.22 show the calculated multiplication factors for various water density. For JRR-3 standard type fuel, the optimum moderation is observed at the condition that the water density is about 0.02g/cm^3 . The calculated multiplication factor at the optimum moderation is 0.939 in 99% confidence level ($k_{\text{eff}} + 3\sigma$), lower than reference value of 0.95. For KUCA flat fuel case, the optimum moderation is observed at the condition that the water density is about 0.001g/cm^3 . The calculated multiplication factor at the optimum moderation is 0.9325 in 99% confidence level ($k_{\text{eff}} + 3\sigma$), lower than reference value of 0.95.

This result indicates that the package is maintained subcritical at any water density.

(II)-Table E.10 Effective multiplication factor for various water density

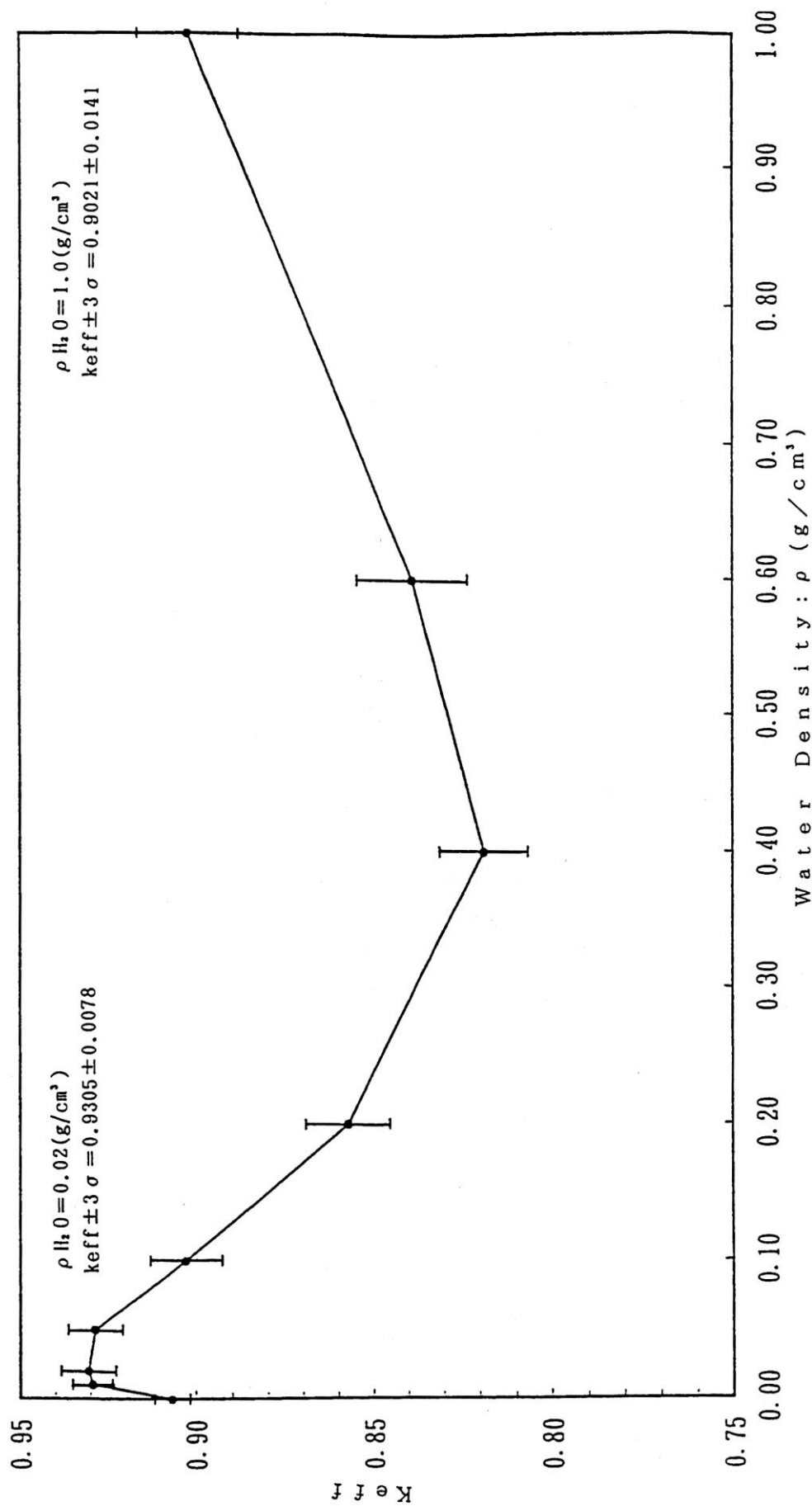
[contained ten JRR-3 standard type fuel elements

(uranium silicon Aluminum dispersion type alloy)]

Water Density (g/cm ³)	Keff	σ	Keff+3 σ
1.00	0.9021	0.0047	0.9162
0.60	0.8391	0.0052	0.8547
0.40	0.8189	0.0041	0.8312
0.20	0.8572	0.0040	0.8692
0.10	0.9028	0.0034	0.9130
0.05	0.9286	0.0026	0.9364
0.02	0.9305	0.0026	0.9383
0.01	0.9294	0.0019	0.9351
0.00	0.9067	0.0017	0.9118

(300 KUCA flat plates in a package)

Water Density (g/cm ³)	Keff	σ	Keff+3 σ
1.00	0.9055	0.003	0.9145
0.5	0.8321	0.0022	0.8387
0.1	0.9208	0.0019	0.9265
0.001	0.9295	0.0010	0.9325
0.00	0.9190	0.0009	0.9216



(II)-Fig. E. 22 Relationship between effective multiplication factor ($k_{eff} \pm 3\sigma$) and water density
 (contained ten JRR-3 standard type fuel elements (uranium silicon Aluminum dispersion type alloy))

E.7.2 Description of KENO-V. a code and KENO=VI code

(1) KENO-V. a code

KENO-V. a, developed by the U.S. ORNL, is a Monte-Carlo criticality calculation code. Based on the multigroup Monte-Carlo method, the KENO code is capable of calculating neutron multiplication factors for complicated systems.

As the library for neutrons cross section, the KENO code uses a library with neutron scattering matrix expressed by Legendre's extended terms (P_L) in multigroup form.

The KENO-IV, the version preceding the KENO-V. a, is only capable of handling primary degrees (P_1) for extension of scattering matrix, while the latest KENO-V. a is capable of handling any degrees. (However, the application only covers primary degrees.) The KENO-V. a has increased accuracy especially in systems where the anisotropy of neutrons' scattering has a great influence on their effective multiplication factor.

The KENO-V. a uses the same basic calculation method for effective multiplication factor as the KENO-IV. This method is based on the assumption that fissile neutrons generated in a field containing fissile material lose their weight in the course of collision with the medium according to their absorption cross section in the medium.

Neutrons will be traced until their weight falls lower than a specified value or until some of the neutrons begin to leak from the system. In the collision in a medium containing fissile material, the weight of fission is recorded and used for the distribution of neutron generations in the next generation. Generating neutrons (usually 300 neutrons) for one generation and repeating the generation of neutrons according to the weight distribution of fission in the preceding generation will bring about a distribution similar to that of actual fissile neutron generations. The effective multiplication factor of the system is the mean of the effective multiplication factors of the different generations.

$$K_{eff} = \frac{\sum_{j=1}^{NPB} \sum_{i=1}^{N_{cou}} W_{t_{ij}} \frac{\nu \Sigma_f}{\Sigma_t}}{\sum_{j=1}^{NPB} W_{t_{oj}}}$$

where NPB : Number of neutrons generated in one generation

N_{COLL}: Number of collisions of neutrons

W_{t_{ij}} : Weight of neutrons at the time of fission

W_{t_{oj}} : Weight of generated neutrons

ν : Number of neutron generations per fission

Σ_f : Macro fissile cross section

Σ_t : Total macro cross section

i : Number of collisions of neutrons

j : Number of neutron generated in one generation

(2) KENO-VI code

KENO-VI is the latest version of the Monte-Carlo criticality calculation code KENO, and is incorporated as Monte-Carlo criticality calculation module in SCALE code system. The calculation procedures are similar to those of KENO-V.a, whereas KENO-VI can handle more complicated geometry.

E.7.3 Explanation of MGCL neutron cross section library and MAIL code

MGCL is the multi-group neutron cross section library generated at JAEA by processing ENDF/B-IV⁽¹⁾ evaluated neutron cross section with SUPERTOG, PIXSES and other cross section processing codes. The energy group structure of MGCL master library is 137 groups.

MGCL master library includes the infinite diluted cross sections, resonance self shielding factors and scattering matrix for sixty seven nuclides. The scattering matrix is represented by p₁ approximation.

MAIL is the computer code to generate macroscopic effective cross section from MGCL in the form used by KENO-IV and ANISN. The heterogeneous effect of resonance self shielding is corrected with Dancoff-Ginsberg factor.

E. 7. 4 References

- (1) Y. Naito, et al. “MGCL-PROCESSUR: A Computer Code System for Processing Multi Group Constant Library MGCL,” JAERI-M9396 (1981).
- (2) L. M. Petrie. et al. “KENO-V a: A Monte Carlo Criticality Program with Super Grouping,” NUREG/CR-200 rev. 3 sec. F-11 (1984).
- (3) SCALE: A Modular Code System for Performing Standardized Computer Analyses for Licensing Evaluation, ORNL/TM-2005/39, Version 5.1, Vols. I-III, November 2006. Available from Radiation Safety Information Computational Center at Oak Ridge National Laboratory as CCC-732.
- (4) Y. Komuro, et al “KENO-IV Code Benchmark Calculation (10) (Critical Experiment of Light Water Type Critical Assembly),” JAERI-M9147(1980) (in Japanese).
- (5) K. Woods, et al. “Critical Experiments of SPERT-D Fuel in Water” , NEA/NSC/DOC(95)03/ II Volume III (1998).
- (6) Y. Nakano, et al. “Neutronics Characteristics of JRR-4 Low Enriched Uranium Core” , Proceedings of 21th International of RERTER (1998).

(II)-F Assessment of the compliance
with the regulation and the notification

(II)-F. Assessment of the compliance with the regulation and the notification

This transported article is in conformity to the relevant items of technical standards stipulated in the regulation and the notification as shown in (II) Table F.1.

(II) Table F.1: Assessment of the compliance with the technical standards stipulated in the regulation and the notification

Item of the regulation	Item of the notification	Explanation	Item corresponding to description in the application form	Remarks
Article 3-1-1	Article 3	Not applicable since this transported article is a BU-type transported article.		
Article 3-1-2	Article 4	Not applicable since this transported article is a BU-type transported article.		
Article 3-1-3	Article 4 and Appended table 1	The nuclear fuel material contained in this transported article corresponds to those other than special-form nuclear fuel materials, and is uranium alloy with enrichment of the fuel material being below 93.3 wt%. Since the amount of radioactivity contained in the cask exceeds the A ₂ value, this transported article corresponds to a BU-type transported article.	(I)-B	
Article 3-2	Article 5	Not applicable since this transported article is a BU-type transported article.		
Article 3-3		Since this transported article is a BU-type transported article, it is subject to the technical standard stipulated in Article 7 of the regulation.	(I)-D	
Article 4		Not applicable since this transported article is a BU-type transported article.		
Article 5		Not applicable since this transported article is a BU-type transported article.		
Article 6		Not applicable since this transported article is a BU-type transported article.		
Article 7-1		<ol style="list-style-type: none"> 1. The maximum weight of this transported article is approximately 950 kg. 2. To lift this transported article, an eye plate shall be used. The eye plate is designed to have a load factor three times the standard type, and is capable of withstanding abrupt lifting and lowering. 3. Except for the eye plate, the transported article is not attached with any hoisting tool that may be used to lift the transported article. 	(II)-A.4.4	Article 4-1

Item of the regulation	Item of the notification	Explanation	Item corresponding to description in the application form	Remarks
Article 7-1 (continued)	Article 9	There is a difference between the natural frequency of this transported article and the frequency expected during the transport, and the article will not resonate during the transport. Therefore, damage such as cracking or breakage due to vibration or the like is unlikely to occur.	(II)-A.4.7	Article 4-2
		This transported article is unlikely to have damage such as cracking or breakage at the temperature and pressure in the general test conditions, which are severer than the temperature and pressure expected during the transport.	(II)-A.5	Article 4-2
		The surface of this transported article is a smooth surface made of stainless steel, and has a structure that enables easy removal of contamination.	(I)-C	Article 4-3
		In this shipping cask, physical or chemical action will not occur between the materials, or between the casket and the fuel elements.	(II)-A.4.1	Article 4-4
		The inner shell of this transported article serves as a sealed boundary for the transported article, and no valve is provided. The lid of the inner shell is covered with the lid of an outer shell. Therefore, the lid of the inner shell will not be carelessly opened.	(II)-C.2.1 (II)-A.4.3	Article 4-5
		The lid of the outer shell is secured to the body of the outer shell with bolts, and is locked and sealed. Therefore, it will not be opened carelessly. Even if the lid were opened, that would be detected.		
		It shall be confirmed that the density of the radioactive material on the surface of this transported article does not exceed the following value in a pre-shipment inspection. 1. Radioactive material emitting alpha ray: 0.4 Bq/cm ² 2. Radioactive material not emitting alpha ray: 4 Bq/cm ²	(IV)-A.2	Article 4-8

Item of the regulation	Item of the notification	Explanation	Item corresponding to description in the application form	Remarks
Article 7-1 (continued)		The loading of fuels in the shipping cask is performed in accordance with prescribed procedures. Further, a content inspection is conducted as the pre-shipment inspection of the transported article. Therefore, no material that may impair the safety of the transported article will be loaded.	(IV)-A.2	Article 4-10
		In this transported article, each side of the circumscribed cube is 10 cm or more as indicated below.	(I)-C (I) Fig. C.1	Article 5-2
		JRF-90Y-950K type Height: approx. 1,800 mm Outer diameter: approx. 840 mm		
		Although the opening/closing section of the transported article is the lid of the inner shell, the lid is covered with the lid of the outer shell. Therefore, it will not be carelessly opened. In addition, the lid of the outer shell is locked and sealed.	(II)-A.4.3	Article 5-3
		The components of this transported article are unlikely to have damage such as cracking or breakage in the temperature range from -40 to +38°C.	(II)-A.3 (II)-A.4.2	Article 5-4
		Even if the ambient pressure reaches 60 kPa, the soundness and the sealability of the inner shell, which is the sealed boundary of this transported article, will be maintained. Therefore, no radioactive material will be leaked from this transported article.	(II)-A.4.6	Article 5-5
		This shipping cask will not contain radioactive material in liquid form.		Article 5-6
		The maximum dose equivalent rate on the surface of the transported article is 0.169 mSv/h, not exceeding 2 mSv/h.	(II)-D.5	Article 5-7
		The maximum dose equivalent rate in a position 1 m distant from the surface of the transported article is 19 µSv/h, not exceeding 100 µSv/h.	(II)-D.5	Article 5-8

Item of the regulation	Item of the notification	Explanation	Item corresponding to description in the application form	Remarks
Article 7-1 (continued)		Not applicable since the maximum amount of radioactivity of this shipping cask is less than 100,000 times the A2 value.	(II)-A.6.4	Article 6-5
Article 7-2	<p>Article 19 Appendix 7 Appendix 4-1</p> <p>Appendix 4-2 Appendix 3-1-i</p> <p>Appendix 3-1-ii</p> <p>Appendix 3-1-ii (1)</p> <p>Appendix 3-1-ii (3)</p>	<p>General test conditions for BU-type transported articles</p> <p>With ambient temperature of 38°C assumed, 800 W/m² is applied as the solar radiant heat to a flat surface, and 400 W/m² to a curved surface, for 24 hours a day in assessment.</p> <p>i. Water spray test The effect of spraying water equivalent to a precipitation of 50 mm/h for one hour is assessed.</p> <p>ii. After the specimen is placed under the condition (i), it is placed under the following condition.</p> <p>Free-fall drop test The maximum total weight of this transported article is approximately 950 kg, and the drop height is 1.2 m. Analysis is conducted so that the maximum damage caused by the drop can be assessed.</p> <p>Stack test Since applying a load equivalent to five times the transported article in self-weight will represent a severer condition, the strength of the inner shell under this condition is assessed.</p>	<p>(II)-B.4.1</p> <p>(II)-A.5.2</p> <p>(II)-A.5.3</p> <p>(II)-A.5.4</p>	

Item of the regulation	Item of the notification	Explanation	Item corresponding to description in the application form	Remarks
Article 7-2 (continued)	Appendix 3-1-ii (4)	<p>Penetration test</p> <p>In this test, a mild steel bar with a weight of 6 kg and a diameter of 3.2 cm was dropped from a height of 1 m to the weakest part of this transported article.</p> <p>The deformation of cushioning in the general test conditions is marginal, and the dose equivalent rate on the surface of the inner shell assumed as the surface of the transported article is far below the reference level of 2 mSv/h. Therefore, the dose equivalent rate on the surface would not significantly increase under the general test conditions.</p>	(II)-A.5.5	Article 5-9-ii
	Article 15	<p>If the transported article were placed under the general test conditions, the sealing performance would not decline. The leakage per hour of radioactive materials would not exceed the A2 value $\times 10^{-6}$.</p>	(II)-D.4	
	Article 9	<p>The temperature of the surface of this transported article is 38°C in the shade, and will not exceed 50°C.</p>	(II)-C.3.1	
		<p>The sealability of this transported article would not decline even under the general test conditions. Therefore, the contamination would not spread, and the contamination density on the surface which was observed in the pre-shipment inspection would not be exceeded.</p>	(II)-B.4.2	
Article 7-3	Article 20 Appendix 8 Appendix 5-1-i	<p>Special test conditions for BU-type transported articles</p> <p>Drop test I</p> <p>The maximum total weight of this transported article is 950 kg. To assess the maximum damage caused by the drop, an analysis is conducted in which the article falls from a height of 9 m to the drop test bench, which has a rigid surface, in the vertical, corner, horizontal and tilt directions.</p>	(I)-A.2	Article 6-2-ii
			(II)-A.6	Article 6-2-iii
			(II)-A.6.1	Article 6-2-iv

Item of the regulation	Item of the notification	Explanation	Item corresponding to description in the application form	Remarks
Article 7-3 (continued)	Appendix 5-1-ii	<p>Drop test II</p> <p>An analysis is conducted in which this transported article falls from a height of 1 m above a mild steel bar in vertical and horizontal drops where the center of gravity of this transported article is directly above the mild steel round bar, so that this transported article receives the maximum damage.</p>	(II)-A.6.2	Article 6-3-i
	Appendix 5-2 -i	<p>Fire resistance test</p> <p>An analysis is conducted in which after this transported article is applied with the same solar radiation heat as the general test conditions at environmental temperature of 38°C and it reaches a thermal equilibrium state, the article is exposed to an environment with radiation heat of 0.9 and temperature of 800°C. In addition, the surface absorptance of the transported article is 0.8.</p>	(II)-A.6.3	
	Appendix 5-2-ii	<p>Calculation is performed for this transported article until all internal temperatures start to fall in a state of natural cooling while the same heat input as the above is applied at environmental temperature of 38°C after the heating is stopped.</p>		
	Appendix 5-3	<p>Immersion test (water depth:15 m)</p> <p>An analysis is conducted in which this transported article was immersed in water at depth of 15 m for eight hours.</p> <p>The soundness of this transported article will not be impaired even in special test conditions, the dose equivalent rate in a position 1 m distant from the surface is 0.019 mSv/h, and the reference value of 10 mSv/h will not be exceeded.</p>	<p>(II)-A.6.4</p> <p>(II)-D.5</p>	

Item of the regulation	Item of the notification	Explanation	Item corresponding to description in the application form	Remarks
Article 7-3 (continued)	Article 17	<p>If this transported article is placed under special test conditions, the outer shell would be partially deformed. However, the sealability of the inner shell would be maintained.</p> <p>The leakage of radioactive material would not exceed the A₂ value per week.</p>	(II)-C.4.2	Article 6-3-ii
Article 7-4		The components of this transported article are unlikely to have damage such as cracking or breakage in the temperature range from -40 to +38°C.	(II)-A.3 (II)-B.4.2	
Article 7-5		For this transported article, no mechanical cooling device will be used. Instead, it has a structure that provides cooling of the content.	(II)-B.1	
Article 7-6		The maximum inner pressure of this transported article is 0.016 MPa [gauge] under the general test conditions, or 0.065 MPa [gauge] under special test conditions, and will not exceed 700 kPa [gauge].	(II)-B.4 (II)-B.5	
Article 8		Not applicable since this transported article is a BU-type transported article.		
Article 9		Not applicable since this transported article is a BU-type transported article.		
Article 10		Not applicable since this transported article is a BU-type transported article.		
Article 11	Article 23	Since this transported article will contain 15 g or more of uranium 235, and the enrichment of uranium 235 will be 19.95 to 93.3%, it corresponds to the requirements for fissionable transported articles.	(I)-B (I)-D	
Article 11-1	Article 24 Appendix 11-1-2	<p>(General test conditions)</p> <p>The effect of spraying water equivalent to a precipitation of 50 mm/h for one hour is assessed.</p> <p>The maximum total weight of this transported article is approximately 950 kg, and the drop height is 1.2 m. An analysis is conducted so that the maximum damage caused by the drop can be assessed.</p>	(II)-A.9.1 (II)-A.9.1	

Item of the regulation	Item of the notification	Explanation	Item corresponding to description in the application form	Remarks
Article 11-1 (continued)	Appendix 11-3	<p>Since applying a load equivalent to five times the transported article in self-weight will represent a severer condition, the strength of the inner shell under this condition is assessed.</p> <p>In this test, a mild steel bar with a weight of 6 kg and a diameter of 3.2 cm was dropped from a height of 1 m to the weakest part of this transported article.</p>	(II)-A.9.1 (II)-A.9.1	
Article 11-1-i		In the drop assessment, no dent containing a cube with a side of 10 cm was formed in the structural member.	(II)-A.9.1	
Article 11-1-ii		Each side of a rectangular solid circumscribed to this transported article will not be below 10 cm.	(II)-A.9.1	
Article 11-2-i, ii and iii	Article 25	With regard to this transported article at the time of normal transport, the conditions for an arranged system under special test conditions are severer in terms of criticality assessment than any of the isolated system conditions, general test conditions and special test conditions. Therefore, the criticality assessment shall be conducted for the arranged system.	(II)-E.3.1 (II)-E.4.4 (II)-E.5	
Article 11-2-iv and v	Article 27	<p>If this transported article were placed under the conditions for an arranged system, the special test conditions for the system are severer in terms of criticality assessment than the general test conditions. Therefore, the arrangement of an infinite number of transported articles is simulated. In addition, the entry of water, which is severer in terms of criticality assessment, is assumed. In such a case, the effective multiplication constant ($K_{eff} + 3\sigma$) would not exceed 0.95.</p> <p>Therefore, subcriticality of this transported article is secured even in an arranged system under special test conditions, which are the severest conditions.</p>	(II)-E.3.1 (II)-E.4.4 (II)-E.5	

Item of the regulation	Item of the notification	Explanation	Item corresponding to description in the application form	Remarks
Article 11-2-iii and v	Article 26 Appendix 12-1-i	The effect of spraying water equivalent to a precipitation of 50 mm/h for one hour is assessed.	(II)-A.9.1	
		The maximum total weight of this transported article is approximately 950 kg, and the drop height is 1.2 m. Analysis is conducted so that the maximum damage caused by the drop can be assessed.	(II)-A.9.1	
		Since applying a load equivalent to five times the transported article in self-weight will represent a severer condition, the strength of the inner shell under this condition is assessed.	(II)-A.9.1	
	Appendix 12-1-ii (1)	In this test, a mild steel bar with a weight of 6 kg and a diameter of 3.2 cm was dropped from a height of 1 m to the weakest part of this transported article.	(II)-A.9.1	
		The maximum total weight of this transported article is 950 kg. To assess the maximum damage caused by the drop, an analysis is conducted in which the article falls from a height of 9 m to the drop test bench, which has a rigid surface, in the vertical, corner, horizontal and tilt directions.	(II)-A.9.2	
	Appendix 12-1-ii (2)	An analysis is conducted in which this transported article falls from a height of 1 m above a mild steel bar in vertical and horizontal drops where the center of gravity of this transported article is directly above the mild steel round bar, so that this transported article receives the maximum damage.	(II)-A.9.2	
	Appendix 12-1-iii	An analysis is conducted in which after this transported article is applied with the same solar radiation heat as the general test conditions at environmental temperature of 38°C and it reaches a thermal equilibrium state, the article is exposed to an environment with radiation heat of 0.9 and temperature of 800°C. In addition, the surface absorptance of the transported article is 0.8.	(II)-A.9.2 (II)-B.5.6	

Item of the regulation	Item of the notification	Explanation	Item corresponding to description in the application form	Remarks
Article 11-2-iii and v (continued)	Appendix 12-1-iv	<p>Calculation is performed for this transported article until all internal temperatures start to fall in a state of natural cooling while the same heat input as the above is applied at environmental temperature of 38°C after the heating is stopped.</p> <p>For this transported article, and analysis is conducted while taking into account the entry of water.</p>	<p>(II)-A.9.2</p> <p>(II)-A.9.2</p>	
Article 11-3		The components of this transported article are unlikely to have damage such as cracking or breakage in the temperature range from -40 to +38°C.	<p>(II)-A.3</p> <p>(II)-A.4.2</p>	

(III) Basic policy for quality management

Chapter III: Basic policy for quality management

The basic policy for this quality management stipulates the requirements for quality assurance activities by reference to the “Guidelines for Quality Assurance on the Safety at Nuclear Power Plant Equipment (JEAC4111-2009).”

A. Quality management system

A.1 General requirements

- (1) In order to comply with the technical criteria of the relevant regulations and design specifications and manufacturing methods described in the application for confirmation regarding transport or application for transport packaging approval, Institute for Integrated Nuclear and Radiation Science, Kyoto University (hereinafter referred as “KURNS”) shall establish, perform and maintain the quality management system (hereinafter referred as “QMS”) concerning design, manufacture, handling, maintenance and transport of the transport packaging and nuclear facilities relevant to handling, maintenance and transportation of transport packaging (hereinafter referred as “transport packaging, etc.”). This quality assurance system shall be improved continuously through management review.
- (2) KURNS shall carry out the following operations:
 - a) clarifying the details of the necessary processes entailed by the QMS (including the results to be achieved by said processes), be able to identify how said processes will be individually applied.
 - b) Determine the order of these processes and their mutual relationships.
 - c) Determine the criteria and methods necessary for ensuring the implementation of processes and the effectiveness of their management.
 - d) Ensure a system that enables the use of the resources and information necessary for the implementation of processes, as well as their monitoring and measurement.
 - e) Monitor, measure, and analyze processes. However, where measurement is difficult, measurement shall not be required.
 - f) Take the necessary measures for obtaining the results of the processes set forth in item (i) and for maintaining effectiveness.
 - g) Render processes and organizations pertaining to the implementation of

quality assurance consistent with the QMS.

- h) Promote safety activities based on findings from the social sciences and behavioral sciences.

A.2 Requirements for documentation

A.2.1 General

In order to establish a QMS pursuant to the provisions of A.1, KURNS shall prepare the following documents and implement the items prescribed in said documents.

- a) A Quality Policy Statement and a Quality Objective Statement.
- b) A document specifying the provisions of the QMS (Quality Assurance Plan).
- c) Documents necessary for ensuring the effective and planned implementation and management of processes.
- d) Procedural manuals and records as defined in the Quality Assurance Plan.

A.2.2 Document management

- (1) KURNS shall manage the documents specified in this document and other documents necessary for the QMS (excluding records; hereinafter referred as “quality management documents”).
- (2) KURNS shall prepare procedural manuals stipulating the controls required for the following operations:
 - a) When issuing quality management documents, to review the validity of said documents and approve their release.
 - b) When updating quality management documents after performing the necessary reviews, to approve said updates.
 - c) To make it possible to identify content changes and the status of the latest revisions to quality management documents.
 - d) When using a revised quality management document, to ensure that systems are able to use the appropriate revised version of said document.
 - e) To ensure that quality management documents are easy to read and in a state such that their contents can be easily grasped.

- f) To identify quality management documents prepared by external bodies and manage their distribution.
- g) To prevent the unintentional use of obsolete quality management documents. In such cases, when retaining said documents, to identify such regardless of their purpose.

A.2.3 Control of records

- (1) As well as clarifying the object of records specified in this document and of records demonstrating compliance with other requirements and effective implementation of the QMS, KURNS shall prepare and manage said records in a searchable format while ensuring that their contents are easy to read and can be easily grasped.
- (2) KURNS shall prepare procedural manuals stipulating necessary controls relating to the identification, preservation, protection, search, retention period, and disposal of the records set forth in the previous paragraph.
- (3) KURNS shall confirm the following items regarding the quality records of the transport packaging:
 - a) Quality records shall include quality records submitted by the manufacturer of the transport packaging,
 - b) Retention periods of the quality records shall be determined with regards to the validity period of the packaging license and design license of the transport packaging.

B. Responsibility of the Applicant

B.1 Commitment of the management

The director of KURNS (hereinafter referred as “Director”), as operating representative, shall demonstrate responsible leadership through his or her involvement in establishing, implementing, and maintaining the effectiveness of the QMS by conducting the following operations:

- a) Establishing a quality policy.
- b) Ensuring the establishment of quality objectives.
- c) Promoting activities that foster a safety culture.
- d) Implementation of management review.
- e) Ensuring systems that are able to utilize resources.
- f) Informing personnel implementing safety activities (hereinafter, “Section personnel”) of the importance of observing the applicable laws and regulations and otherwise ensuring the safety of nuclear energy.

B.2 Responsibility and authority

B.2.1 Responsibility and authority

(1) System

Figure III-B.1 shows the quality assurance organization which performs the duties regarding the quality assurance plan.

(2) Responsibility and authority

The Director shall ensure that the responsibilities and authorities of each Section and Section personnel (including responsibility for explaining the content of safety activities) are defined, documented, and widely understood.

B.2.2 Quality assurance representatives

The director shall grant responsibility and authority for the following operations to personnel responsible for managing and supervising the QMS

(hereinafter, “quality assurance representatives”).

- a) Ensure that processes are established and implemented, and that their effectiveness is maintained.
- b) Report to the director the implementation status of the QMS and any needed improvements.
- c) In each Section, raise awareness about observing the applicable laws and regulations and otherwise ensure the safety of nuclear energy.

B.2.3 Responsibilities and authority of section heads

The Director shall grant responsibility and authority for the following operations to the heads in each Section (hereinafter, “Section Heads”) as the parties responsible for managing and supervising these processes.

- a) Ensure that processes for the individual operations managed by the Section Head are established and implemented, and that their effectiveness is maintained.
- b) Raise awareness regarding individual operations requirements on the part of Section personnel engaged in individual operations managed by the Section Head.
- c) Conduct evaluations regarding the performance of individual operations managed by the Section Head.
- d) Promote activities that foster a safety culture.

B.2.4 Internal audit representative

- (1) The Director shall appoint an internal audit representative.
- (2) The internal audit representative shall perform operations for planning and implementing the internal audit as the responsible personnel of the internal audit.

B.3 Management review

B.3.1 General

- (1) The Director shall, at predefined intervals, review the QMS to confirm its

validity and effectiveness, as well as maintain its effectiveness (including evaluation of room for improvement and the need for changes to the QMS, quality policy, or quality objectives; hereinafter, “management review”).

- (2) KURNS shall arrange for quality assurance representatives to prepare and manage records of the results of the management review.

B.3.2 Input to management review

The Director shall carry out management review based on the following inputs:

- a) Audit results.
- b) Feedback from parties outside KURNS (e.g., external institutions, regulatory agencies, the Kyoto University administration, local residents, and users).
- c) Process implementation status.
- d) The results of inspections of the transport packaging, etc.
- e) Quality objective achievement status.
- f) Implementation status of activities for fostering a safety culture.
- g) Compliance status regarding applicable laws and regulations.
- h) The status of corrective actions (hereinafter understood as remedial actions carried out to prevent the reoccurrence of nonconformities, which in turn are hereinafter understood as states that do not conform to requirements) and preventive actions (hereinafter understood as preventive measures to prevent potential nonconformities.)
- i) Measures taken in response to the results of previous management reviews (follow-up measures).
- j) Changes that may affect the QMS.
- k) Proposals for improvements from each Section or from Section personnel.

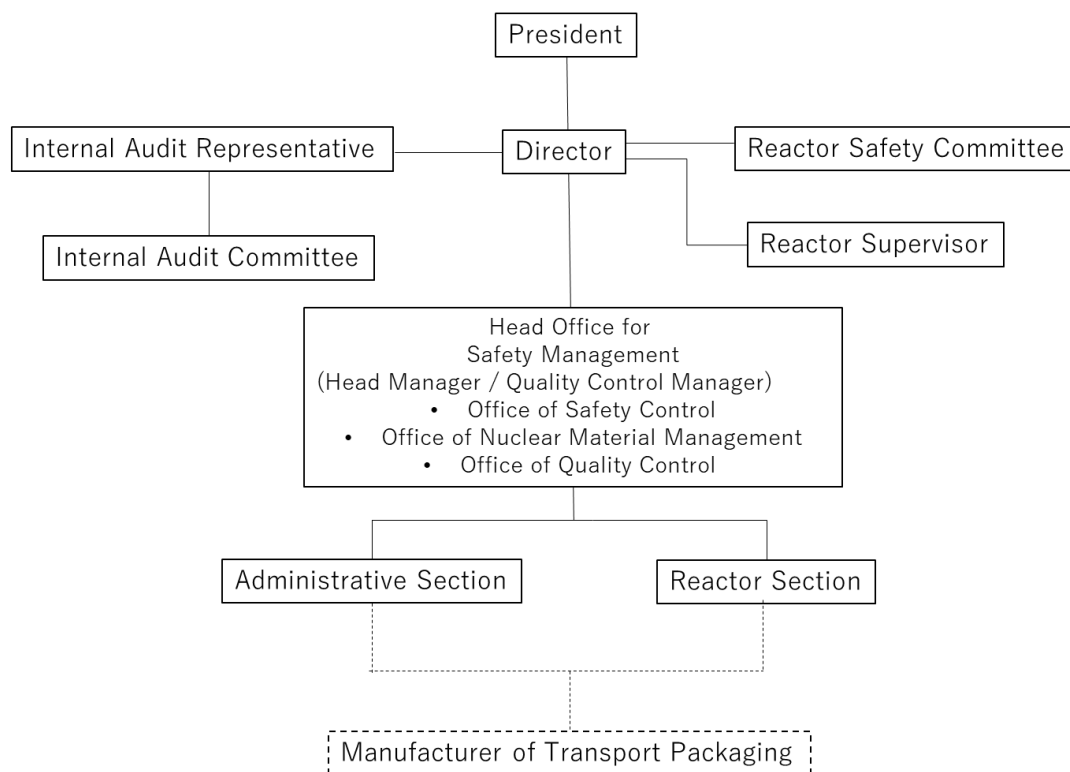
B.3.3 Output from management review

The Director shall obtain information pertaining to the following matters from the management review and take steps as necessary.

- a) Improvements needed to maintain the effectiveness of the QMS and operations.
- b) Improvements to safety activities associated with the planning and

implementation of individual operations.

- c) Resources necessary for ensuring maintenance of the validity and effectiveness of the QMS.



(III)-Fig. B. 1

Quality assurance organization for design of the transport packaging

C. Education and training

C.1 Securing resources

KURNS shall determine and secure the necessary resources for ensuring safety.

C.2 Section personnel

KURNS shall ensure that Sections are staffed with personnel who have demonstrated their abilities sufficiently to satisfy the following requirements.

- a) Have appropriate education and training.
- b) Have the requisite skills and experience.

C.3 Education and training, etc.

KURNS shall undertake the following operations.

- a) Determine the kinds of abilities required by Section personnel.
- b) Clarify the need for education and training among Section personnel.
- c) Provide education and training and otherwise take steps to fulfill the need for education and training set forth in the previous item.
- d) Evaluate the effectiveness of measures set forth in the previous item.
- e) Ensure that Section personnel are aware of the relationship and importance of their own individual operations to achieving quality objectives, and that they recognize ways of making their own contributions.
- f) Prepare and manage appropriate records regarding the education and training, as well as skills and experiences of Section personnel.

D. Design control

D.1 Planning of processes required by individual operations

- (1) KURNS shall formulate and establish plans for the processes required by individual operations for transport packaging etc.
- (2) Plans formulated pursuant to the provisions of the previous paragraph (hereinafter referred as “individual operations plans”) shall be consistent with the requirements of the other processes.
- (3) When formulating individual operations plans, KURNS shall appropriately determine with regard to the following items.
 - a) Quality objectives and individual operations requirements pertaining to individual operations and transport packaging, etc.
 - b) Necessary processes, and quality management documents and resources that are specific to individual operations or transport packaging, etc.
 - c) Necessary verification, validation, monitoring, and measurement, as well as inspection and testing specific to the individual operations or transport packaging, etc., and criteria for determining the compliance of individual operations or transport packaging, etc. (hereinafter, “compliance-determining criteria”).
 - d) Records necessary for verifying that processes pertaining to individual operations and transport packaging, etc., and the results thereof conform to individual operations requirements.
 - e) KURNS shall ensure that outputs relating to the formulation of individual operations plans take forms that correspond to work methods.

D.2 Determination of individual operations requirements

KURNS shall determine the following items as individual operations requirements.

- a) Matters that, although not explicitly stated by outside parties, are known to be necessary requirements for individual operations or transport packaging, etc.
- b) Applicable laws and regulations that concern said individual operations and transport packaging, etc.
- c) Other requirements deemed necessary by KURNS.

D.3 Review of individual operations requirements

- (1) Prior to implementing individual operations or utilizing transport packaging, etc., KURNS shall implement a prior review of individual operations requirements.
- (2) When implementing the review set forth in the previous paragraph, KURNS shall confirm the following items.
 - a) That individual operations requirements have been specified for said individual operations or transport packaging, etc.
 - b) Where the individual operations requirements pertaining to said individual operations or transport packaging, etc. differ from individual operations requirements determined beforehand, those said differences are clarified.
 - c) That KURNS has the ability to comply with the predetermined requirements.
- (3) KURNS shall prepare and manage records pertaining to the results of the review set forth in the first paragraph, as well as records pertaining to the steps taken based on the results of the said review.
- (4) When individual operations requirements are changed, in addition to revising the relevant documents, KURNS shall ensure that the relevant Section personnel are informed of the modified individual operations requirements.

D.4 Transmission of information to external parties

KURNS shall clarify and implement effective methods for the transmission of information to external parties.

D.5 Design and development planning

KURNS, as well as formulating plans for design and development (Hereinafter “design and development plans” understood as the definition of specifications for transport packaging, etc., taking their necessary requirements into consideration.), shall also manage design and development.

- (1) When formulating design and development plans, KURNS shall determine the

following items:

- a) Stages of design and development.
 - b) Review, verification, and validation as appropriate for each stage of design and development.
 - c) The responsibility and authority of Section and Section personnel involved with design and development (including the responsibility to explain the content of safety activities).
- (2) In order to ensure the effective transmission of information and clear assignment of responsibility and authority, KURNS shall manage and supervise communication between the various individuals involved in design and development.
- (3) KURNS shall properly update the design and development plan formulated pursuant to the provisions of the first paragraph in accordance with the progress of design and development.

D.6 Input related to design and development

- (1) As well as determining inputs relating to design and development as listed below with regard to the requirements pertaining to transport packaging, KURNS shall prepare and manage records relating to the pertinent information.
- a) Requirements pertaining to transport packaging with regard to function or performance in accordance with intended usage.
 - b) Information obtained from the prior implementation of similar design and development that is applicable as input to said design and development.
 - c) Applicable laws and regulations.
 - d) Other requirements essential to design and development.
- (2) KURNS shall review and approve the validity of inputs relating to design and development.

D.7 Output related to design and development

- (1) KURNS shall retain outputs related to design and developments in a format that enables verification relative to inputs related to design and development.

- (2) When approving progress from design and development to the next stage in the process, KURNS shall first approve the relevant outputs related to design and developments.
- (3) KURNS shall ensure that outputs related to design and development meet the following conditions.
 - a) Compliance with requirements that constitute inputs related to design and development.
 - b) Provision of appropriate information for procurement, for the implementation of individual operations, and for the use of transport packaging, etc.
 - c) Inclusion of compliance-determining criteria.
 - d) Prescription of specific characteristics of transport packaging, etc.. that are indispensable for the safe and proper use of transport packaging, etc.

D.8 Design and development review

- (1) At the appropriate stage, KURNS shall implement a systematic review of design and development (hereinafter, “design and development review”) including the following items in accordance with the design and development plan.
 - a) Evaluate whether the results of design and development can comply with requirements.
 - b) Where problems with design and development exist, ensure the ability to identify the problematic content in question and propose the necessary measures.
- (2) In the design and development review process, KURNS shall involve representatives of the Sections associated with the design and development stage that is the object of the review in question, as well as experts related to said design and development.
- (3) Where the necessary measures have been taken based on records of the results of design and development review and the results in question, KURNS shall prepare and manage the records thereof.

D.9 Design and development verification

- (1) KURNS shall implement verification in accordance with the design and development plan in order to ensure that outputs related to design and development are in a state of conformance with requirements that are inputs related to the design and development in question. In this case, it shall ascertain conformity with the requirements when proceeding to the next stage in the process in accordance with the design and development plan.
- (2) KURNS shall prepare and manage records of the results of the verification set forth in the preceding paragraph (including records of necessary measures taken based on the results of the verification in question).
- (3) KURNS shall not allow any Section or Section personnel involved in the design and development in question to conduct the verification set forth in the first paragraph.

D.10 Validation of design and development

- (1) In order to ensure that transport packaging comply with the requirements concerning the prescribed performance, purpose of use, and intended usage method, KURNS shall implement the validation of the design and development in question in accordance with the design and development plan as it relates to the transport packaging in question (hereinafter referred to in this article as “design and development validation”).
- (2) When using the transport packaging, KURNS shall first complete design and development validation. However, if it is not possible to carry out validation until after the installation of the transport packaging in question, then design and development validation shall be carried out prior to commencing the use of the transport packaging.
- (3) Where the necessary measures have been taken based on records of the results of design and development validation and the results of the validation in question, KURNS shall prepare and manage the records thereof.

D.11 Control of design and development changes

- (1) When a design and development change has been made, as well as ensuring that the ability to identify the content of said changes, KURNS shall prepare and manage a record pertaining to the change in question.
- (2) When implementing design and development changes, KURNS shall approve these

after first carrying out the appropriate review, verification, and validation.

- (3) KURNS shall ensure that the scope of the review of design and development changes includes evaluation of the impact of the changes in question on transport packaging (including an evaluation of impact on materials and components that constitute the transport packaging in question).
- (4) KURNS shall prepare and manage records relating to the results of the review of changes under the provisions of paragraph 2 (including any records of necessary measures taken based on the results of said review).

E. Manufacturing order of transport packaging

E.1 Quality management plan

KURNS shall establish a quality management plan defining the quality management operation of transport packaging manufacturing, including the quality control of manufacturer and supplier of transport packaging.

E.2 Procurement process

- (1) When ordering the manufacturing of the transport packaging, KURNS shall ensure that the manufacturing of the transport packaging complies with the technical criteria set by law, design specifications specified in application for transport packaging design approval or application for transport packaging approval and manufacturing process specified in application for transport packaging design approval, and shall ensure that externally procured goods and services procured (hereinafter referred as “procured goods, etc.”) shall comply with its own specified requirements pertaining to procured goods, etc. (hereinafter referred as “requirements for procured goods, etc.”).
- (2) KURNS shall ensure the items in the preceding paragraph when KURNS orders the manufacturing of the part(s) of the transport packaging and supplies the part(s) to the manufacturer of the transport packaging.

E.3 Evaluation of the Manufacturer of Transport Packaging

KURNS shall perform the following items:

- (1) Evaluate the ability of the manufacturer of transport packaging to manufacture the transport packaging and select the manufacturer. The following items shall be considered upon evaluating the manufacturer's ability.
 - a) Technology and personnel regarding the transport packaging manufacturing.
 - b) Quality policy, quality management plan of the manufacturer and their implementation status.
 - c) Supply experience of transport packaging or similar products.
 - d) Usage experience and quality records of transport packaging or similar products.
 - e) Evaluation of test products and samples, etc.

- (2) Clarify the method and level of management of the manufacturer performed by KURNS.

E.4 Quality Management Requirement to the Manufacturer

When ordering the manufacturing of transport packaging, KURNS shall clearly instruct the manufacturer of the transport packaging about the following requirements in a document such as a specification sheet, and ensure the manufacturer to implement the requirements:

- a) The manufacturer of the transport packaging shall implement quality control that complies with "E.8 Content of Quality Management by Manufacturer of the Transport Packaging".
- b) Measures shall be taken so that the personnel of KURNS and the regulatory authorities can inspect the manufacturer of the transport packaging and the supplier of the manufacturer of the transport packaging during the manufacture of the transport packaging and confirm the quality control status.
- c) Measures shall be taken so that KURNS can examine and approve the selection criteria for suppliers of manufacturer of the transport packaging. Measures shall be taken so that KURNS can confirm the selection status of the manufacturer of the transport packaging's supplier.
- d) Measures shall be taken to clarify the relationship of responsibilities between business operators involved in the manufacture of transport packaging through contracts.
- e) Measures shall be taken to ensure that the manufacturer of the transport packaging and the supplier of the manufacturer of the transport packaging fully understand the meaning and importance of the numerical values regarding the safety-critical material specifications specified by KURNS.
- f) When using special materials that are of high safety importance in the manufacture of transport packaging, information on the construction, analysis, and inspection methods related to manufacturing shall be exchanged beforehand between the business operators involved in the manufacture of transport packaging and take measures to ensure that technical studies are carried out sufficiently.

- g) In processes that involve multiple business operators regarding the manufacture of transport packaging, clarify the arrangements such as work instructions and delivery agreements and ensure close cooperation.
- h) If a non-conforming product occurs and it is used by rework, etc., notify KURNS in writing and receive instructions for handling.
- i) Immediate reporting and approval of any significant changes in the manufacturer of the transport packaging's manufacturing process.

E.5 Verification of manufacturing of transport packaging

- (1) KURNS shall conduct quality audits on the manufacturer of the transport packaging, understand the status of quality audits by the manufacturer of the transport packaging on suppliers, and directly check the quality control status with the supplier if necessary.
- (2) When inspecting transport packaging, KURNS shall perform witness inspection and record inspections considering the importance of safety and other factors, while considering the existence of public standards and official qualification systems and the status of quality control of manufacturer of the transport packaging and suppliers.
- (3) KURNS shall prepare and implement documents such as inspection plans, inspection procedures, and implementation procedures for quality inspections related to the production and inspections of transport packaging.

E.6 Schedule management and certification of special processes

KURNS shall create and manage the manufacturing schedule and inspection schedule for manufacturing the transport packaging. KURNS shall also certify processes that cannot be sufficiently verified in the subsequent inspection as special processes, and clarify the method of certifying and managing workers and processes.

E.7 Measurement, analysis and improvement

E.7.1 General

KURNS shall formulate and implement a plan concerning processes related to the monitoring, measurement, analysis, and improvements necessary for the following

operations (including applicable methods of inspection and testing [including statistical methods] and the determination of the scope of the application of the methods in question):

- a) Demonstrating conformity with individual operations requirements.
- b) Ensuring the conformity of the QMS and maintaining its effectiveness.

E.7.2 Opinions from outside parties

- (1) As part of the monitoring and measurement of the implementation status of the QMS, KURNS shall grasp the opinions of individuals external to the transport packaging, etc., for ensuring safety.
- (2) KURNS shall clarify its grasp of the opinions referenced in the preceding paragraph, as well as determine methods concerning the reflection of said opinions.

E.7.3 Internal audit

- (1) In order to determine whether the QMS meets the following requirements, KURNS shall implement an internal audit by an Internal Audit Committee at predefined intervals. KURNS shall arrange for an Internal Audit Representative to convene and instruct the Internal Audit Committee.
 - a) KURNS conforms to the requirements of the individual operations plan, the provisions of this document, and the requirements related to the QMS in question.
 - b) Effective implementation and maintenance have been carried out.
- (2) KURNS shall formulate an internal audit implementation plan that takes into consideration the status and importance of the areas and processes targeted by the internal audit, as well as the results of previous audits.
- (3) KURNS shall establish the criteria, scope, frequency, and method of the internal audit.
- (4) KURNS shall ensure objectivity and impartiality in its selection of internal audit committee members and in the implementation of the internal audit.
- (5) KURNS shall not allow the internal audit committee to conduct an internal audit of its own individual operations.
- (6) KURNS shall establish the responsibility, authority, and requirements for formulating and implementing an internal audit implementation plan, as well

as reporting the results of the internal audit and managing the records thereof, in a procedural manual.

- (7) KURNS, in addition to having managers responsible for the areas subjected to internal audit take rapid measures to eliminate any discovered nonconformities and the causes of said nonconformities, shall also arrange for the verification of said measures and the reporting of their results.

E. 7.4 Process monitoring and measurement

- (1) When conducting the monitoring and measurement of processes, KURNS shall apply monitoring and measurement methods suited to the monitoring and measurement of said processes.
- (2) Using the monitoring and measurement methods set forth in the preceding paragraph, KURNS shall demonstrate that processes are able to obtain the results prescribed in the quality management plan and individual operations plans.
- (3) In the event that it is not possible to obtain the results prescribed in the quality management plan and individual operations plans, KURNS shall take appropriate remedial and corrective action to ensure conformity with individual operations requirements.

E. 7.5 Inspection and test

- (1) KURNS shall carry out the inspection and testing of transport packaging in order to verify that the transport packaging conform to requirements.
- (2) KURNS shall carry out the inspection and testing set forth in the previous paragraph at the appropriate stage of processes relating to the implementation of individual operations, according to the individual operations plan and the procedural manuals.
- (3) KURNS shall prepare and manage records, etc., related to the results of inspection and testing, which constitute evidence of conformity with the compliance-determining criteria of inspection and testing.
- (4) KURNS shall prepare and manage records specifying individuals who approve proceeding to the next stage in a process.

- (5) KURNS shall not approve proceeding to the next stage of a process until inspection and testing based on the individual operations plan is completed and found to be free of trouble.
- (6) KURNS shall designate individuals to conduct inspection and testing in accordance with the importance of individual operations and transport packaging. In this case, the neutrality of the individuals who will conduct inspection and testing shall be taken into consideration.

E. 7.6 Management of nonconformity

- (1) In order to prevent individual operations and transport packaging that do not conform to requirements from being neglected, KURNS shall identify the individual operations and transport packaging in question and ensure that they are managed correctly.
- (2) KURNS shall set out management pertaining to the handling of nonconformities and the responsibility and authority associated with such in a procedural manual.
- (3) KURNS shall handle nonconformities using one of the following methods.
 - a) Taking measures to eliminate any nonconformities discovered.
 - b) Approving the implementation of individual operations, the use of transport packaging or advancement to the next stage of a process (hereinafter, “specially adopted measures”).
 - c) Taking measures to prevent the originally intended use or application.
 - d) In the event that a nonconformity is discovered after the implementation of an individual operation, taking appropriate measures against the effects or potential effects of the nonconformity.
- (4) KURNS shall prepare and manage records of the content of nonconformities and of measures (including specially adopted measures) taken against said nonconformities.
- (5) Where a nonconformity has been modified, KURNS shall carry out a secondary verification to confirm conformity with individual operations requirements in the wake of the modification.

E. 7.7 Data analysis

- (1) In order to demonstrate that the QMS is appropriate and effective and to evaluate room for improvement in terms of its effectiveness, KURNS shall determine, collect, and analyze appropriate data (including data obtained from the results of monitoring and measurement and data from other relevant information sources).
- (2) By analyzing the data set forth in the preceding paragraph, KURNS shall obtain information relating to the following items.
 - a) Opinions from parties external to the transport packaging
 - b) Conformity with individual operations requirements
 - c) Characteristics and trends of processes and transport packaging (including those that will serve as the starting point for preventive action)
 - d) The supply capacity of the suppliers of procured goods, etc.

E. 7.8 Improvement

As well as clarifying all items for which changes are necessary for maintaining the validity and effectiveness of the QMS through the utilization of its quality policy, quality objectives, the results of internal auditing, data analysis, corrective actions, preventive actions, and management review, KURNS shall implement the changes in question.

E. 7.9 Corrective actions

- (1) KURNS shall take appropriate corrective action in light of the impact of the nonconformities discovered. In such cases, KURNS shall conduct an analysis for investigating the fundamental causes of matters that have arisen affecting nuclear energy safety (hereinafter, “root cause analysis”) after establishing procedures for doing so.
- (2) KURNS shall prepare a Corrective Action Procedural Manual stipulating the following requirements.
 - a) Review of nonconformities.
 - b) Determination of the causes of nonconformities.
 - c) Evaluation of the necessity of measures for ensuring that nonconformities do not reoccur.
 - d) Determination and implementation of the necessary corrective actions

(including document updates).

- e) In the event that a survey has been carried out regarding corrective actions, recording of the results thereof and of corrective actions taken based on said results.
- f) Review of the corrective actions taken and their effectiveness.

E. 7.10 Preventive actions

- (1) KURNS shall determine and take appropriate preventive action in light of the impact of the potential problems. In such cases, KURNS shall reflect appropriately not only on findings obtained through the implementation of safety activities in its own transport packaging, etc., but also on findings obtained from other facilities.
- (2) KURNS shall prepare a Preventive Action Procedural Manual stipulating the following requirements (including requirements relating to root cause analysis).
 - a) Determination of potential nonconformities and their causes.
 - b) Evaluation of the necessity for preventive action.
 - c) Determination and implementation of the necessary preventive actions.
 - d) In the event that a survey has been carried out regarding preventive actions, record of results thereof and of preventive actions taken based on said results.
 - e) Review of the preventive actions taken and their effectiveness.

E. 8 Content of quality management system by manufacturer of transport packaging

KURNS shall require the following items related to quality management from the manufacturer of transport packaging when placing an order for manufacturing the transport packaging with the manufacturer of transport packaging.

E. 8. 1 Quality management system

E. 8. 1. 1 General

The manufacturer of the transport packaging shall establish, document, implement and maintain a quality management system in order to implement the manufacturing in conformity with the requirements related to the manufacturing of transport packaging.

E. 8. 1. 2 Documentation requirements

E. 8. 1. 2. 1 General

The quality management system documentation shall include a documented statement of quality policy and quality objectives, and E. 8. 1. 2. 2 through E. 8. 1. 2. 4 below.

E. 8. 1. 2. 2 Quality Manual

The manufacturer of the transport packaging shall develop and maintain a quality manual containing a description of the scope of the quality management system, the documented procedures established for the quality management system and the interrelationships between the processes of the quality management system.

E. 8. 1. 2. 3 Document management

The manufacturer of the transport packaging shall control the documentation required by the quality management system. Establish documented procedures that

define the controls required for document approval and review and identification.

E.8.1.2.4 Quality record management

The manufacturer of the transport packaging shall create and maintain readable, identifiable, and searchable quality records. The manufacturer shall establish a documented procedure that defines the controls required for the identification, storage, protection, retrieval, storage period and disposal of quality records. The quality record shall include the quality record submitted by the supplier.

E.8.2 Responsibility of the Manufacturer of the Transport Packaging

E.8.2.1 Chief Executive Commitment

The chief executive of the manufacturer of the transport packaging shall show evidence of its commitment to establishing and implementing a quality management system and continually improving its effectiveness by setting quality policies, ensuring that quality objectives are set, and conducting management reviews.

E.8.2.2 Responsibility and authority

E.8.2.2.1 Responsibility and authority

The chief executive of the manufacturer of the transport packaging shall ensure that the responsibilities and authorities for the operations that affect the quality of the production of the transport packaging are defined and are known to the entire organization.

E.8.2.2.2 Management Representative Officer

The chief executive of the manufacturer of the transport packaging shall appoint a management representative officer who has the responsibility and authority for the implementation of the quality management system from the management personnel level.

E. 8. 2. 3 Management review

The chief of the manufacturer of the transport packaging shall regularly review the quality management system to ensure that it is effective.

E. 8. 3 Resource operation management

E. 8. 3. 1 Provision of personnel

The manufacturer of the transport packaging shall identify and provide the personnel necessary to implement and maintain the quality management system and to continually improve its effectiveness.

E. 8. 3. 2 Education and training

- (1) The manufacturer of the transport packaging shall clarify the competence required for personnel engaged in work that affects the quality of manufacturing of transport packaging, educate and train them to have the necessary competence and maintain the records.
- (2) Persons engaged in the specified work shall be qualified based on appropriate education/training history and experience as necessary.

E. 8. 4 Manufacturing of transport packaging

E. 8. 4. 1 Quality control plan

- (1) The manufacturer of the transport packaging shall establish a quality control plan that defines quality management operations related to the manufacturing of transport packaging, including quality control of suppliers, and formulate a quality control plan.
- (2) The manufacturer of the transport packaging shall consider the following items as appropriate in order to meet the requirements related to the manufacture of transport packaging.
 - a) All control measures, processes, equipment (including inspection equipment), equipment, management resources and technology that are considered necessary to achieve the requirements shall be secured.

- b) Manufacturing process, inspection procedures and documents shall be coordinated.
- c) Quality control and inspection techniques shall be updated as necessary.
- d) Verification method in the transport packaging manufacturing process shall be clarified.
- e) Acceptance criteria shall be clarified.
- f) Quality records shall be created

E. 8. 4. 2 Confirmation of Contract Details

- (1) The manufacturer of the transport packaging shall establish the procedure for confirming the contract content.
- (2) The manufacturer of the transport packaging shall confirm the contents before submitting the quotation specification or before contracting, and confirm that he/she has the ability to meet the contract requirements.

E. 8. 4. 3 Purchasing

E. 8. 4. 3. 1 General

The manufacturer of the transport packaging shall define the procedure for conforming the purchased items (including services; the same shall apply hereinafter) to the requirements. It should be noted that this does not apply to purchased goods manufactured based on JIS or other public standards, or those for which the items to be checked for inspection are simple or general-purpose products, and whose compatibility can be confirmed by inspection at the time of acceptance.

E. 8. 4. 3. 2 Evaluation of the suppliers

The manufacturer of the transport packaging shall implement the following items.

- a) Develop selection criteria for suppliers, evaluate whether suppliers have the ability to meet the requirements of supply contracts, and make selections.

- b) Clarify to the supplier the type and extent of controls performed by the manufacturer of the transport packaging.

E.8.4.3.3 Purchasing data

The manufacturer of the transport packaging shall prepare a purchase document stating the supply requirements and instruct the supplier.

E.8.4.3.4 Purchase verification

- (1) The manufacturer of the transport packaging shall prepare a document such as a guideline for the inspection of purchased products.
- (2) The manufacturer of the transport packaging shall verify the purchased items by performing necessary inspections or other activities.

E.8.4.4 Process control

- (1) The manufacturer of the transport packaging shall carry out the following items when planning and controlling the manufacturing process of transport packaging.
 - a) Develop a written procedure that clarifies the method of manufacturing that may affect quality.
 - b) In each process, use appropriate equipment and ensure an appropriate work environment.
 - c) Perform all processes according to quality control plans, procedures, etc.
 - d) To monitor the characteristic values of processes and products.
 - e) Appropriate maintenance of equipment to maintain continuous process capability.
 - f) In the event of a supplier nonconformity or significant change in the manufacturing process, prompt documentation shall be provided and appropriate action shall be taken.
- (2) The manufacturer of the transport packaging shall certify the process whose results cannot be sufficiently verified by the subsequent inspection as a special process in consultation with the applicant, and clarify the method of certifying and controlling the worker and the process. Records shall be kept as appropriate for the certified processes, equipment and personnel.

E. 8. 4. 5 Identification and traceability

- (1) The manufacturer of the transport packaging shall establish a procedure for identifying the condition of the transport packaging at all stages from receiving the material to manufacturing.
- (2) The manufacturer of the transport packaging shall establish procedures to enable tracking of quality records for individual transport packaging.

E. 8. 4. 6 Managing customer supplies

The manufacturer of the transport packaging shall establish procedures for verification, storage and management of the goods supplied by the applicant for incorporation into the manufactured transport packaging or for related work. For lost or damaged supplies and other supplies not suitable for use, record and report to the applicant.

E. 8. 4. 7 Inspection

E. 8. 4. 7. 1 General

The manufacturer of the transport packaging shall establish the procedure for inspection work. Required inspections and records shall be specified in the quality control plan or procedure manual.

E. 8. 4. 7. 2 Acceptance inspection

The manufacturer of the transport packaging shall not use or process the purchased product until it confirms that the purchased product complies with the requirements.

E. 8. 4. 7. 3 In-process inspection

The manufacturer of the transport packaging shall implement the following items:

- a) Inspect the transport packaging in accordance with the provisions of the quality control plan and procedure manual.
- b) Do not proceed to the next step until the prescribed inspection is completed or the required report is received and verified.

E.8.4.7.4 Final inspection

The manufacturer of the transport packaging shall perform a final inspection in accordance with the quality control plan and procedure manual to confirm that the transport packaging complies with the requirements.

E.8.4.7.5 Inspection record

The manufacturer of the transport packaging shall create and keep an inspection record of the transport packaging. These records shall show whether the inspection has been passed according to the criteria. If the inspection does not pass, apply the procedures for managing nonconforming products.

E.8.4.8 Control of inspection, measurement and test equipment

E.8.4.8.1 General

- (1) The manufacturer of the transport packaging shall define procedures for controlling and calibrating inspection, measurement and test equipment (hereinafter referred to as "measuring equipment, etc."). Use the measuring device according to the measuring ability.
- (2) The manufacturer of the transport packaging shall define the scope and frequency of inspection of measuring devices and keep the records.

E.8.4.8.2 Management procedure

The manufacturer of the transport packaging shall implement the following items:

- a) Clarify the measurement items and the required accuracy, and select appropriate measurement equipment.
- b) To specify calibration of measuring devices.

- c) Calibrate and adjust measuring devices, etc. regularly or before use. If there are no international or national standards for calibration and adjustment, record the standards used for calibration.
- d) Identify the calibration status of the measuring device, etc., by using an appropriate sign.
- e) Keep calibration records of measuring devices.
- f) If the measuring device is discovered to be out of the calibration standard, the validity of the past inspection results shall be evaluated and recorded.
- g) Calibration, inspection, measurement and testing shall be performed under appropriate environmental conditions.
- h) Protect the measuring device etc., from damage and deterioration during handling, maintenance and storage.

E. 8.4.9 Inspection Status

The manufacturer of the transport packaging shall identify the inspection status of the transport packaging in all processes of manufacturing in order to ship only the transport packaging that has passed the inspection, in accordance with the provisions of the quality control plan and the procedure manual.

E. 8.5 Measurement, analysis and improvement

E. 8.5.1 Internal Audit

- (1) The manufacturer of the transport packaging shall conduct internal audits on a regular basis to clarify whether the quality management system is effectively implemented and maintained. The audit plan and its implementation shall be defined in a documented procedure. Auditors shall not audit their own work.
- (2) The person in charge of the audited area shall ensure that any nonconformities found and their causes can be taken without delay. The results of the internal audit shall be input to the management review.

E. 8.5.2 Management of nonconforming products

- (1) The manufacturer of the transport packaging shall ensure to identify and control transport packaging that do not meet the requirements. Controls and associated responsibilities and authorities for handling nonconforming products shall be established in documented procedures.
- (2) Repaired or reworked transport packaging shall be reverified to demonstrate compliance with the requirements.

E. 8. 5. 3 Improvement

E. 8. 5. 3. 1 Corrective Action

- (1) The manufacturer of the transport packaging shall take measures to eliminate the cause of nonconformity in order to prevent recurrence.
- (2) Documented procedure shall be established by the manufacturer to specify requirements for:
 - a) Applicant's complaint and confirmation of nonconforming product report contents.
 - b) Identification of the causes of nonconformities related to transport packaging, processes and quality management systems.
 - c) Assessing the need for action to ensure the prevention of nonconformity recurrence.
 - d) Determination and implementation of necessary measures.
 - e) Recording the results of the actions taken.

E. 8. 5. 3. 2 Preventive Measures

- (1) The manufacturer of the transport packaging shall decide the action to eliminate the cause in order to prevent the occurrence of possible nonconformity.
- (2) The manufacturer shall establish a documented procedure to specify requirements for:
 - a) Identification of possible nonconformities and their causes.
 - b) Assessing the need for action to prevent the occurrence of nonconformities.
 - c) Determination and implementation of necessary actions.
 - d) Recording the results of the actions taken.

F. Handling and Maintenance

F.1 Handling Management

- (1) In order to prevent accidental operation and damage to the transport packaging during handling, KURNS shall establish in a document a handling management method including the following items and manage it appropriately.
 - a) Measures to prevent erroneous operation and damage during inspection and handling of handling equipment.
 - b) Handling conditions for transport packaging.
 - c) Conditions and methods for loading and unloading transport packaging from storage facilities.
 - d) Person in charge of facility management.
- (2) KURNS shall clearly indicate the handling requirements to the person who handles it, and reflect it in the prevention of incorrect operation and damage of the transport packaging.

F.2 Maintenance and storage management

- (1) In order to maintain conformity with the requirements for transport packaging, KURNS shall establish in a document a storage management method that includes the following items and manage them appropriately.
 - a) Measures to prevent damage during storage.
 - b) Storage method and storage area setting in consideration of environmental conditions.
 - c) Inspection during storage.
 - d) Person in charge of facility management.
- (2) KURNS shall clearly indicate the requirements for maintenance and storage management to those who perform maintenance and storage management, and reflect them in the prevention of erroneous operation and damage to the transport packaging.

If the quality management system is reviewed, the revised content shall be applicable.

(IV) Handling methods and maintenance
of nuclear fuel package

(IV)-A Package handling methods

A.1 Method of loading

The contents of this package are loaded in the following manner.

(1) Preparation of the contents

Before being loaded, the contents shall pass a content inspection based on the pre-shipment content inspection indicated in (IV)-A.2.

(2) Loading of contents and installation of inner lid

The packaging shall be transferred by means of handling tools to a location for loading and removal of the outer lid and inner lid. After this operation, the contents prepared in advance shall be loaded into a fuel basket and a top spacer shall be inserted.

After completion of the above operations, the inner lid shall be installed and the inner lid clamping bolt shall be fastened at a specified torque.

(3) Leak-tightness inspection on the inner lid

Leak-tightness inspection on the inner lid shall be conducted.

(4) Installation of an outer lid

The outer lid shall be fitted and fastened by a clamping bolt with a specified torque, and sealed and locked.

A.2 Package inspection prior to shipment

Pre-shipment inspection indicated in (IV)-Table A.1 is performed on each shipment of the package.

A.3 Method for removal

The contents shall be removed from the package in the following procedure.

- (1) Remove the outer lid and the inner lid.
- (2) Remove the upper spacer.
- (3) Remove the contents from the package.
- (4) Install the inner lid and the outer lid.

A.4 Preparation of empty packaging

After the contents are removed from the packaging, conduct radiation control of the inner surface of the packaging, and conduct decontamination as needed. In addition, conduct a visual appearance inspection of the packaging to confirm it has no anomaly, and then store it indoor.

(IV) Table A.1: Procedures for pre-shipment inspection of the package

Item of inspection	Method for inspection	Acceptance criterion
Visual appearance inspection	Visually inspect the appearance of the main body, inner lid and outer lid.	No cracking, abnormal flaw, deformation, etc. is observed.
Lifting inspection	With the package lifted, inspect its appearance.	The eye-plates have no cracking, abnormal flaw, deformation, etc.
Weight inspection	Measure the total weight of the package.	The weight is not more than 950 kg.
Surface density inspection	Measure the surface density of the package by the smear method or the like.	The surface density is not more than 0.4 Bq/cm ² for radioactive materials emitting alpha ray, or not more than 4 Bq/cm ² for radioactive materials not emitting alpha ray.
Dose equivalent rate inspection	With fuel elements loaded, measure the dose equivalent rate for gamma ray and neutron ray.	The sum of the dose equivalent rate for gamma ray and neutron ray is not more than 2 mSv/h on the surface of the package, or not more than 100 μSv/h in a position 1 m distant from the package surface.
Subcriticality inspection	Visually inspect the appearance of the fuel basket.	1. The fuel basket is installed in the prescribed position. 2. No cracking, abnormal flaw, deformation, etc. is observed.
Content inspection	Inspect/measure the type, concentration, volume, appearance and surface density.	1. Type It must be the design approval conditions. 2. Concentration and volume It must be the design approval conditions. 3. Appearance: no anomaly is observed. 4. Surface density: not more than 0.056 Bq/cm ² for radioactive materials emitting alpha ray
Airtight leakage inspection	Apply air pressure of 0.392 MPa [gauge] to the sealed parts of the inner lid for 30 minutes, and measure the pressure drop to determine the leakage rate.	The leakage rate does not exceed 1.09×10^{-2} MPa·cm ³ /s.
Pressure measurement / inspection	The decay heat generated from the contents is minimal, and the vessel's temperature will remain the same as the ambient temperature. Therefore, this inspection shall not be conducted.	
Temperature measurement / inspection	The decay heat generated from the contents is minimal, the pressure in the package will remain constant, and therefore the pressure from inside the package will remain the same as the ambient pressure. Therefore, this inspection shall not be conducted.	

(IV)-B Maintenance requirement

(IV)-B. Maintenance requirements

The transport packaging shall be stored indoor. Periodical self-controlled inspections shall be conducted in accordance with the following instructions at least once every year (at least once every 10 times of use for those used 10 times or more yearly).

B.1 Visual appearance inspection

Perform a visual inspection to confirm that there is no cracking, abnormal flaw, deformation, etc. in the inner and outer surfaces of the main body, fuel basket, inner lid, and outer lid.

B.2 Pressure durability inspection

If a repair or the like that may affect the pressure durability performance has been conducted, install a provisional inner lid and inspect the leakage rate for the main body of the inner shell by pressurized leakage testing (initial inspection pressure: 0.392 MPa [gauge] or more; inspection time: 30 minutes or more) to confirm that the leakage rate is not more than $1.09 \times 10^{-2} \text{ MPa} \cdot \text{cm}^3/\text{s}$.

Subsequently, perform a visual inspection to confirm that there is no cracking, abnormal flaw, deformation, etc. in the inner surface of the main body of the inner shell.

B.3 Airtight leakage inspection

Conduct airtight leakage inspection for the O-ring of the inner lid by pressurized leakage testing (inspection pressure: 0.392 MPa [gauge] or more; inspection time: 30 minutes or more) to confirm that the leakage rate is not more than $1.09 \times 10^{-2} \text{ MPa} \cdot \text{cm}^3/\text{s}$.

B.4 Shielding inspection

This does not apply since no particular shield is used in this transport packaging.

B.5 Subcriticality inspection

Perform visual inspection to confirm that there is no anomaly in the dimensions, shape, etc. of the fuel basket, such as cracking, abnormal flaw, and deformation.

B.6 Thermal inspection

This does not apply since this transport packaging has no particular exothermic body.

B.7 Lifting inspection

With the transport packaging lifted, inspect the appearance of the transport packaging to visually confirm that the eye-plates have no cracking, abnormal flaw, deformation, etc.

B.8 Actuation check/inspection

This does not apply since this transport packaging has no special articles such as valves.

B.9 Maintenance of auxiliary systems

This does not apply since this transport packaging has no auxiliary system.

B.10 Maintenance of the valves, gaskets, etc. of sealing devices

This transport packaging has no valve or the like.

Inspect the O-ring of the inner lid to confirm that it has no cracking, abnormal flaw, deformation, etc. If any anomaly is observed, replace the O-ring.

B.11 Storage of the transport packaging

The transport packaging shall be stored indoor.

B.12 Retention of records

While this transport packaging is in service, retain a record of inspection conducted during fabrication and a record of periodical self-controlled inspection.

B.13 Others

Not Applicable

(V) Important Notice about a safe design and the safe transportation
Not Applicable